MOLECULAR NANOMACHINES OF THE PRESYNAPTIC TERMINAL, VOLUME II

EDITED BY: Silvio O. Rizzoli and Lucia Tabares

PUBLISHED IN: Frontiers in Synaptic Neuroscience

frontiers Research Topics

ISSN 1664-8714
ISBN 978-2-88976-467-9
DOI 10.3389/978-2-88976-467-9

About Frontiers

Frontiers is more than just an open-access publisher of scholarly articles: it is a pioneering approach to the world of academia, radically improving the way scholarly research is managed. The grand vision of Frontiers is a world where all people have an equal opportunity to seek, share and generate knowledge. Frontiers provides immediate and permanent online open access to all its publications, but this alone is not enough to realize our grand goals.

Frontiers Journal Series

The Frontiers Journal Series is a multi-tier and interdisciplinary set of open-access, online journals, promising a paradigm shift from the current review, selection and dissemination processes in academic publishing. All Frontiers journals are driven by researchers for researchers; therefore, they constitute a service to the scholarly community. At the same time, the Frontiers Journal Series operates on a revolutionary invention, the tiered publishing system, initially addressing specific communities of scholars, and gradually climbing up to broader public understanding, thus serving the interests of the lay society, too.

Dedication to Quality

Each Frontiers article is a landmark of the highest quality, thanks to genuinely collaborative interactions between authors and review editors, who include some of the world's best academicians. Research must be certified by peers before entering a stream of knowledge that may eventually reach the public - and shape society; therefore, Frontiers only applies the most rigorous and unbiased reviews.
Frontiers revolutionizes research publishing by freely delivering the most outstanding research, evaluated with no bias from both the academic and social point of view. By applying the most advanced information technologies, Frontiers is catapulting scholarly publishing into a new generation.

What are Frontiers Research Topics?

Frontiers Research Topics are very popular trademarks of the Frontiers Journals Series: they are collections of at least ten articles, all centered on a particular subject. With their unique mix of varied contributions from Original Research to Review Articles, Frontiers Research Topics unify the most influential researchers, the latest key findings and historical advances in a hot research area! Find out more on how to host your own Frontiers Research Topic or contribute to one as an author by contacting the Frontiers Editorial Office: frontiersin.org/about/contact

MOLECULAR NANOMACHINES OF THE PRESYNAPTIC TERMINAL, VOLUME II

Topic Editors:
Silvio O. Rizzoli, Society for Scientific Data Processing, Max Planck Society, Germany
Lucia Tabares, Sevilla University, Spain

Citation: Rizzoli, S. O., Tabares, L., eds. (2022). Molecular Nanomachines of the Presynaptic Terminal, Volume II. Lausanne: Frontiers Media SA.
doi: 10.3389/978-2-88976-467-9

Table of Contents

frontiers | Frontiers in Synaptic Neuroscience

EDITORIAL
published: 07 June 2022
doi: 10.3389/fnsyn.2022.941339

Editorial: Molecular Nanomachines of the Presynaptic Terminal, Volume II

Lucia Tabares[1]* *and Silvio O. Rizzoli*[2]*

[1] Department of Medical Physiology, School of Medicine, University of Seville, Seville, Spain, [2] Instituts für Neuro- und Sinnesphysiologie Zentrum Physiologie und Pathophysiologie, Universitätsmedizin Göttingen Georg-August-Universität, Göttingen, Germany

Keywords: synapse, exocytosis, endocytosis, neurons, nanomachines

Editorial on the Research Topic

Molecular Nanomachines of the Presynaptic Terminal, Volume II

The synapse has been designed and refined during animal evolution for two main processes: (1) to translate and transmit information with exquisite spatio-temporal precision, and (2) to prevent the spread of unspecific signals. This resulted in a highly specialized arrangement of molecules, especially on the presynaptic side, to enable the synapse to respond to these pressures. For example, the exocytosis machinery needs to be exquisitely sensitive to meaningful signals and respond precisely to different stimulation patterns. The endocytosis machinery needs to balance exocytosis to prevent changes in synapse shape and volume, but also needs precision in the selective removal of vesicular material, rather than random uptake of membrane components.

Multiple machines (nanomachines) need to be coordinated to organize this activity and keep it in tune with the long-term needs of the neuron and the synapse. Proteins and vesicles become "used" and need to be eventually degraded, either locally or in lysosomes located elsewhere, which poses significant logistic challenges. Some of these challenges need to be solved within the synaptic vesicle cluster, while others require the re-organization of the synaptic release sites. Moreover, the synapse as a whole needs to maintain its organization and modulate its shape and size dynamically in relation to the activity and plasticity needs of the neuronal network. Actin is among the most important elements that modulate these aspects, being responsible for both vesicle dynamics and maintaining the plasma membrane shape (*via* cortical actin). In addition, the extracellular matrix also participates in the maintenance of synapse shape and connectivity.

Our Research Topic presents a timely and thorough view of many of these synaptic elements, starting at the level of individual proteins, proceeding up to complex plasticity and re-shaping mechanisms. Two of the most abundant proteins of the synapse, synaptobrevin (VAMP2) and synaptophysin, are revised by White and Stowell, who discuss their organization in the synapse, especially in relation to how these molecules impact the traffic of vesicles to the presynaptic membrane and the formation of the fusion complex. The clear conclusion is that these molecules form complexes involved in multiple functions, fully deserving the term "nanomachines."

One long-standing issue has been that such molecules are typically analyzed in static conditions, while their functions are most evident during phases of activity. To solve this problem, Jackson et al. present here the combination of live imaging with structural imaging methods at the super-resolution level. This type of approach enables a thorough functional view of the synaptic complex and should enable many discoveries in the future. At the same time, imaging synaptic proteins can be combined with the direct investigation of other elements, such as the neurotransmitters themselves. For analyzing these components, Lork et al. present chemical imaging methods that can be implemented both in fixed and live cells.

Edited and reviewed by:
P. Jesper Sjöström, McGill University, Canada

***Correspondence:**
Lucia Tabares
ltabares@us.es
Silvio O. Rizzoli
srizzol@gwdg.de

Received: *11 May 2022*
Accepted: *24 May 2022*
Published: *07 June 2022*

Citation:
Tabares L and Rizzoli SO (2022) Editorial: Molecular Nanomachines of the Presynaptic Terminal, Volume II. Front. Synaptic Neurosci. 14:941339. doi: 10.3389/fnsyn.2022.941339

Imaging methods have long served the synaptic exocytosis field and have led, more than a decade ago, to the conclusion that not every exocytosis event is the same as any other. Synaptic vesicles and active zones are heterogenous and specialized for different release flavors, even within the same synapse, as explored by Guzikowski and Kavalali. Nevertheless, all fused vesicles need to be eventually retrieved and re-formed. This process is complex, and also connects to the degradation system in complex fashions involving the endo-lysosomal molecules. The involvement of these molecules in the synaptic vesicle recycling system is analyzed by Ivanova and Cousin. Importantly, as implied above, protein degradation does serve not only the synaptic vesicle cycle but also other synaptic processes. Here the evidence on the involvement of different presynaptic structures with membrane-based protein-degradation pathways is reviewed by Gundelfinger et al., concluding that synaptic vesicles, their endocytic machinery, and the main components of the release sites are strongly connected to degradation pathways.

Synaptic proteins and vesicles are often connected by actin, which participates in many of the dynamic processes of the synapse. Actin is involved in almost all forms of endocytosis, in the vesicle replenishment to the readily releasable pool, the expansion of the fusion pore, and even in vesicular content release, as described by Wu and Chan.

While synaptic vesicles have been known to undergo exo- and endocytose for decades, this is less known for other synaptic components. Surprisingly, extracellular matrix molecules do it as well, in a fashion that relates to synaptic vesicle dynamics (Dankovich and Rizzoli), which presumably represents a new form of plasticity involved in re-shaping the synaptic release sites and adjusting them to the structure of the post-synapse.

The release sites themselves are also complex and dynamic and are functionally linked to and regulated by mitochondria, as Lopez-Manzaneda et al. demonstrate. The mitochondria act mainly by buffering the local Ca^{2+} concentrations, thereby regulating the fusion of the synaptic vesicles during activity bursts (rendering it synchronous or asynchronous). This finding enhances our current understanding of the regulation of the release site function since most previous works have concentrated on Ca^{2+} dynamics related to the entry of ions through membrane channels that are located at the release sites and were therefore thought to be more likely to affect vesicle release than the more distantly located mitochondria. While it is not yet clear whether the mitochondria-based regulation also involves modulation of the release site architecture, Holderith et al. show here that such regulation, including the selective placement and organization of specific proteins, is more common than previously thought. This type of regulation may even be a strong component of presynaptic plasticity since the release sites, along with the synaptic vesicles, are among the primary targets for plasticity-related alterations, as discussed by Shahoha et al.

The works in this topic provide, therefore, a glimpse into the complex organization of the presynapse, from single molecules to plasticity mechanisms. In comparison to the similarly titled topic of 6 years ago, we can conclude that, while the number of targets and nanomachines increased strongly, so did our knowledge of the intricate synaptic dynamics. The major progress in synapse-describing tools that has ensued over the last years also offers the hope that even more quantitative works can be performed in the future, providing an even more precise understanding of the function of this essential brain component.

AUTHOR CONTRIBUTIONS

All authors listed have made a substantial, direct, and intellectual contribution to the work and approved it for publication.

Conflict of Interest: The authors declare that the research was conducted in the absence of any commercial or financial relationships that could be construed as a potential conflict of interest.

Publisher's Note: All claims expressed in this article are solely those of the authors and do not necessarily represent those of their affiliated organizations, or those of the publisher, the editors and the reviewers. Any product that may be evaluated in this article, or claim that may be made by its manufacturer, is not guaranteed or endorsed by the publisher.

frontiers in Synaptic Neuroscience

MINI REVIEW
published: 20 September 2021
doi: 10.3389/fnsyn.2021.740318

Room for Two: The Synaptophysin/Synaptobrevin Complex

Dustin N. White and Michael H. B. Stowell**

MCD Biology, University of Colorado Boulder, Boulder, CO, United States

Synaptic vesicle release is regulated by upwards of 30 proteins at the fusion complex alone, but disruptions in any one of these components can have devastating consequences for neuronal communication. Aberrant molecular responses to calcium signaling at the pre-synaptic terminal dramatically affect vesicle trafficking, docking, fusion, and release. At the organismal level, this is reflected in disorders such as epilepsy, depression, and neurodegeneration. Among the myriad pre-synaptic proteins, perhaps the most functionally mysterious is synaptophysin (SYP). On its own, this vesicular transmembrane protein has been proposed to function as a calcium sensor, a cholesterol-binding protein, and to form ion channels across the phospholipid bilayer. The downstream effects of these functions are largely unknown. The physiological relevance of SYP is readily apparent in its interaction with synaptobrevin (VAMP2), an integral element of the neuronal SNARE complex. SNAREs, soluble NSF attachment protein receptors, comprise a family of proteins essential for vesicle fusion. The complex formed by SYP and VAMP2 is thought to be involved in both trafficking to the pre-synaptic membrane as well as regulation of SNARE complex formation. Recent structural observations specifically implicate the SYP/VAMP2 complex in anchoring the SNARE assembly at the pre-synaptic membrane prior to vesicle fusion. Thus, the SYP/VAMP2 complex appears vital to the form and function of neuronal exocytotic machinery.

Keywords: synaptic fusion, fusion machinery, supercomplex, synaptobrevin, synaptophysin (SYP)

OPEN ACCESS

Edited by:
Lucia Tabares, Sevilla University, Spain

Reviewed by:
Janet E. Richmond, University of Illinois at Chicago, United States
Luís F. Ribeiro, VIB & KU Leuven Center for Brain & Disease Research, Belgium

***Correspondence:**
Dustin N. White
dustin.n.white@colorado.edu
Michael H. B. Stowell
stowellm@colorado.edu

Received: *12 July 2021*
Accepted: *18 August 2021*
Published: *20 September 2021*

Citation:
White DN and Stowell MHB (2021) Room for Two: The Synaptophysin/Synaptobrevin Complex. Front. Synaptic Neurosci. 13:740318. doi: 10.3389/fnsyn.2021.740318

INTRODUCTION

Communication between neurons is a fundamental process of the nervous system. Regulated neurotransmitter release contributes to everything from memory consolidation to mood regulation (Jurado et al., 2013; Kandel et al., 2014; Metzger et al., 2017). Aberrant synaptic release is associated with numerous neurological disorders, and the molecular mechanisms underlying this process are elaborate (Roselli and Caroni, 2015; Körber and Kuner, 2016; Ramos-Miguel et al., 2018). The general role of vesicle and target SNAREs, v-SNAREs and t-SNAREs respectively, in vesicle fusion at the pre-synaptic membrane has been widely studied, but some of the individual components of this pathway are more nebulous (Karmakar et al., 2019). Specifically, SYP, while prolific at most pre-synaptic terminals, has no well-defined role within the synaptic architecture (Marqueze-Pouey et al., 1991). Putative functions of the vesicle membrane protein SYP include vesicular ion channel activity,

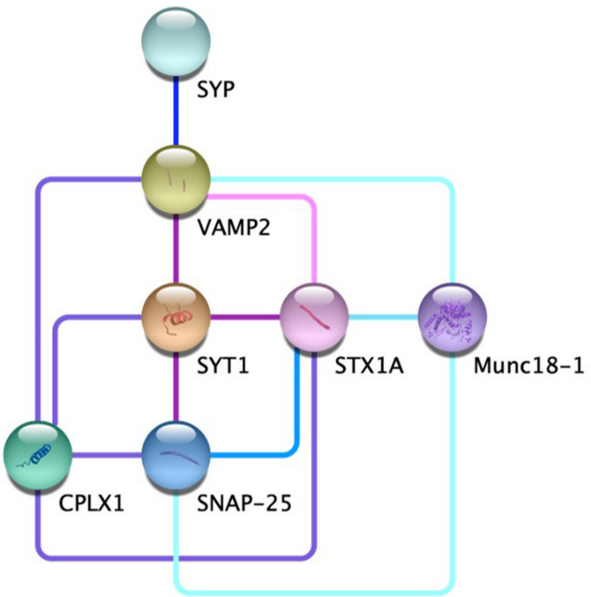

FIGURE 1 | The protein-protein interaction network at the chemical synapse. Direct evidence for the edges displayed for VAMP2-STX1A (Far et al., 1995; Hazzard et al., 1999); VAMP2-SYT1-SNAP25 (Söllner et al., 1993a,b; Chapman et al., 1995; Zhang et al., 2002); VAMP2-SYT1- SYTX1A-CPLX1 (Pabst et al., 2000; Bracher et al., 2002; Chen et al., 2002; Zhou et al., 2017); SYP-VAMP2 (Edelmann et al., 1995; Felkl and Leube, 2008; Gordon et al., 2011; Adams et al., 2015); STX1A-SNAP25 (McMahon and Südhof, 1995; Fasshauer et al., 1997); STX1A-Munc18-1 (Hata et al., 1993; Misura et al., 2000; Zilly et al., 2006; Rickman et al., 2007); VAMP2-SNAP25-Munc18-1 (Carr et al., 1999; Dulubova et al., 2007).

vesicle endocytosis, synaptobrevin trafficking during SNARE assembly, and the kiss-and-run archetype of dense-core vesicle fusion (Gincel and Shoshan-Barmatz, 2002; Kwon and Chapman, 2011; Harper et al., 2017; Chang et al., 2021). Probing these functions has proved difficult, however, due to the compensatory nature of various physin family proteins (Janz et al., 1999). SYP's interaction with VAMP2 is of particular interest; the two proteins form a complex thought to contribute to the characteristic speed and reactivity of synaptic vesicle release (Adams et al., 2015). Recent advances have further illuminated the individual and cooperative roles of SYP and VAMP2 in synaptic vesicle regulation. Recent advances have further illuminated the individual and cooperative roles of SYP and VAMP2 in synaptic vesicle regulation as well as the interaction network between other key players in vesicle fusion (**Figure 1**, **Table 1**; Szklarczyk et al., 2019).

Synaptophysin

Despite its prevalence at the pre-synaptic terminal, synaptophysin's role in vesicular neurotransmission is highly speculative. Synaptophysin (SYP) forms a transmembrane structure on synaptic vesicles similar to canonical gap junctions and mechanosensitive ion channels (Arthur and Stowell, 2007). This structure is concordant with the idea that SYP forms functional ion channels within membranes (Yin et al., 2002). Indeed, SYP multimers reconstituted in phospholipid bilayers are selective for cations and show a preference for potassium (Gincel and Shoshan-Barmatz, 2002). Though past studies saw no change in ion channel activity in response to fluctuation in Ca^{2+} concentration, SYP is known to bind cytoplasmic calcium (Rehm et al., 1986). The importance of calcium-dependent exocytosis in neurotransmitter release is widely accepted, but the specific function of SYP-Ca^{2+} binding is unclear (Karmakar et al., 2019).

In addition to its association with Ca^{2+}, SYP readily binds cholesterol in the plasma membrane. This binding is necessary for the initial formation of synaptic vesicles (Thiele et al., 2000). Further roles for cholesterol in the function of SYP, including regulation of synaptic plasticity and the interaction of synaptophysin with synaptobrevin, have been suggested, but the precise physiology underlying this relationship remains elusive (Mitter et al., 2003; Ya et al., 2013).

Synaptobrevin

VAMP2, syntaxin, and SNAP-25 form the core assembly of SNARE proteins (Brunger, 2005). The collaborative functions of these and other SNARE-associated proteins are necessary for Ca^{2+}-dependent neurotransmitter release at presynaptic terminals (Weber et al., 1998). VAMP2 knockout mice exhibit profoundly reduced rates of vesicle fusion, though fusion is not abrogated entirely (Schoch et al., 2001). While VAMP2 alone may not be necessary for fusion overall, its absence profoundly affects the rate of neurotransmission. Additionally, VAMP2/VAMP3 double knockout results in complete termination of presynaptic vesicle fusion, reinforcing the significance of synaptobrevin and its structural homologs (Borisovska et al., 2005).

VAMP2 may also be required for the maintenance of the readily releasable pool (RRP). Specifically, VAMP2 appears to be associated with the "fast endocytosis" necessary for quick Ca^{2+} signaling. At terminals with depleted RRPs, the rate of vesicle recycling is significantly impacted by the absence of VAMP2 (Deák et al., 2004). "Slow endocytosis" is also VAMP2 dependent, but appears to rely on the activity of additional SNAREs syntaxin and SNAP-25 (Xu et al., 2013a). This dual role of VAMP2 heavily implicates it in the cycle of exo- and endocytosis required to maintain the RRP.

SYP/VAMP2 Complex

Exocytosis

While Ca^{2+} induced exocytosis is widely recognized as the basis of neurotransmitter release, the molecular architecture underlying this process is a point of contention (Berridge, 1998; Neher and Sakaba, 2008; Williams and Smith, 2018). The neuronal SNARE fusion complex at the pre-synaptic plasma membrane results from the assembly of numerous fusion proteins, including syntaxin, SNAP-25, and synaptobrevin (VAMP2; Brunger, 2005). Recent cryoelectron tomographic evidence points to a conserved, symmetric distribution of proteins at primed active zones. While the identity of these proteins is unknown, it is clear that their assembly is dependent

TABLE 1 | Network evidence—STRING false discovery rate (FDR) < 1e-10.

Article title	Author	FDR
Candidate pathway association study in cocaine dependence: the control of neurotransmitter release	Fernàndez-castillo et al. (2012)	1.89E-15
Subtle Interplay between synaptotagmin and complexin binding to the SNARE complex	Xu et al. (2013b)	1.47E-13
Munc18a does not alter fusion rates mediated by neuronal SNAREs, synaptotagmin, and complexin	Zhang et al. (2002)	8.50E-13
Quantitative Proteomic Analysis Reveals Molecular Adaptations in the Hippocampal Synaptic Active Zone of Chronic Mild Stress-Unsusceptible Rats.	Zhou et al. (2015)	9.85E-13
Solution NMR of SNAREs, complexin, and α-synuclein in association with membrane-mimetics	Liang and Tamm (2018)	9.85E-13
MicroRNA-153 impairs presynaptic plasticity by blocking vesicle release following chronic brain hypoperfusion	Yan et al. (2020)	3.15E-11
Ca^{2+}-Triggered Synaptic Vesicle Fusion Initiated by Release of Inhibition	Brunger et al. (2018)	7.38E-11
De novo STXBP1 mutations in mental retardation and nonsyndromic epilepsy	Hamdan et al. (2009)	9.81E-11
The cell adhesion protein CAR is a negative regulator of synaptic transmission	Wrackmeyer et al. (2019)	2.15E-10
Identification of SNARE and cell trafficking regulatory proteins in the salivary glands of the lone star tick, Amblyomma americanum (L.)	Karim et al. (2002)	2.47E-10
Extended Synaptotagmin (ESyt) Triple Knock-Out Mice Are Viable and Fertile without Obvious Endoplasmic Reticulum Dysfunction	Sclip et al. (2016)	2.71E-10
Impaired gene and protein expression of exocytotic soluble N-ethylmaleimide attachment protein receptor complex proteins in pancreatic islets of type 2 diabetic patients.	Ostenson et al. (2006)	3.34E-10
Munc18-1 binding to the neuronal SNARE complex controls synaptic vesicle priming	Deák et al. (2009)	3.34E-10
Munc13 mediates the transition from the closed syntaxin-Munc18 complex to the SNARE complex	Ma et al. (2011)	3.34E-10
The synaptic pathology of cognitive life	Honer et al. (2019)	3.34E-10
A single amino acid mutation in SNAP-25 induces anxiety-related behavior in mouse	Kataoka et al. (2011)	3.90E-10
Re-examining how complexin inhibits neurotransmitter release	Trimbuch et al. (2014)	3.90E-10
Components of the neuronal exocytotic machinery in the anterior pituitary of the ovariectomized ewe and the effects of estrogen in gonadotropes as studied with confocal microscopy.	Thomas et al. (1998)	3.90E-10
The Janus-faced nature of the C(2)B domain is fundamental for synaptotagmin-1 function	Xue et al. (2008)	4.92E-10
Mutations in the Neuronal Vesicular SNARE VAMP2 Affect Synaptic Membrane Fusion and Impair Human Neurodevelopment	Salpietro et al. (2019)	4.92E-10
Munc18-1 is crucial to overcome the inhibition of synaptic vesicle fusion by αSNAP	Stepien et al. (2019)	4.92E-10
GPCR regulation of secretion	Yim et al. (2018)	8.02E-10

on the upstream function of SNARE and SNARE-interacting molecules (Radhakrishnan et al., 2021).

One such complex is formed by SYP and VAMP2. This hexameric complex is thought to provide a template for the assembly of proteins at primed active zones, thereby controlling exocytosis through regulation of VAMP2 binding (Edelmann et al., 1995). The SYP/VAMP2 complex, assembled prior to docking and priming, is functionally suited for this purpose: the early assembly of SYP/VAMP2 facilitates a quick temporal response necessary for Ca^{2+}-mediated exocytosis (Adams et al., 2015). Interestingly, there is evidence that SYP is specifically involved in the *negative* regulation of VAMP2-syntaxin binding, further supporting the importance of synaptophysin in temporal control of SNARE formation (Raja et al., 2019). SYP mutations that affect VAMP2 trafficking are associated with neurodevelopmental disorders, and understanding the molecular sequence of events underlying SYP/VAMP2-mediated trafficking is vital for addressing public health concerns (Harper et al., 2017; John et al., 2021).

Endocytosis

In addition to neurotransmitter release, vesicular recycling at the synaptic cleft is also thought to be influenced by the SYP/VAMP2 complex. Synaptophysin itself is crucial to the maintenance of synaptic vesicle endocytosis; SYP loss-of-function mutations result in severely reduced recycling rates (Kwon and Chapman, 2011). During vesicle recycling, SYP appears to be required for the reuptake of VAMP2 into the pre-synaptic bouton, as well as maintaining appropriate levels of VAMP2 at the pre-synapse (Gordon et al., 2011; Kokotos et al., 2019). Additionally, this relationship is heavily reliant upon the ratio of SYP to VAMP2; disruptions in the physiological balance of the two proteins results in drastically reduced trafficking of VAMP2 back to pre-synaptic vesicles (Gordon et al., 2016).

Endocytosis is primarily dependent on SYP's cytoplasmic C-terminus, which is necessary for the efficient recovery of VAMP2 (Harper et al., 2021). While the direct molecular basis of SYP/VAMP2 binding is becoming clearer, there are several extrinsic factors that contribute to the complex's role in overall synaptic function. A particularly interesting property of the SYP/VAMP2 complex is its dependence on cholesterol, with assembly preferentially occurring in high cholesterol environments (Mitter et al., 2003; Hussain et al., 2019). With further investigation, external components like cholesterol may reveal functional links to some puzzling physiologies. One example is the predilection of synapses for recently synthesized vesicle proteins. Synaptophysin exits the recycling pool relatively quickly following production and is replaced by freshly-synthesized molecules; how this ties into the balance of SYP/VAMP2 is unknown (Truckenbrodt et al., 2018).

Contextual Roles

Many integral pre-synaptic functions remain ambiguously defined at the molecular level. The calcium ion is a key player in vesicular docking and fusion; Ca^{2+} concentration is directly

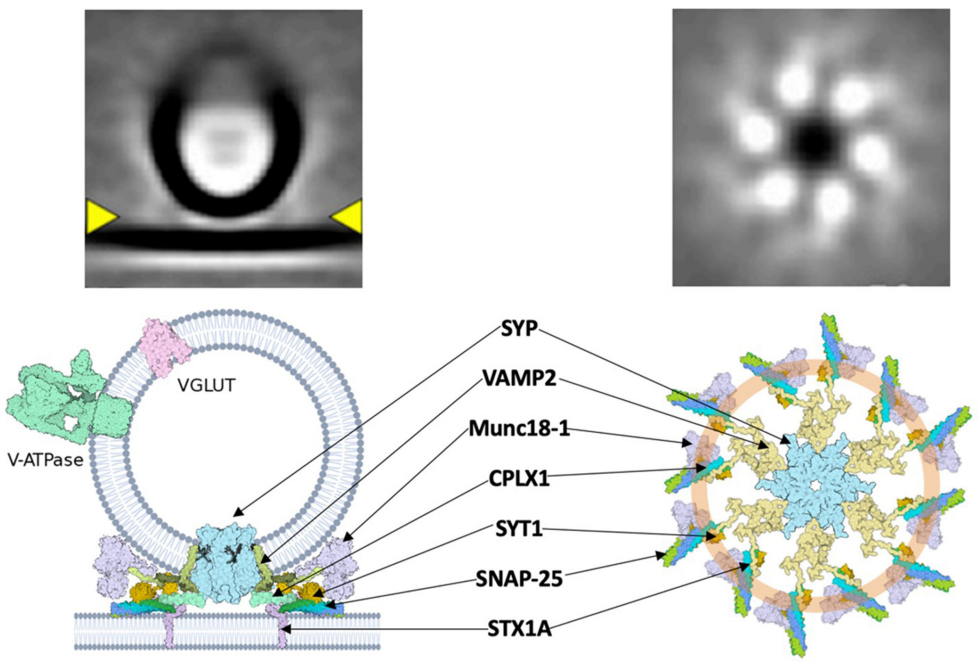

FIGURE 2 | A hypothetical synaptic fusion nanomachine comprised of a multimeric assembly organized by synaptophysin. **Top**, cryo-ET averages of docked synaptic vesicles (Radhakrishnan et al., 2021). **Bottom**, proposed fusion assembly based upon the prior synaptophysin/synaptobrevin complex (Adams et al., 2015) and the buttressed ring model (Rothman et al., 2017).

related to the rate of vesicle recruitment and release (Neher and Sakaba, 2008). The direct role of Ca^{2+} within the pre-synaptic terminal is highly contextual and depends on local signal strength as well as the type of synapse (excitatory vs. inhibitory; Schneggenburger and Neher, 2005; Williams and Smith, 2018). Despite this physiological range, many Ca^{2+} sensors have been identified at the pre-synaptic terminal. Regulation of the readily releasable pool (RRP) is one process that relies upon such Ca^{2+} sensors. The RRP links Ca^{2+} flux to synaptic strength and release probability (Thanawala and Regehr, 2013). In addition, Munc18-1 has been established as a key physiological regulator of cognate SNARE activation (Shen et al., 2007). Munc18-1 contributes to the maintenance of the SNARE complex in the presence of destabilizing factors. This kind of synapse-specific Ca^{2+} response could be important in the molecular regulation of atypical synaptic release.

In addition to traditional synapses, which use a single primary neurotransmitter, so-called dual-release terminals are found in many pathways throughout the brain and are capable of producing and releasing two primary neurotransmitters, such as glutamate and GABA (Vaaga et al., 2014; Root et al., 2018). These terminals release GABA and glutamate at a specific ratio, and disruptions of this ratio are implicated in major depressive disorder and addiction (Shabel et al., 2014; Root et al., 2020). Despite the prevalence and associated pathologies of dual-release neurons, the pre-synaptic machinery regulating most release properties is unknown.

A major connection between dual-release physiology and Ca^{2+}-mediated vesicular release may be found in the SYP/VAMP2 complex and associated superstructures. A central Ca^{2+} sensor, synaptotagmin (syt), is responsible for the induction of synchronous events at the pre-synaptic membrane through regulation of vSNARE activity *via* its C2B domain (Chang et al., 2018). Syt has recently been shown to form a ring-like structure upon which SNAREs are assembled (Rothman et al., 2017). Specifically, the C2AB domain of syt "clamps" the SNARE assembly at the synaptic vesicle (**Figure 2**). This conceptually allows docking of the vesicle at the plasma membrane with the syt ring attached, followed by Ca^{2+}-mediated disassembly of the syt ring upon action potential stimulation and subsequent fusion of vSNAREs to the membrane. This framework could contribute to the previously described speed of SNARE complex assembly, vesicle docking, and fusion. The physiological role of syt extends beyond a simple scaffold, as demonstrated in its ability to negatively regulate the attachment of vSNAREs to their plasma membrane-bound tSNARE targets at low intracellular Ca^{2+} concentrations (Wang et al., 2014). Interestingly, it appears that the syt "ring" acts as a vesicle "landing gear," guiding a pre-synaptic vesicle to specific active zones determined by the concentration of PIP2 (Zhu et al., 2021). The specificity of this docking might elucidate the basis of ratio-based dual-release. If the two neurotransmitters of a dual-release terminal are packaged in separate vesicles, an idea that has recently been contested, then one of the logical methods for regulating the ratio of release is *via* differential trafficking to the pre-synaptic membrane (Wang et al., 2020; Kim et al., 2021). The interaction of syt with the vesicular SYP/VAMP2 complex provides a structural basis for distinct trafficking pathways, but further study is needed to define the precise mechanism. Understanding how the v-SNARE pantheon contributes to dual-release physiology is essential for refining signaling pathways, understanding mood regulation, and discovering targeted treatments for associated disorders. The key to this understanding will come by obtaining high-resolution structure data of the SYP/VAMP complex so that mutational disruption of the complex can be explored functionally. Methods such as cryo-electron tomography and super-resolution microscopy will be vital next steps in analyzing pre-synaptic structures at a sufficient resolution. Questions regarding the spatial arrangement, temporal dynamics, and association kinetics of SNARE-associated complexes are crucial yet remain unanswered.

AUTHOR CONTRIBUTIONS

DW and MS wrote the manuscript and approved it for publication. All authors contributed to the article and approved the submitted version.

FUNDING

This work was supported by the NIH/CU Molecular Biophysics Program and NIH Biophysics Training Grant T32 GM-065103 to DW, and the MCDB Neurodegenerative Disease Fund to MS.

ACKNOWLEDGMENTS

We thank J. Shen for helpful comments.

REFERENCES

Adams, D. J., Arthur, C. P., and Stowell, M. H. B. (2015). Architecture of the synaptophysin/synaptobrevin complex: structural evidence for an entropic clustering function at the synapse. *Sci. Rep.* 5:13659. doi: 10.1038/srep 13659

Arthur, C. P., and Stowell, M. H. B. (2007). Structure of synaptophysin: a hexameric MARVEL domain channel protein. *Structure* 15, 707–714. doi: 10.1016/j.str.2007.04.011

Berridge, M. J. (1998). Neuronal Calcium Signaling. *Neuron* 21, 13–26. doi: 10.1016/s0896-6273(00)80510-3

Borisovska, M., Zhao, Y., Tsytsyura, Y., Glyvuk, N., Takamori, S., Matti, U., et al. (2005). v-SNAREs control exocytosis of vesicles from priming to fusion. *EMBO J.* 24, 2114–2126. doi: 10.1038/sj.emboj.7600696

Bracher, A., Kadlec, J., Betz, H., and Weissenhorn, W. (2002). X-ray structure of a neuronal complexin-snare complex from squid. *J. Biol. Chem.* 277, 26517–26523. doi: 10.1074/jbc.M203460200

Brunger, A. T. (2005). Structure and function of SNARE and SNARE-interacting proteins. *Q. Rev. Biophys.* 38, 1–47. doi: 10.1017/S0033583505004051

Brunger, A. T., Leitz, J., Zhou, Q., Choi, U. B., and Lai, Y. (2018). Ca^{2+}-triggered synaptic vesicle fusion initiated by release of inhibition. *Trends Cell Biol.* 28, 631–645. doi: 10.1016/j.tcb.2018.03.004

Carr, C. M., Grote, E., Munson, M., Hughson, F. M., and Novick, P. J. (1999). Sec1p binds to SNARE complexes and concentrates at sites of secretion. *J. Cell Biol.* 146, 333–344. doi: 10.1083/jcb.146.2.333

Chang, C.-W., Hsiao, Y.-T., and Jackson, M. B. (2021). Synaptophysin regulates fusion pores and exocytosis mode in chromaffin cells. *J. Neurosci.* 41, 3563–3578. doi: 10.1523/JNEUROSCI.2833-20.2021

Chang, S., Trimbuch, T., and Rosenmund, C. (2018). Synaptotagmin-1 drives synchronous Ca^{2+}-triggered fusion by C2B-domain-mediated synaptic-vesicle-membrane attachment. *Nat. Neurosci.* 21, 33–40. doi: 10.1038/s41593-017-0037-5

Chapman, E. R., Hanson, P. I., An, S., and Jahn, R. (1995). Ca^{2+} regulates the interaction between synaptotagmin and syntaxin 1. *J. Biol. Chem.* 270, 23667–23671. doi: 10.1074/jbc.270.40.23667

Chen, X., Tomchick, D. R., Kovrigin, E., Araç, D., Machius, M., Südhof, T. C., et al. (2002). Three-dimensional structure of the complexin/SNARE complex. *Neuron* 33, 397–409. doi: 10.1016/s0896-6273(02)00583-4

Deák, F., Schoch, S., Liu, X., Südhof, T. C., and Kavalali, E. T. (2004). Synaptobrevin is essential for fast synaptic-vesicle endocytosis. *Nat. Cell Biol.* 6, 1102–1108. doi: 10.1038/ncb1185

Deák, F., Xu, Y., Chang, W.-P., Dulubova, I., Khvotchev, M., Liu, X., et al. (2009). Munc18-1 binding to the neuronal SNARE complex controls synaptic vesicle priming. *J. Cell Biol.* 184, 751–764. doi: 10.1083/jcb.200812026

Dulubova, I., Khvotchev, M., Liu, S., Huryeva, I., Südhof, T. C., and Rizo, J. (2007). Munc18-1 binds directly to the neuronal SNARE complex. *Proc. Natl. Acad. Sci. USA* 104, 2697–2702. doi: 10.1073/pnas.0611318104

Edelmann, L., Hanson, P., Chapman, E., and Jahn, R. (1995). Synaptobrevin binding to synaptophysin: a potential mechanism for controlling the exocytotic fusion machine. *EMBO J.* 14, 224–231.

Far, O. E., Charvin, N., Leveque, C., Martin-Moutot, N., Takahashi, M., and Seagar, M. J. (1995). Interaction of a synaptobrevin (VAMP)-syntaxin complex with presynaptic calcium channels. *FEBS Lett.* 361, 101–105. doi: 10.1016/0014-5793(95)00156-4

Fasshauer, D., Bruns, D., Shen, B., Jahn, R., and Brünger, A. T. (1997). A structural change occurs upon binding of syntaxin to SNAP-25. *J. Biol. Chem.* 272, 4582–4590. doi: 10.1074/jbc.272.7.4582

Felkl, M., and Leube, R. E. (2008). Interaction assays in yeast and cultured cells confirm known and identify novel partners of the synaptic vesicle protein synaptophysin. *Neuroscience* 156, 344–352. doi: 10.1016/j.neuroscience.2008.07.033

Fernàndez-castillo, N., Cormand, B., Roncero, C., Sánchez-Mora, C., Grau-Lopez, L., Gonzalvo, B., et al. (2012). Candidate pathway association study in cocaine dependence: The control of neurotransmitter release. *World J. Biol. Psychiatry* 13, 126–134. doi: 10.3109/15622975.2010.551406

Gincel, D., and Shoshan-Barmatz, V. (2002). The synaptic vesicle protein synaptophysin: purification and characterization of its channel activity. *Biophys. J.* 83, 3223–3229. doi: 10.1016/S0006-3495(02)75324-1

Gordon, S. L., Harper, C. B., Smillie, K. J., and Cousin, M. A. (2016). A fine balance of synaptophysin levels underlies efficient retrieval of synaptobrevin II to synaptic vesicles. *PLoS One* 11:e0149457. doi: 10.1371/journal.pone.0149457

Gordon, S. L., Leube, R. E., and Cousin, M. A. (2011). Synaptophysin is required for synaptobrevin retrieval during synaptic vesicle endocytosis. *J. Neurosci.* 31, 14032–14036. doi: 10.1523/JNEUROSCI.3162-11.2011

Hamdan, F. F., Piton, A., Gauthier, J., Lortie, A., Dubeau, F., Dobrzeniecka, S., et al. (2009). De novo STXBP1 mutations in mental retardation and nonsyndromic epilepsy. *Ann. Neurol.* 65, 748–753. doi: 10.1002/ana.21625

Harper, C. B., Blumrich, E.-M., and Cousin, M. A. (2021). Synaptophysin controls synaptobrevin-II retrieval *via* a cryptic C-terminal interaction site. *J. Biol. Chem.* 296:100266. doi: 10.1016/j.jbc.2021.100266

Harper, C. B., Mancini, G. M. S., van Slegtenhorst, M., and Cousin, M. A. (2017). Altered synaptobrevin-II trafficking in neurons expressing a synaptophysin mutation associated with a severe neurodevelopmental disorder. *Neurobiol. Dis.* 108, 298–306. doi: 10.1016/j.nbd.2017.08.021

Hata, Y., Slaughter, C. A., and Südhof, T. C. (1993). Synaptic vesicle fusion complex contains unc-18 homologue bound to syntaxin. *Nature* 366, 347–351. doi: 10.1038/366347a0

Hazzard, J., Südhof, T. C., and Rizo, J. (1999). NMR analysis of the structure of synaptobrevin and of its interaction with syntaxin. *J. Biomol. NMR* 14, 203–207. doi: 10.1023/a:1008382027065

Honer, W. G., Ramos-Miguel, A., Alamri, J., Sawada, K., Barr, A. M., Schneider, J. A., et al. (2019). The synaptic pathology of cognitive life. *Dialogues Clin. Neurosci.* 21, 271–279. doi: 10.31887/DCNS.2019.21.3/whoner

Hussain, G., Wang, J., Rasul, A., Anwar, H., Imran, A., Qasim, M., et al. (2019). Role of cholesterol and sphingolipids in brain development and neurological diseases. *Lipids Health Dis.* 18:26. doi: 10.1186/s12944-019-0965-z

Janz, R., Südhof, T. C., Hammer, R. E., Unni, V., Siegelbaum, S. A., and Bolshakov, V. Y. (1999). Essential roles in synaptic plasticity for synaptogyrin I and synaptophysin I. *Neuron* 24, 687–700. doi: 10.1016/s0896-6273(00)81122-8

John, A., Ng-Cordell, E., Hanna, N., Brkic, D., and Baker, K. (2021). The neurodevelopmental spectrum of synaptic vesicle cycling disorders. *J. Neurochem.* 157, 208–228. doi: 10.1111/jnc.15135

Jurado, S., Goswami, D., Zhang, Y., Molina, A. J. M., Südhof, T. C., and Malenka, R. C. (2013). LTP requires a unique postsynaptic SNARE fusion machinery. *Neuron* 77, 542–558. doi: 10.1016/j.neuron.2012.11.029

Kandel, E. R., Dudai, Y., and Mayford, M. R. (2014). The molecular and systems biology of memory. *Cell* 157, 163–186. doi: 10.1016/j.cell.2014.03.001

Karim, S., Essenberg, R. C., Dillwith, J. W., Tucker, J. S., Bowman, A. S., and Sauer, J. R. (2002). Identification of SNARE and cell trafficking regulatory proteins in the salivary glands of the lone star tick, *Amblyomma americanum* (L.). *Insect Biochem. Mol. Biol.* 32, 1711–1721. doi: 10.1016/s0965-1748(02)00111-x

Karmakar, S., Sharma, L. G., Roy, A., Patel, A., and Pandey, L. M. (2019). Neuronal SNARE complex: a protein folding system with intricate protein-protein interactions and its common neuropathological hallmark, SNAP25. *Neurochem. Int.* 122, 196–207. doi: 10.1016/j.neuint.2018.12.001

Kataoka, M., Yamamori, S., Suzuki, E., Watanabe, S., Sato, T., Miyaoka, H., et al. (2011). A single amino acid mutation in SNAP-25 induces anxiety-related behavior in mouse. *PLoS One* 6:e25158. doi: 10.1371/journal.pone.0025158

Kim, S., Wallace, M., El-Rifai, M., Knudsen, A., and Sabatini, B. (2021). Biophysical demonstration of co-packaging of glutamate and GABA in individual synaptic vesicles in the central nervous system. *bioRxiv* [Preprint]. doi: 10.1101/2021.03.23.436594

Kokotos, A. C., Harper, C. B., Marland, J. R. K., Smillie, K. J., Cousin, M. A., and Gordon, S. L. (2019). Synaptophysin sustains presynaptic performance by preserving vesicular synaptobrevin-II levels. *J. Neurochem.* 151, 28–37. doi: 10.1111/jnc.14797

Körber, C., and Kuner, T. (2016). Molecular machines regulating the release probability of synaptic vesicles at the active zone. *Front. Synaptic Neurosci.* 8:5. doi: 10.3389/fnsyn.2016.00005

Kwon, S. E., and Chapman, E. R. (2011). Synaptophysin regulates the kinetics of synaptic vesicle endocytosis in central neurons. *Neuron* 70, 847–854. doi: 10.1016/j.neuron.2011.04.001

Liang, B., and Tamm, L. K. (2018). Solution NMR of SNAREs, complexin and α-synuclein in association with membrane-mimetics. *Prog. Nucl. Magn. Reson. Spectrosc.* 105, 41–53. doi: 10.1016/j.pnmrs.2018.02.001

Ma, C., Li, W., Xu, Y., and Rizo, J. (2011). Munc13 mediates the transition from the closed syntaxin-Munc18 complex to the SNARE complex. *Nat. Struct. Mol. Biol.* 18, 542–549. doi: 10.1038/nsmb.2047

Marqueze-Pouey, B., Wisden, W., Malosio, M., and Betz, H. (1991). Differential expression of synaptophysin and synaptoporin mRNAs in the postnatal rat central nervous system. *J. Neurosci.* 11, 3388–3397. doi: 10.1523/JNEUROSCI.11-11-03388.1991

McMahon, H. T., and Südhof, T. C. (1995). Synaptic core complex of synaptobrevin, syntaxin and SNAP25 forms high affinity-SNAP binding site. *J. Biol. Chem.* 270, 2213–2217. doi: 10.1074/jbc.270.5.2213

Metzger, M., Bueno, D., and Lima, L. B. (2017). The lateral habenula and the serotonergic system. *Pharmacol. Biochem. Behav.* 162, 22–28. doi: 10.1016/j.pbb.2017.05.007

Misura, K. M., Scheller, R. H., and Weis, W. I. (2000). Three-dimensional structure of the neuronal-Sec1-syntaxin 1a complex. *Nature* 404, 355–362. doi: 10.1038/35006120

Mitter, D., Reisinger, C., Hinz, B., Hollmann, S., Yelamanchili, S. V., Treiber-Held, S., et al. (2003). The synaptophysin/synaptobrevin interaction critically depends on the cholesterol content. *J. Neurochem.* 84, 35–42. doi: 10.1046/j.1471-4159.2003.01258.x

Neher, E., and Sakaba, T. (2008). Multiple roles of calcium ions in the regulation of neurotransmitter release. *Neuron* 59, 861–872. doi: 10.1016/j.neuron.2008.08.019

Ostenson, C.-G., Gaisano, H., Sheu, L., Tibell, A., and Bartfai, T. (2006). Impaired gene and protein expression of exocytotic soluble N-ethylmaleimide attachment protein receptor complex proteins in pancreatic islets of type 2 diabetic patients. *Diabetes* 55, 435–440. doi: 10.2337/diabetes.55.02.06.db04-1575

Pabst, S., Hazzard, J. W., Antonin, W., Südhof, T. C., Jahn, R., Rizo, J., et al. (2000). Selective interaction of complexin with the neuronal snare complex: determination of the binding regions. *J. Biol. Chem.* 275, 19808–19818. doi: 10.1074/jbc.M002571200

Radhakrishnan, A., Li, X., Grushin, K., Krishnakumar, S. S., Liu, J., and Rothman, J. E. (2021). Symmetrical arrangement of proteins under release-ready vesicles in presynaptic terminals. *Proc. Natl. Acad. Sci. USA* 118:e2024029118. doi: 10.1073/pnas.2024029118

Raja, M. K., Preobraschenski, J., Del Olmo-Cabrera, S., Martinez-Turrillas, R., Jahn, R., Perez-Otano, I., et al. (2019). Elevated synaptic vesicle release probability in synaptophysin/gyrin family quadruple knockouts. *eLife* 8:e40744. doi: 10.7554/eLife.40744

Ramos-Miguel, A., Jones, A. A., Sawada, K., Barr, A. M., Bayer, T. A., Falkai, P., et al. (2018). Frontotemporal dysregulation of the SNARE protein interactome is associated with faster cognitive decline in old age. *Neurobiol. Dis.* 114, 31–44. doi: 10.1016/j.nbd.2018.02.006

Rehm, H., Wiedenmann, B., and Betz, H. (1986). Molecular characterization of synaptophysin, a major calcium-binding protein of the synaptic vesicle membrane. *EMBO J.* 5, 535–541.

Rickman, C., Medine, C. N., Bergmann, A., and Duncan, R. R. (2007). Functionally and spatially distinct modes of munc18-syntaxin 1 interaction. *J. Biol. Chem.* 282, 12097–12103. doi: 10.1074/jbc.M700227200

Root, D. H., Barker, D. J., Estrin, D. J., Miranda-Barrientos, J. A., Liu, B., Zhang, S., et al. (2020). Distinct signaling by ventral tegmental area glutamate, gaba and combinatorial glutamate-gaba neurons in motivated behavior. *Cell Rep.* 32:108094. doi: 10.1016/j.celrep.2020.108094

Root, D. H., Zhang, S., Barker, D. J., Miranda-Barrientos, J., Liu, B., Wang, H.-L., et al. (2018). Selective brain distribution and distinctive synaptic architecture of dual glutamatergic-GABAergic neurons. *Cell Rep.* 23, 3465–3479. doi: 10.1016/j.celrep.2018.05.063

Roselli, F., and Caroni, P. (2015). From intrinsic firing properties to selective neuronal vulnerability in neurodegenerative diseases. *Neuron* 85, 901–910. doi: 10.1016/j.neuron.2014.12.063

Rothman, J. E., Krishnakumar, S. S., Grushin, K., and Pincet, F. (2017). Hypothesis—buttressed rings assemble, clamp and release SNAREpins for synaptic transmission. *FEBS Lett.* 591, 3459–3480. doi: 10.1002/1873-3468.12874

Salpietro, V., Malintan, N. T., Llano-Rivas, I., Spaeth, C. G., Efthymiou, S., Striano, P., et al. (2019). Mutations in the neuronal vesicular SNARE VAMP2 affect synaptic membrane fusion and impair human neurodevelopment. *Am. J. Hum. Genet.* 104, 721–730. doi: 10.1016/j.ajhg.2019.02.016

Schneggenburger, R., and Neher, E. (2005). Presynaptic calcium and control of vesicle fusion. *Curr. Opin. Neurobiol.* 15, 266–274. doi: 10.1016/j.conb.2005.05.006

Schoch, S., Deák, F., Königstorfer, A., Mozhayeva, M., Sara, Y., Südhof, T. C., et al. (2001). SNARE function analyzed in synaptobrevin/VAMP knockout mice. *Science* 294, 1117–1122. doi: 10.1126/science.1064335

Sclip, A., Bacaj, T., Giam, L. R., and Südhof, T. C. (2016). Extended synaptotagmin (ESyt) triple knock-out mice are viable and fertile without obvious endoplasmic reticulum dysfunction. *PLoS One* 11:e0158295. doi: 10.1371/journal.pone.0158295

Shabel, S. J., Proulx, C. D., Piriz, J., and Malinow, R. (2014). Mood regulation. GABA/glutamate co-release controls habenula output and is modified by antidepressant treatment. *Science* 345, 1494–1498. doi: 10.1126/science.1250469

Shen, J., Tareste, D. C., Paumet, F., Rothman, J. E., and Melia, T. J. (2007). Selective activation of cognate SNAREpins by Sec1/Munc18 proteins. *Cell* 128, 183–195. doi: 10.1016/j.cell.2006.12.016

Söllner, T., Bennett, M. K., Whiteheart, S. W., Scheller, R. H., and Rothman, J. E. (1993b). A protein assembly-disassembly pathway *in vitro* that may correspond to sequential steps of synaptic vesicle docking, activation and fusion. *Cell* 75, 409–418. doi: 10.1016/0092-8674(93)90376-2

Söllner, T., Whiteheart, S. W., Brunner, M., Erdjument-Bromage, H., Geromanos, S., Tempst, P., et al. (1993a). SNAP receptors implicated in vesicle targeting and fusion. *Nature* 362, 318–324. doi: 10.1038/362318a0

Stepien, K. P., Prinslow, E. A., and Rizo, J. (2019). Munc18-1 is crucial to overcome the inhibition of synaptic vesicle fusion by αSNAP. *Nat. Commun.* 10:4326. doi: 10.1038/s41467-019-12188-4

Szklarczyk, D., Gable, A. L., Lyon, D., Junge, A., Wyder, S., Huerta-Cepas, J., et al. (2019). STRING v11: protein-protein association networks with increased coverage, supporting functional discovery in genome-wide experimental datasets. *Nucleic Acids Res.* 47, D607–D613. doi: 10.1093/nar/gky1131

Thanawala, M. S., and Regehr, W. G. (2013). Presynaptic calcium influx controls neurotransmitter release in part by regulating the effective size of the readily releasable pool. *J. Neurosci.* 33, 4625–4633. doi: 10.1523/JNEUROSCI.4031-12.2013

Thiele, C., Hannah, M. J., Fahrenholz, F., and Huttner, W. B. (2000). Cholesterol binds to synaptophysin and is required for biogenesis of synaptic vesicles. *Nat. Cell Biol.* 2, 42–49. doi: 10.1038/71366

Thomas, S. G., Takahashi, M., Neill, J. D., and Clarke, I. J. (1998). Components of the neuronal exocytotic machinery in the anterior pituitary of the ovariectomised ewe and the effects of oestrogen in gonadotropes as studied with confocal microscopy. *Neuroendocrinology* 67, 244–259. doi: 10.1159/000054320

Trimbuch, T., Xu, J., Flaherty, D., Tomchick, D. R., Rizo, J., and Rosenmund, C. (2014). Re-examining how complexin inhibits neurotransmitter release. *eLife* 3:e02391. doi: 10.7554/eLife.02391

Truckenbrodt, S., Viplav, A., Jähne, S., Vogts, A., Denker, A., Wildhagen, H., et al. (2018). Newly produced synaptic vesicle proteins are preferentially used in synaptic transmission. *EMBO J.* 37:e98044. doi: 10.15252/embj.201798044

Vaaga, C. E., Borisovska, M., and Westbrook, G. L. (2014). Dual-transmitter neurons: functional implications of co-release and co-transmission. *Curr. Opin. Neurobiol.* 29, 25–32. doi: 10.1016/j.conb.2014.04.010

Wang, C., Tu, J., Zhang, S., Cai, B., Liu, Z., Hou, S., et al. (2020). Different regions of synaptic vesicle membrane regulate VAMP2 conformation for the SNARE assembly. *Nat. Commun.* 11:1531. doi: 10.1038/s41467-020-15270-4

Wang, J., Bello, O., Auclair, S. M., Wang, J., Coleman, J., Pincet, F., et al. (2014). Calcium sensitive ring-like oligomers formed by synaptotagmin. *Proc. Natl. Acad. Sci. U S A* 111, 13966–13971. doi: 10.1073/pnas.1415849111

Weber, T., Zemelman, B. V., McNew, J. A., Westermann, B., Gmachl, M., Parlati, F., et al. (1998). SNAREpins: minimal machinery for membrane fusion. *Cell* 92, 759–772. doi: 10.1016/s0092-8674(00)81404-x

Williams, C. L., and Smith, S. M. (2018). Calcium dependence of spontaneous neurotransmitter release. *J. Neurosci. Res.* 96, 335–347. doi: 10.1002/jnr.24116

Wrackmeyer, U., Kaldrack, J., Jüttner, R., Pannasch, U., Gimber, N., Freiberg, F., et al. (2019). The cell adhesion protein CAR is a negative regulator of synaptic transmission. *Sci. Rep.* 9:6768. doi: 10.1038/s41598-019-43150-5

Xu, J., Brewer, K. D., Perez-Castillejos, R., and Rizo, J. (2013b). Subtle interplay between synaptotagmin and complexin binding to the SNARE complex. *J. Mol. Biol.* 425, 3461–3475. doi: 10.1016/j.jmb.2013.07.001

Xu, J., Luo, F., Zhang, Z., Xue, L., Wu, X.-S., Chiang, H.-C., et al. (2013a). SNARE proteins synaptobrevin, SNAP-25 and syntaxin are involved in rapid and slow endocytosis at synapses. *Cell Rep.* 3, 1414–1421. doi: 10.1016/j.celrep.2013.03.010

Xue, M., Ma, C., Craig, T. K., Rosenmund, C., and Rizo, J. (2008). The Janus-faced nature of the C(2)B domain is fundamental for synaptotagmin-1 function. *Nat. Struct. Mol. Biol.* 15, 1160–1168. doi: 10.1038/nsmb.1508

Ya, B.-L., Liu, W.-Y., Ge, F., Zhang, Y.-X., Zhu, B.-L., and Bai, B. (2013). Dietary cholesterol alters memory and synaptic structural plasticity in young rat brain. *Neurol. Sci.* 34, 1355–1365. doi: 10.1007/s10072-012-1241-4

Yan, M.-L., Zhang, S., Zhao, H.-M., Xia, S.-N., Jin, Z., Xu, Y., et al. (2020). MicroRNA-153 impairs presynaptic plasticity by blocking vesicle release following chronic brain hypoperfusion. *Cell Commun. Signal.* 18:57. doi: 10.1186/s12964-020-00551-8

Yim, Y. Y., Zurawski, Z., and Hamm, H. (2018). GPCR regulation of secretion. *Pharmacol. Ther.* 192, 124–140. doi: 10.1016/j.pharmthera.2018.07.005

Yin, Y., Dayanithi, G., and Lemos, J. R. (2002). Ca^{2+}-regulated, neurosecretory granule channel involved in release from neurohypophysial terminals. *J. Physiol.* 539, 409–418. doi: 10.1113/jphysiol.2001.012943

Zhang, X., Kim-Miller, M. J., Fukuda, M., Kowalchyk, J. A., and Martin, T. F. J. (2002). Ca^{2+}-dependent synaptotagmin binding to SNAP-25 is essential for Ca^{2+}-triggered exocytosis. *Neuron* 34, 599–611. doi: 10.1016/s0896-6273(02)00671-2

Zhou, J., Liu, Z., Yu, J., Han, X., Fan, S., Shao, W., et al. (2015). Quantitative proteomic analysis reveals molecular adaptations in the hippocampal synaptic active zone of chronic mild stress-unsusceptible rats. *Int. J. Neuropsychopharmacol.* 19:pyv100. doi: 10.1093/ijnp/pyv100

Zhou, Q., Zhou, P., Wang, A. L., Wu, D., Zhao, M., Südhof, T. C., et al. (2017). The primed SNARE-complexin-synaptotagmin complex for neuronal exocytosis. *Nature* 548, 420–425. doi: 10.1038/nature23484

Zhu, J., McDargh, Z. A., Li, F., Krishnakumar, S., Rothman, J. E., and O'Shaughnessy, B. (2021). Synaptotagmin rings as high sensitivity regulators of synaptic vesicle docking and fusion. [Preprint]. *bioRxiv*. doi: 10.1101/2021.03.12.435193

Zilly, F. E., Sørensen, J. B., Jahn, R., and Lang, T. (2006). Munc18-bound syntaxin readily forms SNARE complexes with synaptobrevin in native plasma membranes. *PLoS Biol.* 4:e330. doi: 10.1371/journal.pbio.0040330

Conflict of Interest: The authors declare that the research was conducted in the absence of any commercial or financial relationships that could be construed as a potential conflict of interest.

Publisher's Note: All claims expressed in this article are solely those of the authors and do not necessarily represent those of their affiliated organizations, or those of the publisher, the editors and the reviewers. Any product that may be evaluated in this article, or claim that may be made by its manufacturer, is not guaranteed or endorsed by the publisher.

frontiers in Synaptic Neuroscience

MINI REVIEW
published: 22 December 2021
doi: 10.3389/fnsyn.2021.796498

Nano-Organization at the Synapse: Segregation of Distinct Forms of Neurotransmission

Natalie J. Guzikowski[1,2] *and Ege T. Kavalali*[1,2]*

[1] Department of Pharmacology, Vanderbilt University, Nashville, TN, United States, [2] Vanderbilt Brain Institute, Vanderbilt University, Nashville, TN, United States

Synapses maintain synchronous, asynchronous, and spontaneous modes of neurotransmission through distinct molecular and biochemical pathways. Traditionally a single synapse was assumed to have a homogeneous organization of molecular components both at the active zone and post-synaptically. However, recent advancements in experimental tools and the further elucidation of the physiological significance of distinct forms of release have challenged this notion. In comparison to rapid evoked release, the physiological significance of both spontaneous and asynchronous neurotransmission has only recently been considered in parallel with synaptic structural organization. Active zone nanostructure aligns with postsynaptic nanostructure creating a precise trans-synaptic alignment of release sites and receptors shaping synaptic efficacy, determining neurotransmission reliability, and tuning plasticity. This review will discuss how studies delineating synaptic nanostructure create a picture of a molecularly heterogeneous active zone tuned to distinct forms of release that may dictate diverse synaptic functional outputs.

Keywords: nanocolumn, spontaneous neurotransmission, asynchronous neurotransmission, synchronous neurotransmission, synaptic transmission and plasticity

OPEN ACCESS

Edited by:
Lucia Tabares,
Seville University, Spain

Reviewed by:
Pei-Lin Cheng,
Academia Sinica, Taiwan

***Correspondence:**
Ege T. Kavalali
ege.kavalali@vanderbilt.edu

Received: *16 October 2021*
Accepted: *19 November 2021*
Published: *22 December 2021*

Citation:
Guzikowski NJ and Kavalali ET (2021) Nano-Organization at the Synapse: Segregation of Distinct Forms of Neurotransmission. Front. Synaptic Neurosci. 13:796498. doi: 10.3389/fnsyn.2021.796498

INTRODUCTION—CLASSICAL VIEW OF SINGLE ACTIVE ZONE SYNAPSES

In the 1960s the canonical synaptic transmission pathway was established; neurotransmission is initiated by an action potential arriving at the presynaptic terminal, presynaptic calcium influx is triggered, synaptic vesicles fuse with the presynaptic membrane and ultimately release neurotransmitter (Katz, 1969; Südhof, 2013). This seminal work set the stage for the investigation of neurotransmission at numerous synapse types across the nervous system in diverse animal models with electrophysiology. This original view of synaptic transmission holds true today albeit with knowledge of the specificity, segregation, and molecular mechanisms that mediate and regulate neurotransmission. Today, three different modes of neurotransmission are categorized by their time scale relative to a stimulus as well as calcium dependence. Action potential dependent release is composed of synchronous and asynchronous phases, where synchronous release strictly adheres to the timing of incoming presynaptic action potentials and asynchronous

release is only loosely coupled to stimulation temporally. In contrast, spontaneous release happens independently of action potentials in a quantal manner, where single synaptic vesicles fuse and release neurotransmitter in a quasi-random fashion (Kavalali, 2015). Studies conducted at the *Drosophila* neuromuscular junction as well as hippocampal synapses have demonstrated that a single active zone is capable of synchronous, asynchronous, and spontaneous release while some synapses exclusively execute spontaneous or evoked neurotransmission, creating a dynamic neuronal network dependent on distinct forms of neurotransmission (Atasoy et al., 2008; Melom et al., 2013; Peled et al., 2014; Reese and Kavalali, 2016). Each of the three modes of neurotransmission rely on distinct molecular frameworks to ultimately accomplish complex information processing (Kononenko and Haucke, 2015; Chanaday and Kavalali, 2017).

Recently, our understanding of neurotransmission has expanded to include both action potential dependent release and spontaneous release which have distinct physiological roles governed by a molecularly heterogeneous active zone (Andreae and Burrone, 2018; Gonzalez-Islas et al., 2018; Kavalali, 2018). The expansion of our synaptic "world-view" to include the nuances of different modes of neurotransmission relays the importance of the molecular pathways and synaptic structures that support release and presents broader implications for learning, memory, as well as associated disease processes. With the continued advancement of tools to probe release segregation, the notion that neurotransmission occurs via distinct pathways has been bolstered. How this segregation of release is maintained by the nano-organization of the synapse to transduce complex information processing will be the focus of this review.

Synaptic Efficacy

The fundamental reason we study the synapse is to understand how one neuron influences its targets. Therefore, to elucidate this process, we must consider how synaptic efficacy is shaped by multiple molecular pathways and different modes of neurotransmission. Synaptic efficacy defined as the ability of a presynaptic input to influence a postsynaptic response is classically considered within the context of action potential induced presynaptic calcium signaling and subsequent neurotransmitter release. The synaptic efficacy of an active zone or release site is traditionally determined by the release probability, the probability that upon arrival of an action potential to the synaptic terminal a synaptic vesicle will fuse and there will be subsequent neurotransmitter release. The size of the readily releasable pool, which includes vesicles docked at the active zone that fuse first in response to stimulation, and the fusion propensity of each synaptic vesicle dictates this release probability and ultimately synaptic strength (Rey et al., 2015; Chanaday and Kavalali, 2018). This view of synaptic strength and synaptic vesicle organization focused solely on evoked neurotransmission assumes a rather homogeneous synaptic vesicle pool and equally homogeneous organization of the active zone. In addition, it excludes other modes of neurotransmission and how their distinct functional roles may shape, guide, or determine synaptic efficacy.

MOLECULAR MECHANISMS OF DISTINCT FORMS OF RELEASE

Historically the organization of synaptic vesicles within the presynaptic terminal was defined by their propensity to fuse in response to stimulation and ultrastructural localization. Thus, creating a pool organization of synaptic vesicles comprised of the readily releasable pool, vesicles that fuse first in response to stimulation, and the reserve pool, the pool that replenishes the readily releasable pool, which shows limited synaptic vesicle trafficking during physiological activity (Alabi and Tsien, 2012). However, this pool organization does not fully account for the dynamics of release with regard to different modes of neurotransmission. Understanding the heterogeneity of synaptic vesicle molecular composition and how this heterogeneity dictates release and trafficking creates a more accurate classification system of synaptic vesicle organization in the presynaptic terminal. The diversity in synaptic vesicle molecular composition of v-SNAREs (vesicle-soluble *N*-ethylmaleimide-sensitive factor (NSF) attachment protein receptor) and calcium sensors distinguishes synaptic vesicle populations indicating that unique molecular compositions may designate synaptic vesicles for different forms of release (**Figure 1**) (Crawford and Kavalali, 2015). Furthermore, there is increasing evidence that different calcium sources mediate distinct modes of release (Kavalali, 2020).

Synaptic Vesicle Associated SNAREs, v-SNAREs

The canonical SNARE complex includes synaptic vesicle associated protein Synaptobrevin 2 (Syb2, also called VAMP2) that forms a complex with the plasma membrane SNAREs synaptosomal-associated protein 25 (SNAP25) and syntaxin 1 to drive rapid action potential-evoked synaptic vesicle fusion (Südhof and Rothman, 2009). Early experiments investigating the selective loss of canonical SNAREs induced large effects on evoked release while spontaneous release was maintained. The genetic deletion of Syb2 in mice caused the loss of calcium dependent evoked release while residual spontaneous release and to some extent asynchronous release were still present (Schoch et al., 2001; Deák et al., 2004). This initial work stimulated further research into which SNAREs are mediating different modes of neurotransmission as molecular perturbations selectively effected spontaneous and evoked release in distinguishable ways.

Fluorescence imaging experiments in conjunction with electrophysiology have shown that Vps10p-tail-interactor-1a (vti1a) containing vesicles traffic in the absence of activity and vesicle-associated membrane protein 7 (VAMP7) containing vesicles also preferentially traffic in response to resting calcium signals, thus both v-SNAREs specifically drive spontaneous release (Hua et al., 2011; Ramirez et al., 2012; Bal et al., 2013; to see a full list of SNAREs associated with the synaptic vesicle proteome; see Takamori et al., 2006). Furthermore, despite both synchronous and asynchronous release being action potential dependent, vesicle-associated membrane protein 4 (VAMP4) selectively maintains asynchronous release demonstrated by

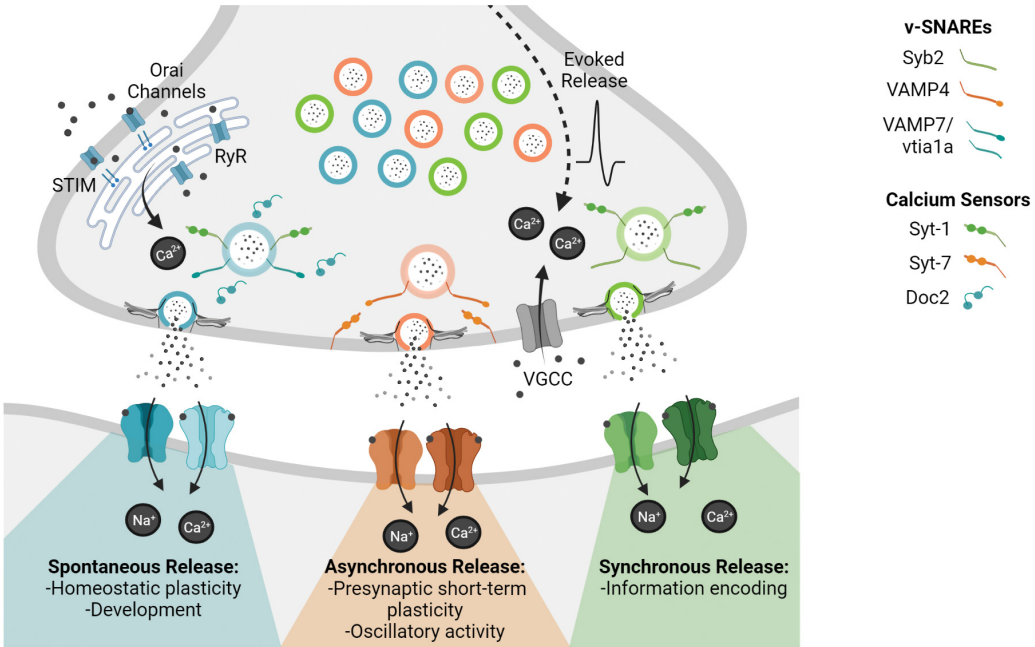

FIGURE 1 | This figure depicts the different modes of neurotransmission and their distinct downstream signaling pathways. Synchronous release transmits precise timing information across the synapse enabling information transfer with fidelity, whereas asynchronous release is thought to regulate short term plasticity and oscillatory activity. In contrast, spontaneous release is action potential independent although it may rely on alternative calcium sources, such as endoplasmic reticulum (ER) mediated calcium via ryanodine receptors (RyR) or store-operated calcium entry via Orai channels activated by the ER calcium sensor STIM. Spontaneous release is thought to play a role in synapse development as well as homeostatic synaptic scaling shaping synaptic efficacy.

differential trafficking with minimal Syb2 trafficking overlap (Raingo et al., 2012). In addition to the functional evidence that these alternative v-SNAREs maintain distinct trafficking pathways, biochemical evidence is consistent with their distinct functions. As for instance VAMP4 forms stable SNARE complexes independent of Syb2 and these complexes do not interact with synaptotagmin-1 and complexins, two protein that are essential for rapid synchronous evoked release (Raingo et al., 2012). The elucidation of specific v-SNAREs that selectively maintain different modes of release reveals a synaptic terminal composed of subpopulations of vesicles defined by their heterogeneous distribution of molecular components (Ramirez et al., 2012; Revelo et al., 2014; Walter et al., 2014). Alternative v-SNAREs act as synaptic vesicle molecular tags for the organization of synaptic vesicles into pools, conferring distinct release properties, downstream functional roles, and the selective regulation of neurotransmitter release (**Figure 1**) (Mori et al., 2021).

Calcium Sensors

Differences in the molecular machinery to maintain synchronous, asynchronous, and spontaneous release extend beyond SNARE machinery and include calcium sensing proteins. The diversity in calcium sensitivity between synchronous, asynchronous, and spontaneous release is complex; with differential degrees of absolute dependence, different sources of calcium mediating release, as well as differential calcium dependences between excitatory and inhibitory spontaneous release (Courtney et al., 2018; Williams and Smith, 2018; Lin et al., 2020).

Synaptotagmins are a family of calcium sensing proteins implicated in synaptic vesicle exocytosis. Synaptotagmin-1 (Syt-1) is required for synchronous release mediating the calcium sensitivity of fast evoked neurotransmitter release. While the loss of Syt-1 impairs synchronous release, it unclamps spontaneous release and augments asynchronous release, regulating release bidirectionally (Maximov and Südhof, 2005; Liu et al., 2009). Syt-1 is a low affinity calcium isoform making it only a reliable calcium sensor following voltage gated calcium channel (VGCC) opening and subsequent nanodomain elevation of calcium. Whereas Synaptotagmin-7 (Syt-7), the proposed asynchronous calcium sensor, has a 10-fold higher calcium affinity than Syt-1, giving it utility on a longer timescale post VGCC opening. Syt-7 loss of function mutations drastically reduce asynchronous release and associated synaptic vesicle trafficking providing the molecular framework for the differential timing of these two types of action potential dependent release (Geppert et al., 1994; Sugita et al., 2002; Bacaj et al., 2013; Li et al., 2017).

Although the precise nature of calcium sensitivity of spontaneous release is still a matter of debate, soluble calcium sensors of the Doc2-like protein family are thought to regulate spontaneous release in addition to synaptotagmin (Groffen et al., 2010; Pang et al., 2011). A quadruple knockdown strategy to eliminate members of the Doc2 family caused a reduction in spontaneous neurotransmission while action potential-evoked neurotransmission remained relatively normal.

This protein loss also caused a subsequent increase in synaptic strength, suggesting that spontaneous neurotransmission is able to communicate independently with the postsynaptic neuron and trigger downstream signaling cascades that regulate the synaptic state (Ramirez et al., 2017). This regulation of release via calcium dynamics shows even more complexity with excitatory spontaneous signaling preferentially regulated by Doc2α and inhibitory spontaneous signaling by both Doc2β and Syt-1 (Courtney et al., 2018).

FUNCTIONAL CONSEQUENCES OF DISTINCT FORMS OF RELEASE

The investigation into molecular components that drive different modes of release implies there are distinct functional consequences for synchronous, asynchronous, and spontaneous release. These studies have addressed why different modes of release are maintained in separable pathways and how they contribute to the physiological function of the synapse. In particular, asynchronous and spontaneous forms of release are poorly understood in comparison to evoked synchronous release, however, recent work has identified dedicated functional roles that are unique and specific to each mode of release.

SPONTANEOUS RELEASE

Spontaneous release events were originally viewed as random errors at the synaptic terminal deviating from canonical action potential dependent release, and described as biological noise (Fatt and Katz, 1950). However recent evidence suggests that spontaneous release has a specialized role in both regulating synapse and circuit development in addition to the maintenance of synapse dynamics in several organisms (Huntwork and Littleton, 2007; Choi et al., 2014; Andreae and Burrone, 2015; Banerjee et al., 2021). Furthermore recent findings on the role of aberrant spontaneous neurotransmission in neurological disease as well as ketamine's rapid antidepressant action arising from spontaneous release modulation reflect the utility of different modes of release at the synapse (Autry et al., 2011; Alten et al., 2021). Ultimately revealing spontaneous neurotransmission as an autonomous mode of release involved in a broad range of functions (Kavalali and Monteggia, 2020).

Development

Early stages of development are characterized by high levels of spontaneous release and resting synaptic vesicle cycling as compared to minimal evoked release (Molnár et al., 2002; Andreae et al., 2012). Previously the importance of spontaneous activity in synapse formation has been speculative due to the lack of a proposed function of developmentally elevated spontaneous release (Andreae and Burrone, 2018). However, key studies at the *Drosophila* neuromuscular junction during development have demonstrated how the frequency of spontaneous release events are directly correlated with synaptic structure. Experimentally facilitating miniature postsynaptic currents (mPSCs) leads to the subsequent increase in presynaptic boutons and the blockade of mPSCs leads to abnormal neuromuscular junctions characterized by reduced growth and surface area (Choi et al., 2014). In addition, spontaneous glutamate release events are thought to regulate dendritic arbors by acting as cues for dendritic outgrowth, a process not modulated by evoked release (Andreae and Burrone, 2015). Spontaneous release maintains these developmental pathways that are not controlled by evoked release delineating spontaneous release specific biochemical pathways (**Figure 1**; Andreae and Burrone, 2018).

Homeostatic Plasticity

In response to global changes in neuronal activity synaptic weights are up- or down-scaled to maintain homeostatic set points of neurotransmission. This homeostatic synaptic scaling maintains the relative differences in synaptic weights between synapses on a neuron, vital for information processing, while still allowing the system to adapt to environmental levels of activity (Turrigiano and Nelson, 2004; Kavalali and Monteggia, 2020). Global changes in activity elicited by complete suppression of action potentials (tetrodotoxin treatment) or conversely disinhibition (bicuculine treatment) can regulate this scaling phenomenon by up or down regulation of postsynaptic receptor density. However, synaptic scaling can also be triggered by alterations in action potential independent neurotransmitter release or via direct manipulation of neurotransmission without gross changes in activity levels (Gonzalez-Islas et al., 2018).

Reduction in N-methyl-D-aspartate receptor (NMDAR) mediated miniature excitatory postsynaptic currents (mEPSCs) via postsynaptic manipulations triggers Eukaryotic Elongation Factor 2 Kinase mediated synaptic upscaling via local dendritic translation (Sutton et al., 2006; Aoto et al., 2008; Reese and Kavalali, 2015). Not only is this NMDAR synaptic scaling pathway separable from the canonical NMDAR mediated long term potentiation (LTP) pathway but it is also implicated as a substrate for disease intervention in major depressive disorder (Lin et al., 2018). In parallel the loss of spontaneous specific release machinery, vti1a and VAMP7, triggers synaptic scaling of α-amino-3-hydroxy-5-methyl-4-isoxazolepropionic acid receptors (AMPARs) as reflected by increased mEPSC amplitudes (Crawford et al., 2017). Furthermore, the blockade of spontaneous γ-aminobutyric acid (GABA)-ergic signaling leads to multiplicative downscaling at excitatory synapses via brain-derived neurotrophic factor transcription and signaling, demonstrating an exclusive role of spontaneous release in the relationship between excitatory and inhibitory synapses (Horvath et al., 2021). These specific pre- and post-synaptic perturbations ultimately reveal how spontaneous release functions to maintain basal levels of synaptic efficacy, through separable mechanisms from evoked release (**Figure 1**).

ASYNCHRONOUS RELEASE

Plasticity

Due to the slow dynamics of asynchronous release–vesicle fusion occurring with 10–100 ms delay after an action

potential –it is speculated to impact synaptic plasticity. However, neuron and synapse specific diversity in the degree of asynchronous release make the generalization of the physiological significance of asynchronous release difficult. Syt-7, putative asynchronous calcium sensor, is required for short-term presynaptic facilitation at some synapses (Jackman et al., 2016). While at fast synapses, with minimal asynchronous release, Syt-7 is not required for short-term plasticity but the fidelity of synchronous release allowing for prolonged synaptic signaling (Luo and Südhof, 2017).

Information Encoding

Fast synchronous release is often thought to be the main mode of information transfer due to its tight temporal coupling with presynaptic action potentials. Nevertheless, loss of synchronous neurotransmission by *in vivo* knockdown of Syt-1 in the hippocampus still allowed the acquisition of fear memories, albeit with impairments, suggesting that asynchronous release detected after Syt-1 loss-of-function is still sufficient to encode the majority of the memory. While this result does not negate the importance of release timing in brain circuits, it indicates that action potential bursts and subsequent asynchronous release can be critical drivers for information encoding (Xu et al., 2012).

Oscillatory Activity

Understanding the degree of asynchronous release in different neuronal subtypes provides insight into the molecular diversity and input specificity of inhibitory interneurons in the hippocampal circuit. Cholecystokinin (CCK)–expressing GABAergic interneurons (innervate pyramidal cells at soma and proximal dendrites) are characterized by high asynchronous activity as compared to other interneuron subtypes. Therefore their prolonged asynchronous GABA release generates long lasting inhibition that modulates circuit activity (Hefft and Jonas, 2005). Based on CCK–expressing GABAergic interneurons' role in maintaining low frequency oscillations of the hippocampus, their prominent asynchronous release is suspected to play a key role in generating hippocampal theta rhythms (Klausberger and Somogyi, 2008; Rozov et al., 2019). Delineating the physiological function of asynchronous release demonstrates its unique and specific role creating the context to further study the molecular underpinnings of each mode of release (**Figure 1**).

NANOSTRUCTURE

The molecular diversity of synaptic vesicles as well as distinct functional roles of each mode of release challenge the notion of a molecularly homogeneous organization within the synaptic terminal. The proposed structure of the synapse now incorporates the nano-organization of proteins throughout the synapse, including protein density gradients in the active zone, synaptic cleft, receptor localization, and postsynaptic density creating a physical trans-synaptic alignment of proteins termed a nano-column (Tang et al., 2016). Synaptic nanocolumns are suspected to have a role in facilitating release differentially providing the framework at which the synapse is able to maintain different modes of release via parallel pathways.

DISTINCT POSTSYNAPTIC TARGETS

Excitatory Synapses

The application of use dependent drugs and optical imaging have demonstrated that different modes of neurotransmission target distinct postsynaptic receptors (Atasoy et al., 2008; Melom et al., 2013; Peled et al., 2014). Initial studies at excitatory synapses took advantage of use dependent receptor blockers to probe postsynaptic receptor segregation. The application of use dependent NMDAR blocker, MK-801, demonstrated a near complete segregation of NMDAR response to spontaneous and evoked glutamate release (Atasoy et al., 2008; Reese and Kavalali, 2016). The use of philanthotoxin, use dependent blocker of GluR2 lacking AMPARs, extended this notion to evoked and spontaneous glutamate release dependent activation of distinct sets of AMPARs (Sara et al., 2011; Peled et al., 2014). These results demonstrate the independence of evoked and spontaneous release probabilities as well as spatial segregation of the two forms of release.

Inhibitory Synapses

Despite accumulating evidence of nano-organization at excitatory synapses, segregation of distinct forms of release at the inhibitory synapse is relatively under-investigated. The distinct functional roles of evoked and spontaneous release at excitatory synapses provides rationale for robust segregation, however, the degree of segregation and functional outcomes of evoked and spontaneous inhibitory signaling are unknown. A recent study has uncovered partial segregation of evoked and spontaneous release at an inhibitory synapse. The utilization of picrotoxin, a use dependent $GABA_AR$ channel blocker, demonstrated that approximately 40% of $GABA_ARs$ are exclusively activated by evoked release (Horvath et al., 2020).

Historically the main role of inhibitory signaling has been cast as modulating excitatory neurotransmission and regulating a neuron's propensity to fire action potentials. However, only recently has the biochemical signaling of inhibitory neurotransmission been addressed due to the few known targets of chloride. The discovery that with-no-lysine kinases (WNKs) function as chloride sensors and second messenger cascades downstream of GABAergic chloride current provide insight into the dynamic nature of the inhibitory synapse (Piala et al., 2014; Heubl et al., 2017; Chen et al., 2019). Further adding to the complexity of the inhibitory synapse, GABAergic signaling is excitatory during early development, influencing synapse plasticity and growth to generate functional circuits (Ben-Ari, 2002). Understanding if there are common principles governing nanostructure and the segregation of release at inhibitory synapses as seen at excitatory synapses is crucial, however, it remains unclear if a partial segregation mediates differential signaling of inhibitory spontaneous and evoked neurotransmission and how this segregation is achieved (Horvath et al., 2020).

Neurotransmitter Receptor Dynamics

The nanocolumn organization discussed above allows for concentrated increases in neurotransmitter at designated regions along the active zone, aligned with specific receptor subpopulations. The significance of transient localized increases in neurotransmitter is bolstered by studies investigating the segregation of release via receptor activation, neurotransmitter receptor dynamics, and synaptic plasticity.

To understand the implications of synaptic nanocolumns, it is first important to establish the essential role of the site of neurotransmitter release and receptor localization in determining the efficacy of neurotransmission. The traditional picture of the synapse assumes a homogeneous structure whereby synaptic strength is governed by the number of receptors in the postsynaptic density and neurotransmitter is released at any place within the active zone (Lisman et al., 2007). Under previous assumptions neurotransmitter release activated the same subset of receptors regardless of its mode or timing, however, the dynamics of glutamate diffusion and AMPAR activation challenge this notion. The probability of AMPAR activation declines with distance from glutamate release due to both the low affinity of AMPARs for glutamate and the rapid diffusion of neurotransmitters following release (Franks et al., 2003; Raghavachari and Lisman, 2004). Modeling has predicted that the necessary concentration of glutamate to activate AMPARs following synaptic vesicle fusion is extremely brief and localized whereby presynaptic release most likely creates a "hotspot" of neurotransmitter activating only a subset of receptors (Biederer et al., 2017). Thus, now the prevailing view is both the location and timing of glutamate release is important for determining how information is transmitted at excitatory synapses.

Plasticity

Synaptic plasticity involves both pre- and post-synaptic mechanisms that employ numerous molecules and signaling cascades. However, if we focus on receptor mediated postsynaptic potentiation we see how nano-organization at the synapse can be vital, where not just the number of postsynaptic receptors, but also receptor location is a critical determinant of synaptic strength and efficacy. For instance, during LTP induction, it has been reported that preventing AMPAR surface diffusion markedly impairs potentiation *in vitro* in addition to inhibiting behavioral aspects of contextual learning (Penn et al., 2017). Modeling predicts that increasing receptor density is more efficient than merely increasing synaptic area as the same degree of AMPAR current potentiation can be achieved by reducing inter-receptor distances by 30–35% or by increasing AMPAR number by 100–200% (Franks et al., 2003; Savtchenko and Rusakov, 2014).

However, not until the advent of super resolution microscopy has the nanoscale organization of a synapse been explicitly linked to synaptic strength. With super resolution microscopy these earlier proposals were validated with the visualization of intra-synapse AMPAR clusters. Chemical LTP induction lead to nano-domain alignment alterations of increased postsynaptic density protein 95 (PSD-95) density followed by trans-synaptic re-alignment within nanoclusters (Tang et al., 2016). In addition, structural plasticity, changes in spine and bouton size in response to activity paradigms, is related to synaptic molecular architecture. In that synaptic reorganization is modular, whereby increases in spine size are accompanied by the addition of individual nano-modules (Hruska et al., 2018; **Figure 2**). These studies collectively posit that purely re-distribution of receptors can alter synaptic strength and this reorganization can be a more resource effective means for postsynaptic potentiation.

MOLECULAR COMPONENTS THAT MEDIATE NANO-ORGANIZATION

As discussed above, all different modes of release have distinct functional roles, specific synaptic vesicle fusion machinery, and target distinct postsynaptic receptors, but how this organization is maintained structurally in a single active zone synapse remains poorly understood. The advancement of super resolution light microscopy techniques in conjunction with cryogenic electron microscopy (EM) approaches have uncovered prominent nano-organization at single synapses supported by molecular nano-scaffolds that link pre- and post-synaptic compartments providing a platform that privileges different regions of the synapse for evoked release.

Early optical studies hinted at synaptic nano-organization while examining clustering dynamics of receptor subpopulations. Relative to the extrasynaptic space, AMPARs are organized in nanodomains where the number of clusters increases with synapse size (MacGillavry et al., 2013; Biederer et al., 2017). These clusters are mobile and dynamic as AMPARs can diffuse in and out although they demonstrate an overall stability creating a dynamic environment of AMPAR localization (Nair et al., 2013). Therefore, it has become evident that the distribution of receptors in the excitatory postsynaptic density is not homogeneous whereby AMPARs and NMDARs are both arranged in clusters (Goncalves et al., 2020). Moreover, these receptor clusters are found in areas enriched in postsynaptic proteins providing a proteomic network supporting nanoscale receptor organization (MacGillavry et al., 2013). A principal protein of interest is PSD-95 due to both its role in anchoring AMPARs via TARP binding and its co-enrichment with AMPAR clusters at the postsynaptic density (PSD) (Chen et al., 2011; MacGillavry et al., 2013; Nair et al., 2013; Tang et al., 2016). Consequently, PSD-95 is thought to be the master organizer of excitatory postsynaptic organization facilitating the heterogeneous enrichment of receptors and other scaffolding proteins such as GKAP, Shank, and Homer, creating a range of protein expression within the postsynaptic neuron (Tang et al., 2016; Biederer et al., 2017).

A recent study demonstrated that presynaptic loci with a high density of proteins vital for vesicle priming and fusion (such as RIM1/2, Munc13, and bassoon) were associated with parallel postsynaptic gradients of PSD-95 and AMPARs (Tang et al., 2016). Here, presynaptic RIM1/2 clusters show the largest degree of correspondence with postsynaptic PSD-95 whereas presynaptic Munc13 and Bassoon show weaker association

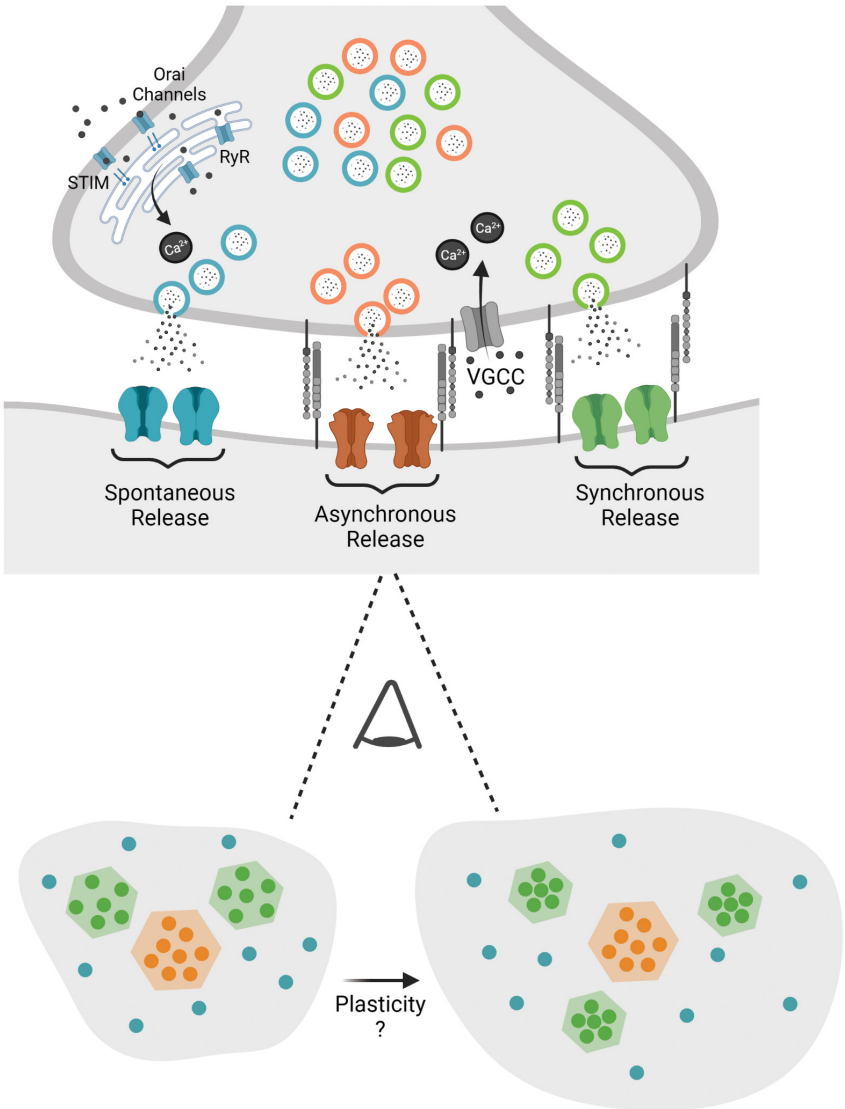

FIGURE 2 | This figure depicts the nanostructure that is proposed to privilege different modes of release at the synapse, with evoked release supported by specific structural elements (i.e., neurexin and LRRTM2). When viewing the synapse from above one proposal states that evoked release is clustered in confined areas, while asynchronous release is clustered toward the center and spontaneous release is distributed over a larger area of the synapse. Potential plasticity processes may alter nanostructure with increased spine size and a parallel increase in nano-modules as well as increased postsynaptic scaffold and receptor density within nanocolumns.

with their postsynaptic scaffold counterparts. These findings establish a trans-synaptic nanocolumn model via co-alignment and enrichment of both pre- and post-synaptic proteomes. This nanocolumn organization facilities concentrated increases in neurotransmitter at designated points along the active zone aligned with specific receptor subpopulations providing the substrate for the functionality of different types of release.

CORRESPONDENCE BETWEEN NANOSTRUCTURE AND FUNCTION

The organization of the synapse in nanocolumns deconstructs the classical homogeneous view of single active zone synapses and proposes a heterogeneous molecular platform that favors different modes of release at different regions governing distinct downstream biochemical signaling pathways. A substructure within the active zone that is privileged for evoked release was defined by the co-enrichment of pre- and post-synaptic proteins defined by high local RIM1, PSD-95, and GluA2 density. The mapping of evoked and spontaneous synaptic vesicle fusion in relation to the molecular layout of these key proteins demonstrated evoked fusion is privileged at areas of dense postsynaptic ensembles and spontaneous release happens within a greater area of the active zone (**Figure 2**). Active zone regions with the highest likelihood of release are aligned to the densest AMPAR areas, optimizing the potency of neurotransmission

(Tang et al., 2016). This work demonstrated AMPARs are enriched within 80 nm nanodomains aligned with presynaptic RIM nanodomains, however, how AMPAR clusters opposed to release sites are maintained across the synapse was originally unclear.

The extracellular cleavage of leucine rich repeat transmembrane 2 (LRRTM2), a cell adhesion molecule that binds postsynaptic PSD-95 and presynaptic neurexin, has recently been demonstrated to be vital in regulating this pre- and post-synaptic alignment. The acute proteolytic cleavage LRRTM2, disrupting extracellular neurexin binding, led to the rapid repositioning of AMPARs away from RIM nanodomains, specifically reducing the amplitude of evoked PSCs while spontaneous release was unaffected. The enrichment of LRRTM2 in the nanocolumn upholds release and receptor nanoclustering by facilitating the alignment of AMPARs for evoked release (Ramsey et al., 2021). Ultimately demonstrating LRRTM2 as a structural link mediating the trans-synaptic alignment necessary for evoked neurotransmitter release (**Figure 2**). The bias of these defined nanocolumns toward one mode of release bolsters the premise that different modes of release activate different postsynaptic receptors and provides a substrate for plasticity. However, multiple questions still remain. First of all, synaptic nanostructure has been shown to facilitate evoked release, however, it is unknown if there are molecular platforms in place to support spontaneous release. Furthermore, are there other trans-synaptic molecules enriched in nanocolumns? If so, what is their role in development? In addition, are there other mechanisms besides direct interactions supporting pre- and post-synaptic domains, i.e., steric hinderance (Biederer et al., 2017) that impact nano-organization? Lastly how does this synaptic nanostructure relate to synaptic vesicle pools? As discussed above synaptic vesicle pools are defined by their molecular identity but how do nanodomains traffic and facilitate release at distinct fusions sites of molecularly diverse synaptic vesicles?

Recent development of a system that allowed for stimulation followed by the immediate high-pressure freezing of the sample, "zap-and-freeze," allowed for the spatial and temporal analysis of both synchronous and asynchronous release at the active zone. Series of electron micrographs of synaptic ultrastructure revealed a distinct spatial organization of vesicle fusion following stimulation, with synchronous release happening throughout the active zone and asynchronous release, vesicles that fuse 11 ms after stimulation, concentrated at the center (**Figure 2**; Kusick et al., 2020). The functional significance of this segregation of action potential induced release was investigated in regard to subtypes of glutamate receptors that have a heterogeneous organization on the post synapse.

Excitatory synapses typically express three subtypes of glutamate receptors; NMDARs, AMPARs, and metabotropic glutamate receptors that display a centralized, peripheral, and dispersed organization within the PSD, respectively (Goncalves et al., 2020). The location of NMDARs is of particular interest due to the necessity of not only glutamate binding but postsynaptic depolarization, to relieve magnesium pore blockade, for receptor activation (Seeburg et al., 1995). The ultrastructural analysis of synaptic fusion pits and postsynaptic receptors delineated AMPARs cluster at the periphery and NMDARs at the center of the PSD. Further computer modeling revealed the spatial organization of fusion sites with specific receptors, where asynchronous release is privileged adjacent to where NMDARs are localized (Li et al., 2021). The temporal difference of synchronous and asynchronous release is suspected to facilitate NMDAR activation. Thus, providing new evidence deviating from the canonical view of NMDAR activation via spike timing dependent plasticity but NMDAR activation in the same active zone by the same spike due to the trans-synaptic alignment of release sites and receptors (Li et al., 2021).

These studies outline a synaptic organization of nanocolumn clusters supporting evoked release where asynchronous release is preferentially localized to the center of the synapse and spontaneous release happening throughout the synapse (**Figure 2**). Modular nanocolumn synaptic organization implies a design principle that may ultimately mediate the segregation of release, shape synaptic efficacy, determine neurotransmission reliability, and tune plasticity.

FUTURE DIRECTIONS: TECHNOLOGY AND TOOLS

The largest challenge with understanding the ultrastructure of the synapse in relation to neurotransmission is synaptic structures are too small for traditional light microscopy methods while physiological processes are fast and dynamic (Biederer et al., 2017). Use-dependent pharmacology to investigate the segregation of release primarily at excitatory hippocampal synapses have set the stage for advanced techniques to uncover synaptic nanostructure. However, these fundamental techniques should not be overlooked but employed to study inhibitory synapses as well as other synapse types to form a complete picture of synaptic organization throughout the brain.

The advent of super resolution microscopy has allowed us to overcome the diffraction limit of light and probe the nanoscale organization of the synapse with fluorescence microscopy. In addition, cryogenic electron microscopy (cryo-EM) techniques allow for the visualization of molecules providing great insight into the morphology of cells and confirmations of proteins. However, at this point cryo-EM does not endow the molecular specificity that fluorescence microscopy offers, and super resolution microscopy does not provide high resolution characterization of synaptic ultra-structure. Whilst super resolution microscopy and cryo-EM are great imaging tools, they do not provide the temporal resolution needed to see physiological synaptic processes in real time. Therefore, electrophysiology still has paramount importance and utility today due to its unparalleled temporal resolution, making it a technique that should be employed in addition to imaging to understand fundamental organizing principles of the synapse. An approach that has recently linked synapse nanostructure

to function is cryo-EM visualization of synaptic vesicle fusion coined "zap and freeze" (Kusick et al., 2020). One of the largest draw backs of EM is it cannot be conducted on live tissue. Nevertheless, this method has been used to characterize synaptic ultrastructure directly following stimulation by reconstructing a series of events from snapshots (Kusick et al., 2020). However, it remains a challenge to visualize spontaneous release using these approaches as these fusion events are not under the experimenter's control.

In order to fully elucidate the function of synaptic nanoscale organization, methods that provide molecular information as well as the monitoring of synaptic vesicle release and retrieval must be used in parallel. Nanometer level resolution has changed the field of neuroscience giving us the tools to further study how synaptic nanostructure underlies function, however, novel tools and further insight are necessary to causally link these nano-structural elements to synaptic signaling.

AUTHOR CONTRIBUTIONS

NG and EK wrote and edited this article. Both authors contributed to the article and approved the submitted version.

FUNDING

This work was supported by the National Institute of Mental Health (Grant MH066198 to EK and T32 MH064913 to NG).

ACKNOWLEDGMENTS

We would like to thank Drs. Richard Sando and Qiangjun Zhou for helpful feedback during the writing process. **Figures 1** and **2** were created with BioRender.com.

REFERENCES

Alabi, A. A., and Tsien, R. W. (2012). Synaptic vesicle pools and dynamics. *Cold Spring Harb. Perspect. Biol.* 4:a013680. doi: 10.1101/cshperspect.a013680

Alten, B., Zhou, Q., Shin, O.-H., Esquivies, L., Lin, P.-Y., White, K. I., et al. (2021). Role of aberrant spontaneous neurotransmission in SNAP25-associated encephalopathies. *Neuron* 109, 59–72.e5. doi: 10.1016/j.neuron.2020.10.012

Andreae, L. C., and Burrone, J. (2015). Spontaneous neurotransmitter release shapes dendritic arbors via long-range activation of NMDA receptors. *Cell Rep.* 10, 873–882. doi: 10.1016/j.celrep.2015.01.032

Andreae, L. C., and Burrone, J. (2018). The role of spontaneous neurotransmission in synapse and circuit development. *J. Neurosci. Res.* 96, 354–359. doi: 10.1002/jnr.24154

Andreae, L. C., Fredj, N. B., and Burrone, J. (2012). Independent vesicle pools underlie different modes of release during neuronal development. *J. Neurosci.* 32, 1867–1874. doi: 10.1523/JNEUROSCI.5181-11.2012

Aoto, J., Nam, C. I., Poon, M. M., Ting, P., and Chen, L. (2008). Synaptic signaling by all-trans retinoic acid in homeostatic synaptic plasticity. *Neuron* 60, 308–320. doi: 10.1016/j.neuron.2008.08.012

Atasoy, D., Ertunc, M., Moulder, K. L., Blackwell, J., Chung, C., Su, J., et al. (2008). Spontaneous and evoked glutamate release activates two populations of NMDA receptors with limited overlap. *J. Neurosci.* 28, 10151–10166. doi: 10.1523/JNEUROSCI.2432-08.2008

Autry, A. E., Adachi, M., Nosyreva, E., Na, E. S., Los, M. F., Cheng, P., et al. (2011). NMDA receptor blockade at rest triggers rapid behavioural antidepressant responses. *Nature* 475, 91–95. doi: 10.1038/nature10130

Bacaj, T., Wu, D., Yang, X., Morishita, W., Zhou, P., Xu, W., et al. (2013). Synaptotagmin-1 and synaptotagmin-7 trigger synchronous and asynchronous phases of neurotransmitter release. *Neuron* 80, 947–959. doi: 10.1016/j.neuron.2013.10.026

Bal, M., Leitz, J., Reese, A. L., Ramirez, D. M. O., Durakoglugil, M., Herz, J., et al. (2013). Reelin mobilizes a VAMP7-dependent synaptic vesicle pool and selectively augments spontaneous neurotransmission. *Neuron* 80, 934–946. doi: 10.1016/j.neuron.2013.08.024

Banerjee, S., Vernon, S., Jiao, W., Choi, B. J., Ruchti, E., Asadzadeh, J., et al. (2021). Miniature neurotransmission is required to maintain Drosophila synaptic structures during ageing. *Nat. Commun.* 12:4399. doi: 10.1038/s41467-021-24490-1

Ben-Ari, Y. (2002). Excitatory actions of gaba during development: the nature of the nurture. *Nat. Rev. Neurosci.* 3, 728–739. doi: 10.1038/nrn920

Biederer, T., Kaeser, P. S., and Blanpied, T. A. (2017). Trans-cellular nano-alignment of synaptic function. *Neuron* 96, 680–696. doi: 10.1016/j.neuron.2017.10.006

Chanaday, N. L., and Kavalali, E. T. (2017). How do you recognize and reconstitute a synaptic vesicle after fusion? *F1000Res* 6:1734. doi: 10.12688/f1000research.12072.1

Chanaday, N. L., and Kavalali, E. T. (2018). Presynaptic origins of distinct modes of neurotransmitter release. *Curr. Opin. Neurobiol.* 51, 119–126. doi: 10.1016/j.conb.2018.03.005

Chen, J.-C., Lo, Y.-F., Lin, Y.-W., Lin, S.-H., Huang, C.-L., and Cheng, C.-J. (2019). WNK4 kinase is a physiological intracellular chloride sensor. *Proc. Natl. Acad. Sci. U.S.A* 116, 4502–4507. doi: 10.1073/pnas.1817220116

Chen, X., Nelson, C. D., Li, X., Winters, C. A., Azzam, R., Sousa, A. A., et al. (2011). PSD-95 is required to sustain the molecular organization of the postsynaptic density. *J. Neurosci.* 31, 6329–6338. doi: 10.1523/JNEUROSCI.5968-10.2011

Choi, B. J., Imlach, W. L., Jiao, W., Wolfram, V., Wu, Y., Grbic, M., et al. (2014). Miniature neurotransmission regulates Drosophila synaptic structural maturation. *Neuron* 82, 618–634. doi: 10.1016/j.neuron.2014.03.012

Courtney, N. A., Briguglio, J. S., Bradberry, M. M., Greer, C., and Chapman, E. R. (2018). Excitatory and inhibitory neurons utilize different Ca^{2+} sensors and sources to regulate spontaneous release. *Neuron* 98, 977–991.e5. doi: 10.1016/j.neuron.2018.04.022

Crawford, D. C., and Kavalali, E. T. (2015). Molecular underpinnings of synaptic vesicle pool heterogeneity. *Traffic* 16, 338–364. doi: 10.1111/tra.12262

Crawford, D. C., Ramirez, D. M. O., Trauterman, B., Monteggia, L. M., and Kavalali, E. T. (2017). Selective molecular impairment of spontaneous neurotransmission modulates synaptic efficacy. *Nat. Commun,* 8:14436. doi: 10.1038/ncomms14436

Deák, F., Schoch, S., Liu, X., Südhof, T. C., and Kavalali, E. T. (2004). Synaptobrevin is essential for fast synaptic-vesicle endocytosis. *Nat. Cell Biol.* 6, 1102–1108. doi: 10.1038/ncb1185

Fatt, P., and Katz, B. (1950). Some observations on biological noise. *Nature* 166, 597–598. doi: 10.1038/166597a0

Franks, K. M., Stevens, C. F., and Sejnowski, T. J. (2003). Independent sources of quantal variability at single glutamatergic synapses. *J. Neurosci.* 23, 3186–3195. doi: 10.1523/JNEUROSCI.23-08-03186.2003

Geppert, M., Goda, Y., Hammer, R. E., Li, C., Rosahl, T. W., Stevens, C. F., et al. (1994). Synaptotagmin I: a major Ca2+ sensor for transmitter release at a central synapse. *Cell* 79, 717–727. doi: 10.1016/0092-8674(94)90556-8

Goncalves, J., Bartol, T. M., Camus, C., Levet, F., Menegolla, A. P., Sejnowski, T. J., et al. (2020). Nanoscale co-organization and coactivation of AMPAR, NMDAR, and mGluR at excitatory synapses. *Proc. Natl. Acad. Sci. U.S.A.* 117, 14503–14511. doi: 10.1073/pnas.1922563117

Gonzalez-Islas, C., Bülow, P., and Wenner, P. (2018). Regulation of synaptic scaling by action potential-independent miniature neurotransmission. *J. Neurosci. Res.* 96, 348–353. doi: 10.1002/jnr.24138

Groffen, A. J., Martens, S., Arazola, R. D., Cornelisse, L. N., Lozovaya, N., de Jong, A. P. H., et al. (2010). Doc2b is a high-affinity Ca^{2+} sensor for spontaneous neurotransmitter release. *Science* 327, 1614–1618. doi: 10.1126/science.1183765

Hefft, S., and Jonas, P. (2005). Asynchronous GABA release generates long-lasting inhibition at a hippocampal interneuron-principal neuron synapse. *Nat. Neurosci.* 8, 1319–1328. doi: 10.1038/nn1542

Heubl, M., Zhang, J., Pressey, J. C., Al Awabdh, S., Renner, M., Gomez-Castro, F., et al. (2017). GABA A receptor dependent synaptic inhibition rapidly tunes KCC2 activity via the Cl - -sensitive WNK1 kinase. *Nat. Commun.* 8:1776. doi: 10.1038/s41467-017-01749-0

Horvath, P. M., Chanaday, N. L., Alten, B., Kavalali, E. T., and Monteggia, L. M. (2021). A subthreshold synaptic mechanism regulating BDNF expression and resting synaptic strength. *Cell Rep.* 36:109467. doi: 10.1016/j.celrep.2021.109467

Horvath, P. M., Piazza, M. K., Monteggia, L. M., and Kavalali, E. T. (2020). Spontaneous and evoked neurotransmission are partially segregated at inhibitory synapses. *Elife* 9:e52852. doi: 10.7554/eLife.52852

Hruska, M., Henderson, N., Le Marchand, S. J., Jafri, H., and Dalva, M. B. (2018). Synaptic nanomodules underlie the organization and plasticity of spine synapses. *Nat. Neurosci.* 21, 671–682. doi: 10.1038/s41593-018-0138-9

Hua, Z., Leal-Ortiz, S., Foss, S. M., Waites, C. L., Garner, C. C., Voglmaier, S. M., et al. (2011). v-SNARE composition distinguishes synaptic vesicle pools. *Neuron* 71, 474–487. doi: 10.1016/j.neuron.2011.06.010

Huntwork, S., and Littleton, J. T. (2007). A complexin fusion clamp regulates spontaneous neurotransmitter release and synaptic growth. *Nat. Neurosci.* 10, 1235–1237. doi: 10.1038/nn1980

Jackman, S. L., Turecek, J., Belinsky, J. E., and Regehr, W. G. (2016). The calcium sensor synaptotagmin 7 is required for synaptic facilitation. *Nature* 529, 88–91. doi: 10.1038/nature16507

Katz, B. (1969). *The Release of Neural Transmitter Substances*. Liverpool: Liverpool University Press.

Kavalali, E. T. (2015). The mechanisms and functions of spontaneous neurotransmitter release. *Nat. Rev. Neurosci.* 16, 5–16. doi: 10.1038/nrn3875

Kavalali, E. T. (2018). Spontaneous neurotransmission: a form of neural communication comes of age. *J. Neurosci. Res.* 96, 331–334. doi: 10.1002/jnr.24207

Kavalali, E. T. (2020). Neuronal Ca2+ signalling at rest and during spontaneous neurotransmission. *J. Physiol.* 598, 1649–1654. doi: 10.1113/JP276541

Kavalali, E. T., and Monteggia, L. M. (2020). Targeting homeostatic synaptic plasticity for treatment of mood disorders. *Neuron* 106, 715–726. doi: 10.1016/j.neuron.2020.05.015

Klausberger, T., and Somogyi, P. (2008). Neuronal Diversity and temporal dynamics: the unity of hippocampal circuit operations. *Science* 321, 53–57. doi: 10.1126/science.1149381

Kononenko, N. L., and Haucke, V. (2015). Molecular mechanisms of presynaptic membrane retrieval and synaptic vesicle reformation. *Neuron* 85, 484–496. doi: 10.1016/j.neuron.2014.12.016

Kusick, G. F., Chin, M., Raychaudhuri, S., Lippmann, K., Adula, K. P., Hujber, E. J., et al. (2020). Synaptic vesicles transiently dock to refill release sites. *Nat. Neurosci.* 23, 1329–1338. doi: 10.1038/s41593-020-00716-1

Li, S., Raychaudhuri, S., Lee, S. A., Brockmann, M. M., Wang, J., Kusick, G., et al. (2021). Asynchronous release sites align with NMDA receptors in mouse hippocampal synapses. *Nat. Commun.* 12:677. doi: 10.1038/s41467-021-21004-x

Li, Y. C., Chanaday, N. L., Xu, W., and Kavalali, E. T. (2017). Synaptotagmin-1- and synaptotagmin-7-dependent fusion mechanisms target synaptic vesicles to kinetically distinct endocytic pathways. *Neuron* 93, 616–631.e3. doi: 10.1016/j.neuron.2016.12.010

Lin, P.-Y., Chanaday, N. L., Horvath, P. M., Ramirez, D. M. O., Monteggia, L. M., and Kavalali, E. T. (2020). VAMP4 maintains a Ca2+-sensitive pool of spontaneously recycling synaptic vesicles. *J. Neurosci.* 40, 5389–5401. doi: 10.1523/JNEUROSCI.2386-19.2020

Lin, P.-Y., Kavalali, E. T., and Monteggia, L. M. (2018). Genetic dissection of presynaptic and postsynaptic BDNF-TrkB signaling in synaptic efficacy of CA3-CA1 synapses. *Cell Rep.* 24, 1550–1561. doi: 10.1016/j.celrep.2018.07.020

Lisman, J. E., Raghavachari, S., and Tsien, R. W. (2007). The sequence of events that underlie quantal transmission at central glutamatergic synapses. *Nat. Rev. Neurosci.* 8, 597–609. doi: 10.1038/nrn2191

Liu, H., Dean, C., Arthur, C. P., Dong, M., and Chapman, E. R. (2009). Autapses and networks of hippocampal neurons exhibit distinct synaptic transmission phenotypes in the absence of synaptotagmin I. *J. Neurosci.* 29, 7395–7403. doi: 10.1523/JNEUROSCI.1341-09.2009

Luo, F., and Südhof, T. C. (2017). Synaptotagmin-7-mediated asynchronous release boosts high-fidelity synchronous transmission at a central synapse. *Neuron* 94, 826–839.e3. doi: 10.1016/j.neuron.2017.04.020

MacGillavry, H. D., Song, Y., Raghavachari, S., and Blanpied, T. A. (2013). Nanoscale scaffolding domains within the postsynaptic density concentrate synaptic AMPA receptors. *Neuron* 78, 615–622. doi: 10.1016/j.neuron.2013.03.009

Maximov, A., and Südhof, T. C. (2005). Autonomous function of synaptotagmin 1 in triggering synchronous release independent of asynchronous release. *Neuron* 48, 547–554. doi: 10.1016/j.neuron.2005.09.006

Melom, J. E., Akbergenova, Y., Gavornik, J. P., and Littleton, J. T. (2013). Spontaneous and evoked release are independently regulated at individual active zones. *J. Neurosci.* 33, 17253–17263. doi: 10.1523/JNEUROSCI.3334-13.2013

Molnár, Z., López-Bendito, G., Small, J., Partridge, L. D., Blakemore, C., and Wilson, M. C. (2002). Normal development of embryonic thalamocortical connectivity in the absence of evoked synaptic activity. *J. Neurosci.* 22, 10313–10323. doi: 10.1523/JNEUROSCI.22-23-10313.2002

Mori, Y., Takenaka, K., Fukazawa, Y., and Takamori, S. (2021). The endosomal Q-SNARE, Syntaxin 7, defines a rapidly replenishing synaptic vesicle recycling pool in hippocampal neurons. *Commun. Biol.* 4:981. doi: 10.1038/s42003-021-02512-4

Nair, D., Hosy, E., Petersen, J. D., Constals, A., Giannone, G., Choquet, D., et al. (2013). Super-resolution imaging reveals that AMPA receptors inside synapses are dynamically organized in nanodomains regulated by PSD95. *J. Neurosci.* 33, 13204–13224. doi: 10.1523/JNEUROSCI.2381-12.2013

Pang, Z. P., Bacaj, T., Yang, X., Zhou, P., Xu, W., and Südhof, T. C. (2011). Doc2 supports spontaneous synaptic transmission by a Ca2+-independent mechanism. *Neuron* 70, 244–251. doi: 10.1016/j.neuron.2011.03.011

Peled, E. S., Newman, Z. L., and Isacoff, E. Y. (2014). Evoked and spontaneous transmission favored by distinct sets of synapses. *Curr. Biol.* 24, 484–493. doi: 10.1016/j.cub.2014.01.022

Penn, A. C., Zhang, C. L., Georges, F., Royer, L., Breillat, C., Hosy, E., et al. (2017). Hippocampal LTP and contextual learning require surface diffusion of AMPA receptors. *Nature* 549, 384–388. doi: 10.1038/nature23658

Piala, A. T., Moon, T. M., Akella, R., He, H., Cobb, M. H., and Goldsmith, E. J. (2014). Chloride sensing by WNK1 involves inhibition of autophosphorylation. *Sci. Signal.* 7:ra41. doi: 10.1126/scisignal.2005050

Raghavachari, S., and Lisman, J. E. (2004). Properties of quantal transmission at CA1 synapses. *J. Neurophysiol.* 92, 2456–2467. doi: 10.1152/jn.00258.2004

Raingo, J., Khvotchev, M., Liu, P., Darios, F., Li, Y. C., Ramirez, D. M. O., et al. (2012). VAMP4 directs synaptic vesicles to a pool that selectively maintains asynchronous neurotransmission. *Nat. Neurosci.* 15, 738–745. doi: 10.1038/nn.3067

Ramirez, D. M. O., Crawford, D. C., Chanaday, N. L., Trauterman, B., Monteggia, L. M., and Kavalali, E. T. (2017). Loss of Doc2-dependent spontaneous neurotransmission augments glutamatergic synaptic strength. *J. Neurosci.* 37, 6224–6230. doi: 10.1523/JNEUROSCI.0418-17.2017

Ramirez, D. M. O., Khvotchev, M., Trauterman, B., and Kavalali, E. T. (2012). Vti1a identifies a vesicle pool that preferentially recycles at rest and maintains spontaneous neurotransmission. *Neuron* 73, 121–134. doi: 10.1016/j.neuron.2011.10.034

Ramsey, A. M., Tang, A.-H., LeGates, T. A., Gou, X.-Z., Carbone, B. E., Thompson, S. M., et al. (2021). Subsynaptic positioning of AMPARs by LRRTM2 controls synaptic strength. *Sci. Adv.* 7:eabf3126. doi: 10.1126/sciadv.abf3126

Reese, A. L., and Kavalali, E. T. (2015). Spontaneous neurotransmission signals through store-driven Ca(2+) transients to maintain synaptic homeostasis. *Elife* 4:e09262. doi: 10.7554/eLife.09262

Reese, A. L., and Kavalali, E. T. (2016). Single synapse evaluation of the postsynaptic NMDA receptors targeted by evoked and spontaneous neurotransmission. *eLife* 5:e21170. doi: 10.7554/eLife.21170

Revelo, N. H., Kamin, D., Truckenbrodt, S., Wong, A. B., Reuter-Jessen, K., Reisinger, E., et al. (2014). A new probe for super-resolution imaging of

membranes elucidates trafficking pathways. *J. Cell Biol.* 205, 591–606. doi: 10.1083/jcb.201402066

Rey, S. A., Smith, C. A., Fowler, M. W., Crawford, F., Burden, J. J., and Staras, K. (2015). Ultrastructural and functional fate of recycled vesicles in hippocampal synapses. *Nat. Commun.* 6:8043. doi: 10.1038/ncomms9043

Rozov, A., Bolshakov, A. P., and Valiullina-Rakhmatullina, F. (2019). The ever-growing puzzle of asynchronous release. *Front. Cell. Neurosci.* 13:28. doi: 10.3389/fncel.2019.00028

Sara, Y., Bal, M., Adachi, M., Monteggia, L. M., and Kavalali, E. T. (2011). Use-dependent AMPA receptor block reveals segregation of spontaneous and evoked glutamatergic neurotransmission. *J. Neurosci.* 31, 5378–5382. doi: 10.1523/JNEUROSCI.5234-10.2011

Savtchenko, L. P., and Rusakov, D. A. (2014). Moderate AMPA receptor clustering on the nanoscale can efficiently potentiate synaptic current. *Philos. Trans. R. Soc. Lond. B Biol. Sci.* 369:20130167. doi: 10.1098/rstb.2013.0167

Schoch, S., Deák, F., Königstorfer, A., Mozhayeva, M., Sara, Y., Südhof, T. C., et al. (2001). SNARE function analyzed in synaptobrevin/VAMP knockout mice. *Science* 294, 1117–1122. doi: 10.1126/science.1064335

Seeburg, P. H., Burnashev, N., Köhr, G., Kuner, T., Sprengel, R., and Monyer, H. (1995). The NMDA receptor channel: molecular design of a coincidence detector. *Recent Prog. Horm. Res.* 50, 19–34. doi: 10.1016/b978-0-12-571150-0.50006-8

Südhof, T. C. (2013). Neurotransmitter release: the last millisecond in the life of a synaptic vesicle. *Neuron* 80, 675–690. doi: 10.1016/j.neuron.2013.10.022

Südhof, T. C., and Rothman, J. E. (2009). Membrane fusion: grappling with SNARE and SM proteins. *Science* 323, 474–477. doi: 10.1126/science.1161748

Sugita, S., Shin, O.-H., Han, W., Lao, Y., and Südhof, T. C. (2002). Synaptotagmins form a hierarchy of exocytotic Ca(2+) sensors with distinct Ca(2+) affinities. *EMBO J.* 21, 270–280. doi: 10.1093/emboj/21.3.270

Sutton, M. A., Ito, H. T., Cressy, P., Kempf, C., Woo, J. C., and Schuman, E. M. (2006). Miniature neurotransmission stabilizes synaptic function via tonic suppression of local dendritic protein synthesis. *Cell* 125, 785–799. doi: 10.1016/j.cell.2006.03.040

Takamori, S., Holt, M., Stenius, K., Lemke, E. A., Grønborg, M., Riedel, D., et al. (2006). Molecular anatomy of a trafficking organelle. *Cell* 127, 831–846. doi: 10.1016/j.cell.2006.10.030

Tang, A.-H., Chen, H., Li, T. P., Metzbower, S. R., MacGillavry, H. D., and Blanpied, T. A. (2016). A trans-synaptic nanocolumn aligns neurotransmitter release to receptors. *Nature* 536, 210–214. doi: 10.1038/nature19058

Turrigiano, G. G., and Nelson, S. B. (2004). Homeostatic plasticity in the developing nervous system. *Nat. Rev. Neurosci.* 5, 97–107. doi: 10.1038/nrn1327

Walter, A. M., Kurps, J., de Wit, H., Schöning, S., Toft-Bertelsen, T. L., Lauks, J., et al. (2014). The SNARE protein vti1a functions in dense-core vesicle biogenesis. *EMBO J.* 33, 1681–1697. doi: 10.15252/embj.201387549

Williams, C. L., and Smith, S. M. (2018). Calcium dependence of spontaneous neurotransmitter release. *J. Neurosci. Res.* 96, 335–347. doi: 10.1002/jnr.24116

Xu, W., Morishita, W., Buckmaster, P. S., Pang, Z. P., Malenka, R. C., and Südhof, T. C. (2012). Distinct neuronal coding schemes in memory revealed by selective erasure of fast synchronous synaptic transmission. *Neuron* 73, 990–1001. doi: 10.1016/j.neuron.2011.12.036

Conflict of Interest: The authors declare that the research was conducted in the absence of any commercial or financial relationships that could be construed as a potential conflict of interest.

Publisher's Note: All claims expressed in this article are solely those of the authors and do not necessarily represent those of their affiliated organizations, or those of the publisher, the editors and the reviewers. Any product that may be evaluated in this article, or claim that may be made by its manufacturer, is not guaranteed or endorsed by the publisher.

frontiers in Synaptic Neuroscience

ORIGINAL RESEARCH
published: 10 February 2022
doi: 10.3389/fnsyn.2021.773209

Selective Enrichment of Munc13-2 in Presynaptic Active Zones of Hippocampal Pyramidal Cells That Innervate mGluR1α Expressing Interneurons

*Noemi Holderith[1], Mohammad Aldahabi[1,2] and Zoltan Nusser[1]**

[1] *Institute of Experimental Medicine, Eotvos Lorand Research Network, Budapest, Hungary,* [2] *János Szentágothai School of Neurosciences, Semmelweis University, Budapest, Hungary*

Selective distribution of proteins in presynaptic active zones (AZs) is a prerequisite for generating postsynaptic target cell type-specific differences in presynaptic vesicle release probability (P_V) and short-term plasticity, a characteristic feature of cortical pyramidal cells (PCs). In the hippocampus of rodents, somatostatin and mGluR1α expressing interneurons (mGluR1α+ INs) receive small, facilitating excitatory postsynaptic currents (EPSCs) from PCs and express Elfn1 that trans-synaptically recruits mGluR7 into the presynaptic AZ of PC axons. Here we show that Elfn1 also has a role in the selective recruitment of Munc13-2, a synaptic vesicle priming and docking protein, to PC AZs that innervate mGluR1α+ INs. In Elfn1 knock-out mice, unitary EPSCs (uEPSCs) in mGluR1α+ INs have threefold larger amplitudes with less pronounced short-term facilitation, which might be the consequence of the loss of either mGluR7 or Munc13-2 or both. Conditional genetic deletion of Munc13-2 from CA1 PCs results in the loss of Munc13-2, but not mGluR7 from the AZs, and has no effect on the amplitude of uEPSCs and leaves the characteristic short-term facilitation intact at PC to mGluR1α+ IN connection. Our results demonstrate that Munc13-1 alone is capable of imposing low P_V at PC to mGluR1α+ IN synapses and Munc13-2 has yet an unknown role in this synapse.

Keywords: hippocampus, CA1, O-LM interneuron, paired recordings, multiplexed postembedding immunohistochemistry, vesicle release probability, short-term plasticity

OPEN ACCESS

Edited by:
Lucia Tabares, Seville University, Spain

Reviewed by:
Jose Luis Nieto-Gonzalez, Instituto de Biomedicina de Sevilla (IBiS), HUVR/Spanish National Research Council (CSIC)/Universidad de Sevilla, Spain
Marcial Camacho, Universidad de La Laguna, Spain

****Correspondence:***
Zoltan Nusser
nusser@koki.hu

Received: *09 September 2021*
Accepted: *27 December 2021*
Published: *10 February 2022*

Citation:
Holderith N, Aldahabi M and Nusser Z (2022) Selective Enrichment of Munc13-2 in Presynaptic Active Zones of Hippocampal Pyramidal Cells That Innervate mGluR1α Expressing Interneurons. Front. Synaptic Neurosci. 13:773209. doi: 10.3389/fnsyn.2021.773209

INTRODUCTION

Postsynaptic target cell type-dependent differences in synaptic efficacy and short-term plasticity of excitatory synapses (Ali and Thomson, 1997, 1998; Reyes et al., 1998; Scanziani et al., 1998; Sun et al., 2005) have profound impacts on cortical network dynamics (Pouille and Scanziani, 2004). The first identified molecule with postsynaptic target cell type-dependent location in the presynaptic active zone (AZ) of pyramidal cells (PCs) was mGluR7. It was found to be

selectively enriched in hippocampal PC AZs that innervate somatostatin (Som) and mGluR1α expressing interneurons (mGluR1α+ IN; Shigemoto et al., 1996) and its constitutive activity contributes to the low postsynaptic response amplitude of this synapse (Losonczy et al., 2003). Interestingly, mGluR7 is recruited into the AZ by Elfn1 (extracellular leucine-rich repeat and fibronectin type III domain containing 1) which is selectively expressed by Som/mGluR1α+ INs and located in the excitatory postsynaptic densities where Elfn1 trans-synaptically binds and activates mGluR7 (Sylwestrak and Ghosh, 2012; Tomioka et al., 2014; Stachniak et al., 2019). Ectopic expression of Elfn1 in parvalbumin expressing INs (PV+ INs) in the hippocampus changed the short-term plasticity from depression to moderate facilitation through an unknown mechanism (Sylwestrak and Ghosh, 2012).

Although presynaptic neurotransmitter receptors could powerfully influence neurotransmitter release and short-term plasticity, in the presence of a large number of presynaptic receptor blockers synapses still show very diverse functional properties. This diversity is likely the consequence of the heterogeneous molecular components of the AZ matrix that mediate synaptic vesicles (SVs) docking, priming, and release (Sudhof, 2012). Among these, members of the Munc13 protein family are essential for SV docking and priming (Augustin et al., 1999b; Varoqueaux et al., 2002; Siksou et al., 2007) and Munc13-containing supramolecular complexes constitute the docking/release sites in the AZs (Sakamoto et al., 2018). Three closely related Munc13 genes are present in mammals (Brose et al., 1995), out of which two, Munc13-1 and Munc13-2, are expressed in hippocampal PCs (Rosenmund et al., 2002). The C-terminal part of the proteins shares common domain structures, which is functionally essential for their priming activity and are structurally homologous to vesicle tethering factors (Basu et al., 2005; Stevens et al., 2005; Li et al., 2011). Munc13-1 has one while Munc13-2 has two major splice variants with different N-terminal regions: the brain-specific bMunc13-2 and the ubiquitously expressed ubMunc13-2 both of which are expressed in CA1 PCs (Brose et al., 1995; Augustin et al., 1999b; Betz et al., 2001; Breustedt et al., 2010; Kawabe et al., 2017). Experiments in cultured autaptic neurons suggest that Munc13-1 and Munc13-2 bestow different short-term plasticity to the synapses. In 90% of the axon terminals of cultured PCs, Munc13-1 primed vesicles have high P_v and the synapses display short-term depression while in 10% of boutons, the presence of Munc13-2, in the absence of Munc13-1, confers low P_v and short-term facilitation (Rosenmund et al., 2002). As this correlation appears to hold in other synapses (Cooper et al., 2012; Man et al., 2015), the following concept emerged: high P_v synapses that show short-term depression are equipped with Munc13-1 which enables tight docking of readily releasable SVs, while low P_v synapses that display short-term facilitation employ Munc13-2 and vesicles are loosely docked and require intracellular $[Ca^{2+}]$ increase to become release competent (Neher and Brose, 2018). Munc13-2 immunolabeling in the hippocampus showed an uneven distribution of the protein with strong staining in the stratum oriens of the CA1 area (Kawabe et al., 2017) where most of the dendrites of mGluR1α+ INs are located, raising the question whether the low P_v of CA1 PC to mGluR1α+ IN synapses could be the consequence of the presence of Munc13-2 as a priming factor?

MATERIALS AND METHODS

Animals

Two young adult male Wistar rats (P30, 42), 3 adult (P50) male C57BL/6J mice, 47 adult (P50-60) Tg(Chrna2-Cre)OE25Gsat/Mmucd (RRID:MMRRC_036502-UCD, on C57BL/6J background (Leao et al., 2012) crossed with reporter line Ai9 [Gt(ROSA)26Sor_CAG/LSL_tdTomato], 15 adult (P50–70) male C57BL/6N-*Elfn1*$^{tm1.1(KOMP)Vlcg}$/MbpMmucd (RRID:MMRRC_047527-UCD, on C57BL/6N background (Tomioka et al., 2014) and 5 heterozygous littermate control mice, and 35 adult P50–70 C57BL/6N-*Unc13b*$^{TM1a(KOMP)Wtsi}$/MbpMmucd (RRID:MMRRC_050292-UCD, on C57BL/6N background) were used. Mice of both sexes were used. The animals were housed in the vivarium of the Institute of Experimental Medicine in a normal 12 h/12 h light/dark cycle and had access to water and food *ad libitum*. All the experiments were carried out in accordance with the Hungarian Act of Animal Care and Experimentation 40/2013 (II.14) and with the ethical guidelines of the Animal Committee of the Institute of Experimental Medicine, Budapest.

Virus Injection

Mice were anesthetized with a mixture of ketamine, xylasine, pypolphene (0.625, 6.25, 1.25 mg/ml respectively, 10 μl/g body weight). The pAAV-Ef1a-mCherry-IRES-Cre was a gift from Karl Deisseroth (1.8×10^{13} Addgene viral prep # 55632-AAV8[1]; RRID:Addgene_55632) (Fenno et al., 2014) or pENN.AAV.CamKII 0.4.Cre.SV40 was a gift from James M. Wilson (Addgene viral prep # 105558-AAv9[2]; RRID:Addgene_105558) (1:10 dilution 2.8×10^{13}, Penn Vector Core) were injected into the dorsal hippocampus (200 nl, coordinates from the Bregma in mm: antero posterior/dorso ventral/lateral: 2.1/1.1/1.3 and/or 2.2/1.5/1.2). After 2 weeks, the mice were either perfused or *in vitro* acute slices were prepared from the dorsal hippocampus as below.

Slice Preparation and Electrophysiological Recordings

The following animals were used: 44 adult (P50-60) Tg(Chrna2-Cre)OE25Gsat/Mmucd (RRID:MMRRC_036502-UCD, on C57Bl/6J background) crossed with reporter line Ai9 [Gt(ROSA)26Sor_CAG/LSL_tdTomato]; 10 adult P50-70 C57BL/6N-*Elfn1*$^{tm1.1(KOMP)Vlcg}$/MbpMmucd. Nineteen adult P50-70 C57BL/6N-*Unc13b*$^{TM1a(KOMP)Wtsi}$/MbpMmucd mice were injected with pAAV-Ef1a-mCherry-IRES-Cre more than 2 weeks prior to the slice preparation. Mice were stably anesthetized with a ketamine, xylasine, and pypolphene cocktail (0.625, 6.25, 1.25 mg/ml, respectively, 10 μl/g body weight), and

[1]http://n2t.net/addgene:55632

[2]http://n2t.net/addgene:105558

then decapitated; the brain was quickly removed and placed into an ice-cold cutting solution containing the following (in mM): sucrose, 205.2; KCl, 2.5; $NaHCO_3$, 26; $CaCl_2$, 0.5; $MgCl_2$, 5; NaH_2PO_4, 1.25; and glucose, 10, saturated with 95% O_2 and 5% CO_2. Coronal slices (300 μm thick) were then cut from the dorsal hippocampus using a Leica Vibratome (VT1200S) and were incubated in a submerged-type holding chamber in an artificial cerebral spinal fluid (ACSF) containing the following (in mM): NaCl, 126; KCl, 2.5; $NaHCO_3$, 26; $CaCl_2$, 2; $MgCl_2$, 2; NaH_2PO_4, 1.25; and glucose, 10, saturated with 95% O_2 and 5% CO_2, pH 7.2–7.4, at 36°C for 30 min, then kept at 22–24°C until use. Recordings were performed in the same ACSF supplemented with 2 μM AM251 to block presynaptic CB1 receptors at 32°C up to 6 h after slicing.

Cells were visualized using infrared differential interference contrast (DIC) imaging on a Nikon Eclipse FN1 microscope with a 40X water immersion objective (NA = 0.8). CA1 PCs were identified from their position and morphology, and the virally expressed mCherry was identified using fluorescent illumination. Whole-cell current-clamp recordings were performed from CA1 PCs using MultiClamp 700B amplifiers (Molecular Devices). Recorded traces were filtered at 3–4 kHz and digitized online at 50 kHz. Patch pipettes (resistance 3–6 MΩ) were pulled from thick-walled borosilicate glass capillaries with an inner filament. Intracellular solution contained the following (in mM): K-gluconate, 130; KCl, 5; $MgCl_2$, 2; EGTA, 0.05; creatine phosphate, 10; HEPES, 10; ATP, 2; GTP, 1; and biocytin, 7; glutamate, 10 (for presynaptic PCs only) pH = 7.3; 290–300 mOsm. Pyramidal cells were held at –65 mV (with a maximum of ± 100 pA DC current) and trains of 3 APs at 40 Hz were evoked with 1.2–1.5 ms-long depolarizing current pulses (1.5–2 nA). Peak amplitude and full width at half-maximal amplitude of the APs were monitored and the cells were rejected if any of these parameters changed greater than 10%. Postsynaptic O-LM cells were identified in the stratum oriens of the CA1 region by tdTomato fluorescence in the Tg(Chrna2-Cre)OE25Gsat/Mmucd animals crossed with reporter line Ai9 or by their morphology and firing pattern obtained with de- or hyperpolarizing square current injections (600 ms, from –250 to 300 pA with 50 pA steps). Paired whole-cell recordings were performed with a dual-channel amplifier (MultiClamp 700B; Axon Instruments, CA, United States). Data were filtered at 3–4 kHz (Bessel filter), digitized online at 50 kHz, recorded and analyzed using pClamp 10.3 (Molecular Devices, CA, United States). Postsynaptic INs were held at –65 mV (with a maximum of ± 200 pA DC current) in the voltage-clamp mode with the access resistance below 20 MOhm.

Tissue Processing

After recordings, the slices were fixed in a solution containing 4% formaldehyde (FA, Molar Chemicals, Budapest, Hungary), 0.2% picric acid in 0.1 M phosphate buffer (PB), pH = 7.4, at 4°C for 12 h. Immunolabeling was carried out without re-sectioning. Slices were washed in 0.1 M PB and blocked in normal goat serum (NGS, 10%; Vector Laboratories, CA, United States) for 1 h made up in Tris-buffered saline (TBS; pH 7.4), incubated in the solutions of the primary antibodies: guinea pig anti-mGluR1α (1:1,000, Frontier Institute Co., Ltd.; Cat# mGluR1a-GP-Af660, RRID:AB_2531897), or a cocktail of this Ab and a mouse anti-Cre Ab (IgG1, 1:1,000, Millipore, Cat# MAB3120, RRID:AB_2085748); diluted in TBS containing 2% NGS and 0.2% TritonX-100. Biocytin was visualized with Cy3-conjugated streptavidin (1:1,000; Jackson Immunoresearch Laboratories, PA, United States, RRID:AB_2337244). After several washes, the following secondary antibodies were applied: Alexa488-conjugated goat anti-mouse IgG1 (Jackson Immunoresearch Laboratories, PA, United States, Code: 115-547-185, RRID:AB_2632534), and Cy5-conjugated donkey anti-guinea pig IgGs (Jackson Immunoresearch, Code 706-175-148, RRID: AB_2340462). Sections were mounted in Vectashield. Image stacks were acquired with an Olympus FV1000 confocal microscope with 20x and 60x (oil immersion) objectives. A PC was considered virally infected if its nucleus had a detectable Cre signal. A cell was considered an O-LM cell, if the axon arborized in the stratum lacunosum-moleculare.

Processing of Perfusion-Fixed Tissue

Two young-adult Wistar rats (P30, 42), 3 adult (P50) male C57BL/6J mice, 3 adult (P50–60) Tg(Chrna2-Cre)OE25Gsat/Mmucd, (RRID:MMRRC_036502-UCD, on C57BL/6J background) crossed with reporter line Ai9 [Gt(ROSA)26Sor_CAG/LSL_tdTomato], 5 adult (P50–70) male C57BL/6N-*Elfn1*$^{tm1.1(KOMP)Vlcg}$/MbpMmucd (RRID:MMRRC_047527-UCD, on C57BL/6N background) and 5 heterozygous littermate control mice, and 16 adult P50-70 C57BL/6N-*Unc13b*$^{TM1a(KOMP)Wtsi}$/MbpMmucd (RRID:MMRRC_050292-UCD, on C57BL/6N background) were deeply anesthetized and transcardially perfused with a fixative containing 1% FA (Molar Chemicals, Budapest, Hungary) and 0.2% picric acid in 0.1 M PB or in 0.1 M sodium acetate buffer for 15–20 min. The brains were then quickly removed from the skull and placed in 0.1 M PB. Next, 60–100 μm thick sections were cut from the dorsal hippocampus. After blocking in NGS or normal donkey serum (NDS, 10%) for 1 h made up in TBS, the sections were incubated in the following primary antibodies: guinea pig anti-mGluR1α (1:1,000; Frontier Institute Co., Ltd, Nittobo Medical Co. Ltd, Tokyo, Japan; Cat# mGluR1a-GP-Af660, RRID:AB_2531897), goat anti-mGluR1α (1:1,000, Frontier Institute Co., Ltd; Cat# mGluR1a-Go-Af1220, RRID:AB_2571800), rabbit anti-Munc13-1 (1:500, Synaptic Systems, Göttingen, Germany; Cat# 126113, RRID:AB_887734); rabbit anti-Munc13-2 (1:250; Synaptic Systems, Göttingen, Germany; Cat# 126203, RRID:AB_2619807, recognizing the brain-specific isoform, bMunc13-2), rabbit anti-mGluR7 (1:1,000; Millipore, MA, United States; Cat# 07-239, RRID: AB_310459), rabbit anti-Elfn2 (1:500, Sigma-Aldrich, MO, United States, Cat# HPA000781, RRID: AB_1079280) that recognizes both Elfn1 and Elfn 2 (Sylwestrak and Ghosh, 2012), rabbit anti-Elfn1 (1:500; Synaptic Systems, Göttingen, Germany; Cat#448-003, RRID:AB_2884915), guinea pig anti-mGluR7b (1:1,000 gift from Prof. Shigemoto, Shigemoto et al., 1997) diluted in TBS containing 2% NGS or NDS and 0.2% TritonX-100. After several washes, the following secondary antibodies were applied: Cy3-conjugated donkey

anti-guinea pig (Cat#: 706-165-148, RRID: AB_2340460) or donkey anti-goat IgG (Cat#: 705-165-147, RRID: AB_2307351) and Cy5-conjugated donkey anti-rabbit IgG (Cat#711-175-152, RRID: AB_2340607; all from Jackson Immunoresearch Laboratories, PA, United States). Sections were either mounted in Vectashield or processed for multiplexed postembedding immunolabeling (see the section below). Image stacks were acquired with an Olympus FV1000 confocal microscope (Olympus Europa SE & Co., Hamburg, Germany) with 20x and 60x (oil immersion) objectives.

Multiplexed Postembedding Immunolabeling

For details of this method (see Holderith et al., 2020). Briefly, sections following a preembedding immunoreaction (see the section above) for mGluR1α (1:1,000 visualized with Cy3-coupled donkey anti-goat Ab) and Munc13-2 (1:250; visualized with Cy5-coupled donkey anti-rabbit Ab) were washed several times in 0.1 M PB, dehydrated (without treatment with OsO_4), and embedded into Durcupan. Preembedding immunolabeling of Munc13-2 was essential, because after epoxy embedding, our antibody did not recognize its epitope. 500 nm thick serial sections of the stratum oriens containing double immunolabeled IN dendrites were cut from the top 5 μm of the sections (to avoid heterogeneity from potential unequal penetration of the antibody into the tissue) and placed onto Superfrost Ultra plus slides. First, selected regions of interest (ROIs) were analyzed and imaged with Olympus FV1000 confocal microscope at high magnifications (60X objective; NA = 1.35). The resin was etched with Na-ethanolate (saturated solution of NaOH in absolute ethanol) for 5 min, then rinsed with 96% ethanol, and finally rinsed with distilled water. Retrieval of the proteins were carried out in 0.02 M Tris Base (pH = 9) containing 0.5% sodium dodecyl sulfate (SDS) at 80°C for 60 min. After several washes in TBS containing 0.05–0.1% Triton X-100 (TBST, pH = 7.6), the sections were blocked in TBST containing 6% Blotto A (Santa Cruz Biotechnology), 10% NGS, and 1% BSA (Sigma) for 30 min, then incubated in the guinea pig primary Ab against Munc13-1 (1:500, Synaptic Systems, Göttingen, Germany; Cat# 126104, RRID: AB_2619806) diluted in a blocking solution at room temperature, overnight. After several washes in TBST, the secondary Ab (Alexa 488 donkey anti-guinea pig, 1:200, Jackson ImmunoResearch Laboratories, PA, United States, Cat# 706-545-148, RRID: AB_2340472) was applied in TBST containing 10% of blocking solution for 2 h. After several washes in TBST, the slides were rinsed with distilled water, and the sections were mounted in SlowFade Diamond (Invitrogen, MA, United States). Images of ROIs were taken with an Olympus FV1000 confocal microscope and a 60x (oil immersion) objective or with an Abberior ExpertLine confocal microscope and a 100x (oil immersion) objective. Immunoglobulins were removed with a 5-min incubation in TBS containing 1% SDS (pH = 7.7) at 80°C. After 5 min of washing in TBST, new rounds of immunolabeling were performed using a guinea pig anti-PSD95 Ab (1:500, Synaptic Systems, Göttingen, Germany; Cat# 124014, RRID: AB_2619800), a guinea pig anti-panAMPA receptor Ab (1:100 Frontiers Cat#Af580; RRID: AB_257161), a chicken anti-Bassoon Ab (1:200 Synaptic Systems, Göttingen, Germany; Cat#141-016; RRID: AB_2661779), a guinea pig anti-Cav2.1 Ab (1:100 Synaptic Systems, Göttingen, Germany; Cat#152 205; RRID: AB_2619842), and finally with a guinea pig anti-Rim1/2 Ab (1:100 Synaptic Systems, Göttingen, Germany; Cat#140-205; RRID:AB_2631216) with the appropriate Alexa488-coupled secondary Abs (Alexa488-coupled donkey anti-guinea pig, 1:200; Jackson ImmunoResearch Laboratories, PA, United States; as above or Alexa488-coupled goat anti-chicken, 1:200; Jackson ImmunoResearch Laboratories, PA, United States, Cat# 103-545-155, RRID: AB_2337390).

Quantitative Image Analysis

Confocal images were imported in ImageJ where circular ROIs (for postembedding immunolabeling) were placed over synaptic fluorescent clusters and over the unlabeled neuropil to determine the specific and non-specific labeling, respectively. The integral of the fluorescence was measured, and the background was subtracted for each ROI. For postembedding multiplexed labeling, images of the serial 500 nm thick sections were aligned using a custom-made module of ImageJ ("HyperStackStitcher;" available on the web site).[3] To pool data from different experiments obtained with different confocal microscopes and laser settings, PSD95- normalized intensities of each immunosignal were further normalized to the population mean of the random synapses.

To quantify Munc13-2, Elfn, mGluR7, and mGluR1α immunolabeling intensity in Elfn KO and virally injected animals, freehand contour ROIs were used to outline mGluR1α+ dendrites in both the KO and the control or the injected and the contralateral hemispheres with same microscope settings and in the same depth of the tissue. The integral of the fluorescence was measured, and the background was subtracted for each ROI. About 40–150 ROIs were measured per animal.

Statistical Analyses

Data are presented as mean ± SD and median throughout this study. All data were tested for normality using Shapiro–Wilk test. Non-normally distributed datasets were compared with Mann–Whitney *U*-test. Correlations were determined with Spearman's rank correlation and the regression coefficient (r_s); related *p*-values were calculated from two-tailed Student's *t*-distribution. For multiple comparison, Kruskal–Wallis ANOVA was used with *post hoc* Dunn's test. Statistically significant difference was assumed at $p < 0.05$.

Materials

All the chemicals are obtained from Sigma, unless otherwise stated.

[3]http://nusserlab.hu/software.html

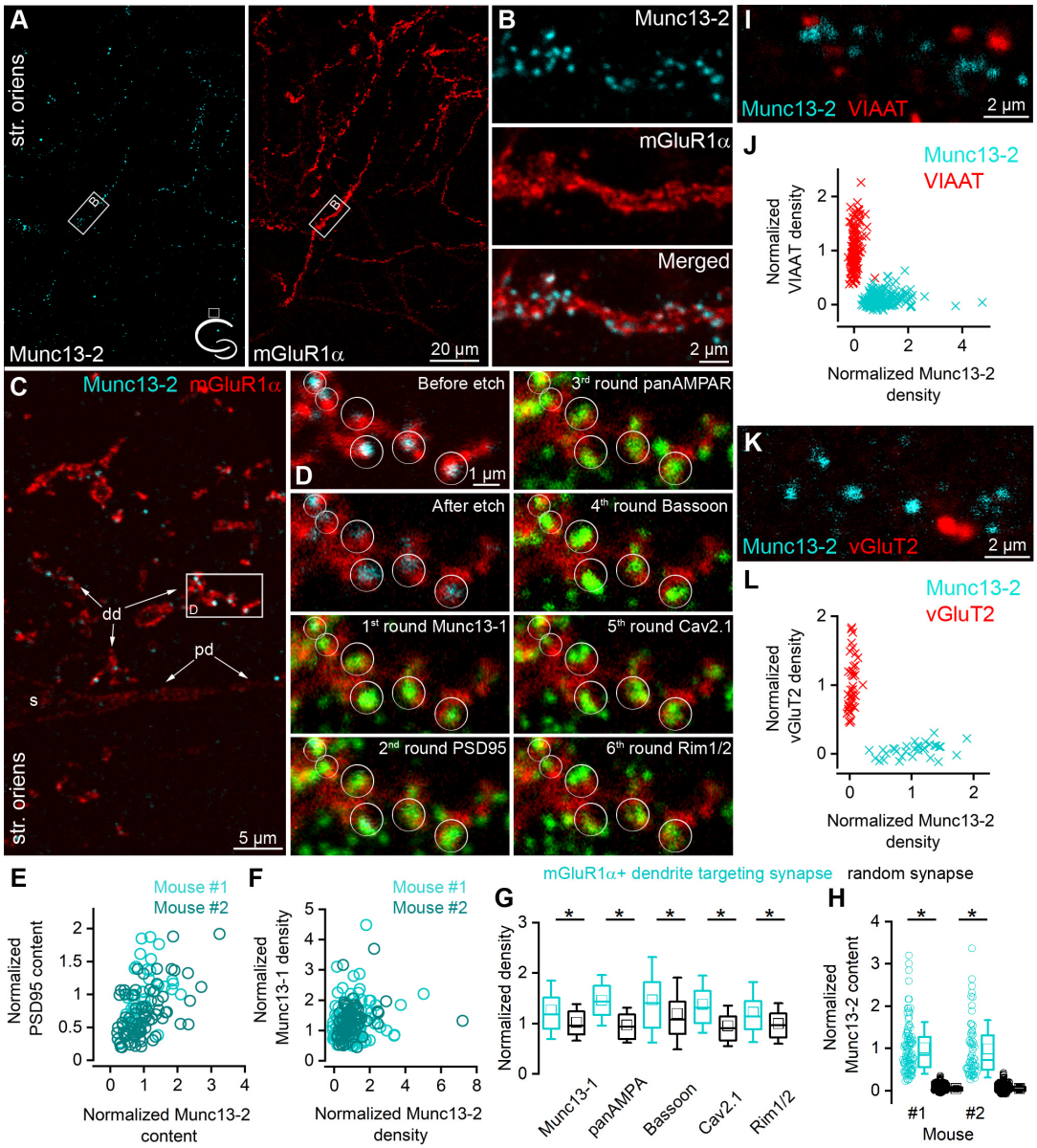

FIGURE 1 | Munc13-2 immunolabeling is enriched on mGluR1α immunopositive dendrites. **(A)** Double immunolabeling for Munc13-2 (left, cyan) and mGluR1α (right, red) in the dorsal hippocampal CA1 region of the mouse (cartoon indicates the location of the region) shows similar distribution in the stratum oriens. Maximum intensity projection of six confocal images separated by 1 μm. **(B)** A dendritic segment of an mGluR1α immunopositive IN (white boxes on **A**) is shown at a higher magnification, which is decorated by Munc13-2 immunopositive puncta. Maximum intensity projection of three confocal images separated by 1 μm. **(C)** 500 nm thick epoxy resin embedded section with preembedding immunolabeling for Munc13-2 (cyan) and mGluR1α (red) shows that Munc13-2 immunopositive puncta preferentially located on the small diameter of mGluR1α+ (distal) dendrites (dd), and mainly avoid the soma (s) and a proximal dendrite (pd) in the hippocampus of the mouse. Boxed area is enlarged on panel **(D)**. **(D)** Multiplexed postembedding immunolabeling carried out on the section shown in panel **(G)**. Munc13-2 immunopositive puncta marked by circles (representing ROIs for quantification) along the mGluR1α immunolabeled dendrite are immunopositive for Munc13-1, PSD95, AMPA receptors, Bassoon, Cav2.1,and Rim1/2 (all pseudo colored to green). Note that the intensity of Munc13-2 immunolabeling varies substantially. Alignment of sections after each round was based on mGluR1α immunolabeling (red). Numbers represent the labeling rounds during the multiplexed labeling. **(E)** All of the Munc13-2 immunopositive puncta contain PSD95 immunosignal. Their amount shows positive correlations (Spearman correlation $r = 0.48$ and 0.55, $n = 40$ in mouse #1 and $n = 80$ in mouse #2). **(F)** Correlations between the density of the Munc13-2 and Munc13-1 in individual AZs (each data point represents an AZ, $n = 114$ in mouse #1 and $n = 80$ in mouse #2; Spearman correlation $r = 0.16$ and 0.34). **(G)** mGluR1α IN targeting synapses have significantly larger (*) Munc13-1, AMPA receptors, Bassoon, Cav2.1 and Rim1/2 densities than those found in randomly selected glutamatergic synapses in the str. oriens ($p = 1.5 \times 10^{-5}$, 5.5×10^{-24}, 1.5×10^{-4}, 6.6×10^{-16}, 1.3×10^{-5}, respectively, MW-*U*-test). Box plots represent median and 25/75 percentiles, square represent the mean value, whiskers represent SD. All immunolabelings were normalized to PSD95 intensity on panels **(F,G)**. **(H)** The Munc13-2 content of randomly selected synapses is only $4 \pm 7\%$ and $4 \pm 10\%$ (in two mice; $p = 0$ for both MW-*U*-test) of that of synapses on mGluR1α+ dendrites. **(I–L)** Munc13-2 immunolabeling (cyan) does not colocalize either with vesicular inhibitory amino acid transporter (VIAAT, red) **(I,J**, $n = 152$ Munc13-2 and 222 VIAAT positive profiles in 2 mice) or with vesicular glutamate transporter-2 (vGluT2, red) **(K,L)**, $n = 43$ Munc13-2 and 33 vGluT2 positive profiles in 1 mouse). Single confocal images **(I,K)**. str. oriens, stratum oriens.

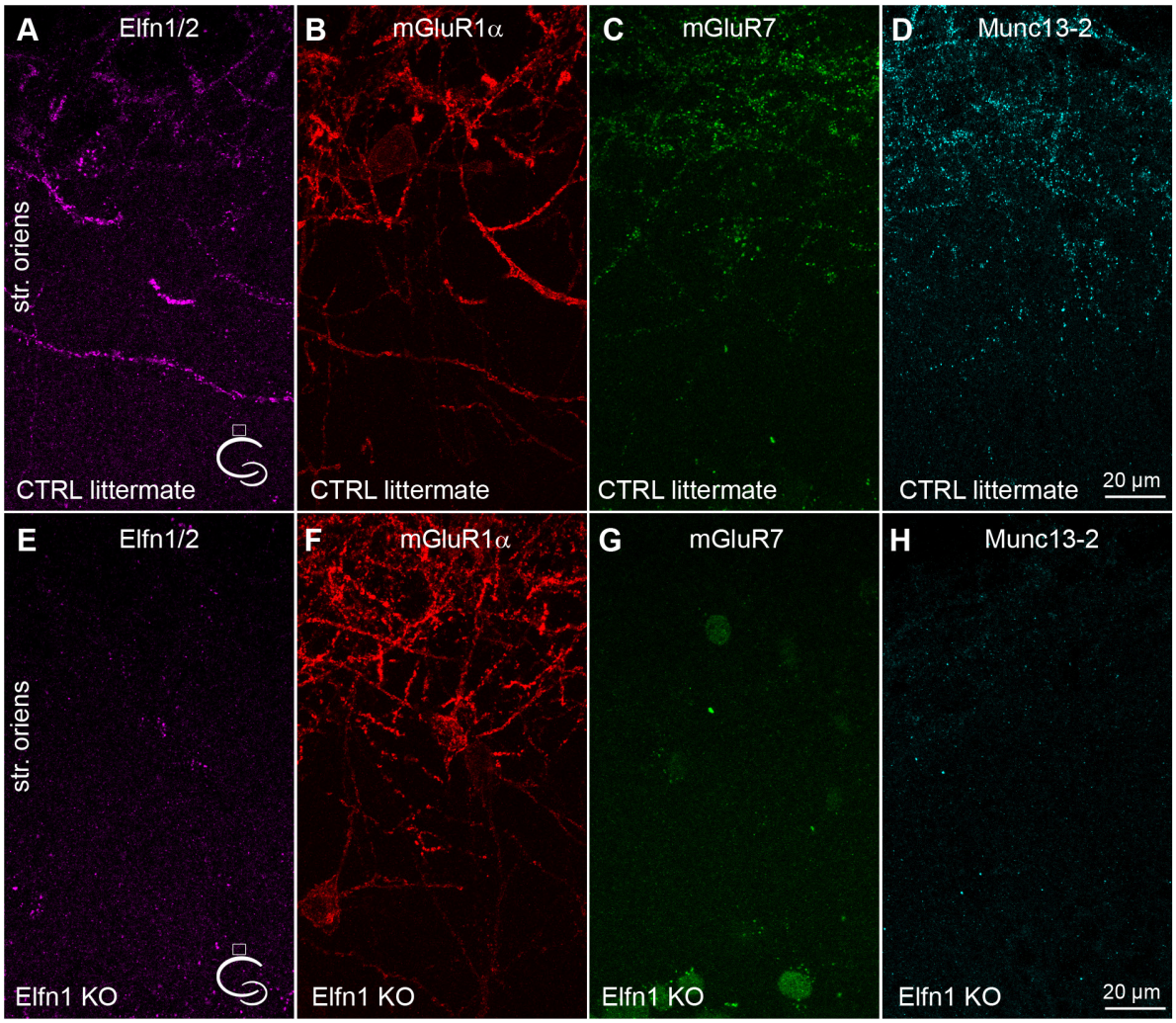

FIGURE 2 | Munc13-2 and mGluR7 are missing in Elfn1 knock-out mice. **(A–D)** Immunolabeling for Elfn1/2 **(A)**, mGluR1α **(B)**, mGluR7 **(C)** and Munc13-2 **(D)** in the dorsal CA1 region of a littermate control mouse shows intense labeling of IN dendrites in the str. oriens. **(E–H)** same as **(A–D)** in an Elfn1 KO mouse. No specific immunolabeling is detected for Elfn1/2 **(E)**, mGluR7 **(G)** and Munc13-2 **(H)**. Cartoons indicate the location of the region. Maximum intensity projection of 20 confocal images separated by 1 μm. str. oriens, stratum oriens.

RESULTS

Munc13-2 Is Selectively Present in Synapses-Innervating mGluR1α+ Dendrites

Immunostaining of bMunc13-2 (brain specific isoform of the Munc13-2, referred as Munc13-2 in the study) in the dorsal hippocampus of adult mice [**Figure 1**, n = 3 C57BL6/J, n = 3 Tg(Chrna2-Cre)OE25Gsat/Mmucd, Leao et al., 2012] crossed with the reporter line Ai9 [Gt(ROSA)26Sor_CAG/LSL_tdTomato] and rats (n = 2, **Supplementary Figure 1**) revealed punctate labeling of neuronal processes in the stratum oriens and in the alveus of the CA1 area. Double immunofluorescent labeling of Munc13-2 and mGluR1α demonstrated that most of the Munc13-2 immunopositive puncta decorate mGluR1α+ dendrites and the majority of the mGluR1α+ dendrites are decorated by Munc13-2 puncta (**Figures 1A,B**). Since mGluR7 is present in presynaptic glutamatergic AZs that innervate mGluR1α+ INs (Shigemoto et al., 1996) and has a rather similar labeling pattern to that of Munc13-2, we performed colocalization of these two proteins. The majority of the mGluR7b puncta along the small diameter dendrites were Munc13-2 immunopositive and vice versa, and most Munc13-2 puncta were labeled for mGluR7b in rat (**Supplementary Figures 1C,D**). This suggested that Munc13-2 is present in excitatory synapses.

To further test the molecular composition of these Munc13-2 immunopositive synapses in mice, we applied postembedding multiplexed immunolabeling of a number of synaptic proteins on ultrathin sections obtained from epoxy resin-embedded

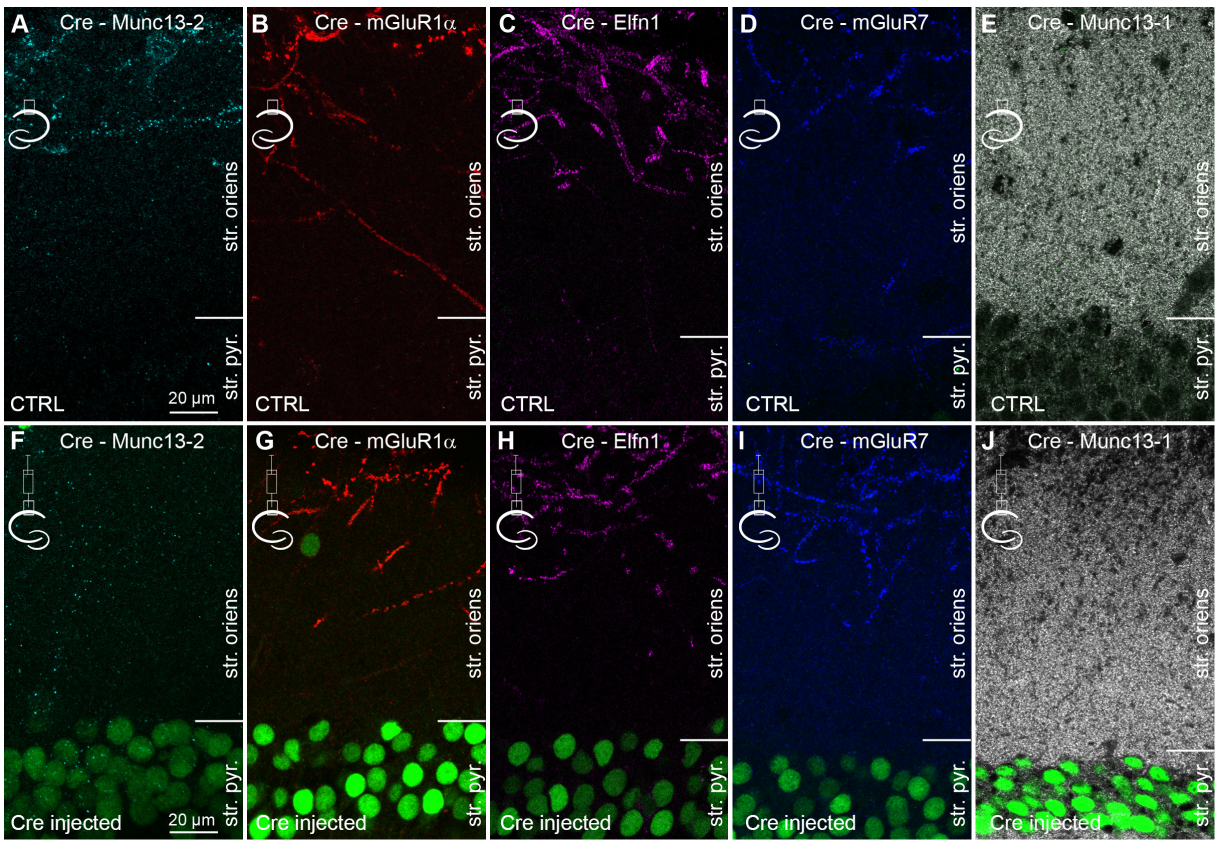

FIGURE 3 | Conditional knock-out of Munc13-2 does not change the expression and distribution of Elfn1 and mGluR7. **(A–E)** Double immunolabeling for Cre and either Munc13-2 **(A)** or mGluR1α **(B)**, or Elfn1 **(C)** or mGluR7 **(D)** or Munc13-1 **(E)** in the dorsal CA1 area of the non-injected hemisphere. **(F–J)** Same as in **(A–E)**, but the images are from the hemisphere that has been injected with AAV expressing Cre-recombinase. Immunolabeled Cre (green) is visible in most CA1 PC nuclei (green). Note the lack of immunolabeling for Munc13-2 in the outer part of the stratum oriens, demonstrating the efficient removal of the protein, while there is no detectable change in the immunolabeling for mGluR1α, Elfn1, mGluR7, and Munc13-1. Maximum intensity projection of 4 confocal images separated by 1 µm. str. pyr, stratum pyramidale; str. oriens, stratum oriens.

tissue (Holderith et al., 2020) that had been immunolabeled for Munc13-2 and mGluR1α. We discovered that dehydration and resin embedding without OsO_4 treatment retains the preembedding immunosignal when the reactions are visualized with Cy3- or Cy5-coupled secondary antibodies (**Figure 1C**). In 500 nm thick epoxy resin-embedded sections, Munc13-2 immunopositive puncta were clearly visible as they surrounded mGluR1α+ small diameter dendrites but spared the perisomatic and proximal dendritic membranes (**Figure 1C**). Following the removal of the resin with Na-ethanolate and antigen retrieval with an SDS solution, we immunolabeled the sections, first for Munc13-1, imaged the ROI, eluted the immunoglobulins, and relabeled the sections for PSD95, then for AMPA receptors, Bassoon, Cav2.1 voltage-gated Ca^{2+} channel (VGCC) subunit, and finally for Rim1/2 (**Figure 1D**). Qualitative assessment of the images revealed that the Munc13-2 positive puncta were immunopositive for all of these synaptic proteins, but to a different degree. We then quantified the fluorescent intensities for each protein in circular ROIs placed over the Munc13-2 positive puncta. We found that all Munc13-2 positive puncta contained PSD95 immunosignal (**Figure 1E**, n = 40 and 80 puncta in two mice) indicating that they are excitatory glutamatergic synapses. As the amount of PSD95 correlates almost perfectly with the size of the synapse (Cane et al., 2014; Karlocai et al., 2021), we normalized the immunosignal for each synaptic protein to that of PSD95 of the same synapse, resulting in density values that should be independent of the synapse size. To compare the data from different experiments, Munc13-2 density values were further normalized to the population mean of randomly selected synapses. Following this normalization, Munc13-2 density values displayed large variability (coefficient of variation: CV = 0.87 and 0.86 for mouse #1 and #2, respectively) among individual synapses and they did not correlate with normalized Munc13-1 density values (**Figure 1F**), suggesting that their amounts in the AZ are independently regulated. Interestingly, the PSD95 normalized densities of Munc13-1, AMPA receptors, Bassoon, Cav2.1, and Rim1/2 were significantly higher in synapses on mGluR1α+ dendrites compared to the randomly selected surrounding synapses (Munc13-1: 1.27 ± 0.58; AMPAR: 1.46 ± 0.50; Bassoon: 1.47 ± 0.85; Cav2.1: 1.38 ± 0.57; Rim1/2: 1.22 ± 0.6, n = 194 mGluR1α targeting and n = 160 random synapses from 2 mice; **Figure 1G**). To assess the

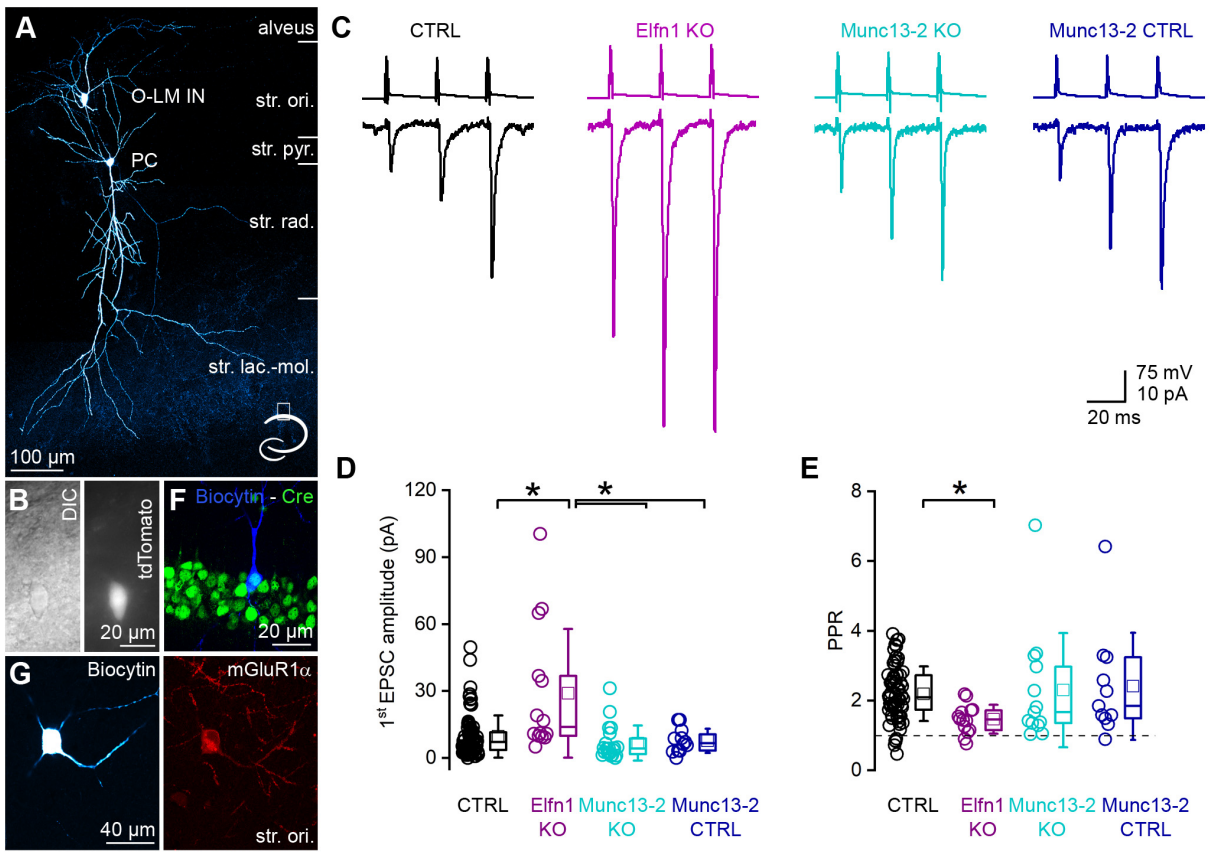

FIGURE 4 | Removal of Munc13-2 does not change the peak amplitude and short-term plasticity of unitary EPSCs between CA1 PCs and mGluR1α expressing INs. **(A)** *In vitro* whole-cell patch-clamp recorded and biocytin filled CA1 PC and O-LM IN. The axonal arbor of the IN is visible in the stratum lacunosum-moleculare. Cartoon depicts the location of the cells within the hippocampus. **(B)** DIC image of the O-LM IN shown in panel **(A)** (left) and fluorescent tdTomato signal of the same cell (right). **(C)** Unitary EPSCs (lower traces) evoked by a train of 3 APs @ 40 Hz in a presynaptic CA1 PC (upper traces) recorded in postsynaptic O-LM INs in the dorsal CA1 region of the hippocampus. Black traces are from a control, magenta traces from an Elfn1 knock-out, cyan traces from a Munc13-2 conditional knock-out, dark blue traces from a Munc13-2 conditional knock-out littermate control. **(D)** The first EPSC is significantly larger (*) in the Elfn1 knock-out mouse than in any of the controls or in the Munc13-2 conditional knock-out mice ($p = 5.44 \times 10^{-4}$, Kruskal-Wallis ANOVA, *post hoc* Dunn's test: $p = 0.003$, 0.00024, 0.041, ctrl vs. Elfn KO, Elfn KO vs. Munc13-2 KO, Elfn KO vs. Munc13-2 ctrl, respectively) while there is no change in the peak amplitude in the Munc13-2 conditional knock-out mouse compared to any of the controls (Kruskal–Wallis ANOVA, *post hoc* Dunn's test $p = 0.49$ and 1, ctrl vs. Munc13-2 KO, control vs. Munc13-2 control). **(E)** The short-term facilitation is significantly less pronounced in the Elfn1 knock-out mouse ($p = 0.0065$, Kruskal-Wallis ANOVA, *post hoc* Dunn's test: $p = 0.0034$, ctrl vs. Elfn knock-out) while there is no change in the short-term plasticity in the Munc13-2 conditional knock-out mouse compared to any of the controls (Kruskal-Wallis ANOVA, *post hoc* Dunn's test, $p = 1$, ctrl vs. Munc13-2 KO, Munc13-2 KO vs. Munc13-2 control). **(F)** *In vitro* recorded and biocytin filled PC (blue) expressing Cre-recombinase (green) that is localized to the PC nucleus. Single confocal image. **(G)** A biocytin filled IN with truncated axon (left) expresses mGluR1α (right red). Maximum intensity projection of four confocal images separated by 1 µm. Box plots represent median and 25/75 percentiles, square represent the mean value, whiskers represent SD. str. ori., stratum oriens, str. pyr., stratum pyramidale, str. rad., stratum radiatum, str. lac.-mol., stratum lacunosum-moleculare.

selectivity of the Munc13-2 expression in mGluR1α+ dendrites targeting synapses, we measured their Munc13-2 content and compared them with that of randomly selected synapses in the surrounding neuropil in 2 mice ($n = 101$ and $n = 60$ mGluR1α+ dendrite targeting synapses, and $n = 1{,}000$ and $n = 500$ random synapses). Our quantification revealed that only 4 ± 6% and 4 ± 10% of the immunoreactivity found in mGluR1α+ dendrite targeting synapses are present in the surrounding randomly sampled synapses (**Figure 1H**).

Munc13-2 did not colocalize with vesicular inhibitory amino acid transporter (VIAAT; **Figures 1I,J**, $n = 152$ Munc13-2, and $n = 222$ VIAAT positive puncta in 2 mice, and **Supplementary Figure 1F** in 1 rat) or with vesicular glutamate transporter-2 (vGluT2; **Figures 1K,L**, $n = 43$ Munc13-2 and $n = 33$ vGluT2 positive puncta in 1 mouse, **Supplementary Figure 1G** in 1 rat). This indicates that most of the Munc13-2 labeled puncta are present on the axon terminals of local (CA1 and/or CA3) PCs.

Lack of Munc13-2 Puncta in the Stratum Oriens of Elfn1 Knock-Out Mice

Elfn1 has been shown to be selectively expressed in Som/mGluR1α+ hippocampal INs (Sylwestrak and Ghosh, 2012), where it recruits mGluR7 to the presynaptic AZ (Tomioka et al., 2014; Stachniak et al., 2019). The selective knock-down of Elfn1 from these INs results in a decreased short-term

facilitation. Next, we tested the potential role of Elfn1 in the above-described selective recruitment of Munc13-2. In five Elfn1 knock-out (KO) mice, immunolabeling of Elfn1/2 were clearly absent in the stratum oriens/alveus (**Figures 2A,E**). Quantitative measurement of Elfn1 immunolabeling showed a 97.7 ± 0.53% decrease in KO mice (n = 5) compared to the control littermates (n = 4) demonstrating that our antibody against Elfn1/2 provides specific labeling here for Elfn1 and also that the protein is missing in the KO mice. In line with previous results, we also found that immunolabeling of mGluR7 is dramatically reduced compared to the littermate heterozygous controls (**Figures 2C,G**) without any apparent change in the postsynaptic mGluR1α expression (**Figures 2B,F**, 107 ± 16% of control littermates, n = 5 KO mice, n = 4 control mice). Finally, we found that immunolabeling of Munc13-2 is apparently absent in the KO mice (3.7 ± 1.7% of control littermates; n = 5 KO mice and n = 4 control mice) compared to the littermate controls where punctate Munc13-2 immunolabeling is clearly visible along the mGluR1α+ dendrites (**Figures 2D,H**). The lack of both mGluR7 and Munc13-2 in Elfn1 KO mice raises the question whether the increased P_v at the PC-Som+ IN synapses found following Elfn1 knock-down is attributable to the lack of either mGluR7, or that of Munc13-2, or both.

Conditional Knock-Out of Munc13-2 From CA1 Pyramidal Cells Does Not Affect mGluR7 Expression

To investigate the contribution of Munc13-2 to the properties of CA1 PC to mGluR1α+ IN synapses, Munc13-2 was conditionally knocked out from CA1 PCs in sixteen C57BL/6N-*Unc13b*$^{TM1a(KOMP)Wtsi}$/MbpMmucd mice with Cre-recombinase expressing AAVs injected unilaterally into the dorsal hippocampus (**Figure 3**). After 14 days, the mice were transcardially perfused and Cre expression was visualized with an anti-Cre antibody (**Figure 3** and **Supplementary Figure 2**). In the non-injected hemisphere, no detectable anti-Cre immunoreactivity was observed in the nuclei of CA1 PCs and the immunolabeling patterns of Munc13-2, mGluR1α, Elfn1, mGluR7, and Munc13-1 (**Figures 3A–E**) were indistinguishable from those seen in the control mice and rats (**Figure 1** and **Supplementary Figure 1**). In the central part of the injected area, the nuclei of apparently every PC were intensely labeled for Cre-recombinase and the mGluR1α+ dendrite associated specific immunosignal for Munc13-2 decreased by 92 ± 10% in the stratum oriens/alveus (n = 3 mice, **Supplementary Figure 2G** and **Figure 3F**). At the edges of the injection zone, the frequency of Cre-immunopositive nuclei decreased and Munc13-2 labeled structures emerged (**Supplementary Figures 2A–C**). In contrast, despite the expression of Cre and the lack of Munc13-2, the labeling patterns and the intensity of labeling for mGluR1α, Elfn1, mGluR7, and Munc13-1 were unchanged (**Figures 3G–J** and **Supplementary Figure 2G**, 101 ± 18%, 104 ± 5%, 104 ± 4%, 99 ± 1% of controls, respectively. n = 3 mice for mGluR1α, Elfn1, mGluR7, n = 2 mice for Munc13-1). In our injections, neither CA3 nor subicular PCs were transfected with Cre-expressing AAVs. Our results demonstrate that the majority of Munc13-2 immunosignal in the stratum oriens of the dorsal CA1 area originates from the axons of CA1 PCs and 2 weeks is sufficient for the significant removal of the protein from these synapses.

Conditional Removal of Munc13-2 From CA1 Pyramidal Cells Leaves Unitary Excitatory Postsynaptic Currents in mGluR1α+ INs Unchanged

Postsynaptic responses between CA1 PCs and mGluR1α+ INs have small amplitudes and display marked short-term facilitation. We recorded from a large population of connected CA1 PC to mGluR1α+ IN pairs in a transgenic mouse line that expresses the red fluorescent protein, tdTomato in O-LM INs in the stratum oriens of the CA1 region (**Figures 4A,B**). This allowed us to efficiently select mGluR1α+ /O-LM INs (50 out of 52 *post hoc* identified INs had O-LM morphology, and only 2 were bistratified cells, **Figure 4A**). We recorded unitary excitatory postsynaptic currents (uEPSCs) evoked by a short train of presynaptic action potentials (APs) at 40 Hz (**Figure 4C**, black). The first uEPSC had a small amplitude (9.6 ± 9.4 pA, median = 7.2 pA, n = 80 pairs in 44 mice; **Figure 4D**, black) and the paired pulse ratio (PPR, 2nd uEPSC/1st uEPSC) was 2.19 ± 0.78 (median = 2.09, n = 66 in 38 animals, in 14 cell pairs, the 1st uEPSC peak amplitude was 0 pA, precluding the calculation of the PPR, **Figure 4E**, black). The amplitude of the 3rd uEPSC increased further resulting in a third uEPSC/first uEPSC ratio of 2.99 ± 1.25 (median = 2.74, n = 66 in 38 mice). In Elfn1 KO mice, the amplitude of the first uEPSC was significantly larger (29.0 ± 28.9 pA, median = 13.9 pA, n = 14 pairs in 10 mice; **Figures 4C,D** magenta) than that in the control mice. In these KO animals, presumed mGluR1α+ /O-LM INs were preselected based on the location, size, shape of their somata, and on their firing patterns upon DC current injections. Following the recordings, we characterized the cells *post hoc* and found that 10 out of 14 cells had O-LM morphology and the remaining 4 cells had truncated axon, but they were immunopositive for mGluR1α. The 3-times increase in the first uEPSC is accompanied by a significant decrease of the PPR (1.46 ± 0.41, n = 14 pairs in 10 mice; **Figure 4E**). As discussed above, the altered uEPSCs in Elfn1 KO mice could be the consequence of the loss of mGluR7 and/or Munc13-2. To address the contribution of Munc13-2, we performed paired recordings between CA1 PCs and presumed mGluR1α+ /O-LM INs in slices from conditional Munc13-2 KO mice in which the dorsal CA1 region was injected with Cre- and mCherry-expressing AAVs. In these animals, PCs were selected based on the expression of mCherry, and the presence of Cre-recombinase in the recorded PCs was verified *post hoc* by immunolabeling for Cre. Only those pairs were included where the Cre immunopositivity was unequivocally identified in the presynaptic PC (**Figure 4F**). Similar to the Elfn1 KO mice, in this transgenic line, mGluR1α+ /O-LM INs were selected in the slice based on the same criteria as described above and were molecularly and morphologically characterized *post hoc* (10 out of 20 cells were O-LM cells, 10 out of 20 cells have truncated axons, but they were immunopositive for mGluR1α; **Figure 4G**). The first uEPSC of the short train had a

small amplitude (6.7 ± 7.9 pA, median = 4.3 pA, n = 20 pairs in 13 animals) which was not significantly different from that recorded in the control mice (**Figure 4D**). The amplitudes of the second (14.0 ± 13.7 pA, median = 7.1 pA) and the third uEPSCs (18.7 ± 19.9 pA, median = 7.6 pA) were also similar to those in the control, resulting in a PPR of 2.30 ± 1.64 (median = 1.66, n = 13 pairs in 10 mice, for 7 cell pairs the amplitude of the 1st uEPSC peak was 0 pA, precluding the calculation of the PPR; **Figure 2E**), which was not significantly different from that in the control. Since the Munc13-2 KO mice had a different genetic background (C57BL/6N) compared to the control mice (C57BL/6J), we recorded from the contralateral, non-injected hemisphere of Munc13-2 conditional KO mice as an independent control population and found that the amplitude (first: 7.7 ± 5.5 pA, median = 6.7 pA; second: 17.0 ± 11.8 pA, median = 17.3 pA; third: 27.1 ± 18.6 pA, median = 27.1 pA, n = 12 pairs in 6 mice, **Figures 4C,D**) and PPR (2.4 ± 1.5; **Figure 4E**) of uEPSCs were not significantly different from those recorded from the control or the Munc13-2 KO mice.

DISCUSSION

In the present manuscript, we describe that: (1) bMunc13-2 is selectively enriched in AZs of CA1 PC axon terminals that target mGluR1α+ INs (mainly O-LM INs). (2) Munc13-1 is also present in Munc13-2 containing CA1 PC AZs, together with Rim1/2, Cav2.1, and Bassoon. (3) Elfn1 is expressed by the postsynaptic mGluR1α+ INs and trans-synaptically recruits not only mGluR7, but also Munc13-2 into AZs. (4) Conditional genetic deletion of Munc13-2 does not change the distribution of either Elfn1 or its presynaptic signaling partner, mGluR7. (5) CA1 PC to mGluR1α+ /O-LM IN synapses lacking Munc13-2 display very similar functional properties compared to Munc13-2 containing control synapses.

Postsynaptic responses made by hippocampal PCs onto mGluR1α+ /O-LM INs display marked short-term facilitation upon repetitive stimulation (Ali and Thomson, 1998; Biro et al., 2005). Despite several studies aiming to reveal the mechanisms of how facilitation is manifested at this synapse, the key molecular mechanism remains still elusive. A selective enrichment of mGluR7 in these presynaptic AZs had been described over two decades ago (Shigemoto et al., 1996) and the contribution of constitutively active group III mGluRs (including mGluR7) to the small EPSC amplitude has been reported (Losonczy et al., 2003). However, neither pharmacological block nor genetic manipulations that remove mGluR7 increased the EPSC amplitude markedly enough at this synapse, leaving the characteristic short-term facilitation intact (Sylwestrak and Ghosh, 2012; Tomioka et al., 2014; Stachniak et al., 2019). A previous study from our laboratory (Eltes et al., 2017) and the study by Koester and Johnston (2005) described smaller [Ca^{2+}] transients in the PC terminals synapsing on Som/mGluR1α+ dendrites compared to those that synapse PV+ INs. However, this difference in [Ca^{2+}] is unlikely to be responsible for the low P_v at this synapse, because the application of 4-aminopyridin elevated the presynaptic [Ca^{2+}] in boutons innervating mGluR1α+ INs to reach that found in boutons innervating PV expressing INs, but the EPSCs, though increased, still remained small and facilitating at PC to mGluR1α+ IN synapses (Holderith et al., unpublished observation). A longer coupling distance between SVs and presynaptic VGCCs was also suggested as a potential mechanism of the low P_v at cortical PC to Som+ IN synapses (Rozov et al., 2001), but freeze-fracture replica immunolabeling experiments could not confirm different nano-topologies at the hippocampal PC to mGluR1α+ vs. PC to PV+ IN synapses (Lorincz et al., unpublished observation), suggesting that a different coupling distance as a key mechanism is also unlikely.

Since none of the above-mentioned mechanisms seems to be key in setting the P_v exceptionally low at PC to Som/mGluR1α+ IN synapses, we tested the subcellular distribution of presynaptic proteins with critical roles in SV docking/priming and tried to find whether any of them has a postsynaptic cell type-dependent distribution in PC axons. Munc13-2 showed a punctate labeling in the stratum oriens of the dorsal hippocampal CA1 area, and our colocalization experiments revealed that it is selectively enriched in the AZs of local CA1 PC boutons that innervate mGluR1α+ INs. To our knowledge, this is the third example (mGluR7: Shigemoto et al., 1996 and mGluR8: Ferraguti et al., 2005) of such postsynaptic target cell type-specific distribution of presynaptic molecules in cortical networks, suggesting that this phenomenon might be more common than previously envisaged. Munc13s are essential synaptic vesicle priming factors and are indispensable for synaptic vesicle fusion (Augustin et al., 1999b; Varoqueaux et al., 2002; Sudhof and Rizo, 2011). They form a tripartite complex with RIMs and RIM-binding proteins that collaborate to recruit VGCCs and SVs to the AZ (Wang et al., 1997; Betz et al., 2001; Schoch et al., 2002; Andrews-Zwilling et al., 2006; Kaeser et al., 2011; Brockmann et al., 2019, 2020). Out of the three isoforms expressed in the CNS (Munc13-1 to Munc13-3), Munc13-1 has the broadest distribution, while Munc13-2 and 3 have more restricted and largely non-overlapping expression patterns (Augustin et al., 1999a). Several studies investigated the functional roles of Munc13s in the heterologous expression systems or neuronal cultures (Rhee et al., 2002; Rosenmund et al., 2002; Varoqueaux et al., 2002; Van De Bospoort et al., 2012). For example, Rosenmund et al. (2002) demonstrated that in cultured hippocampal neurons, Munc13-1 is likely to contribute to the tight docking of vesicles and confer high P_v, whereas in Munc13-2 containing AZs, SVs are loosely docked and have low P_v. Based on these results and the preferential location of Munc13-2 in AZs innervating mGluR1α+ INs, we hypothesized that this Munc isoform will have a key role in setting the P_v low in this synapse. However, to our surprise, the conditional removal of Munc13-2 from CA1 PCs (in an intact neuronal network) had no apparent effect on the P_v of the CA1 PC to mGluR1α+ IN synapses. Similar results were found at mouse photoreceptor ribbon synapses, where Munc13-2 is the only Munc13 isoform present (Cooper et al., 2012), although this synapse differs from the conventional synapses in many ways. A similar lack of effect was found however at Schaffer collateral input onto CA1 PCs (Breustedt et al., 2010) and in

the calyx of Held (Chen et al., 2013) in Munc13-2 KO animals. Although, it should be noted that the amount of bMunc13-2 is low in Schaffer collateral to CA1 PC synapses in control animals, therefore the lack of effect in the KO is not that surprising. Furthermore, in the same Munc13-2 KO animals, an apparent reduction of P_v was found at the hippocampal mossy fiber synapses onto CA3 PCs (Breustedt et al., 2010). Munc13-2 knock down with shRNA from glutamatergic input onto amygdala PCs increases P_v (Gioia et al., 2016), indicating a complex role of Munc13-2 in SV priming, probably depending on its interactive partners in the protein complex of the AZ. Here we show that CA1 PC to mGluR1α+ IN synapses also contain Munc13-1, which requires Rim1/2 and Rim binding protein for the efficient priming activity (Deng et al., 2011; Brockmann et al., 2020). Thus, the lack of Rim1/2 at this synapse could provide an explanation for the low P_v. We directly tested this hypothesis using multiplexed immunolabeling of Munc13-2 positive synapses on mGluR1α+ INs and found that Rim1/2 has an even higher density in this synapse compared to that found in the surrounding synapses that are likely to be on PC spines. Thus, we conclude that Munc13-1 must have additional interactive partners or regulatory pathways that adjust its efficacy in priming SVs in a target cell type-dependent manner.

Although, knocking down the expression of Elfn1 with shRNA did not turn EPSCs on Som+ INs depressing there was a reduction in the paired pulse facilitation, indicating some change in the P_v of the synapse (Sylwestrak and Ghosh, 2012), which was later attributed to the lack of presynaptic mGluR7 (Tomioka et al., 2014; Stachniak et al., 2019). Here, we tested how the expression of the specifically located Munc13-2 in the AZs innervating mGluR1α+ INs is altered in the Elfn1 KO mice. Our results revealed that Munc13-2 is enriched in CA1 PC to mGluR1α+ IN synapses in an Elfn1-dependent manner. Removal of Elfn1 results in the loss of mGluR7 and Munc13-2 and a threefold increase in the peak amplitude of PC to mGluR1α+ /O-LM IN uEPSCs and a decreased short-term facilitation. To distinguish whether the functional effect is due to the lack of constitutive mGluR7 activity or lack of Munc13-2, we conditionally removed Munc13-2 (both bMunc13-2 and ubMunc13-2 isoforms) from these synapses by injecting Cre-recombinase expressing AAVs into the dorsal hippocampal CA1 area of the transgenic mouse line in which the Munc13-2 exons, 15–17 are placed between two loxP sites. As no effect of Munc13-2 removal was found on uEPSC amplitudes and PPRs, we conclude that the functional effects of removing Elfn1 from Som/mGluR1α+ INs are the sole consequence of the lack of mGluR7. This is in line with the results of pharmacological block of group III mGluRs that has a very similar effect in EPSC amplitudes (Losonczy et al., 2003).

In summary, although the hippocampal CA1 PC to mGluR1α+ /O-LM IN synapses contain Munc13-2 at high concentration, it does not play a role in setting the P_v unusually low, indicating that Munc13-1 is capable of "ill-priming" SVs or there are additional molecules that prevent tightly docked vesicles from being released, the identity of which is to be discovered.

DATA AVAILABILITY STATEMENT

The raw data supporting the conclusions of this article will be made available by the authors, without undue reservation.

ETHICS STATEMENT

The animal study was reviewed and approved by the Animal Committee of the Institute of Experimental Medicine, Budapest.

AUTHOR CONTRIBUTIONS

NH and ZN designed the experiments and wrote the manuscript. MA performed the *in vitro* paired recording and analyzed the data. NH performed some paired recordings and all immunolocalization experiments and analyzed the data. All authors contributed to the article and approved the submitted version.

FUNDING

ZN was the recipient of the European Research Council Advanced Grant (ERC-AG 787157) and the Hungarian National Brain Research Program (NAP2.0) grant. The financial support from these funding bodies was gratefully acknowledged.

ACKNOWLEDGMENTS

We thank Dóra Ronaszéki for her excellent technical assistance, Bence Kókay and Eszter Sipos (Central Viral Unit, Institute of Experimental Medicine) for the injection of AAV construct.

SUPPLEMENTARY MATERIAL

The Supplementary Material for this article can be found online at: https://www.frontiersin.org/articles/10.3389/fnsyn.2021.773209/full#supplementary-material

REFERENCES

Ali, A. B., and Thomson, A. M. (1997). Brief train depression and facilitation at pyramidal-interneurone connections in slices of rat hippocampus; paired recordings with biocytin filling. *J. Physiol.* 9:501.

Ali, A. B., and Thomson, A. M. (1998). Facilitating pyramid to horizontal oriens-alveus interneurone inputs: dual intracellular recordings in slices of rat hippocampus. *J. Physiol.* 507, 185–199. doi: 10.1111/j.1469-7793.1998.185bu.x

Andrews-Zwilling, Y. S., Kawabe, H., Reim, K., Varoqueaux, F., and Brose, N. (2006). Binding to Rab3A-interacting molecule RIM regulates the presynaptic recruitment of Munc13-1 and ubMunc13-2. *J. Biol. Chem.* 281, 19720–19731.doi: 10.1074/jbc.M601421200

Augustin, I., Betz, A., Herrmann, C., Jo, T., and Brose, N. (1999a). Differential expression of two novel Munc13 proteins in rat brain. *Biochem. J.* 337, 363–371.

Augustin, I., Rosenmund, C., Sudhof, T. C., and Brose, N. (1999b). Munc13-1 is essential for fusion competence of glutamatergic synaptic vesicles. *Nature* 400, 457–461. doi: 10.1038/22768

Basu, J., Shen, N., Dulubova, I., Lu, J., Guan, R., Guryev, O., et al. (2005). A minimal domain responsible for Munc13 activity. *Nat. Struct. Mol. Biol.* 12, 1017–1018. doi: 10.1038/nsmb1001

Betz, A., Thakur, P., Junge, H. J., Ashery, U., Rhee, J. S., Scheuss, V., et al. (2001). Functional interaction of the active zone proteins Munc13-1 and RIM1 in synaptic vesicle priming. *Neuron* 30, 183–196. doi: 10.1016/s0896-6273(01)00272-0

Biro, A. A., Holderith, N. B., and Nusser, Z. (2005). Quantal size is independent of the release probability at hippocampal excitatory synapses. *J. Neurosci.* 25, 223–232. doi: 10.1523/JNEUROSCI.3688-04.2005

Breustedt, J., Gundlfinger, A., Varoqueaux, F., Reim, K., Brose, N., and Schmitz, D. (2010). Munc13-2 differentially affects hippocampal synaptic transmission and plasticity. *Cereb. Cortex* 20, 1109–1120. doi: 10.1093/cercor/bhp170

Brockmann, M. M., Maglione, M., Willmes, C. G., Stumpf, A., Bouazza, B. A., Velasquez, L. M., et al. (2019). RIM-BP2 primes synaptic vesicles via recruitment of Munc13-1 at hippocampal mossy fiber synapses. *Elife* 8:e43243. doi: 10.7554/eLife.43243

Brockmann, M. M., Zarebidaki, F., Camacho, M., Grauel, M. K., Trimbuch, T., Sudhof, T. C., et al. (2020). A Trio of Active Zone Proteins Comprised of RIM-BPs. *Cell Rep.* 32:107960. doi: 10.1016/j.celrep.2020.107960

Brose, N., Hofmann, K., Hata, Y., and Sudhof, T. C. (1995). Mammalian homologues of Caenorhabditis elegans unc-13 gene define novel family of C2-domain proteins. *J. Biol. Chem.* 270, 25273–25280. doi: 10.1074/jbc.270.42.25273

Cane, M., Maco, B., Knott, G., and Holtmaat, A. (2014). The relationship between PSD-95 clustering and spine stability *in vivo*. *J. Neurosci.* 34, 2075–2086. doi: 10.1523/JNEUROSCI.3353-13.2014

Chen, Z., Cooper, B., Kalla, S., Varoqueaux, F., and Young, S. M. Jr. (2013). The Munc13 proteins differentially regulate readily releasable pool dynamics and calcium-dependent recovery at a central synapse. *J. Neurosci.* 33, 8336–8351. doi: 10.1523/JNEUROSCI.5128-12.2013

Cooper, B., Hemmerlein, M., Ammermuller, J., Imig, C., Reim, K., Lipstein, N., et al. (2012). Munc13-independent vesicle priming at mouse photoreceptor ribbon synapses. *J. Neurosci.* 32, 8040–8052. doi: 10.1523/JNEUROSCI.4240-11.2012

Deng, L., Kaeser, P. S., Xu, W., and Sudhof, T. C. (2011). RIM proteins activate vesicle priming by reversing autoinhibitory homodimerization of Munc13. *Neuron* 69, 317–331. doi: 10.1016/j.neuron.2011.01.005

Eltes, T., Kirizs, T., Nusser, Z., and Holderith, N. (2017). Target Cell Type-Dependent Differences in Ca2 + Channel Function Underlie Distinct Release Probabilities at Hippocampal Glutamatergic Terminals. *J. Neurosci.* 37, 1910–1924. doi: 10.1523/JNEUROSCI.2024-16.2017

Fenno, L. E., Mattis, J., Ramakrishnan, C., Hyun, M., Lee, S. Y., He, M., et al. (2014). Targeting cells with single vectors using multiple-feature Boolean logic. *Nat. Methods* 11, 763–772. doi: 10.1038/nmeth.2996

Ferraguti, F., Klausberger, T., Cobden, P., Baude, A., Roberts, J. D., Szucs, P., et al. (2005). Metabotropic glutamate receptor 8-expressing nerve terminals target subsets of GABAergic neurons in the hippocampus. *J. Neurosci.* 25, 10520–10536. doi: 10.1523/JNEUROSCI.2547-05.2005

Gioia, D. A., Alexander, N. J., and Mccool, B. A. (2016). Differential Expression of Munc13-2 Produces Unique Synaptic Phenotypes in the Basolateral Amygdala of C57BL/6J and DBA/2J Mice. *J. Neurosci.* 36, 10964–10977. doi: 10.1523/JNEUROSCI.1785-16.2016

Holderith, N., Heredi, J., Kis, V., and Nusser, Z. (2020). A High-Resolution Method for Quantitative Molecular Analysis of Functionally Characterized Individual Synapses. *Cell Rep.* 32:107968. doi: 10.1016/j.celrep.2020.107968

Kaeser, P. S., Deng, L., Wang, Y., Dulubova, I., Liu, X., Rizo, J., et al. (2011). RIM proteins tether Ca2 + channels to presynaptic active zones via a direct PDZ-domain interaction. *Cell* 144, 282–295. doi: 10.1016/j.cell.2010.12.029

Karlocai, M. R., Heredi, J., Benedek, T., Holderith, N., Lorincz, A., and Nusser, Z. (2021). Variability in the Munc13-1 content of excitatory release sites. *Elife* 10:e67468. doi: 10.7554/eLife.67468

Kawabe, H., Mitkovski, M., Kaeser, P. S., Hirrlinger, J., Opazo, F., Nestvogel, D., et al. (2017). ELKS1 localizes the synaptic vesicle priming protein bMunc13-2 to a specific subset of active zones. *J. Cell Biol.* 216, 1143–1161. doi: 10.1083/jcb.201606086

Koester, H. J., and Johnston, D. (2005). Target cell-dependent normalization of transmitter release at neocortical synapses. *Science* 308, 863–866. doi: 10.1126/science.1100815

Leao, R. N., Mikulovic, S., Leao, K. E., Munguba, H., Gezelius, H., Enjin, A., et al. (2012). OLM interneurons differentially modulate CA3 and entorhinal inputs to hippocampal CA1 neurons. *Nat. Neurosci.* 15, 1524–1530. doi: 10.1038/nn.3235

Li, W., Ma, C., Guan, R., Xu, Y., Tomchick, D. R., and Rizo, J. (2011). The crystal structure of a Munc13 C-terminal module exhibits a remarkable similarity to vesicle tethering factors. *Structure* 19, 1443–1455. doi: 10.1016/j.str.2011.07.012

Losonczy, A., Somogyi, P., and Nusser, Z. (2003). Reduction of excitatory postsynaptic responses by persistently active metabotropic glutamate receptors in the hippocampus. *J. Neurophysiol.* 89, 1910–1919. doi: 10.1152/jn.00842.2002

Man, K. N., Imig, C., Walter, A. M., Pinheiro, P. S., Stevens, D. R., Rettig, J., et al. (2015). Identification of a Munc13-sensitive step in chromaffin cell large dense-core vesicle exocytosis. *Elife* 4:e10635. doi: 10.7554/eLife.10635

Neher, E., and Brose, N. (2018). Dynamically Primed Synaptic Vesicle States: key to Understand Synaptic Short-Term Plasticity. *Neuron* 100, 1283–1291. doi: 10.1016/j.neuron.2018.11.024

Pouille, F., and Scanziani, M. (2004). Routing of spike series by dynamic circuits in the hippocampus. *Nature* 429, 717–723. doi: 10.1038/nature02615

Reyes, A., Lujan, R., Rozov, A., Burnashev, N., Somogyi, P., and Sakmann, B. (1998). Target-cell-specific facilitation and depression in neocortical circuits. *Nat. Neurosci.* 1, 279–285. doi: 10.1038/1092

Rhee, J. S., Betz, A., Pyott, S., Reim, K., Varoqueaux, F., Augustin, I., et al. (2002). Beta phorbol ester- and diacylglycerol-induced augmentation of transmitter release is mediated by Munc13s and not by PKCs. *Cell* 108, 121–133. doi: 10.1016/s0092-8674(01)00635-3

Rosenmund, C., Sigler, A., Augustin, I., Reim, K., Brose, N., and Rhee, J. S. (2002). Differential control of vesicle priming and short-term plasticity by Munc13 isoforms. *Neuron* 33, 411–424. doi: 10.1016/s0896-6273(02)00568-8

Rozov, A., Burnashev, N., Sakmann, B., and Neher, E. (2001). Transmitter release modulation by intracellular Ca2 + buffers in facilitating and depressing nerve terminals of pyramidal cells in layer 2/3 of the rat neocortex indicates a target cell-specific difference in presynaptic calcium dynamics. *J. Physiol.* 531, 807–826. doi: 10.1111/j.1469-7793.2001.0807h.x

Sakamoto, H., Ariyoshi, T., Kimpara, N., Sugao, K., Taiko, I., Takikawa, K., et al. (2018). Synaptic weight set by Munc13-1 supramolecular assemblies. *Nat. Neurosci.* 21, 41–49. doi: 10.1038/s41593-017-0041-9

Scanziani, M., Gahwiler, B. H., and Charpak, S. (1998). Target cell-specific modulation of transmitter release at terminals from a single axon. *Proc. Natl. Acad. Sci. U.S.A.* 95, 12004–12009. doi: 10.1073/pnas.95.20.12004

Schoch, S., Castillo, P. E., Jo, T., Mukherjee, K., Geppert, M., Wang, Y., et al. (2002). RIM1alpha forms a protein scaffold for regulating neurotransmitter release at the active zone. *Nature* 415, 321–326. doi: 10.1038/415321a

Shigemoto, R., Kinoshita, A., Wada, E., Nomura, S., Ohishi, H., Takada, M., et al. (1997). Differential presynaptic localization of metabotropic glutamate receptor subtypes in the rat hippocampus. *J. Neurosci.* 17, 7503–7522. doi: 10.1523/JNEUROSCI.17-19-07503.1997

Shigemoto, R., Kulik, A., Roberts, J. D., Ohishi, H., Nusser, Z., Kaneko, T., et al. (1996). Target-cell-specific concentration of a metabotropic glutamate receptor in the presynaptic active zone. *Nature* 381, 523–525. doi: 10.1038/381523a0

Siksou, L., Rostaing, P., Lechaire, J. P., Boudier, T., Ohtsuka, T., Fejtova, A., et al. (2007). Three-dimensional architecture of presynaptic terminal cytomatrix. *J. Neurosci.* 27, 6868–6877. doi: 10.1523/JNEUROSCI.1773-07.2007

Stachniak, T. J., Sylwestrak, E. L., Scheiffele, P., Hall, B. J., and Ghosh, A. (2019). Elfn1-Induced Constitutive Activation of mGluR7 Determines Frequency-Dependent Recruitment of Somatostatin Interneurons. *J. Neurosci.* 39, 4461–4474. doi: 10.1523/JNEUROSCI.2276-18.2019

Stevens, D. R., Wu, Z. X., Matti, U., Junge, H. J., Schirra, C., Becherer, U., et al. (2005). Identification of the minimal protein domain required for priming activity of Munc13-1. *Curr. Biol.* 15, 2243–2248. doi: 10.1016/j.cub.2005.10.055

Sudhof, T. C. (2012). The presynaptic active zone. *Neuron* 75, 11–25. doi: 10.1016/j.neuron.2012.06.012

Sudhof, T. C., and Rizo, J. (2011). Synaptic vesicle exocytosis. *Cold Spring Harb. Perspect. Biol.* 3:a005637.

Sun, H. Y., Lyons, S. A., and Dobrunz, L. E. (2005). Mechanisms of target-cell specific short-term plasticity at Schaffer collateral synapses onto interneurones versus pyramidal cells in juvenile rats. *J. Physiol.* 568, 815–840. doi: 10.1113/jphysiol.2005.093948

Sylwestrak, E. L., and Ghosh, A. (2012). Elfn1 regulates target-specific release probability at CA1-interneuron synapses. *Science* 338, 536–540. doi: 10.1126/science.1222482

Tomioka, N. H., Yasuda, H., Miyamoto, H., Hatayama, M., Morimura, N., Matsumoto, Y., et al. (2014). Elfn1 recruits presynaptic mGluR7 in trans and its loss results in seizures. *Nat. Commun.* 5:4501. doi: 10.1038/ncomms5501

Van De Bospoort, R., Farina, M., Schmitz, S. K., De Jong, A., De Wit, H., Verhage, M., et al. (2012). Munc13 controls the location and efficiency of dense-core vesicle release in neurons. *J. Cell Biol.* 199, 883–891. doi: 10.1083/jcb.201208024

Varoqueaux, F., Sigler, A., Rhee, J. S., Brose, N., Enk, C., Reim, K., et al. (2002). Total arrest of spontaneous and evoked synaptic transmission but normal synaptogenesis in the absence of Munc13-mediated vesicle priming. *Proc. Natl. Acad. Sci. U.S.A.* 99, 9037–9042. doi: 10.1073/pnas.122623799

Wang, Y., Okamoto, M., Schmitz, F., Hofmann, K., and Sudhof, T. C. (1997). Rim is a putative Rab3 effector in regulating synaptic-vesicle fusion. *Nature* 388, 593–598. doi: 10.1038/41580

Conflict of Interest: The authors declare that the research was conducted in the absence of any commercial or financial relationships that could be construed as a potential conflict of interest.

frontiers in Synaptic Neuroscience

ORIGINAL RESEARCH
published: 15 February 2022
doi: 10.3389/fnsyn.2022.830583

Correlative Live-Cell and Super-Resolution Imaging to Link Presynaptic Molecular Organisation With Function

Rachel E. Jackson[1,2*†], *Benjamin Compans*[1,2*†] *and Juan Burrone*[1,2*]

[1] *Centre for Developmental Neurobiology, Institute of Psychiatry, Psychology and Neuroscience, King's College London, London, United Kingdom,* [2] *MRC Centre for Neurodevelopmental Disorders, Institute of Psychiatry, Psychology and Neuroscience, King's College London, London, United Kingdom*

Information transfer at synapses occurs when vesicles fuse with the plasma membrane to release neurotransmitters, which then bind to receptors at the postsynaptic membrane. The process of neurotransmitter release varies dramatically between different synapses, but little is known about how this heterogeneity emerges. The development of super-resolution microscopy has revealed that synaptic proteins are precisely organised within and between the two parts of the synapse and that this precise spatiotemporal organisation fine-tunes neurotransmission. However, it remains unclear if variability in release probability could be attributed to the nanoscale organisation of one or several proteins of the release machinery. To begin to address this question, we have developed a pipeline for correlative functional and super-resolution microscopy, taking advantage of recent technological advancements enabling multicolour imaging. Here we demonstrate the combination of live imaging of SypHy-RGECO, a unique dual reporter that simultaneously measures presynaptic calcium influx and neurotransmitter release, with *post hoc* immunolabelling and multicolour single molecule localisation microscopy, to investigate the structure-function relationship at individual presynaptic boutons.

Keywords: synapse, super-resolution imaging, neurotransmitter release, calcium, active zone (AZ), correlative imaging

OPEN ACCESS

Edited by:
Lucia Tabares,
Seville University, Spain

Reviewed by:
Matteo Fossati,
Institute of Neuroscience, National Research Council (CNR), Italy
Vincenzo Marra,
University of Leicester, United Kingdom

***Correspondence:**
Rachel E. Jackson
rachel.jackson@kcl.ac.uk
Benjamin Compans
benjamin.compans@kcl.ac.uk
Juan Burrone
juan.burrone@kcl.ac.uk

† These authors have contributed equally to this work and share first authorship

Received: *07 December 2021*
Accepted: *12 January 2022*
Published: *15 February 2022*

Citation:
Jackson RE, Compans B and Burrone J (2022) Correlative Live-Cell and Super-Resolution Imaging to Link Presynaptic Molecular Organisation With Function. Front. Synaptic Neurosci. 14:830583. doi: 10.3389/fnsyn.2022.830583

INTRODUCTION

Synapses are remarkably heterogenous subcellular compartments, formed of a presynaptic terminal and a postsynaptic element that vary in structure, function and molecular composition. At the presynaptic terminal, calcium influx through voltage gated calcium channels (VGCCs) triggers the fusion of a neurotransmitter-filled synaptic vesicle (SV) with the plasma membrane at the active zone (AZ), a specialised site containing the necessary machinery for vesicle tethering, docking and release (Südhof, 2012). Individual synapses display a high degree of heterogeneity in all stages of this process, differing in their expression of calcium channel subtypes (Luebke et al., 1993; Wheeler et al., 1994; Reid et al., 1997; Gasparini et al., 2001), the level of calcium influx (Ermolyuk et al., 2012) and the sensitivity of release to calcium (Ermolyuk et al., 2012; Jackson and Burrone, 2016; Rebola et al., 2019). Most importantly, neurotransmitter release is a probabilistic process, with SV

fusion occurring with a release probability (P_r) that varies widely between synapses (Murthy et al., 1997). Presynaptic boutons are also heterogenous in their structure, such as volume and shape, as well as in their sub-synaptic features, such as AZ area and the number of neurotransmitter-filled vesicles, including their distribution in different vesicle pools (Schikorski and Stevens, 1997; Holderith et al., 2012). Although several of these aspects of presynaptic structure correlate with functional measures, our understanding of this important relationship remains incomplete, in part due to the technical challenges associated with studying both structure and function at the level of the individual synapse. The small size of presynaptic structures, below the spatial resolution limit of light microscopy, requires the use of electron or super-resolution microscopy, whilst the small and rapid events associated with neurotransmitter release require highly sensitive probes with good temporal resolution. It is therefore necessary to combine imaging modalities to uncover how structure informs function at the chemical synapse.

Methods to Study Synapse Function

Our fundamental understanding of presynaptic function comes from classical electrophysiological studies that identified the quantal nature of neurotransmitter release (del Castillo and Katz, 1954) and its relationship with calcium influx (Dodge and Rahamimoff, 1967). Whilst electrophysiological techniques have since been refined to enable recording from individual presynaptic terminals, including small central boutons (Novak et al., 2013), imaging techniques remain the simplest approach to study synapses in the large numbers required to understand their heterogeneity. For this, a range of chemical indicators and genetically encoded reporters have been developed to measure two key aspects of presynaptic function, calcium influx and neurotransmitter release (reviewed in Wang et al., 2019). More recently, the development of genetically encoded voltage indicators has also allowed imaging of the shape of the AP along axons and at individual boutons (Hoppa et al., 2014; Sabater et al., 2021).

Reporters of neurotransmitter release consist of a pH-sensitive form of GFP (pHluorin), typically fused to the luminal domain of a synaptic vesicle protein such as VAMP2 (Miesenböck et al., 1998), synaptophysin (Granseth et al., 2006), or VGLUT1 (Voglmaier et al., 2006). The pHluorin fluorescence is quenched at the acidic pH inside the vesicle and undergoes a 20-fold increase upon vesicle fusion and exposure to the extracellular medium at pH7.4 (Sankaranarayanan et al., 2000). Variants of these probes now include the addition of an invariant fluorophore (tdimer2) for normalisation of the pHluorin signal (Ratio-sypHy, Rose et al., 2013) as well as red-shifted pHluorin analogues for multicolour imaging (Li and Tsien, 2012; Liu et al., 2021). More recently, fluorescent sensors that bind glutamate or GABA have been constructed (Marvin et al., 2013, 2018, 2019) to directly sense neurotransmitter release.

The most widely used genetically encoded calcium indicators are the GCaMP family (Nakai et al., 2001), which have undergone numerous iterations to improve sensitivity and kinetics. Red-shifted calcium indicators have also been produced, such as RGECO and RCaMP1, from which jRCaMP1a and jRGECO1a have been developed (reviewed in Wang et al., 2019). Many of these probes have been targeted to specific subcellular compartments, including the presynaptic terminal (Dreosti et al., 2009; Walker et al., 2013). To monitor both presynaptic calcium influx and neurotransmitter release simultaneously we constructed SypHy-RGECO (Jackson and Burrone, 2016), a dual sensor probe which also provides an optical measure of the calcium dependence of release with single synapse resolution.

This range of tools has been essential in demonstrating the heterogeneity of synapse function, but to understand the underlying structural features that govern it, they must be combined with tools that provide information on synapse morphology and molecular organisation.

Methods to Study Synapse Structure

Electron microscopy (EM) provided the first insights into synapse structure, revealing the existence and arrangement of SVs within a presynaptic terminal, the electron dense AZ with tethered vesicles poised for release and the opposing postsynaptic density (PSD) (Harris and Weinberg, 2012), now known to precisely cluster neurotransmitter receptors (Nair et al., 2013). Although unparalleled in its spatial resolution, EM does not provide information on the distribution of molecules unless combined with immunogold labelling which remains challenging to achieve with high labelling efficiency. Cryo-electron tomography holds great promise to study the structure of the synapse and its proteins in their native state but remains a specialised and experimentally demanding technique.

Over the last two decades, super-resolution microscopy (SRM) has emerged as a tool that allows examination of protein organisation at the nanoscale using standard fluorescent labelling approaches (reviewed in Sigal et al., 2018). Whilst it does not reach the spatial resolution of EM, it is a vast improvement over conventional light microscopy, provides information on the nanoscale organisation of molecules and is more amenable to higher throughput imaging. SRM has shown that several key AZ proteins such as Bassoon (Dani et al., 2010; Glebov et al., 2017), RIM1/2 (Tang et al., 2016; Haas et al., 2018) and Munc13 (Sakamoto et al., 2018) are arranged into subsynaptic domains (SSDs), as are postsynaptic proteins including PSD95 (Fukata et al., 2013; MacGillavry et al., 2013; Nair et al., 2013) and AMPA receptors (Nair et al., 2013). VGCCS have been shown to be highly dynamic at the presynaptic membrane, but transiently stabilise into SSDs at the AZ through protein interactions (Schneider et al., 2015; Heck et al., 2019). Importantly, SRM has brought the pre- and post-synaptic compartments together at the nanoscale by uncovering a novel arrangement in which RIM1/2 and PSD-95 SSDs align across the synaptic cleft, creating a transsynaptic nanocolumn for the efficient transfer of information across the cleft (Tang et al., 2016; Haas et al., 2018). In an intriguing twist to this arrangement, the nanoscale organisation of synaptic proteins was also shown to be plastic, suggesting an important role of subsynaptic domains in regulating synaptic function (Tang et al., 2016; Glebov et al., 2017; Hruska et al., 2018; Heck et al., 2019; Compans et al., 2021). However, the link between nanoscale

organisation of synaptic molecules and synapse function is only just beginning to be understood.

Studying the Structure-Function Relationship at the Synapse

Correlative light and electron microscopy studies have revealed that release probability is tightly coupled to the number of docked vesicles, which constitutes the readily releasable pool (RRP) (Murthy et al., 2001; Branco et al., 2010), and that both properties correlate with area of the AZ (Holderith et al., 2012). Whilst these correlations are maintained within synapses from a single type of neuron, synapses from different neuron types but with similar ultrastructural features, such as number of docked vesicles, display different release probabilities (Xu-Friedman et al., 2001).

Neurotransmitter release is driven by calcium influx such that the average release probability of a vesicle in the RRP is correlated with the size of the calcium transient (Ermolyuk et al., 2012). The number of VGCCs also scales linearly with AZ area and release probability in some synapse types (Holderith et al., 2012; Miki et al., 2017). However, weak cerebellar granule cell synapses express greater numbers of Cav2.1 channels than the stronger stellate cell synapses, but these channels are located at a greater distance from SV release sites and are therefore less effective at initiating neurotransmitter release (Rebola et al., 2019). This relationship can be further complicated by the expression of different calcium channel subtypes (Wheeler et al., 1994; Reid et al., 1997; Gasparini et al., 2001) and splice isoforms (reviewed in Lipscombe et al., 2013) that display different dynamics at the plasma membrane as well as distinct biophysical properties, which affect P_r (Heck et al., 2019). In addition, molecular crowding may affect the recruitment and retention of calcium channels in the plasma membrane. For example, blockade of neuronal activity causes a decrease in the density of Bassoon clusters at the active zone and the preferential recruitment of Cav2.1 to synapses with lower density (Glebov et al., 2017). Taken together it is clear that both the number of synaptic proteins and their spatial relationships are important in determining synaptic function.

A key spatial relationship at the synapse is the alignment of pre and postsynaptic protein clusters across the synaptic cleft in transsynaptic nanocolumns, which define the SSDs at which neurotransmitter release will maximally activate postsynaptic receptors (Nair et al., 2013; Tang et al., 2016; Haas et al., 2018). Until recently it was thought that the AZ constituted a single release site, however precise localisation of vesicle fusion using vGlut-pHluorin has revealed that there are multiple hotspots for release at each AZ, ranging from 5 to 14 (Maschi and Klyachko, 2017). Combining this with live SRM has shown that these hotspots are marked by dense nanoclusters of RIM1/2 (Tang et al., 2016), a protein whose levels at the AZ have been intimately linked to P_r (Holderith et al., 2012), and constitute distinct release sites. Munc13-1 and syntaxin-1 are similarly organised into SSDs, and their numbers also correlate with the number of release sites as well as the number of vesicles in the RRP (Sakamoto et al., 2018). However, in contrast to previous studies (Branco et al., 2010; Holderith et al., 2012), the number of Munc13-1 molecules, and consequently the number of release sites and RRP size, did not correlate with P_r at individual synapses (Sakamoto et al., 2018), suggesting that our understanding of the relationship between the molecular composition of release sites and release probability remains incomplete.

Many studies relating synaptic nanoscale structure with function have done so using indirect methods (Glebov et al., 2017) and only a few have attempted to combine SRM techniques and functional imaging at the same synapses (Tang et al., 2016; Sakamoto et al., 2018; Holderith et al., 2020), despite the insight this type of correlation can provide. Here we present a correlative approach combining live imaging of SypHy-RGECO, a genetically encoded reporter that simultaneously measures calcium influx and neurotransmitter release (Jackson and Burrone, 2016), with multicolour 3D-dSTORM using spectral demixing (Testa et al., 2010; Platonova et al., 2015). Using the well-characterised presynaptic proteins Bassoon and Cav2.1, we provide proof of principle that both nanoscale organisation and functional measures can be investigated at the level of individual boutons.

MATERIALS AND METHODS

An overview of the pipeline for functional and 3D-dSTORM correlative imaging is shown in **Figure 1**.

Step 1: Preparation of Hippocampal Neurons on Gridded Dishes

Hippocampi were dissected from E18.5 Wistar rat embryos (Charles River Laboratories, United Kingdom), treated with trypsin (Worthington, United Kingdom) at 0.5 mg/ml and triturated with fire-polished Pasteur pipettes. Dissociated cells (80–100k) were plated onto 35 mm low profile Grid500 μ-dishes (Ibidi, Germany) pre-treated with 100 μg/mL poly-D-lysine (Sigma, United Kingdom) and 10 μg/mL laminin (Thermo Fisher Scientific, United Kingdom). Neurons were maintained in Neurobasal media supplemented with 2% B27, 2% foetal bovine serum, 1% glutamax, and 1% penicillin/streptomycin (all Thermo Fisher Scientific, United Kingdom) in a 37°C humidified incubator with 5% CO_2. After 3 days *in vitro* (DIV) the media was exchanged for serum and antibiotic-free media.

Step 2: Transfection With SypHy-RGECO

At 7DIV, neurons were transfected with CAMKII:SypHy-RGECO [Jackson and Burrone, 2016, Addgene plasmid #84078, subcloned under a minimal CAMKII promoter in the vector backbone of pAAV-CW3SL-EGFP, a gift from Bong-Kiun Kaang (Choi et al., 2014), Addgene plasmid #61463] using Effectene, following the manufacturer's protocol (QIAGEN, United Kingdom). Expression of SypHy-RGECO under the minimal CAMKII promoter should be restricted to excitatory neurons.

Step 3: Live Imaging of SypHy-RGECO

Neurons were imaged live at DIV17-21 on an inverted Olympus IX71 microscope equipped with a 60x/1.42 NA oil objective, with

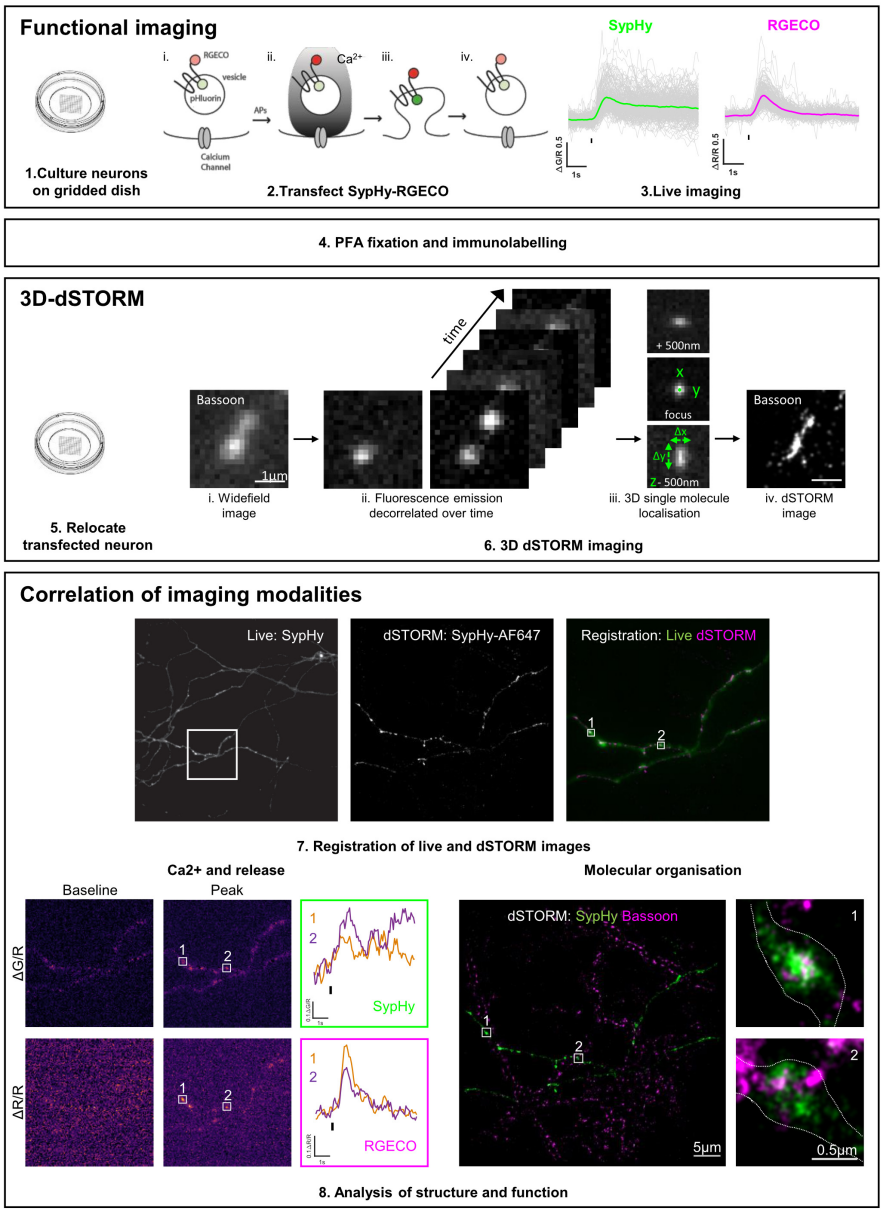

FIGURE 1 | Functional and 3D-dSTORM correlative imaging pipeline. (1–3) Preparation of neurons for functional imaging of a presynaptic calcium and vesicle release sensor (SypHy-RGECO). (4) Fixation and immunolabelling of neurons. (5–6) Relocation and super-resolution (dSTORM) imaging of SypHy-RGECO + ve neurons. (7–8) Registration between imaging modalities, analysis of calcium influx (RGECO) and neurotransmitter release (SypHy) and nanoscale organisation of synaptic proteins (dSTORM), followed by single synapse correlation between modalities.

a heated stage and objective to maintain the bath temperature at 32 ± 2°C. The growth media was replaced with HEPES buffered saline (HBS; 139 mM NaCl, 2.5 mM KCl, 10 mM HEPES, 10 mM D-Glucose, 2 mM $CaCl_2$, 1.3 mM $MgCl_2$; pH7.3 at 32°C, 290 mOsmol) supplemented with 10 μM NBQX, 25 μM APV and 10 μM Gabazine (Tocris, United Kingdom) to prevent recurrent activity. Images were acquired with an ORCA-Flash4.0 V2 C11440-22CU scientific CMOS camera (Hamamatsu Photonics, Japan) using HCImageLive Software (Hamamatsu Photonics) and the camera was cooled to approximately −20°C with an Exos2 water cooling system (Koolance, United States). The triggering of LEDs, camera acquisition and stimulation were controlled externally through Clampex software (pCLAMP10, Molecular Devices, United States) and a Master-8 programmable stimulator (A.M.P.I, Israel).

A GFP-positive cell was identified, and an extracellular parallel bipolar electrode (FHC, United States) was positioned with the tips on either side of the soma using a PatchStar Motorised Micromanipulator (Scientifica, United Kingdom). A 10-action potential (AP) stimulation at 20 Hz was delivered by an SD9

stimulator (Grass Technologies, United States) using 10 pulses of 9.5–10 V for 1 ms, a stimulus previously shown to elicit a single AP per pulse (Sabater et al., 2021). Imaging was performed with a dual band-pass filter set optimised for EGFP and mCherry (#59022, Chroma Technology, United States) and with LED excitation light sources of 470 and 585 nm (CoolLED, United Kingdom) set at 70 and 100% power, for pHluorin and RGECO fluorophores, respectively. The full frame was acquired with 4 × 4 binning (pixel size = 433 nm), alternating 20 ms exposures of the 470 and 585 nm LEDs with a 20 ms interval between frames, resulting in a final acquisition rate of 12.5 Hz for each channel.

Step 4: Immunofluorescence

Immediately after live imaging, neurons were fixed with 4 or 1% PFA (for Cav2.1 labelling) for 10 min at room temperature (RT). Neurons were washed in PBS 3 times and 50 mM NH_4Cl in PBS was applied as a quenching agent, followed by a further 3 washes in PBS. Dishes were stored in PBS at 4°C in the dark until staining. Neurons were permeabilised with 0.1% TritonX-100 in PBS for 10 min, washed three times in PBS and placed in blocking solution (2% BSA in PBS) for 60 min at room temperature (RT). Cells were incubated with primary antibodies diluted in blocking solution for 60 min at RT then washed three times in blocking solution for 5 min each. Secondary antibodies and nanobodies in blocking solution were applied for 60 min at RT and cells were washed three times in block and 3 times in PBS for 5 min each. Cells were kept in PBS at 4°C in the dark until STORM imaging.

Step 5–6: Relocate Neurons for Multicolour 3D-dSTORM Imaging

dSTORM imaging was performed using a spectral-demixing SAFeRedSTORM module (Abbelight, France) mounted on an Olympus IX3 equipped with an oil-immersion objective (100 × 1.49NA oil immersion, Olympus, United Kingdom) and fibre-coupled 642 nm laser (450 mW, Errol). Fluorescent signal was collected with two ORCA-fusion sCMOS cameras (Hamamatsu). A longpass dichroic beam splitter (700 nm; Chroma Technology) was used to split the emission light on the two cameras. 3D-dSTORM imaging was performed by using cylindrical lenses placed before each camera.

The imaging buffer contained 1 mL Glucose Base (10% Glucose, 0.1% Glycerol), 125 μL of Enzyme Buffer (42 μg/mL Catalase (C100, Sigma), 1 mg/mL Glucose oxidase (G2133, Sigma), 50% Glycerol, 20 mM Tris-HCl pH7.5, 4 mM TCEP (C4706, Sigma), 25 mM KCl) and 125 μL of 1 M MEA-HCl (pH∼8 with NaOH, M6500, Sigma). This allowed a final concentration of 4 μg/mL of Catalase and 100 μg/mL of Glucose oxidase, and a final concentration of 100 mM of reducing agent MEA. The final pH was adjusted to fall between pH7.6 and pH8. To limit the contact of the imaging buffer with oxygen, the ibidi dish well was sealed with a 25 mm glass coverslip.

Image acquisition was driven by NEO software (Abbelight). The image stack contained 60,000 frames of a selected ROI of 512 × 512 pixels (pixel size = 97 nm). Cross-correlation was used to correct for lateral drifts. Super-resolution images (.tiff) with a pixel size of 10 nm and localisation files (.csv) were obtained using NEO_analysis software (Abbelight).

Step 7: Image Registration and Synapse Correlation

A maximum z-projection of the live SypHy channel and the reconstructed dSTORM image of the amplified GFP signal were registered using landmark selection and affine transformation in Matlab (Mathworks, script available at https://github.com/jburrone/Jackson-Compans-and-Burrone). Individual synapses that were clearly defined in both images and well aligned in the registration were manually selected and included in correlative analysis.

Step 8: Analysis of Structure and Function

8a: Analysis of Live Images

Images saved in CXD format were converted to TIFF files and split into two separate channels using FIJI (ImageJ). Images were analysed using custom written Matlab scripts (Mathworks, script available upon request). Regions of interest (ROIs, 5 × 5 pixels) were selected for each punctum of SypHy fluorescence and a 15 × 15 pixel ROI was used to calculate background fluorescence. Mean background-subtracted fluorescence intensity values were calculated for each ROI in both SypHy(G) and RGECO(R) channels. Traces were smoothed by averaging over a sliding window of 4 frames. Baseline fluorescence (G_0 and R_0) was measured as the mean of 15 frames prior to the stimulus. ΔG and ΔR values were calculated by the change in signal intensity from the baseline, with the peak responses defined as the maximum ΔG and ΔR within 15 frames of the stimulus. Puncta in which the ΔR response to the 10AP at 20 Hz stimulus was greater than three times the standard deviation of the baseline were considered responding synapses and were included in further analysis, regardless of whether there was a measurable ΔG response. ΔG and ΔR responses were both normalised to the baseline R_0 fluorescence, which represents the overall levels of reporter at the synapse.

8b: Multicolour 3D-dSTORM Analysis

Point Clouds Analyst software (PoCA, Levet et al., 2015, 2019) was used to identify SypHy-RGECO, Cav2.1 and Bassoon clusters from localised molecule coordinates. First a Voronoi diagram was applied to draw 3D polygons of various sizes centred on the localised molecules for each colour separately. Automatic segmentation was performed to detect clusters for each protein (colour1: SypHy-RGECO to identify presynaptic boutons and colour2: Bassoon or Cav2.1). Clusters for each colour were thresholded based on their density (δ_i^1 for colour1 and δ_i^2 for colour2) with respect to the average density of the dataset for each colour, such that $\delta_i^1 \geq 1\delta_d$ and $\delta_i^2 \geq 1\delta_d$. All selected neighbouring molecules within a maximum distance between neighbours of 200 and 100 nm were considered as forming a cluster when having a minimum number of 200 and 20 molecules for colour1 and colour2, respectively. The colocalisation between SypHy-RGECO and Bassoon or Cav2.1

was computed from the overlapping clusters. We found that some colour2 clusters (Bassoon or Cav2.1) were not automatically detected as colocalising with colour 1 (SypHy-RGECO) clusters even though they clearly formed part of the same synapse. There are multiple reasons for this, including the segmentation thresholds used, which limit the extent of the overlap between colours, and the fact that SypHy-RGECO labels synaptic vesicles and does not cover the entirety of the presynaptic volume. We therefore manually verified and corrected for any missed colocalisations, then extracted cluster volume and density of molecules for colour1 and colour2 from all synapses. Synapses with no colour2 cluster or ambiguous clusters that could not be manually verified were excluded.

8c: Correlation of Live and dSTORM Analysis

Functional responses (ΔG/R, ΔR/R and the ratio ΔG/ΔR) and structural parameters (number of detections and cluster volume and density) were analysed for correlation using Matlab (Mathworks, United States) and Prism 9 (GraphPad, United States), across all synapses selected during image registration (step 7) that passed the inclusion criteria in both imaging modalities (steps 8a and b).

RESULTS

The first imaging step in our pipeline (see section "Materials and Methods" and **Figure 1**) is to simultaneously measure calcium influx and neurotransmitter release by performing live imaging of SypHy-RGECO, a probe that localises to presynaptic boutons, seen as clear puncta along the axons of hippocampal neurons (**Figure 2A**). Axonal regions were imaged whilst the soma of the transfected cell was stimulated with a parallel bipolar electrode using 10 pulses that induce single APs (Sabater et al., 2021), a stimulus which lies within the linear range for both reporters (Jackson and Burrone, 2016). Puncta in which the change in RGECO fluorescence was greater than 3S.D. of the baseline were considered functional synapses and included in later analysis (magenta traces, **Figure 2A**). Using the same criterion for sypHy responses, almost a quarter of synapses (23.27%) did not display measurable neurotransmitter release to a 10AP stimulus despite experiencing a calcium influx, suggesting they had a low release probability (white vs. green traces, **Figure 2A**). When neurotransmitter release could be quantified, individual synaptic ΔG/R and ΔR/R responses exhibited a wide range of amplitudes, which were positively correlated (**Figure 2B**). However, due to the spread of points within this correlation, individual synapses with the same level of calcium influx could display different levels of neurotransmitter release (**Figure 2C**). This can be quantified using the ratio ΔG/ΔR, a measure of the calcium-dependence of release (**Figure 2D**).

To relocate the same synapses after fixation and staining, we used both their grid position and axonal morphology. We first amplified the SypHy signal using an anti-GFP antibody and an AF488-coupled secondary antibody and labelled endogenous Bassoon with a primary and CF680-coupled secondary antibody suitable for dSTORM imaging. SypHy-RGECO + ve boutons

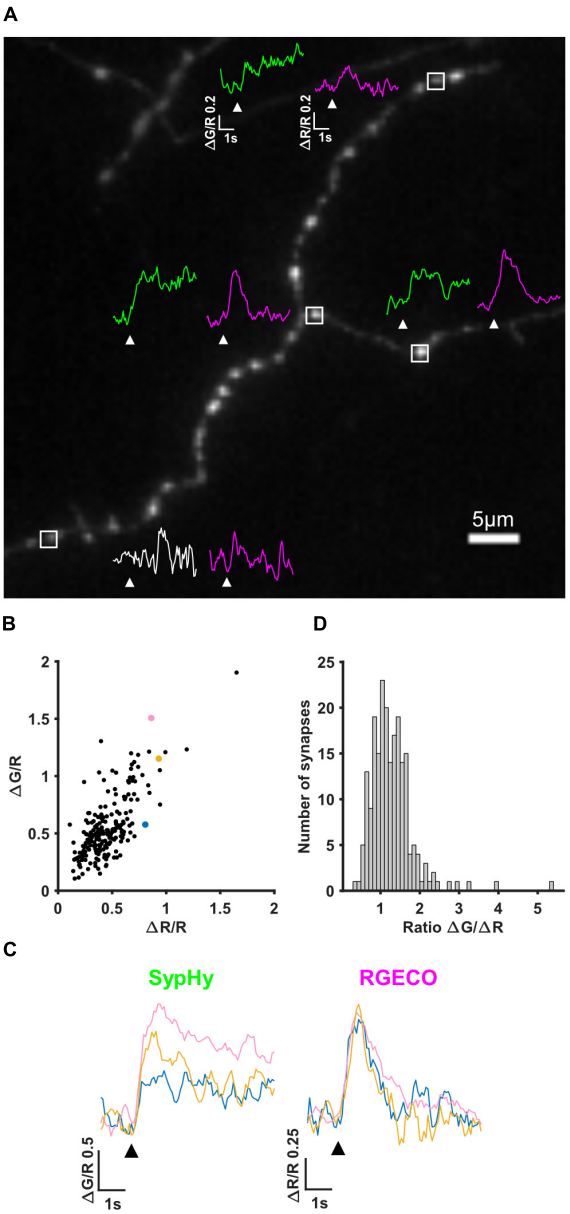

FIGURE 2 | SypHy-RGECO responses to 10AP stimuli. **(A)** Image of an axon transfected with SypHy-RGECO (green channel (SypHy) shown). Representative traces of SypHy (ΔG/R, green/white) and RGECO (ΔR/R, magenta) responses to 10AP stimuli are shown for boutons with a detectable calcium influx (peak response greater than 3SD of the baseline), associated with SV release (green traces) or failure to release (bottom synapse, white trace) assessed using the same threshold. White boxes indicate selected boutons, all traces shown on the same scale, white arrows indicate stimulation. **(B)** Cells were stimulated with a 10AP 20 Hz stimulus. The change in fluorescence from baseline (ΔG and ΔR) was normalised to the basal RGECO fluorescence (R) for each synapse. ΔG/R and ΔR/R responses from all synapses show a positive correlation (Spearman's rank correlation, $r = 0.633$, $p = < 0.0001$, $n = 211$ synapses). **(C)** SypHy (left) and RGECO (right) traces from 3 synapses (coloured points in **B**) with a similar amount of calcium influx (RGECO) in response to a 10AP stimulus but a different level of neurotransmitter release (SypHy). Black arrows indicate stimulation. **(D)** Distribution of the ratio ΔG/ΔR indicating the calcium dependence of release (for the synapses shown in **B**).

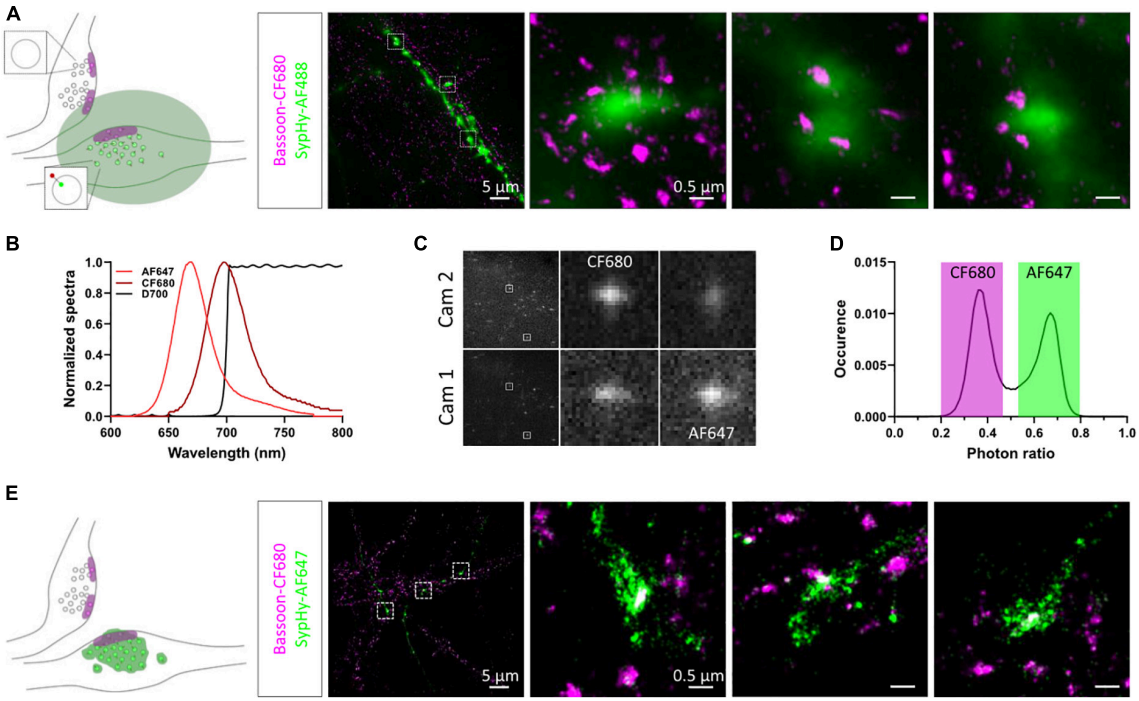

FIGURE 3 | Multicolour 3D-dSTORM to investigate synaptic protein nanoscale organisation. **(A)** Left panel: schematic of two presynaptic bouton labelled for active zone protein Bassoon resolved with dSTORM. Only one of the two boutons expresses SypHy-RGECO (zoomed synaptic vesicle). The green area represents the diffracted signal from GFP staining imaged with conventional widefield fluorescence microscopy. Right panel: representative example of a widefield image of a SypHy-RGECO + ve axon immunolabelled with AF488 (green) overlaid with a dSTORM image of endogenous Bassoon (magenta) immunolabelled with CF680. Zoomed examples of 3 boutons are shown (square box). **(B)** Emission spectra of AF647 (light red) and CF680 (dark red), and transmission profile of D700 dichroic (black). **(C)** Example images of single emitters obtained from the 2 cameras on our SD-dSTORM system and zoomed examples of 2 single emitters. AF647 intensity is stronger on camera 1 than camera 2. CF680 intensity is stronger on camera 2 than camera 1. **(D)** Distribution of single emitters according to their photon ratio $[I_{cam1}/(I_{cam2} + I_{cam1})]$ allows separation of AF647 and CF680 detections. **(E)** Left panel: schematic of two presynaptic bouton labelled for Bassoon resolved with dSTORM. Only one of the two boutons expresses SypHy-RGECO (zoomed synaptic vesicle). The green area represents the super-resolved signal from GFP staining imaged with SD-dSTORM. Right panel: representative example of multicolour 3D-dSTORM of a SypHy-RGECO + axon immunolabelled with AF647 (green) and endogenous Bassoon (magenta) immunolabelled with CF680. Zoomed examples of 3 boutons are shown (square box).

were identified and a widefield image was acquired in the green channel. 3D-dSTORM was then performed for CF680 and the super-resolved image of Bassoon was reconstructed and overlaid on the diffracted GFP image (**Figure 3A**). Due to the low resolution of the GFP image, chromatic aberrations and the high density of axons in the culture, identifying colocalisation between Bassoon subsynaptic domains (SSDs) and SypHy-RGECO + ve boutons was difficult. To overcome these limits and avoid misidentification, we took advantage of spectral demixing dSTORM (SD-dSTORM) to perform multicolour super-resolution imaging. SD-dSTORM uses fluorophores excitable with a single wavelength (here 642 nm) but with a small shift in their emission spectrum (**Figure 3B**). Using a long-pass dichroic to split the emission of fluorescence from single emitters onto two cameras, a photon ratio can be calculated to assign the detection to one of the fluorophores (Testa et al., 2010; Platonova et al., 2015; **Figures 3C,D** and **Supplementary Movie 1**). As SD-dSTORM uses fluorophores with similar emission wavelengths, chromatic aberrations are negligible compared to more classical multicolour SRM that requires further image processing. Using this technique increased the resolution of SypHy-RGECO + boutons and improved identification of their associated Bassoon SSDs (**Figure 3E**).

To further enhance the localisation precision of the SypHy-RGECO + vesicular pool, we used GFP nanobodies directly coupled with AF647. As expected, due to the reduced distance between SypHy and AF647 (Früh et al., 2021), we observed a net reduction in SypHy cluster volume with nanobody labelling compared to classical primary/secondary staining (**Supplementary Figures 1A–C**). However, after 1% PFA fixation required for labelling Cav2.1, nanobody staining appeared weaker and did not easily allow relocation of SypHy-RGECO + ve neurons for dSTORM imaging, correct registration of image modalities or confident identification of presynaptic boutons (**Supplementary Figure 1A**, top panel). When compared to nanobody staining following 4% PFA fixation, used for Bassoon labelling, the staining following 1% PFA fixation was less reliable, as shown by the decreased number of detections of AF647 per SypHy-RGECO cluster (**Supplementary Figures 1A,D**). Since under these conditions the GFP nanobody was likely undersampling the labelling of SypHy, we continued to use the classical primary and secondary antibody labelling approach,

which appeared to be less sensitive to fixing conditions and improved the correlation between the number of SypHy-RGECO detections in dSTORM and the RGECO baseline (R_0) in live imaging (**Supplementary Figures 1E–G**). Whilst the primary aim of super-resolving SypHy was to precisely identify live-imaged boutons and their associated proteins of interest, we were also able to investigate the relationship between presynaptic functional properties and SypHy-RGECO detections in neurons labelled with the polyclonal antibody. As this reporter is mostly expressed on SVs, the number and volume of the SypHy-RGECO cluster will be proportional to the total pool of vesicles. We did not observe any correlation between SV release ($\Delta G/R$) or calcium influx ($\Delta R/R$) and either the number or volume of SypHy detections (**Supplementary Figure 2**).

Two colour super-resolution images of either Cav2.1 or Bassoon together with SypHy-RGECO showed that both AZ proteins are organised in sub-synaptic domains (SSDs), such that a single SypHy-RGECO cluster, representing an individual bouton, could contain anywhere from 1 to 6 Cav2.1 (mean = 1.6, **Figure 4A**) or Bassoon SSDs (mean = 1.7, **Figure 4B**). Point Clouds Analyst, a method for 3D two-colour segmentation based on single molecule detection densities (PoCA, Levet et al., 2015, 2019), was used to identify SypHy-RGECO clusters and their associated Bassoon or Cav2.1 SSDs. In most cases, the identification of Bassoon or Cav2.1 SSDs within a SypHy-RGECO cluster was straight forward (**Supplementary Figure 3C**). In a few cases, segmentation limits meant that associated SSDs were not automatically identified (**Supplementary Figures 3D,E**). Where possible, these were manually corrected, otherwise synapses were excluded from further analysis. This analysis showed that synapses with more than one Cav2.1 SSD had bigger SypHy cluster volumes (**Figure 4C**), a difference that was even more noticeable for synapses with multiple Bassoon SSDs (**Figure 4D**). Interestingly, in synapses with multiple SSDs, the individual clusters of both Cav2.1 and Bassoon display a slight but significant decrease in density compared to those from synapses with single SSDs (**Supplementary Figure 4**). Together these observations suggest that synapses can use multiple strategies for protein organisation such as forming one or multiple SSDs with different densities of crowding. These types of observation would not be possible using conventional fluorescence microscopy, highlighting the advantage of using SRM to investigate synaptic protein organisation.

As VGCCs are directly involved in neurotransmitter release, we next investigated the potential link between Cav2.1 nanoscale organisation, one major subtype of VGCC found at synaptic boutons, and SV release at individual synapses. The number of Cav2.1 SSDs varied considerably across boutons, ranging from 1 to 6 SSDs, with around 60% of analysed synapses containing only a single Cav2.1 SSD (**Figure 5A**). We separated synapses into two groups according to the presence of a single or multiple Cav2.1 SSDs. For both groups, we observed a similar positive correlation between $\Delta G/R$ and $\Delta R/R$ (**Figure 5B**). Within this correlation, the spread of the responses indicates a variation in the calcium-dependence of release between synapses, quantified by the ratio $\Delta G/\Delta R$. We compared the distribution of $\Delta G/\Delta R$ between synapses with single or multiple Cav2.1 SSDs and found no significant difference (**Figure 5C**). As we did not observe any correlation between Cav2.1 SSD properties and the level of calcium influx or neurotransmitter release (**Supplementary Figure 5**), we next split synapses based on their release properties—those with detectable levels of neurotransmitter release in response to a 10AP stimulus and those that do not exhibit any detectable release despite showing robust Ca^{2+} influx. No difference in the number of Cav2.1 SSDs, nor in SSD properties were observed between synapses which released and those which did not (**Figures 5D–F**). Our findings indicate that Cav2.1 abundance or spatial distribution are not a good predictor for measures of presynaptic function.

The probability of neurotransmitter release was previously shown to correlate well with active zone area (Holderith et al., 2012). We therefore investigated the relationship between Bassoon, one of the main presynaptic scaffolding proteins, and presynaptic function. Around 55% of synapses contained a single Bassoon SSD, with the rest of the synapses containing from 2 to 5 SSDs, much like our observations for Cav2.1 (**Figure 6A**). A similar positive correlation was found between $\Delta G/R$ and $\Delta R/R$ for synapses with single and multiple Bassoon SSDs (**Figure 6B**) and again, there was no difference in the relationship between Ca^{2+} and release between the two group of synapses when comparing the distributions of the ratio $\Delta G/\Delta R$ (**Figure 6C**). We also found no correlation between Bassoon SSD properties and the levels of release or calcium influx, with the exception that in synapses with multiple Bassoon SSDs, the number of Bassoon detections was negatively correlated with the calcium dependence of release ($\Delta G/\Delta R$) (**Supplementary Figure 6**). However, when comparing synapses with detectable levels of release to those where release is not detectable, we observed differences in the nanoscale organisation of Bassoon. Releasing synapses tended to have fewer Bassoon SSDs (**Figure 6D**), as well as less Bassoon detections per synapse (**Figure 6F**). There was, however, no difference in the mean density of Bassoon distribution (**Figure 6E**).

DISCUSSION

In this study we have described the use of a correlative approach combining functional imaging and multicolour 3D-dSTORM to investigate presynaptic structure and function at individual synapses. Using this method, we examined the nanoscale organisation of Bassoon and the VGCC Cav2.1. We found that these proteins are organised into SSDs, of which there can 1–6 per synapse (mean = 1.7 and 1.6, respectively), in agreement with previous studies using SRM (dSTORM Bassoon = 1.5, Tang et al., 2016; STED 1–4 Bassoon SSD, Hruska et al., 2018) and immunogold-EM (1–5 Cav2.1 SSD; Miki et al., 2017). In synapses with a single SSD, the density of the protein cluster was increased in comparison to the individual densities of the multiple SSDs, suggesting different strategies can be employed to arrange the same number of total proteins. At present it is not clear what determines the strategy at different synapses and further examination of the co-organisation of protein SSDs will be needed.

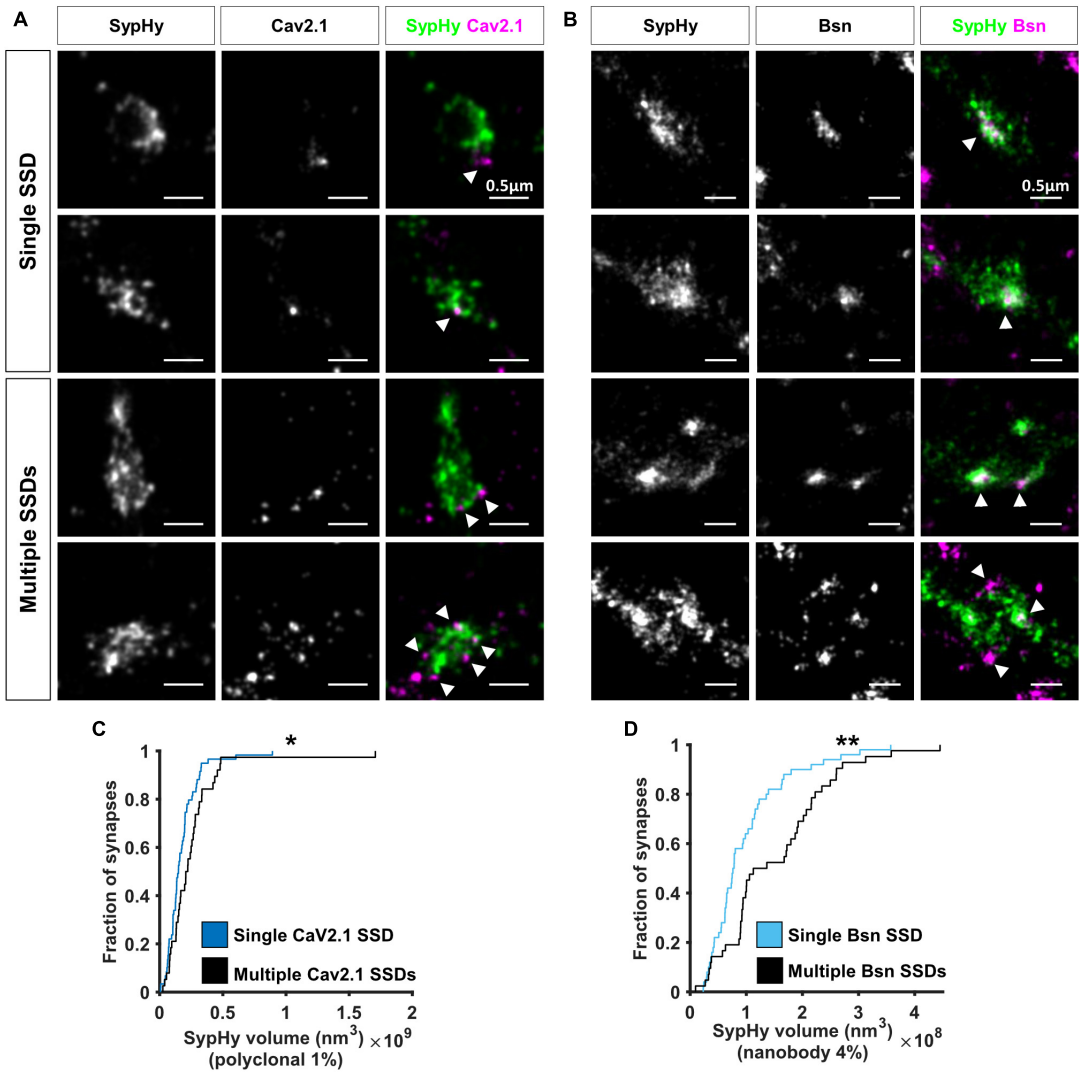

FIGURE 4 | Nanoscale organisation of Cav2.1 and Bassoon in SypHy-RGECO + ve boutons. **(A,B)** Examples of SypHy-RGECO + ve boutons labelled for SypHy-AF647 (left panels) and Cav2.1-CF680 (A: middle panels) or Bassoon-CF680 (**B**, middle panels) imaged with SD-dSTORM. Merged images of SypHy (green) and Cav2.1 (**A**, magenta) or Bassoon (**B**, magenta) are shown in the right panels. White arrows indicate Cav2.1 or Bassoon subsynaptic domains (SSD). Synapses can contain a single (top panels) or multiple SSDs (lower panels). **(C)** Cumulative distribution of SypHy cluster volume labelled with polyclonal anti-GFP and AF647-coupled secondary antibodies after 1%PFA fixation, for synapses with single or multiple Cav2.1 SSDs (Kolmogorov-Smirnov test, $p = 0.025$, $n_{single} = 59$, $n_{multi} = 38$). **(D)** Cumulative distribution of SypHy cluster volume labelled with AF647-coupled anti-GFP nanobody after 4%PFA fixation, for synapses with single or multiple Bassoon SSDs (Kolmogorov-Smirnov test, $p = 0.004$, $n_{single} = 50$, $n_{multi} = 42$). $^*p < 0.05$ and $^{**}p < 0.01$.

We found no correlation between the mean density or total number of Cav2.1 localisations and the levels of either calcium influx or neurotransmitter release. However, immunogold labelling in CA3-CA3 recurrent synapses has previously shown that the number of Cav2.1 channels correlates with AZ area, which in turn correlates with P_r (Holderith et al., 2012). In our study, the population of synapses we sampled from was more heterogeneous, since the promoter driving the expression of SypHy-RGECO could be expressed in any excitatory hippocampal neuron, which may account for any difference between the studies. Importantly, the calcium channel subtypes responsible for calcium influx have been shown to vary between synapses, adding another level of heterogeneity. Cav2.1, Cav2.2, and Cav2.3 have all been shown to support presynaptic calcium influx in glutamatergic terminals (Luebke et al., 1993; Wheeler et al., 1994; Gasparini et al., 2001), and the proportions of VGCC subtypes varied not only across hippocampal regions (Parajuli et al., 2012) but, more intriguingly, across synapses themselves, even when these synapses belong to the same neuron (Reid et al., 1997). In addition, it has been shown that postsynaptic cell identity can also influence presynaptic calcium influx and neurotransmitter release properties (Éltes et al., 2017). This heterogeneity in the complement of VGCC types, where some synapses are almost entirely reliant on one subtype, whilst

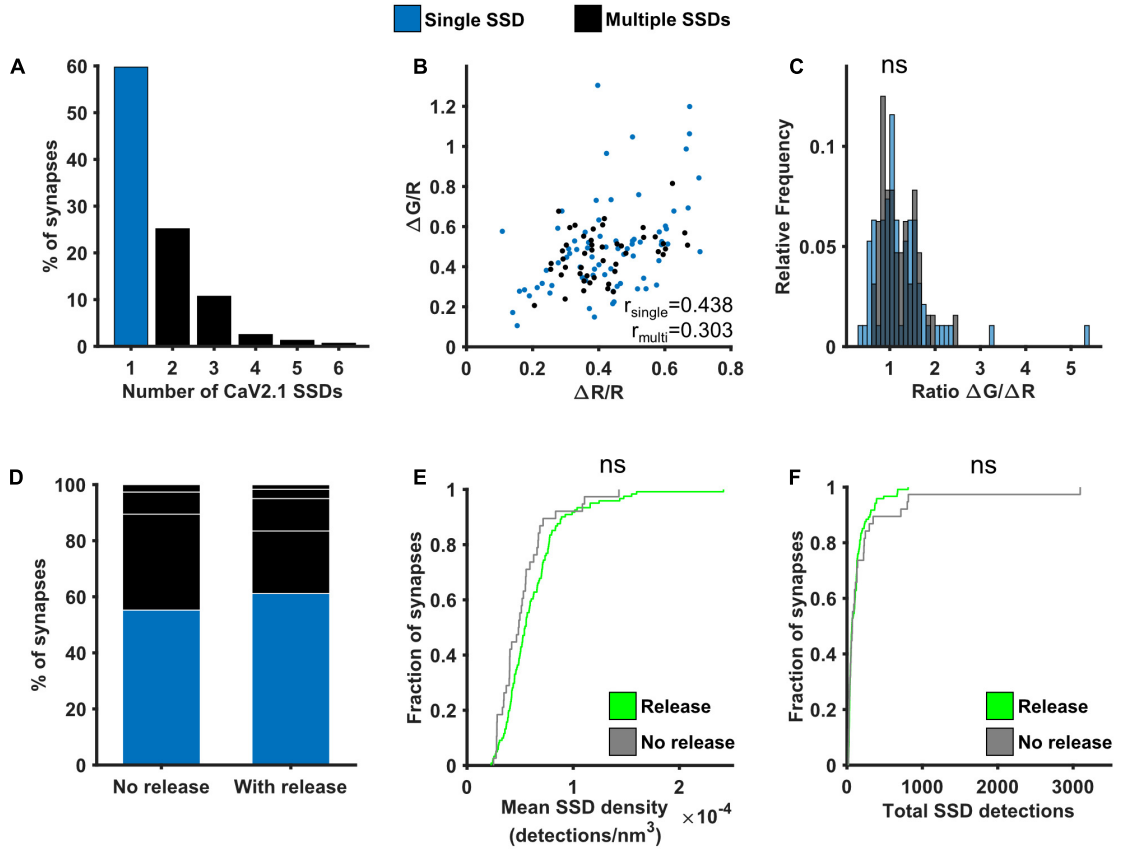

FIGURE 5 | Effect of Cav2.1 nanoscale organisation on neurotransmitter release. **(A)** Distribution of the number of Cav2.1 SSDs per synapse. **(B)** ΔG/R and ΔR/R responses from synapses *post hoc* labelled for Cav2.1 and identified as containing a single (blue) or multiple Cav2.1 SSDs (black) show a positive correlation (Spearman's rank correlation, r_{single} = 0.439, $p < 0.0001$, n_{single} = 74 synapses; r_{multi} = 0.303, $p < 0.0001$, n_{multi} = 47 synapses). **(C)** Distribution of the ratio ΔG/ΔR for the two group of synapses. Distributions are not significantly different (Kolmogorov-Smirnov test, p = 0.657, n_{single} = 74, n_{multi} = 47). **(D)** Percentage of synapses with single or multiple Cav2.1 SSDs in synapses without detectable release (left, n = 38) or with release (right, n = 121). White lines indicate separation of multiple SSDs by number. **(E)** Cumulative frequency distribution of the mean density of detections in Cav2.1 SSDs per synapse (number of detections/nm^3) in synapses with (green) or without (grey) detectable release to a 10AP stimulus (Kolmogorov-Smirnov test, p = 0.122, $n_{release}$ = 121, $n_{norelease}$ = 38). **(F)** Cumulative frequency distribution of the total number of detections in Cav2.1 SSDs per synapse in synapses with (green) or without (grey) detectable release to a 10AP stimulus (Kolmogorov-Smirnov test, p = 0.820, $n_{release}$ = 121, $n_{norelease}$ = 38).

others utilise a mixed population (Reid et al., 1997; Scheuber et al., 2004), needs to be better understood at the single synapse level. The complexity increases even further at the level of neurotransmitter release. In addition to VGCC number and composition, neurotransmitter release is known to be regulated by the spatial coupling of VGCCs and docked SVs (Eggermann et al., 2012; Rebola et al., 2019). The precise positioning of calcium channels next to docked vesicles is thought to be regulated by an ensemble of proteins such as RIM, ELKS and Munc13 (Wang et al., 2000; Kaeser et al., 2011; Dong et al., 2018; Quade et al., 2019) as well as the diffusive behaviour of VGCCs at the plasma membrane (Schneider et al., 2015; Heck et al., 2019). Any or all of these factors could contribute to the lack of correlation observed between Cav2.1 and functional parameters. It would be particularly interesting to use the same correlative approach to explore how the diverse complement of VGCC subtypes modulates synapse function, as well as the link between vesicle position and specific calcium channel subtypes.

Similarly, we found no correlation between the levels of Bassoon and either calcium influx or neurotransmitter release, in agreement with studies using other correlative methods (Holderith et al., 2020). We previously found that Bassoon clustering density was negatively correlated with neurotransmitter release and hypothesised this was due to a molecular crowding effect that limited the recruitment of other AZ proteins such as RIM and Cav2.1 (Glebov et al., 2017). Here, although we did not observe a negative correlation, we did find a significant increase in Bassoon detections and a larger proportion of multiple Bassoon SSDs in the small subset of synapses without detectable neurotransmitter release, consistent with increased Bassoon enrichment limiting presynaptic function. Furthermore, in synapses with multiple Bassoon SSDs in which release could be quantified, both the number and volume of Bassoon detections negatively correlated with the ratio ΔG/ΔR, a measure of the calcium dependence of release, suggesting a complex interplay between the spatial relationships of the AZ matrix

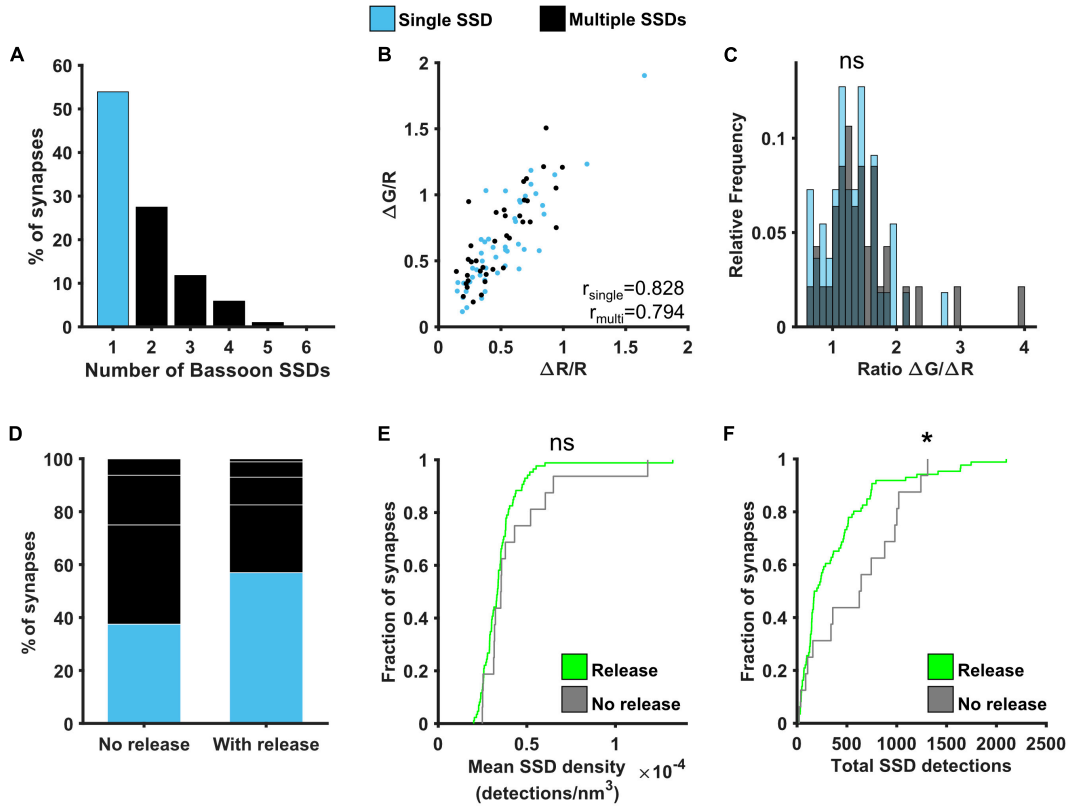

FIGURE 6 | Effect of Bassoon nanoscale organisation on neurotransmitter release. **(A)** Distribution of the number of Bassoon SSDs per synapse. **(B)** ΔG/R and ΔR/R responses from synapses *post hoc* labelled for Bassoon and identified as containing a single (blue) or multiple (black) Bassoon SSDs show a positive correlation (Spearman's rank correlation, r_{single} = 0.828, $p < 0.001$, n_{single} = 49 synapses, r_{multi} = 0.794, $p < 0.001$, n_{multi} = 37 synapses). **(C)** Distribution of the ratio ΔG/ΔR for the two group of synapses. Distributions are not significantly different (Kolmogorov-Smirnov test, p = 0.575, n_{single} = 49, $n_{multiple}$ = 37). **(D)** Percentage of synapses with single or multiple Bassoon SSDs in synapses without detectable release (left, n = 16) or with release (right, n = 86). White lines indicate separation of multiple SSDs by number. **(E)** Cumulative frequency distribution of the mean density of detections in Bassoon SSDs per synapse (number of detections/nm^3) in synapses with (green) or without (grey) detectable release to a 10AP stimulus (Kolmogorov-Smirnov test, p = 0.355, $n_{release}$ = 86, $n_{norelease}$ = 16). **(F)** Cumulative frequency distribution of the total number of detections in Bassoon SSDs per synapse in synapses with (green) or without (grey) detectable release to a 10AP stimulus (Kolmogorov-Smirnov test, p = 0.041, $n_{release}$ = 86, $n_{norelease}$ = 16). *$p < 0.05$.

and VGCCs and neurotransmitter release, which will require further investigation.

Using the number of SypHy detections obtained with dSTORM as a proportional measure of the total vesicle pool, we also saw no correlation with release or calcium influx, in agreement with EM studies showing the size of the total vesicle pool does not correlate with P_r, and that bouton volume shows only a weak relationship (Branco et al., 2010; Holderith et al., 2012).

Whilst the proteins we examined in this study showed few significant correlations with presynaptic functional measures, we have provided proof of principle of a correlative approach that can be used to examine functional properties and nanoscale protein organisation at individual presynaptic boutons. Nevertheless, there are some limitations to this technique which must be considered. First, as with all types of image analysis, detection thresholds must be applied. Here, using Voronoi segmentation for dSTORM imaging, we excluded low density detections that may arise from non-specific background or from isolated molecules that are not part of a cluster, perhaps because they are diffusing. By their nature these detections would not significantly alter the total number of counts and they are unlikely to substantially contribute to synapse function since they represent a minority of detections when compared to the larger clusters of protein. For SypHy, the highest density localisations arise from the total pool of SVs, which can be localised away from the AZ (Marra et al., 2012), hence this segmentation method may exclude localisations from surface stranded protein or individual SVs docked at the AZ. As the SSDs of Bassoon and Cav2.1 are located at the AZ, in some synapses they did not overlap with the segmented cluster of SypHy and had to be manually selected as belonging to the same bouton by visually inspecting individual SypHy localisations. If there was any ambiguity as to which SSD was associated with a SypHy cluster the synapse was excluded (**Supplementary Figure 3**). Second, despite applying manual correction, we still found a significant number of SypHy-RGECO positive synapses without any Cav2.1 or Bassoon SSD, for which there are several

possible explanations. The protein may not have been present at the bouton, which is more likely in the case of Cav2.1 as it is known that different synapses can preferentially express other Cav2 subtypes (Reid et al., 1997). This is unlikely the case for Bassoon as it is thought to be ubiquitously expressed at synapses, although boutons lacking Bassoon maintain some enrichment of VGCCs and capacity to release (Davydova et al., 2014). Another explanation could be that the protein was expressed, but at a level below our detection threshold. Whilst we used standard immunolabelling techniques with commercially conjugated antibodies that offer high efficiency labelling, this may also vary between proteins and samples. Finally, the z-range in which we can localise fluorophores is limited to ∼1 um and depending on the size and orientation of the bouton in relation to the focal plane, the SSD of Bassoon or Cav2.1 may lie outside of this range. This limitation could possibly mean that some synapses were incorrectly classified as containing a single rather than multiple SSDs. This could occur if the synapse was sufficiently large to extend beyond the 1um range or the AZ SSD was detected only at the edge of the focal range and extended beyond it, which is only likely to be the case in a small proportion of synapses.

For functional imaging we used SypHy-RGECO, due to its ability to measure two aspects of presynaptic function simultaneously. Again, thresholding must be applied for both SypHy and RGECO channels, and some synapses display a calcium response but not a measurable release. We interpret these as having low release probability, as there may be a response that cannot be distinguished from baseline noise. There is a possibility that these are silent presynaptic terminals (Crawford and Mennerick, 2012), but to determine this would require using a stronger stimulus or more sensitive indicators to improve response detection, such as iGlusNFR for neurotransmitter release (Marvin et al., 2013, 2018, 2019) and GCaMP8 (Zhang et al., 2020) or jRCaMP1a/jRGECO1a (Dana et al., 2016) for calcium influx. Our correlative approach would work equally well with any of these reporters. In addition, whilst we used a 10AP stimulation protocol, which provides a robust response within the linear range for both reporters (Jackson and Burrone, 2016), different stimulation protocols could be employed to explore synaptic function in more depth than presented here.

The correlative approach would also be applicable to link function with the organisation of other synaptic proteins of interest and could be adapted to use different SRM methods. The main drawback of dSTORM imaging is the limited number of proteins that can be imaged at once. Here we have used two-colour imaging, with one channel occupied by GFP labelling for SypHy-RGECO, which is necessary to precisely relocate the same boutons. However, SD-dSTORM could allow the addition of a third fluorophore to examine two proteins of interest alongside GFP. In the dense protein environment of the presynapse, where proteins of interest are in very close proximity, care must be taken to ensure that single molecule localisation without crosstalk is achieved. Alternatively, Exchange-PAINT, SIM or the more recently developed MINFLUX could be used to improve the multiplexing possibilities of this technique, despite their own limitations (Jungmann et al., 2014; Gwosch et al., 2020; Butkevich et al., 2021). Live-SRM or single particle tracking could also add further important information about the dynamics of the nanoscale organisation of synaptic proteins and its role in regulating the calcium-dependence of release (Heine and Holcman, 2020).

Overall, we have demonstrated a flexible method that combines two imaging modalities at the same synapse to investigate functional properties and nanoscale organisation. Large numbers of synapses can be examined using this approach, enabling the wide range of synaptic heterogeneity to be explored, which will be necessary to fully understand the synaptic structure-function link.

DATA AVAILABILITY STATEMENT

The raw data supporting the conclusions of this article will be made available by the authors, without undue reservation.

ETHICS STATEMENT

Ethical review and approval was not required for the animal study because only schedule 1 procedures performed by a competent individual were used in these studies, which are exempt under the Animals (Scientific Procedures) Act 1986.

AUTHOR CONTRIBUTIONS

RJ, BC, and JB designed experiments, edited, and approved the manuscript. RJ performed and analysed functional experiments. BC performed and analysed dSTORM experiments. RJ and BC drafted the manuscript. All authors contributed to the article and approved the submitted version.

FUNDING

This research was funded in whole, or in part, by the Wellcome Trust (Grant No. 215508/Z/19/Z to JB). For the purpose of open access, the authors have applied a CC BY public copyright license to any Author-Accepted Manuscript version arising from this submission. This work was additionally funded by an IBIN grant to RJ and BC and an MCSA-IF fellowship to BC.

ACKNOWLEDGMENTS

We would like to thank Nicolas Bourg and Abbelight for the SAFeRedSTORM module and software, Olympus for the IX3 microscope, Florian Levet and Jean-Baptiste Sibarita (IINS, Bordeaux University) for PoCA software and Marcio Guiomar de Oliveira for preparation of dissociated hippocampal neurons.

SUPPLEMENTARY MATERIAL

The Supplementary Material for this article can be found online at: https://www.frontiersin.org/articles/10.3389/fnsyn.2022.830583/full#supplementary-material

REFERENCES

Branco, T., Marra, V., and Staras, K. (2010). Examining size-strength relationships at hippocampal synapses using an ultrastructural measurement of synaptic release probability. *J. Struct. Biol.* 172, 203–210. doi: 10.1016/j.jsb.2009.10.014

Butkevich, A. N., Weber, M., Cereceda Delgado, A. R., Ostersehlt, L. M., D'Este, E., and Hell, S. W. (2021). Photoactivatable fluorescent dyes with hydrophilic caging groups and their use in multicolor nanoscopy. *J. Am. Chem. Soc.* 143, 18388–18393. doi: 10.1021/jacs.1c09999

Choi, J.-H., Yu, N.-K., Baek, G.-C., Bakes, J., Seo, D., Nam, H. J., et al. (2014). Optimization of AAV expression cassettes to improve packaging capacity and transgene expression in neurons. *Mol. Brain* 7:17. doi: 10.1186/1756-6606-7-17

Compans, B., Camus, C., Kallergi, E., Sposini, S., Martineau, M., Butler, C., et al. (2021). NMDAR-dependent long-term depression is associated with increased short term plasticity through autophagy mediated loss of PSD-95. *Nat. Commun.* 12:2849. doi: 10.1038/s41467-021-23133-9

Crawford, D. C., and Mennerick, S. (2012). Presynaptically silent synapses: dormancy and awakening of presynaptic vesicle release. *Neuroscientist* 18, 216–223. doi: 10.1177/1073858411418525

Dana, H., Mohar, B., Sun, Y., Narayan, S., Gordus, A., Hasseman, J. P., et al. (2016). Sensitive red protein calcium indicators for imaging neural activity. *eLife* 5:e12727. doi: 10.7554/eLife.12727

Dani, A., Huang, B., Bergan, J., Dulac, C., and Zhuang, X. (2010). Superresolution imaging of chemical synapses in the brain. *Neuron* 68, 843–856. doi: 10.1016/j.neuron.2010.11.021

Davydova, D., Marini, C., King, C., Klueva, J., Bischof, F., Romorini, S., et al. (2014). Bassoon specifically controls presynaptic P/Q-type Ca2+ channels via RIM-binding protein. *Neuron* 82, 181–194. doi: 10.1016/j.neuron.2014.02.012

del Castillo, J., and Katz, B. (1954). Quantal components of the end-plate potential. *J. Physiol.* 124, 560–573. doi: 10.1113/jphysiol.1954.sp005129

Dodge, F. A., and Rahamimoff, R. (1967). Co-operative action of calcium ions in transmitter release at the neuromuscular junction. *J. Physiol.* 193, 419–432. doi: 10.1113/jphysiol.1967.sp008367

Dong, W., Radulovic, T., Goral, R. O., Thomas, C., Suarez Montesinos, M., Guerrero-Given, D., et al. (2018). CAST/ELKS proteins control voltage-gated Ca 2+ channel density and synaptic release probability at a mammalian central synapse. *Cell Rep.* 24, 284.e6–293.e6. doi: 10.1016/j.celrep.2018.06.024

Dreosti, E., Odermatt, B., Dorostkar, M. M., and Lagnado, L. (2009). A genetically encoded reporter of synaptic activity in vivo. *Nat. Methods* 6, 883–889. doi: 10.1038/nmeth.1399

Eggermann, E., Bucurenciu, I., Goswami, S. P., and Jonas, P. (2012). Nanodomain coupling between Ca 2+ channels and sensors of exocytosis at fast mammalian synapses. *Nat. Rev. Neurosci.* 13, 7–21. doi: 10.1038/nrn3125

Éltes, T., Kirizs, T., Nusser, Z., and Holderith, N. (2017). Target cell type-dependent differences in Ca2+ channel function underlie distinct release probabilities at hippocampal glutamatergic terminals. *J. Neurosci.* 37, 1910–1924. doi: 10.1523/JNEUROSCI.2024-16.2017

Ermolyuk, Y. S., Alder, F. G., Henneberger, C., Rusakov, D. A., Kullmann, D. M., and Volynski, K. E. (2012). Independent regulation of basal neurotransmitter release efficacy by variable Ca2+ influx and bouton size at small central synapses. *PLoS Biol.* 10:e1001396. doi: 10.1371/journal.pbio.1001396

Früh, S. M., Matti, U., Spycher, P. R., Rubini, M., Lickert, S., Schlichthaerle, T., et al. (2021). Site-specifically-labeled antibodies for super-resolution microscopy reveal *In Situ* linkage errors. *ACS Nano* 15, 12161–12170. doi: 10.1021/acsnano.1c03677

Fukata, Y., Dimitrov, A., Boncompain, G., Vielemeyer, O., Perez, F., and Fukata, M. (2013). Local palmitoylation cycles define activity-regulated postsynaptic subdomains. *J. Cell Biol.* 202, 145–161. doi: 10.1083/jcb.201302071

Gasparini, S., Kasyanov, A. M., Pietrobon, D., Voronin, L. L., and Cherubini, E. (2001). Presynaptic R-Type calcium channels contribute to fast excitatory synaptic transmission in the rat hippocampus. *J. Neurosci.* 21, 8715–8721. doi: 10.1523/JNEUROSCI.21-22-08715.2001

Glebov, O. O., Jackson, R. E., Winterflood, C. M., Owen, D. M., Barker, E. A., Doherty, P., et al. (2017). Nanoscale structural plasticity of the active zone matrix modulates presynaptic function. *Cell Rep.* 18, 2715–2728. doi: 10.1016/j.celrep.2017.02.064

Granseth, B., Odermatt, B., Royle, S. J. J., and Lagnado, L. (2006). Clathrin-mediated endocytosis is the dominant mechanism of vesicle retrieval at hippocampal synapses. *Neuron* 51, 773–786. doi: 10.1016/j.neuron.2006.08.029

Gwosch, K. C., Pape, J. K., Balzarotti, F., Hoess, P., Ellenberg, J., Ries, J., et al. (2020). MINFLUX nanoscopy delivers 3D multicolor nanometer resolution in cells. *Nat. Methods* 17, 217–224. doi: 10.1038/s41592-019-0688-0

Haas, K. T., Compans, B., Letellier, M., Bartol, T. M., Grillo-Bosch, D., Sejnowski, T. J., et al. (2018). Pre-post synaptic alignment through neuroligin-1 tunes synaptic transmission efficiency. *eLife* 7:e31755. doi: 10.7554/eLife.31755

Harris, K. M., and Weinberg, R. J. (2012). Ultrastructure of synapses in the mammalian brain. *Cold Spring Harb. Perspect. Biol.* 4:a005587. doi: 10.1101/cshperspect.a005587

Heck, J., Parutto, P., Ciuraszkiewicz, A., Bikbaev, A., Freund, R., Mitlöhner, J., et al. (2019). Transient confinement of CaV2.1 Ca2+-Channel splice variants shapes synaptic short-term plasticity. *Neuron* 103, 66.e12–79.e12. doi: 10.1016/j.neuron.2019.04.030

Heine, M., and Holcman, D. (2020). Asymmetry between pre- and postsynaptic transient nanodomains shapes neuronal communication. *Trends Neurosci.* 43, 182–196. doi: 10.1016/j.tins.2020.01.005

Holderith, N., Heredi, J., Kis, V., and Nusser, Z. (2020). A high-resolution method for quantitative molecular analysis of functionally characterized individual synapses. *Cell Rep.* 32:107968. doi: 10.1016/j.celrep.2020.107968

Holderith, N., Lorincz, A., Katona, G., Rózsa, B., Kulik, A., Watanabe, M., et al. (2012). Release probability of hippocampal glutamatergic terminals scales with the size of the active zone. *Nat. Neurosci.* 15, 988–997. doi: 10.1038/nn.3137

Hoppa, M. B., Gouzer, G., Armbruster, M., and Ryan, T. A. (2014). Control and plasticity of the presynaptic action potential waveform at small CNS nerve terminals. *Neuron* 84, 778–789. doi: 10.1016/j.neuron.2014.09.038

Hruska, M., Henderson, N., Le Marchand, S. J., Jafri, H., and Dalva, M. B. (2018). Synaptic nanomodules underlie the organization and plasticity of spine synapses. *Nat. Neurosci.* 21, 671–682. doi: 10.1038/s41593-018-0138-9

Jackson, R. E., and Burrone, J. (2016). Visualizing presynaptic calcium dynamics and vesicle fusion with a single genetically encoded reporter at individual synapses. *Front. Synaptic Neurosci.* 8:21. doi: 10.3389/fnsyn.2016.00021

Jungmann, R., Avendaño, M. S., Woehrstein, J. B., Dai, M., Shih, W. M., and Yin, P. (2014). Multiplexed 3D cellular super-resolution imaging with DNA-PAINT and Exchange-PAINT. *Nat. Methods* 11, 313–318. doi: 10.1038/nmeth.2835

Kaeser, P. S., Deng, L., Wang, Y., Dulubova, I., Liu, X., Rizo, J., et al. (2011). RIM proteins tether Ca2+ Channels to presynaptic active zones via a direct PDZ-Domain interaction. *Cell* 144, 282–295. doi: 10.1016/j.cell.2010.12.029

Levet, F., Hosy, E., Kechkar, A., Butler, C., Beghin, A., Choquet, D., et al. (2015). SR-Tesseler: a method to segment and quantify localization-based super-resolution microscopy data. *Nat. Methods* 12, 1065–1071. doi: 10.1038/nmeth.3579

Levet, F., Julien, G., Galland, R., Butler, C., Beghin, A., Chazeau, A., et al. (2019). A tessellation-based colocalization analysis approach for single-molecule localization microscopy. *Nat. Commun.* 10:2379. doi: 10.1038/s41467-019-10007-4

Li, Y., and Tsien, R. W. (2012). pHTomato, a red, genetically encoded indicator that enables multiplex interrogation of synaptic activity. *Nat. Neurosci.* 15, 1047–1053. doi: 10.1038/nn.3126

Lipscombe, D., Allen, S. E., and Toro, C. P. (2013). Control of neuronal voltage-gated calcium ion channels from RNA to protein. *Trends Neurosci.* 36, 598–609. doi: 10.1016/j.tins.2013.06.008

Liu, A., Huang, X., He, W., Xue, F., Yang, Y., Liu, J., et al. (2021). pHmScarlet is a pH-sensitive red fluorescent protein to monitor exocytosis docking and fusion steps. *Nat. Commun.* 12:1413. doi: 10.1038/s41467-021-21666-7

Luebke, I., Dunlap, K., and Turner, T. J. (1993). Multiple calcium channel types control glutamatergic synaptic transmission in the hippocampus. *Neuron* 11, 895–902. doi: 10.1016/0896-6273(93)90119-c

MacGillavry, H. D., Song, Y., Raghavachari, S., and Blanpied, T. A. (2013). Nanoscale scaffolding domains within the postsynaptic density concentrate synaptic ampa receptors. *Neuron* 78, 615–622. doi: 10.1016/j.neuron.2013.03.009

Marra, V., Burden, J. J., Thorpe, J. R., Smith, I. T., Smith, S. L., Häusser, M., et al. (2012). A preferentially segregated recycling vesicle pool of limited size supports neurotransmission in native central synapses. *Neuron* 76, 579–589. doi: 10.1016/j.neuron.2012.08.042

Marvin, J. S., Borghuis, B. G., Tian, L., Cichon, J., Harnett, M. T., Akerboom, J., et al. (2013). An optimized fluorescent probe for visualizing glutamate neurotransmission. *Nat. Methods* 10, 162–170. doi: 10.1038/nmeth.2333

Marvin, J. S., Scholl, B., Wilson, D. E., Podgorski, K., Kazemipour, A., Müller, J. A., et al. (2018). Stability, affinity, and chromatic variants of the glutamate sensor iGluSnFR. *Nat. Methods* 15, 936–939. doi: 10.1038/s41592-018-0171-3

Marvin, J. S., Shimoda, Y., Magloire, V., Leite, M., Kawashima, T., Jensen, T. P., et al. (2019). A genetically encoded fluorescent sensor for in vivo imaging of GABA. *Nat. Methods* 16, 763–770. doi: 10.1038/s41592-019-0471-2

Maschi, D., and Klyachko, V. A. (2017). Spatiotemporal regulation of synaptic vesicle fusion sites in central synapses. *Neuron* 94, 65.e3–73.e3. doi: 10.1016/j.neuron.2017.03.006

Miesenböck, G., de Angelis, D. A., and Rothman, J. E. (1998). Visualizing secretion and synaptic transmission with pH-sensitive green fluorescent proteins. *Nature* 394, 192–195. doi: 10.1038/28190

Miki, T., Kaufmann, W. A., Malagon, G., Gomez, L., Tabuchi, K., Watanabe, M., et al. (2017). Numbers of presynaptic Ca2+ channel clusters match those of functionally defined vesicular docking sites in single central synapses. *Proc. Natl. Acad. Sci. U.S.A.* 114, E5246–E5255. doi: 10.1073/pnas.1704470114

Murthy, V. N., Schikorski, T., Stevens, C. F., and Zhu, Y. (2001). Inactivity produces increases in neurotransmitter release and synapse size. *Neuron* 32, 673–682. doi: 10.1016/S0896-6273(01)00500-1

Murthy, V. N., Sejnowski, T. J., and Stevens, C. F. (1997). Heterogeneous release properties of visualized individual hippocampal synapses. *Neuron* 18, 599–612. doi: 10.1016/S0896-6273(00)80301-3

Nair, D., Hosy, E., Petersen, J. D., Constals, A., Giannone, G., Choquet, D., et al. (2013). Super-resolution imaging reveals that AMPA receptors inside synapses are dynamically organized in nanodomains regulated by PSD95. *J. Neurosci.* 33, 13204–13224. doi: 10.1523/JNEUROSCI.2381-12.2013

Nakai, J., Ohkura, M., and Imoto, K. (2001). A high signal-to-noise Ca2+ probe composed of a single green fluorescent protein. *Nat. Biotechnol.* 19, 137–141. doi: 10.1038/84397

Novak, P., Gorelik, J., Vivekananda, U., Shevchuk, A. I., Ermolyuk, Y. S., Bailey, R. J., et al. (2013). Nanoscale-targeted patch-clamp recordings of functional presynaptic ion channels. *Neuron* 79, 1067–1077. doi: 10.1016/j.neuron.2013.07.012

Parajuli, L. K., Nakajima, C., Kulik, A., Matsui, K., Schneider, T., Shigemoto, R., et al. (2012). Quantitative regional and ultra structural localization of the Ca v2.3 subunit of R-type calcium channel in mouse brain. *J. Neurosci.* 32, 13555–13567. doi: 10.1523/JNEUROSCI.1142-12.2012

Platonova, E., Winterflood, C. M., and Ewers, H. (2015). A simple method for GFP- and RFP-based dual color single-molecule localization microscopy. *ACS Chem. Biol.* 10, 1411–1416. doi: 10.1021/acschembio.5b00046

Quade, B., Camacho, M., Zhao, X., Orlando, M., Trimbuch, T., Xu, J., et al. (2019). Membrane bridging by Munc13-1 is crucial for neurotransmitter release. *eLife* 8:e42806. doi: 10.7554/eLife.42806

Rebola, N., Reva, M., Kirizs, T., Szoboszlay, M., Lőrincz, A., Moneron, G., et al. (2019). Distinct nanoscale calcium channel and synaptic vesicle topographies contribute to the diversity of synaptic function. *Neuron* 104, 693.e9–710.e9. doi: 10.1016/j.neuron.2019.08.014

Reid, C. A., Clements, J. D., and Bekkers, J. M. (1997). Nonuniform distribution of Ca 2 channel subtypes on presynaptic terminals of excitatory synapses in hippocampal cultures. *J. Neurosci.* 17, 2738–2745. doi: 10.1523/JNEUROSCI.17-08-02738.1997

Rose, T., Schoenenberger, P., Jezek, K., and Oertner, T. G. (2013). Developmental refinement of vesicle cycling at schaffer collateral synapses. *Neuron* 77, 1109–1121. doi: 10.1016/j.neuron.2013.01.021

Sabater, V. G., Rigby, M., and Burrone, J. (2021). Voltage-gated potassium channels ensure action potential shape fidelity in distal axons. *J. Neurosci.* 41, 5372–5385. doi: 10.1523/JNEUROSCI.2765-20.2021

Sakamoto, H., Ariyoshi, T., Kimpara, N., Sugao, K., Taiko, I., Takikawa, K., et al. (2018). Synaptic weight set by Munc13-1 supramolecular assemblies. *Nat. Neurosci.* 21, 41–55. doi: 10.1038/s41593-017-0041-9

Sankaranarayanan, S., de Angelis, D., Rothman, J. E., and Ryan, T. A. (2000). The use of pHluorins for optical measurements of presynaptic activity. *Biophys. J.* 79, 2199–2208. doi: 10.1016/S0006-3495(00)76468-X

Scheuber, A., Miles, R., and Poncer, J. C. (2004). Presynaptic Cav2.1 and Cav2.2 differentially influence release dynamics at hippocampal excitatory synapses. *J. Neurosci.* 24, 10402–10409. doi: 10.1523/JNEUROSCI.1664-04.2004

Schikorski, T., and Stevens, C. F. (1997). Quantitative ultrastructural analysis of hippocampal excitatory synapses. *J. Neurosci.* 17, 5858–5867. doi: 10.1523/JNEUROSCI.17-15-05858.1997

Schneider, R., Hosy, E., Kohl, J., Klueva, J., Choquet, D., Thomas, U., et al. (2015). Mobility of calcium channels in the presynaptic membrane. *Neuron* 86, 672–679. doi: 10.1016/j.neuron.2015.03.050

Sigal, Y. M., Zhou, R., and Zhuang, X. (2018). Visualizing and discovering cellular structures with super-resolution microscopy. *Science* 361, 880–887. doi: 10.1126/science.aau1044

Südhof, T. C. (2012). The presynaptic active zone. *Neuron* 75, 11–25. doi: 10.1016/j.neuron.2012.06.012

Tang, A. H., Chen, H., Li, T. P., Metzbower, S. R., MacGillavry, H. D., and Blanpied, T. A. (2016). A trans-synaptic nanocolumn aligns neurotransmitter release to receptors. *Nature* 536, 210–214. doi: 10.1038/nature19058

Testa, I., Wurm, C. A., Medda, R., Rothermel, E., von Middendorf, C., Fölling, J., et al. (2010). Multicolor fluorescence nanoscopy in fixed and living cells by exciting conventional fluorophores with a single wavelength. *Biophys. J.* 99, 2686–2694. doi: 10.1016/j.bpj.2010.08.012

Voglmaier, S. M., Kam, K., Yang, H., Fortin, D. L., Hua, Z., Nicoll, R. A., et al. (2006). Distinct endocytic pathways control the rate and extent of synaptic vesicle protein recycling. *Neuron* 51, 71–84. doi: 10.1016/j.neuron.2006.05.027

Walker, A. S., Burrone, J., and Meyer, M. P. (2013). Functional imaging in the zebrafish retinotectal system using RGECO. *Front. Neural Circuits* 7:34. doi: 10.3389/fncir.2013.00034

Wang, W., Kim, C. K., and Ting, A. Y. (2019). Molecular tools for imaging and recording neuronal activity. *Nat. Chem. Biol.* 15, 101–110. doi: 10.1038/s41589-018-0207-0

Wang, Y., Sugita, S., and Südhof, T. C. (2000). The RIM/NIM family of neuronal C2 domain proteins: interactions with Rab3 and a new class of Src homology 3 domain proteins. *J. Biol. Chem.* 275, 20033–20044. doi: 10.1074/jbc.M909008199

Wheeler, D. B., Randall, A., and Tsien, R. W. (1994). Roles of N-type and Q-type Ca2+ channels in supporting hippocampal synaptic transmission. *Science* 264, 107–111. doi: 10.1126/science.7832825

Xu-Friedman, M. A., Harris, K. M., and Regehr, W. G. (2001). Three-dimensional comparison of ultrastructural characteristics at depressing and facilitating synapses onto cerebellar purkinje cells. *J. Neurosci.* 21, 6666–6672. doi: 10.1523/JNEUROSCI.21-17-06666.2001

Zhang, Y., Rózsa, M., Bushey, D., Zheng, J., Reep, D., Broussard, G. J., et al. (2020). jGCaMP8: a new suite of fast and sensitive calcium indicators. doi: 10.25378/janelia.13148243

Conflict of Interest: The authors declare that the research was conducted in the absence of any commercial or financial relationships that could be construed as a potential conflict of interest.

Publisher's Note: All claims expressed in this article are solely those of the authors and do not necessarily represent those of their affiliated organizations, or those of the publisher, the editors and the reviewers. Any product that may be evaluated in this article, or claim that may be made by its manufacturer, is not guaranteed or endorsed by the publisher.

frontiers in Synaptic Neuroscience

REVIEW
published: 25 February 2022
doi: 10.3389/fnsyn.2022.826098

Synaptic Vesicle Recycling and the Endolysosomal System: A Reappraisal of Form and Function

Daniela Ivanova[1,2,3]* *and Michael A. Cousin*[1,2,3]*

[1] Centre for Discovery Brain Sciences, University of Edinburgh, Edinburgh, United Kingdom, [2] Muir Maxwell Epilepsy Centre, University of Edinburgh, Edinburgh, United Kingdom, [3] Simons Initiative for the Developing Brain, University of Edinburgh, Edinburgh, United Kingdom

The endolysosomal system is present in all cell types. Within these cells, it performs a series of essential roles, such as trafficking and sorting of membrane cargo, intracellular signaling, control of metabolism and degradation. A specific compartment within central neurons, called the presynapse, mediates inter-neuronal communication via the fusion of neurotransmitter-containing synaptic vesicles (SVs). The localized recycling of SVs and their organization into functional pools is widely assumed to be a discrete mechanism, that only intersects with the endolysosomal system at specific points. However, evidence is emerging that molecules essential for endolysosomal function also have key roles within the SV life cycle, suggesting that they form a continuum rather than being isolated processes. In this review, we summarize the evidence for key endolysosomal molecules in SV recycling and propose an alternative model for membrane trafficking at the presynapse. This includes the hypotheses that endolysosomal intermediates represent specific functional SV pools, that sorting of cargo to SVs is mediated via the endolysosomal system and that manipulation of this process can result in both plastic changes to neurotransmitter release and pathophysiology via neurodegeneration.

Keywords: vesicle, endocytosis, endosome, trafficking, presynapse, lysosome

OPEN ACCESS

Edited by:
Lucia Tabares, Seville University, Spain

Reviewed by:
Rafael Fernández-Chacón, Institute of Biomedicine of Seville (CSIC), Spain
Cláudia Guimas Almeida, New University of Lisbon, Portugal

***Correspondence:**
Daniela Ivanova
D.Ivanova@ed.ac.uk
Michael A. Cousin
M.Cousin@ed.ac.uk

Received: *30 November 2021*
Accepted: *03 February 2022*
Published: *25 February 2022*

Citation:
Ivanova D and Cousin MA (2022) Synaptic Vesicle Recycling and the Endolysosomal System: A Reappraisal of Form and Function. Front. Synaptic Neurosci. 14:826098. doi: 10.3389/fnsyn.2022.826098

INTRODUCTION

Compartmentalization in eukaryotic cells enables efficient spatiotemporal control of multiple parallel cellular processes by concentrating the required factors in confined microenvironments that provide the best conditions for these processes to proceed. The endomembrane system, which includes the majority of membrane-bound organelles and the plasma membrane, plays a key role in segregating the intracellular environment into functional hubs. However, organelles do not operate as autonomous modules and without a regulated exchange of molecules between the compartments, their overall function would soon be compromised. Therefore, all membrane-bound organelles engage in extensive communication that coordinates their functions and enables long-term maintenance of cellular homeostasis.

The Endolysosomal System

The endolysosomal system is a dynamic network of intracellular membranous organelles, where the endocytic, biosynthetic, and degradative pathways intersect (Maxfield and McGraw, 2004; Grant and Donaldson, 2009). This collection of organelles is a key sorting station distributing cargo to different membrane domains, a signaling hub regulating cellular metabolism and an intermediate to degradation (Klumperman and Raposo, 2014; Naslavsky and Caplan, 2018). The endolysosomal

system has been extensively studied in non-neuronal cells, however, in neurons its characteristics remain relatively ambiguous and poorly defined (Andres-Alonso et al., 2021; Kuijpers et al., 2021a). In non-neuronal cells, the highly heterogeneous collection of organelles which constitutes the endolysosomal system is generally classified into several compartments, including early endosome (EE), recycling endosome (RE), late endosome (LE), and lysosome (Maxfield and McGraw, 2004; Klumperman and Raposo, 2014; Naslavsky and Caplan, 2018). It is still a matter of debate whether these heterogeneous compartments with overlapping, but also unique, set of proteins are distinct organelles or a series of structures that undergo maturation and "evolve" from each other.

The EE is a major station for sorting of cargo previously internalized by endocytosis. Some cargos are recycled via a rapid recycling pathway directly from EE, whereas others are trafficked to specialized RE, or endocytic recycling compartment, which is often but not always clustered in the perinuclear region, beside the microtubule-organizing center of the cell (Grant and Donaldson, 2009; Naslavsky and Caplan, 2018). In contrast to EEs, from which cargo can be recycled directly to the plasma membrane, the RE is involved in the "slow" recycling of internalized cargo (Li and DiFiglia, 2012). LEs are a group of organelles structurally and functionally related to lysosomes. Like lysosomes, LEs play a key role in protein degradation and are also essential components of the autophagy pathway (Scott et al., 2014). In addition, they are required for nutrient sensing and transport of cholesterol and other lipids to other membranous organelles in the cell (Scott et al., 2014). Lysosomes are the main waste disposal system of the cell, degrading materials delivered by autophagy or endocytosis into their basic building blocks. In addition, they participate in multiple other cellular processes, including regulation of metabolic signaling, gene expression, plasma membrane repair and lipid sensing and trafficking (Luzio et al., 2007; Saftig and Klumperman, 2009; Ballabio and Bonifacino, 2020).

Synaptic Vesicle Recycling

The recycling of neurotransmitter-containing synaptic vesicles (SVs) at nerve terminals is one of the most extensively studied cellular pathways in central neurons. This process is essential for the neuronal communication, with even small perturbations resulting in a series of neurodevelopmental, neurodegenerative disorders or death (Bonnycastle et al., 2021; Overhoff et al., 2021). SVs are small 50 nm organelles that accumulate neurotransmitter via specialized transporters that are coupled to an intraluminal protonmotive force generated by V-type ATPases on the SV membrane. Neurotransmitter-filled SVs undergo a series of molecular events before they are triggered to fuse with the presynaptic plasma membrane during synaptic stimulation. These include a physical attachment to the plasma membrane (docking), a transition to fusion competency (priming), and calcium-triggered fusion (exocytosis) (Brunger et al., 2018; Rizo, 2018). After fusion, SV proteins and membrane are retrieved via endocytosis that is triggered by neuronal activity and proceeds at different speeds and locations in the nerve terminal (Chanaday et al., 2019).

Within central nerve terminals, three pools of SVs have been described based on their availability for release, the readily releasable pool (RRP), recycling pool and resting/reserve pool. A fourth pool, termed "super pool," that is shared between neighboring *en passant* boutons and trafficked along the axon, has also been reported (Staras et al., 2010; Herzog et al., 2011; Zhang et al., 2019). Furthermore, several studies have suggested that separate SV pools drive different forms of neurotransmitter release (e.g., spontaneous, evoked synchronous and evoked asynchronous release) (Chanaday and Kavalali, 2018). However, this concept remains controversial, and has been refuted by others (Hua et al., 2010). This controversy may in large part be due to the fact that the majority of current studies focus on SV recycling as an isolated process. Our understanding of how the SV cycle integrates in the general endomembrane system in neurons and the functional implications of its communication with other membrane trafficking pathways, remains limited. Specifically, very little is known about the biogenesis and maintenance of the SV cluster across the lifespan of the neuron. Furthermore, fundamental questions about the mechanisms that mediate turnover of SV components also remain unanswered. These questions cannot be adequately addressed unless a more holistic understanding of the SV cycle and its place in the general endomembrane system in neurons is developed.

However, this important question is difficult to address, since there are only a few distinctive molecular markers that define EE and especially RE, which has made the characterization of their cellular localization and function a challenging endeavor. Defining EE and RE, their function in neuronal cells, and in particular in synaptic terminals, has proven to be a monumental task, partly due to the reductionist approach to SV recycling largely adopted by the field. Although it has its place, the fixation on detail often leads to inability to "see the wood for the trees."

There is accumulating evidence to suggest that SV recycling and axonal endolysosomal trafficking are both structurally and functionally linked. However, the extent to which they are entangled is difficult to envision because of the lack of a conceptual framework that juxtaposes the two pathways in synaptic terminals. In this review, we propose an alternative interpretation of SV recycling by proposing that the SV pool is an integral part of the endolysosomal system in neurons, with equivalents of EE, RE, LE, and lysosomes functioning in concert at the presynapse, and supporting not only synaptic transmission, but the overall health of the neuron. In doing so, we will discuss the current evidence for crosstalk and potential overlap between the endolysosomal system and the SV recycling pathway, by examining the role of endolysosomal molecules in SV recycling which form the foundation of a series of testable hypotheses for future studies.

ENDOCYTOSIS AND EARLY ENDOSOMES

Endocytosis

The first stage of the endolysosomal pathway is endocytosis. Due to its capacity to regulate the surface expression and

internalization of membrane and soluble molecules, endocytosis is a fundamental cellular mechanism that regulates a multitude of cellular processes, including uptake of nutrients, cell signaling, establishment of cellular polarity, cell motility, and neurotransmission (Conner and Schmid, 2003; Doherty and McMahon, 2009). Although clathrin-dependent endocytosis is the most studied and best characterized endocytosis pathway, owing to their high capacity, clathrin-independent mechanisms are now recognized as the main route for internalization of cargo, responsible for the majority (∼70%) of membrane and fluid uptake into the cell (Howes et al., 2010; Renard and Boucrot, 2021). Neurons and synaptic terminals are no exception from this rule. There is accumulating evidence, that clathrin-independent, bulk membrane retrieval is also the dominant pathway for membrane retrieval in central nerve terminals across a range of stimuli, but particularly during intense neuronal activity (Clayton et al., 2008; Kononenko et al., 2014). During this endocytic process, known as activity-dependent bulk endocytosis (ADBE), endosomes are formed directly from the plasma membrane (bulk endosomes) with SVs subsequently regenerated from these compartments (Kokotos and Cousin, 2015). Clathrin still performs an essential role in the reformation of SVs and selection of SV cargo, however, there is an emerging consensus that this occurs at the level of the internalized endosome, rather than at the plasma membrane (Watanabe et al., 2014; Kononenko and Haucke, 2015). The formation of endosomes can occur at different timescale from tens of milliseconds (e.g., the recently reported ultrafast endocytosis) to tens of seconds, depending on the strength of the stimulus input (Watanabe et al., 2013, 2018; Soykan et al., 2017). The lack of clathrin dependence of SV endocytosis is particularly pertinent in experiments performed at physiological temperatures (Kononenko et al., 2014; Watanabe et al., 2014; Delvendahl et al., 2016). In these conditions, the relatively slow assembly of the clathrin coat means that clathrin-mediated budding events that originate on the plasma membrane are finalized on the endosome, due to the rapid invagination of these structures. Several other forms of endocytosis have been proposed to operate at the presynapse: e.g., clathrin-independent endocytosis (CIE) (Soykan et al., 2016), clathrin-independent and calcium-independent endocytosis (Orlando et al., 2019) and "kiss-and-run" (Stevens and Williams, 2000; He et al., 2006; Zhang et al., 2009). However, they either represent the same process of clathrin-independent bulk membrane retrieval under a different name (CIE) or their existence and contribution to presynaptic function at typical small central nerve terminals remains a matter of debate ("kiss-and-run") (Granseth et al., 2006; LoGiudice and Matthews, 2006; Wu et al., 2014).

Early Endosome Function

Classical EEs in non-neuronal cells are marked by a series of molecules with specific functional roles. For example, they typically contain a high concentration of the lipid phosphatidylinositol 3-phosphate (PI(3)P), generated by the PI3-kinase VPS34 (Grant and Donaldson, 2009). VPS34 is a class III phosphatidylinositol 3-kinase that uses phosphatidylinositol as a substrate to generate PI(3)P. Previous studies have revealed an important role for VPS34 in EE-sorting and autophagy (Dall'Armi et al., 2013; Raiborg et al., 2013). Accumulation of PI(3)P is required for the recruitment of proteins to EEs that contain a FYVE PI(3)P-binding domain, such as early endosomal antigen 1 (EEA1) and rabenosyn-5. EEA1 functions as a tethering molecule that together with the endosomal soluble N-ethylmaleimide attachment protein receptor (SNARE) proteins controls the maturation of EE and their homotypic fusion (Maxfield and McGraw, 2004). SNARE proteins are classified as either Q- or R-SNAREs dependent on the presence of highly conserved glutamine or arginine residues at the center of their SNARE motif that drives fusion (Jahn and Scheller, 2006). Typically, R-SNAREs reside on the vesicular membrane whereas Q-SNAREs reside on target membranes. Rabenosyn-5 is also required for early endosomal fusion. In addition, rabenosyn-5, associates with another important class of EE-associated proteins, the dynamin-like EHD (Eps15 Homology Domain) ATPases, to regulate the transport of cargo from EEs to REs (Naslavsky and Caplan, 2011).

Another layer of identity for the organelles in the endolysosomal system is provided by the small Rab GTPases. They are considered "deciphers of organelle identity" and serve as platforms for recruitment of specific molecular machineries that confer unique functional characteristics to the particular organelles they bind to Stenmark (2009). The Rab GTPases that typically associate with EEs include Rab4, Rab5, Rab10, Rab14, Rab21, and Rab22 (Stenmark, 2009). It has been suggested that Rab proteins on EE cluster in district membrane microdomains. However, the precise mechanisms by which proteins are clustered into these domains remain poorly understood.

The SNARE-based vesicle fusion system is key for endosomal fusion and transport. After cargo proteins have been sorted into EE subdomains, a process of budding and fission of tubulovesicular structures occurs and the newly formed vesicles are trafficked to their target organelle (Grant and Donaldson, 2009). Some of the most important early endosomal SNAREs involved in homotypic and heterotypic endosomal fusion include VAMP4, syntaxin 6, syntaxin 12 (called syntaxin 13 in rat), and Vti1a. The R-SNARE VAMP4 and the Q-SNAREs syntaxin 6, syntaxin 12, and Vti1a predominantly localize at the trans-Golgi network (TGN), but are also found at the plasma membrane, EE and RE, with VAMP4 and syntaxin 6 also present on lysosome-related secretory organelles (Maxfield and McGraw, 2004). All four are implicated in the homotypic fusion of EEs by forming a SNARE complex with each other. In addition, VAMP4 and Vti1a have a central role in the retrograde endosome-to- TGN transport (Johannes and Popoff, 2008; Hirata et al., 2015). This pathway is important for recycling of molecules to the TGN, that in turn enable efficient anterograde transport of transmembrane proteins. Both VAMP4 and Vti1a are involved in maintaining the ribbon structure of the TGN (Shitara et al., 2013).

Early Endosome and Synaptic Vesicle Recycling

When considering the role of EEs in SV recycling, a key question to address is—are any of the molecules mentioned above implicated in this process? Many of the EE markers outlined

above are enriched in nerve terminals and some have links to SV recycling.

In neuronal axons, PI3-kinase activity is important for long-range trafficking, actin-based membrane ruffling and bulk membrane retrieval in growth cones, all of which support axonal outgrowth during neuronal development (Bonanomi et al., 2008; Zhou et al., 2013; Lorenzo et al., 2014). In mature presynaptic boutons, PI3-kinase activity supports actin remodeling and a signaling cascade linked to ADBE (Holt et al., 2003; Nicholson-Fish et al., 2016). Furthermore, inhibition of PI3-kinase activity stalls SV recycling and results in the appearance of numerous cisternae in synaptic terminals (Rizzoli and Betz, 2002; Richards et al., 2004). Presynaptic PI3-kinase activity is coupled to membrane depolarization and calcium influx, in a similar manner to SV recycling (Nicholson-Fish et al., 2016). PI3-kinase activity is also associated with the SV protein synapsin and it is required for optimal replenishment of the RRP from the reserve pool (Cousin et al., 2003). However it should be noted that the PI3-kinase activity associated with synapsin was from Class I PI3-kinases [which generate $PI(3,4,5)P_3$], whereas the activity required for classical EE function is via Class III [which generate PI(3)P]. Although, FYVE-domain-containing proteins, such as EEA1 and rabenosyn-5 were reported to show a polarized distribution to the somato-dendritic domain, they have been detected in axons (Selak et al., 2004; Ackermann et al., 2019; Goto-Silva et al., 2019). However, more research is warranted to shed light on their exact presynaptic function. Finally, biochemical studies examining endosomes purified from AP1 (adaptor protein 1) σ knockout mice suggest that VPS34 is required for the maturation of LE and lysosomes (multivesicular bodies) in axons via a mechanism which involves sorting at presynaptic endosomes mediated by ADP-ribosylation factor GTPase activating protein 1 and Rab5 GDP/GTP exchange factor (Candiello et al., 2016). This implies that, in presynaptic terminals, PI3-kinase activity may be at the core of a mechanism operating at the presynaptic endosomes which coordinates both generation of functional SVs and degradative pathways.

More than 11 distinct Rabs, including most of the early endosomal Rabs, were detected on the surface of highly purified SV membranes (Pavlos et al., 2010; Pavlos and Jahn, 2011). The best characterized early endosomal Rab, Rab5, is present in a subpopulation of SVs at the presynapse, with its manipulation resulting in alterations to SV recycling. For example, overexpression of Rab5 reduced the size of the recycling SV pool in hippocampal neurons by 50 % (Star et al., 2005), whereas dominant negative Rab5 expression impaired SV recycling (Shimizu et al., 2003; Wucherpfennig et al., 2003). Furthermore, wild-type and constitutively active Rab5 rescued defective SV endocytosis produced by knockdown of the protein kinase leucine rich repeat kinase 2 (LRRK2) (Shin et al., 2008). Another early endosome Rab, Rab4, traffics bidirectionally within the axon and is enriched at synapses, with a reduction in its anterograde trafficking resulting in aberrant synaptic morphology (Dey et al., 2017; White et al., 2020). Therefore, classical EE Rabs are present at the presynapse and modulate the SV life cycle, providing further evidence of crosstalk and functional integration.

A number of endosomal SNAREs are implicated in SV recycling. For example, a series of early endosome Q-SNARE proteins (Vti1a, syntaxin-6 and syntaxin-13) visit the presynaptic plasma membrane during brief stimulation or baseline activity, suggesting that endosomal SNAREs were present on SVs (Hoopmann et al., 2010; Ramirez et al., 2012). Vti1a resides on SVs that recycle at rest and sustain spontaneous neurotransmission (Ramirez et al., 2012). More recently, Vti1a (and Vti1b) were implicated in regulation of SV- and dense-core vesicle fusion at the presynapse by modulating secretory cargo sorting at the TGN (Emperador-Melero et al., 2018). The endosomal R-SNARE VAMP4, is present on highly purified SVs (Takamori et al., 2006), however, it does not readily visit the cell surface during neuronal activity (Raingo et al., 2012; Nicholson-Fish et al., 2015; Ivanova et al., 2021). VAMP4 has been proposed to control discrete forms of neurotransmission (Raingo et al., 2012; Lin et al., 2020), however, a more global role has recently been identified. This role is of a negative regulator of SV release probability (Pr), with VAMP4 levels on SVs controlled via both ADBE and downstream endolysosomal processing (Ivanova et al., 2021). Altogether, this highlights EE proteins as an integral component and a key modulator of SV recycling.

Retromer Function

The retromer protein complex is a critical component of the machinery mediating sorting and trafficking from EE (Seaman, 2012; Burd and Cullen, 2014). It was first characterized in yeast as a complex involved in the retrograde trafficking of membrane proteins, from peripheral endosomes to the TGN (Seaman et al., 1998), but a role in the trafficking of cargo to the plasma membrane has also been described (Small and Petsko, 2015). It consists of two main parts, the cargo-selection complex (CSC) and the tubulation module. In mammals, the two modules are not tightly coupled and can function independently. The CSC is composed of three proteins VPS26, VPS29, and VPS35, whereas the tubulation module is a heterodimer of the BAR (Bin, Amphiphysin, Rvs)-containing sorting nexins SNX1/SNX2 and SNX5/SNX6 (Seaman, 2012; Gallon and Cullen, 2015).

It is assumed that the GTPase activity of dynamin is important for scission of retromer-containing vesicles at EEs (Naslavsky and Caplan, 2018). Association of EHD ATPases and several of their endocytic interaction partners (e.g., syndapin and MICAL-like protein 1) with retromer in domains where vesicles are being generated at EE has also been shown (Gokool et al., 2007; Naslavsky and Caplan, 2011; McKenzie et al., 2012). It was suggested that both motor pulling by different fission complexes and the force generated by the WASH-mediated nucleation of actin, are important for the budding of vesicles from EE (Derivery et al., 2009; Jia et al., 2012; Capitani and Baldari, 2021).

Retromer and Synaptic Vesicle Recycling

The retromer complex and EHD are ubiquitously expressed in the nervous system, and they are both enriched in the presynaptic compartment (Jakobsson et al., 2011; Li and DiFiglia, 2012; Inoshita et al., 2017). Retromer function is essential for neuronal development and constitutive knockout of VPS35 is embryonically lethal, whereas heterozygous knockout hinders the

development of both axons and dendrites (Wen et al., 2011; Tian et al., 2015). Investigation of the effect of VPS35 knockdown on presynaptic function in mouse hippocampal neurons, failed to detect any deficits in SV exo- and endocytosis (Vazquez-Sanchez et al., 2018). However, deletion of VPS35 in Drosophila larvae led to a reduced number and altered morphology of SVs in motor terminals which was accompanied by enhanced rundown of synaptic transmission, suggesting a functional role of retromer in SV recycling (Inoshita et al., 2017). However, given the apparent discrepancy between these two model systems, further studies are required to adjudicate on the precise function of retromer in the SV cycle. Interestingly, retromer dysfunction is involved in the pathoetiology of neurodegenerative diseases such as Alzheimer's and Parkinson's disease, a common early hallmark of which is disruption of presynaptic function (Small and Petsko, 2015).

EHD1 is also linked to SV recycling. In addition to a potential negative regulation of SV exocytosis (Wei et al., 2010), EHD1 is required for clathrin-independent endocytosis. For example, its removal at the lamprey giant reticulospinal synapse, blocks SV endocytosis due to defective dynamin-induced membrane tubulation (Jakobsson et al., 2011). Furthermore EHDs associate with syndapins (Braun et al., 2005), F-BAR-proteins with pivotal role in ADBE and SV reformation at bulk endosomes (Clayton et al., 2009; Koch D. et al., 2011; Quan et al., 2012; Cheung and Cousin, 2019).

RECYCLING ENDOSOME

Recycling Endosome Function

An alternative mechanism for trafficking of cargo from the EE to the RE involves a process of organelle maturation. This mechanism does not require generation of vesicles from the EE and their fusion with the RE, but the entire EE changes its identity and matures to RE by acquiring a set of characteristic proteins, such as Rab11, Rab35, cellubrevin (VAMP3), ADP-ribosylation factor 6 (Arf6), and EHD1 (Grant and Donaldson, 2009). There are no typical resident proteins that define REs. Thus, rather than a "stable" compartment that receives cargo from the EE, the RE can be viewed as the residual organelle that remains from the EE after cargo sorting to LEs. As stated above, the major function of REs is as a trafficking intermediate for cargo proteins that normally undergo recycling to the plasma membrane. In most cell types, REs are a collection of tubule-vesicular structures of approximately 60 nm in diameter that localize to the perinuclear region in the vicinity of microtubule-organizing center (Li and DiFiglia, 2012; Goldenring, 2015). However, the perinuclear distribution of REs does not seem to be essential for their function and in some cells, REs are dispersed throughout the cytoplasm (Joensuu et al., 2017; Naslavsky and Caplan, 2018).

Rab11 has been broadly accepted as the main regulator of slow recycling through REs and its function is implicated in the recycling of a vast array of membrane proteins ranging from cell adhesion molecules to membrane receptors and ion channels (Li and DiFiglia, 2012). How Rab11 exerts its function in the regulation of RE trafficking is not well established, however. One prediction is that Rab11 controls the formation of vesicles from RE by recruiting EHD1 and its interactors, such as syndapin2, that collectively promote fission of cargo carriers (Naslavsky and Caplan, 2011; Li and DiFiglia, 2012). RE have been reported to also function as a sorting intermediate for proteins synthesized at the TGN that are destined for secretion (Murray et al., 2005). The integrity of the R-SNARE VAMP3/cellubrevin and Rab11 functions were shown to be crucial for the RE-mediated secretion of newly synthesized proteins (Murray et al., 2005).

The GTPase Arf6 is another molecular marker regulating the endocytic trafficking through RE whose function is essential in all cell types for multiple cellular events, including regulation of cell shape, cytokinesis, cell migration, and tumor cell invasion (Sheehan and Waites, 2019). Rab35 is also required for recycling previously endocytosed cargo to the plasma membrane as part of the RE system (Klinkert and Echard, 2016). Intricate reciprocal antagonistic processes regulate the active/inactive state of both Rab35 and Arf6, suggesting these GTPases are key effectors in RE function (Sheehan and Waites, 2019).

As stated above, a systematic investigation of RE has been challenging because of the difficulties identifying unique molecular tags for this organelle. The challenge to decipher the molecular basis of the RE points to the possibility that REs are not a single organelle but a constellation of interconnected, semi-autonomous organelles that collectively coordinate the trafficking of specific cargos to the plasma membrane. Therefore, it is easy to envisage that specializations of this system exist within different cell types and cellular compartments and account for regulation of the trafficking of compartment-specific cargo molecules.

Recycling Endosomes and Synaptic Vesicle Recycling

There is accumulating evidence that key components of the RE machinery, such as Rab35, Arf6, and their effectors, perform important roles in both SV recycling and processing of SV cargo. For example, *Drosophila* hypomorphic mutants for the Rab35 GAP, *skywalker,* display a large increase in presynaptic endosomes during neuronal activity (Uytterhoeven et al., 2011). Constitutively active Rab5, 23, and 35 mutants all phenocopied this defect, suggesting a key role of EE/RE effectors in SV recycling. The human *skywalker* orthologue TBC1 Domain Family Member 24 (TBC1D24) appears to perform a parallel role in mammalian nerve terminals. For example, its depletion caused defective growth cone endocytosis and axonal initial segment maturation resulting in altered action potential firing (Aprile et al., 2019). In addition, neurons from mice haploinsufficient for TBC1D24 displayed dysfunctional SV endocytosis, with a threefold increase in the volume of presynaptic endosomes, consistent with the phenotype in *Drosophila sky* mutants (Finelli et al., 2019). Interestingly, similar SV recycling phenotypes are observed in neurons in which endogenous Arf6 was depleted (Tagliatti et al., 2016). Since TBC1D24 regulates the activation state of Arf6 (Falace et al., 2014; Aprile et al., 2019), this suggests that Arf6 represses trafficking via endosomal SV recycling routes, whereas Rab35 promotes endosomal recycling. In support, depletion of the Rab35 guanine nucleotide exchange factor connecdenn in primary neuronal culture greatly reduces

endocytosis during strong stimulation (Allaire et al., 2006). In addition, the Rab35/Arf6 system controls the degradation of specific SV cargos. For example, increased endosomal flux via *skywalker* increases the functional size of the RRP, due to rejuvenation of specific SV cargo components (Uytterhoeven et al., 2011). Furthermore, interference with this endosomal sorting route restored RRP size (Fernandes et al., 2014).

Rab11 is associated with both REs and LE/lysosomes, and has also been linked to SV recycling, mainly in model organisms. In these studies, Rab11 performs a facilitatory role. For example, its knockdown in *C. elegans* resulted in SV endocytosis defects (Han et al., 2017), whereas its expression in either a *Drosophila* model of Huntington's Disease or Vps35 null flies restored the SV size to control levels (Steinert et al., 2012; Inoshita et al., 2017). In mammalian neurons, overexpression of constitutively active Rab11 mutants facilitated SV endocytosis (Kokotos et al., 2018). Therefore, molecules essential for RE function are also required for optimal SV endocytosis and cargo trafficking at the presynapse. This suggests that REs are fully integrated into the SV recycling system and even that some SVs that undergo spontaneous and evoked fusion may in fact be considered as a type of REs.

LATE ENDOSOMES/LYSOSOMES

Late Endosome/Lysosome Function

Molecular discrimination between LEs and lysosomes is challenging because of the absence of selective molecular markers between these organelles. However, these compartments have different origins. LEs are formed from dynamic EEs as endocytic carrier vesicles, which undergo a conversion during which the small GTPase Rab5 is exchanged for Rab7 (Stoorvogel et al., 1991; Rink et al., 2005). Similar to other types of endosomes, they are a heterogeneous group of organelles. One specific kind of LE contains lumenal vesicles and are often described as multi-vesicular bodies (MVB) (Piper and Katzmann, 2007). The sorting of ubiquitinated membrane proteins into intralumenal vesicles and the mechanism by which MVB are formed, which typically involves the function of the ESCRT (endosomal sorting complexes required for transport) complexes, has been extensively discussed elsewhere (Hurley, 2008, 2015; Wollert and Hurley, 2010; Vietri et al., 2020).

Lysosomes on the other hand, are the terminal degradative compartment for cargo internalized through endocytosis and intracellular cargo segregated during autophagy. Lysosomes are formed from the TGN, in a process during which lysosomal transmembrane proteins are delivered directly to the lysosome, whereas newly synthesized acid hydrolases are transported to the lysosome through an endosomal intermediate (Saftig and Klumperman, 2009). The indirect route allows TGN recycling of the mannose-6-phosphate receptor, which binds to the mannose-6-phosphate tag on the acid hydrolases and sorts them to the lysosome. Lysosomes are, essentially, storage containers for degradative enzymes, which periodically fuse with late endosomes, autophagosomes, or other hybrid organelles (amphisomes), to form a compartment in which degradation occurs (Ballabio and Bonifacino, 2020). The regeneration of functional lysosomes from these compartments after degradation is another route for maintaining the lysosomal pool and cellular homeostasis (Yang and Wang, 2021). However, the function of lysosomes is not restricted to degradation of cellular components: they can also undergo regulated exocytosis in response to an increase in the intracellular calcium concentration (Martinez et al., 2000). Lysosome exocytosis is believed to supply extra membrane for plasma membrane repair (Reddy et al., 2001), which is an essential homeostatic mechanism that prevents cell death and progression of multiple diseases (Zhen et al., 2021).

Similar to other fusion events, fusion of lysosomes or late endosomes with the plasma membrane is a sequential process that proceeds through different stages: tethering, formation of a trans-SNARE complex and fusion (Luzio et al., 2007). Organelle tethering is a prerequisite step for fusion, during which membrane organelles form links with each other. The composition of the tethers responsible for LE-lysosome fusion has not been completely established, but homotypic fusion and protein sorting complex, which is recruited by Rab7, is likely one of the components (Fernandes et al., 2014). Following tethering, the formation of a SNARE complex bridges across the two membranes and enables fusion. Compelling evidence exists that the Q-SNAREs syntaxin-7, syntaxin-8, and Vti1b are essential for both, homotypic late endosome fusion and heterotypic late endosome-lysosome fusion, whereas the R-SNARE VAMP7 is specifically required for late endosome-lysosome fusion (Luzio et al., 2010). VAMP7 also mediates fusion of lysosomes with the plasma membrane (Rao et al., 2004). The N-terminal longin domain of VAMP7 is a critical regulatory site for its endosomal sorting. The kinetics and the extent of the calcium-dependent fusion of lysosomes with the plasma membrane are regulated by the calcium sensor synaptotagmin-7 (Syt7) (Martinez et al., 2000).

Late Endosome/Lysosomes and Synaptic Vesicle Recycling

In neurons, LEs formed at the synapse undergo progressive acidification and further maturation toward a lysosomal identity during their retrograde transport to the cell body (Deinhardt et al., 2006; Maday et al., 2012; Cheng et al., 2015). In agreement with this model, organelles with increasing levels of acidity are observed from distal to proximal axons (Overly and Hollenbeck, 1996). The controversy surrounding the presence of *bone fide* lysosomes at the presynapse is compounded by the fact that common markers of lysosomes such as LAMP1 are present on many non-lysosomal compartments (Vukoja et al., 2018). However, it is clear that fusion of either LEs, lysosomes, or vesicles containing lysosome markers, occurs at distal axons and is both calcium- and SNARE-dependent, with both Syt7 acting as the calcium sensor and VAMP7 as the R-SNARE on the LE/lysosome membrane (Arantes and Andrews, 2006).

Evidence has been accumulating that both Syt7 and VAMP7 (and potentially by extension LEs) are integrated in the SV life cycle. VAMP7 is targeted to SVs via an interaction with its longin domain to the adaptor complex

AP3 (Scheuber et al., 2006). Interestingly, the VAMP7 longin domain interferes with the formation of SNARE complexes with a variety of Q-SNARE partners (Martinez-Arca et al., 2003), providing a potential explanation for why VAMP7 fails to visit the cell surface during action potential stimulation (Hua et al., 2011; Ramirez et al., 2012). However, VAMP7-containing vesicles may support spontaneous SV fusion, since increased cell surface trafficking occurs in resting neurons. In support, expression of VAMP7 lacking its longin domain increases spontaneous SV fusion, suggesting that VAMP7 may be required for this event (Hua et al., 2011). Furthermore, modulation of spontaneous SV fusion events by the signaling molecule reelin was abolished on depletion of endogenous VAMP7 (Bal et al., 2013), suggesting that VAMP7-mediated fusion events occur at the presynapse and can be modulated.

Almost all of the proposed presynaptic functions for Syt7 are dependent on its role as a calcium sensor. For example, Syt7 is postulated to be the calcium sensor for store-operated channel entry-mediated presynaptic calcium increases from the endoplasmic reticulum (ER), which augment spontaneous glutamate release (Chanaday et al., 2021). In addition, Syt7 is proposed to replenish the RRP via a calcium-dependent interaction with calmodulin (Liu et al., 2014). Syt7 is also a candidate calcium sensor for asynchronous release, with the extent of this release modulated by the copy number ratio between fast binding, but low affinity calcium sensors such as Syt1 and slower, higher affinity sensors such as Syt7 (Maximov et al., 2008; Bacaj et al., 2013; Weber et al., 2014; Luo et al., 2015; Li et al., 2017).

Syt7 has also been linked to SV endocytosis. Early studies revealed that Syt7 overexpression increased the number of presynaptic endosomes (Virmani et al., 2003), with subsequent studies reporting slowed SV endocytosis in neurons overexpressing the sensor (Li et al., 2017). Interestingly, Syt7 knockdown was sufficient to restore normal SV endocytosis kinetics in Syt1 knockdown neurons, again suggesting a functional link between the two calcium sensors. These results suggest that Syt7 might facilitate endosomal recycling pathways such as ADBE. Syt7 trafficking is largely refractory to stimulation (Dean et al., 2012; Weber et al., 2014), in agreement with its predominant plasma membrane localization (Sugita et al., 2001; Maximov et al., 2008; Dean et al., 2012; Li et al., 2017). This atypical localization may explain some of the disparate functions ascribed to this calcium sensor. Recent evidence supports this view, with the plasma membrane localization of Syt7 critical for its control of multiple aspects of the SV life cycle (Vevea et al., 2021). In these studies, targeting Syt7 to either the plasma membrane or lysosome-associated membrane glycoprotein 1 (LAMP1)-positive vesicles, but not SVs, rescued the functional deficits observed in Syt7 knockout neurons. Plasma membrane targeting of Syt7 was dependent on its cleavage via γ-secretase and palmitoylation (Vevea et al., 2021), directly placing LEs and the endolysosomal system at the regulatory center of SV recycling.

The presence of two of the most abundant LE/lysosomal markers, VAMP7 and Syt7, in the SV pool suggests that lysosome-related organelles are intermingled in the pool of SVs, however, what could be their role? The evidence implicating LEs/lysosomes in regulation of local protein degradation is sparse. For example, LAMP1-containing organelles in distal axons have different acidity from the LAMP1-containing organelles in proximal axons indicating that they might have lower degradative capacity (Overly and Hollenbeck, 1996; Lie et al., 2021). In contrast, the ESCRT machinery is implicated in activity-dependent degradation of a subset of SV proteins via a pathway that requires Rab35 (Sheehan et al., 2016). Furthermore, cathepsins were detected in distal axons in the *Drosophila* brain and two parallel pathways, a Rab7-independent and a Rab7-dependent pathway were shown to specifically mediate synaptic degradation of SV proteins and membrane proteins, respectively (Jin et al., 2018). One study described a selective localization of the lysosomal protease cathepsin D to GABA-ergic presynapses and implicated it in the control of endocytic trafficking and GABA-ergic neurotransmission (Li et al., 2019). However, an argument against differential distribution of this lysosomal enzyme to inhibitory presynapses is the observation that cathepsin D knockout mice have global deficits in presynaptic ultrastructure (Partanen et al., 2008; Koch S. et al., 2011) and markedly decreased frequency of miniature excitatory postsynaptic currents, mEPSCs (Koch S. et al., 2011). Therefore, cathepsin D-containing lysosome-related organelles are present at both glutamatergic and GABA-ergic synapses and contribute to excitatory and inhibitory neurotransmission.

However, whether there are lysosomes with degradative capacity present at mammalian presynaptic terminals and what their contribution is, if any, to local degradation is currently unknown.

AUTOPHAGY FUNCTION AND SYNAPTIC VESICLE RECYCLING

Another key axonal retrograde membrane trafficking route, fully integrated in the endolysosomal system, is the autophagy pathway. The generation of autophagosomes in synaptic terminals involves the sequential recruitment and activation of a series of protein complexes, with the main membrane donor being the endoplasmic reticulum [summarized in Kuijpers et al. (2021a), Overhoff et al. (2021)]. Indeed, when autophagy is disrupted via the loss of the key molecule autophagy protein 5 (Atg5), there is increased calcium release from presynaptic ER, resulting in enhanced excitatory neurotransmission (Kuijpers et al., 2021b). Synaptic autophagosome formation appears to be a constitutive process, unlike nutrient starvation-triggered events in non-neuronal cells (Maday and Holzbaur, 2014) and may aid the turnover/degradation of SVs and their cargos (Ravikumar et al., 2010; Maday et al., 2012). Maturation of autophagosomes into autolysosomes involves their fusion with degradative lysosomes and retrograde transport toward the cell body (Itakura et al., 2012; Takáts et al., 2013). Alternatively, they can also fuse with LE to form amphisomes, which perform discrete signaling roles, particularly when transporting growth factor receptors (Villarroel-Campos et al., 2018; Andres-Alonso et al., 2019). As

outlined above, manipulation of the autophagy pathway results in altered neurotransmission, implicating this pathway as another control point in the SV life cycle. Furthermore, autophagy also requires proteins with defined roles in SV recycling and clathrin-independent endocytosis pathways (Milosevic et al., 2011; Pechstein et al., 2015; Kroll et al., 2019), such as endophilin and synaptojanin-1 (Soukup et al., 2016; Soukup and Verstreken, 2017; Vanhauwaert et al., 2017). In addition, the active zone protein bassoon modulates autophagy via sequestration of the Atg5 (Okerlund et al., 2017). This suggests that both SV recycling and autophagy pathways are intricately linked in terms of both function and molecular requirements.

DISCUSSION

The question whether SV recycling involves an endosomal intermediate is surprisingly still a matter of debate (Jähne et al., 2015), even when one considers that most, if not all, reported EE, RE, and LE markers are present in the SV pool and with many having direct effects on presynaptic function. Furthermore, the ever-increasing subdivision of functional SV pools described above suggests that the presynapse harbors a collection of functionally diverse organelles with distinct molecular compositions, not all of which engage directly in neurotransmission. This leads to the question, how inter-dependent are SV recycling and the endolysosomal system, and perhaps more provocatively, are these apparently different processes part of the same cellular continuum? In the section below, we outline a series of hypotheses, supported by the current literature which provide a potentially unifying model for membrane trafficking at the presynapse.

How Homogenous Are Synaptic Vesicles and Are Many Recycling Endosomes/Late Endosomes in Disguise?

REs are a heterogeneous population of tubulovesicular membrane-bound organelles ∼60–100 nm in diameter (Willingham and Pastan, 1980; Willingham et al., 1984). An argument against a potential link between REs and SVs is the morphological uniformity of SVs that has been observed in multiple studies and attributed to the functioning of specific endocytic mechanisms (Zhang et al., 1998; Shimizu et al., 2003; Koo et al., 2015; Ivanova et al., 2020). However, electron microscopy (EM) studies from ultrathin sections have shown that the size of SVs exists in a range from 25 to 80 nm (Fox, 1988; Harris and Sultan, 1995). It is not always possible to reconstruct membrane continuity from such ultrathin sections and therefore the length at which SVs extend is difficult to appreciate. Contrary to the prevailing view that SVs have only a spherical shape, studies exist showing that SVs may not be morphologically uniform. Pleomorphic vesicles have been described in early EM studies, mostly as a marker for inhibitory synapses (Uchizono, 1965 and more recently, Koo et al., 2015; Li et al., 2019). With the advent of new technologies (e.g., cryo-EM and electron tomography) there is increasing evidence that tubule-shaped ellipsoidal vesicles are present at both excitatory and inhibitory synapses (Tao et al., 2018). Therefore, similarly to REs, SVs show a degree of morphological heterogeneity, with a diameter that ranges within tens of nanometers.

SVs are also functionally diverse and molecularly heterogeneous. Previous bulk biochemical approaches described the protein composition of a prototypical SV (Takamori et al., 2006; Wilhelm et al., 2014; Wittig et al., 2021). While providing insight into the molecular composition of an average SV, an important caveat of these bulk proteomic studies is that the cellular fractions that were analyzed represent averages of a diverse array of synapses and SVs. The copy number of common SV proteins, such as synaptobrevin2, synaptophysin, and synaptogyrin, in individual SVs shows a significant inter-vesicle variability, as revealed by single molecular quantification approaches (Mutch et al., 2011). Another important limitation of these early proteomic studies is that they have a bias toward proteins with high abundance, while underrepresented proteins with essential functions, often remain undetected. More recent studies report a longer list of proteins found in isolated synaptosomes, with low abundance proteins (less than 1 copy per SV) being the dominant fraction (Taoufiq et al., 2020). All of this suggests that different proteins are likely differentially distributed to different SV subpopulations. The presence of a multitude of endolysosomal molecules in the total SV pool that exert fine control over different steps of the SV cycle therefore strongly supports the notion that the two systems form a continuum (**Figure 1**).

The disparity of endolysosomal molecules within the SV pool (**Table 1**) suggests that some vesicles previously assumed to be SVs may in fact be intermediates of the endolysosomal pathway. In support, SVs are functionally similar to REs, as they are involved in slow, regulated and constitutive recycling of SV cargo to the plasma membrane. Furthermore, a handful of molecular markers characteristic for RE have been implicated in SV function as discussed above. For instance, the Rab35/Arf6 axis directly impacts SV composition and function. Furthermore the RE marker, Rab11 impacts calcium-regulated exocytosis of dense core vesicles and SVs and integrates regulated and constitutive exocytosis in neurons and neuroendocrine cells (Khvotchev et al., 2003), while facilitating SV endocytosis modes in central nerve terminals (Kokotos et al., 2018). The only described R-SNARE associated with RE, cellubrevin, is a structural homologue of the most abundant SV R-SNARE, synaptobrevin2 (McMahon et al., 1993). It quantitatively co-isolates with synaptophysin, when expressed in a heterologous system, suggesting that both localize on the same vesicles (McMahon et al., 1993). In further support of the hypothesis that some recycling SVs may be the equivalent of the RE in the presynaptic terminal, cellubrevin fully rescues synaptic transmission when expressed in synaptobrevin2-deficient neurons (Deák et al., 2006).

Similarly, LE/lysosome fusion events may be responsible for a series of functional outputs ascribed to particular SV subpopulations. The mobilization of the resting SV pool is of particular interest, since the LE/lysosome effectors VAMP7

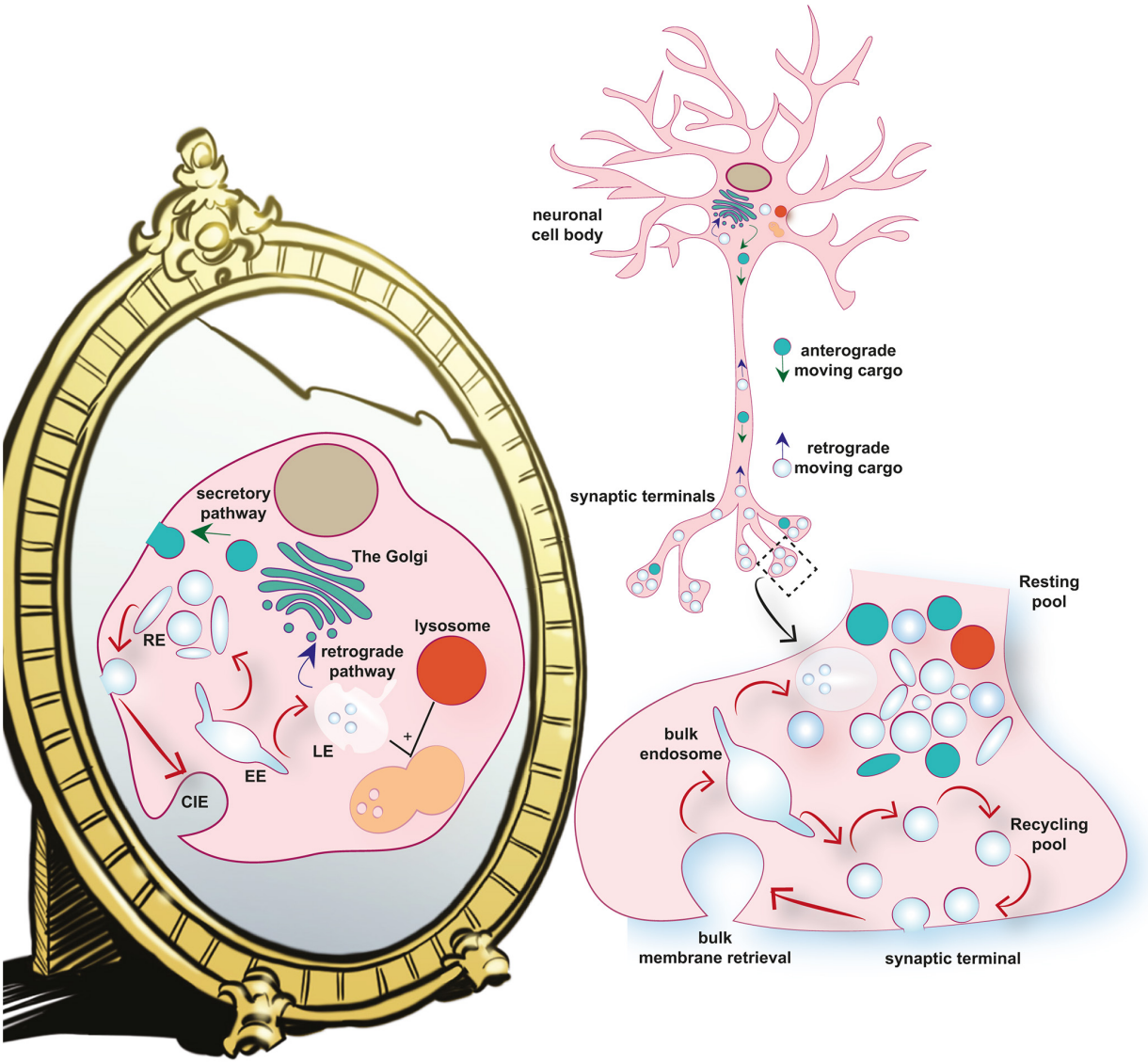

FIGURE 1 | The SV life cycle as a mirror image of the general endolysosomal system. **(A)** The endolysosomal system consists of a set of membrane-bound compartments that undergo dynamic interconversion. At the center of this system is the Golgi apparatus, which is a steady-state organelle that apart from a central sorting hub in the secretory pathway, functions as an important quality control checkpoint that constantly receives cargo from the plasma membrane and the peripheral endosomes. The endolysosomal system is comprised of: (1). Early endosomes (EEs). EEs are organelles that receive membrane cargos and solutes from the extracellular environment through endocytosis. The main mode of endocytosis in most cells is clathrin-independent endocytosis (CIE). The EE sorts these cargos into recycling or degradative compartments of the cell. (2). Recycling endosomes (REs). REs are compartments involved in the slow constitutive and regulated recycling of cargo to the plasma membrane. (3). Late endosomes (LEs). The central role of LEs is sorting of ubiquitinated membrane proteins into intralumenal vesicles which form multi vesicular bodies (MVBs). MVBs fuse with lysosomes to form a degradative compartment in which protein cargos and intralumenal vesicles are degraded. LEs are also involved in the retrograde retrieval of cargo molecules from the plasma membrane and other endosomes to the Golgi apparatus. (4). Lysosomes are membrane-bound organelles that degrade and recycle cellular waste. In addition, they play an important role in cellular signaling and energy metabolism. **(B)** The dominant endocytosis modes operating at the central nerve terminals (ADBE and ultrafast endocytosis) are CIE pathways. The bulk endosome is emerging as a central sorting station, which similarly to the EE, sorts cargos to either the Recycling pool or the Resting pool. The Recycling pool (similarly to the REs) is implicated in the constitutive (spontaneous) and regulated (evoked) recycling of cargos to the plasma membrane. The Resting pool is likely a collection of functionally and molecularly heterogeneous membrane-bound organelles, which likely includes endolysosomal intermediates such as LE and lysosomes, which may or may not have a full degradative capacity. The membrane-bound organelles at the synapse are connected to endolysosomal organelles in neuronal cell bodies (the Golgi apparatus and the degradative lysosome) through antero- and retrograde-trafficking along the axon.

and Syt7 are both represented in this SV pool. For example, the calcium-dependent nature of the VAMP7-dependent fusion events evoked by reelin (Bal et al., 2013), is reminiscent of ionophore-evoked lysosome fusion in non-neuronal cells. This may have great relevance, since the plasma membrane deposition of Syt7 impacts a series of SV recycling events (Vevea et al.,

2021), suggesting lysosome fusion is a prerequisite for optimal presynaptic function. However, the reciprocal control of the resting SV pool by the calcium-activated protein phosphatase calcineurin and the protein kinase cyclin-dependent kinase 5 (Kim and Ryan, 2010) appears to operate in a reverse manner for lysosome fusion (Medina et al., 2015; Ishii et al., 2019). Therefore, more work is required to determine the specific molecular nature of the organelles that undergo regulated fusion at the presynapse.

A Reappraisal of the Synaptic Vesicle Pool Nomenclature

The concept of SV pools was introduced as a model to explain the functional diversity of SVs present in the presynaptic terminal and their distinct contribution to different forms of neurotransmitter release (Alabi and Tsien, 2012). As hypothesized above, the ever-increasing complexity of SV subpopulations that contribute to specific functional fusion or release events suggests a disparate composition of the total SV pool, with potentially direct contributions from different endolysosomal organelles. The SV pool model has proven its utility for describing the plasticity of neurotransmitter release in terms of changes of SV pool sizes (Kim and Ryan, 2010; Rey et al., 2020). However, as with any model, it has its limitations (Neher, 2015). The main limitation is that it remains too deterministic in its original interpretation, and in specific cases, it postulates that distinct pools with specific molecular composition mediate different forms of release (Crawford and Kavalali, 2015). In reality, the dynamic behavior of complex biological systems, such as the SV life cycle, is inherently stochastic. Molecules are randomly distributed to different SV populations and complex regulatory mechanisms guide probabilistic outcomes. Because of this, qualitatively similar functional outcomes may arise from the interactions of different and varied number of molecules, each present on SVs in a small absolute quantity.

The pool model also fails to explain why the resting pool both *in vitro* and *in vivo* cannot be released even after extensive periods of synaptic stimulation (Alabi and Tsien, 2012). The reluctant nature of these SVs to participate in activity-dependent recycling suggest that they might be endosomes that have roles other than a direct contribution to neurotransmitter release. For instance, these resting SVs might function as a reservoir of molecules that can be incorporated into the recycling pool on demand (during sorting, as discussed below) to allow plastic changes of SV composition and function (Denker et al., 2011). In addition, part of the resting pool, may in fact be comprised of a series of endolysosomal intermediates primed for transport to neuronal cell bodies and the degradative pathways (**Figure 1**).

In many cases, the pool model comes short in providing a good correlation between morphology and function. Thus, loss of function of molecules, such as synaptobrevin2 (Deák et al., 2004), munc-13 (Varoqueaux et al., 2002), munc-18 (Verhage et al., 2000), and calcium channels (Held et al., 2020), that strongly reduce or eliminate any forms of neurotransmitter release, does not have any major impact on synaptic ultrastructure and the number of SVs per synaptic terminal. In contrast, the integrity of the SV cluster is compromised when the function of key endosomal sorting proteins is abrogated (Glyvuk et al., 2010; Tagliatti et al., 2016). This implies that the SV pool and its clustering at the synapse are driven by intrinsic programs in the neuron and SV recycling is not essential for maintaining its integrity.

Contrary to the pool model, SV fusion and neurotransmitter release are likely an emerging property of a small subset of the endolysosomes orchestrated in the presynaptic terminal that has been selected through evolution to support the central function of the nervous system, neuronal communication. Indeed, the ultrastructural organization of excitatory presynaptic terminals that developed in complete absence of glutamate release (due to Cre-induced expression of tetanus toxin), was largely preserved, with a normal number of SVs and led to normal refinement of connectivity in the developing brain (Sando et al., 2017; Sigler et al., 2017). Furthermore, the universal excitatory (glutamate, aspartate, and cysteic acid) and inhibitory neurotransmitters (GABA, glycine), are amino acids and the endolysosomal system is a well-established storage site for free amino acids (Russnak et al., 2001; Abu-Remaileh et al., 2017). Some of these intralumenal amino acids are a key element of a central endolysosomal mechanism for nutrient sensing and metabolic control that operates in virtually all cells and organs (Lawrence and Zoncu, 2019). Furthermore, the transport of classical neurotransmitters and neuromodulators into SVs is driven by members of the solute carrier family of transporters (SLC) (Schuldiner et al., 1995; Anne and Gasnier, 2014), that are broadly expressed in various endolysosomal structures and are essential to vital processes within and outside the nervous system (Serrano-Saiz et al., 2020). In addition to their ability to transport amino acids, some of these channels operate as ion channels and regulate the ion gradients and acidification of endosomes (Martineau et al., 2017). The import of neurotransmitters could therefore be considered a by-product of the establishment of these electrochemical gradients, that have additional roles in the functioning of endosomes.

Additional support for the hypothesis that the SV pool is not an autonomous module, operating independently in isolated synaptic terminals, is provided by the existence of a superpool of SVs. Although it is generally accepted that the SV pool and recycling are local, synapse-specific phenomena, overwhelming evidence exists that the pool is not confined to a particular synapse, but spans multiple synapses in a single axon (Staras et al., 2010). Photobleaching and photoactivation experiments have demonstrated that recycling SVs, and synaptic proteins in general, quickly redistribute among neighboring synapses and even between synapses and neuronal cell bodies (Tsuriel et al., 2006; Staras et al., 2010; Ivanova et al., 2015). Thus, the SV pool is shared among many synapses and consists of multiple interconnected organelles that continuously shuttle (in both directions) between axons and neuronal cell bodies. Based on this, a different model emerges, in which the SV pool can be presented as a collection of molecularly heterogeneous endosomes. Owing to the accumulation of specific sets of molecules during the elaborate process of endosomal sorting, a small fraction of these endosomes engages in regulated (evoked) as well as constitutive (spontaneous) release in the confines of

TABLE 1 | Common endolysosomal proteins present in the SV proteome.

Protein	SV recycling role	Endolysosomal role	Presence on SVs
Syntaxin-6	Activity-dependent trafficking to plasma membrane (Hoopmann et al., 2010)	Endosome fusion (Maxfield and McGraw, 2004; Grant and Donaldson, 2009)	Yes (Takamori et al., 2006)
Syntaxin-7	Not determined	LE fusion (Luzio et al., 2010)	Yes (Takamori et al., 2006; Taoufiq et al., 2020)
Syntaxin-8	Not determined	LE fusion (Luzio et al., 2010)	Yes (Taoufiq et al., 2020)
Syntaxin-12	Activity-dependent trafficking to plasma membrane (Hoopmann et al., 2010)	Endosome fusion (Grant and Donaldson, 2009)	Yes (Takamori et al., 2006; Taoufiq et al., 2020)
Rab-4	Not determined	Axonal transport (Stenmark, 2009)	Yes (Takamori et al., 2006; Pavlos et al., 2010; Taoufiq et al., 2020)
Rab-5	Required for efficient SV recycling/SV cargo processing (Shimizu et al., 2003; Wucherpfennig et al., 2003; Star et al., 2005; Shin et al., 2008)	EE fusion/maturation (Stenmark, 2009)	Yes (Takamori et al., 2006; Pavlos et al., 2010; Taoufiq et al., 2020)
Rab-7	Not determined	EE to LE maturation (Stenmark, 2009)	Yes (Takamori et al., 2006; Pavlos et al., 2010; Taoufiq et al., 2020)
		LE fusion (Luzio et al., 2010)	
Rab-8	Not determined	Axonal transport (Stenmark, 2009)	Yes (Takamori et al., 2006; Pavlos et al., 2010; Taoufiq et al., 2020)
Rab-10	LDCV secretion (Sasidharan et al., 2012)	TGN to plasma membrane transport (Stenmark, 2009)	Yes (Takamori et al., 2006; Pavlos et al., 2010)
Rab-11	Facilitation of SV endocytosis/recycling (Steinert et al., 2012; Han et al., 2017; Kokotos et al., 2018)	RE maturation (Grant and Donaldson, 2009; Stenmark, 2009)	Yes (Takamori et al., 2006; Pavlos et al., 2010; Taoufiq et al., 2020)
Rab-14	Not determined	TGN to EE transport (Stenmark, 2009)	Yes (Takamori et al., 2006; Pavlos et al., 2010)
Rab-21	Not determined	EE to LE transport (Stenmark, 2009)	Yes (Takamori et al., 2006; Pavlos et al., 2010; Taoufiq et al., 2020)
Rab-35	Required for efficient SV recycling/SV cargo processing (Uytterhoeven et al., 2011; Sheehan et al., 2016)	RE fusion/maturation (Grant and Donaldson, 2009; Stenmark, 2009; Sheehan and Waites, 2019)	Yes (Takamori et al., 2006; Pavlos et al., 2010; Taoufiq et al., 2020)
EHD1	Required for ADBE (Jakobsson et al., 2011)	EE to RE transport (Grant and Donaldson, 2009; Naslavsky and Caplan, 2011)	Yes (Taoufiq et al., 2020)
Vti1a	Spontaneous SV fusion (Ramirez et al., 2012)	Endosome fusion (Maxfield and McGraw, 2004)	Yes (Takamori et al., 2006; Taoufiq et al., 2020)
	Activity-dependent trafficking to plasma membrane (Hoopmann et al., 2010)		
	SV fusion via TGN cargo trafficking (Emperador-Melero et al., 2018)	Retrograde TGN transport (Johannes and Popoff, 2008)	
Vti1b	SV fusion via TGN cargo trafficking (Emperador-Melero et al., 2018)	LE/lysosome fusion (Luzio et al., 2010)	Yes (Taoufiq et al., 2020)
AP1	Control of SV composition via SV cargo clearance (Candiello et al., 2016; Ivanova et al., 2021)	Cargo selection for retrograde transport (Grant and Donaldson, 2009)	Yes (Takamori et al., 2006)

(Continued)

TABLE 1 | (Continued)

Protein	SV recycling role	Endolysosomal role	Presence on SVs
VPS26	Not determined	Retromer cargo selection (Seaman, 2012; Burd and Cullen, 2014)	No
VPS29	Not determined	Retromer cargo selection (Seaman, 2012; Burd and Cullen, 2014)	Yes (Taoufiq et al., 2020)
VPS35	Facilitation of SV recycling (Inoshita et al., 2017)	Retromer cargo selection (Seaman, 2012; Burd and Cullen, 2014)	No
VPS34	Bulk endosome cargo sorting (Candiello et al., 2016)	Endosome to TGN transport (Grant and Donaldson, 2009)	No
SNX1	Not determined	Retromer tubulation (Seaman, 2012; Burd and Cullen, 2014)	Yes (Taoufiq et al., 2020)
SNX5	Not determined	Retromer tubulation (Seaman, 2012; Burd and Cullen, 2014)	Yes (Takamori et al., 2006; Taoufiq et al., 2020)
SNX6	Not determined	Retromer tubulation (Seaman, 2012; Burd and Cullen, 2014)	Yes (Taoufiq et al., 2020)
Arf6	Repression of SV recycling/SV cargo processing (Allaire et al., 2006)	RE maturation (Grant and Donaldson, 2009; Sheehan and Waites, 2019)	Yes (Taoufiq et al., 2020)
TBC1D24	Required for efficient SV recycling/SV cargo processing (Uytterhoeven et al., 2011; Fernandes et al., 2014; Finelli et al., 2019)	Rab35 GTPase activating protein (Uytterhoeven et al., 2011)	No
		Control of Arf6 activity (Falace et al., 2014; Aprile et al., 2019)	
Syt7	RRP Replenishment (Liu et al., 2014)	LE/lysosome fusion (Martinez et al., 2000; Arantes and Andrews, 2006)	Yes (Taoufiq et al., 2020)
	Asynchronous release (Maximov et al., 2008; Bacaj et al., 2013; Weber et al., 2014; Luo and Südhof, 2017)		
	Spontaneous release (Chanaday et al., 2021)		
	Facilitation of ADBE (Virmani et al., 2003; Li et al., 2017)		
VAMP3	Not determined	RE fusion (Grant and Donaldson, 2009)	Yes (Takamori et al., 2006; Taoufiq et al., 2020)
VAMP4	Control of Pr (Ivanova et al., 2021)	Endosome fusion (Maxfield and McGraw, 2004)	Yes (Takamori et al., 2006; Taoufiq et al., 2020)
	Required for ADBE (Nicholson-Fish et al., 2015; Ivanova et al., 2021)		
	Asynchronous release (Raingo et al., 2012)	Retrograde TGN transport (Johannes and Popoff, 2008)	
	Spontaneous release (Raingo et al., 2012; Lin et al., 2020)		
VAMP7	Spontaneous SV fusion (Hua et al., 2011; Ramirez et al., 2012; Bal et al., 2013)	LE/lysosome fusion (Rao et al., 2004; Arantes and Andrews, 2006; Luzio et al., 2010)	Yes (Takamori et al., 2006; Taoufiq et al., 2020)
ATG5	Not determined	Presynaptic autophagy (Kuijpers et al., 2021a; Overhoff et al., 2021)	No
Endophilin	Required for SV uncoating (Gad et al., 2000; Milosevic et al., 2011; Pechstein et al., 2015)	Presynaptic autophagy (Soukup et al., 2016; Soukup and Verstreken, 2017)	Yes (Taoufiq et al., 2020)

(Continued)

TABLE 1 | (Continued)

Protein	SV recycling role	Endolysosomal role	Presence on SVs
	Required for SV endocytosis (Gad et al., 2000; Sundborger et al., 2011; Watanabe et al., 2018)		
	Calcium influx and SV recycling (Kroll et al., 2019; Gowrisankaran et al., 2020)		
LAMP1	Not determined	Maintenance of lysosome integrity (Saftig and Klumperman, 2009)	Yes (Takamori et al., 2006; Taoufiq et al., 2020)

Many endolysosomal proteins are part of the cohort of molecules present in highly purified SV fractions. This table reports common endolysosomal molecules, their proposed role in the SV life cycle and their presence on purified SVs.

a specific synapse (Kaeser and Regehr, 2014; Chanaday and Kavalali, 2018). However, the SV cycle is nested in a larger cycle that encompasses membrane-bound organelles that reside in both, presynaptic sites and neuronal cell bodies.

Lessons Learned From Studying the Trafficking of the Endosomal R-SNARE VAMP4 at the Presynapse

As described above, VAMP4 is an endosomal R-SNARE implicated in homo- and heterotypic endosomal fusion which continuously shuttles between endosomes and the TGN in non-neuronal cells. In neurons it is enriched at the TGN as well as in distal axons. In nerve terminals, the majority of VAMP4 is sorted during ADBE to vesicles that are refractory to synaptic stimulation (Nicholson-Fish et al., 2015; Ivanova et al., 2021). Retrograde axonal trafficking of VAMP4 on vesicles that are positive for Rab7 (presumably LEs) mediates its continuous retrieval from nerve terminals and recycles it back to neuronal cell bodies. A small fraction of the VAMP4 pool is present on SVs that undergo activity-dependent exocytosis (recycling SVs) and its abundance in the SV pool inversely correlates with SV fusion (Ivanova et al., 2021). Thus, VAMP4 is an example of a protein that shows a wide distribution to different membrane-bound organelles, once again highlighting the interconnectedness of the endolysosomal system and SVs.

Activity-dependent SV endocytosis modes such as ultrafast endocytosis and ADBE are the dominant mechanism for SV cargo and membrane retrieval at central synaptic terminals (Chanaday et al., 2019). Therefore, the great majority of SVs mobilized during synaptic activity recycles through a common endosomal intermediate, the bulk endosome. To mediate efficient neurotransmitter release, recycling SVs must garner a specific set of proteins in a certain stoichiometric ratio. However, a systematic model of the molecular mechanisms underpinning differential protein sorting during SV recycling is currently missing. Di-leucine and tyrosine-based motifs are known to be involved in endolysosomal targeting of proteins (Bonifacino and Traub, 2003), such as with VAMP4, whose cytoplasmic domain possesses a di-leucine motif which mediates its AP1-dependent sorting to endosomes and lysosome-related organelles (Peden et al., 2001). The presence of a di-leucine signal in VAMP4 is likely the underlying reason for its limited localization to recycling SVs and its enrichment on bulk endosomes (Nicholson-Fish et al., 2015).

However, there is no common sorting motif responsible for selective targeting of proteins to the recycling SV pool. This might indicate the existence of distinct sorting mechanisms for each individual SV cargo. An alternative model stipulates that removal of molecules is more important than selective incorporation of proteins for generating of SVs with an optimal complement of proteins for recycling. According to this model, recycling SVs, exactly like REs, are the remnants of bulk endosomes (the equivalent of EE) that persist after cargo sorting to LE. The incorporation of classic endolysosomal proteins, such as VAMP4, in the SV pool makes endolysosomal sorting a prerequisite step in the reformation of SVs. Based on the similarity between EEs and synaptic bulk endosomes, it is easy to envisage that following endocytic retrieval, the newly formed bulk endosomes mature to a dynamic sorting compartment by undergoing heterotypic fusion with pre-existing vesicles/endolysosomes from the resting SV pool. This hypothesis is supported by *in vitro* data showing that newly endocytosed SVs undergo homotypic fusion and are capable of fusing with early endosomes isolated from other cell types (Rizzoli et al., 2006). However, despite the increasing level of innovation in the imaging tools that drive rapid advancement in cellular neurobiology, currently there is no *in cellulo* data supporting endosomal fusion at the presynapse. More than anything else, this indicates the urgent need for developing of sufficiently sensitive techniques that break the diffraction barrier but simultaneously allow real-time visualization of membrane trafficking in the confinements of the conventional chemical synapse.

Despite these currently insurmountable technical limitations, we recently showed (indirectly, through studying VAMP4 trafficking at the presynapse) that intermixing of cargos retrieved through endocytosis with classic endolysosomal cargos, presumably prior to endolysosomal sorting, can introduce molecular heterogeneity in SV composition and drive plasticity of neurotransmitter release (Ivanova et al., 2021). This attunes synaptic transmission to both the history of presynaptic activity, and the functionality status of the quality control mechanisms operating throughout the endolysosomal system.

More importantly, endolysosomal sorting during SV recycling provides a potential conduit for a constitutive, use-dependent turnover of SV components. In support, blocking the sorting of VAMP4 to LEs, using a dominant negative form of Rab7, increased its synaptic expression and slowed down its synaptic turnover (Ivanova et al., 2021). Interestingly, the same intervention also increased the synaptic expression of synaptophysin, although to a lesser extent. Therefore, it is tempting to speculate that active sorting of classic endolysosomal proteins, such as VAMP4, to LEs may promote passive retrieval of SV cargos that do not necessarily possess sorting determinants for targeting to LEs/lysosomes. This can provide a stochastic, pre-emptive mechanism for removal of SV cargos that have participated in recycling (that has been speculated to exist Truckenbrodt et al., 2018) which continuously rejuvenates the SV proteome and thereby maintains synaptic integrity and function.

Cycling Back to Neuronal Cell Bodies; Potential Impact of Re-trafficking to the Trans-Golgi Network and Somatic Lysosomes on Presynaptic Function, Lessons Learned From Models of Disease

The rapid redistribution of SV proteins between neighboring synapses (in a matter of minutes; Tsuriel et al., 2006; Staras et al., 2010) and between synapses and neuronal cell bodies (in a matter of hours Tsuriel et al., 2006; Ivanova et al., 2015) observed using various live-imaging approaches, indicates a very rapid axonal turnover of SV components. However, this is at odds with the very slow metabolic turnover of SV proteins, which ranges from several days to several weeks *in vitro* and *in vivo*, respectively (Dorrbaum et al., 2018). This suggests that SV proteins may undergo multiple rounds of trafficking between synapses and neuronal cell bodies before being directed to any of the degradative routes. Although synapses are located at a considerable distance from neuronal cell bodies, owing to the function of motor proteins the communication between them is a very rapid and efficient process (Guedes-Dias and Holzbaur, 2019). However, why would neurons support such a metabolically-expensive strategy to continuously shuttle vesicles and molecules between distal synapses and neuronal cell bodies?

The TGN, which is a central sorting hub in the secretory pathway, is also emerging as a major protein quality control checkpoint (Briant et al., 2017; Hellerschmied et al., 2019; Sun and Brodsky, 2019). Similarly to the quality control systems operating in the ER, specialized molecular machineries residing in the TGN perform protein surveillance and funnel damaged, misfolded or aggregated proteins into pathways that either attempt repair or sequester and degrade the damaged proteins (typically through lysosomal degradation) (Sun and Brodsky, 2019). Therefore, continuous retrograde trafficking and recycling through the TGN of plasma membrane proteins and proteins that normally localize to other endolysosomal compartments, will allow a periodical reevaluation of their state (**Figure 2**).

This hypothesis that recycling of synaptic proteins to the TGN is essential for synapse integrity, is strongly supported by the key role of retromer in maintaining synaptic health and its involvement in the progression of neurodegenerative diseases such as Alzheimer's and Parkinson's disease (Small and Petsko, 2015). Multiple genetic studies have linked both Alzheimer's and Parkinson's disease to a number of retromer-associated proteins and enhancement of the retromer function was neuroprotective against the pathology of these slowly progressing neurodegenerative diseases (Vilariño-Güell et al., 2011; Wen et al., 2011; Small and Petsko, 2015; McMillan et al., 2017; Brodin and Shupliakov, 2018). The neuroprotective role of the retromer complex is believed to be coupled to its role in retrieving cargo from the plasma membrane and the endosome back to the TGN. However, whether the retrograde trafficking from synaptic endosomes to the TGN is limited to specific cargos or is a more widespread phenomenon with a major impact on synaptic function, remains an open question.

In the light of this hypothesis, one possible function for presynaptic LEs/lysosomes is sorting of SV cargos during SV recycling and directing them to trafficking pathways that carry them back to the soma where they can be subjected to quality control sampling (at the TGN) and/or degradation by somatic lysosomes. This is supported by the clear functional link between lysosomal function and presynaptic health. Neurodegenerative processes associated with lysosomal dysfunction, as in lysosomal storage diseases (LSD), are usually presynaptically initiated and neurodegeneration in these conditions can be curbed by re-establishing presynaptic function (Sambri et al., 2017). SV exo- and endocytosis are severely compromised by lysosomal storage dysfunction. Thus, in several LSD mouse models (Twitcher mice, Niemann-Pick disease type C1, and Mucopolysaccharidosis type 3A), axonal transport of SV-positive vesicles, SV exo-and endocytosis are critically impaired (Xu et al., 2010; Pressey et al., 2012; Wilkinson et al., 2012; Teixeira et al., 2014; Sambri et al., 2017; Bayó-Puxan et al., 2018). This is associated with reduction or aggregation of SV proteins and axonal swelling which results in compromised neurotransmission. Some of these deficits can be partly attributed to interference with the function of presynaptic autophagy (and reduced fusion of autophagosomes and lysosomes). However, the severe presynaptic phenotypes in LSD mouse models, strongly suggest that the SV cycle is a loop within a loop, and that it is structurally and functionally integrated in the general endolysosomal system of the neuron. Therefore, deficits at either end of the system will compromise the function of the whole system.

Outlook

Transitioning from a purely analytic approach to SV recycling to a more systemic one at a molecular level, which recognizes and studies the SV cycle as an integral part of the endomembrane system of the neuron is key for answering outstanding questions in the field by setting the right priorities for future research. Some of these questions are: Which are the cell-biological

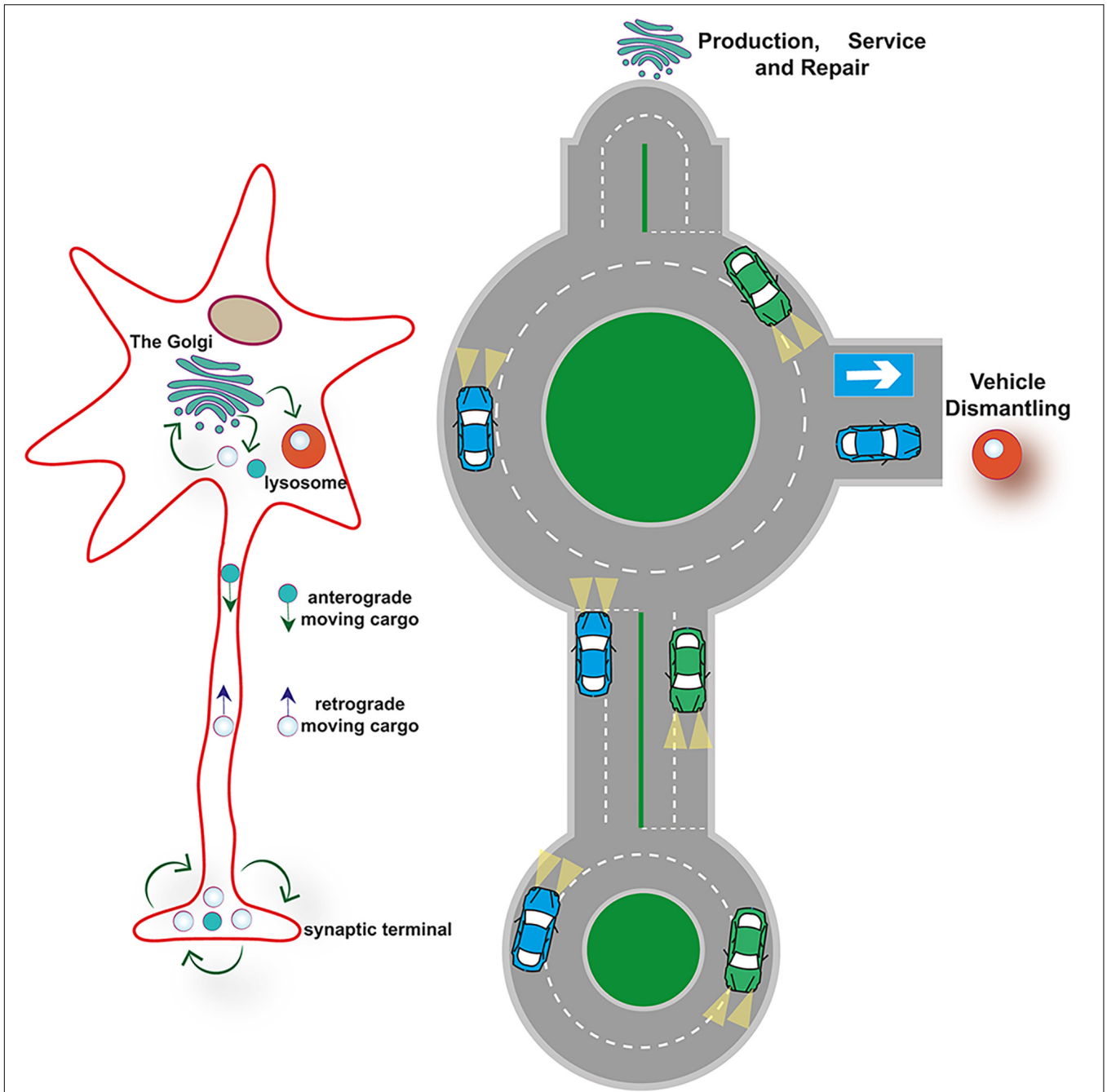

FIGURE 2 | SV recycling is nested in the endolysosomal system. SV recycling is a nested cycle within a larger cycle that encompasses membrane-bound organelles that reside in both, presynaptic sites (the Recycling and Resting pool) and neuronal cell bodies (the Golgi apparatus and degradative lysosomes). The Golgi apparatus performs protein surveillance and funnels cargos to pathways that either repair damage or degrade old and damaged proteins (the lysosome).

mechanisms underlying the assembly and removal of the presynaptic specializations? What drives the use-dependent structural and functional presynaptic plasticity that alters the information coding capacity of the neuron? What mediates the ongoing turnover of SV components which sustains synaptic integrity and function over the lifespan of the neuron? How does previous experience impact these events and is this process tuneable to external signals? Furthermore, multiple neurological disorders ranging from neurodevelopmental autism spectrum disorders and epilepsy to slowly progressing neurodegenerative disorders can be linked to deficits in endolysosomal function and concomitant presynaptic malfunction. To prevent or delay the onset of such disorders and assist in developing targeted therapies in the future, disentangling the systems that regulate these

complex diseases is key and requires examining the interplay among the underlying factors at a molecular level.

AUTHOR CONTRIBUTIONS

DI conceived the topic. DI and MC wrote all drafts of the manuscript. Both authors contributed to the article and approved the submitted version.

FUNDING

Research discussed in this review was funded in part by the Wellcome Trust [Investigator Award to MC (204954/Z/16/Z)].

ACKNOWLEDGMENTS

We thank Federico De Luca for help with the artwork.

REFERENCES

Abu-Remaileh, M., Wyant, G. A., Kim, C., Laqtom, N. N., Abbasi, M., Chan, S. H., et al. (2017). Lysosomal metabolomics reveals V-ATPase- and mTOR-dependent regulation of amino acid efflux from lysosomes. *Science* 358, 807–813. doi: 10.1126/science.aan6298

Ackermann, F., Schink, K. O., Bruns, C., Izsvák, Z., Hamra, F. K., Rosenmund, C., et al. (2019). Critical role for Piccolo in synaptic vesicle retrieval. *Elife* 8:e46629. doi: 10.7554/eLife.46629

Alabi, A. A., and Tsien, R. W. (2012). Synaptic vesicle pools and dynamics. *Cold Spring Harb. Perspect. Biol.* 4:a013680. doi: 10.1101/cshperspect.a013680

Allaire, P. D., Ritter, B., Thomas, S., Burman, J. L., Denisov, A. Y., Legendre-Guillemin, V., et al. (2006). Connecdenn, a novel DENN domain-containing protein of neuronal clathrin-coated vesicles functioning in synaptic vesicle endocytosis. *J. Neurosci.* 26, 13202–13212. doi: 10.1523/jneurosci.4608-06.2006

Andres-Alonso, M., Ammar, M. R., Butnaru, I., Gomes, G. M., Acuna Sanhueza, G., Raman, R., et al. (2019). SIPA1L2 controls trafficking and local signaling of TrkB-containing amphisomes at presynaptic terminals. *Nat. Commun.* 10:5448. doi: 10.1038/s41467-019-13224-z

Andres-Alonso, M., Kreutz, M. R., and Karpova, A. (2021). Autophagy and the endolysosomal system in presynaptic function. *Cell Mol. Life Sci.* 78, 2621–2639. doi: 10.1007/s00018-020-03722-5

Anne, C., and Gasnier, B. (2014). Vesicular neurotransmitter transporters: mechanistic aspects. *Curr. Top. Membr.* 73, 149–174. doi: 10.1016/b978-0-12-800223-0.00003-7

Aprile, D., Fruscione, F., Baldassari, S., Fadda, M., Ferrante, D., Falace, A., et al. (2019). TBC1D24 regulates axonal outgrowth and membrane trafficking at the growth cone in rodent and human neurons. *Cell Death Differ.* 26, 2464–2478. doi: 10.1038/s41418-019-0313-x

Arantes, R. M., and Andrews, N. W. (2006). A role for synaptotagmin VII-regulated exocytosis of lysosomes in neurite outgrowth from primary sympathetic neurons. *J. Neurosci.* 26, 4630–4637. doi: 10.1523/jneurosci.0009-06.2006

Bacaj, T., Wu, D., Yang, X., Morishita, W., Zhou, P., Xu, W., et al. (2013). Synaptotagmin-1 and synaptotagmin-7 trigger synchronous and asynchronous phases of neurotransmitter release. *Neuron* 80, 947–959. doi: 10.1016/j.neuron.2013.10.026

Bal, M., Leitz, J., Reese, A. L., Ramirez, D. M., Durakoglugil, M., Herz, J., et al. (2013). Reelin mobilizes a VAMP7-dependent synaptic vesicle pool and selectively augments spontaneous neurotransmission. *Neuron* 80, 934–946. doi: 10.1016/j.neuron.2013.08.024

Ballabio, A., and Bonifacino, J. S. (2020). Lysosomes as dynamic regulators of cell and organismal homeostasis. *Nat. Rev. Mol. Cell Biol.* 21, 101–118. doi: 10.1038/s41580-019-0185-4

Bayó-Puxan, N., Terrasso, A. P., Creyssels, S., Simão, D., Begon-Pescia, C., Lavigne, M., et al. (2018). Lysosomal and network alterations in human mucopolysaccharidosis type VII iPSC-derived neurons. *Sci. Rep.* 8:16644. doi: 10.1038/s41598-018-34523-3

Bonanomi, D., Fornasiero, E. F., Valdez, G., Halegoua, S., Benfenati, F., Menegon, A., et al. (2008). Identification of a developmentally regulated pathway of membrane retrieval in neuronal growth cones. *J. Cell Sci.* 121(Pt 22), 3757–3769. doi: 10.1242/jcs.033803

Bonifacino, J. S., and Traub, L. M. (2003). Signals for sorting of transmembrane proteins to endosomes and lysosomes. *Annu. Rev. Biochem.* 72, 395–447. doi: 10.1146/annurev.biochem.72.121801.161800

Bonnycastle, K., Davenport, E. C., and Cousin, M. A. (2021). Presynaptic dysfunction in neurodevelopmental disorders: insights from the synaptic vesicle life cycle. *J. Neurochem.* 157, 179–207. doi: 10.1111/jnc.15035

Braun, A., Pinyol, R., Dahlhaus, R., Koch, D., Fonarev, P., Grant, B. D., et al. (2005). EHD proteins associate with syndapin I and II and such interactions play a crucial role in endosomal recycling. *Mol. Biol. Cell* 16, 3642–3658. doi: 10.1091/mbc.e05-01-0076

Briant, K., Johnson, N., and Swanton, E. (2017). Transmembrane domain quality control systems operate at the endoplasmic reticulum and Golgi apparatus. *PLoS One* 12:e0173924. doi: 10.1371/journal.pone.0173924

Brodin, L., and Shupliakov, O. (2018). Retromer in synaptic function and pathology. *Front. Synaptic. Neurosci.* 10:37. doi: 10.3389/fnsyn.2018.00037

Brunger, A. T., Choi, U. B., Lai, Y., Leitz, J., and Zhou, Q. (2018). Molecular mechanisms of fast neurotransmitter release. *Annu. Rev. Biophys.* 47, 469–497. doi: 10.1146/annurev-biophys-070816-034117

Burd, C., and Cullen, P. J. (2014). Retromer: a master conductor of endosome sorting. *Cold Spring Harb. Perspect. Biol.* 6:a016774. doi: 10.1101/cshperspect.a016774

Candiello, E., Kratzke, M., Wenzel, D., Cassel, D., and Schu, P. (2016). AP-1/sigma1A and AP-1/sigma1B adaptor-proteins differentially regulate neuronal early endosome maturation via the Rab5/Vps34-pathway. *Sci. Rep.* 6:29950. doi: 10.1038/srep29950

Capitani, N., and Baldari, C. T. (2021). F-Actin dynamics in the regulation of endosomal recycling and immune synapse assembly. *Front. Cell Dev. Biol.* 9:670882. doi: 10.3389/fcell.2021.670882

Chanaday, N. L., and Kavalali, E. T. (2018). Presynaptic origins of distinct modes of neurotransmitter release. *Curr. Opin. Neurobiol.* 51, 119–126. doi: 10.1016/j.conb.2018.03.005

Chanaday, N. L., Cousin, M. A., Milosevic, I., Watanabe, S., and Morgan, J. R. (2019). The synaptic vesicle cycle revisited: new insights into the modes and mechanisms. *J. Neurosci.* 39, 8209–8216. doi: 10.1523/JNEUROSCI.1158-19.2019

Chanaday, N. L., Nosyreva, E., Shin, O. H., Zhang, H., Aklan, I., Atasoy, D., et al. (2021). Presynaptic store-operated Ca(2+) entry drives excitatory spontaneous neurotransmission and augments endoplasmic reticulum stress. *Neuron* 109, 1314.e–1332.e. doi: 10.1016/j.neuron.2021.02.023

Cheng, X. T., Zhou, B., Lin, M. Y., Cai, Q., and Sheng, Z. H. (2015). Axonal autophagosomes recruit dynein for retrograde transport through fusion with late endosomes. *J. Cell Biol.* 209, 377–386. doi: 10.1083/jcb.201412046

Cheung, G., and Cousin, M. A. (2019). Synaptic vesicle generation from activity-dependent bulk endosomes requires a dephosphorylation-dependent dynamin-syndapin interaction. *J. Neurochem.* 151, 570–583. doi: 10.1111/jnc.14862

Clayton, E. L., Anggono, V., Smillie, K. J., Chau, N., Robinson, P. J., and Cousin, M. A. (2009). The phospho-dependent dynamin-syndapin interaction triggers activity-dependent bulk endocytosis of synaptic vesicles. *J. Neurosci.* 29, 7706–7717. doi: 10.1523/jneurosci.1976-09.2009

Clayton, E. L., Evans, G. J., and Cousin, M. A. (2008). Bulk synaptic vesicle endocytosis is rapidly triggered during strong stimulation. *J. Neurosci.* 28, 6627–6632. doi: 10.1523/jneurosci.1445-08.2008

Conner, S. D., and Schmid, S. L. (2003). Regulated portals of entry into the cell. *Nature* 422, 37–44. doi: 10.1038/nature01451

Cousin, M. A., Malladi, C. S., Tan, T. C., Raymond, C. R., Smillie, K. J., and Robinson, P. J. (2003). Synapsin I-associated phosphatidylinositol 3-kinase mediates synaptic vesicle delivery to the readily releasable pool. *J. Biol. Chem.* 278, 29065–29071. doi: 10.1074/jbc.M302386200

Crawford, D. C., and Kavalali, E. T. (2015). Molecular underpinnings of synaptic vesicle pool heterogeneity. *Traffic* 16, 338–364. doi: 10.1111/tra.12262

Dall'Armi, C., Devereaux, K. A., and Di Paolo, G. (2013). The role of lipids in the control of autophagy. *Curr. Biol.* 23, R33–R45. doi: 10.1016/j.cub.2012.10.041

Deák, F., Schoch, S., Liu, X., Südhof, T. C., and Kavalali, E. T. (2004). Synaptobrevin is essential for fast synaptic-vesicle endocytosis. *Nat. Cell Biol.* 6, 1102–1108. doi: 10.1038/ncb1185

Deák, F., Shin, O. H., Kavalali, E. T., and Südhof, T. C. (2006). Structural determinants of synaptobrevin 2 function in synaptic vesicle fusion. *J. Neurosci.* 26, 6668–6676. doi: 10.1523/jneurosci.5272-05.2006

Dean, C., Dunning, F. M., Liu, H., Bomba-Warczak, E., Martens, H., Bharat, V., et al. (2012). Axonal and dendritic synaptotagmin isoforms revealed by a pHluorin-syt functional screen. *Mol. Biol. Cell* 23, 1715–1727. doi: 10.1091/mbc.E11-08-0707

Deinhardt, K., Salinas, S., Verastegui, C., Watson, R., Worth, D., Hanrahan, S., et al. (2006). Rab5 and Rab7 control endocytic sorting along the axonal retrograde transport pathway. *Neuron* 52, 293–305. doi: 10.1016/j.neuron.2006.08.018

Delvendahl, I., Vyleta, N. P., von Gersdorff, H., and Hallermann, S. (2016). Fast, temperature-sensitive and clathrin-independent endocytosis at central synapses. *Neuron* 90, 492–498. doi: 10.1016/j.neuron.2016.03.013

Denker, A., Kröhnert, K., Bückers, J., Neher, E., and Rizzoli, S. O. (2011). The reserve pool of synaptic vesicles acts as a buffer for proteins involved in synaptic vesicle recycling. *Proc. Natl. Acad. Sci. U.S.A.* 108, 17183–17188. doi: 10.1073/pnas.1112690108

Derivery, E., Sousa, C., Gautier, J. J., Lombard, B., Loew, D., and Gautreau, A. (2009). The Arp2/3 activator WASH controls the fission of endosomes through a large multiprotein complex. *Dev. Cell* 17, 712–723. doi: 10.1016/j.devcel.2009.09.010

Dey, S., Banker, G., and Ray, K. (2017). Anterograde transport of rab4-associated vesicles regulates synapse organization in *Drosophila*. *Cell Rep.* 18, 2452–2463. doi: 10.1016/j.celrep.2017.02.034

Doherty, G. J., and McMahon, H. T. (2009). Mechanisms of endocytosis. *Annu. Rev. Biochem.* 78, 857–902. doi: 10.1146/annurev.biochem.78.081307.110540

Dorrbaum, A. R., Kochen, L., Langer, J. D., and Schuman, E. M. (2018). Local and global influences on protein turnover in neurons and glia. *Elife* 7:e34202. doi: 10.7554/eLife.34202

Emperador-Melero, J., Huson, V., van Weering, J., Bollmann, C., Fischer von Mollard, G., Toonen, R. F., et al. (2018). Vti1a/b regulate synaptic vesicle and dense core vesicle secretion via protein sorting at the Golgi. *Nat. Commun.* 9:3421. doi: 10.1038/s41467-018-05699-z

Falace, A., Buhler, E., Fadda, M., Watrin, F., Lippiello, P., Pallesi-Pocachard, E., et al. (2014). TBC1D24 regulates neuronal migration and maturation through modulation of the ARF6-dependent pathway. *Proc. Natl. Acad. Sci. U.S.A.* 111, 2337–2342. doi: 10.1073/pnas.1316294111

Fernandes, A. C., Uytterhoeven, V., Kuenen, S., Wang, Y. C., Slabbaert, J. R., Swerts, J., et al. (2014). Reduced synaptic vesicle protein degradation at lysosomes curbs TBC1D24/sky-induced neurodegeneration. *J. Cell Biol.* 207, 453–462. doi: 10.1083/jcb.201406026

Finelli, M. J., Aprile, D., Castroflorio, E., Jeans, A., Moschetta, M., Chessum, L., et al. (2019). The epilepsy-associated protein TBC1D24 is required for normal development, survival and vesicle trafficking in mammalian neurons. *Hum. Mol. Genet.* 28, 584–597. doi: 10.1093/hmg/ddy370

Fox, G. Q. (1988). A morphometric analysis of synaptic vesicle distributions. *Brain Res.* 475, 103–117. doi: 10.1016/0006-8993(88)90203-x

Gad, H., Ringstad, N., Löw, P., Kjaerulff, O., Gustafsson, J., Wenk, M., et al. (2000). Fission and uncoating of synaptic clathrin-coated vesicles are perturbed by disruption of interactions with the SH3 domain of endophilin. *Neuron* 27, 301–312. doi: 10.1016/s0896-6273(00)00038-6

Gallon, M., and Cullen, P. J. (2015). Retromer and sorting nexins in endosomal sorting. *Biochem. Soc. Trans.* 43, 33–47. doi: 10.1042/bst20140290

Glyvuk, N., Tsytsyura, Y., Geumann, C., D'Hooge, R., Huve, J., Kratzke, M., et al. (2010). AP-1/sigma1B-adaptin mediates endosomal synaptic vesicle recycling, learning and memory. *EMBO J.* 29, 1318–1330. doi: 10.1038/emboj.2010.15

Gokool, S., Tattersall, D., and Seaman, M. N. J. (2007). EHD1 interacts with retromer to stabilize SNX1 tubules and facilitate endosome-to-Golgi retrieval. *Traffic* 8, 1873–1886. doi: 10.1111/j.1600-0854.2007.00652.x

Goldenring, J. R. (2015). Recycling endosomes. *Curr. Opin. Cell Biol.* 35, 117–122. doi: 10.1016/j.ceb.2015.04.018

Goto-Silva, L., McShane, M. P., Salinas, S., Kalaidzidis, Y., Schiavo, G., and Zerial, M. (2019). Retrograde transport of Akt by a neuronal Rab5-APPL1 endosome. *Sci. Rep.* 9:2433. doi: 10.1038/s41598-019-38637-0

Gowrisankaran, S., Houy, S., Del Castillo, J. G. P., Steubler, V., Gelker, M., Kroll, J., et al. (2020). Endophilin-A coordinates priming and fusion of neurosecretory vesicles via intersectin. *Nat. Commun.* 11:1266. doi: 10.1038/s41467-020-14993-8

Granseth, B., Odermatt, B., Royle, S. J., and Lagnado, L. (2006). Clathrin-mediated endocytosis is the dominant mechanism of vesicle retrieval at hippocampal synapses. *Neuron* 51, 773–786. doi: 10.1016/j.neuron.2006.08.029

Grant, B. D., and Donaldson, J. G. (2009). Pathways and mechanisms of endocytic recycling. *Nat. Rev. Mol. Cell Biol.* 10, 597–608. doi: 10.1038/nrm2755

Guedes-Dias, P., and Holzbaur, E. L. F. (2019). Axonal transport: driving synaptic function. *Science* 366:eaaw9997. doi: 10.1126/science.aaw9997

Han, M., Zou, W., Chang, H., Yu, Y., Zhang, H., Li, S., et al. (2017). A Systematic RNAi screen reveals a novel role of a spindle assembly checkpoint protein bugz in synaptic transmission in C. elegans. *Front. Mol. Neurosci.* 10:141. doi: 10.3389/fnmol.2017.00141

Harris, K. M., and Sultan, P. (1995). Variation in the number, location and size of synaptic vesicles provides an anatomical basis for the nonuniform probability of release at hippocampal CA1 synapses. *Neuropharmacology* 34, 1387–1395. doi: 10.1016/0028-3908(95)00142-s

He, L., Wu, X. S., Mohan, R., and Wu, L. G. (2006). Two modes of fusion pore opening revealed by cell-attached recordings at a synapse. *Nature* 444, 102–105. doi: 10.1038/nature05250

Held, R. G., Liu, C., Ma, K., Ramsey, A. M., Tarr, T. B., De Nola, G., et al. (2020). Synapse and active zone assembly in the absence of presynaptic Ca(2+) channels and Ca(2+) entry. *Neuron* 107:e669. doi: 10.1016/j.neuron.2020.05.032

Hellerschmied, D., Serebrenik, Y. V., Shao, L., Burslem, G. M., and Crews, C. M. (2019). Protein folding state-dependent sorting at the Golgi apparatus. *Mol. Biol. Cell* 30, 2296–2308. doi: 10.1091/mbc.E19-01-0069

Herzog, E., Nadrigny, F., Silm, K., Biesemann, C., Helling, I., Bersot, T., et al. (2011). In vivo imaging of intersynaptic vesicle exchange using VGLUT1 Venus knock-in mice. *J. Neurosci.* 31, 15544–15559. doi: 10.1523/jneurosci.2073-11.2011

Hirata, T., Fujita, M., Nakamura, S., Gotoh, K., Motooka, D., Murakami, Y., et al. (2015). Post-Golgi anterograde transport requires GARP-dependent endosome-to-TGN retrograde transport. *Mol. Biol. Cell* 26, 3071–3084. doi: 10.1091/mbc.E14-11-1568

Holt, M., Cooke, A., Wu, M. M., and Lagnado, L. (2003). Bulk membrane retrieval in the synaptic terminal of retinal bipolar cells. *J. Neurosci.* 23, 1329–1339. doi: 10.1523/jneurosci.23-04-01329.2003

Hoopmann, P., Punge, A., Barysch, S. V., Westphal, V., Buckers, J., Opazo, F., et al. (2010). Endosomal sorting of readily releasable synaptic vesicles. *Proc. Natl. Acad. Sci. U.S.A.* 107, 19055–19060. doi: 10.1073/pnas.1007037107

Howes, M. T., Kirkham, M., Riches, J., Cortese, K., Walser, P. J., Simpson, F., et al. (2010). Clathrin-independent carriers form a high capacity endocytic sorting system at the leading edge of migrating cells. *J. Cell Biol.* 190, 675–691. doi: 10.1083/jcb.201002119

Hua, Y., Sinha, R., Martineau, M., Kahms, M., and Klingauf, J. (2010). A common origin of synaptic vesicles undergoing evoked and spontaneous fusion. *Nat. Neurosci.* 13, 1451–1453. doi: 10.1038/nn.2695

Hua, Z., Leal-Ortiz, S., Foss, S. M., Waites, C. L., Garner, C. C., Voglmaier, S. M., et al. (2011). V-SNARE composition distinguishes synaptic vesicle pools. *Neuron* 71, 474–487. doi: 10.1016/j.neuron.2011.06.010

Hurley, J. H. (2008). ESCRT complexes and the biogenesis of multivesicular bodies. *Curr. Opin. Cell Biol.* 20, 4–11. doi: 10.1016/j.ceb.2007.12.002

Hurley, J. H. (2015). ESCRTs are everywhere. *Embo J.* 34, 2398–2407. doi: 10.15252/embj.201592484

Inoshita, T., Arano, T., Hosaka, Y., Meng, H., Umezaki, Y., Kosugi, S., et al. (2017). Vps35 in cooperation with LRRK2 regulates synaptic vesicle endocytosis through the endosomal pathway in *Drosophila*. *Hum. Mol. Genet.* 26, 2933–2948. doi: 10.1093/hmg/ddx179

Ishii, S., Matsuura, A., and Itakura, E. (2019). Identification of a factor controlling lysosomal homeostasis using a novel lysosomal trafficking probe. *Sci. Rep.* 9:11635. doi: 10.1038/s41598-019-48131-2

Itakura, E., Kishi-Itakura, C., and Mizushima, N. (2012). The hairpin-type tail-anchored SNARE syntaxin 17 targets to autophagosomes for fusion with endosomes/lysosomes. *Cell* 151, 1256–1269. doi: 10.1016/j.cell.2012.11.001

Ivanova, D., Dirks, A., Montenegro-Venegas, C., Schone, C., Altrock, W. D., Marini, C., et al. (2015). Synaptic activity controls localization and function of CtBP1 via binding to Bassoon and Piccolo. *EMBO J.* 34, 1056–1077. doi: 10.15252/embj.201488796

Ivanova, D., Dobson, K. L., Gajbhiye, A., Davenport, E. C., Hacker, D., Ultanir, S. K., et al. (2021). Control of synaptic vesicle release probability via VAMP4 targeting to endolysosomes. *Sci. Adv.* 7:eabf3873. doi: 10.1126/sciadv.abf3873

Ivanova, D., Imig, C., Camacho, M., Reinhold, A., Guhathakurta, D., Montenegro-Venegas, C., et al. (2020). CtBP1-Mediated Membrane Fission Contributes to Effective Recycling of Synaptic Vesicles. *Cell Rep.* 30, 2444–2459.e7. doi: 10.1016/j.celrep.2020.01.079

Jahn, R., and Scheller, R. H. (2006). SNAREs–engines for membrane fusion. *Nat. Rev. Mol. Cell Biol.* 7, 631–643. doi: 10.1038/nrm2002

Jähne, S., Rizzoli, S. O., and Helm, M. S. (2015). The structure and function of presynaptic endosomes. *Exp. Cell Res.* 335, 172–179. doi: 10.1016/j.yexcr.2015.04.017

Jakobsson, J., Ackermann, F., Andersson, F., Larhammar, D., Löw, P., and Brodin, L. (2011). Regulation of synaptic vesicle budding and dynamin function by an EHD ATPase. *J. Neurosci.* 31, 13972–13980. doi: 10.1523/jneurosci.1289-11.2011

Jia, D., Gomez, T. S., Billadeau, D. D., and Rosen, M. K. (2012). Multiple repeat elements within the FAM21 tail link the WASH actin regulatory complex to the retromer. *Mol. Biol. Cell* 23, 2352–2361. doi: 10.1091/mbc.E11-12-1059

Jin, E. J., Kiral, F. R., Ozel, M. N., Burchardt, L. S., Osterland, M., Epstein, D., et al. (2018). Live observation of two parallel membrane degradation pathways at axon terminals. *Curr. Biol.* 28, 1027.e–1038.e. doi: 10.1016/j.cub.2018.02.032

Joensuu, M., Martínez-Mármol, R., Padmanabhan, P., Glass, N. R., Durisic, N., Pelekanos, M., et al. (2017). Visualizing endocytic recycling and trafficking in live neurons by subdiffractional tracking of internalized molecules. *Nat. Protoc.* 12, 2590–2622. doi: 10.1038/nprot.2017.116

Johannes, L., and Popoff, V. (2008). Tracing the retrograde route in protein trafficking. *Cell* 135, 1175–1187. doi: 10.1016/j.cell.2008.12.009

Kaeser, P. S., and Regehr, W. G. (2014). Molecular mechanisms for synchronous, asynchronous, and spontaneous neurotransmitter release. *Annu. Rev. Physiol.* 76, 333–363. doi: 10.1146/annurev-physiol-021113-170338

Khvotchev, M. V., Ren, M., Takamori, S., Jahn, R., and Südhof, T. C. (2003). Divergent functions of neuronal Rab11b in Ca2+-regulated versus constitutive exocytosis. *J. Neurosci.* 23, 10531–10539. doi: 10.1523/jneurosci.23-33-10531.2003

Kim, S. H., and Ryan, T. A. (2010). CDK5 serves as a major control point in neurotransmitter release. *Neuron* 67, 797–809. doi: 10.1016/j.neuron.2010.08.003

Klinkert, K., and Echard, A. (2016). Rab35 GTPase: a central regulator of phosphoinositides and f-actin in endocytic recycling and beyond. *Traffic* 17, 1063–1077. doi: 10.1111/tra.12422

Klumperman, J., and Raposo, G. (2014). The complex ultrastructure of the endolysosomal system. *Cold Spring Harb. Perspect. Biol.* 6:a016857. doi: 10.1101/cshperspect.a016857

Koch, D., Spiwoks-Becker, I., Sabanov, V., Sinning, A., Dugladze, T., Stellmacher, A., et al. (2011). Proper synaptic vesicle formation and neuronal network activity critically rely on syndapin I. *Embo J.* 30, 4955–4969. doi: 10.1038/emboj.2011.339

Koch, S., Molchanova, S. M., Wright, A. K., Edwards, A., Cooper, J. D., Taira, T., et al. (2011). Morphologic and functional correlates of synaptic pathology in the cathepsin D knockout mouse model of congenital neuronal ceroid lipofuscinosis. *J. Neuropathol. Exp. Neurol.* 70, 1089–1096. doi: 10.1097/NEN.0b013e318238fc28

Kokotos, A. C., and Cousin, M. A. (2015). Synaptic vesicle generation from central nerve terminal endosomes. *Traffic* 16, 229–240. doi: 10.1111/tra.12235

Kokotos, A. C., Peltier, J., Davenport, E. C., Trost, M., and Cousin, M. A. (2018). Activity-dependent bulk endocytosis proteome reveals a key presynaptic role for the monomeric GTPase Rab11. *Proc. Natl. Acad. Sci. U.S.A.* 115, E10177–E10186. doi: 10.1073/pnas.1809189115

Kononenko, N. L., and Haucke, V. (2015). Molecular mechanisms of presynaptic membrane retrieval and synaptic vesicle reformation. *Neuron* 85, 484–496. doi: 10.1016/j.neuron.2014.12.016

Kononenko, N. L., Puchkov, D., Classen, G. A., Walter, A. M., Pechstein, A., Sawade, L., et al. (2014). Clathrin/AP-2 mediate synaptic vesicle reformation from endosome-like vacuoles but are not essential for membrane retrieval at central synapses. *Neuron* 82, 981–988. doi: 10.1016/j.neuron.2014.05.007

Koo, S. J., Kochlamazashvili, G., Rost, B., Puchkov, D., Gimber, N., Lehmann, M., et al. (2015). Vesicular synaptobrevin/VAMP2 levels guarded by AP180 control efficient neurotransmission. *Neuron* 88, 330–344. doi: 10.1016/j.neuron.2015.08.034

Kroll, J., Jaime Tobón, L. M., Vogl, C., Neef, J., Kondratiuk, I., König, M., et al. (2019). Endophilin-A regulates presynaptic Ca(2+) influx and synaptic vesicle recycling in auditory hair cells. *Embo J.* 38:116. doi: 10.15252/embj.2018100116

Kuijpers, M., Azarnia Tehran, D., Haucke, V., and Soykan, T. (2021a). The axonal endolysosomal and autophagic systems. *J. Neurochem.* 158, 589–602. doi: 10.1111/jnc.15287

Kuijpers, M., Kochlamazashvili, G., Stumpf, A., Puchkov, D., Swaminathan, A., Lucht, M. T., et al. (2021b). Neuronal autophagy regulates presynaptic neurotransmission by controlling the axonal endoplasmic reticulum. *Neuron* 109, 299.e–313.e. doi: 10.1016/j.neuron.2020.10.005

Lawrence, R. E., and Zoncu, R. (2019). The lysosome as a cellular centre for signalling, metabolism and quality control. *Nat. Cell Biol.* 21, 133–142. doi: 10.1038/s41556-018-0244-7

Li, X., and DiFiglia, M. (2012). The recycling endosome and its role in neurological disorders. *Prog. Neurobiol.* 97, 127–141. doi: 10.1016/j.pneurobio.2011.10.002

Li, X., Qin, L., Li, Y., Yu, H., Zhang, Z., Tao, C., et al. (2019). Presynaptic endosomal cathepsin d regulates the biogenesis of GABAergic synaptic vesicles. *Cell Rep.* 28, 1015.e–1028.e. doi: 10.1016/j.celrep.2019.06.006

Li, Y. C., Chanaday, N. L., Xu, W., and Kavalali, E. T. (2017). Synaptotagmin-1- and synaptotagmin-7-dependent fusion mechanisms target synaptic vesicles to kinetically distinct endocytic pathways. *Neuron* 93, 616.e–631.e. doi: 10.1016/j.neuron.2016.12.010

Lie, P. P. Y., Yang, D. S., Stavrides, P., Goulbourne, C. N., Zheng, P., Mohan, P. S., et al. (2021). Post-Golgi carriers, not lysosomes, confer lysosomal properties to pre-degradative organelles in normal and dystrophic axons. *Cell Rep.* 35:109034. doi: 10.1016/j.celrep.2021.109034

Lin, P. Y., Chanaday, N. L., Horvath, P. M., Ramirez, D. M. O., Monteggia, L. M., and Kavalali, E. T. (2020). VAMP4 maintains a Ca(2+)-sensitive pool of spontaneously recycling synaptic vesicles. *J. Neurosci.* 40, 5389–5401. doi: 10.1523/JNEUROSCI.2386-19.2020

Liu, H., Bai, H., Hui, E., Yang, L., Evans, C. S., Wang, Z., et al. (2014). Synaptotagmin 7 functions as a Ca2+-sensor for synaptic vesicle replenishment. *Elife* 3:e01524. doi: 10.7554/eLife.01524

LoGiudice, L., and Matthews, G. (2006). The synaptic vesicle cycle: is kissing overrated? *Neuron* 51, 676–677. doi: 10.1016/j.neuron.2006.09.004

Lorenzo, D. N., Badea, A., Davis, J., Hostettler, J., He, J., Zhong, G., et al. (2014). A PIK3C3-ankyrin-B-dynactin pathway promotes axonal growth and multiorganelle transport. *J. Cell Biol.* 207, 735–752. doi: 10.1083/jcb.201407063

Luo, F., and Südhof, T. C. (2017).). Synaptotagmin-7-mediated asynchronous release boosts high-fidelity synchronous transmission at a central synapse. *Neuron* 94, 826.e–839.e. doi: 10.1016/j.neuron.2017.04.020

Luo, F., Bacaj, T., and Südhof, T. C. (2015). Synaptotagmin-7 is essential for Ca2+-triggered delayed asynchronous release but not for Ca2+-dependent vesicle priming in retinal ribbon synapses. *J. Neurosci.* 35, 11024–11033. doi: 10.1523/jneurosci.0759-15.2015

Luzio, J. P., Gray, S. R., and Bright, N. A. (2010). Endosome-lysosome fusion. *Biochem. Soc. Trans.* 38, 1413–1416. doi: 10.1042/bst0381413

Luzio, J. P., Pryor, P. R., and Bright, N. A. (2007). Lysosomes: fusion and function. *Nat. Rev. Mol. Cell Biol.* 8, 622–632. doi: 10.1038/nrm2217

Maday, S., and Holzbaur, E. L. (2014). Autophagosome biogenesis in primary neurons follows an ordered and spatially regulated pathway. *Dev. Cell* 30, 71–85. doi: 10.1016/j.devcel.2014.06.001

Maday, S., Wallace, K. E., and Holzbaur, E. L. (2012). Autophagosomes initiate distally and mature during transport toward the cell soma in primary neurons. *J. Cell Biol.* 196, 407–417. doi: 10.1083/jcb.201106120

Martineau, M., Guzman, R. E., Fahlke, C., and Klingauf, J. (2017). VGLUT1 functions as a glutamate/proton exchanger with chloride channel activity in hippocampal glutamatergic synapses. *Nat. Commun.* 8:2279. doi: 10.1038/s41467-017-02367-6

Martinez, I., Chakrabarti, S., Hellevik, T., Morehead, J., Fowler, K., and Andrews, N. W. (2000). Synaptotagmin VII regulates Ca(2+)-dependent exocytosis of lysosomes in fibroblasts. *J. Cell Biol.* 148, 1141–1149. doi: 10.1083/jcb.148.6.1141

Martinez-Arca, S., Rudge, R., Vacca, M., Raposo, G., Camonis, J., Proux-Gillardeaux, V., et al. (2003). A dual mechanism controlling the localization and function of exocytic v-SNAREs. *Proc. Natl. Acad. Sci. U.S.A.* 100, 9011–9016. doi: 10.1073/pnas.1431910100

Maxfield, F. R., and McGraw, T. E. (2004). Endocytic recycling. *Nat. Rev. Mol. Cell Biol.* 5, 121–132. doi: 10.1038/nrm1315

Maximov, A., Lao, Y., Li, H., Chen, X., Rizo, J., Sørensen, J. B., et al. (2008). Genetic analysis of synaptotagmin-7 function in synaptic vesicle exocytosis. *Proc. Natl. Acad. Sci. U.S.A.* 105, 3986–3991. doi: 10.1073/pnas.0712372105

McKenzie, J. E., Raisley, B., Zhou, X., Naslavsky, N., Taguchi, T., Caplan, S., et al. (2012). Retromer guides STxB and CD8-M6PR from early to recycling endosomes. EHD1 guides STxB from recycling endosome to Golgi. *Traffic* 13, 1140–1159. doi: 10.1111/j.1600-0854.2012.01374.x

McMahon, H. T., Ushkaryov, Y. A., Edelmann, L., Link, E., Binz, T., Niemann, H., et al. (1993). Cellubrevin is a ubiquitous tetanus-toxin substrate homologous to a putative synaptic vesicle fusion protein. *Nature* 364, 346–349. doi: 10.1038/364346a0

McMillan, K. J., Korswagen, H. C., and Cullen, P. J. (2017). The emerging role of retromer in neuroprotection. *Curr. Opin. Cell Biol.* 47, 72–82. doi: 10.1016/j.ceb.2017.02.004

Medina, D. L., Di Paola, S., Peluso, I., Armani, A., De Stefani, D., Venditti, R., et al. (2015). Lysosomal calcium signalling regulates autophagy through calcineurin and TFEB. *Nat. Cell Biol.* 17, 288–299. doi: 10.1038/ncb3114

Milosevic, I., Giovedi, S., Lou, X., Raimondi, A., Collesi, C., Shen, H., et al. (2011). Recruitment of endophilin to clathrin-coated pit necks is required for efficient vesicle uncoating after fission. *Neuron* 72, 587–601. doi: 10.1016/j.neuron.2011.08.029

Murray, R. Z., Kay, J. G., Sangermani, D. G., and Stow, J. L. (2005). A role for the phagosome in cytokine secretion. *Science* 310, 1492–1495. doi: 10.1126/science.1120225

Mutch, S. A., Kensel-Hammes, P., Gadd, J. C., Fujimoto, B. S., Allen, R. W., Schiro, P. G., et al. (2011). Protein quantification at the single vesicle level reveals that a subset of synaptic vesicle proteins are trafficked with high precision. *J. Neurosci.* 31, 1461–1470. doi: 10.1523/jneurosci.3805-10.2011

Naslavsky, N., and Caplan, S. (2011). EHD proteins: key conductors of endocytic transport. *Trends Cell Biol.* 21, 122–131. doi: 10.1016/j.tcb.2010.10.003

Naslavsky, N., and Caplan, S. (2018). The enigmatic endosome - sorting the ins and outs of endocytic trafficking. *J. Cell Sci.* 131:jcs216499. doi: 10.1242/jcs.216499

Neher, E. (2015). Merits and limitations of vesicle pool models in view of heterogeneous populations of synaptic vesicles. *Neuron* 87, 1131–1142. doi: 10.1016/j.neuron.2015.08.038

Nicholson-Fish, J. C., Cousin, M. A., and Smillie, K. J. (2016). Phosphatidylinositol 3-kinase couples localised calcium influx to activation of Akt in central nerve terminals. *Neurochem. Res.* 41, 534–543. doi: 10.1007/s11064-015-1663-5

Nicholson-Fish, J. C., Kokotos, A. C., Gillingwater, T. H., Smillie, K. J., and Cousin, M. A. (2015). VAMP4 is an essential cargo molecule for activity-dependent bulk endocytosis. *Neuron* 88, 973–984. doi: 10.1016/j.neuron.2015.10.043

Okerlund, N. D., Schneider, K., Leal-Ortiz, S., Montenegro-Venegas, C., Kim, S. A., Garner, L. C., et al. (2017). Bassoon controls presynaptic autophagy through Atg5. *Neuron* 93, 897.e–913.e. doi: 10.1016/j.neuron.2017.01.026

Orlando, M., Schmitz, D., Rosenmund, C., and Herman, M. A. (2019). Calcium-independent exo-endocytosis coupling at small central synapses. *Cell Rep.* 29, 3767.e–3774.e. doi: 10.1016/j.celrep.2019.11.060

Overhoff, M., De Bruyckere, E., and Kononenko, N. L. (2021). Mechanisms of neuronal survival safeguarded by endocytosis and autophagy. *J. Neurochem.* 157, 263–296. doi: 10.1111/jnc.15194

Overly, C. C., and Hollenbeck, P. J. (1996). Dynamic organization of endocytic pathways in axons of cultured sympathetic neurons. *J. Neurosci.* 16, 6056–6064. doi: 10.1523/jneurosci.16-19-06056.1996

Partanen, S., Haapanen, A., Kielar, C., Pontikis, C., Alexander, N., Inkinen, T., et al. (2008). Synaptic changes in the thalamocortical system of cathepsin D-deficient mice: a model of human congenital neuronal ceroid-lipofuscinosis. *J. Neuropathol. Exp. Neurol.* 67, 16–29. doi: 10.1097/nen.0b013e31815f3899

Pavlos, N. J., and Jahn, R. (2011). Distinct yet overlapping roles of Rab GTPases on synaptic vesicles. *Small GTPases* 2, 77–81. doi: 10.4161/sgtp.2.2.15201

Pavlos, N. J., Grønborg, M., Riedel, D., Chua, J. J., Boyken, J., Kloepper, T. H., et al. (2010). Quantitative analysis of synaptic vesicle Rabs uncovers distinct yet overlapping roles for Rab3a and Rab27b in Ca2+-triggered exocytosis. *J. Neurosci.* 30, 13441–13453. doi: 10.1523/jneurosci.0907-10.2010

Pechstein, A., Gerth, F., Milosevic, I., Jäpel, M., Eichhorn-Grünig, M., Vorontsova, O., et al. (2015). Vesicle uncoating regulated by SH3-SH3 domain-mediated complex formation between endophilin and intersectin at synapses. *EMBO Rep.* 16, 232–239. doi: 10.15252/embr.201439260

Peden, A. A., Park, G. Y., and Scheller, R. H. (2001). The Di-leucine motif of vesicle-associated membrane protein 4 is required for its localization and AP-1 binding. *J. Biol. Chem.* 276, 49183–49187. doi: 10.1074/jbc.M106646200

Piper, R. C., and Katzmann, D. J. (2007). Biogenesis and function of multivesicular bodies. *Annu. Rev. Cell Dev. Biol.* 23, 519–547. doi: 10.1146/annurev.cellbio.23.090506.123319

Pressey, S. N., Smith, D. A., Wong, A. M., Platt, F. M., and Cooper, J. D. (2012). Early glial activation, synaptic changes and axonal pathology in the thalamocortical system of Niemann-Pick type C1 mice. *Neurobiol. Dis.* 45, 1086–1100. doi: 10.1016/j.nbd.2011.12.027

Quan, A., Xue, J., Wielens, J., Smillie, K. J., Anggono, V., Parker, M. W., et al. (2012). Phosphorylation of syndapin I F-BAR domain at two helix-capping motifs regulates membrane tubulation. *Proc. Natl. Acad. Sci. U.S.A.* 109, 3760–3765. doi: 10.1073/pnas.1108294109

Raiborg, C., Schink, K. O., and Stenmark, H. (2013). Class III phosphatidylinositol 3-kinase and its catalytic product PtdIns3P in regulation of endocytic membrane traffic. *Febs J.* 280, 2730–2742. doi: 10.1111/febs.12116

Raingo, J., Khvotchev, M., Liu, P., Darios, F., Li, Y. C., Ramirez, D. M., et al. (2012). VAMP4 directs synaptic vesicles to a pool that selectively maintains asynchronous neurotransmission. *Nat. Neurosci.* 15, 738–745. doi: 10.1038/nn.3067

Ramirez, D. M., Khvotchev, M., Trauterman, B., and Kavalali, E. T. (2012). Vti1a identifies a vesicle pool that preferentially recycles at rest and maintains spontaneous neurotransmission. *Neuron* 73, 121–134. doi: 10.1016/j.neuron.2011.10.034

Rao, S. K., Huynh, C., Proux-Gillardeaux, V., Galli, T., and Andrews, N. W. (2004). Identification of SNAREs involved in synaptotagmin VII-regulated lysosomal exocytosis. *J. Biol. Chem.* 279, 20471–20479. doi: 10.1074/jbc.M400798200

Ravikumar, B., Sarkar, S., Davies, J. E., Futter, M., Garcia-Arencibia, M., Green-Thompson, Z. W., et al. (2010). Regulation of mammalian autophagy in physiology and pathophysiology. *Physiol. Rev.* 90, 1383–1435. doi: 10.1152/physrev.00030.2009

Reddy, A., Caler, E. V., and Andrews, N. W. (2001). Plasma membrane repair is mediated by Ca(2+)-regulated exocytosis of lysosomes. *Cell* 106, 157–169. doi: 10.1016/s0092-8674(01)00421-4

Renard, H. F., and Boucrot, E. (2021). Unconventional endocytic mechanisms. *Curr. Opin. Cell Biol.* 71, 120–129. doi: 10.1016/j.ceb.2021.03.001

Rey, S., Marra, V., Smith, C., and Staras, K. (2020). Nanoscale remodeling of functional synaptic vesicle pools in hebbian plasticity. *Cell Rep.* 30, 2006–2017.e3. doi: 10.1016/j.celrep.2020.01.051

Richards, D. A., Rizzoli, S. O., and Betz, W. J. (2004). Effects of wortmannin and latrunculin A on slow endocytosis at the frog neuromuscular junction. *J. Physiol.* 557(Pt 1), 77–91. doi: 10.1113/jphysiol.2004.062158

Rink, J., Ghigo, E., Kalaidzidis, Y., and Zerial, M. (2005). Rab conversion as a mechanism of progression from early to late endosomes. *Cell* 122, 735–749. doi: 10.1016/j.cell.2005.06.043

Rizo, J. (2018). Mechanism of neurotransmitter release coming into focus. *Protein Sci.* 27, 1364–1391. doi: 10.1002/pro.3445

Rizzoli, S. O., and Betz, W. J. (2002). Effects of 2-(4-morpholinyl)-8-phenyl-4H-1-benzopyran-4-one on synaptic vesicle cycling at the frog neuromuscular junction. *J. Neurosci.* 22, 10680–10689. doi: 10.1523/jneurosci.22-24-10680.2002

Rizzoli, S. O., Bethani, I., Zwilling, D., Wenzel, D., Siddiqui, T. J., Brandhorst, D., et al. (2006). Evidence for early endosome-like fusion of recently endocytosed synaptic vesicles. *Traffic* 7, 1163–1176. doi: 10.1111/j.1600-0854.2006.00466.x

Russnak, R., Konczal, D., and McIntire, S. L. (2001). A family of yeast proteins mediating bidirectional vacuolar amino acid transport. *J. Biol. Chem.* 276, 23849–23857. doi: 10.1074/jbc.M008028200

Saftig, P., and Klumperman, J. (2009). Lysosome biogenesis and lysosomal membrane proteins: trafficking meets function. *Nat. Rev. Mol. Cell Biol.* 10, 623–635. doi: 10.1038/nrm2745

Sambri, I., D'Alessio, R., Ezhova, Y., Giuliano, T., Sorrentino, N. C., Cacace, V., et al. (2017). Lysosomal dysfunction disrupts presynaptic maintenance and restoration of presynaptic function prevents neurodegeneration in lysosomal storage diseases. *EMBO Mol. Med.* 9, 112–132. doi: 10.15252/emmm.201606965

Sando, R., Bushong, E., Zhu, Y., Huang, M., Considine, C., Phan, S., et al. (2017). Assembly of excitatory synapses in the absence of glutamatergic neurotransmission. *Neuron* 94, 312–313. doi: 10.1016/j.neuron.2017.03.047

Sasidharan, N., Sumakovic, M., Hannemann, M., Hegermann, J., Liewald, J. F., Olendrowitz, C., et al. (2012). RAB-5 and RAB-10 cooperate to regulate neuropeptide release in Caenorhabditis elegans. *Proc. Natl. Acad. Sci. U.S.A.* 109, 18944–18949. doi: 10.1073/pnas.1203306109

Scheuber, A., Rudge, R., Danglot, L., Raposo, G., Binz, T., Poncer, J. C., et al. (2006). Loss of AP-3 function affects spontaneous and evoked release at hippocampal mossy fiber synapses. *Proc. Natl. Acad. Sci. U.S.A.* 103, 16562–16567. doi: 10.1073/pnas.0603511103

Schuldiner, S., Shirvan, A., and Linial, M. (1995). Vesicular neurotransmitter transporters: from bacteria to humans. *Physiol. Rev.* 75, 369–392. doi: 10.1152/physrev.1995.75.2.369

Scott, C. C., Vacca, F., and Gruenberg, J. (2014). Endosome maturation, transport and functions. *Semin. Cell Dev. Biol.* 31, 2–10. doi: 10.1016/j.semcdb.2014.03.034

Seaman, M. N. (2012). The retromer complex - endosomal protein recycling and beyond. *J. Cell Sci.* 125(Pt 20), 4693–4702. doi: 10.1242/jcs.103440

Seaman, M. N., McCaffery, J. M., and Emr, S. D. (1998). A membrane coat complex essential for endosome-to-Golgi retrograde transport in yeast. *J. Cell Biol.* 142, 665–681. doi: 10.1083/jcb.142.3.665

Selak, S., Braun, J. E., and Fritzler, M. J. (2004). Characterization of early endosome antigen 1 in neural tissues. *Biochem. Biophys. Res. Commun.* 323, 1334–1342. doi: 10.1016/j.bbrc.2004.09.010

Serrano-Saiz, E., Vogt, M. C., Levy, S., Wang, Y., Kaczmarczyk, K. K., Mei, X., et al. (2020). SLC17A6/7/8 vesicular glutamate transporter homologs in nematodes. *Genetics* 214, 163–178. doi: 10.1534/genetics.119.302855

Sheehan, P., and Waites, C. L. (2019). Coordination of synaptic vesicle trafficking and turnover by the Rab35 signaling network. *Small GTPases* 10, 54–63. doi: 10.1080/21541248.2016.1270392

Sheehan, P., Zhu, M., Beskow, A., Vollmer, C., and Waites, C. L. (2016). Activity-dependent degradation of synaptic vesicle proteins requires Rab35 and the ESCRT pathway. *J. Neurosci.* 36, 8668–8686. doi: 10.1523/JNEUROSCI.0725-16.2016

Shimizu, H., Kawamura, S., and Ozaki, K. (2003). An essential role of Rab5 in uniformity of synaptic vesicle size. *J. Cell Sci.* 116(Pt 17), 3583–3590. doi: 10.1242/jcs.00676

Shin, N., Jeong, H., Kwon, J., Heo, H. Y., Kwon, J. J., Yun, H. J., et al. (2008). LRRK2 regulates synaptic vesicle endocytosis. *Exp. Cell Res.* 314, 2055–2065. doi: 10.1016/j.yexcr.2008.02.015

Shitara, A., Shibui, T., Okayama, M., Arakawa, T., Mizoguchi, I., Sakakura, Y., et al. (2013). VAMP4 is required to maintain the ribbon structure of the Golgi apparatus. *Mol. Cell Biochem.* 380, 11–21. doi: 10.1007/s11010-013-1652-4

Sigler, A., Oh, W. C., Imig, C., Altas, B., Kawabe, H., Cooper, B. H., et al. (2017). Formation and maintenance of functional spines in the absence of presynaptic glutamate release. *Neuron* 94, 304.e–311.e. doi: 10.1016/j.neuron.2017.03.029

Small, S. A., and Petsko, G. A. (2015). Retromer in Alzheimer disease. Parkinson disease and other neurological disorders. *Nat. Rev. Neurosci.* 16, 126–132. doi: 10.1038/nrn3896

Soukup, S. F., and Verstreken, P. (2017). EndoA/Endophilin-A creates docking stations for autophagic proteins at synapses. *Autophagy* 13, 971–972. doi: 10.1080/15548627.2017.1286440

Soukup, S. F., Kuenen, S., Vanhauwaert, R., Manetsberger, J., Hernández-Díaz, S., Swerts, J., et al. (2016). A LRRK2-dependent endophilinA phosphoswitch is critical for macroautophagy at presynaptic terminals. *Neuron* 92, 829–844. doi: 10.1016/j.neuron.2016.09.037

Soykan, T., Kaempf, N., Sakaba, T., Vollweiter, D., Goerdeler, F., Puchkov, D., et al. (2017). Synaptic vesicle endocytosis occurs on multiple timescales and is mediated by formin-dependent actin assembly. *Neuron* 93, 854–856. doi: 10.1016/j.neuron.2017.02.011

Soykan, T., Maritzen, T., and Haucke, V. (2016). Modes and mechanisms of synaptic vesicle recycling. *Curr. Opin. Neurobiol.* 39, 17–23. doi: 10.1016/j.conb.2016.03.005

Star, E. N., Newton, A. J., and Murthy, V. N. (2005). Real-time imaging of Rab3a and Rab5a reveals differential roles in presynaptic function. *J. Physiol.* 569(Pt 1), 103–117. doi: 10.1113/jphysiol.2005.092528

Staras, K., Branco, T., Burden, J. J., Pozo, K., Darcy, K., Marra, V., et al. (2010). A vesicle superpool spans multiple presynaptic terminals in hippocampal neurons. *Neuron* 66, 37–44. doi: 10.1016/j.neuron.2010.03.020

Steinert, J. R., Campesan, S., Richards, P., Kyriacou, C. P., Forsythe, I. D., and Giorgini, F. (2012). Rab11 rescues synaptic dysfunction and behavioural deficits in a *Drosophila* model of Huntington's disease. *Hum. Mol. Genet.* 21, 2912–2922. doi: 10.1093/hmg/dds117

Stenmark, H. (2009). Rab GTPases as coordinators of vesicle traffic. *Nat. Rev. Mol. Cell Biol.* 10, 513–525. doi: 10.1038/nrm2728

Stevens, C. F., and Williams, J. H. (2000). "Kiss and run" exocytosis at hippocampal synapses. *Proc. Natl. Acad. Sci. U.S.A.* 97, 12828–12833. doi: 10.1073/pnas.230438697

Stoorvogel, W., Strous, G. J., Geuze, H. J., Oorschot, V., and Schwartz, A. L. (1991). Late endosomes derive from early endosomes by maturation. *Cell* 65, 417–427. doi: 10.1016/0092-8674(91)90459-c

Sugita, S., Han, W., Butz, S., Liu, X., Fernández-Chacón, R., Lao, Y., et al. (2001). Synaptotagmin VII as a plasma membrane Ca(2+) sensor in exocytosis. *Neuron* 30, 459–473. doi: 10.1016/s0896-6273(01)00290-2

Sun, Z., and Brodsky, J. L. (2019). Protein quality control in the secretory pathway. *J. Cell Biol.* 218, 3171–3187. doi: 10.1083/jcb.201906047

Sundborger, A., Soderblom, C., Vorontsova, O., Evergren, E., Hinshaw, J. E., and Shupliakov, O. (2011). An endophilin-dynamin complex promotes budding of clathrin-coated vesicles during synaptic vesicle recycling. *J. Cell Sci.* 124(Pt 1), 133–143. doi: 10.1242/jcs.072686

Tagliatti, E., Fadda, M., Falace, A., Benfenati, F., and Fassio, A. (2016). Arf6 regulates the cycling and the readily releasable pool of synaptic vesicles at hippocampal synapse. *Elife* 5:10116. doi: 10.7554/eLife.10116

Takamori, S., Holt, M., Stenius, K., Lemke, E. A., Gronborg, M., Riedel, D., et al. (2006). Molecular anatomy of a trafficking organelle. *Cell* 127, 831–846. doi: 10.1016/j.cell.2006.10.030

Takáts, S., Nagy, P., Varga, Á, Pircs, K., Kárpáti, M., Varga, K., et al. (2013). Autophagosomal syntaxin17-dependent lysosomal degradation maintains neuronal function in *Drosophila*. *J. Cell Biol.* 201, 531–539. doi: 10.1083/jcb.201211160

Tao, C. L., Liu, Y. T., Sun, R., Zhang, B., Qi, L., Shivakoti, S., et al. (2018). Differentiation and characterization of excitatory and inhibitory synapses by cryo-electron tomography and correlative microscopy. *J. Neurosci.* 38, 1493–1510. doi: 10.1523/jneurosci.1548-17.2017

Taoufiq, Z., Ninov, M., Villar-Briones, A., Wang, H. Y., Sasaki, T., Roy, M. C., et al. (2020). Hidden proteome of synaptic vesicles in the mammalian brain. *Proc. Natl. Acad. Sci. U.S.A.* 117, 33586–33596. doi: 10.1073/pnas.2011870117

Teixeira, C. A., Miranda, C. O., Sousa, V. F., Santos, T. E., Malheiro, A. R., Solomon, M., et al. (2014). Early axonal loss accompanied by impaired endocytosis, abnormal axonal transport, and decreased microtubule stability occur in the model of Krabbe's disease. *Neurobiol. Dis.* 66, 92–103. doi: 10.1016/j.nbd.2014.02.012

Tian, Y., Tang, F. L., Sun, X., Wen, L., Mei, L., Tang, B. S., et al. (2015). VPS35-deficiency results in an impaired AMPA receptor trafficking and decreased dendritic spine maturation. *Mol. Brain* 8:70. doi: 10.1186/s13041-015-0156-4

Truckenbrodt, S., Viplav, A., Jahne, S., Vogts, A., Denker, A., Wildhagen, H., et al. (2018). Newly produced synaptic vesicle proteins are preferentially used in synaptic transmission. *EMBO J.* 37:e98044. doi: 10.15252/embj.201798044

Tsuriel, S., Geva, R., Zamorano, P., Dresbach, T., Boeckers, T., Gundelfinger, E. D., et al. (2006). Local sharing as a predominant determinant of synaptic matrix molecular dynamics. *PLoS Biol.* 4:e271. doi: 10.1371/journal.pbio.0040271

Uchizono, K. (1965). Characteristics of excitatory and inhibitory synapses in the central nervous system of the cat. *Nature* 207, 642–643. doi: 10.1038/207642a0

Uytterhoeven, V., Kuenen, S., Kasprowicz, J., Miskiewicz, K., and Verstreken, P. (2011). Loss of skywalker reveals synaptic endosomes as sorting stations for synaptic vesicle proteins. *Cell* 145, 117–132. doi: 10.1016/j.cell.2011.02.039

Vanhauwaert, R., Kuenen, S., Masius, R., Bademosi, A., Manetsberger, J., Schoovaerts, N., et al. (2017). The SAC1 domain in synaptojanin is required for autophagosome maturation at presynaptic terminals. *Embo J.* 36, 1392–1411. doi: 10.15252/embj.201695773

Varoqueaux, F., Sigler, A., Rhee, J. S., Brose, N., Enk, C., Reim, K., et al. (2002). Total arrest of spontaneous and evoked synaptic transmission but normal synaptogenesis in the absence of Munc13-mediated vesicle priming. *Proc. Natl. Acad. Sci. U.S.A.* 99, 9037–9042. doi: 10.1073/pnas.122623799

Vazquez-Sanchez, S., Bobeldijk, S., Dekker, M. P., van Keimpema, L., and van Weering, J. R. T. (2018). VPS35 depletion does not impair presynaptic structure and function. *Sci. Rep.* 8:2996. doi: 10.1038/s41598-018-20448-4

Verhage, M., Maia, A. S., Plomp, J. J., Brussaard, A. B., Heeroma, J. H., Vermeer, H., et al. (2000). Synaptic assembly of the brain in the absence of neurotransmitter secretion. *Science* 287, 864–869. doi: 10.1126/science.287.5454.864

Vevea, J. D., Kusick, G. F., Courtney, K. C., Chen, E., Watanabe, S., and Chapman, E. R. (2021). Synaptotagmin 7 is targeted to the axonal plasma membrane through γ-secretase processing to promote synaptic vesicle docking in mouse hippocampal neurons. *Elife* 10:e67261. doi: 10.7554/eLife.67261

Vietri, M., Radulovic, M., and Stenmark, H. (2020). The many functions of ESCRTs. *Nat. Rev. Mol. Cell Biol.* 21, 25–42. doi: 10.1038/s41580-019-0177-4

Vilariño-Güell, C., Wider, C., Ross, O. A., Dachsel, J. C., Kachergus, J. M., Lincoln, S. J., et al. (2011). VPS35 mutations in Parkinson disease. *Am. J. Hum. Genet.* 89, 162–167. doi: 10.1016/j.ajhg.2011.06.001

Villarroel-Campos, D., Schiavo, G., and Lazo, O. M. (2018). The many disguises of the signalling endosome. *FEBS Lett.* 592, 3615–3632. doi: 10.1002/1873-3468.13235

Virmani, T., Han, W., Liu, X., Südhof, T. C., and Kavalali, E. T. (2003). Synaptotagmin 7 splice variants differentially regulate synaptic vesicle recycling. *Embo J.* 22, 5347–5357. doi: 10.1093/emboj/cdg514

Vukoja, A., Rey, U., Petzoldt, A. G., Ott, C., Vollweiter, D., Quentin, C., et al. (2018). Presynaptic biogenesis requires axonal transport of lysosome-related vesicles. *Neuron* 99, 1216.e–1232.e. doi: 10.1016/j.neuron.2018.08.004

Watanabe, S., Mamer, L. E., Raychaudhuri, S., Luvsanjav, D., Eisen, J., Trimbuch, T., et al. (2018). Synaptojanin and endophilin mediate neck formation during ultrafast endocytosis. *Neuron* 98, 1184.e–1197.e. doi: 10.1016/j.neuron.2018.06.005

Watanabe, S., Rost, B. R., Camacho-Perez, M., Davis, M. W., Sohl-Kielczynski, B., Rosenmund, C., et al. (2013). Ultrafast endocytosis at mouse hippocampal synapses. *Nature* 504, 242–247. doi: 10.1038/nature12809

Watanabe, S., Trimbuch, T., Camacho-Perez, M., Rost, B. R., Brokowski, B., Sohl-Kielczynski, B., et al. (2014). Clathrin regenerates synaptic vesicles from endosomes. *Nature* 515, 228–233. doi: 10.1038/nature13846

Weber, J. P., Toft-Bertelsen, T. L., Mohrmann, R., Delgado-Martinez, I., and Sørensen, J. B. (2014). Synaptotagmin-7 is an asynchronous calcium sensor for synaptic transmission in neurons expressing SNAP-23. *PLoS One* 9:e114033. doi: 10.1371/journal.pone.0114033

Wei, S., Xu, Y., Shi, H., Wong, S. H., Han, W., Talbot, K., et al. (2010). EHD1 is a synaptic protein that modulates exocytosis through binding to snapin. *Mol. Cell Neurosci.* 45, 418–429. doi: 10.1016/j.mcn.2010.07.014

Wen, L., Tang, F. L., Hong, Y., Luo, S. W., Wang, C. L., He, W., et al. (2011). VPS35 haploinsufficiency increases Alzheimer's disease neuropathology. *J. Cell Biol.* 195, 765–779. doi: 10.1083/jcb.201105109

White, J. A. II, Krzystek, T. J., Hoffmar-Glennon, H., Thant, C., Zimmerman, K., Iacobucci, G., et al. (2020). Excess Rab4 rescues synaptic and behavioral dysfunction caused by defective HTT-Rab4 axonal transport in Huntington's disease. *Acta Neuropathol. Commun.* 8:97. doi: 10.1186/s40478-020-00964-z

Wilhelm, B. G., Mandad, S., Truckenbrodt, S., Krohnert, K., Schafer, C., Rammner, B., et al. (2014). Composition of isolated synaptic boutons reveals the amounts of vesicle trafficking proteins. *Science* 344, 1023–1028. doi: 10.1126/science.1252884

Wilkinson, F. L., Holley, R. J., Langford-Smith, K. J., Badrinath, S., Liao, A., Langford-Smith, A., et al. (2012). Neuropathology in mouse models of mucopolysaccharidosis type I. IIIA and IIIB. *PLoS One* 7:e35787. doi: 10.1371/journal.pone.0035787

Willingham, M. C., and Pastan, I. (1980). The receptosome: an intermediate organelle of receptor mediated endocytosis in cultured fibroblasts. *Cell* 21, 67–77. doi: 10.1016/0092-8674(80)90115-4

Willingham, M. C., Hanover, J. A., Dickson, R. B., and Pastan, I. (1984). Morphologic characterization of the pathway of transferrin endocytosis and recycling in human KB cells. *Proc. Natl. Acad. Sci. U.S.A.* 81, 175–179. doi: 10.1073/pnas.81.1.175

Wittig, S., Ganzella, M., Barth, M., Kostmann, S., Riedel, D., Pérez-Lara, Á, et al. (2021). Cross-linking mass spectrometry uncovers protein interactions and functional assemblies in synaptic vesicle membranes. *Nat. Commun.* 12:858. doi: 10.1038/s41467-021-21102-w

Wollert, T., and Hurley, J. H. (2010). Molecular mechanism of multivesicular body biogenesis by ESCRT complexes. *Nature* 464, 864–869. doi: 10.1038/nature08849

Wu, L. G., Hamid, E., Shin, W., and Chiang, H. C. (2014). Exocytosis and endocytosis: modes, functions, and coupling mechanisms. *Annu. Rev. Physiol.* 76, 301–331. doi: 10.1146/annurev-physiol-021113-170305

Wucherpfennig, T., Wilsch-Bräuninger, M., and González-Gaitán, M. (2003). Role of Drosophila Rab5 during endosomal trafficking at the synapse and evoked neurotransmitter release. *J. Cell Biol.* 161, 609–624. doi: 10.1083/jcb.200211087

Xu, S., Zhou, S., Xia, D., Xia, J., Chen, G., Duan, S., et al. (2010). Defects of synaptic vesicle turnover at excitatory and inhibitory synapses in Niemann-Pick C1-deficient neurons. *Neuroscience* 167, 608–620. doi: 10.1016/j.neuroscience.2010.02.033

Yang, C., and Wang, X. (2021). Lysosome biogenesis: regulation and functions. *J. Cell Biol.* 220:e202102001. doi: 10.1083/jcb.202102001

Zhang, B., Koh, Y. H., Beckstead, R. B., Budnik, V., Ganetzky, B., and Bellen, H. J. (1998). Synaptic vesicle size and number are regulated by a clathrin adaptor protein required for endocytosis. *Neuron* 21, 1465–1475. doi: 10.1016/s0896-6273(00)80664-9

Zhang, Q., Li, Y., and Tsien, R. W. (2009). The dynamic control of kiss-and-run and vesicular reuse probed with single nanoparticles. *Science* 323, 1448–1453. doi: 10.1126/science.1167373

Zhang, X. M., François, U., Silm, K., Angelo, M. F., Fernandez-Busch, M. V., Maged, M., et al. (2019). A proline-rich motif on VGLUT1 reduces synaptic vesicle super-pool and spontaneous release frequency. *Elife* 8:e50401. doi: 10.7554/eLife.50401

Zhen, Y., Radulovic, M., Vietri, M., and Stenmark, H. (2021). Sealing holes in cellular membranes. *Embo J.* 40:e106922. doi: 10.15252/embj.2020106922

Zhou, C., Li, C., Li, D., Wang, Y., Shao, W., You, Y., et al. (2013). BIG1, a brefeldin A-inhibited guanine nucleotide-exchange protein regulates neurite development via PI3K-AKT and ERK signaling pathways. *Neuroscience* 254, 361–368. doi: 10.1016/j.neuroscience.2013.09.045

Conflict of Interest: The authors declare that the research was conducted in the absence of any commercial or financial relationships that could be construed as a potential conflict of interest.

Publisher's Note: All claims expressed in this article are solely those of the authors and do not necessarily represent those of their affiliated organizations, or those of the publisher, the editors and the reviewers. Any product that may be evaluated in this article, or claim that may be made by its manufacturer, is not guaranteed or endorsed by the publisher.

frontiers in Synaptic Neuroscience

REVIEW
published: 04 March 2022
doi: 10.3389/fnsyn.2022.841704

Multiple Roles of Actin in Exo- and Endocytosis

Ling-Gang Wu and Chung Yu Chan*

National Institute of Neurological Disorders and Stroke, Bethesda, MD, United States

Cytoskeletal filamentous actin (F-actin) has long been considered a molecule that may regulate exo- and endocytosis. However, its exact roles remained elusive. Recent studies shed new light on many crucial roles of F-actin in regulating exo- and endocytosis. Here, this progress is reviewed from studies of secretory cells, particularly neurons and endocrine cells. These studies reveal that F-actin is involved in mediating all kinetically distinguishable forms of endocytosis, including ultrafast, fast, slow, bulk, and overshoot endocytosis, likely *via* membrane pit formation. F-actin promotes vesicle replenishment to the readily releasable pool most likely *via* active zone clearance, which may sustain synaptic transmission and overcome short-term depression of synaptic transmission during repetitive firing. By enhancing plasma membrane tension, F-actin promotes fusion pore expansion, vesicular content release, and a fusion mode called shrink fusion involving fusing vesicle shrinking. Not only F-actin, but also the F-actin assembly pathway, including ATP hydrolysis, N-WASH, and formin, are involved in mediating these roles of exo- and endocytosis. Neurological disorders, including spinocerebellar ataxia 13 caused by Kv3.3 channel mutation, may involve impairment of F-actin and its assembly pathway, leading in turn to impairment of exo- and endocytosis at synapses that may contribute to neurological disorders.

Keywords: actin, exocytosis, endocytosis, synaptic transmission, neurological disorder

OPEN ACCESS

Edited by:
Lucia Tabares,
University of Seville, Spain

Reviewed by:
Silvio O. Rizzoli,
Society for Scientific Data Processing,
Max Planck Society, Germany
Helena Haque Chowdhury,
University of Ljubljana, Slovenia

****Correspondence:***
Ling-Gang Wu
wul@ninds.nih.gov

Received: *22 December 2021*
Accepted: *11 February 2022*
Published: *04 March 2022*

Citation:
Wu L-G and Chan CY (2022) Multiple Roles of Actin in Exo- and Endocytosis. Front. Synaptic Neurosci. 14:841704. doi: 10.3389/fnsyn.2022.841704

INTRODUCTION

Vesicle exocytosis releases neurotransmitters and hormones to mediate important functions, such as synaptic transmission, stress responses, and immune responses (Wu et al., 2014; Chang et al., 2017; Brunger et al., 2018; Sharma and Lindau, 2018). After exocytosis, fused vesicles must be retrieved *via* endocytosis, which recycles vesicles and thus sustains exocytosis in secretory cells, particularly in nerve terminals (Wu et al., 2014; Kononenko and Haucke, 2015; Gan and Watanabe, 2018). Half a century of studies identified many core exo- and endocytic proteins, such as SNARE proteins, synaptotagmin, and dynamin (Jahn and Fasshauer, 2012; Kaksonen and Roux, 2018; Mettlen et al., 2018). However, the role of actin in the exo- and endocytosis of secretory cells remained not well understood despite it being one of the most abundant cytoskeletal proteins (Cingolani and Goda, 2008; Li et al., 2018).

Studies over the past three decades led to proposals that actin is involved in many steps of exo- and endocytosis in secretory cells. These potential roles include vesicle clustering in nerve terminals, physical barrier to prevent vesicle docking at the plasma membrane, facilitation of vesicle mobilization to the readily releasable pool (RRP) that seems to contradict its physical barrier function, fusion pore expansion, vesicle merging at the plasma membrane, and endocytosis that

recycles vesicles (Cingolani and Goda, 2008; Li et al., 2018). With respect to its vesicle clustering role, filamentous actin (F-actin), together with synapsin, has long been proposed to provide a cytoskeletal scaffold linking vesicles together, leading to formation of vesicle clusters in nerve terminals (reviewed in Cingolani and Goda, 2008). Recent studies suggest that synapsin alone can form a distinct liquid phase in an aqueous environment, which may catalyze vesicle clustering at nerve terminals (Milovanovic et al., 2018). Microinjection of reagents that bind to the intrinsically disordered region of synapsin causes dispersal of synaptic vesicle clusters, suggesting that liquid-liquid phase separation may mediate synaptic vesicle clustering (Pechstein et al., 2020). These results suggest re-examination of the role of F-actin in vesicle clustering in the future. Accordingly, this topic will not be further discussed here.

With respect to its physical barrier role, early studies showed that disruption of actin polymerization increases the frequency of spontaneous and evoked transmitter release at synapses and in endocrine cells, suggesting that F-actin behind the plasma membrane may restrain docking of vesicles at release sites (Aunis and Bader, 1988; Morales et al., 2000; Trifaro et al., 2000; Chowdhury et al., 2002; Malacombe et al., 2006; Cingolani and Goda, 2008). In neuroendocrine cells, the region of cytosol adjacent to the plasma membrane contains the most actin filaments, called the cortical actin network (reviewed in Meunier and Gutierrez, 2016). This cortical actin network may act as a physical barrier that opposes vesicle access to release sites, as shown in studies of chemicals that stabilize or inhibit actin polymerization (Wen et al., 2011; Meunier and Gutierrez, 2016). The physical barrier function has been systematically surveyed in several excellent reviews (Meunier and Gutierrez, 2016; Papadopulos, 2017; Li et al., 2018). Thus, readers are referred to these reviews for more detailed discussion of the physical barrier function. This review focuses on actin's roles in mediating endocytosis, facilitating replenishment of the RRP, promoting fusion pore expansion, and merging vesicles with the plasma membrane. Potential mechanisms that may reconcile the apparent conflict between actin's physical barrier function versus facilitatory role in RRP replenishment are also suggested.

ACTIN IS CRUCIAL FOR ALL KINETICALLY DISTINGUISHABLE FORMS OF ENDOCYTOSIS

Early studies regarding actin's role in endocytosis in secretory cells reached different conclusions as to whether actin is needed and at which step(s). For example, at lamprey giant synapses, latrunculin B, which disrupts actin polymerization, causes accumulation of clathrin-coated pits and vesicles (Shupliakov et al., 2002; Bourne et al., 2006), whereas latrunculin A (Lat A), which also disrupts actin polymerization, does not affect endocytosis as measured using FM1-43 uptake (Bleckert et al., 2012). At frog neuromuscular junctions, Lat A reduces FM1-43 uptake into nerve terminals (Richards et al., 2004). Whether this effect is caused by inhibition of endocytosis or exocytosis has not been distinguished. On the other hand, cytochalasin D, which inhibits actin polymerization, does not affect FM1-43 uptake or release, implying that actin may not be needed for endocytosis at frog neuromuscular junctions (Betz and Henkel, 1994). At hippocampal synapses, Lat A does not affect endocytosis after action potential trains (Li and Murthy, 2001; Sankaranarayanan et al., 2003; Hua et al., 2011). At goldfish retinal bipolar synapses, latrunculin B and cytochalasin D do not inhibit endocytosis over a time course $<\sim$20 s, but may slow down bulk endocytosis (Holt et al., 2003). Lat A inhibits fast endocytosis at mossy fiber boutons (Delvendahl et al., 2016) and ultrafast endocytosis at hippocampal synapses (Watanabe et al., 2014). These pharmacological studies do not reach a consensus regarding the effect of actin blockers on endocytosis at the same synapse, at different synapses, or for different endocytic modes. However, these studies rely on actin blockers, and some studies use only one blocker at one concentration. False-positive or -negative results owing to off-target effects or difficulty blocking actin polymerization in live cells might contribute to these apparent controversial results (Bleckert et al., 2012). In the following, we review more recent studies that used genetic combined with pharmacological approaches to study actin's endocytic role in mammalian cells.

There are six actin isoforms in mammalian cells. β-Cytoplasmic actin (β-actin), encoded by *Actb*, and γ-cytoplasmic actin (γ-actin), encoded by *Actg1,* are ubiquitously expressed and are the major isoforms in the nervous system (**Figure 1A**; Herman, 1993; Cheever and Ervasti, 2013). β- or γ-actin knockout at two types of nerve terminals in mice, the calyx of Held and hippocampal boutons, were generated (Wu et al., 2016). At the giant calyx of Held nerve terminal, capacitance measurements reveal four kinetically different forms of endocytosis, including slow endocytosis (tens of seconds), rapid or fast endocytosis (a few seconds), bulk endocytosis (forming vesicles larger than regular vesicles), and endocytosis overshoot (retrieving more vesicles than were exocytosed) (Sun and Wu, 2001; Sun et al., 2002; Yamashita et al., 2005, 2010; Renden and Von Gersdorff, 2007; Xu et al., 2008; Hosoi et al., 2009; Wu et al., 2009; Xue et al., 2012). At cultured small conventional hippocampal boutons, endocytosis can be measured with imaging of pH-sensitive pHluorin attached to synaptic vesicle proteins (Sankaranarayanan and Ryan, 2000; Wienisch and Klingauf, 2006; Balaji and Ryan, 2007; Sun et al., 2010; Zhang et al., 2013; Kavalali and Jorgensen, 2014; Chanaday and Kavalali, 2018).

Capacitance measurements at calyces reveal that β- or γ-actin knockout inhibits slow endocytosis, rapid endocytosis (**Figures 1B,C**), bulk endocytosis (detected as the large downward capacitance shift; **Figure 1D**), and endocytosis overshoot (**Figure 1D**; Wu et al., 2016). Electron microscopy and pHluorin imaging at hippocampal synapses show that β- or γ-actin knockout inhibits slow endocytosis and endosome-like structure formation due to bulk endocytosis (Wu et al., 2016). Thus, actin is crucial in mediating rapid, slow, bulk, and overshoot endocytosis. An actin mutant with a polymerization defect could not rescue endocytosis in boutons lacking β-actin, suggesting that polymerized actin, which is known to exert mechanical forces (Mund et al., 2018), is involved in generating

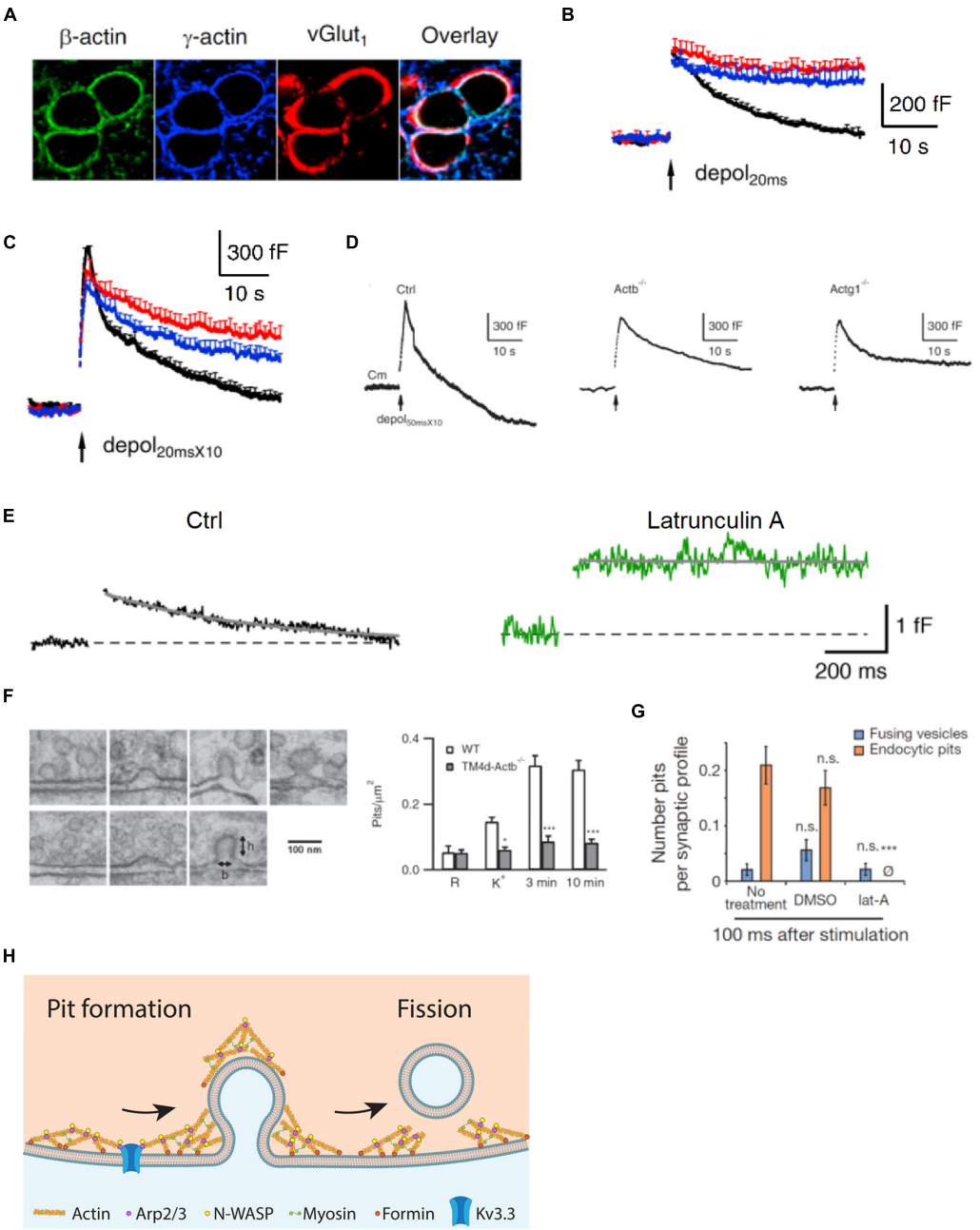

FIGURE 1 | Actin is involved in mediating ultrafast, fast, slow, bulk, and overshoot endocytosis at synapses likely by facilitating membrane pit formation. **(A)** Antibody staining of β-actin, γ-actin, and vesicular glutamate transporter 1 ($vGluT_1$) in calyx of Held nerve terminals. **(B)** Actin involvement in slow endocytosis: mean capacitance (Cm) traces (mean + SEM) induced by a 20 ms depolarization from –80 to +10 mV ($depol_{20\ ms}$, arrow) in calyces of wild-type (black), $Actb^{-/-}$ (red), and $Actg1^{-/-}$ (blue) mice. $Depol_{20\ ms}$ induces slow endocytosis in wild-type calyces. **(C)** Actin involvement in rapid (or fast) endocytosis: similar arrangement as in **B** except that the stimulus was 10 $depol_{20\ ms}$ at 10 Hz ($depol_{20\ msX10}$), which induces rapid (or fast) endocytosis in wild-type calyces. **(D)** Actin involvement in bulk endocytosis and endocytosis overshoot: sampled Cm induced by $depol_{50\ msX10}$ (10 $depol_{50\ ms}$ at 10 Hz) with 5.5 mM calcium in the bath from wild-type (Ctrl), β-actin $(Actb)^{-/-}$, and γ-actin $(Actg1)^{-/-}$ calyces. $Depol_{50\ msX10}$ induces bulk endocytosis (a large step of downward capacitance shift) and endocytosis overshoot in Ctrl. **(E)** Actin involvement in very fast endocytosis: averaged Cm response to single action potentials in Ctrl (black) and in the presence of latrunculin A (Lat A, green). Gray solid lines are exponential fits to the Cm decay. **(F)** Left: electron microscopy images of membrane pits of various shapes obtained during or after high potassium chloride (KCl) application from either wild-type (WT) or $Actb^{-/-}$ hippocampal cultures. Right: the number of pits before (R) and after KCl application (K^+, 0 min; 3 min and 10 min) in wild-type (WT) control and $Actb^{-/-}$ hippocampal synapses (mean + SEM). *$p < 0.05$; ***$p < 0.001$ (t-test). The data show that β-actin knockout inhibits pit formation. **(G)** Actin involvement in ultrafast pit formation: average number of exocytic pits (blue) and endocytic pits (orange) in cells treated with latrunculin A (Lat A) or dimethyl sulfoxide (DMSO). ***$p < 0.001$ (t-test). **(H)** Schematic diagram showing the involvement of F-actin and its nucleation factors, such as Kv3.3 potassium channel, Arp2/3, formin, and myosin II in all kinetically distinguishable forms of endocytosis, including ultrafast, fast, slow, bulk, and overshoot endocytosis. Panels **A–D,F** are adapted from Wu et al. (2016) with permission. Panel **E** is adapted from Delvendahl et al. (2016) with permission. Panel **G** is adapted from Watanabe et al. (2013) with permission.

forces needed for endocytosis (Wu et al., 2016). Actin knockout does not affect the rate of fission pore closure during bulk endocytosis at calyces but inhibits membrane pit formation at hippocampal synapses (**Figure 1F**), suggesting that F-actin may exert mechanical force to bend membrane and thereby generate membrane pits (Wu et al., 2016). Taken together, these findings indicate that polymerized actin may mediate rapid, slow, bulk, and overshoot endocytosis by providing mechanical forces to bend membrane (Wu et al., 2016).

This suggestion, supported by genetic evidence, is consistent with pharmacological evidence that Lat A inhibits a very fast form of endocytosis with a time constant of ∼0.5 s recorded with capacitance measurements at cerebellar and hippocampal mossy fiber boutons (**Figure 1E**; Delvendahl et al., 2016). Lat A also inhibits ultrafast pit formation detected with electron microscopy combined with rapid freezing after optogenetic stimulation at hippocampal synapses (**Figure 1G**), which suggests involvement of F-actin in ultrafast endocytosis (Watanabe et al., 2013). Taken together, these results indicate that F-actin may be involved in mediating all distinguishable forms of endocytosis at synapses, including ultrafast, fast, slow, bulk, and overshoot endocytosis *via* its role in pit generation (**Figure 1H**).

This possibility, inferred from studies of secretory cells, may not generalize to non-secretory vesicle endocytosis in mammalian cells, where F-actin is thought to be needed to overcome membrane tension only when plasma membrane tension is high (Merrifield et al., 2005; Yarar et al., 2005; Ferguson et al., 2009; Saffarian et al., 2009; Boulant et al., 2011). However, it is consistent with actin's role during endocytosis in yeast, which possess a cell wall, where actin polymerization from the plasma membrane toward the cytosol has been suggested to generate a force pushing and elongating the neck, forming a tube-shape pit (Picco et al., 2015; Kaksonen and Roux, 2018; Mund et al., 2018). Whether this mechanism applies to mammalian cells, which do not contain cell walls, remains to be determined. Imaging F-actin dynamics during endocytic membrane pit formation in real time, a very recent study in mammalian chromaffin cells suggests that F-actin may providing a point-pulling force at the center of the endocytic zone to pull membrane inward, forming membrane pits together with dynamin (Shin et al., 2022).

Many factors are involved in nucleating F-actin. Neural Wiskott-Aldrich-syndrome protein (N-WASP) may activate actin-related protein 2/3 complex (Arp2/3) to form branched actin networks together with myosin, whereas formins are involved in forming linear actin filaments (Cingolani and Goda, 2008; Kononenko and Haucke, 2015; Kaksonen and Roux, 2018). Myosin II inhibitor blebbistatin suppresses endocytosis at hippocampal and calyx of Held synapses, suggesting that myosin II-dependent F-actin nucleation is involved in mediating endocytosis (Yue and Xu, 2014; Soykan et al., 2017). Consistent with this suggestion, knockout of myosin IIB or application of blebbistatin reduces horseradish peroxidase uptake that may reflect endocytosis at hippocampal synapses (Chandrasekar et al., 2013). To investigate the function of actomyosin, actin nucleation, which precedes F-actin assembly, has been studied with pharmacological approaches and gene knockdown (Soykan et al., 2017). Inhibition of formin-mediated assembly of linear actin filaments by the selective inhibitor SMIFH2 (Ganguly et al., 2015) in turn inhibits endocytosis at hippocampal and calyx-type synapses (Soykan et al., 2017). Similarly, shRNA-mediated knockdown of the diaphanous-related formin mDia1 slows synaptic vesicle endocytosis (Soykan et al., 2017). These results suggest that formin-dependent actin filament assembly may regulate synaptic vesicle endocytosis (Soykan et al., 2017).

Recent studies reveal an unexpected relationship between potassium channels and endocytosis mediated by nucleation of F-actin at synapses (Zhang et al., 2016; Wu et al., 2021). Since the discovery of potassium channels, the physiological and pathological impact of potassium channels has been attributed to their ion conductance, which sets the cell membrane potential and repolarizes the membrane during action potentials (Kaczmarek and Zhang, 2017). For example, Kv3 family channels are generally considered to regulate neurotransmitter release by repolarizing the membrane during action potentials (Kaczmarek and Zhang, 2017). A recent study reports a crucial function of these channels independent of their ion conductance – by organizing the F-actin cytoskeleton in nerve terminals, Kv3.3 protein facilitates rapid and slow endocytosis at hippocampal and calyx of Held synapses (Wu et al., 2021). The extended cytoplasmic C-terminal domain of Kv3.3 at the plasma membrane binds to and thereby recruits beneath the plasma membrane the Arp2/3, which is involved in nucleating the cortical F-actin cytoskeleton (Zhang et al., 2016; Wu et al., 2021). The channel mutation G592R Kv3.3 causes Kv3.3 to fail to bind Arp2/3, and thus disrupts the ability of the channel to nucleate F-actin in nerve terminals, resulting in inhibition of synaptic vesicle endocytosis (Zhang et al., 2016; Wu et al., 2021). Since this mutation may cause spinocerebellar ataxia 13 (Middlebrooks et al., 2013), inhibition of synaptic vesicle endocytosis by disruption of F-actin nucleation may contribute to the generation of spinocerebellar ataxia 13 (Wu et al., 2021).

Figure 1H provides a schematic summary of the role of actin and its assembly pathways in mediating synaptic vesicle endocytosis. The implications of the studies discussed above are integrated in the figure to show the involvement of F-actin and F-actin nucleation factors, such as Kv3.3, Arp2/3, formin, and myosin II, in all kinetically distinguishable forms of endocytosis.

ACTIN FACILITATES VESICLE REPLENISHMENT TO THE READILY RELEASABLE POOL

After release of vesicles at active zone release sites, they must be replenished. This process, called vesicle mobilization or replenishment to the RRP, is crucial to sustain synaptic transmission and minimize short-term synaptic depression during repetitive firing (Wang and Kaczmarek, 1998; Schneggenburger et al., 1999; Wu and Borst, 1999; Sakaba and Neher, 2001; Von Gersdorff and Borst, 2002; Zucker and Regehr, 2002; Xu and Wu, 2005; He et al., 2009). At the calyx of Held synapse, the rate of RRP replenishment can be measured experimentally with a pair of depolarizing pulses of ∼20–50 ms, each of which can completely deplete the

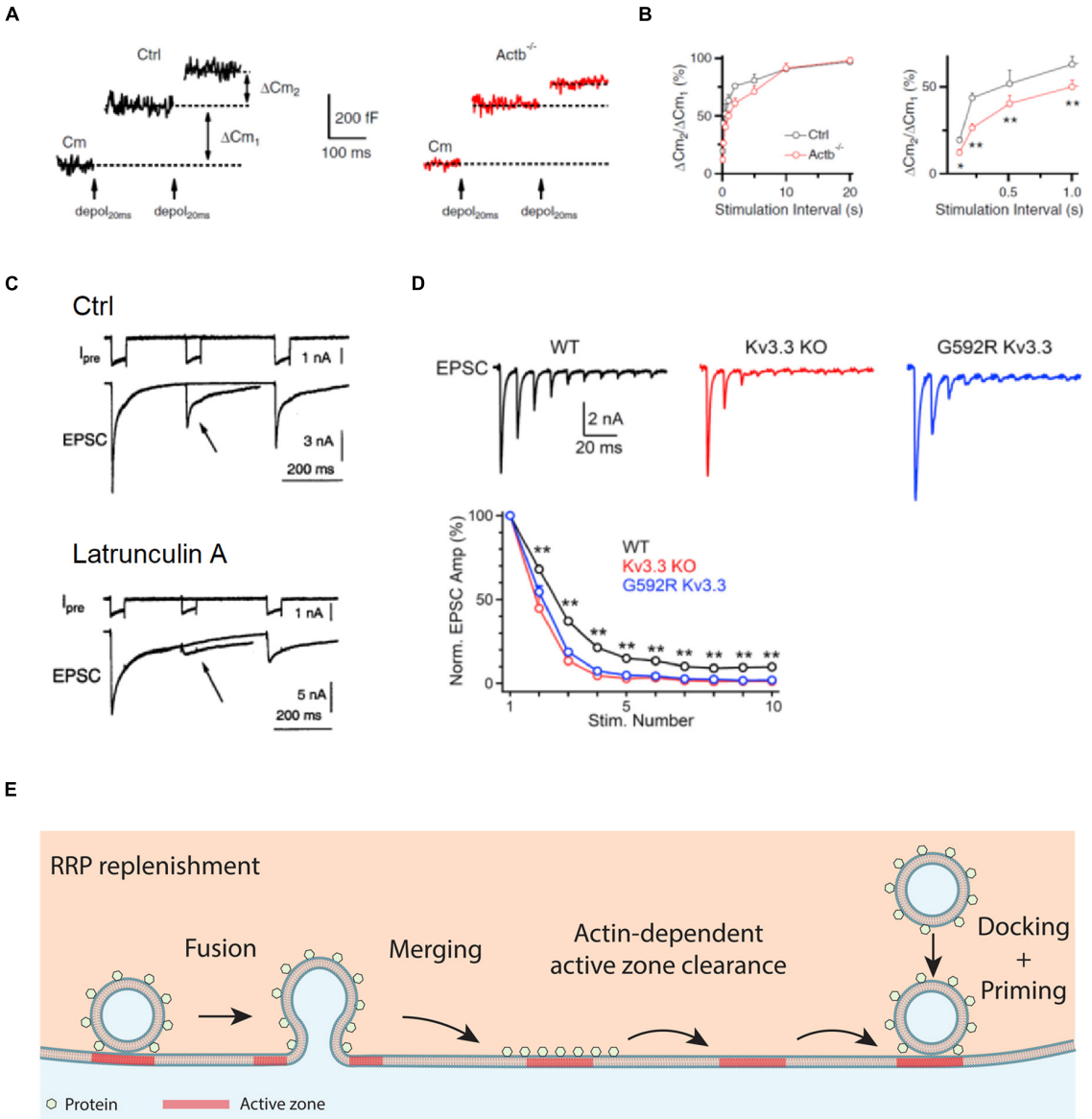

FIGURE 2 | Actin promotes RRP replenishment likely by facilitating active zone clearance. **(A)** Sampled Cm traces induced by a pair of $depol_{20\ ms}$ at an interval of 200 ms in a control (Ctrl, left) and an $Actb^{-/-}$ (right) calyx. Measurements of the capacitance jumps induced by the first and second $depol_{20\ ms}$ (ΔCm_1 and ΔCm_2) are schematically shown. **(B)** Left: the ratio between the second and first ΔCm ($\Delta Cm_2/\Delta Cm_1$) during a pair of $depol_{20\ ms}$ plotted versus paired-pulse interval at control and $Actb^{-/-}$ calyces. Right: same as in left but plotting the interval between 0 and 1 s. $^*p < 0.05$; $^{**}p < 0.01$ (*t*-test). The data in **A,B** show that β-actin knockout reduces ΔCm2/ΔCm1. **(C)** Top: a dual pulse of 50 ms (to 0 mV) was applied at different intervals (200 and 500 ms) to the calyx. Presynaptic calcium currents (Ipre) and excitatory postsynaptic currents (EPSCs) are shown. Bottom: similar arrangement as in the top, but with the presynaptic pipette solution containing Lat A to inhibit actin polymerization. Arrows indicate that latrunculin A inhibits EPSC induced by a second pulse. **(D)** The Kv3.3 channel regulates EPSCs during repetitive action potential firing: sampled EPSCs (top) and the amplitude of EPSCs (bottom, mean + SEM) induced by 10 action potentials at 100 Hz at the calyx of wild-type mice, $Kv3.3^{-/-}$ mice, and mice with a mutation (Kv3.3 G592R) that causes spinocerebellar ataxia 13 and inhibits F-actin nucleation at the calyx. **(E)** Schematic diagram showing that the F-actin cytoskeleton may facilitate active zone clearance and thus RRP replenishment. RRP replenishment may involve active zone clearance, vesicle docking, and vesicle priming that makes the docked vesicle release-ready. Panels **A,B** are adapted from Wu et al. (2016) with permission. Panel **C** is adapted from Sakaba and Neher (2003) with permission. Panel **D** is adapted from Wu et al. (2021) with permission.

RRP (**Figures 2A–C**; Wu and Borst, 1999; Sakaba and Neher, 2001; Wu et al., 2016). The exocytosis induced by the second pulse applied at various intervals after the first pulse may thus indicate the time course of RRP replenishment (**Figures 2A–C**). It has been found that the RRP replenishment is suppressed by a variety of manipulations that inhibit F-actin, including knockout of the β-actin or γ-actin gene (**Figures 2A,B**), Lat A that inhibits F-actin polymerization (**Figure 2C**), Kv3.3 that disrupts F-actin nucleation, and mutation of Kv3.3 that causes spinocerebellar ataxia and inhibits F-actin nucleation at nerve

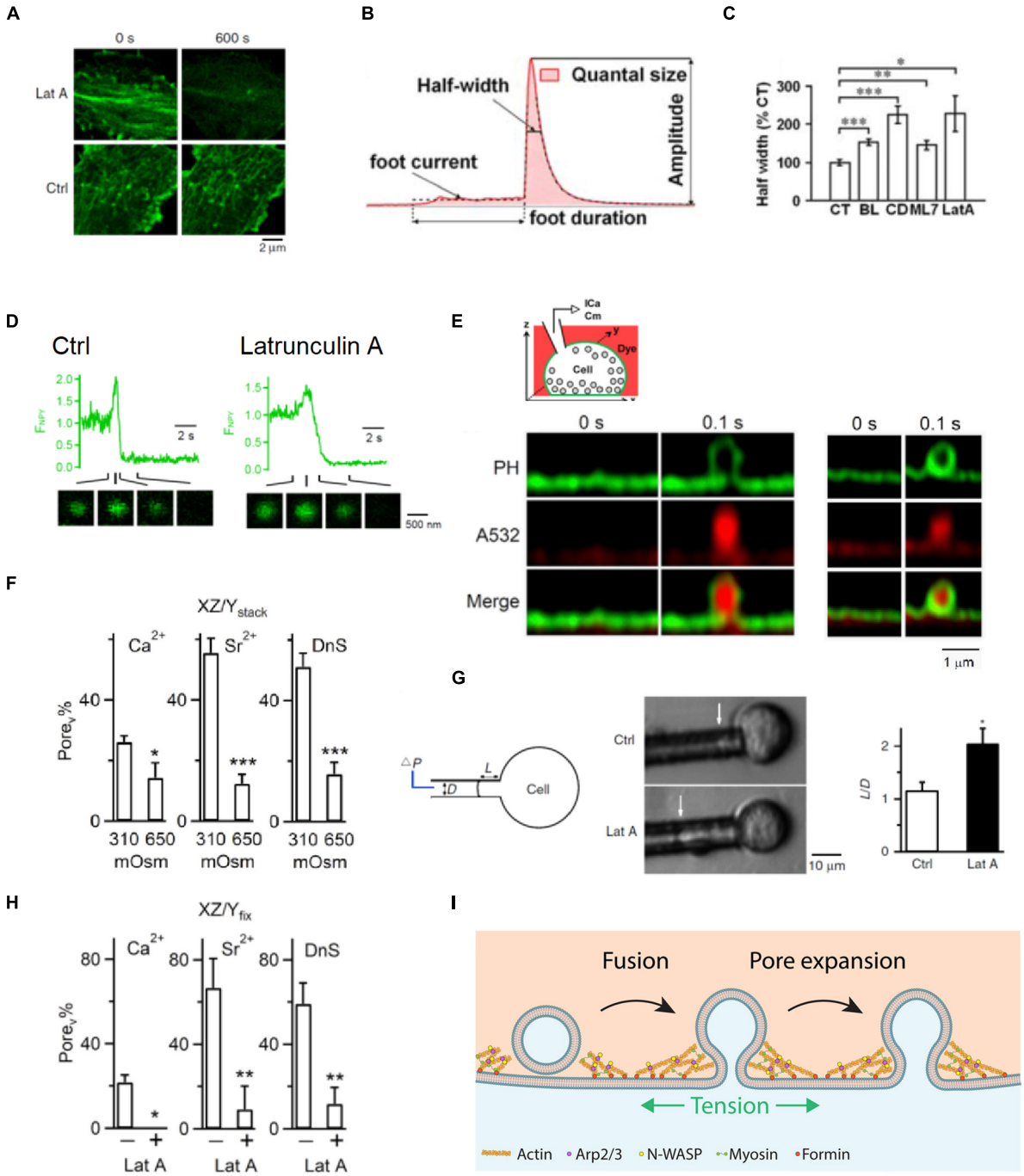

FIGURE 3 | F-actin promotes fusion pore expansion by enhancing plasma membrane tension. **(A)** Latrunculin A (Lat A) reduces F-actin: sampled Lifeact-labeled F-actin at the cell bottom of bovine adrenal chromaffin cells before (0 s, left) and 600 s after (right) application of Lat A (3 µM) or a control (Ctrl) solution. **(B)** A single amperometric spike along with the five parameters: quantal size Q (pC), half-width (ms), peak amplitude (pA), foot signal duration (ms), and mean foot current (pA). **(C)** Half-width (mean ± SEM) of amperometric spikes in control (CT) or in the presence of blebbistatin (BL), cytochalasin D (CD), ML-7 (ML7), or Lat A. Data normalized to the mean in control. *$p < 0.05$; **$p < 0.01$; ***$p < 0.001$ (*t*-test). **(D)** Lat A slows down neuropeptide Y-EGFP (NPY-EGFP) release from single vesicles: fluorescence of NPY-EGFP (F_{NPY}) from single vesicles in Ctrl (left) and in the presence of Lat A (right). Decay indicates release of neuropeptide Y-EGFP. NPY-EGFP images at times indicated are also shown. The initial increase of NPY-EGFP fluorescence is due to fusion pore opening that increases the vesicular lumen pH. **(E)** Top: setup drawing. Cell membrane is labeled with the phospholipase C ΔPH domain attached with mNeonGreen (PH_G, green), whereas the bath solution contains Atto 532 (A532, red, pseudo-color). Bottom left: STED PH_G/A532 images immediately before (time 0) and after fusion during imaging every 0.1 s. PH_G-labeled fusion pore is visible. The stimulation was a depolarization from –80 to +10 mV for 1 s ($depol_{1\ s}$). Bottom right: similar to left panel but showing a pore not visible to STED microscopy. **(F)** The percentage of fusion pores induced by $depol_{1s}$ that are visible to STED microscopy ($Pore_v$%) at 310 or 650 mOsm (bath

(Continued)

FIGURE 3 | solution) in calcium (Ca^{2+}), strontium (Sr^{2+}), or dynasore (DnS, with 5 mM Ca^{2+}). $Pore_v$ was detected with PH_G STED imaging as shown in **E**. Data show that 650 mOsm reduces $Pore_v$%. **(G)** Latrunculin A (Lat A) reduces membrane tension. Left: drawings of the micropipette aspiration technique. Negative pressure (ΔP) in the pipette (with a diameter D) draws the cell membrane into the pipette by a length L. Middle: pipette-aspirated cells (bright-field images) in the absence (Ctrl) and presence of Lat A (0.5 μM). Arrows indicate membrane projection (L) into the micropipette (ΔP = 500 Pa). Right: normalized projection length (L/D, mean + SEM) for aspirated cells in the absence (Ctrl) or presence of Lat A (0.5 μM). *p = 0.011 (t-test). **(H)** Lat A inhibits $Pore_v$ (fusion pore visible to STED microscopy) percentage: the percentage of $Pore_v$ ($Pore_v$%) in the absence (–) or presence (+) of 3 μM Lat A in a bath containing Ca^{2+}, Sr^{2+}, or DnS. $Pore_v$ was detected with STED imaging of PH_G as shown in panel **E**. **(I)** Schematic drawing showing that F-actin cytoskeleton enhances plasma membrane tension and thus promotes fusion pore expansion that releases vesicular contents rapidly and completely. Promotion of fusion pore expansion does not necessarily flatten the fusion pore, explained in more detail in **Figure 4**. Panels **A,D,G** are adapted from Wen et al. (2016) with permission. Panels **B,C** are adapted from Berberian et al. (2009) with permission. Panel **E,F,H** are adapted from Shin et al. (2018) with permission.

terminals (Sakaba and Neher, 2003; Wu et al., 2016, 2021). These results suggest that F-actin facilitates RRP replenishment and impact F-actin nucleation may contribute to the generation of neurological disorders.

Since RRP replenishment sustains synaptic transmission during repetitive firing, suppression of RRP replenishment by inhibition of F-actin predicts severe short-term depression of synaptic transmission. This prediction was verified by measurements of the excitatory postsynaptic current (EPSC) during repetitive firing in Kv3.3 knockout or G592R Kv3.3 knock-in mice, in which F-actin nucleation at nerve terminals is impaired (**Figure 2D**; Wu et al., 2021). Taken together, these results suggest that F-actin opposes short-term depression, and thus helps to sustain synaptic transmission during repetitive firing.

Given that inhibition of endocytosis by the block of dynamin, calmodulin, calcium influx, and SNARE proteins slows down RRP replenishment, it has been suggested that endocytosis facilitates RRP replenishment *via* clearance of the active zone as perturbed by exocytosis (Hosoi et al., 2009; Wu et al., 2009, 2014; Neher, 2010; Sun et al., 2010; Hua et al., 2013; Xu et al., 2013). Accordingly, actin involvement in endocytosis and RRP replenishment suggests that F-actin promotes RRP replenishment by facilitating active zone clearance (**Figure 2E**; Wu et al., 2016). Therefore, impairment of RRP replenishment may contribute to the generation of spinocerebellar ataxia 13 and other neurological disorders caused by impairments of F-actin nucleation or assembly.

The exact mechanism of how actin and endocytosis mediate active zone clearance remains unclear. Annexin A2, a calcium-, actin-, and lipid-binding protein involved in exocytosis, may induce actin bundling that seems essential for generating active exocytotic sites in chromaffin cells (Gabel et al., 2015). Such a mechanism might provide hints about how F-actin facilitates replenishment of the RRP.

Actin's role in facilitating RRP replenishment is apparently in conflict with its physical barrier function, which has been suggested based on an observed increase in spontaneous and evoked vesicular content release after inhibition of actin polymerization (Aunis and Bader, 1988; Morales et al., 2000; Trifaro et al., 2000; Chowdhury et al., 2002; Malacombe et al., 2006; Cingolani and Goda, 2008). This discrepancy could be reconciled if the RRP replenishment reflects mostly the active zone clearance, but not solely just vesicle movement to the docking site. The RRP is functionally defined as a pool of vesicles that can be depleted by a brief depolarization (Von Gersdorff and Borst, 2002; Neher and Sakaba, 2008; Wu et al., 2014). For example, at the calyx of Held, the RRP is defined as the vesicles being released by a 20 or 50 ms depolarization or about 20 action potentials at 100–300 Hz (Wang and Kaczmarek, 1998; Schneggenburger et al., 1999; Wu and Borst, 1999; Sakaba and Neher, 2001; Sun and Wu, 2001). The number of vesicles in the RRP, estimated with capacitance measurements (Sun and Wu, 2001; Sun et al., 2002), could be larger than the number of morphologically docked vesicles observed with electron microscopy (Sätzler et al., 2002; Taschenberger et al., 2002). Thus, RRP replenishment may reflect not only physical movement of vesicles from the cytosol to the plasma membrane docking site, but also the summed activity of active zone clearance, vesicle docking, and subsequent vesicle priming to become release-ready. Accordingly, we suggest that within the time scale of seconds after RRP depletion, F-actin cytoskeleton may help in active zone clearance that facilitates RRP replenishment. In a longer time scale and likely a longer distance, F-actin cytoskeleton may serve as a physical barrier for vesicles deep inside the cytosol to move toward the plasma membrane. This suggestion may reconcile the apparent controversy surrounding F-actin regarding its facilitatory role in RRP replenishment and its inhibitory function in vesicle movement toward the plasma membrane. Verifying this suggestion in the future may require imaging and quantification of individual vesicle movements toward, and fusion at, the plasma membrane release site in live cells.

FILAMENTOUS ACTIN PROMOTES FUSION PORE EXPANSION AND THUS CONTENT RELEASE BY ENHANCING MEMBRANE TENSION

Filamentous actin blockers that reduce F-actin (**Figure 3A**) and myosin II inhibitors slow down catecholamine release as detected with amperometry (**Figures 3B,C**; Neco et al., 2008; Berberian et al., 2009; Olivares et al., 2014) and prolong release of vesicular lumen protein neuropeptide Y-EGFP as detected with imaging in chromaffin cells (**Figure 3D**; Wen et al., 2016). These results suggest that F-actin speeds up vesicular content release in chromaffin cells. How does F-actin facilitate vesicular content release? Recent studies addressed this question by direct visualization of fusion pore opening, expansion, constriction and closure with super-resolution stimulated emission depletion

(STED) microscopy at a neuroendocrine cell, the adrenal chromaffin cell containing ∼180–720 nm diameter vesicles (**Figure 3E**; Wen et al., 2016; Zhao et al., 2016; Shin et al., 2018). It has been observed that fusion pore size may vary between 0 and 490 nm within 26 ms to seconds (Shin et al., 2018). These pore dynamics are crucial in determining the efficiency of vesicular cargo release and vesicle retrieval (Shin et al., 2018). They are generated by competition between mechanisms

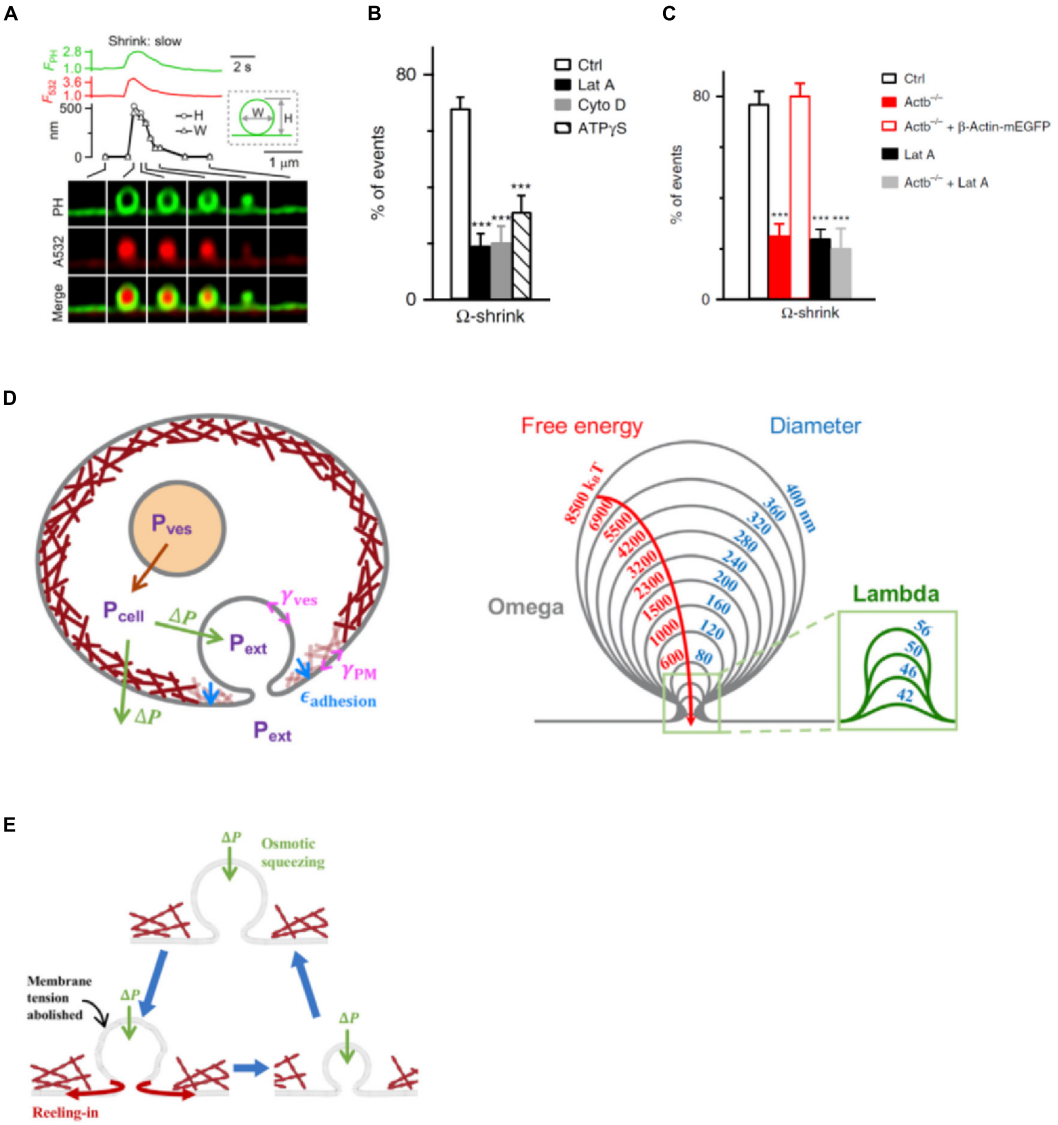

FIGURE 4 | Actin promotes shrink fusion by enhancing plasma membrane tension. **(A)** PH_G-labeled Ω-profile fluorescence (F_{PH}; normalized to baseline), A532 spot fluorescence (F_{532}; normalized to baseline), PH_G-labeled Ω-profile height (H; circles), PH_G-labeled Ω-profile width (W; triangles), and sampled images at times indicated with lines showing shrink fusion. The experimental setup is the same as that shown in **Figure 3E**. **(B)** Percentages (mean + SEM) of fusion events undergoing Ω-shrink fusion in Ctrl or in the presence of 3 µM Lat A (***$p < 0.001$), 4 µM Cyto D (***$p < 0.001$), or ATPγS (2 mM, replacing 2 mM ATP in the whole-cell pipette; ***$p < 0.001$) (*t*-test). **(C)** Percentages (mean + SEM) of Ω-shrink fusion induced by whole-cell calcium (1.5 µM) dialysis in Ctrl, $Actb^{-/-}$ cells, $Actb^{-/-}$ cells overexpressed with β-Actin–mEGFP, Ctrl cells treated with Lat A (Lat A), and $Actb^{-/-}$ cells treated with Lat A. ***$p < 0.001$ (*t*-test). **(D)** Left: schematic of the model (not to scale). Cells maintain an outward (swelling) osmotic pressure $\Delta P = P_{cell} - P_{ext}$ (green arrows), with cell pressure P_{cell} exceeding extracellular pressure P_{ext}. Intact vesicles maintain swelling pressure (red arrow), with vesicle pressure $P_{ves} > P_{cell}$. Following fusion with plasma membrane (PM), rapid equilibration between vesicle lumen and extracellular medium is assumed, so $P_{ves} = P_{ext}$. The vesicle osmotic pressure then equals ΔP but is now an inward squeezing pressure. The model calculates the vesicle tension, γ_{ves}, while the PM tension, γ_{PM}, and the adhesion energy $\varepsilon_{adhesion}$ to the actin cortex (maroon layer adjacent to PM) are taken from experiment. Right: predicted shrink fusion sequence. Computed vesicle shapes and free energies for squeezing pressure $\Delta P = 100$ Pa and the indicated effective diameters *D* (such that vesicle area equals πD^2). A transition occurs at $D = 56$ nm from Ω to Λ shape (defined as a profile lacking overhang). **(E)** Shrink fusion mechanism predicted by the model. Osmotic squeezing deflates the vesicular Ω-shape profile and abolishes its membrane tension, so the Ω-profile's membrane is reeled into the PM by PM tension and PM adhesion to the actin cortex. Panels **A,D,E** are adapted from Shin et al. (2020) with permission. Panels **B,C** are adapted from Wen et al. (2016) with permission.

for pore expansion and mechanisms for pore constriction and closure (Shin et al., 2018). Increasing the extracellular solution osmolarity, which shrinks the cell size and thus may reduce plasma membrane tension (Wen et al., 2016), reduces the initial fusion pore size as measured with STED microscopy (**Figure 3F**; Shin et al., 2018). Lat A, which reduces F-actin and plasma membrane tension as measured with the pipette aspiration technique in chromaffin cells (**Figure 3G**; Wen et al., 2016), also reduces the initial fusion pore size as measured with STED microscopy (**Figure 3H**; Shin et al., 2018). Thus, F-actin promotes fusion pore expansion by enhancing plasma membrane tension (Shin et al., 2018), explaining why F-actin facilitates vesicular content release (**Figure 3I**).

FILAMENTOUS ACTIN PROMOTES SHRINK FUSION

For many decades, two fusion modes were thought to control hormone and transmitter release (Ceccarelli et al., 1973; Heuser and Reese, 1981; Alabi and Tsien, 2013; Wu et al., 2014). One facilitates release *via* fusion pore dilation and flattening, called full-collapse fusion. The other limits release by closing a narrow fusion pore, called kiss-and-run or close-fusion (Ceccarelli et al., 1973; Chiang et al., 2014; Zhao et al., 2016). With super-resolution STED microscopy to visualize fusion modes of dense-core vesicles in neuroendocrine cells, it has been found, surprisingly, that facilitation of release is not mediated by full-collapse, but rather shrink fusion, in which the Ω-profile generated by vesicle fusion shrinks, but maintains a large non-dilating pore until the Ω-profile is undetectable (**Figure 4A**; Chiang et al., 2014; Wen et al., 2016; Shin et al., 2018, 2021). Inhibition of F-actin polymerization by Lat A, cytochalasin D, or β-actin knockout significantly reduces plasma membrane tension (**Figure 3G**) and shrink fusion percentage (**Figures 4B,C**; Wen et al., 2016; Shin et al., 2020). Such an inhibition of shrink fusion can be mimicked by a decrease in plasma membrane tension (*via* increasing the extracellular solution osmolarity) and can be rescued by an increase in plasma membrane tension (*via* decreasing the extracellular solution osmolarity) (Wen et al., 2016). These results suggest that F-actin is essential in mediating shrink fusion (Wen et al., 2016). Furthermore, it has been shown that the F-actin assembly pathway, including N-WASP, formin, and hydrolysis of the energy molecule ATP is involved in mediating shrink fusion (Wen et al., 2016). Inhibition of F-actin leads to accumulation of Ω-shape profiles at the active zone of lamprey synapses, suggesting that F-actin also facilitates merging of fusing vesicles at the plasma membrane, likely also *via* shrink fusion (Wen et al., 2016).

How does F-actin-provided membrane tension mediate shrink fusion? A recent study found that the swelling osmotic pressure maintained by cells, the positive intracellular-to-extracellular osmotic pressure difference, may squeeze the Ω-profile and reduce the Ω-profile membrane tension, generating a tension gradient from the plasma membrane to the Ω-profile that reels Ω-profile membrane into the plasma membrane (**Figures 4D,E**; Shin et al., 2020). The requirement of the plasma-membrane-to-Ω-profile tension gradient explains why F-actin-dependent plasma membrane tension is needed to mediate shrink fusion (Wen et al., 2016). As the fused vesicle medium equilibrates with the extracellular medium, the squeezing pressure is equal to the swelling osmotic pressure of the cell (Diz-Munoz et al., 2010; Boulant et al., 2011; Stewart et al., 2011; Tsujita et al., 2015; Wen et al., 2016). With squeezing

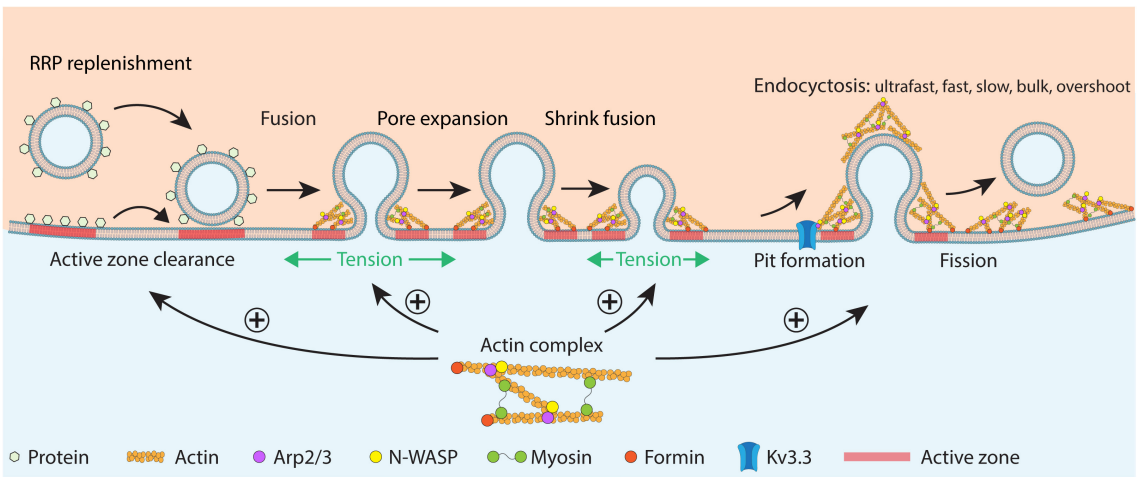

FIGURE 5 | Schematic summary of F-actin's functions in RRP replenishment, fusion pore expansion, fused vesicle merging *via* shrink fusion, and all distinguishable forms of endocytosis in secretory cells. The schematic drawing shows RRP replenishment involving active zone clearance, vesicle docking and priming, fusion pore opening, fusion pore expansion that releases vesicular contents, shrink fusion that merges fused vesicles at the plasma membrane, and classical endocytosis involving pit formation and fission of the pit. F-actin promotes (1) RRP replenishment likely by facilitating active zone clearance, (2) fusion pore expansion by enhancing the plasma membrane tension, (3) shrink fusion by providing membrane tension to reel of fusing vesicular membrane, and (4) endocytosis likely by generating forces needed for pit formation. Actin nucleation factors, including Kv3.3, N-WASP, Arp2/3, myosin II, and formin are also involved in these processes. This cartoon represents a synthesis of many suggestions derived from the many studies discussed in this review.

force and membrane-reeling-in force, Ω-profile shrinking is energetically favored over full-collapse fusion (**Figures 4D,E**), explaining why shrink fusion is selected over full-collapse fusion to merge fusing vesicles at the plasma membrane.

Given that the swelling osmotic pressure and cortical F-actin required for mediating shrink fusion are general properties of cells (Dai and Sheetz, 1999; Diz-Munoz et al., 2010; Boulant et al., 2011; Stewart et al., 2011; Tsujita et al., 2015; Wen et al., 2016), shrink fusion may in fact replace the widely believed-to-be dominant full-collapse fusion in many cell types. It should be noted that as the fusion-generated Ω-profile shrinks at the final stage, the Ω-profile may undergo a transition to a Λ- or dome-shape profile (Shin et al., 2020). This observation has led to the proposal of a shrink-collapse fusion mode, in which Ω-profile shrinking is followed by a transition to a Λ-profile, which in turn is followed by flattening/merging (Shin et al., 2020). This mode unifies the apparent contradiction between shrink fusion and full-collapse fusion.

It has been proposed that small synaptic vesicles, with diameters in the range of ∼20–60 nm, may undergo shrink-collapse fusion, with shrinking as the major component for larger synaptic vesicles and collapse as the primary component for smaller synaptic vesicles. Supporting this proposal, inhibition of F-actin assembly with Lat A, cytochalasin D, or an inhibitor of the formin-dependent F-actin assembly reduces F-actin at nerve terminals and causes accumulation of Ω-profiles at the active zone of lamprey giant synapses (Wen et al., 2016), suggesting that F-actin is also involved in merging small synaptic vesicles, likely *via* facilitating shrink fusion or shrink-collapse fusion.

CONCLUSION AND FUTURE RESEARCH QUESTIONS

Recent studies reveal an essential role of F-actin in mediating all kinetically distinguishable forms of endocytosis, including ultrafast, fast, slow, bulk, and overshoot endocytosis (**Figure 5**). Ultrastructural examination and real-time imaging suggest that F-actin is involved in pit formation, a critical step of endocytosis that has just been visualized in real time in live cells (Shin et al., 2021, 2022). The essential role of F-actin in mediating endocytosis may facilitate active zone clearance that may in turn promote RRP replenishment (**Figure 5**). RRP replenishment sustains synaptic transmission and overcomes short-term depression during repetitive firing at synapses. Facilitation of RRP replenishment *via* active zone clearance within seconds after exocytosis is different from the physical barrier function F-actin performs on a much longer time scale during vesicle movement from deep inside the cytosol to the plasma membrane. Such a difference might reconcile the apparent conflict of F-actin's roles between facilitation of RRP replenishment and being a physical barrier that blocks vesicle movement. Recent studies also showed that F-actin promotes rapid and complete vesicular content release by increasing plasma membrane tension, which facilitates fusion pore expansion (**Figure 5**). By increasing plasma membrane tension, F-actin reels off fusing vesicle membrane and thus mediates shrink fusion together with the swelling osmotic pressure of the cell that squeezes the fusing Ω-profile (**Figure 5**). In conclusion, F-actin is essential in (1) mediating all forms of endocytosis and the RRP replenishment that together sustain synaptic transmission, (2) expanding the fusion pore to promote vesicular content release, and (3) mediating shrink fusion or shrink-collapse fusion that merges fusing vesicles with the plasma membrane (**Figure 5**). Not only actin, but also the actin assembly pathway, including N-WASH-dependent branched F-actin assembly and formin-dependent linear F-actin assembly are involved in mediating these functions of F-actin. A mutation in the Kv3.3 potassium channel, which causes spinocerebellar ataxia 13, inhibits F-actin nucleation, endocytosis, and RRP replenishment and enhances short-term synaptic depression at synapses (Wu et al., 2021), suggesting that impairment of F-actin's roles in exo- and endocytosis may contribute to neurological disorders.

While recent studies reveal important roles of F-actin in regulating exo- and endocytosis, how F-actin generates forces to mediate endocytosis and pit formation remains not well understood. How actin facilitates active zone clearance and thus RRP replenishment also remains unclear, owing to the difficulty of visualizing active zone clearance in live synapses (Hua et al., 2013). To what extent impairment of F-actin assembly and nucleation plays a role in generating neurological disorders is not well understood. How the cell uses F-actin to shrink fusing Ω-profiles at release sites, but also to generate endocytic pits at endocytic sites, apparently contradictory functions, is also not well understood. It would be of great interest to address these questions in the future.

AUTHOR CONTRIBUTIONS

L-GW designed and wrote the manuscript. CYC participated in writing the manuscript. Both authors contributed to manuscript revision, read, and approved the submitted version.

FUNDING

This work was supported by the National Institute of Neurological Disorders and Stroke Intramural Research Program (ZIA NS003009-16 and ZIA NS003105-11 to L-GW).

REFERENCES

Alabi, A. A., and Tsien, R. W. (2013). Perspectives on kiss-and-run: role in exocytosis, endocytosis, and neurotransmission. *Annu. Rev. Physiol.* 75, 393–422. doi: 10.1146/annurev-physiol-020911-153305

Aunis, D., and Bader, M. F. (1988). The cytoskeleton as a barrier to exocytosis in secretory cells. *J. Exp. Biol.* 139, 253–266. doi: 10.1242/jeb.139.1.253

Balaji, J., and Ryan, T. A. (2007). Single-vesicle imaging reveals that synaptic vesicle exocytosis and endocytosis are coupled by a single stochastic mode. *Proc. Natl. Acad. Sci. U.S.A* 104, 20576–20581. doi: 10.1073/pnas.0707574105

Berberian, K., Torres, A. J., Fang, Q., Kisler, K., and Lindau, M. (2009). F-actin and myosin II accelerate catecholamine release from chromaffin granules. *J. Neurosci.* 29, 863–870. doi: 10.1523/JNEUROSCI.2818-08.2009

Bleckert, A., Photowala, H., and Alford, S. (2012). Dual pools of actin at presynaptic terminals. *J. Neurophysiol.* 107, 3479–3492. doi: 10.1152/jn.00789.2011

Boulant, S., Kural, C., Zeeh, J. C., Ubelmann, F., and Kirchhausen, T. (2011). Actin dynamics counteract membrane tension during clathrin-mediated endocytosis. *Nat. Cell Biol.* 13, 1124–1131. doi: 10.1038/ncb2307

Bourne, J., Morgan, J. R., and Pieribone, V. A. (2006). Actin polymerization regulates clathrin coat maturation during early stages of synaptic vesicle recycling at lamprey synapses. *J. Comp. Neurol.* 497, 600–609. doi: 10.1002/cne.21006

Brunger, A. T., Choi, U. B., Lai, Y., Leitz, J., and Zhou, Q. (2018). Molecular Mechanisms of Fast Neurotransmitter Release. *Annu. Rev. Biophys.* 47, 469–497. doi: 10.1146/annurev-biophys-070816-034117

Ceccarelli, B., Hurlbut, W. P., and Mauro, A. (1973). Turnover of transmitter and synaptic vesicles at the frog neuromuscular junction. *J. Cell Biol.* 57, 499–524. doi: 10.1083/jcb.57.2.499

Chanaday, N. L., and Kavalali, E. T. (2018). Optical detection of three modes of endocytosis at hippocampal synapses. *Elife* 7:e36097. doi: 10.7554/eLife.36097

Chandrasekar, I., Huettner, J. E., Turney, S. G., and Bridgman, P. C. (2013). Myosin II regulates activity dependent compensatory endocytosis at central synapses. *J. Neurosci.* 33, 16131–16145. doi: 10.1523/JNEUROSCI.2229-13.2013

Chang, C. W., Chiang, C. W., and Jackson, M. B. (2017). Fusion pores and their control of neurotransmitter and hormone release. *J. Gen. Physiol.* 149, 301–322. doi: 10.1085/jgp.201611724

Cheever, T. R., and Ervasti, J. M. (2013). Actin isoforms in neuronal development and function. *Int. Rev. Cell Mol. Biol.* 301, 157–213. doi: 10.1016/B978-0-12-407704-1.00004-X

Chiang, H. C., Shin, W., Zhao, W. D., Hamid, E., Sheng, J., Baydyuk, M., et al. (2014). Post-fusion structural changes and their roles in exocytosis and endocytosis of dense-core vesicles. *Nat. Commun.* 5:3356.

Chowdhury, H. H., Kreft, M., and Zorec, R. (2002). Distinct effect of actin cytoskeleton disassembly on exo- and endocytic events in a membrane patch of rat melanotrophs. *J. Physiol.* 545, 879–886. doi: 10.1113/jphysiol.2002.028043

Cingolani, L. A., and Goda, Y. (2008). Actin in action: the interplay between the actin cytoskeleton and synaptic efficacy. *Nat. Rev. Neurosci.* 9, 344–356. doi: 10.1038/nrn2373

Dai, J., and Sheetz, M. P. (1999). Membrane tether formation from blebbing cells. *Biophys. J.* 77, 3363–3370. doi: 10.1016/S0006-3495(99)77168-7

Delvendahl, I., Vyleta, N. P., Von Gersdorff, H., and Hallermann, S. (2016). Fast, Temperature-Sensitive and Clathrin-Independent Endocytosis at Central Synapses. *Neuron* 90, 492–498. doi: 10.1016/j.neuron.2016.03.013

Diz-Munoz, A., Krieg, M., Bergert, M., Ibarlucea-Benitez, I., Muller, D. J., Paluch, E., et al. (2010). Control of directed cell migration *in vivo* by membrane-to-cortex attachment. *PLoS Biol.* 8:e1000544. doi: 10.1371/journal.pbio.1000544

Ferguson, S. M., Raimondi, A., Paradise, S., Shen, H., Mesaki, K., Ferguson, A., et al. (2009). Coordinated actions of actin and BAR proteins upstream of dynamin at endocytic clathrin-coated pits. *Dev. Cell* 17, 811–822. doi: 10.1016/j.devcel.2009.11.005

Gabel, M., Delavoie, F., Demais, V., Royer, C., Bailly, Y., Vitale, N., et al. (2015). Annexin A2-dependent actin bundling promotes secretory granule docking to the plasma membrane and exocytosis. *J. Cell Biol.* 210, 785–800. doi: 10.1083/jcb.201412030

Gan, Q., and Watanabe, S. (2018). Synaptic Vesicle Endocytosis in Different Model Systems. *Front. Cell Neurosci.* 12:171. doi: 10.3389/fncel.2018.00171

Ganguly, A., Tang, Y., Wang, L., Ladt, K., Loi, J., Dargent, B., et al. (2015). A dynamic formin-dependent deep F-actin network in axons. *J. Cell Biol.* 210, 401–17. doi: 10.1083/jcb.201506110

He, L., Xue, L., Xu, J., Mcneil, B. D., Bai, L., Melicoff, E., et al. (2009). Compound vesicle fusion increases quantal size and potentiates synaptic transmission. *Nature* 459, 93–97. doi: 10.1038/nature07860

Betz, W. J., and Henkel, A. (1994). Okadaic acid disrupts clusters of synaptic vesicles in frog motor nerve terminals. *J. Cell Biol.* 124, 843–854. doi: 10.1083/jcb.124.5.843

Herman, I. M. (1993). Actin isoforms. *Curr. Opin. Cell Biol.* 5, 48–55.

Heuser, J. E., and Reese, T. S. (1981). Structural changes after transmitter release at the frog neuromuscular junction. *J. Cell Biol.* 88, 564–580. doi: 10.1083/jcb.88.3.564

Holt, M., Cooke, A., Wu, M. M., and Lagnado, L. (2003). Bulk membrane retrieval in the synaptic terminal of retinal bipolar cells. *J. Neurosci.* 23, 1329–1339. doi: 10.1523/JNEUROSCI.23-04-01329.2003

Hosoi, N., Holt, M., and Sakaba, T. (2009). Calcium dependence of exo- and endocytotic coupling at a glutamatergic synapse. *Neuron* 63, 216–229. doi: 10.1016/j.neuron.2009.06.010

Hua, Y., Woehler, A., Kahms, M., Haucke, V., Neher, E., and Klingauf, J. (2013). Blocking endocytosis enhances short-term synaptic depression under conditions of normal availability of vesicles. *Neuron* 80, 343–349. doi: 10.1016/j.neuron.2013.08.010

Hua, Z., Leal-Ortiz, S., Foss, S. M., Waites, C. L., Garner, C. C., Voglmaier, S. M., et al. (2011). v-SNARE composition distinguishes synaptic vesicle pools. *Neuron* 71, 474–487. doi: 10.1016/j.neuron.2011.06.010

Jahn, R., and Fasshauer, D. (2012). Molecular machines governing exocytosis of synaptic vesicles. *Nature* 490, 201–207. doi: 10.1038/nature11320

Kaczmarek, L. K., and Zhang, Y. (2017). Kv3 Channels: enablers of Rapid Firing, Neurotransmitter Release, and Neuronal Endurance. *Physiol. Rev.* 97, 1431–1468. doi: 10.1152/physrev.00002.2017

Kaksonen, M., and Roux, A. (2018). Mechanisms of clathrin-mediated endocytosis. *Nat. Rev. Mol. Cell Biol.* 19, 313–326.

Kavalali, E. T., and Jorgensen, E. M. (2014). Visualizing presynaptic function. *Nat. Neurosci.* 17, 10–16. doi: 10.1038/nn.3578

Kononenko, N. L., and Haucke, V. (2015). Molecular mechanisms of presynaptic membrane retrieval and synaptic vesicle reformation. *Neuron* 85, 484–496. doi: 10.1016/j.neuron.2014.12.016

Li, P., Bademosi, A. T., Luo, J., and Meunier, F. A. (2018). Actin Remodeling in Regulated Exocytosis: toward a Mesoscopic View. *Trends Cell Biol.* 28, 685–697. doi: 10.1016/j.tcb.2018.04.004

Li, Z., and Murthy, V. N. (2001). Visualizing postendocytic traffic of synaptic vesicles at hippocampal synapses. *Neuron* 31, 593–605. doi: 10.1016/s0896-6273(01)00398-1

Malacombe, M., Bader, M. F., and Gasman, S. (2006). Exocytosis in neuroendocrine cells: new tasks for actin. *Biochim. Biophys. Acta* 1763, 1175–1183. doi: 10.1016/j.bbamcr.2006.09.004

Merrifield, C. J., Perrais, D., and Zenisek, D. (2005). Coupling between clathrin-coated-pit invagination, cortactin recruitment, and membrane scission observed in live cells. *Cell* 121, 593–606. doi: 10.1016/j.cell.2005.03.015

Mettlen, M., Chen, P. H., Srinivasan, S., Danuser, G., and Schmid, S. L. (2018). Regulation of Clathrin-Mediated Endocytosis. *Annu. Rev. Biochem.* 87, 871–896.

Meunier, F. A., and Gutierrez, L. M. (2016). Captivating New Roles of F-Actin Cortex in Exocytosis and Bulk Endocytosis in Neurosecretory Cells. *Trends Neurosci.* 39, 605–613. doi: 10.1016/j.tins.2016.07.003

Middlebrooks, J. C., Nick, H. S., Subramony, S. H., Advincula, J., Rosales, R. L., Lee, L. V., et al. (2013). Mutation in the kv3.3 voltage-gated potassium channel causing spinocerebellar ataxia 13 disrupts sound-localization mechanisms. *PLoS One* 8:e76749. doi: 10.1371/journal.pone.0076749

Milovanovic, D., Wu, Y., Bian, X., and De Camilli, P. (2018). A liquid phase of synapsin and lipid vesicles. *Science* 361, 604–607. doi: 10.1126/science.aat5671

Morales, M., Colicos, M. A., and Goda, Y. (2000). Actin-dependent regulation of neurotransmitter release at central synapses. *Neuron* 27, 539–550. doi: 10.1016/s0896-6273(00)00064-7

Mund, M., Van Der Beek, J. A., Deschamps, J., Dmitrieff, S., Hoess, P., Monster, J. L., et al. (2018). Systematic Nanoscale Analysis of Endocytosis Links Efficient Vesicle Formation to Patterned Actin Nucleation. *Cell* 174:e817. doi: 10.1016/j.cell.2018.06.032

Neco, P., Fernandez-Peruchena, C., Navas, S., Gutierrez, L. M., De Toledo, G. A., and Ales, E. (2008). Myosin II contributes to fusion pore expansion during exocytosis. *J. Biol. Chem.* 283, 10949–10957. doi: 10.1074/jbc.M709058200

Neher, E. (2010). What is Rate-Limiting during Sustained Synaptic Activity: vesicle Supply or the Availability of Release Sites. *Front. Synaptic. Neurosci.* 2:144. doi: 10.3389/fnsyn.2010.00144

Neher, E., and Sakaba, T. (2008). Multiple roles of calcium ions in the regulation of neurotransmitter release. *Neuron* 59, 861–872. doi: 10.1016/j.neuron.2008.08.019

Olivares, M. J., Gonzalez-Jamett, A. M., Guerra, M. J., Baez-Matus, X., Haro-Acuna, V., Martinez-Quiles, N., et al. (2014). Src Kinases Regulate De Novo Actin Polymerization during Exocytosis in Neuroendocrine Chromaffin Cells. *PLoS One* 9:e99001. doi: 10.1371/journal.pone.0099001

Papadopulos, A. (2017). Membrane shaping by actin and myosin during regulated exocytosis. *Mol. Cell Neurosci.* 84, 93–99. doi: 10.1016/j.mcn.2017.05.006

Pechstein, A., Tomilin, N., Fredrich, K., Vorontsova, O., Sopova, E., Evergren, E., et al. (2020). Vesicle Clustering in a Living Synapse Depends on a Synapsin Region that Mediates Phase Separation. *Cell Rep.* 30:e2593. doi: 10.1016/j.celrep.2020.01.092

Picco, A., Mund, M., Ries, J., Nedelec, F., and Kaksonen, M. (2015). Visualizing the functional architecture of the endocytic machinery. *Elife* 4:e04535. doi: 10.7554/eLife.04535

Renden, R., and Von Gersdorff, H. (2007). Synaptic vesicle endocytosis at a CNS nerve terminal: faster kinetics at physiological temperatures and increased endocytotic capacity during maturation. *J. Neurophysiol.* 98, 3349–3359. doi: 10.1152/jn.00898.2007

Richards, D. A., Rizzoli, S. O., and Betz, W. J. (2004). Effects of wortmannin and latrunculin A on slow endocytosis at the frog neuromuscular junction. *J. Physiol.* 557, 77–91. doi: 10.1113/jphysiol.2004.062158

Saffarian, S., Cocucci, E., and Kirchhausen, T. (2009). Distinct dynamics of endocytic clathrin-coated pits and coated plaques. *PLoS Biol.* 7:e1000191. doi: 10.1371/journal.pbio.1000191

Sakaba, T., and Neher, E. (2001). Calmodulin mediates rapid recruitment of fast-releasing synaptic vesicles at a calyx-type synapse. *Neuron* 32, 1119–1131. doi: 10.1016/s0896-6273(01)00543-8

Sakaba, T., and Neher, E. (2003). Involvement of actin polymerization in vesicle recruitment at the calyx of Held synapse. *J. Neurosci.* 23, 837–846. doi: 10.1523/JNEUROSCI.23-03-00837.2003

Sankaranarayanan, S., Atluri, P. P., and Ryan, T. A. (2003). Actin has a molecular scaffolding, not propulsive, role in presynaptic function. *Nat. Neurosci.* 6, 127–135. doi: 10.1038/nn1002

Sankaranarayanan, S., and Ryan, T. A. (2000). Real-time measurements of vesicle-SNARE recycling in synapses of the central nervous system. *Nat. Cell Biol.* 2, 197–204. doi: 10.1038/35008615

Sätzler, K., Sohl, L., Bollmann, J. H., Borst, J. G. G., Frotscher, M., Sakmann, B., et al. (2002). Three-dimensional reconstruction of a calyx of Held and its postsynaptic principal neuron in the medial nucleus of the trapezoid body. *J Neurosci.* 22, 10567–10579. doi: 10.1523/JNEUROSCI.22-24-10567.2002

Schneggenburger, R., Meyer, A. C., and Neher, E. (1999). Released fraction and total size of a pool of immediately available transmitter quanta at a calyx synapse. *Neuron* 23, 399–409. doi: 10.1016/s0896-6273(00)80789-8

Sharma, S., and Lindau, M. (2018). The fusion pore, 60 years after the first cartoon. *FEBS Lett.* 592, 3542–3562. doi: 10.1002/1873-3468.13160

Shin, W., Arpino, G., Thiyagarajan, S., Su, R., Ge, L., Mcdargh, Z., et al. (2020). Vesicle Shrinking and Enlargement Play Opposing Roles in the Release of Exocytotic Contents. *Cell Rep.* 30:e427. doi: 10.1016/j.celrep.2019.12.044

Shin, W., Ge, L., Arpino, G., Villarreal, S. A., Hamid, E., Liu, H., et al. (2018). Visualization of Membrane Pore in Live Cells Reveals a Dynamic-Pore Theory Governing Fusion and Endocytosis. *Cell* 173, 934–945. doi: 10.1016/j.cell.2018.02.062

Shin, W., Wei, L., Arpino, G., Ge, L., Guo, X., Chan, C. Y., et al. (2021). Preformed Omega-profile closure and kiss-and-run mediate endocytosis and diverse endocytic modes in neuroendocrine chromaffin cells. *Neuron* 109:e3115. doi: 10.1016/j.neuron.2021.07.019

Shin, W., Zucker, B., Kundu, N., Lee, S. H., Shi, B., Guo, X., et al. (2022). Molecular mechanics underlying flat-to-round membrane budding in live secretory cells. *BioRxiv* [preprint].

Shupliakov, O., Bloom, O., Gustafsson, J. S., Kjaerulff, O., Low, P., Tomilin, N., et al. (2002). Impaired recycling of synaptic vesicles after acute perturbation of the presynaptic actin cytoskeleton. *Proc. Natl. Acad. Sci. U.S.A.* 99, 14476–14481. doi: 10.1073/pnas.212381799

Soykan, T., Kaempf, N., Sakaba, T., Vollweiter, D., Goerdeler, F., Puchkov, D., et al. (2017). Synaptic Vesicle Endocytosis Occurs on Multiple Timescales and Is Mediated by Formin-Dependent Actin Assembly. *Neuron* 93, 854–866. doi: 10.1016/j.neuron.2017.02.011

Stewart, M. P., Helenius, J., Toyoda, Y., Ramanathan, S. P., Muller, D. J., and Hyman, A. A. (2011). Hydrostatic pressure and the actomyosin cortex drive mitotic cell rounding. *Nature* 469, 226–230. doi: 10.1038/nature09642

Sun, J. Y., and Wu, L. G. (2001). Fast kinetics of exocytosis revealed by simultaneous measurements of presynaptic capacitance and postsynatpic currents at a central synapse. *Neuron* 30, 171–182. doi: 10.1016/s0896-6273(01)00271-9

Sun, J. Y., Wu, X. S., and Wu, L. G. (2002). Single and multiple vesicle fusion induce different rates of endocytosis at a central synapse. *Nature* 417, 555–559. doi: 10.1038/417555a

Sun, T., Wu, X. S., Xu, J., Mcneil, B. D., Pang, Z. P., Yang, W., et al. (2010). The role of calcium/calmodulin-activated calcineurin in rapid and slow endocytosis at central synapses. *J. Neurosci.* 30, 11838–11847. doi: 10.1523/JNEUROSCI.1481-10.2010

Taschenberger, H., Leao, R. M., Rowland, K. C., Spirou, G. A., and Von Gersdorff, H. (2002). Optimizing synaptic architecture and efficiency for high-frequency transmission. *Neuron* 36, 1127–1143. doi: 10.1016/s0896-6273(02)01137-6

Trifaro, J., Rose, S. D., Lejen, T., and Elzagallaai, A. (2000). Two pathways control chromaffin cell cortical F-actin dynamics during exocytosis. *Biochimie* 82, 339–352. doi: 10.1016/s0300-9084(00)00193-0

Tsujita, K., Takenawa, T., and Itoh, T. (2015). Feedback regulation between plasma membrane tension and membrane-bending proteins organizes cell polarity during leading edge formation. *Nat. Cell Biol.* 17, 749–758. doi: 10.1038/ncb3162

Von Gersdorff, H., and Borst, J. G. G. (2002). Short-term plasticity at the calyx of Held. *Nat. Rev. Neurosci.* 3, 53–64.

Wang, L. Y., and Kaczmarek, L. K. (1998). High-frequency firing helps replenish the readily releasable pool of synaptic vesicles. *Nature* 394, 384–388. doi: 10.1038/28645

Watanabe, S., Rost, B. R., Camacho-Perez, M., Davis, M. W., Sohl-Kielczynski, B., Rosenmund, C., et al. (2013). Ultrafast endocytosis at mouse hippocampal synapses. *Nature* 504, 242–247. doi: 10.1038/nature12809

Watanabe, S., Trimbuch, T., Camacho-Perez, M., Rost, B. R., Brokowski, B., Sohl-Kielczynski, B., et al. (2014). Clathrin regenerates synaptic vesicles from endosomes. *Nature* 515, 228–233. doi: 10.1038/nature13846

Wen, P. J., Grenklo, S., Arpino, G., Tan, X., Liao, H. S., Heureaux, J., et al. (2016). Actin dynamics provides membrane tension to merge fusing vesicles into the plasma membrane. *Nat. Commun.* 7:12604. doi: 10.1038/ncomms12604

Wen, P. J., Osborne, S. L., Zanin, M., Low, P. C., Wang, H. T., Schoenwaelder, S. M., et al. (2011). Phosphatidylinositol(4,5)bisphosphate coordinates actin-mediated mobilization and translocation of secretory vesicles to the plasma membrane of chromaffin cells. *Nat. Commun.* 2:491. doi: 10.1038/ncomms1500

Wienisch, M., and Klingauf, J. (2006). Vesicular proteins exocytosed and subsequently retrieved by compensatory endocytosis are nonidentical. *Nat. Neurosci.* 9, 1019–1027. doi: 10.1038/nn1739

Wu, L. G., and Borst, J. G. G. (1999). The reduced release probability of releasable vesicles during recovery from short-term synaptic depression. *Neuron* 23, 821–832. doi: 10.1016/s0896-6273(01)80039-8

Wu, L. G., Hamid, E., Shin, W., and Chiang, H. C. (2014). Exocytosis and endocytosis: modes, functions, and coupling mechanisms. *Annu. Rev. Physiol.* 76, 301–331. doi: 10.1146/annurev-physiol-021113-170305

Wu, X. S., Lee, S. H., Sheng, J., Zhang, Z., Zhao, W. D., Wang, D., et al. (2016). Actin Is Crucial for All Kinetically Distinguishable Forms of Endocytosis at Synapses. *Neuron* 92, 1020–1035. doi: 10.1016/j.neuron.2016.10.014

Wu, X. S., Mcneil, B. D., Xu, J., Fan, J., Xue, L., Melicoff, E., et al. (2009). Ca(2+) and calmodulin initiate all forms of endocytosis during depolarization at a nerve terminal. *Nat. Neurosci.* 12, 1003–1010. doi: 10.1038/nn.2355

Wu, X. S., Subramanian, S., Zhang, Y., Shi, B., Xia, J., Li, T., et al. (2021). Presynaptic Kv3 channels are required for fast and slow endocytosis of synaptic vesicles. *Neuron* 109, e935. doi: 10.1016/j.neuron.2021.01.006

Xu, J., Luo, F., Zhang, Z., Xue, L., Wu, X. S., Chiang, H. C., et al. (2013). SNARE proteins synaptobrevin, SNAP-25, and syntaxin are involved in rapid and slow endocytosis at synapses. *Cell Rep.* 3, 1414–1421. doi: 10.1016/j.celrep.2013.03.010

Xu, J., Mcneil, B., Wu, W., Nees, D., Bai, L., and Wu, L. G. (2008). GTP-independent rapid and slow endocytosis at a central synapse. *Nat. Neurosci.* 11, 45–53. doi: 10.1038/nn2021

Xu, J., and Wu, L. G. (2005). The decrease in the presynaptic calcium current is a major cause of short-term depression at a calyx-type synapse. *Neuron* 46, 633–645. doi: 10.1016/j.neuron.2005.03.024

Xue, L., Mcneil, B. D., Wu, X. S., Luo, F., He, L., and Wu, L. G. (2012). A membrane pool retrieved *via* endocytosis overshoot at nerve terminals: a study of its retrieval mechanism and role. *J. Neurosci.* 32, 3398–3404. doi: 10.1523/JNEUROSCI.5943-11.2012

Yamashita, T., Eguchi, K., Saitoh, N., Von Gersdorff, H., and Takahashi, T. (2010). Developmental shift to a mechanism of synaptic vesicle endocytosis requiring nanodomain Ca2+. *Nat. Neurosci.* 13, 838–844. doi: 10.1038/nn.2576

Yamashita, T., Hige, T., and Takahashi, T. (2005). Vesicle endocytosis requires dynamin-dependent GTP hydrolysis at a fast CNS synapse. *Science* 307, 124–127. doi: 10.1126/science.1103631

Yarar, D., Waterman-Storer, C. M., and Schmid, S. L. (2005). A dynamic actin cytoskeleton functions at multiple stages of clathrin-mediated endocytosis. *Mol. Biol. Cell* 16, 964–975.

Yue, H. Y., and Xu, J. (2014). Myosin light chain kinase accelerates vesicle endocytosis at the calyx of Held synapse. *J. Neurosci.* 34, 295–304. doi: 10.1523/JNEUROSCI.3744-13.2014

Zhang, Y., Zhang, X. F., Fleming, M. R., Amiri, A., El-Hassar, L., Surguchev, A. A., et al. (2016). Kv3.3 Channels Bind Hax-1 and Arp2/3 to Assemble a Stable Local Actin Network that Regulates Channel Gating. *Cell* 165, 434–448. doi: 10.1016/j.cell.2016.02.009

Zhang, Z., Wang, D., Sun, T., Xu, J., Chiang, H. C., Shin, W., et al. (2013). The SNARE proteins SNAP25 and synaptobrevin are involved in endocytosis at hippocampal synapses. *J. Neurosci.* 33, 9169–9175. doi: 10.1523/JNEUROSCI.0301-13.2013

Zhao, W. D., Hamid, E., Shin, W., Wen, P. J., Krystofiak, E. S., Villarreal, S. A., et al. (2016). Hemi-fused structure mediates and controls fusion and fission in live cells. *Nature* 534, 548–552. doi: 10.1038/nature18598

Zucker, R. S., and Regehr, W. G. (2002). Short-term synaptic plasticity. *Annu. Rev. Physiol.* 64, 355–405.

Conflict of Interest: The authors declare that the research was conducted in the absence of any commercial or financial relationships that could be construed as a potential conflict of interest.

Publisher's Note: All claims expressed in this article are solely those of the authors and do not necessarily represent those of their affiliated organizations, or those of the publisher, the editors and the reviewers. Any product that may be evaluated in this article, or claim that may be made by its manufacturer, is not guaranteed or endorsed by the publisher.

frontiers in Synaptic Neuroscience

REVIEW
published: 08 March 2022
doi: 10.3389/fnsyn.2022.854956

The Synaptic Extracellular Matrix: Long-Lived, Stable, and Still Remarkably Dynamic

Tal M. Dankovich[1,2]* *and Silvio O. Rizzoli*[1,3]*

[1]*University Medical Center Göttingen, Institute for Neuro- and Sensory Physiology, Göttingen, Germany,* [2]*International Max Planck Research School for Neuroscience, Göttingen, Germany,* [3]*Biostructural Imaging of Neurodegeneration (BIN) Center & Multiscale Bioimaging Excellence Center, Göttingen, Germany*

In the adult brain, synapses are tightly enwrapped by lattices of the extracellular matrix that consist of extremely long-lived molecules. These lattices are deemed to stabilize synapses, restrict the reorganization of their transmission machinery, and prevent them from undergoing structural or morphological changes. At the same time, they are expected to retain some degree of flexibility to permit occasional events of synaptic plasticity. The recent understanding that structural changes to synapses are significantly more frequent than previously assumed (occurring even on a timescale of minutes) has called for a mechanism that allows continual and energy-efficient remodeling of the extracellular matrix (ECM) at synapses. Here, we review recent evidence for such a process based on the constitutive recycling of synaptic ECM molecules. We discuss the key characteristics of this mechanism, focusing on its roles in mediating synaptic transmission and plasticity, and speculate on additional potential functions in neuronal signaling.

Keywords: ECM, synapse, plasticity, tenascin, recycling

OPEN ACCESS

Edited by:
Martin Heine,
Johannes Gutenberg University Mainz, Germany

Reviewed by:
Lorenzo A. Cingolani,
Italian Institute of Technology (IIT), Italy
Villers Agnes,
University of Mons, Belgium

***Correspondence:**
Tal M. Dankovich
tal.dankovich@med.uni-goettingen.de
Silvio O. Rizzoli
srizzoli@gwdg.de

Received: *14 January 2022*
Accepted: *16 February 2022*
Published: *08 March 2022*

Citation:
Dankovich TM and Rizzoli SO (2022) The Synaptic Extracellular Matrix: Long-Lived, Stable, and Still Remarkably Dynamic. Front. Synaptic Neurosci. 14:854956. doi: 10.3389/fnsyn.2022.854956

INTRODUCTION

An increasing number of studies are showing that synaptic function is strongly influenced by their local environment, including the molecules or cellular components in their vicinity. As a result, the classical synaptic framework (consisting of the pre- and postsynaptic compartments only) has gradually been extended to include the neighboring astrocytic processes (the "tripartite synapse"; Araque et al., 1999) and, ultimately, also the surrounding extracellular matrix (ECM; the "tetrapartite synapse"; Dityatev et al., 2006). Nowadays, the synaptic ECM is recognized to play an essential role in physiological synaptic transmission as well as in plasticity, and its dysregulation has been linked to synaptopathies in a wide variety of brain disorders (Bonneh-Barkay and Wiley, 2009; Pantazopoulos and Berretta, 2016; Ferrer-Ferrer and Dityatev, 2018). An important property of this ECM is that its molecules are among the longest-lived in the brain, which renders this structure extremely stable (Toyama et al., 2013; Dörrbaum et al., 2018; Fornasiero et al., 2018), and while this quality makes the ECM well-suited to provide long-term support to synapses, both functionally and structurally, it is seemingly ill-suited to allow for very frequent synaptic changes. However, increasingly more studies are showing that changes to synaptic structure can be extremely frequent, even in the adult brain (Berning et al., 2012; Willig et al., 2014; Wegner et al., 2018). In light of these observations, one would expect a mechanism to be in place for maintaining sufficient flexibility of the ECM at synapses, to allow for ongoing structural plasticity. In this review, we discuss a novel mechanism proposed to provide such flexibility, in the form of molecular recycling of ECM

components at synapses (Dankovich et al., 2021). We begin by briefly reviewing the various roles of ECM components at the tetrapartite synapse and the existing model for ECM remodeling, followed by a discussion on the plausibility of ECM recycling and its potential implications for our current understanding of synaptic signaling.

ORGANIZATION OF THE ECM AT SYNAPSES

In the adult brain, the major components of the neuronal ECM are a family of chondroitin sulfate proteoglycans (CSPGs) called lecticans, and their binding partners: the glycoprotein tenascin-R (TNR) and the glycosaminoglycan hyaluronic acid. Together, these organize into an extensive lattice where long chains of hyaluronan form a backbone for lecticans to bind, and these are thoroughly cross-linked through extensive interactions with TNR (Ruoslahti, 1996). Hyaluronan remains attached to the transmembrane synthase that produces it, which effectively tethers these structures to the surface of the plasma membrane (Dityatev et al., 2010; Sorg et al., 2016). ECM lattices can be found throughout neuronal surfaces, albeit with variations in the relative abundance of the various components and the density of these structures. Particularly dense conformations can be found in the form of perineuronal nets (PNNs) that enwrap the soma and proximal dendrites of a subgroup of neurons, while more diffuse conformations are found pan-neuronally, including finer segments of the neurites and the perisynaptic spaces (Dityatev and Schachner, 2003). In addition to secreted molecules, synapses are also associated with a variety of membrane-bound molecules that interact with the nearby ECM. One well-studied example is the integrin family of ECM receptors, which play an important role in the modulation of actin-associated proteins, and therefore act as a link between the ECM and the neuronal cytoskeleton, allowing these ECM ligands to act as modulators of synaptic structure (Shi and Ethell, 2006; Park and Goda, 2016). Besides the various ECM receptors that are present in the synaptic membrane, there is also growing evidence that many membrane-bound components of the synaptic transmission machinery, such as neurotransmitter receptors, can interact with ECM molecules at the synapse. In the following section, we review some of this evidence, and discuss the potential role of these interactions in modulating various aspects of synaptic function.

ROLES OF THE ECM AT THE TETRAPARTITE SYNAPSE

Stabilization and Maintenance of Synapses

Expectedly, the perisynaptic ECM provides a steric hindrance to the diffusion of transmembrane molecules at the synapse (**Figure 1**). *In vitro*, postsynaptic AMPA-type glutamate receptors become significantly less mobile after ∼2–3 weeks in culture, which also corresponds to the time at which structured ECM begins to appear on the neuronal surfaces (Borgdorff and Choquet, 2002; John et al., 2006). Disrupting the ECM through enzymatic cleavage of hyaluronan was shown to partially restore this juvenile level of mobility (Frischknecht et al., 2009). Interestingly, this effect was not limited to AMPA receptors, since the authors also reported a reduction in the mobility of green fluorescent protein (GFP) that was artificially introduced into the membrane, suggesting that the ECM at synapses stands as a diffusion barrier to a wide variety of membrane-associated proteins (Frischknecht et al., 2009). For the presynapse, evidence for ECM-mediated stabilization of membrane proteins comes from studies of synapses in the auditory pathway. In cochlear inner hair cell synapses, a deficiency in the lectican brevican leads to a misalignment of presynaptic calcium channels, resulting in a mild hearing loss (Sonntag et al., 2018). In the calyx of Held synapses, a loss of brevican results in altered dynamics in synaptic transmission that are also consistent with a change in the organization of presynaptic calcium channels (Blosa et al., 2015). Taken together, these findings suggest that the ECM-imposed hindrance of diffusion is necessary for the functional organization of synaptic transmission machinery.

In addition to hindering protein diffusion, it also appears that the ECM constricts the mobility and outgrowth of the synapse itself. Application of CSPG-cleaving enzymes *in vitro* and *in vivo* has been shown to result in the outgrowth of dendritic spine heads, and an enhancement of spine motility (Orlando et al., 2012; de Vivo et al., 2013). Mechanistically, such a treatment may act not only to release the constraint placed by the ECM, but is also likely to interfere with direct interactions between ECM molecules and synaptic transmembrane proteins that contribute to synapse stabilization. For example, integrin receptors containing the β1 subunit are known to promote spine maintenance through the modulation of the actin cytoskeleton, and are also known to interact with TNR and CSPGs (Liao et al., 2008; Tan et al., 2011; Sloan Warren et al., 2012). Similarly, the hyaluronan receptor CD44 has been shown to affect spine structure through its modulation of actin cytoskeleton regulators. Furthermore, a knockdown of this receptor was shown to reduce the number of presynapses labeled by the active zone marker bassoon (Roszkowska et al., 2016). It remains to be determined whether the interaction of these ECM receptors with their ligands is necessary for their stabilization of the synapse.

Modulation of Postsynaptic Plasticity

ECM molecules have also been shown to directly modulate the activity of machinery involved in synaptic plasticity (**Figure 1**). In many synapses, plasticity-related changes are instigated through the activity-dependent opening of NMDA receptors (NMDARs), which results in an influx of calcium and, subsequently, the long-term potentiation of postsynaptic responses (LTP; Herring and Nicoll, 2016). A number of studies have demonstrated that the activation of postsynaptic β1 integrins is necessary for the initiation and maintenance of LTP, both by modulating the actin cytoskeleton to allow dendritic spine head enlargement and, presumably, resulting in an augmentation of NMDA-mediated currents (Bernard-Trifilo et al., 2005; Kramar et al., 2006; Rex et al., 2009). Accordingly, mice that harbor a neuron-specific deficiency in β1 integrins have impaired NMDAR-dependent LTP (Chan et al., 2006; Huang et al., 2006). It should be noted, however, that the demonstration of an integrin-dependent

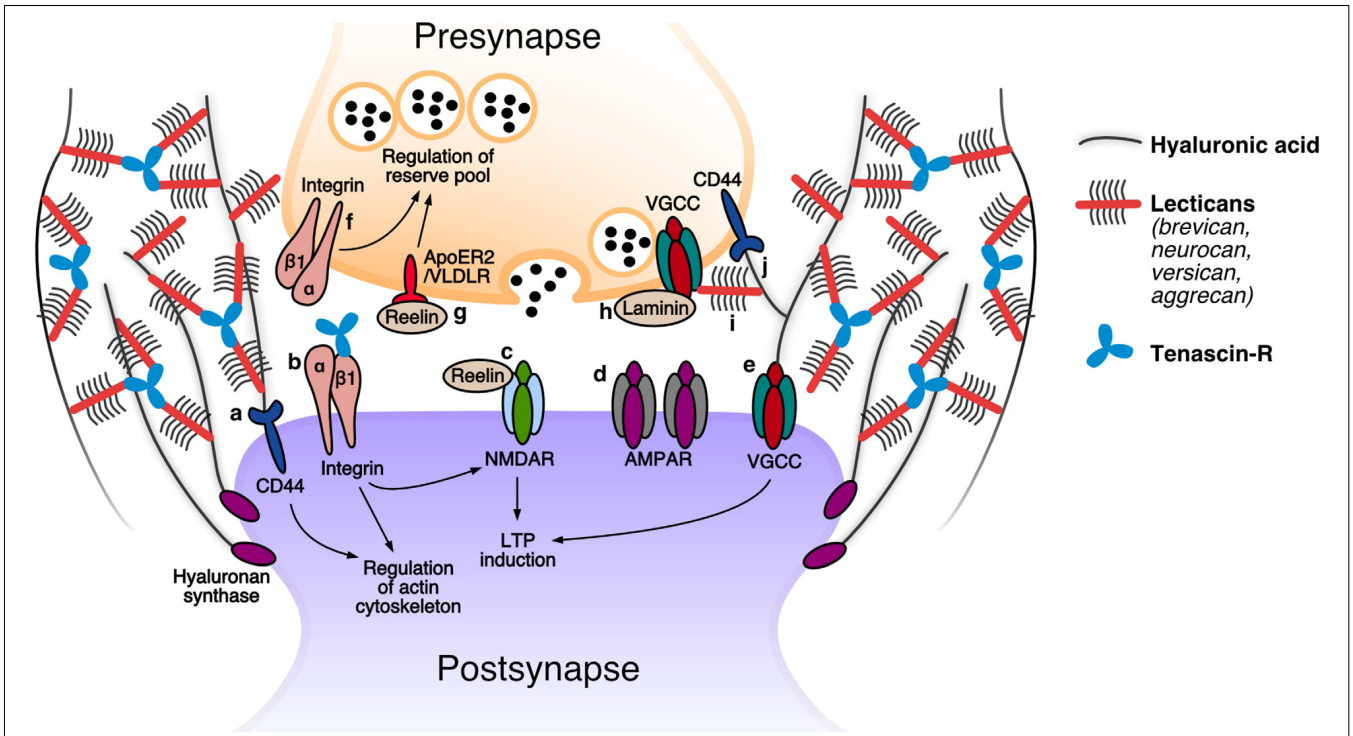

FIGURE 1 | The tetrapartite synapse: speculated roles of extracellular matrix (ECM) molecules. **Postsynapse: (a)** The receptor for hyaluronan CD44 was demonstrated to modulate the activity of actin-associated proteins and thereby promote the stabilization of dendritic spines (Roszkowska et al., 2016). **(b)** β1 integrin receptors are proposed to contribute to LTP by modulating NMDAR-mediated currents, and play a role in spine restructuring and stabilization by modulating the actin cytoskeleton. An interaction has been reported between β1 integrins and tenascin-R (TNR) (Bernard-Trifilo et al., 2005; Liao et al., 2008; Tan et al., 2011; Sloan Warren et al., 2012). **(c)** Increased levels of reelin augment NMDAR-mediated currents, leading to enhanced LTP responses (Weeber et al., 2002; Rogers et al., 2011). **(d)** The hyaluronan-based perisynaptic ECM restricts the lateral mobility of AMPARs (Frischknecht et al., 2009). **(e)** Hyaluronan regulates VGCC-dependent plasticity by modulating these channels (Kochlamazashvili et al., 2010). **Presynapse: (f)** Presynaptic β1 integrin receptors are presumed to regulate the reserve pool of synaptic vesicles (Huang et al., 2006). **(g)** Reelin activation of its ApoER2 and VLDLR receptors modulates reserve pool synaptic vesicles (Bal et al., 2013). **(h)** Presynaptic active zone proteins are anchored at the membrane through putative interactions with β2 laminins (such as with VGCCs; Nishimune et al., 2004; Hunter et al., 2019). **(i)** The presence of perisynaptic brevican is essential for a correct alignment of presynaptic VGCCs in front of the postsynaptic density (Sonntag et al., 2018). **(j)** CD44, the receptor for hyaluronan, was shown to be present presynaptically and is essential for presynapse stability (Roszkowska et al., 2016). Modified from Dankovich (2021).

modulation of NMDARs relied on short integrin ligand (RGD) peptides that have since been shown to directly act on these receptors (Cingolani et al., 2008). It, therefore, remains to be established whether such modulations also take place at the physiological level.

An additional ECM component that has been implicated in LTP is the secreted glycoprotein reelin (generally known for its role in early brain development; D'Arcangelo, 2014). Several studies have shown that reelin supplementation results in enhanced LTP responses, likely due to its ability to modulate NMDAR-mediated currents. In addition, mice deficient in reelin were found to have impairments in LTP (Weeber et al., 2002; Beffert et al., 2005; Qiu et al., 2006; Rogers et al., 2011). Lastly, it is worth mentioning that additional, NMDAR-independent LTP mechanisms have also been linked to ECM modulation. For example, both hyaluronan and tenascin-C were shown to modulate a form of LTP that depends on signaling through postsynaptic L-type voltage-gated calcium channels (LVGCCs; Evers et al., 2002; Kochlamazashvili et al., 2010).

Besides *bona fide* plasticity mechanisms, synapses also have "metaplasticity" mechanisms in place that allow them to modify their predisposition to undergo plasticity. This is often achieved through an adjustment of a neuron's basal level of excitation, which can act to temper the threshold for LTP induction (Abraham and Bear, 1996). The ECM glycoprotein TNR has been linked to such metaplasticity mechanisms due to its ability to modulate GABA-mediated inhibitory transmission, an important determinant of basal neuronal activity. TNR-deficient mice have elevated levels of basal excitatory transmission and hence a metaplastic increase in the LTP induction threshold (Saghatelyan et al., 2001; Nikonenko et al., 2003; Bukalo et al., 2007). It is possible that TNR exerts its modulation through direct interaction with $GABA_B$ receptors (Kruse et al., 1985; Saghatelyan et al., 2001, 2003).

Modulation of Synaptic Vesicle Release

As for the postsynapse, studies have also demonstrated that the ECM can directly modulate the presynaptic machinery involved in synaptic vesicle release (**Figure 1**). Recent evidence

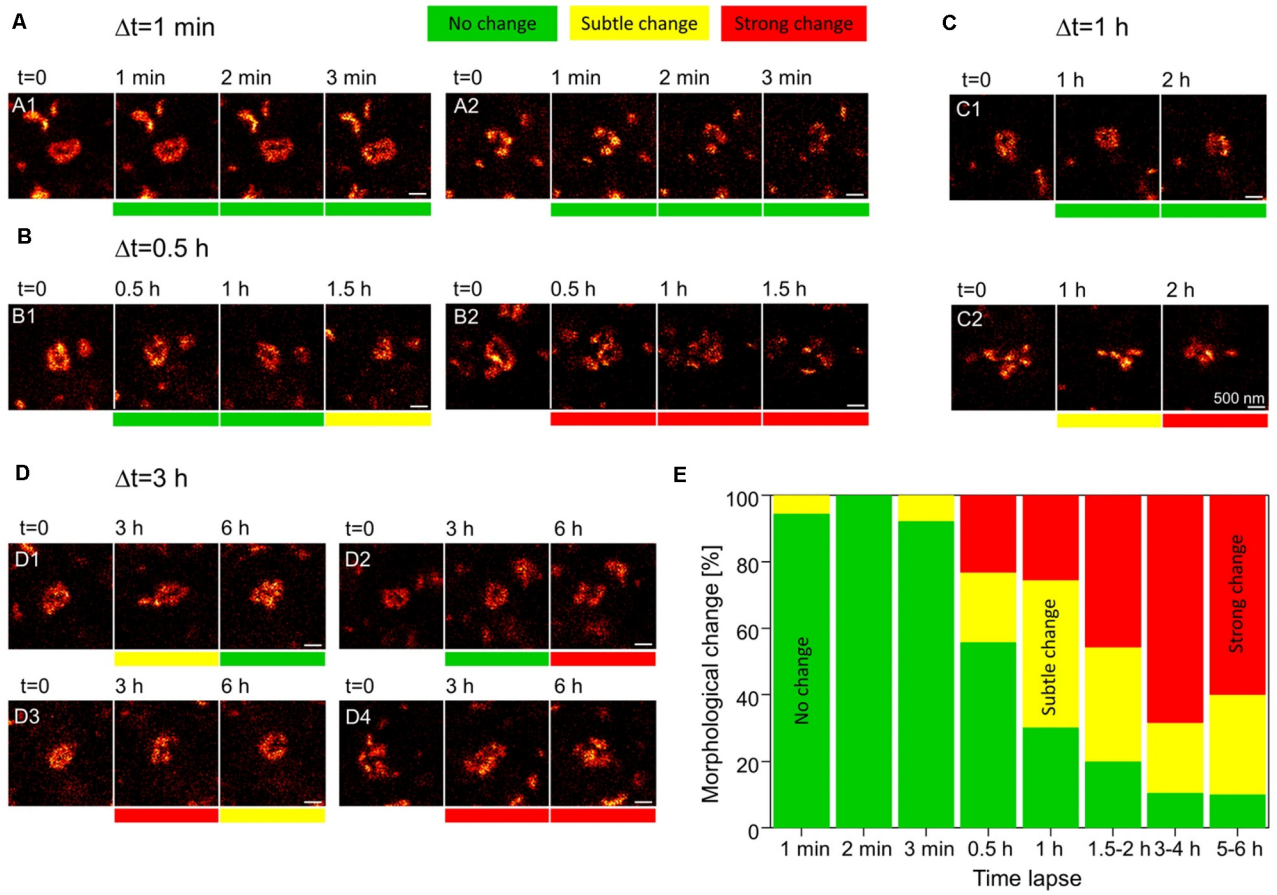

FIGURE 2 | Rapid dynamics of the postsynaptic density (PSD) in dendritic spines. Knock-in mice in which the postsynaptic density protein PSD95 was fused to a fluorescent reporter were used to track the morphology of the PSD. Individual dendritic spines in the visual cortex were imaged using live stimulated emission depletion (STED) microscopy for up to 6 h. **(A)** At a time interval of 1 min, no morphological changes to PSD assemblies are observed. **(B,C)** At higher intervals of 30 min to 2 h, morphological changes can be seen at some synapses **(B2,C2)**, while others appear to remain stable **(B1,C1)**. **(D)** At synapses imaged up to 6 h, PSD assemblies may undergo morphological changes and then return to their original structure **(D1)**, remain unchanged for several hours and only then undergo a morphological change **(D2)**, or undergo multiple morphological changes over the course of several hours **(D3,D4)**. Scale bars = 500 nm. **(E)** Quantification of the % of either no change, subtle and strong changes to the morphology of postsynaptic assemblies of PSD95 for increasing imaging time intervals. *N* = 4 mice; *n* = 18 (1–2 min), 13 (3 min), 43 (0.5–1 h), 35 (1.2–2 h), 10 (5–6 h) PSD95 assemblies imaged. Adapted with permission from Wegner et al. (2018; http://creativecommons.org/licenses/by/4.0/).

suggests that laminins, which have largely been studied in the context of brain development, are essential for the organization of presynaptic release machinery at synapses in the adult brain. In the retina, a deficiency in laminin β2 disrupted the spatial organization of a variety of presynaptic components, while their expression level remained unchanged (Hunter et al., 2019). It is possible that laminin β2 molecules achieve this function through direct interactions with the extracellular region of one or more of these components (e.g., they are known to bind presynaptic calcium channels at neuromuscular junction synapses; Nishimune et al., 2004). In addition to prospective interactions with release machinery, laminins may also interact with the synaptic vesicles themselves. At neuromuscular junctions, laminin α5 subunits were found to interact with the synaptic vesicle protein 2 (SV2), which plays a role in priming synaptic vesicles for their release (Son et al., 2000; Chang and Sudhof, 2009). Since laminin α5 was recently also shown to be present at central synapses, it is possible to imagine that it also plays a role in synaptic vesicle release in the brain (Omar et al., 2017). Besides these direct interactions with key synapse components, it is also possible that laminins carry out some of their functions indirectly, through an interaction with ECM receptors such as integrins (Carlson et al., 2010; Nirwane and Yao, 2018). For example, β1 integrins (known to bind laminin α5) were shown to be present at hippocampal presynapses (Mortillo et al., 2012). Furthermore, a neuron-specific deficiency in β1 integrin results in altered synaptic responses that are congruent with a reduced mobilization of vesicles belonging to the reserve pool (i.e., vesicles that are released only rarely under physiological conditions; Huang et al., 2006).

An additional ECM molecule that has been implicated in the modulation of synaptic vesicle release is reelin. A study by Bal and colleagues demonstrated that the application of

reelin *in vitro* results in a significant increase in spontaneous vesicle release. Evidence suggests this is due to an increase in presynaptic calcium levels, possibly as a result of the interaction between reelin and its receptors ApoER2 and VLDLR (Bal et al., 2013). Interestingly, the authors also found that reelin specifically mobilizes vesicles enriched with the synaptic vesicle protein VAMP7, which are generally believed to be "reserve pool" vesicles (Hua et al., 2011). Similar to the findings for β1 integrins described above, this demonstrates that the ECM is capable of differentially modulating synaptic vesicle pools.

ECM REMODELING AT THE SYNAPSE

Since the ECM is integral to synapse stabilization and maintenance, events of synaptic plasticity are likely to require extensive remodeling of these components at synapses. The currently prevailing notion is that ECM remodeling takes place through proteolytic cleavage of these molecules by locally secreted enzymes, followed by the integration of newly-synthesized ECM molecules. One well-studied example is the local synaptic secretion of matrix metalloproteinase 9 (MMP9) at the onset of LTP, which was shown to be necessary for the accompanying structural plasticity of dendritic spines (Nagy et al., 2006; Wang et al., 2008; Gawlak et al., 2009; Michaluk et al., 2011; Dziembowska et al., 2012). MMP9 can be subsequently deactivated through the parallel secretion of tissue inhibitor of metalloproteinase1 (TIMP1), allowing this cleavage to be transient (Okulski et al., 2007; Magnowska et al., 2016).

While proteolysis-dependent ECM remodeling comprises a tightly controlled mechanism for mediating synaptic plasticity, it is expected to become metabolically expensive when employed very frequently. It is therefore difficult to reconcile this mechanism with the emerging understanding that structural synaptic plasticity is an extremely frequent event: as demonstrated by multiple super-resolution imaging experiments, synaptic morphology can change drastically within just minutes to hours (e.g., **Figure 2**; Berning et al., 2012; Testa et al., 2012; Willig et al., 2014; Wegner et al., 2018). If every structural fluctuation at synapses were to involve proteolysis and *de novo* synthesis of the ECM, this mechanism would necessitate a relatively fast turnover of these molecules, bringing them close to the lifetimes of other synaptic components that are affected by plasticity, as the postsynaptic receptors. Nevertheless, experimental evidence suggests that ECM molecules are among the longest-lived in the brain (see **Table 1** below, for examples of ECM protein lifetimes *in vivo*, Toyama et al., 2013; Dörrbaum et al., 2018; Fornasiero et al., 2018), far longer-lived than the average pre- or postsynaptic protein. It is, therefore, highly likely that additional mechanisms of ECM remodeling exist that do not require a continual turnover of ECM molecules.

TABLE 1 | Average lifetimes of select extracellular matrix (ECM) and synaptic proteins (as reported in Fornasiero et al., 2018).

Protein	Half-life in adult mouse brain (days, range for several regions shown)
Brevican	17–31
Neurocan	20–97
Aggrecan	24
Versican	49–687
Tenascin-R	39–74
Synaptic proteins:	
SNAP25	3–4
VAMP2	11–15
Synaptotagmin1	9–10
NMDA receptors	3–7
AMPA receptors	6–15
PSD95	13–16
Homer1	13–14

RECYCLING OF SYNAPTIC ECM

A novel mechanism of ECM remodeling was presented in a recent study by Dankovich and colleagues, based on the recycling of ECM molecules at the synapse. The authors proposed that these molecules are constitutively internalized into neurons, and subsequently resurface and re-integrate into the ECM around synapses (Dankovich et al., 2021). A complete recycling loop was described for the glycoprotein TNR, which spans ∼3 days (**Figure 3**).

In further support of this mechanism, it was found that recycling TNR molecules are significantly enriched at synaptic regions, while more stable TNR molecules are present throughout the neuronal surface. In addition, it was demonstrated that TNR recycling is tightly linked to synaptic activity and strength: the amount of recycling TNR molecules detected at the neuronal surface increased following treatment with an activity-enhancing drug (the $GABA_A$ channel blocker bicuculline) and decreased following treatment with activity-reducing drugs (the AMPA and NMDA channel blockers CNQX and AP5). The authors further established this link at the synapses themselves. To do so, they labeled actively recycling synaptic vesicles using antibodies against the lumenal domain of synaptotagmin1 (Syt1) as a proxy for local synaptic activity (Kraszewski et al., 1996; Wilhelm et al., 2010; Truckenbrodt et al., 2018; Gürth et al., 2020). Using stimulated emission depletion (STED) microscopy, they confirmed that local synaptic activity is significantly correlated to the extent of recycling. In a second experiment, the authors stained the neurons with lipophilic dye to reveal synaptic membranes, and found a second significant correlation between the extent of TNR recycling and the size of the postsynaptic head (which is known to be an important correlate of synaptic strength; Humeau and Choquet, 2019; **Figure 4**).

An interesting point to consider is the timespan of the TNR recycling loop (∼3 days), which is considerably longer than that of other, well-studied recycling molecules (Bretscher, 1989; Koenig and Edwardson, 1997; Bridgewater et al., 2012). The authors provided a partial answer by metabolically labeling glycans with azide-carrying sugars and then visualizing these with fluorophores using a click chemistry reaction (Saka et al., 2014). This experiment revealed that recycling TNR molecules appear to become re-glycosylated throughout their intracellular trafficking route. This finding was further supported by immunostainings showing that intracellular

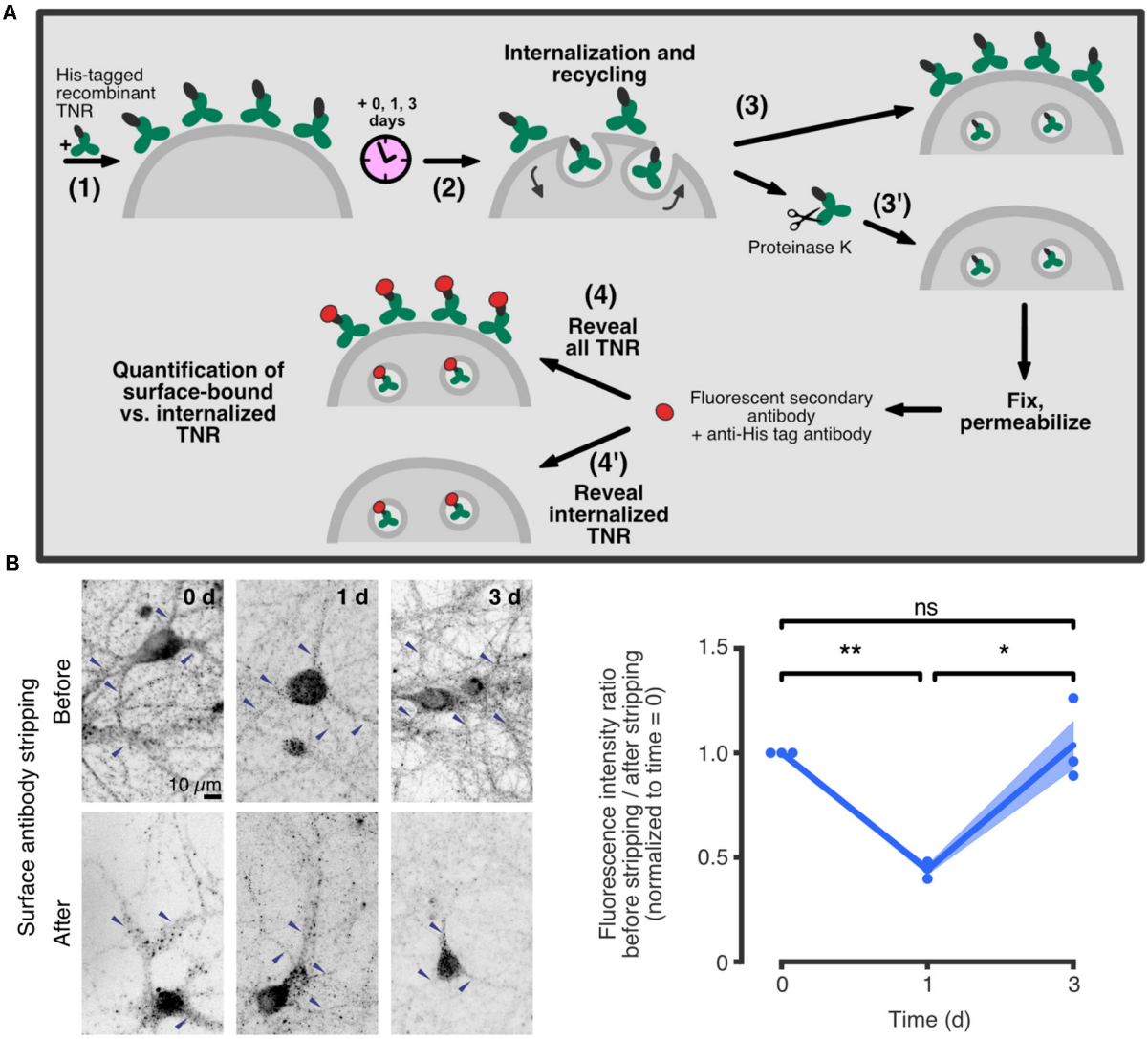

FIGURE 3 | TNR recycles in neurons over ~3 days. **(A)** A schematic of an assay to assess TNR recycling. (1) Cultured hippocampal neurons were pulsed with recombinant His-tagged TNR, which was then allowed to potentially internalize and recycle for a period of 0–3 days (2). After the incubation period, the neurons were immediately fixed (3), or fixed following treatment with proteinase K to strip away all surface-bound recombinant TNR molecules (3'). Following permeabilization treatment, the neurons were immunostained using antibodies against the His-tag to visualize all recombinant TNR (4), or the internalized recombinant TNR only (4'). **(B)** Immediately after pulsing the neurons with recombinant TNR, the staining was visibly reduced by the surface stripping, indicating that the majority of the molecules were surface-bound. One day after the pulse, the signal was similar for non-stripped and stripped neurons, indicating that most molecules had been internalized. Three days after the pulse, surface stripping visibly reduced the staining once again, indicating that a portion of recombinant TNR molecules had recycled back to the surface. Blue arrowheads indicate labeledTNR in neurites. Scale bar = 10 μm. Statistical significance was evaluated with repeated-measures one-way ANOVA ($F_{1.044,\ 2.088}$ = 28, 6, $^*p$ = 0.03), followed by Fisher's LSD ("0 days" vs. "1 day": $^{**}p$ = 0.002; "1 day" vs. "3 days": $^*p$ = 0.027; "0 days" vs. "3 days": p = 0.775). N = 3 independent experiments. In the plot, lines represent the means, shaded areas represent the SEM, and dots represent individual experiments. Adapted from Dankovich et al. (2021) with permission from Springer Nature (http://creativecommons.org/licenses/by/4.0/).

recycling TNRs colocalize with somatic endoplasmic reticulum and Golgi apparatus following their internalization. Pathways of re-glycosylation have not been widely investigated, but there are several reports of this process occurring in non-neural cells (for example, in liver cells; Kreisel et al., 1988; Volz et al., 1995; Porwoll et al., 1998). While the biological function of this process remains to be established, one simple possibility is that it serves to repair the wear and tear of frequently recycling molecules without the need to replace their protein core. It is also possible that the glycans residues themselves play a role in the recycling process by functioning in the sorting of the proteins, as has been shown in non-neural cells (Scheiffele et al., 1995).

Besides their internalization for the purpose of re-glycosylation, it is also interesting to consider that ECM molecules may be internalized to activate intracellular signaling cascades. Recent findings have shown that several types of

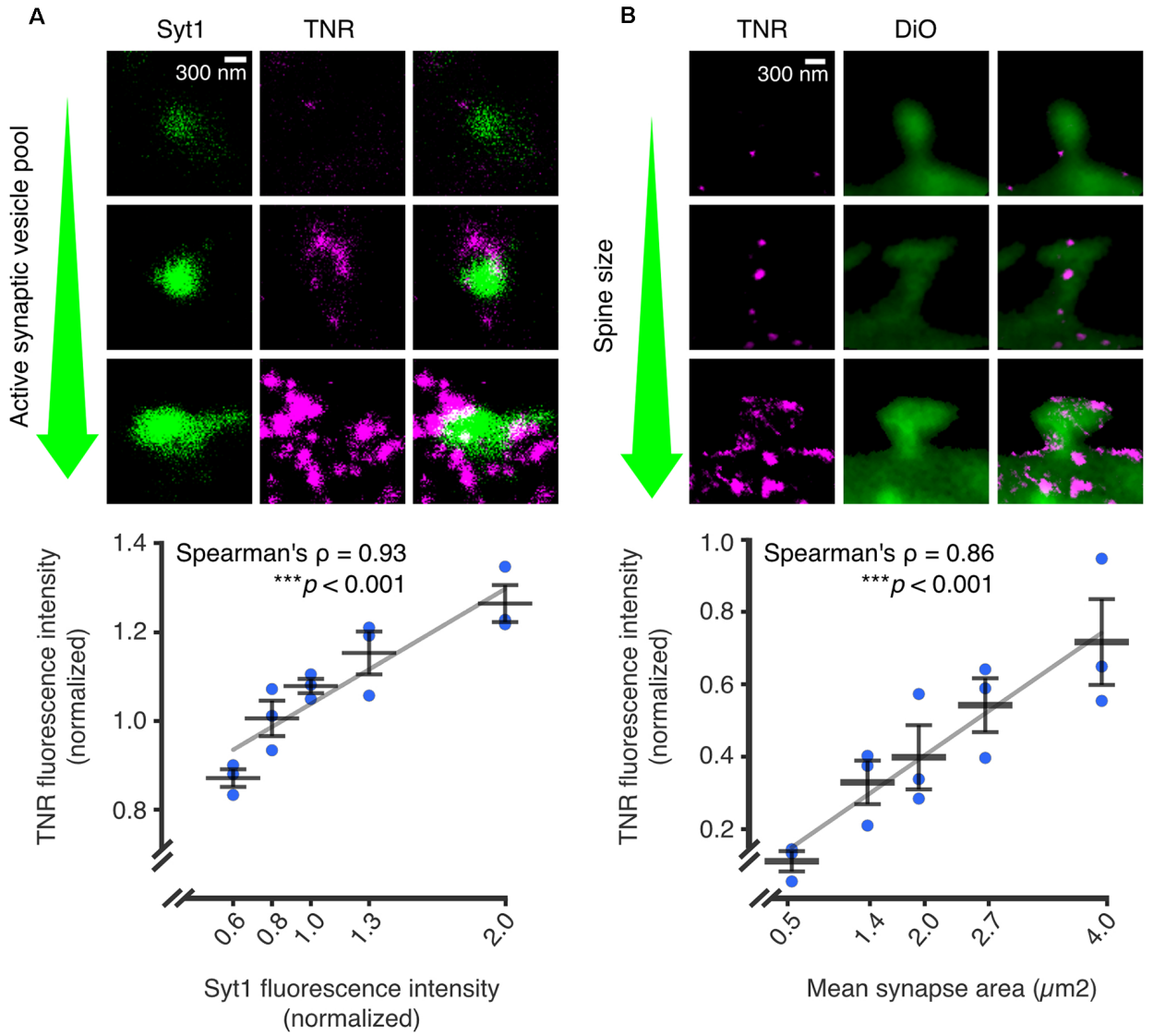

FIGURE 4 | The abundance of recycling TNR molecules at synapses is correlated to synaptic weight. Recycling TNR epitopes were labeled using a live immunostaining-based assay. First, all surface-bound epitopes are blocked with unlabeled antibodies against TNR. After a period of time, newly-emerged epitopes are revealed with the same TNR antibodies conjugated to fluorophores. **(A)** Newly-emerged TNR epitopes were labeled 12 h after surface-blocking (magenta). At the same time, actively recycling synaptic vesicles were labeled with antibodies against the lumenal domain of synaptotagmin1 (Syt1; green), as a proxy for synaptic activity. Shown are three exemplary synapses with increasingly larger active vesicle pools, imaged in confocal (Syt1) and STED (TNR). The mean fluorescence intensities of TNR and Syt1, normalized to the medians of each respective experiment, are plotted against each other. The values for Syt1 were divided into five bins containing equal numbers of synapses. Quantification of the correlation between the intensities demonstrates a strong link between the size of the active vesicle pool and the amount of recycling TNR epitopes ($N = 3$ independent experiments, >1,100 synapses imaged per datapoint, Spearman's $\rho = 0.927$, $^{***}p < 0.001$). **(B)** Newly-emerged TNRs were labeled in a similar fashion to panel a (magenta), and the neuronal membranes were visualized by incubation with the lipophilic dye DiO (green). Shown are exemplary images of postsynapses with increasingly larger head sizes. The mean fluorescence intensities of TNR and the mean synapse area, normalized to the medians of each respective experiment, are plotted against each other. The values for the synapse area were divided into five bins containing equal numbers of synapses. Quantification of the correlation between the intensities demonstrates a strong link between the size of the dendritic spine and the amount of recycling TNR epitopes (N = independent experiments, >280 synapses imaged per datapoint, Spearman's $\rho = 0.862$, $^{***}p < 0.001$. Scale bars = 300 nm. The data shown in the plots represent the means (long horizontal lines) ± SEM (short horizontal lines), with individual dots indicating separate experiments. Adapted from Dankovich et al. (2021) with permission from Springer Nature (http://creativecommons.org/licenses/by/4.0/).

cell-surface receptors can undergo post-endocytic "internalized activation", i.e., trigger distinct signaling activation from within intracellular compartments (Wang et al., 2021). It is, therefore, possible to imagine that internalized ECM-bound receptors may trigger signaling cascades related to, for example, synaptic plasticity.

The findings discussed in this review demonstrate that the neural ECM, while composed of extremely stable components,

needs to remain far more freely modifiable than previously expected, due to the high rate of synapse changes in the living brain. The only solution proposed so far to this problem remains the possibility that the ECM molecules have an ability to be recycled. While this concept is novel in the context of synaptic plasticity, it has, in fact, already been reported in other cell types for the process of fibrillogenesis (Varadaraj et al., 2017). In the respective study, it was demonstrated that the ECM protein fibronectin could be internalized through the activity of integrin and TGF-β receptors, and then subsequently recycled re-integrated into extracellular fibrils. While this is the only demonstration, to our knowledge, of a complete recycling loop of an ECM molecule, many additional studies also add credence to the concept of ECM recycling at synapses. These include reports of ECM molecules that undergo internalization (e.g., Coopman et al., 1996; Tammi et al., 2001; Shi and Sottile, 2008; Lobert et al., 2010; Leonoudakis et al., 2014), demonstrations that ECM receptors are present at synapses (e.g., Kramár et al., 2002; Huang et al., 2006; Roszkowska et al., 2016; Izumi et al., 2017; Apóstolo et al., 2020; Briatore et al., 2020), and reports that synapses contain the machinery for trafficking recycling molecules in an activity-dependent manner (Tang, 2008; Gürth et al., 2020; Helm et al., 2021). Nevertheless, additional demonstrations of the recycling of ECM molecules in neurons are anticipated in the future. We expect such studies to rely on creative probes developed for studying molecular recycling *in vivo*, and on the current explosion in the development of high-resolution imaging methods, including tools that enable long-term imaging with limited phototoxicity (e.g., Bodén et al., 2021).

CONCLUSION

Recycling mechanisms at synapses are well-studied for presynaptic vesicle release, where such a process is crucial for maintaining continuous neurotransmission without the need for a constant supply of vesicles. In a similar fashion, ECM recycling may also serve to preserve energy at the synapse by allowing continuous remodeling without the need for *de novo* synthesis and secretion of ECM components. While the energy gain is clear in the case of synaptic vesicles, it is not entirely obvious whether this also holds true for ECM recycling. Conceivably, this process also serves additional functions, for example, in cellular signaling. Considering that it appears to be largely synaptic and tightly linked to local activity, it is possible to imagine that this mechanism is intimately involved in synaptic function. In agreement with this claim, it was shown that perturbing TNR recycling with large antibody aggregates interfered severely with synaptic vesicle release and resulted in structural changes to the postsynapse (Dankovich et al., 2021). We predict that such perturbations to ECM recycling would also have implications for synaptic plasticity, both at the structural and the molecular level, and may also manifest in brain disorders. Hopefully, future studies will shed light on these ideas and reveal additional molecular details on the involvement of ECM recycling in synaptic function.

AUTHOR CONTRIBUTIONS

The manuscript was conceived by TD and SR, written by TD and revised by SR. All authors contributed to the article and approved the submitted version.

FUNDING

This work was funded by a grant from the German Research Foundation (Deutsche Forschungsgemeinschaft) to SR, SFB1286/A03.

REFERENCES

Abraham, W. C., and Bear, M. F. (1996). Metaplasticity: the plasticity of synaptic plasticity. *Trends Neurosci.* 19, 126–130. doi: 10.1016/s0166-2236(96)80018-x

Apóstolo, N., Smukowski, S. N., Vanderlinden, J., Condomitti, G., Rybakin, V., ten Bos, J., et al. (2020). Synapse type-specific proteomic dissection identifies IgSF8 as a hippocampal CA3 microcircuit organizer. *Nat. Commun.* 11:5171. doi: 10.1038/s41467-020-18956-x

Araque, A., Parpura, V., Sanzgiri, R. P., and Haydon, P. G. (1999). Tripartite synapses: glia, the unacknowledged partner. *Trends Neurosci.* 22, 208–215. doi: 10.1016/s0166-2236(98)01349-6

Bal, M., Leitz, J., Reese, A. L., Ramirez, D. M. O., Durakoglugil, M., Herz, J., et al. (2013). Reelin mobilizes a VAMP7-dependent synaptic vesicle pool and selectively uagments spontaneous neurotransmission. *Neuron* 80, 934–946. doi: 10.1016/j.neuron.2013.08.024

Beffert, U., Weeber, E. J., Durudas, A., Qiu, S., Masiulis, I., Sweatt, J. D., et al. (2005). Modulation of synaptic plasticity and memory by Reelin involves differential splicing of the lipoprotein receptor Apoer2. *Neuron* 47, 567–579. doi: 10.1016/j.neuron.2005.07.007

Bernard-Trifilo, J. A., Kramár, E. A., Torp, R., Lin, C. Y., Pineda, E. A., Lynch, G., et al. (2005). Integrin signaling cascades are operational in adult hippocampal synapses and modulate NMDA receptor physiology. *J. Neurochem.* 93, 834–849. doi: 10.1111/j.1471-4159.2005.03062.x

Berning, S., Willig, K. I., Steffens, H., Dibaj, P., and Hell, S. W. (2012). Nanoscopy in a living mouse brain. *Science* 335:551. doi: 10.1126/science.1215369

Blosa, M., Sonntag, M., Jäger, C., Weigel, S., Seeger, J., Frischknecht, R., et al. (2015). The extracellular matrix molecule brevican is an integral component of the machinery mediating fast synaptic transmission at the calyx of held. *J. Physiol.* 593, 4341–4360. doi: 10.1113/JP270849

Bodén, A., Pennacchietti, F., Coceano, G., Damenti, M., Ratz, M., and Testa, I. (2021). Volumetric live cell imaging with three-dimensional parallelized RESOLFT microscopy. *Nat. Biotechnol.* 39, 609–618. doi: 10.1007/s10661-022-09820-0

Bonneh-Barkay, D., and Wiley, C. A. (2009). Brain extracellular matrix in neurodegeneration. *Brain Pathol.* 19, 573–585. doi: 10.1111/j.1750-3639.2008.00195.x

Borgdorff, A. J., and Choquet, D. (2002). Regulation of AMPA receptor lateral movements. *Nature* 417, 649–653. doi: 10.1038/nature00780

Bretscher, M. S. (1989). Endocytosis and recycling of the fibronectin receptor in CHO cells. *EMBO J.* 8, 1341–1348.

Briatore, F., Pregno, G., Di Angelantonio, S., Frola, E., De Stefano, M. E., Vaillend, C., et al. (2020). Dystroglycan mediates clustering of essential GABAergic components in cerebellar purkinje cells. *Front. Mol. Neurosci.* 13:164. doi: 10.3389/fnmol.2020.00164

Bridgewater, R. E., Norman, J. C., and Caswell, P. T. (2012). Integrin trafficking at a glance. *J. Cell Sci.* 125, 3695–3701. doi: 10.1242/jcs.095810

Bukalo, O., Schachner, M., and Dityatev, A. (2007). Hippocampal metaplasticity induced by deficiency in the extracellular matrix glycoprotein tenascin-R. *J. Neurosci.* 27, 6019–6028. doi: 10.1523/JNEUROSCI.1022-07.2007

Carlson, S. S., Valdez, G., and Sanes, J. R. (2010). Presynaptic calcium channels and α3-integrins are complexed with synaptic cleft laminins, cytoskeletal elements and active zone components. *J. Neurochem.* 115, 654–666. doi: 10.1111/j.1471-4159.2010.06965.x

Chan, C. S., Weeber, E. J., Zong, L., Fuchs, E., Sweatt, J. D., and Davis, R. L. (2006). β1-integrins are required for hippocampal AMPA receptor-dependent synaptic transmission, synaptic plasticity and working memory. *J. Neurosci.* 26, 223–232. doi: 10.1523/JNEUROSCI.4110-05.2006

Chang, W.-P., and Sudhof, T. C. (2009). SV2 renders primed synaptic vesicles competent for Ca2+-induced exocytosis. *J. Neurosci.* 29, 883–897. doi: 10.1523/JNEUROSCI.4521-08.2009

Cingolani, L. A., Thalhammer, A., Yu, L. M. Y., Catalano, M., Ramos, T., Colicos, M. A., et al. (2008). Activity-dependent regulation of synaptic AMPA receptor composition and abundance by β3 integrins. *Neuron* 58, 749–762. doi: 10.1016/j.neuron.2008.04.011

Coopman, P. J., Thomas, D. M., Gehlsen, K. R., and Mueller, S. C. (1996). Integrin alpha 3 beta 1 participates in the phagocytosis of extracellular matrix molecules by human breast cancer cells. *Mol. Biol. Cell* 7, 1789–1804. doi: 10.1091/mbc.7.11.1789

D'Arcangelo, G. (2014). Reelin in the years: controlling neuronal migration and maturation in the mammalian brain. *Adv. Neurosci.* 2014, 1–19. doi: 10.1155/2014/597395

Dankovich, T. M. (2021). *Recycling as a Mechanism for Extracellular Matrix Remodeling at the Synapse*. Doctoral thesis. Göttingen, Germany: Georg-August-Universität Göttingen.

Dankovich, T. M., Kaushik, R., Olsthoorn, L. H. M., Petersen, G. C., Giro, P. E., Kluever, V., et al. (2021). Extracellular matrix remodeling through endocytosis and resurfacing of Tenascin-R. *Nat. Commun.* 12:7129. doi: 10.1038/s41467-021-27462-7

de Vivo, L., Landi, S., Panniello, M., Baroncelli, L., Chierzi, S., Mariotti, L., et al. (2013). Extracellular matrix inhibits structural and functional plasticity of dendritic spines in the adult visual cortex. *Nat. Commun.* 4:1484. doi: 10.1038/ncomms2491

Dityatev, A., Frischknecht, R., and Seidenbecher, C. I. (2006). "Extracellular matrix and synaptic functions," in *Cell Communication in Nervous and Immune System* (Berlin Heidelberg: Springer), 69–97.

Dityatev, A., and Schachner, M. (2003). Extracellular matrix molecules and synaptic plasticity. *Nat. Rev. Neurosci.* 4, 456–468. doi: 10.1038/nrn1115

Dityatev, A., Schachner, M., and Sonderegger, P. (2010). The dual role of the extracellular matrix in synaptic plasticity and homeostasis. *Nat. Rev. Neurosci.* 11, 735–746. doi: 10.1038/nrn2898

Dörrbaum, A. R., Kochen, L., Langer, J. D., and Schuman, E. M. (2018). Local and global influences on protein turnover in neurons and glia. *eLife* 7:e34202. doi: 10.7554/eLife.34202

Dziembowska, M., Milek, J., Janusz, A., Rejmak, E., Romanowska, E., Gorkiewicz, T., et al. (2012). Activity-dependent local translation of matrix metalloproteinase-9. *J. Neurosci.* 32:14538. doi: 10.1523/JNEUROSCI.6028-11.2012

Evers, M. R., Salmen, B., Bukalo, O., Rollenhagen, A., Bösl, M. R., Morellini, F., et al. (2002). Impairment of L-type Ca^{2+} channel-dependent forms of hippocampal synaptic plasticity in mice deficient in the extracellular matrix glycoprotein tenascin-C. *J. Neurosci.* 22, 7177–7194. doi: 10.1523/JNEUROSCI.22-16-07177.2002

Ferrer-Ferrer, M., and Dityatev, A. (2018). Shaping synapses by the neural extracellular matrix. *Front. Neuroanat.* 12:40. doi: 10.3389/fnana.2018.00040

Fornasiero, E. F., Mandad, S., Wildhagen, H., Alevra, M., Rammner, B., Keihani, S., et al. (2018). Precisely measured protein lifetimes in the mouse brain reveal differences across tissues and subcellular fractions. *Nat. Commun.* 9:4230. doi: 10.1038/s41467-018-06519-0

Frischknecht, R., Heine, M., Perrais, D., Seidenbecher, C. I., Choquet, D., and Gundelfinger, E. D. (2009). Brain extracellular matrix affects AMPA receptor lateral mobility and short-term synaptic plasticity. *Nat. Neurosci.* 12, 897–904. doi: 10.1038/nn.2338

Gawlak, M., Górkiewicz, T., Gorlewicz, A., Konopacki, F. A., Kaczmarek, L., and Wilczynski, G. M. (2009). High resolution *in situ* zymography reveals matrix metalloproteinase activity at glutamatergic synapses. *Neuroscience* 158, 167–176. doi: 10.1016/j.neuroscience.2008.05.045

Gürth, C. M., Dankovich, T. M., Rizzoli, S. O., and D'Este, E. (2020). Synaptic activity and strength are reflected by changes in the post-synaptic secretory pathway. *Sci. Rep.* 10:20576. doi: 10.1038/s41598-020-77260-2

Helm, M. S., Dankovich, T. M., Mandad, S., Rammner, B., Jähne, S., Salimi, V., et al. (2021). A large-scale nanoscopy and biochemistry analysis of postsynaptic dendritic spines. *Nat. Neurosci.* 24, 1151–1162. doi: 10.1038/s41593-021-00874-w

Herring, B. E., and Nicoll, R. A. (2016). Long-term potentiation: from CaMKII to AMPA receptor trafficking. *Annu. Rev. Physiol.* 78, 351–365. doi: 10.1146/annurev-physiol-021014-071753

Hua, Z., Leal-Ortiz, S., Foss, S. M., Waites, C. L., Garner, C. C., Voglmaier, S. M., et al. (2011). v-SNARE composition distinguishes dynaptic vesicle pools. *Neuron* 71, 474–487. doi: 10.1016/j.neuron.2011.06.010

Huang, Z., Shimazu, K., Woo, N. H., Zang, K., Muller, U., Lu, B., et al. (2006). Distinct roles of the beta1-class integrins at the developing and the mature hippocampal excitatory synapse. *J. Neurosci.* 26, 11208–11219. doi: 10.1523/JNEUROSCI.3526-06.2006

Humeau, Y., and Choquet, D. (2019). The next generation of approaches to investigate the link between synaptic plasticity and learning. *Nat. Neurosci.* 22, 1536–1543. doi: 10.1038/s41593-019-0480-6

Hunter, D. D., Manglapus, M. K., Bachay, G., Claudepierre, T., Dolan, M. W., Gesuelli, K. A., et al. (2019). CNS synapses are stabilized trans-synaptically by laminins and laminin-interacting proteins. *J. Comp. Neurol.* 527, 67–86. doi: 10.1002/cne.24338

Izumi, Y., Wakita, S., Kanbara, C., Nakai, T., Akaike, A., and Kume, T. (2017). Integrin α5β1 expression on dopaminergic neurons is involved in dopaminergic neurite outgrowth on striatal neurons. *Sci. Rep.* 7:42111. doi: 10.1038/srep42111

John, N., Krügel, H., Frischknecht, R., Smalla, K. H., Schultz, C., Kreutz, M. R., et al. (2006). Brevican-containing perineuronal nets of extracellular matrix in dissociated hippocampal primary cultures. *Mol. Cell. Neurosci.* 31, 774–784. doi: 10.1016/j.mcn.2006.01.011

Kochlamazashvili, G., Henneberger, C., Bukalo, O., Dvoretskova, E., Senkov, O., Lievens, P. M. J., et al. (2010). The extracellular matrix molecule hyaluronic acid regulates hippocampal synaptic plasticity by modulating postsynaptic L-type Ca^{2+} channels. *Neuron* 67, 116–128. doi: 10.1016/j.neuron.2010.05.030

Koenig, J. A., and Edwardson, J. M. (1997). Endocytosis and recycling of G protein-coupled receptors. *Trends Pharmacol. Sci.* 18, 276–287. doi: 10.1016/s0165-6147(97)01091-2

Kramár, E. A., Bernard, J. A., Gall, C. M., and Lynch, G. (2002). Alpha3 integrin receptors contribute to the consolidation of long-term potentiation. *Neuroscience* 110, 29–39. doi: 10.1016/s0306-4522(01)00540-1

Kramar, E. A., Lin, B., Rex, C. S., Gall, C. M., and Lynch, G. (2006). Integrin-driven actin polymerization consolidates long-term potentiation. *Proc. Natl. Acad. Sci. U S A* 103, 5579–5584. doi: 10.1073/pnas.0601354103

Kraszewski, K., Daniell, L., Mundigl, O., and De Camilli, P. (1996). Mobility of synaptic vesicles in nerve endings monitored by recovery from photobleaching of synaptic vesicle-associated fluorescence. *J. Neurosci.* 16, 5905–5913. doi: 10.1523/JNEUROSCI.16-19-05905.1996

Kreisel, W., Hanski, C., Tran-Thi, T. A., Katz, N., Decker, K., Reutter, W., et al. (1988). Remodeling of a rat hepatocyte plasma membrane glycoprotein. De- and reglycosylation of dipeptidyl peptidase IV. *J. Biol. Chem.* 263, 11736–11742. doi: 10.1016/S0021-9258(18)37845-1

Kruse, J., Keilhauer, G., Faissner, A., Timpl, R., and Schachner, M. (1985). The J1 glycoprotein—a novel nervous system cell adhesion molecule of the L2/HNK-1 family. *Nature* 316, 146–148. doi: 10.1038/316146a0

Leonoudakis, D., Huang, G., Akhavan, A., Fata, J. E., Singh, M., Gray, J. W., et al. (2014). Endocytic trafficking of laminin is controlled by dystroglycan and disrupted in cancers. *J. Cell Sci.* 127, 4894–4903. doi: 10.1242/jcs.152728

Liao, H., Huang, W., Schachner, M., Guan, Y., Guo, J., Yan, J., et al. (2008). β 1 integrin-mediated effects of tenascin-R domains EGFL and FN6–8 on neural stem/progenitor cell proliferation and differentiation *in vitro*. *J. Biol. Chem.* 283, 27927–27936. doi: 10.1074/jbc.M804764200

Lobert, V. H., Brech, A., Pedersen, N. M., Wesche, J., Oppelt, A., Malerød, L., et al. (2010). Ubiquitination of α5β1 integrin controls fibroblast migration through lysosomal degradation of fibronectin-integrin complexes. *Dev. Cell* 19, 148–159. doi: 10.1016/j.devcel.2010.06.010

Magnowska, M., Gorkiewicz, T., Suska, A., Wawrzyniak, M., Rutkowska-Wlodarczyk, I., Kaczmarek, L., et al. (2016). Transient ECM protease activity promotes synaptic plasticity. *Sci. Rep.* 6:27757. doi: 10.1038/srep27757

Michaluk, P., Wawrzyniak, M., Alot, P., Szczot, M., Wyrembek, P., Mercik, K., et al. (2011). Influence of matrix metalloproteinase MMP-9 on dendritic spine morphology. *J. Cell Sci.* 124, 3369–3380. doi: 10.1242/jcs.090852

Mortillo, S., Elste, A., Ge, Y., Patil, S. B., Hsiao, K., Huntley, G. W., et al. (2012). Compensatory redistribution of neuroligins and N-cadherin following deletion of synaptic β1-integrin. *J. Comp. Neurol.* 520, 2041–2052. doi: 10.1002/cne.23027

Nagy, V., Bozdagi, O., Matynia, A., Balcerzyk, M., Okulski, P., Dzwonek, J., et al. (2006). Matrix metalloproteinase-9 is required for hippocampal late-phase long-term potentiation and memory. *J. Neurosci.* 26, 1923–1934. doi: 10.1523/JNEUROSCI.4359-05.2006

Nikonenko, A., Schmidt, S., Skibo, G., Brückner, G., and Schachner, M. (2003). Tenascin-R-deficient mice show structural alterations of symmetric perisomatic synapses in the CA1 region of the hippocampus. *J. Comp. Neurol.* 456, 338–349. doi: 10.1002/cne.10537

Nirwane, A., and Yao, Y. (2018). Laminins and their receptors in the CNS. *Biol. Rev. Camb. Philos. Soc.* 94, 283–306. doi: 10.1111/brv.12454.

Nishimune, H., Sanes, J. R., and Carlson, S. S. (2004). A synaptic laminin-calcium channel interaction organizes active zones in motor nerve terminals. *Nature* 432, 580–587. doi: 10.1038/nature03112

Okulski, P., Jay, T. M., Jaworski, J., Duniec, K., Dzwonek, J., Konopacki, F. A., et al. (2007). TIMP-1 abolishes MMP-9-dependent long-lasting long-term potentiation in the prefrontal cortex. *Biol. Psychiatry* 62, 359–362. doi: 10.1016/j.biopsych.2006.09.012

Omar, M. H., Campbell, M. K., Xiao, X., Zhong, Q., Brunken, W. J., Miner, J. H., et al. (2017). CNS neurons deposit laminin α5 to stabilize synapses. *Cell Rep.* 21, 1281–1292. doi: 10.1016/j.celrep.2017.10.028

Orlando, C., Ster, J., Gerber, U., Fawcett, J. W., and Raineteau, O. (2012). Perisynaptic chondroitin sulfate proteoglycans restrict structural plasticity in an integrin-dependent manner. *J. Neurosci.* 32, 18009–18017. doi: 10.1523/JNEUROSCI.2406-12.2012

Pantazopoulos, H., and Berretta, S. (2016). In sickness and in health: perineuronal nets and synaptic plasticity in psychiatric disorders. *Neural Plast.* 2016:9847696. doi: 10.1155/2016/9847696

Park, Y. K., and Goda, Y. (2016). Integrins in synapse regulation. *Nat. Rev. Neurosci.* 17, 745–756. doi: 10.1038/nrn.2016.138

Porwoll, S., Loch, N., Kannicht, C., Nuck, R., Grunow, D., Reutter, W., et al. (1998). Cell surface glycoproteins undergo postbiosynthetic modification of their N -Glycans by stepwise demannosylation. *J. Biol. Chem.* 273, 1075–1085. doi: 10.1074/jbc.273.2.1075

Qiu, S., Korwek, K. M., Pratt-Davis, A. R., Peters, M., Bergman, M. Y., and Weeber, E. J. (2006). Cognitive disruption and altered hippocampus synaptic function in Reelin haploinsufficient mice. *Neurobiol. Learn. Mem.* 85, 228–242. doi: 10.1016/j.nlm.2005.11.001

Rex, C. S., Chen, L. Y., Sharma, A., Liu, J., Babayan, A. H., Gall, C. M., et al. (2009). Different Rho GTPase-dependent signaling pathways initiate sequential steps in the consolidation of long-term potentiation. *J. Cell Biol.* 186, 85–97. doi: 10.1083/jcb.200901084

Rogers, J. T., Rusiana, I., Trotter, J., Zhao, L., Donaldson, E., Pak, D. T. S., et al. (2011). Reelin supplementation enhances cognitive ability, synaptic plasticity and dendritic spine density. *Learn. Mem.* 18, 558–564. doi: 10.1101/lm.2153511

Roszkowska, M., Skupien, A., Wójtowicz, T., Konopka, A., Gorlewicz, A., Kisiel, M., et al. (2016). CD44: A novel synaptic cell adhesion molecule regulating structural and functional plasticity of dendritic spines. *Mol. Biol. Cell* 27, 4055–4066. doi: 10.1091/mbc.E16-06-0423

Ruoslahti, E. (1996). Brain extracellular matrix. *Glycobiology* 6, 489–492. doi: 10.1093/glycob/6.5.489

Saghatelyan, A. K., Dityatev, A., Schmidt, S., Schuster, T., Bartsch, U., and Schachner, M. (2001). Reduced perisomatic inhibition, increased excitatory transmission and impaired long-term potentiation in mice deficient for the extracellular matrix glycoprotein tenascin-R. *Mol. Cell. Neurosci.* 17, 226–240. doi: 10.1006/mcne.2000.0922

Saghatelyan, A. K., Snapyan, M., Gorissen, S., Meigel, I., Mosbacher, J., Kaupmann, K., et al. (2003). Recognition molecule associated carbohydrate inhibits postsynaptic GABAB receptors: a mechanism for homeostatic regulation of GABA release in perisomatic synapses. *Mol. Cell. Neurosci.* 24, 271–282. doi: 10.1016/s1044-7431(03)00163-5

Saka, S. K., Honigmann, A., Eggeling, C., Hell, S. W., Lang, T., and Rizzoli, S. O. (2014). Multi-protein assemblies underlie the mesoscale organization of the plasma membrane. *Nat. Commun.* 5:4509. doi: 10.1038/ncomms5509

Scheiffele, P., Peränen, J., and Simons, K. (1995). N-glycans as apical sorting signals in epithelial cells. *Nature* 378, 96–98. doi: 10.1038/378096a0

Shi, Y., and Ethell, I. M. (2006). Integrins control dendritic spine plasticity in hippocampal neurons through NMDA receptor and Ca^{2+}/calmodulin-dependent protein kinase II-mediated actin reorganization. *J. Neurosci.* 26, 1813–1822. doi: 10.1523/JNEUROSCI.4091-05.2006

Shi, F., and Sottile, J. (2008). Caveolin-1-dependent β1 integrin endocytosis is a critical regulator of fibronectin turnover. *J. Cell Sci.* 121, 2360–2371. doi: 10.1242/jcs.014977

Sloan Warren, M., Bradley, W. D., Gourley, S. L., Lin, Y. C., Simpson, M. A., Reichardt, L. F., et al. (2012). Integrin β1 signals through Arg to regulate postnatal dendritic arborization, synapse density and behavior. *J. Neurosci.* 32, 2824–2834. doi: 10.1523/JNEUROSCI.3942-11.2012

Son, Y.-J., Scranton, T. W., Sunderland, W. J., Baek, S. J., Miner, J. H., Sanes, J. R., et al. (2000). The synaptic vesicle protein SV2 is complexed with an α5-containing laminin on the nerve terminal surface. *J. Biol. Chem.* 275, 451–460. doi: 10.1074/jbc.275.1.451

Sonntag, M., Blosa, M., Schmidt, S., Reimann, K., Blum, K., Eckrich, T., et al. (2018). Synaptic coupling of inner ear sensory cells is controlled by brevican-based extracellular matrix baskets resembling perineuronal nets. *BMC Biol.* 16:99. doi: 10.1186/s12915-018-0566-8

Sorg, B. A., Berretta, S., Blacktop, J. M., Fawcett, J. W., Kitagawa, H., Kwok, J. C. F., et al. (2016). Casting a wide net: role of perineuronal nets in neural plasticity. *J. Neurosci.* 36, 11459–11468. doi: 10.1523/JNEUROSCI.2351-16.2016

Tammi, R., Rilla, K., Pienimäki, J.-P., MacCallum, D. K., Hogg, M., Luukkonen, M., et al. (2001). Hyaluronan enters keratinocytes by a novel endocytic route for catabolism. *J. Biol. Chem.* 276, 35111–35122. doi: 10.1074/jbc.M103481200

Tan, C. L., Kwok, J. C. F., Patani, R., Ffrench-Constant, C., Chandran, S., and Fawcett, J. W. (2011). Integrin activation promotes axon growth on inhibitory chondroitin sulfate proteoglycans by enhancing integrin signaling. *J. Neurosci.* 31, 6289–6295. doi: 10.1523/JNEUROSCI.0008-11.2011

Tang, B. L. (2008). Emerging aspects of membrane traffic in neuronal dendrite growth. *Biochim. Biophys. Acta* 1783, 169–176. doi: 10.1016/j.bbamcr.2007.11.011

Testa, I., Urban, N. T., Jakobs, S., Eggeling, C., Willig, K. I., and Hell, S. W. (2012). Nanoscopy of living brain slices with low light levels. *Neuron* 75, 992–1000. doi: 10.1016/j.neuron.2012.07.028

Toyama, B. H., Savas, J. N., Park, S. K., Harris, M. S., Ingolia, N. T., Yates, J. R., et al. (2013). Identification of long-lived proteins reveals exceptional stability of essential cellular structures. *Cell* 154, 971–982. doi: 10.1016/j.cell.2013.07.037

Truckenbrodt, S., Viplav, A., Jähne, S., Vogts, A., Denker, A., Wildhagen, H., et al. (2018). Newly produced synaptic vesicle proteins are preferentially used in synaptic transmission. *EMBO J.* 37:e98044. doi: 10.15252/embj.201798044

Varadaraj, A., Jenkins, L. M., Singh, P., Chanda, A., Snider, J., Lee, N. Y., et al. (2017). TGF-β triggers rapid fibrillogenesis *via* a novel TβRII-dependent fibronectin-trafficking mechanism. *Mol. Biol. Cell* 28, 1195–1207. doi: 10.1091/mbc.E16-08-0601

Volz, B., Orberger, G., Porwoll, S., Hauri, H. P., and Tauber, R. (1995). Selective reentry of recycling cell surface glycoproteins to the biosynthetic

pathway in human hepatocarcinoma HepG2 cells. *J. Cell Biol.* 130, 537–551. doi: 10.1083/jcb.130.3.537

Wang, W., Bian, J., Sun, Y., and Li, Z. (2021). The new fate of internalized membrane receptors: internalized activation. *Pharmacol. Ther.* doi: 10.1016/j.pharmthera.2021.108018. [Online ahead of print].

Wang, X., Bozdagi, O., Nikitczuk, J. S., Zhai, Z. W., Zhou, Q., and Huntley, G. W. (2008). Extracellular proteolysis by matrix metalloproteinase-9 drives dendritic spine enlargement and long-term potentiation coordinately. *Proc. Natl. Acad. Sci. U S A* 105, 19520–19525. doi: 10.1073/pnas.0807248105

Weeber, E. J., Beffert, U., Jones, C., Christian, J. M., Förster, E., David Sweatt, J., et al. (2002). Reelin and apoE receptors cooperate to enhance hippocampal synaptic plasticity and learning. *J. Biol. Chem.* 277, 39944–39952. doi: 10.1074/jbc.M205147200

Wegner, W., Mott, A. C., Grant, S. G. N., Steffens, H., and Willig, K. I. (2018). *In vivo* STED microscopy visualizes PSD95 sub-structures and morphological changes over several hours in the mouse visual cortex. *Sci. Rep.* 8:219. doi: 10.1038/s41598-017-18640-z

Wilhelm, B. G., Groemer, T. W., and Rizzoli, S. O. (2010). The same synaptic vesicles drive active and spontaneous release. *Nat. Neurosci.* 13, 1454–1456. doi: 10.1038/nn.2690

Willig, K. I., Steffens, H., Gregor, C., Herholt, A., Rossner, M. J., and Hell, S. W. (2014). Nanoscopy of filamentous actin in cortical dendrites of a living mouse. *Biophys. J.* 106, L01–L03. doi: 10.1016/j.bpj.2013.11.1119

Conflict of Interest: The authors declare that the research was conducted in the absence of any commercial or financial relationships that could be construed as a potential conflict of interest.

Publisher's Note: All claims expressed in this article are solely those of the authors and do not necessarily represent those of their affiliated organizations, or those of the publisher, the editors and the reviewers. Any product that may be evaluated in this article, or claim that may be made by its manufacturer, is not guaranteed or endorsed by the publisher.

frontiers in Synaptic Neuroscience

REVIEW
published: 17 March 2022
doi: 10.3389/fnsyn.2022.829354

Organization of Presynaptic Autophagy-Related Processes

Eckart D. Gundelfinger[1,2,3†], Anna Karpova[1,3†], Rainer Pielot[2,3†], Craig C. Garner[4,5†] and Michael R. Kreutz[1,3,6,7†]*

[1] Research Group Neuroplasticity, Leibniz Institute for Neurobiology, Magdeburg, Germany, [2] Institute of Pharmacology and Toxicology, Medical Faculty, Otto von Guericke University, Magdeburg, Germany, [3] Center for Behavioral Brain Sciences (CBBS), Magdeburg, Germany, [4] German Center for Neurodegenerative Diseases (DZNE), Berlin, Germany, [5] Charité – Universitätsmedizin Berlin, Berlin, Germany, [6] Center for Molecular Neurobiology (ZMNH), University Hospital Hamburg-Eppendorf, Hamburg, Germany, [7] German Center for Neurodegenerative Diseases (DZNE), Magdeburg, Germany

Brain synapses pose special challenges on the quality control of their protein machineries as they are far away from the neuronal soma, display a high potential for plastic adaptation and have a high energy demand to fulfill their physiological tasks. This applies in particular to the presynaptic part where neurotransmitter is released from synaptic vesicles, which in turn have to be recycled and refilled in a complex membrane trafficking cycle. Pathways to remove outdated and damaged proteins include the ubiquitin-proteasome system acting in the cytoplasm as well as membrane-associated endolysosomal and the autophagy systems. Here we focus on the latter systems and review what is known about the spatial organization of autophagy and endolysosomal processes within the presynapse. We provide an inventory of which components of these degradative systems were found to be present in presynaptic boutons and where they might be anchored to the presynaptic apparatus. We identify three presynaptic structures reported to interact with known constituents of membrane-based protein-degradation pathways and therefore may serve as docking stations. These are (i) scaffolding proteins of the cytomatrix at the active zone, such as Bassoon or Clarinet, (ii) the endocytic machinery localized mainly at the peri-active zone, and (iii) synaptic vesicles. Finally, we sketch scenarios, how presynaptic autophagic cargos are tagged and recruited and which cellular mechanisms may govern membrane-associated protein turnover in the presynapse.

Keywords: autophagy, endolysosomal system, active zone (AZ), Bassoon, endocytic zone, synaptic vesicle (SV), amphisome, presynaptic proteostasis

OPEN ACCESS

Edited by:
Lucia Tabares, Seville University, Spain

Reviewed by:
Oleg Shupliakov, Karolinska Institutet, Sweden
Volker Haucke, Freie Universität Berlin, Germany

***Correspondence:**
Eckart D. Gundelfinger
egundelf@lin-magdeburg.de

†ORCID:
Eckart D. Gundelfinger
orcid.org/0000-0001-9377-7414
Anna Karpova
orcid.org/0000-0001-7423-4764
Rainer Pielot
orcid.org/0000-0002-9681-3318
Craig C. Garner
orcid.org/0000-0003-1970-5417
Michael R. Kreutz
orcid.org/0000-0003-0575-6950

Received: *05 December 2021*
Accepted: *04 January 2022*
Published: *17 March 2022*

Citation:
Gundelfinger ED, Karpova A, Pielot R, Garner CC and Kreutz MR (2022) Organization of Presynaptic Autophagy-Related Processes. Front. Synaptic Neurosci. 14:829354. doi: 10.3389/fnsyn.2022.829354

INTRODUCTION

Brain synapses can have long lifetimes (e.g., Holtmaat et al., 2005; Qiao et al., 2016) and display an enormous potential for plasticity (e.g., Citri and Malenka, 2008; Yang and Calakos, 2013). They also have a very high energy demand to maintain their functions (e.g., Harris et al., 2012), a situation that poses additional metabolic stress on synaptic protein components and requires an efficient

Abbreviations: AZ, active zone; BAR domain, Bin-Amphiphysin-Rvs domain; CMA, chaperone-mediated autophagy; NMJ, neuromuscular junction; PAS, pre-autophagosomal structure (also: phagophore assembly site); Peri-AZ, periactive zone, = main endocytic zone; SV, synaptic vesicle; SN, SuperNova; S/T, Serine/Threonine; UPS, Ubiquitin-Proteasome-System.

management of proteostasis. This applies in particular to the presynaptic compartment with its apparatus for regulated neurotransmitter release, which rapidly and efficiently recycles releasable neurotransmitter-filled synaptic vesicles (SVs). Biosynthesis of presynaptic components occurs predominantly in the neuronal soma, where they are packaged into specific precursor organelles and are actively transported along the axon to presynaptic sites (for a review see Rizalar et al., 2021). The lifespan of presynaptic proteins varies with half-lives ranging from a few hours to several days (Hakim et al., 2016; Fornasiero et al., 2018; Cohen and Ziv, 2019), which is very short compared to the lifespan of neurons and synapses. Hence, presynaptic proteins must be continuously replaced in a specific and highly coordinated manner.

Three main systems are in place to mediate this turnover, i.e., the ubiquitin-proteasome system (UPS) acting in the cytoplasm (Rinetti and Schweizer, 2010; Lazarevic et al., 2011; Waites et al., 2013; Cohen and Ziv, 2017; Soykan et al., 2021), and the endolysosomal pathway and autophagy-related processes acting via degradative membranous organelles (Azarnia Tehran et al., 2018; Jin et al., 2018; Boecker and Holzbaur, 2019; Kuijpers et al., 2020; Lieberman and Sulzer, 2020; Andres-Alonso et al., 2021; Soykan et al., 2021; **Figure 1A**). Various autophagic pathways exist in parallel. These comprise macroautophagy, which can act in bulk or selective modes (including ER-phagy, aggrephagy and mitophagy) as well as chaperone-mediated autophagy (CMA) and microautophagy (Stavoe and Holzbaur, 2019). In this review, we will focus mainly on presynaptic macroautophagy, but will also consider constituents of other pathways of membrane-associated protein turnover. Macroautophagy (from here on referred to as autophagy) starts with the formation of a phagophore at a phagophore assembly site (PAS) and the recruitment of membranes from various sources via ATG9-containing vesicles (**Figure 1B**; Dikic and Elazar, 2018). Recruitment of cargo into the autophagosome is mediated via specific receptors/adaptors that bind ATG8-like proteins, which are anchored to the phagophore membrane via conjugation to phosphatidylethanolamine (e.g., Deng et al., 2017; Dikic and Elazar, 2018; Gatica et al., 2018). One major way of determining cargoes for autophagy is the conjugation of poly-ubiquitin chains, but there are also selective modes of autophagy that function independently of ubiquitination (Khaminets et al., 2016). On the other hand, ubiquitination is also involved in the tagging of proteins for proteasomal and endolysosomal degradation. This is achieved via several hundreds of E3-ubiquitin ligases encoded by mammalian genomes and makes them important surveyors of the various pathways of proteostasis (Wang and Le, 2019). In this regard, we will also address the question of which E3 ligases may mediate aspects of presynaptic autophagy.

AUTOPHAGOSOME BIOGENESIS IN AXONS

In their axonal compartment, neurons entertain a steady process of basal autophagy (**Figure 1B**). Phagophore formation during basal autophagy is largely restricted to distal axons where autophagosomes are constitutively generated and then retrogradely transported toward the cell soma in a Dynein-dependent manner to fuse with lysosomes (Cheng et al., 2015; Maday and Holzbaur, 2016). Autophagy occurs at a basal level in all cells, but it can be up-regulated during stress, starvation, or infection. In neurons, however, conflicting reports have been published on whether neurons are sensitive (Boland et al., 2008; Nixon et al., 2008; Young et al., 2009; Alirezaei et al., 2010; Rubinsztein and Nixon, 2010; Hernandez et al., 2012; Catanese et al., 2018) or insensitive (Mizushima et al., 2004; Tsvetkov et al., 2010; Maday and Holzbaur, 2016; Kulkarni et al., 2020) to nutrient deprivation and/or mTOR inhibition. Likewise, the ordered recruitment of assembly factors for phagophore formation and maturation has been studied in much less detail for neuronal autophagy, but seems to be reminiscent of what has been found in non-neuronal cells (Maday and Holzbaur, 2014). The continuous formation of autophagosomes under steady-state conditions of neuronal signaling has led to the notion that autophagy is involved in homeostatic processes of proteostasis, particularly in axons. In fact, the primary membrane donor for the biogenesis of autophagosomes in distal axons is the endoplasmic reticulum (ER; Maday and Holzbaur, 2014). In very recent work, it was shown that the ER is also the main substrate for neuronal autophagy and that ER-phagy is important maintaining the integrity of axonal ER calcium stores and calcium release through ryanodine receptors (Kuijpers et al., 2021). In this contribution to the review series on 'Molecular Nanomachines of the Presynaptic Terminal', we will first examine which constituents of autophagic processes, as well as other interacting membrane-associated pathways of protein turnover, have been detected in presynaptic compartments to date, and how are they organized to fulfill their functions.

AUTOPHAGY-RELATED AND ENDOLYSOSOMAL PROTEINS IN THE PRESYNAPSE

To assess the presence of components of the autophagic and the endolysosomal protein degradation systems as well as major elements contributing to chaperone-mediated autophagy (CMA) in brain synapses, we assembled, based on the relevant literature, a list of proteins contributing to membrane-based degradation pathways. More than 90 proteins and protein complexes were identified (**Table 1**), which were inspected for their localization in synapses and, in particular, in presynaptic compartments by examining whether they are included in relevant databases, i.e., the SynProt database of synaptic proteins[1] (Pielot et al., 2012), and the synaptic gene ontology database SynGO, an expert-curated knowledge base of synaptic proteins[2] (Koopmans et al., 2019). In addition, we checked whether their presence in the presynapse has been reported otherwise. One important source was a study on the so-called hidden proteome of SVs

[1] www.synprot.de

[2] www.syngoportal.org

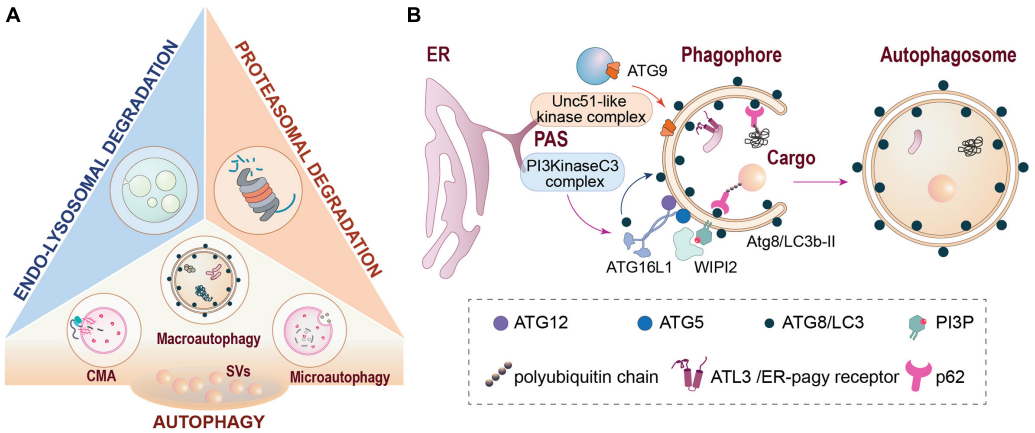

FIGURE 1 | Major pathways of cellular proteostasis. **(A)** Major degradative pathways at the presynapse include proteasomal degradation, endo-lysosomal degradation and different types of autophagy. **(B)** Schematic representation of autophagosome formation and cargo recruitment into autophagosomes via autophagy receptors such as p62/SQMTS1 or ATL3. CMA, chaperone-mediated autophagy; ER, endoplasmic reticulum; PAS, phagophore assembly site (also designated as pre-autophagosomal structure); SVs, synaptic vesicles.

that identified dozens of SV-resident and SV-visitor proteins of the autophagic and endolysosomal pathways (Taoufiq et al., 2020). About 50% of the proteins listed in **Table 1** are present in the SynProt databases, which include proteins identified in synaptic proteome studies (SynProt classics) and in studies on the proteomes of presynaptic compartments (PreProt). About one third of the proteins/protein complexes are found in SynGO, which provides a much higher and expert-evaluated resolution with respect to the compartmental localization of the identified proteins. In essence, we could assign many of the entries included in **Table 1** to the presynaptic compartment. A closer inspection of these proteins allowed us to draw conclusions on the major presynaptic structures involved in the anchoring for the autophagic machinery. These include the cytomatrix at the active zone (CAZ) of neurotransmitter release, represented by the CAZ scaffolding protein Bassoon, the endocytic machinery mainly localized peripherally to the active zone (AZ), the peri-AZ, and SVs (**Figure 2A**). Many of the identified proteins that are included in SynGO can be functionally assigned to presynaptic biological processes related to the SV cycle and SV endocytosis (**Figure 2B**).

BASSOON, A DOCKING STATION FOR PROTEIN TURNOVER PATHWAYS AT THE ACTIVE ZONE

The AZ of neurotransmitter release is characterized by a prominent electron-dense meshwork of proteins, the CAZ, that organizes the regulated fusion of SVs with the presynaptic cell membrane (Garner et al., 2000; Gundelfinger and Fejtova, 2012; Sudhof, 2012; Ackermann et al., 2015). Two related multidomain proteins, Bassoon and Piccolo, serve among others as major scaffolding proteins of the CAZ (Gundelfinger et al., 2016). Knock-down of these two proteins has severe effects on the maintenance and integrity of neuronal synapses, which is in part mediated by their interaction with the E3 ubiquitin ligase Siah1 (Waites et al., 2013). More recent studies have shown that while Piccolo has important functions in SV retrieval (Ackermann et al., 2019), Bassoon contributes important binding sites for components of the proteosomal and the autophagic proteostasis pathways. Thus, Bassoon binds, in addition to Siah1, also the proteasomal subunit PSMB4 (alias β7) and thereby controls proteasome assembly (Montenegro-Venegas et al., 2021) as well as the autophagy protein ATG5, part of an E3-like protein ligase, and thus negatively regulates presynaptic autophagy (Okerlund et al., 2017). As will be detailed below, knockout of Bassoon causes increased ubiquitination of various presynaptic proteins, including various SV proteins, and enhances presynaptic autophagy (Hoffmann-Conaway et al., 2020) as well as proteasome activity (Montenegro-Venegas et al., 2021). Interestingly, the E3 ubiquitin ligase Parkin, an enzyme that is also involved in mitophagy and has been implicated in early onset Parkinsonism (Kitada et al., 1998; Dikic and Elazar, 2018), seems to antagonize Bassoon in this function (Montenegro-Venegas et al., 2020). How exactly Parkin acts in this context is unclear, as to date no physical interaction between Parkin and Bassoon has been detected. Interestingly, Parkin ubiquitinates constituents of the endocytic systems in the presynapse, including Synaptojanin-1, Endophilin-A and Dynamin-1 (Cao et al., 2014; Soukup et al., 2018). This could set the framework for the search for relevant functional interactions between Bassoon and the endocytic machinery to control induction of autophagy in the presynapse.

Overall, the findings discussed above suggest that Bassoon is a negative regulator of presynaptic autophagy and the UPS in the presynapse, and as such may act as an anchoring and control point of these two protein turnover pathways. It should be noted, in this context, that Bassoon itself, in contrast to Piccolo, is subject to autophagic degradation upon nutrient limitation in primary neuronal cultures (Catanese et al., 2018). This suggests

TABLE 1 | Proteins related to autophagic and endolysosomal processes.

Protein	UniProt acc.# (name); alternative names	Present in SynProt[a]	Present in Hidden SV Proteome[b]	Present in SynGO[c]	Localization in Synapse[d]	Function/Remarks	Selected references
AMBRA1	A2AH22 (AMRA1_MOUSE); Activating molecule in BECN1-regulated autophagy protein 1	No	No	No	n.d.	Part of the autophagy nucleation complex	(Fimia et al., 2007; Dikic and Elazar, 2018; Tomoda et al., 2020)
Annexin A7	Q07076 (ANXA7_MOUSE), Annexin-7; Synexin	Yes	Yes SV-visitor	No	Synapse SV	Autophagy, promotes membrane fusion	(Taoufiq et al., 2020)
AP-2	P17426 (AP2A1_MOUSE), P17427 (AP2A2_MOUSE), Q9DBG3 (AP2B1_MOUSE), P84091 (AP2M1_MOUSE), P62743 (AP2S1_MOUSE); Adaptor protein AP-2 complex subunits mu, alpha-1, alpha-2, beta1 and sigma	Yes	Yes SV-resident	Yes	Synapse, Presynapse, Peri-AZ SV	Adaptor for Clathrin-mediated membrane fission. Together with CALM, AP-2 mediates formation of autophagosomes/signaling amphisomes; present in SV preparations.	(Boyken et al., 2013; Tian et al., 2014; Weingarten et al., 2014; Kononenko et al., 2017; Wang et al., 2017; Azarnia Tehran et al., 2018; Taoufiq et al., 2020)
Arf6	P62331 (ARF6_MOUSE); ADP-ribosylation factor 6;	Yes	Yes SV-visitor	Yes	Presynapse Postsynapse SV	Small GTPase antagonizes Rab35 in SV recycling; regulates autophagy by interplay with Synj1 and/or phospholipase D	(Moreau et al., 2012; George et al., 2016; Sheehan and Waites, 2019)
Arl8	Q9CQW2 (ARL8B_MOUSE); ADP-ribosylation factor-like protein 8B;	Yes (8A,B)	Yes (8A,B) SV-visitor	(Yes) BP only	Synapse, Presynapse SV, AZ	Present in synaptic vesicle (SV) and active zone (AZ) preparations; anterograde transport of lysosome-related vesicles	(Takamori et al., 2006; Boyken et al., 2013; Vukoja et al., 2018; Farfel-Becker et al., 2019; De Pace et al., 2020; Borchers et al., 2021)
ATG2a	Q6P4T0 (ATG2A_MOUSE); Autophagy-related protein 2 homolog A; ortholog: D3ZT64 (D3ZT64_RAT, formerly XP_219529)	Yes	(Yes) low abundance P2'-fraction	No	Synapse, Synaptosome Presynapse, SV	Present in SV protein preparation; Transfers phospholipids to the phagophore.	(Takamori et al., 2006) (Soukup et al., 2016; Sawa-Makarska et al., 2020; Chang et al., 2021)
ATG3	Q9CPX6 (ATG3_MOUSE); Autophagy-related protein 3. Ubiquitin-like-conjugating enzyme ATG3; Short name: APG3-like	No	P2'-fraction	No	Synapse	E2-like enzyme of the ubiquitin-like conjugation system; ATG3 can be recruited to membranes by EndoA	(Soukup et al., 2016; Vijayan and Verstreken, 2017; Dikic and Elazar, 2018; Hill and Colon-Ramos, 2020)
ATG4 family	Q9U1N6 (ATG42_CAEEL); Q8C9S8 (ATG4A_MOUSE) etc.; Cysteine proteases ATG4A-D	No	No	No	n.d.	Cysteine proteases of the ubiquitin-like conjugation system; *C. elegans*: A TG-4.2 involved in autophagosome clearance	(Dikic and Elazar, 2018; Hill et al., 2019; Hill and Colon-Ramos, 2020)
ATG5	Q99J83 (ATG5_MOUSE), Autophagy protein 5; APG5-like	No	No	No	Synapse, Presynapse	Part of the ATG12-ATG5-ATG16L1 E3-like complex of the Ubiquitin-like conjugation system; binds AZ protein Bassoon; colocalizes with presynaptic markers in primary neurons; ATG5-KO in neurons induces axonal ER-phagy.	(Vijayan and Verstreken, 2017; Dikic and Elazar, 2018; Tomoda et al., 2020; Andres-Alonso et al., 2021; Chang et al., 2021) (Okerlund et al., 2017; Kuijpers et al., 2021; Soykan et al., 2021)
ATG7	Q9D906 (ATG7_MOUSE); Ubiquitin-like modifier-activating enzyme ATG7; Autophagy-related protein 7; APG7-like	No	P2'-fraction	No	Synapse Synaptosome	E1-like enzyme of the Ubiquitin-like conjugation system; ATG7 deficiency has severe effects on presynaptic function.	(Komatsu et al., 2007; Vijayan and Verstreken, 2017; Dikic and Elazar, 2018; Lieberman and Sulzer, 2020; Overhoff et al., 2021)
ATG9A	Q68FE2 (ATG9A_MOUSE); Autophagy-related protein 9A; APG9-like 1;	Yes	Yes SV-resident	Yes	Synapse, Presynapse; SV, AZ, Peri-AZ	Lipid scramblase involved in autophagosome biogenesis; present in SV preparations (SV-resident repertoire); likely to be involved in SV autophagy.	(Boyken et al., 2013; Stavoe et al., 2016; Guardia et al., 2020; Hill and Colon-Ramos, 2020; Maeda et al., 2020; Sawa-Makarska et al., 2020; Chang et al., 2021)
ATG10	Q8R1P4 (ATG10_MOUSE); Ubiquitin-like-conjugating enzyme ATG10; Autophagy-related protein 10	No	No	No	n.d.	E2-like enzyme of the ubiquitin-like conjugation system; conjugates ATG12 on ATG5.	(Dikic and Elazar, 2018; Stavoe and Holzbaur, 2019)
ATG12	Q9CQY1 (ATG12_MOUSE); Ubiquitin-like protein ATG12; Autophagy-related protein 12; APG12-like	No	No	No	n.d.	Part of the ATG12-ATG5-ATG16L1 E3-like complex of the Ubiquitin-like conjugation system;	(Vijayan and Verstreken, 2017; Dikic and Elazar, 2018; Chang et al., 2021)
ATG13	Q91YI1 (ATG13_MOUSE); Autophagy-related protein 13	No	No	No	n.d.	Adaptor protein within the ULK/ATG1 complex	(Dikic and Elazar, 2018; Hill and Colon-Ramos, 2020; Tomoda et al., 2020)

(Continued)

TABLE 1 | (Continued)

Protein	UniProt acc.# (name); alternative names	Present in SynProt[a]	Present in Hidden SV Proteome[b]	Present in SynGO[c]	Localization in Synapse[d]	Function/Remarks	Selected references
ATG14/ATG14L	Q8CDJ3 (BAKOR_MOUSE) Beclin 1-associated autophagy-related key regulator; Autophagy-related protein 14-like protein	No	No	No	n.d.	Part of the PIK3C3 complex; and promotes autophagosome-endolysosome fusion.	(Diao et al., 2015; Dikic and Elazar, 2018; Hill and Colon-Ramos, 2019)
ATG16L1	Q8C0J2 (A16L1_MOUSE); Autophagy-related protein 16-1; APG16-like 1	Yes	Yes SV-visitor	No	Synapse; Presynapse, SV	Part of the ATG12-ATG5-ATG16L1 E3-like complex of Ub-like conjugation system; may be linked to SV autophagy.	(Binotti et al., 2015; Dikic and Elazar, 2018; Hill and Colon-Ramos, 2020; Chang et al., 2021)
ATG101	Q9D8Z6 (ATGA1_MOUSE); Q9VWQ1 (Q9VWQ1_DROME); Autophagy-related protein 101	No	P2'-fraction	No	Synapse Synaptosome	Part of the ULK/ATG1 complex	(Dikic and Elazar, 2018; Chang et al., 2021)
ATL2/3	Q6PA06 (ATLA2_MOUSE); Atlastin-2; ADP-ribosylation factor-like protein 6-interacting protein 2; Q91YH5 (ATLA3_MOUSE); Atlastin-3	Yes (ATL2)	Yes ATL2: SV-visitor ATL3: SV-visitor	No	Synapse, Presynapse SV	Recruitment and stabilization of ATG1 complex at the FIP200-ATG13–specified autophagosome formation sites on ER. Adaptor for ER-phagy; required for presynaptic function at larval NMJ.	(De Gregorio et al., 2017; Andres-Alonso et al., 2021; Liu et al., 2021; Wojnacki et al., 2021)
BAG3	Q9JLV1 (BAG3_MOUSE); BAG family molecular chaperone regulator 3; Bcl-2-associated athanogene 3	Yes	P2'-fraction	No	Synapse Synaptosome	Co-chaperonin for HSC70, interacts with synaptopodin	(Sturner and Behl, 2017; Ji et al., 2019)
Bassoon	O88737 (BSN_MOUSE); AZ scaffold protein Bassoon.	Yes	Yes SV-visitor	Yes	Presynapse, AZ, SV	Recruits ATG5 to the presynaptic AZ; functionally interacts with Parkin.	(Okerlund et al., 2017; Vijayan and Verstreken, 2017; Hill and Colon-Ramos, 2020; Hoffmann-Conaway et al., 2020; Andres-Alonso et al., 2021)
Beclin-1/ATG6	O88597 (BECN1_MOUSE), Beclin-1	No	Yes SV-visitor	No	Presynape SV	Core subunit of the PI3KinaseC3 complex; regulates Vps34 lipid kinase;	(Dikic and Elazar, 2018)
CALM/PICALM	Q7M6Y3 (PICAL_MOUSE); Phosphatidylinositol-binding Clathrin assembly protein; Clathrin assembly lymphoid myeloid leukemia	Yes	Yes SV-visitor	Yes	Presynapse; Peri-AZ, SV	Autophagic sorting adaptor; endocytic adaptor;	(Takamori et al., 2006; Tian et al., 2013; Azarnia Tehran et al., 2018)
CISD2	Q9CQB5 (CISD2_MOUSE); CDGSH iron-sulfur domain-containing protein 2; Miner 1; NAF-1	No	Yes SV-visitor	No	Presynapse SV	Regulator of autophagy; contributes to control of Beclin-1.	(Chang et al., 2010; Shen et al., 2021)
DFCP1/Zfyve1	Q810J8 (ZFYV1_MOUSE); Zinc finger FYVE domain-containing protein 1	No	Yes SV-visitor	No	Presynapse SV	PI3P- binding protein; enriched in omegasomes of the ER	(Dikic and Elazar, 2018; Hill and Colon-Ramos, 2020)
DENND3	A2RT67 (DEND3_MOUSE); DENN domain-containing protein 3	No	No	No	n.d.	Actin-binding guanine nucleotide exchange factor for Rab12 activated by ULK1 and required for autophagy	(Xu et al., 2015, 2018; Wojnacki and Galli, 2018; Wei and Duan, 2019)
Endophilin-A/EndoA	Q62420 (SH3G2_MOUSE); Endophilin A1, A2; Q8T390 (SH3G3_DROME); Endophilin-A; SH3 domain-containing GRB2-like protein;	Yes	Yes SV-visitor	Yes	Presynapse; SV Peri-AZ	Endocytic adaptor essential for SV recycling; forms docking stations for autophagic proteins at synapses.	(Murdoch et al., 2016; Soukup et al., 2016, 2018; Vijayan and Verstreken, 2017; Azarnia Tehran et al., 2018)
Endophilin-B1	Q9JK48 (SHLB1_MOUSE); SH3 domain-containing GRB2-like protein B1; BIF-1	No	Yes SV-visitor	No	Presynapse, SV,	Associates with PI3KC3-C2 and regulates ATG9a trafficking	(Takahashi et al., 2011; Taoufiq et al., 2020)
FADD	Q61160 (FADD_MOUSE); FAS-associated death domain protein	No	No	No	n.d.	Death domain protein that directly interacts with ATG5,	(Pyo et al., 2005)
FAM134B	Q8VE91 (RETR1_MOUSE); Reticulophagy regulator 1; family with sequence similarity 134 member B;	No	No	No	n.d.	Adaptor for ER-phagy	(Khaminets et al., 2015; Stavoe and Holzbaur, 2019; Andres-Alonso et al., 2021)
FIP200/Rb1cc1	Q9ESK9 (RBCC1_MOUSE); RB1-inducible coiled-coil protein 1; FAK family kinase-interacting protein of 200 kDa	Yes	P2'-fraction	No	Synapse, Synaptosome	Part of the ULK/ATG1 complex	(Dikic and Elazar, 2018; Lieberman and Sulzer, 2020; Tomoda et al., 2020)
FBXO32	Q9CPU7 (FBX32_MOUSE); F-box only protein 32; Atrogin-1	No	No	No	n.d.	E3-ubiquitin ligase; interacts with endophilin-A to control autophagosome formation and protein homeostasis.	(Murdoch et al., 2016; Azarnia Tehran et al., 2018)

(Continued)

TABLE 1 | (Continued)

Protein	UniProt acc.# (name); alternative names	Present in SynProt[a]	Present in Hidden SV Proteome[b]	Present in SynGO[c]	Localization in Synapse[d]	Function/Remarks	Selected references
GABARAPs/ ATG8-like	Q9DCD6 (GBRAP_MOUSE); GABA receptor associated protein; Q8R3R8 (GBRL1_MOUSE); P60521 (GBRL2_MOUSE); GABARP-like 1, 2; LGG-1 and LGG-2 in *C. elegans*	Yes GABARAPL1 GABARAPL2	GABARAP, GABARAPL1, GABARAPL2 P2'-fraction	No	Synapse, Synaptosome Presynapse	Lipidated ATG8-like proteins that are key factors for various autophagic processes. In *C. elegans* localized in presynapse	(Dikic and Elazar, 2018; Hill et al., 2019; Martens and Fracchiolla, 2020)
HSC70	P63017 (HSP7C_MOUSE); Heat shock cognate 71 kDa protein; Heat shock 70 kDa protein 8 (Hspa8)	Yes	Yes SV-visitor	Yes	Synapse, Presynapse	Cytosolic protein guiding KEFRQ-proteins to chaperone-mediated autophagy (CMA)	(Uytterhoeven et al., 2015; Kaushik and Cuervo, 2018; Andres-Alonso et al., 2021)
HOPS complex	Q91W86 (VPS11_MOUSE)	Yes	Yes SV-visitor	Yes	Presynapse, AZ	Homotypic fusion and vacuole protein sorting complex; involved in the fusion events of late endosomes and lysosomes.	(Jiang et al., 2014; Dikic and Elazar, 2018; van der Beek et al., 2019)
Vps11	Q920Q4 (VPS16_MOUSE)	Yes	Yes SV-visitor	Yes	Presynapse		
Vps16/Vps33A	Q9D2N9 (VP33A_MOUSE)	Yes	Yes SV-visitor	No	Presynapse		
Vps18	Q8R307 (VPS18_MOUSE)	Yes	Yes SV-visitor	Yes	Presynapse		
Vps39	Q8R5L3 (VPS39_MOUSE)	Yes	P2'-fraction	No	Synaptosome		
Vps41	Q5KU39 (VPS41_MOUSE); VAM2	Yes	P2'-fraction	No	Synaptosome		
Huntingtin/Htt	P42859 (HD_MOUSE), Huntington disease protein homolog;	Yes	Yes SV-visitor	Yes	Synapse, Presynapse; SV	Scaffolding adaptor recruited to autophagosomes	(Deng et al., 2017; Stavoe and Holzbaur, 2018; Cason et al., 2021)
JIP1	Q9WVI9 (JIP1_MOUSE); c-Jun-amino-terminal kinase-interacting protein 1; JNK-interacting protein 1; Islet brain 1 [IB-1]	Yes	No	No	Synapse (Axon)	Motor adaptor for autophagosome	(Saudou and Humbert, 2016; Stavoe and Holzbaur, 2018; Hill and Colon-Ramos, 2020; Cason et al., 2021)
JIP3	Q9ESN9 (JIP3_MOUSE); C-Jun-amino-terminal kinase-interacting protein 3; Unc-16; Mapk8ip3	Yes	P2'-fraction	No	Synapse Synaptosome (Axon)	Motor adaptor for autophagosome	(Hill et al., 2019; Hill and Colon-Ramos, 2020; Cason et al., 2021)
LAMP1,	P11438 (LAMP1_MOUSE); Lysosome-associated membrane glycoprotein 1; CD107 antigen-like family member A	Yes	Yes SV-visitor	Yes	Presynapse, SV	Marker for degradative autophagy-lysosomal organelles	(De Leo et al., 2016; Vukoja et al., 2018; Hill and Colon-Ramos, 2020) but see also (Cheng et al., 2015)
LAMP2(A)	P17047 (LAMP2_MOUSE); Lysosome-associated membrane glycoprotein 2; CD107 antigen-like family member B	No	Yes SV-visitor	No	Presynapse, SV	LAMP2A is chiefly involved in CMA	(Wang et al., 2017; Issa et al., 2018; Kaushik and Cuervo, 2018)
LC3/ATG8	Q9CQV6 (MLP3B_MOUSE); Autophagy-related ubiquitin-like modifier LC3 B; Microtubule-associated proteins 1A/1B light chain 3B; Map1lc3b.	Yes	Yes SV-visitor	Yes	Synapse, Presynapse	Lipidated ATG8-like proteins that are key factors for various autophagic processes; LGG in *C. elegans*;	(Dikic and Elazar, 2018; Hill and Colon-Ramos, 2020; Martens and Fracchiolla, 2020)
LRRK1	Q3UHC2 (LRRK1_MOUSE); Leucine-rich repeat serine/threonine-protein kinase 1	No	No	No	–	Regulates autophagy via TBC1D2-dependent Rab7 inactivation	(Toyofuku et al., 2015)
LRRK2	Q5S006 (LRRK2_MOUSE); Leucine-rich repeat serine/threonine-protein kinase 2; Dardarin	Yes	No	Yes	Synapse, Presynapse	LRRK2 acts on key actors of the SV cycle; among them endophilin A, a main anchor for autophagic proteins	(Soukup et al., 2016, 2018; Azarnia Tehran et al., 2018; Taylor and Alessi, 2020; Piccoli and Volta, 2021)
mTOR	Q9JLN9 (MTOR_MOUSE); Serine/threonine-protein kinase mTOR; mechanistic target of rapamycin;	Yes	Yes SV-visitor	Yes	Synapse, Postsynapse SV fraction	Regulates various cellular processes including autophagy	(Bockaert and Marin, 2015)

(Continued)

TABLE 1 | (Continued)

Protein	UniProt acc.# (name); alternative names	Present in SynProt[a]	Present in Hidden SV Proteome[b]	Present in SynGO[c]	Localization in Synapse[d]	Function/Remarks	Selected references
MYCBP2	Q7TPH6 (MYCB2_MOUSE); E3 ubiquitin-protein ligase MYCBP2; Pam/highwire/rpm-1 protein	Yes	Yes SV-visitor	No	Presynapse SV fraction	E3 ligase upstream of ULK1/Unc51	(Grill et al., 2016; Crawley et al., 2019)
NBR1	P97432 (NBR1_MOUSE); Next to BRCA1 gene 1 protein	No	No	No	–	Autophagy receptor	(Kirkin et al., 2009; Deng et al., 2017; Dikic and Elazar, 2018)
NDP52	A2A6M5 (CACO2_MOUSE); Calcium-binding and coiled-coil domain-containing protein 2; Nuclear domain 10 protein 52	No	No	No	–	Autophagy receptor	(Deng et al., 2017; Dikic and Elazar, 2018; Chang et al., 2021)
NRBF2	Q8VCQ3 (NRBF2_MOUSE) Nuclear receptor-binding factor 2	No	No	No	–	Assembles with PI3KC3, Autophagosome maturation, Rab7 effector	(Cai et al., 2021)
OPTN	Q8K3K8 (OPTN_MOUSE) Optineurin	No	No	No	–	Autophagy receptor	(Deng et al., 2017; Dikic and Elazar, 2018; Chang et al., 2021)
OCRL	Q6NVF0 (OCRL_MOUSE) Inositol polyphosphate 5-phosphatase OCRL	No	Yes SV-visitor	No	Presynapse SV fraction	Lipid phosphatase, controls autophagosome-lysosome fusion	(De Leo et al., 2016; Marat and Haucke, 2016; Palamiuc et al., 2020)
Parkin	Q9WVS6 (PRKN_MOUSE); E3 ubiquitin-protein ligase parkin	Yes	No	Yes	Synapse, Presynapse, SV	E3 ubiquitin-protein ligase involved in mitophagy and together with Bassoon controls SV protein degradation.	(Mouatt-Prigent et al., 2004; Dikic and Elazar, 2018; Soukup et al., 2018; Hoffmann-Conaway et al., 2020)
p62/SQSTM1	Q64337 (SQSTM_MOUSE) Sequestosome-1, Ubiquitin-binding protein p62	No	P2'-fraction	No	Synapse, Synaptosome Presynapse	Autophagy receptor Presynaptic localization in primary neurons.	(Deng et al., 2017; Dikic and Elazar, 2018; Soukup et al., 2018) (Okerlund et al., 2017)
p115/Uso1	Q9Z1Z0 (USO1_MOUSE), General vesicular transport factor p115; Protein USO1 homolog; Transcytosis-associated protein	Yes	P2'-fraction	No	Synapse, Synaptosome	Associates with PI3KC3complex I	(Dikic and Elazar, 2018)
PHLPP1	Q8CHE4 (PHLP1_MOUSE), Pleckstrin homology domain leucine-rich repeat-containing protein phosphatase 1; PH domain-containing family E member 1	No	No	No	n.d.	Phosphatase in CMA; dephosphorylates e.g., AKT1	(Arias et al., 2015; Kaushik and Cuervo, 2018)
PLEKHG5	Q66T02 (PKHG5_MOUSE) Pleckstrin homology domain-containing family G member 5; Synectin-binding RhoA exchange factor; Tech	Yes	No	(Yes) only BP	Presynapse	Regulates autophagy of SV; Guanine exchange factor (GEF) that regulates the activity of Rab26.	(Lüningschrör et al., 2017; Hill and Colon-Ramos, 2020; Andres-Alonso et al., 2021)
PLEKHM1	Q7TSI1 (PKHM1_MOUSE); Pleckstrin homology domain-containing family M member 1	No	No	No	n.d.	Rab7 and Arl8 effector; recruits HOPS complex to autophagosome	(Hill and Colon-Ramos, 2020; Andres-Alonso et al., 2021; Borchers et al., 2021)
Rab7	P51150 (RAB7A_MOUSE), Ras-related protein Rab-7a	Yes	Yes SV-Visitor	Yes	Presynapse, SV	Small GTPase with key role for the maturation of late endosomes and autophagosomes	(Hyttinen et al., 2013; Weingarten et al., 2014; Hill and Colon-Ramos, 2020; Borchers et al., 2021; Xing et al., 2021)
Rab11a	P62492 (RB11A_MOUSE); Ras-related protein Rab-11A	No	Yes SV-visitor	Yes	Postsynapse Presynapse SV	Rab of recycling endosomes (RE); involved in phagophore formation from RE	(Binotti et al., 2016; Puri et al., 2018; Wei and Duan, 2019)

(Continued)

TABLE 1 | (Continued)

Protein	UniProt acc.# (name); alternative names	Present in SynProt[a]	Present in Hidden SV Proteome[b]	Present in SynGO[c]	Localization in Synapse[d]	Function/Remarks	Selected references
Rab12	P35283 (RAB12_MOUSE); Ras-related protein Rab-12	No	Yes SV-visitor	No	Presynapse, SV	Rab involved in autophagy initiation; LRRK2 substrate	(Takamori et al., 2006; Matsui and Fukuda, 2013; Wei and Duan, 2019; Taoufiq et al., 2020)
Rab24	P35290 (RAB24_MOUSE); Ras-related protein Rab-24; Rab-16;	Yes	Yes SV-visitor	No	Synapse Presynapse SV	Facilitates clearance of autophagic compartments;	(Yla-Anttila et al., 2015; Wei and Duan, 2019)
Rab26	Q504M8 (RAB26_MOUSE); Ras-related protein Rab26	Yes	Yes SV-resident	Yes	Synapse Presynapse, SV	Links SV to autophagy pathway; in complex with Plekhg5;	(Binotti et al., 2015; Lüningschrör et al., 2017; Wang et al., 2017; Andres-Alonso et al., 2021; Kohrs et al., 2021)
Rab35	Q6PHN9 (RAB35_MOUSE); Ras-related protein Rab-35	Yes	Yes SV-visitor	Yes	Synapse, Presynapse, SV	Small GTPase controlling SV turnover; acts via NDP52	(Sheehan et al., 2016; Minowa-Nozawa et al., 2017; Soukup et al., 2018; Wei and Duan, 2019)
Rab37	Q9JKM7 (RAB37_MOUSE); Ras-related protein Rab-37	Yes	Yes SV-visitor	No	Synapse Presynapse SV	Interacts with ATG5 and regulates ATG5-12-16 complex assembly	(Sheng et al., 2018; Wei and Duan, 2019)
Rab39a	Q8BHD0 (RB39A_MOUSE); Ras-related protein Rab-39A	Yes	Yes SV-visitor	No	Presynapse SV	Interacts with PIK3C3 and negatively regulates autophagosome formation;	(Behrends et al., 2010; Boyken et al., 2013; Seto et al., 2013)
RHEB	Q921J2 (RHEB_MOUSE); GTP-binding protein Rheb; Ras homolog enriched in brain	Yes	Yes SV-visitor	Yes	Postsynapse Preynapse SV	Small GTPase in mTORC1 signaling pathway	(Bockaert and Marin, 2015)
RTN3	Q9ES97 (RTN3_MOUSE); Reticulon-3;	Yes	Yes SV-visitor	Yes	Presynapse SV	ER protein involved in ER-phagy	(Weingarten et al., 2014; Grumati et al., 2018; Beese et al., 2019; Stavoe and Holzbaur, 2019; Kuijpers et al., 2021; Wojnacki et al., 2021)
RUSC2	Q80U22 (RUSC2_MOUSE); RUN and SH3 domain-containing protein 2; Iporin	No	No	No	n.d.	Regulates association of ATG9a with kinesin motor	(Guardia et al., 2021)
SIPA1L2	Q80TE4 (SI1L2_MOUSE); Signal-induced proliferation-associated 1-like protein 2; SPAR2	Yes	P2'-fraction	No	Synaptosome Presynapse	Rap-GTPase activating protein (RapGAP); component of signaling amphisome; co-traffics with Snapin; colocalized with synaptophysin in presynapses.	(Andres-Alonso et al., 2019, 2021)
SNAP29	Q9ERB0 (SNP29_MOUSE); Synaptosomal-associated protein 29,	Yes	Yes SV-resident	Yes	Presynapse, SV	Autophagosome fusion with endolysosome	(Itakura et al., 2012; Diao et al., 2015; Andres-Alonso et al., 2021)
Snapin	Q9Z266 (SNAPN_MOUSE); SNARE-associated protein Snapin; Biogenesis of lysosome-related organelles complex 1 subunit 7; BLOC-1S7.	Yes	P2'-fraction	Yes	Synaptosome Presynapse	Motor adaptor that coordinates retrograde transport and late endosomal-lysosomal trafficking	(Cai et al., 2010; Kuijpers et al., 2020; Andres-Alonso et al., 2021)

(Continued)

TABLE 1 | (Continued)

Protein	UniProt acc.# (name); alternative names	Present in SynProt[a]	Present in Hidden SV Proteome[b]	Present in SynGO[c]	Localization in Synapse[d]	Function/Remarks	Selected references
SNX4	Q91YJ2 (SNX4_MOUSE); Sorting nexin-4; ATG24	Yes	(Yes) P2'-fraction	Yes	Synaptosome Presynaptic endosome SV	Phosphatidylinositol 3-phosphate-binding protein that controls ATG9A recycling and autophagy	(Ravussin et al., 2021)
Synaptojanins	Q8CHC4 (SYNJ1_MOUSE); Q9D2G5 (SYNJ2_MOUSE); Synaptojanin-1, -2; Synaptic inositol 1,4,5-trisphosphate 5-phosphatase 1, 2.	Yes (both isoforms)	Yes (Synj1) SV-visitor	Yes (both isoforms)	Presynapse SV fraction	Lipid phosphatase that is essential for maturation of autophagosmes in presynaptic boutons	(Vanhauwaert et al., 2017; Azarnia Tehran et al., 2018; Soukup et al., 2018)
Synaptopodin	Q8CC35 (SYNPO_MOUSE);	Yes	Yes SV-visitor	Yes	Postsynapse Presynapse? SV	In cooperation with BAG3 affects fusion between autophagosomes and lysosomes.	(Ji et al., 2019; Taoufiq et al., 2020)
Stx17	Q9D0I4 (STX17_MOUSE); Syntaxin-17;	No	Yes SV-visitor	No	SV fraction	Autophagosome fusion with endolysosome	(Itakura et al., 2012; Jiang et al., 2014; Diao et al., 2015; Andres-Alonso et al., 2021)
Tax1bp1	Q3UKC1 (TAXB1_MOUSE); Tax1-binding protein 1 homolog	No	P2'-fraction	No	Synaptosome	Autophagy receptor; Ubiquitin-binding protein that mediates autophagosome induction	(Whang et al., 2017; Chang et al., 2021)
TBC1D24/ Skywalker	Q3UUG6 (TBC24_MOUSE); TBC1 domain family member 24; Q9VIH7 (SKY_DROME); GTPase-activating protein skywalker	Yes	P2'-fraction	Yes	Synapse Presynapse	GTPase activating protein controlling SV turnover; acts on Rab35; regulates autophagy via TRAPP complex and ATG9	(Fernandes et al., 2014; Lamb et al., 2016; Soukup et al., 2018; Soykan et al., 2021)
TBC1D2	B1AVH7 (TBD2A_MOUSE); TBC1 domain family member 2A; Armus	No	No	(Yes) only BP	Synapse	GTPase-activating protein for RAB7A	(Toyofuku et al., 2015; Jaber et al., 2016)
TBK1	Q9WUN2 (TBK1_MOUSE); Serine/threonine-protein kinase TBK1; TANK-binding kinase 1	Yes	P2'-fraction	No	Synapse	Regulates together with Rab35 NDP52 recruitment to promote mitophagy and maturation of autophagosomes.	(Minowa-Nozawa et al., 2017)
Tecpr1	Q80VP0 (TCPR1_MOUSE) Tectonin beta-propeller repeat-containing protein 1	No	Yes SV-resident	No	Presynapse SV	Autophagosome maturation mediated by TECPR1 and the ATG12-ATG5 conjugate;	(Chen et al., 2012; Wetzel et al., 2020)
TRAPP complex TRAPPC8	Q9Y2L5 (TPPC8_HUMAN); Trafficking protein particle complex 8	No	Yes SV-resident	No	Presynapse SV	TRAPPC8 is the mammalian ortholog a yeast autophagy-specific TRAPP subunit. It interacts with TBC1D24 to regulate ATG9 trafficking;	(Lamb et al., 2016)
Tsc2	Q61037 (TSC2_MOUSE); Tuberin; Tuberous sclerosis 2 protein homolog	Yes	P2'-fraction	Yes	Synapse Synaptosome Postsynapse	Controls mTORC1 signaling; TSC2 is regulated by WIPI3 and FIP200; heterozygous loss of TSC2 function impairs spine development.	(Tang et al., 2014; Bakula et al., 2017; Dikic and Elazar, 2018; Tomoda et al., 2020)
Ubqln2	Q9QZM0 (UBQL2_MOUSE) Ubiquilin-2; Chap1; DSK2 homolog; PLIC-2	No	P2'-fraction	No	Synaptosome	Ubiquitn binding autophagy receptor	(Deng et al., 2017; Lin et al., 2021)
ULKs/ATG1-like ULK1 ULK2 ULK3	O70405 (ULK1_MOUSE); Unc51-like kinase 1; Serine/threonine-protein kinase ULK1//Q9QY01 (ULK2_MOUSE); Unc-51-like kinase 2	No	(Yes) ULK3 P2'-fraction	No	Synaptosome (SV)	Initiation of autophagy; ULK2 has important role for excitation-inhibition balance in the brain	(Lee and Tournier, 2011; Alers et al., 2012; Dikic and Elazar, 2018; Sumitomo et al., 2018; Tomoda et al., 2020; Chang et al., 2021)

(Continued)

TABLE 1 | (Continued)

Protein	UniProt acc.# (name); alternative names	Present in SynProt[a]	Present in Hidden SV Proteome[b]	Present in SynGO[c]	Localization in Synapse[d]	Function/Remarks	Selected references
Uvrag	Q8K245 (UVRAG_MOUSE); UV radiation resistance-associated protein	No	Yes SV-visitor	No	Presynapse SV	Regulatory component of PIK3C2; involved in maturation of autophagosomes;	(Mercer and Tooze, 2021)
VAMP7	P70280 (VAMP7_MOUSE); Vesicle-associated membrane protein 7; Synaptobrevin-like protein 1; TI-VAMP	Yes	Yes SV-resident	Yes	Presynapse SV	Overlapping functions with VAMP8, SNARE of secretory lysosomes in astrocytes.	(Verderio et al., 2012; Toyofuku et al., 2015; Hill and Colon-Ramos, 2020; Tian et al., 2021; Wojnacki et al., 2021)
VAMP8	O70404 (VAMP8_MOUSE); Vesicle-associated membrane protein 8	No	No	No	n.d.	SNARE involved in autophagosome fusion with endolysosome together with STX17 and SNAP29	(Itakura et al., 2012; Diao et al., 2015; Andres-Alonso et al., 2021; Tian et al., 2021)
Vps13 (a,c,d)	Q5H8C4 (VP13A_MOUSE); Vacuolar protein sorting-associated protein 13A	No	Yes (13d) P2'-fraction (13a,c)	No	Synaptosome Presynapse SV	ATG2-like protein involved in ER-phagy.	(Chen et al., 2020; Chang et al., 2021)
Vps15/PIK3R4	Q8VD65 (PI3R4_MOUSE); Phosphoinositide 3-kinase regulatory subunit 4;	No	Yes SV-visitor	No	Presynapse SV	Regulatory subunit in the PI3KC3 complex;	(Mercer and Tooze, 2021)
Vps33B	P59016 (VP33B_MOUSE); Vacuolar protein sorting-associated protein 33B	No	Yes SV-visitor	Yes	Presynapse, SV	belongs to class C core vacuole/endosome tethering (CORVET) complex, which is mainly implicated in endosomal fusion	(Takamori et al., 2006; Jiang et al., 2014; van der Beek et al., 2019)
Vps34/PIK3C3	Q6PF93 (PK3C3_MOUSE); Phosphatidylinositol 3-kinase catalytic subunit type 3; Vps34	No	Yes SV-resident	No	Presynapse SV	Catalytic component of PIK3C3–C1; colocalizes with synaptophysin at synapses.	(Inaguma et al., 2016; Jaber et al., 2016; Dikic and Elazar, 2018)
Vps35	Q9EQH3 (VPS35_MOUSE); Vacuolar protein sorting-associated protein 35; Vesicle protein sorting 35	Yes	P2'-fraction	Yes	Synapse Synaptosome Presynapse, Peri-AZ	Component of the retromer complex; involved in SV endocytosis in cooperation with LRRK2. Knock-down causes accumulation of ATG9a on endolysosomes	(Inoshita et al., 2017; Kaushik and Cuervo, 2018; Ravussin et al., 2021)
WDFY3/ALFY	Q6VNB8 (WDFY3_MOUSE), WD repeat and FYVE domain-containing protein 3, Autophagy-linked FYVE protein	No	Yes SV-visitor	No	Presynapse SV	Autophagy receptor; mainly for aggrephagy,	(Deng et al., 2017; Stavoe and Holzbaur, 2019)
WDR47	Q8CGF6 (WDR47_MOUSE); WD repeat-containing protein 47; Neuronal enriched MAP interacting protein	Yes	P2'-fraction	No	Synapse Synaptosome	Negatively regulates association of ATG9a with kinesin motor; essential for autophagy	(Kannan et al., 2017; Tomoda et al., 2020; Guardia et al., 2021)
WDR91	Q7TMQ7 (WDR91_MOUSE); WD repeat-containing protein 91	Yes	No	No	Synapse	Rab7 effector, regulates lysosome fusion.	(Borchers et al., 2021; Xing et al., 2021)
WIPI2/ATG18a	Q80W47 (WIPI2_MOUSE); WD repeat domain phosphoinositide-interacting protein 2	No	P2'-fraction	No	Synapse, Synaptosome	Involved in early steps of phagophore formation, recruits ATG12-ATG5-ATG16L1 E3-like complex.	(Vanhauwaert et al., 2017; Dikic and Elazar, 2018; Stavoe et al., 2019)
WIPI3/WDR45B WIPI4/WDR45	Q9CR39 (WIPI3_MOUSE) Q91VM3 (WIPI4_MOUSE); WD repeat domain phosphoinositide-interacting protein 3/4; WD repeat-containing protein 45/45B	No	P2'-fraction	No	Synaptosome	Components of the autophagy machinery	(Bakula et al., 2017; Wan et al., 2020)

AZ, active zone; BP, annotated for biological processes; CMA, chaperone-mediated autophagy; SV, synaptic vesicle; n.d., not detected in synapses; P2', Synaptosomal Protein Preparation (Taoufiq et al., 2020).
[a]*www.synprot.de (Pielot et al., 2012).*
[b]*As reported by Taoufiq et al. (2020).*
[c]*www.syngoportal.org (Koopmans et al., 2019).*
[d]*As taken from the databases or as referred to in remarks/function column.*

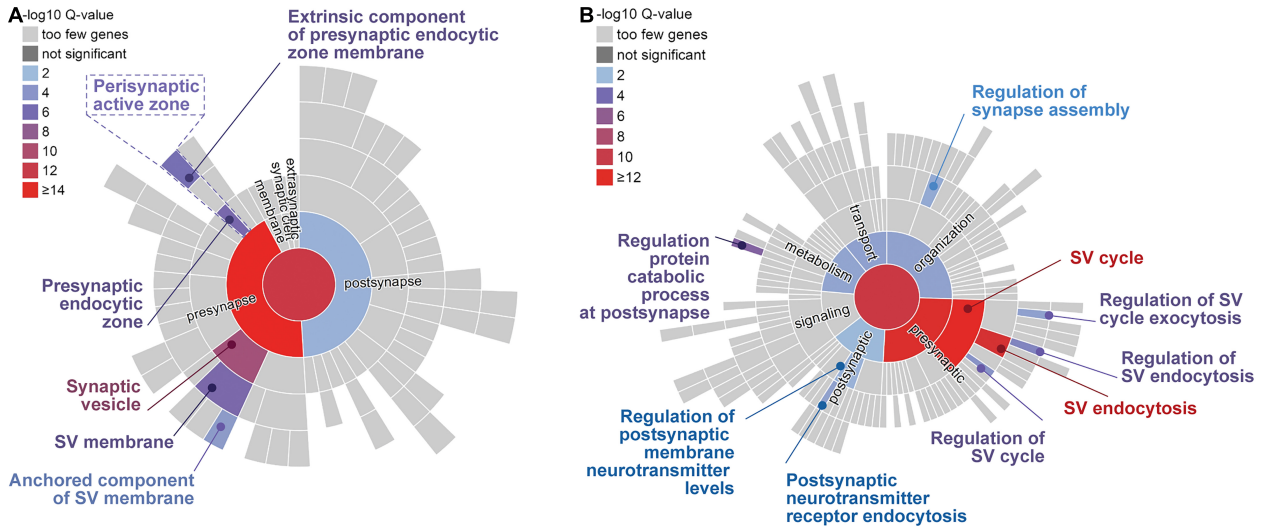

FIGURE 2 | Sunburst plots of gene enrichment analyses for autophagy-related genes/proteins included in SynGO (Koopmans et al., 2019). Significantly enriched cellular components **(A)** and biological processes **(B)** are indicated by color code. The top-level terms of the Gene Ontology (GO) term tree are represented by the inner circle; the second level of the term tree is denoted by the innermost ring and so on. Presynaptic structures **(A)** and processes, like synaptic vesicle (SV) cycle and SV endocytosis **(B)** are significantly over-represented. Note, autophagy-related terms were not annotated in the database. Database entries for cellular components and for biological processes were considered as indicated in **Table 1**.

that Bassoon may be highly feed-back regulated by the processes that it controls.

Interestingly, in *C. elegans*, another active zone protein, Clarinet, was recently reported to regulate presynaptic autophagy (Xuan et al., 2017, 2021). Clarinet is a large AZ protein that occurs in three different isoforms of about 9,000, 3,000, and 1,000 amino acids in length, that is required for proper synapse function. All three isoforms share a PDZ and a C2 domain similar to mammalian Piccolo, and Clarinet's long and short isoforms are supposed to organize SV recruitment and clustering at the presynaptic AZ (Xuan et al., 2017). An elegant follow-up study by the same lab, uploaded recently onto the bioRxiv server, demonstrates that the long Clarinet isoform controls presynaptic autophagy by regulating ATG9 trafficking at the peri-active endocytic zone (Xuan et al., 2021). These observations further support the concept that large scaffolding proteins of presynaptic AZs couple exo- and endocytic zones at neurotransmitter release sites (Gundelfinger et al., 2003; Haucke et al., 2011) and can have essential roles in organizing presynaptic autophagy processes.

CONSTITUENTS OF THE ENDOCYTIC MACHINERY ASSOCIATED WITH PRESYNAPTIC AUTOPHAGY

A tight linkage between autophagic and endocytic factors has been suggested previously (Soukup and Verstreken, 2017; Vijayan and Verstreken, 2017; Azarnia Tehran et al., 2018). Here, we discuss proteins involved in endocytic processes in neurons that have also been implicated in membranous organelle-based protein turnover as listed in **Table 1**. Endophilin-A/EndoA, a BAR-domain protein that is able to sense and modify membrane curvature, is crucially involved in Clathrin-dependent and -independent retrieval of membranes following the fusion SVs with the presynaptic AZ (Milosevic et al., 2011; Boucrot et al., 2015; Watanabe et al., 2018). More recent studies also suggest a function for Endophilins A in exocytosis of neurosecretory vesicles (Gowrisankaran et al., 2020) and the coordination of exo- and endocytic processes in presynapses (Kroll et al., 2019). Compensatory endocytosis associated with neurotransmitter release occurs primarily next to the AZ at the so-called peri-AZ (Haucke et al., 2011; Cano and Tabares, 2016). Two studies, one in *Drosophila* (Soukup et al., 2016) and the other one in mice (Murdoch et al., 2016) have identified Endophilin-A also as major player in generating initiation sites for autophagy. The former study showed that phosphorylation of the BAR domain of Endophilin-A by the leucine-rich repeat S/T protein kinase LRRK2 leads to membrane deformation putatively opening entry sites for the autophagy-related protein ATG3. ATG3 in turn can conjugate LC3/ATG8 to phosphatidyl-ethanolamine in the membrane, promoting progression of autophagosome formation (Soukup and Verstreken, 2017). Utilizing mutants for all three EndoA genes in the mouse genome, the second study revealed that partial or complete Endophilin-A-deficiency leads to age-dependent neurodegenerative changes in the brain and up-regulation of the E3 ubiquitin ligase FBXO32. Endophilins-A are essential for autophagosome formation and their proper interplay with FBXO32 coordinates the balance between autophagosomal and UPS-mediated protein turnover and maintains neuronal health (Murdoch et al., 2016). However, to date, FBXO32 has not yet been detected in the presynapse.

Synaptojanins are lipid phosphatases acting on phosphatidylinositols. In particular, the brain-enriched isoform Synaptojanin-1 is recruited to Endophilin-A complexes and, in

the SV cycle, is required for Clathrin uncoating after endocytosis (Cremona et al., 1999; Verstreken et al., 2003). More recently, studies on the *Drosophila* larval neuromuscular junction revealed that an inactivating mutation in the SAC1 domain, one of the two enzymatically active lipid phosphatase domains of Synaptojanin, causes accumulation of lipid-binding protein ATG18a on nascent autophagosomes (Vanhauwaert et al., 2017). Interestingly, this mutation does not interfere with SV cycling. Similarly, accumulation of WIPI2, the mammalian ortholog of ATG18a, occurs in neurons derived from induced pluripotent stem cells from a human patient with the same mutation (Vanhauwaert et al., 2017).

The heterooligomeric AP-2 complex is also involved in Clathrin-mediated endocytosis during SV recycling, where it can act at the cell membrane or at a bulk-endocytosed membrane compartment (McMahon and Boucrot, 2011; Kononenko et al., 2014). In addition, AP-2 in cooperation with CALM/PICALM has been implicated in autophagic degradation of the C-terminal fragment of the amyloid precursor protein (APP), thus contributing to the clearance of the Alzheimer-related Aβ peptide (Tian et al., 2013). APP is a cell adhesion molecule that has been detected as a constituent of the presynaptic AZ (Lassek et al., 2013). Moreover, AP-2 can directly interact with ATG9A, a multispan transmembrane protein delivering membrane material for phagophore formation and extension (Imai et al., 2016; Dikic and Elazar, 2018). This interaction appears essential for the trafficking of ATG9A through the recycling endosome and making it available for the autophagy process (Imai et al., 2016). Similarly, delivery of ATG16L1 and in turn ATG12-ATG5 to the phagophore depends on Clathrin and AP-2 (Ravikumar et al., 2010), indicating a key role for AP-2 in autophagy initiation and progression.

Recent studies have revealed that AP-2, in conjunction with the RapGTPase-activating protein (RapGAP) SIPA1L2, serve unexpected roles in the transport of autophagosomes that contain actively signaling BDNF-activated TrkB receptors (Kononenko et al., 2017; Andres-Alonso et al., 2019). AP2 and SIPA1L2 link the TrkB receptor to a Dynein motor for retrograde trafficking via a direct interaction with Snapin, a component of the BLOC-1 complex (see below). Interestingly, SIPA1L2 concurrently associates via LC3 to Rab7-positive amphisomes and binding to LC3 promotes RapGAP activity. Endosomes fuse with autophagosomes to form amphisomes, and this step is required for the degradation of some proteins and the overall function of autophagy and the endosomal system (Cheng et al., 2015). Amphisomes are transient intermediate organelles that in non-neuronal cells rapidly enter a lysosomal-degradative pathway. However, in distal axons mature lysosomes are rare and therefore TrkB-LC3-SIPA1L2-AP2-carrying amphisomes have a longer lifespan. They thus can traffic retrogradely along axons and visit presynaptic boutons. Intriguingly, motility and signaling of amphisomes are controlled by SIPA1L2, whose RapGAP activity reduces the trafficking velocity near boutons (Andres-Alonso et al., 2019). Collectively, these data suggest that retrograde transport of BDNF/TrkB in neuronal amphisomes is involved in plasticity-relevant local signaling at presynaptic boutons and this process seems tightly coupled to autophagy.

LRRK2 is a crucial enzyme with roles in intracellular membrane trafficking, including functions in the SV cycle, autophagy and the endolysosomal system (Taylor and Alessi, 2020; Piccoli and Volta, 2021). VPS35 is the cargo binding component of the retromer complex, which can serve multiple functions in synapses (Brodin and Shupliakov, 2018). VPS35 is an upstream regulator of LRRK2 and, as LRRK2, it is linked to various neurodegenerative diseases including Parkinson's disease. Inoshita et al. (2017) studied the functional interaction of these two proteins at the *Drosophila* larval neuromuscular junction. Here, they could be localized peripherally to the AZ and inside presynaptic boutons, where they are essential for proper SV retrieval (Inoshita et al., 2017). VPS35 constructs carrying a Parkinson's disease-associated mutation were unable to complement this endocytotic function in VPS35 null mutants. Tight interaction of the Rab7-LRRK2 pathway and the retromer complex was also observed in fly and rat neurons, where overexpression of wildtype, but not mutant, VPS35 protein was able to rescue Parkinson-related sorting defects (MacLeod et al., 2013).

Proteins discussed in this section, i.e., Endophilin-A, Synaptojanin, AP-2, CALM/PICALM, LRRK2 and VPS35, are all associated with endocytic functions within the SV cycle (cf. **Table 1**). Evidently, they also contribute to the delivery of key components into membrane-based protein degradation processes. However, the spatial organization of this latter machinery and the question of where within the boutons phagophore assembly is initiated remains to be clarified. Similarly, the crosstalk between SV recycling and autophagic and endocytic pathways needs further attention (see also Overhoff et al., 2021).

COMPONENTS OF MEMBRANE-BASED PROTEIN TURNOVER PATHWAYS ASSOCIATED WITH SYNAPTIC VESICLES

A link between SV cycling and membrane trafficking processes controlling proteostasis is also indicated by the finding that constituents of autophagy and endolysosomal degradation pathways are associated with SV protein preparations (Takamori et al., 2006; Boyken et al., 2013; Taoufiq et al., 2020). These are also listed in **Table 1** and include, e.g., small GTPases like Rab7, Rab11a, Rab12, Rab24, Rab26, Rab35, Rab37, Rab39a, Arf6 and the ADP-ribosylation factor-like GTPase Arl8, the SNARE proteins SNAP-29, Stx17 and VAMP7, constituents of the phosphatidylinositol 3-kinase class III (PIK3C3) complex (Vps34, Vps15, Beclin-1, CISD2, Uvrag), as well as other autophagy-related proteins, i.e., ATG2a, ATG9A, ATG16L1, LC3/ATG8, Tecpr1, and autophagy the receptors WDFY3/ALFY, components of the TRAPP complex and various others. Altogether, Taoufiq et al. (2020) identified ∼40 autophagy-related proteins within the hidden SV proteome, eleven of them in the SV-resident repertoire, while the others were defined as SV-visitors by the authors (**Figure 3**).

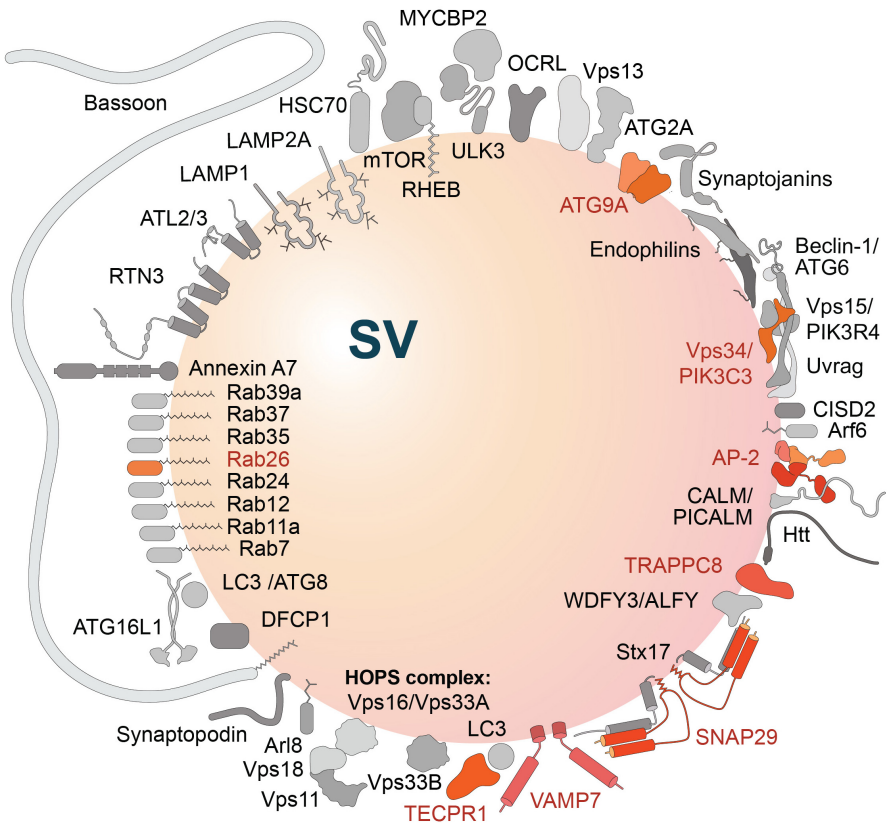

FIGURE 3 | Autophagy-related proteins detected in the hidden proteome of synaptic vesicles (SV) (Taoufiq et al., 2020). Proteins of the SV-resident repertoire are indicated in different shades of orange; proteins defined by the authors as SV-visitors are gray-shaded. Note, the large active zone scaffolding protein Bassoon may be anchored to SVs via N-terminal myristoylation (Dresbach et al., 2003).

Of particular interest is the presence of ATG9 in SVs (Boyken et al., 2013; Taoufiq et al., 2020), a lipid scramblase that is involved in early steps of phagophore formation (Rao et al., 2016; Guardia et al., 2020; Maeda et al., 2020; Matoba and Noda, 2020; Matoba et al., 2020; Orii et al., 2021). Here, it may play a central role in organizing presynaptic autophagy in cooperation with the endocytic machinery (see below).

Rab26 is associated with a subset of recycled SVs, directing them for autophagic degradation (Binotti et al., 2015). This is modulated by the Pleckstrin homology containing family member 5 (PLEKHG5), which acts as guanine exchange factor (GEF) for Rab26. In motoneurons, the lack of PLEKHG5 leads to defective axon growth and impaired SV autophagy, a mechanism that may underlie motoneuron disease (Lüningschrör et al., 2017; Lüningschrör and Sendtner, 2018).

The presence of Arl8 in SV preparations is interesting as this protein has been characterized as a factor associated with anterogradely transported degradative lysosomes (Farias et al., 2017; Farfel-Becker et al., 2019). Vukoja et al. (2018) have proposed that SV precursors may share lysosomal membrane markers, but are distinct from bona fide lysosomes. Another, more recent study reported that Arl8 is involved exclusively in the anterograde transport of lysosomes (De Pace et al., 2020). In addition, Arl8 is involved in controlling fusion of autophagosomes with lysosomes (see Lieberman and Sulzer, 2020), where it may contribute to SV turnover via axonal autolysosomes.

SNAP-29 is regarded as an integral protein of vesicular membranes in the molecular SV model (Takamori et al., 2006; Taoufiq et al., 2020). In addition, SNAP-29, together with VAMP8, are considered as late endosomal/lysosomal SNAREs involved in the fusion with autophagosomes upon forming a SNARE complex with autophagosomal SNARE Syntaxin 17 (Itakura et al., 2012; Hill and Colon-Ramos, 2020).

In addition, multiple constituents of the endocytic machinery and the AZ, such as AP-2 complex, Bassoon, CALM, Endophilin-A, Endophilin-B1, Synaptojanin and VPS35, are associated with SV preparations (**Table 1**). Further proteins detected in SV preparations include the lysosomal-associated membrane protein LAMP1, the E3-ubiquitin ligase Parkin, Vps33B, a protein associated with late endosomes, as well as the Annexin A7. These proteins are mainly considered as visitor proteins associated with a subset of SVs (**Figure 3**). In many cases, however, their (pre-)synaptic localization has been reported utilizing immunocytochemistry.

A number of additional proteins with known functions in autophagic and/or endolysosomal degradative pathways could be localized to presynaptic structures as extracted

from published literature (**Table 1**; SynGO database). Among them are:

- Atlastin2/3, which are involved in initiation of phagophore formation by guiding the Unc51-like kinase (ULK1) complex to the ER (Liu et al., 2021).
- Multiple GABARAPs that, as LC3, belong to the family of ATG8-like proteins that can be conjugated to phosphatidylethanolamine and are required for phagophore extension and closure (e.g., Martens and Fracchiolla, 2020).
- ATG5 that together with ATG12 and ATG16L forms an E3-like complex for the conjugation of ATG8/LC3 family members to phosphatidylethanolamine (Chang et al., 2021).
- Vps34, the catalytic kinase subunit of the lipid kinase PIK3C3-Complex 1, acting in phagophore nucleation (Dikic and Elazar, 2018; Chang et al., 2021).
- Sorting nexin 4 (SNX4)/ATG24B, a PI3P-binding protein controlling the recycling of ATG9A for reuse in phagophore formation (Ravussin et al., 2021).
- The cargo adaptors p62/SQSTM1 and Huntingtin (Deng et al., 2017).
- Snapin, a subunit of the BLOC-1 complex, which functions as a motor adaptor that coordinates retrograde transport and late endosomal-lysosomal trafficking (Cai et al., 2010). Moreover, Dynein-Snapin-mediated retrograde transport was reported to promote clearance of presynaptic mitophagosomes (Han et al., 2020).
- TBC1D24/skywalker, a GTPase-activating protein acting on Rab35 in the endolysosomal pathway (Fernandes et al., 2014; Wang et al., 2017) as well as on the small GTPase Arf6, which antagonizes Rab35 in SV recycling from early endosomes (Sheehan et al., 2016; Sheehan and Waites, 2019).
- Arf6, which in addition has been reported as a regulator of autophagosome formation by controlling phosphatidylinositol 4,5-bisphosphate (PIP2) generation and in turn phospholipase D activity (Moreau et al., 2012) and to rescue aberrant autophagosome formation in Synaptojanin-1-deficient in zebrafish cone photoreceptors (George et al., 2016). This includes Arf6 into the list of players in endocytosis-associated initiation of autophagy.
- Components of the HOPS (Homotypic fusion and vacuole protein sorting) complex involved in the fusion of late endosomal and lysosomal compartments (Jiang et al., 2014; van der Beek et al., 2019).
- Reticulon-3 (RTN3), which is involved in ER-phagy (Beese et al., 2019; Stavoe et al., 2019).
- HSC70, a cytosolic chaperonin of the HSP70 family that is involved in microautophagy and chaperone-mediated autophagy (CMA) (Kaushik and Cuervo, 2018), which is known to contribute significantly to the regulation of synaptic protein levels (Uytterhoeven et al., 2015).

Many of the autophagy-related proteins associated with the presynaptic endocytic machinery, the SV proteome, or other presynaptic structures are phospholipid-binding and -modifying proteins. These include, e.g., various subunits of PI3 kinases, PI phosphatases synaptojanin and OCRL, the lipid scramblase ATG9, lipid transfer protein ATG2a, as well as various other phospholipid binding proteins (**Table 1**). This indicates the significance of the metabolism of phospholipids in general and phosphoinositides in particular for the proper performance of presynaptic autophagy-related processes (for a detailed review see Marat and Haucke, 2016; Palamiuc et al., 2020).

Based on this inventory of autophagy-related proteins present at the presynapse (**Figure 4**), we can now start discussing potential cellular mechanisms of membrane-associated protein turnover in this compartment.

TAGGING AND RECRUITMENT OF PRESYNAPTIC AUTOPHAGIC CARGOS

A central feature of autophagic function is the recruitment and degradation of aged and damaged proteins and membranous organelles. As in most forms of autophagy in different cells and organisms, presynaptic boutons seem to use the ubiquitination system to tag proteins not only for proteasomal degradation, but also in many instances for their removal by autophagy. This versatile system is capable of attaching specific ubiquitin chains to substrates, and this ubiquitination coding plays an essential role in recruitment to autophagic structures (Deng et al., 2017; Kwon and Ciechanover, 2017). The process of substrate ubiquitination requires the regulated activation of several key component of this tagging system, including the ubiquitin activating enzyme E1, the ubiquitin conjugating enzymes E2 and the E3 adaptor/ligases (Nandi et al., 2006; Ding and Shen, 2008). While there is only one E1 enzyme in mammalian cells, there are tens of E2s and hundreds of E3s (Li et al., 2008; Kawabe and Stegmuller, 2021). Of these, E3s are posited to provide substrate specificity, while the E2s define the type of poly-ubiquitin chain (Kwon and Ciechanover, 2017). These poly-ubiquitin determinants are then recognized by a variety of adaptor proteins that mediate the recruitment of tagged cargos into specific degradation pathways. For example, during autophagy the p62/SQSTM1 adaptor protein is capable of recognizing K63-poly-ubiquitined proteins for their engulfment into autophagic organelles (Linares et al., 2013).

Fundamental questions related to presynaptic autophagy are: which of the many E2 and E3 ligases contribute to presynaptic proteostasis? Further, when are they used and how are they regulated? A number of presynaptic E3 ligases (e.g., Scrapper, FBXO45) have been identified that trigger the removal/destruction of AZ proteins including RIM1, Munc13 or Munc18 via the proteasome (Yao et al., 2007; Tada et al., 2010; Martin et al., 2014). Less is known about which E3s regulate the removal of integral SV proteins. As mentioned above, studies of boutons lacking the presynaptic AZ proteins Piccolo and Bassoon have led to the identification of two E3s, Siah1 and Parkin, linked to the removal of SV proteins via the autophagy degradative system (Waites et al., 2013; Okerlund et al., 2017; Hoffmann-Conaway et al., 2020). Mechanistically, these AZ proteins seem to act as negative regulators of these enzymes. This is best exemplified in studies of Bassoon knockout mice, where the total pool of SVs per bouton is dramatically reduced, which can be restored by knocking down the expression of either Siah1 or

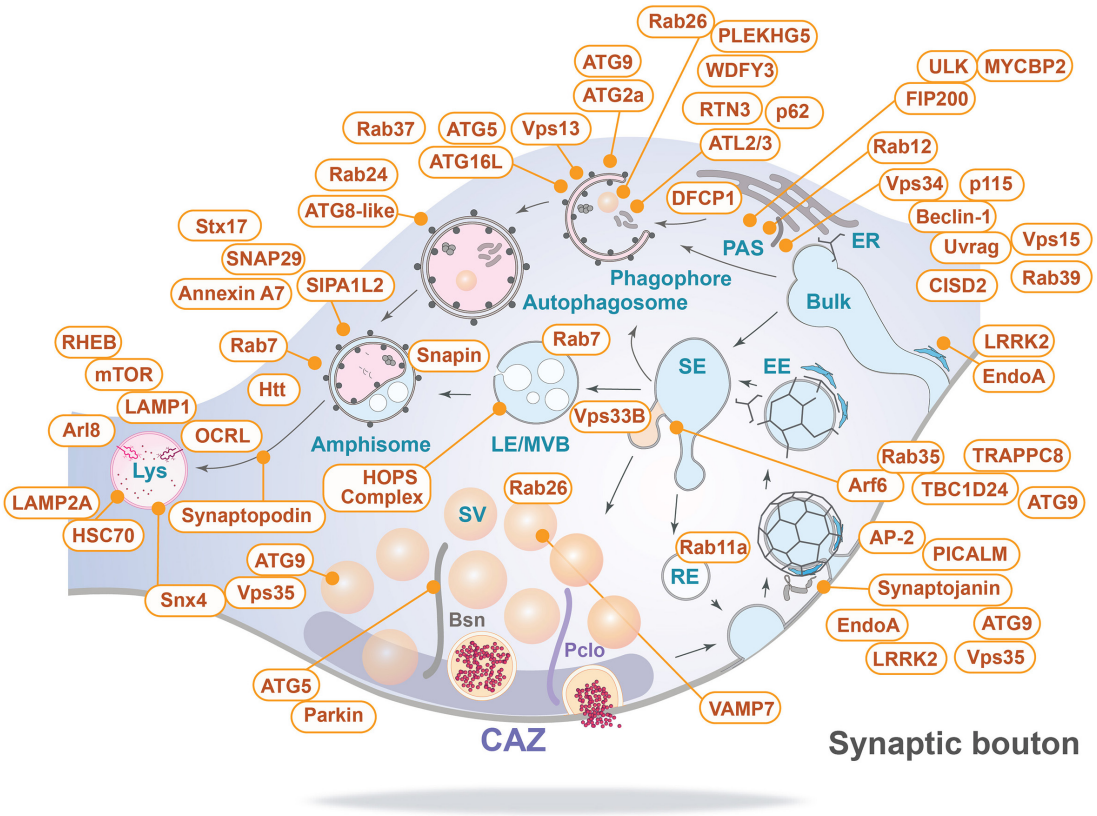

FIGURE 4 | Inventory of autophagy-related proteins detected in presynaptic boutons and their relevant sites of action (for details see text and **Table 1**). Bsn, Bassoon; CAZ, cytomatrix at the active zone; EE, early endosome; ER, endoplasmic reticulum; LE/MVB, late endosome/multi-vesicular body; Lys, lysosome; PAS, phagophore assembly site/pre-autophagosomal structure; Pclo, Piccolo; RE, recycling endosome; SE, sorting endosome; and Bulk indicates bulk endocytosis.

Parkin (Hoffmann-Conaway et al., 2020), indicating that Bassoon normally counteracts their actions (**Figure 5**). For Siah1 this is supported by experiments showing that it directly binds the zinc finger domains in Bassoon, which inhibits Siah1 ubiquitination activity (Waites et al., 2013).

Hints to the substrates of these enzymes come from proteomic studies on synaptosomes isolated from the cortex of Bassoon-deficient mice (Hoffmann-Conaway et al., 2020). These studies identified a dramatic increase in ubiquitinated peptides from SV proteins and proteins involved in SV fusion with the presynaptic membrane, including SNAP25, Synaptotagmin 1, SV2, V-ATPase, VAMP2 and Syntaxin1b. Moreover, autophagy appears to be the major degradative pathway employed, as autophagic vacuoles, but not multi-vesicular bodies, accumulated in these boutons, and inhibiting autophagy restores SV pool size (Hoffmann-Conaway et al., 2020). Intriguingly, this study also found that the Ubiquitin-conjugating enzyme UBE2N was hyper-ubiquitinated. This is highly relevant, as UBE2N is an ubiquitin conjugating enzyme directly involved in creating K63-poly-ubiquitin chains (David et al., 2010), which can tag proteins for degradation via autophagy (Linares et al., 2013). UBE2N can also cooperate with both Siah1 and Parkin (Markson et al., 2009; Fiesel et al., 2014; Geisler et al., 2014). Another E3 ligase, HERC1, was proposed to dysregulate presynaptic pathways and to potentially affect SV autophagy, yet the mode of action is unclear (Montes-Fernandez et al., 2020). This highlights a general challenge for the field.

Given the plethora of known E3 ligases, it will be critical to define which of these are selectively involved in presynaptic autophagy, versus, for example, proteasomal and/or endolysosomal systems. Given the ability of these E3 enzymes to bind various E2s, this will be a daunting, but important challenge. Equally important will be the identification of their associated substrates. In the studies on synapses lacking Bassoon a poignant subset of SV proteins became hyper-ubiquitinated, but to what end? In another study, only a subset of SV proteins was selectively degraded by the endolysosomal system during high synaptic activity conditions (Sheehan et al., 2016), begging the question of which E2s and E3s direct these pathways of destruction.

While it is attractive to consider that there is a high specificity in the clearance systems for particular aspects of presynaptic proteostasis, it is far more likely that there is high flexibility and crosstalk between the different systems, including autophagy, endolysosomal or proteasomal degradation systems, that participate in the removal of different subsets of presynaptic proteins or organelles, like SVs, as was demonstrated for the degradation/turnover of other cellular systems. For example, ATG5-deficient neurons can survive and

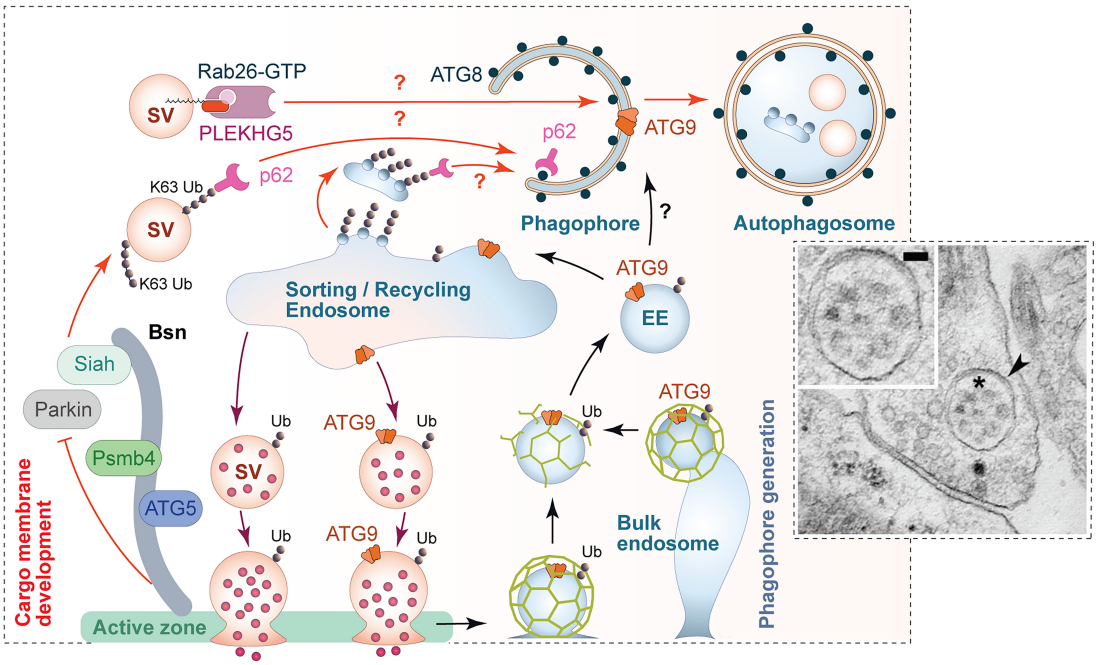

FIGURE 5 | Scenario for the regulation of presynaptic autophagy. Autophagy within presynaptic boutons appears to be locally regulated and mediated via the convergence of two major facets of autophagy. (1) Local tagging of aged and/or damaged proteins/organelles by the ubiquitination system. The active zone protein Bassoon is one regulator of this process by scaffolding E3 ligases such as Siah1 and Parkin. Bassoon can also control the induction of phagophore formation by inhibiting the activity of ATG5 and proteasome function via its binding to Psmb4 proteasomal subunit. (2) The formation of phagophore membranes, which requires an interplay between numerous proteins essential for the regulated conjugation of ATG8/LC3 to membranes containing the integral membrane protein ATG9. Many of these proteins are part of the hidden proteome of SVs (see **Figure 3**) and thus available for the rapid production of these membranes. This aspect of autophagy seems to be coupled to synaptic activity and the sorting and recycling of SV proteins through early endosomes. While not well understood, this compartment is well positioned to not only sort healthy ensembles of proteins regenerating functional SVs, but also damaged ubiquitinated proteins for engulfment into newly forming phagophores. This latter step requires the small GTPase Rab26 and its guanine exchange factor PLEKHG5, as well as autophagy adaptor proteins, like p62/SQSTM1, which binds both poly-ubiquitin chains and ATG8s. The inserted electron micrograph demonstrates the uptake of entire SV-like structures (asterisk) into autophagic vacuoles (arrowhead) within a presynapse (taken from Hoffmann-Conaway et al., 2020; size bar, 50 nm). Finally, the sorting/recycling endosomes also appears to function in the regeneration of SV-like membranes that carry ATG9, providing autophagic support for boutons in subsequent rounds of neurotransmitter release.

still display SV recycling (Negrete-Hurtado et al., 2020). Actually, they rather accumulate ER in axons and increase excitatory neurotransmission (Kuijpers et al., 2021) indicating flexibility and compensatory potential in the system.

From a functional perspective, there are several schools of thought: (i) that presynaptic autophagy primarily operates on a slow time scale for the basal removal of aging and/or defective proteins and membranous organelles, (ii) that it is directly involved in the destruction of SVs during high activity, and/or (iii) that it responds to eliminate proteins/membranes following acute and chronic stress or insults.

A key to solving some of these issues lies in how fast and with what specificity presynaptic autophagy can operate. Utilizing the light-activated free-radical generating protein SuperNova (SN) tethered to different SV proteins, it was recently shown that through the acute damage of these proteins, presynaptic autophagy could be induced in minutes and to depend on ubiquitination (Hoffmann et al., 2019). Here, the clearance mechanisms operated with high-specificity, directing the destruction of the SN-tagged protein (SN-synaptophysin or SN-synaptotagmin) to autophagy, but leaving other SV proteins in action. Intriguingly, such acute ROS-mediated damage had real-time effects on synaptic transmission only when autophagy was simultaneously inhibited with drugs or ATG5 knockdown (Hoffmann et al., 2019). One can thus conclude that the presynaptic autophagy machinery is capable of operating in real-time and can be highly selective, removing only damaged and ubiquitinated proteins ensuring the health and functionality of presynaptic boutons. Consistent with studies on boutons lacking Bassoon, these studies highlight the role of the ubiquitination system in tagging proteins for their elimination by autophagy. They also illustrate that the generation of ubiquitin-tagged damaged proteins is in and of itself a key driver of presynaptic autophagy. Potential cellular mechanisms associated with the sorting and delivery of these tagged proteins into newly formed phagophore membranes are discussed below. A point of consideration is the observation that, in boutons lacking Bassoon, autophagophore organelles contain seemingly intact SVs (**Figure 5**), indicating that whole SVs can also become cargos for autophagic destruction. From a ubiquitination perspective, this could be a consequence of the dramatic increase in the ubiquitination of many SV proteins due to the loss of Bassoon

and the activation of Siah1 and Parkin, which then decorate the surface of SVs making them attractive as a cargo for engulfment (Hoffmann-Conaway et al., 2020).

CELLULAR MECHANISMS GOVERNING PRESYNAPTIC AUTOPHAGY

The ability of presynaptic boutons to engage the autophagy degradative system in real-time to maintain its functionality, raise fundamental questions of how this is temporally and spatial achieved. At its most basic level, the ability of autophagy to operate in a spatially restricted manner requires the machinery to be present. Clearly there are two major arms to this process: (i) the sensing and tagging of misfolded or damaged proteins by ubiquitination, and (ii) the formation of autophagophore membranes capable of engulfing these cargos. As we have seen, some of the enzymes involved in the ligation of ubiquitin are scaffolded to components of the AZ cytoskeletal matrix, e.g., Bassoon and Piccolo (Waites et al., 2013; Okerlund et al., 2017; Hoffmann-Conaway et al., 2020).

Interestingly, many of the proteins critical for autophagophore formation are associated either with the perisynaptic endocytic zone, SVs or scaffold proteins of the AZ **(Figure 4)**. Hints to how these might be linked together come from observations in *C. elegans* and *Drosophila* showing that there are hotspots of autophagosome formation in close proximity to or directly within presynaptic terminals (Soukup et al., 2016; Stavoe et al., 2016; Neisch et al., 2017; Vanhauwaert et al., 2017). Also, in mammals, many, but not all, constituents of the autophagic machinery have been detected reliably in synaptic boutons (**Table 1**). For example, of the Unc51-like kinases required for initiation of phagophore formation, only ULK3 has been detected in synaptosomes together with other components of the ULK complex, i.e., FIP100 or ATG101 (Taoufiq et al., 2020). This seems consistent with the observation that ULK1 and ULK2 are not essential for constitutive autophagy in the young murine brain (Wang et al., 2018) and hint to a function of ULK3 in (pre-)synaptic autophagy. Moreover, constituents of the PI3-Kinase C3 complex, including Vps34 and Beclin-1, have been found associated with SV preparations (**Figure 3**; Taoufiq et al., 2020). Further, there is compelling evidence that components of SV recycling interact with autophagy-related proteins (George et al., 2016; Soukup and Verstreken, 2017; Vanhauwaert et al., 2017), and core components of autophagosomes, including the membrane-delivering protein ATG9, are present in presynaptic boutons (Boyken et al., 2013; Stavoe et al., 2016). This suggests that the local biogenesis of autophagosomes could start at endocytic zones, following SV endocytosis or shortly thereafter when SV proteins pass through early and recycling endosome membranes, where quality control process sort out corrupted proteins.

Actually, membrane trafficking and protein sorting within boutons may be critical for autophagosome formation. Thus, the ATG9 is not only an integral component of the SV membrane (Boyken et al., 2013; Taoufiq et al., 2020), but is also the only transmembrane protein in the core machinery for autophagy (Lang et al., 2000; Noda et al., 2000; Young et al., 2006). A recent study deposited on the bioRxiv server actually suggests that SVs also directly may donate lipids to autophagosomes (Yang et al., 2020; Xuan et al., 2021). These authors propose that ATG9 is transported in vesicles generated at the trans-Golgi network to the presynaptic membrane, which undergo exo-endocytosis prior to accumulation at the peri-AZ and/or autophagosome formation. Mutations that prevent exocytosis (e.g., in *UNC13, UNC18* genes) or endocytosis (e.g., in *AP1, AP2*, or *SDPN-1/Syndapin 1* genes) negatively interfere with activity-dependent synaptic autophagy associated with the SV cycle (Imai et al., 2016; Yang et al., 2020; Xuan et al., 2021). Taken together the data suggest that membrane trafficking of ATG9 could couple the SV cycle to activity-dependent presynaptic autophagy. However, as mentioned above, SVs can also be recruited directly into autophagophores vi Rab26 and PLEKHG5 (Binotti et al., 2015; Lüningschrör et al., 2017; **Figure 5**).

How does neuronal activity and nutrient depletion affect presynaptic autophagy? Starvation/nutrient depletion usually induces autophagy via mTOR signaling (Bockaert and Marin, 2015). As stated above, it remains controversial whether and how strongly starvation affects presynaptic autophagy. At *Drosophila* larval NMJs, both starvation and increased neuronal activity induces ATG8 accumulation in presynaptic boutons (Soukup et al., 2016; Vanhauwaert et al., 2017). Similarly, mTOR inhibition by rapamycin induces autophagy at dopaminergic release sites and is associated with decreased SV numbers and evoked dopamine release (Hernandez et al., 2012). Furthermore, Catanese et al. (2018) report disorganized SV pools and rapid degradation of Bassoon upon nutrient limitation in rodent primary neuronal cultures. Re-supplementation of glucose can restore SV pools, but does not rescue Bassoon levels. In contrast, there are multiple studies reporting no or only minor effects on presynaptic autophagy (Mizushima et al., 2004; Maday and Holzbaur, 2016). The relative resistance of some neurons to autophagy induction in the presynaptic/axonal compartment by starvation/nutrient depletion may have various reasons that should be tested in future: one may be that presynaptic mTOR signaling is dominated by mTORC2 (McCabe et al., 2020), which is not linked to starvation-induced autophagy; another one could be that presynaptic autophagy (partly) depends on ULK3 (see above), while amino acid starvation-induced autophagy is controlled by ULK1/2 (Cheong et al., 2011) in a subset of neurons.

There is strong evidence for neuronal activity being a major factor regulating presynaptic autophagy. Thus, it is known that neuronal activity, and the recycling of SVs carrying key autophagic molecules, might contribute to the assembly of autophagosomes within boutons. Consistently, KCl stimulation has been shown to induce axonal autophagy and enhances retrograde autophagy flux in hippocampal primary neurons (Wang et al., 2015). Of note, activity can also engage the endolysosomal/ESCRT system to degrade subsets of SV protein (Sheehan et al., 2016).

At the organismal level, various studies imply that autophagy has a major impact on learning and memory (Shehata and Inokuchi, 2014; Liang and Sigrist, 2018; Hwang et al., 2019; Liang, 2019). However, in most cases it is impossible to assign these

effects to neurons or even neuronal compartments where the relevant autophagic effect on memory formation is expressed. A particular case of presynaptic autophagic dysfunction seems to be the *tambaleante (tbl)* mouse, where the HERC1 E3 ubiquitin ligase is mutated. Among other phenotypes these mice display poor performance hippocampus-dependent learning including novel-object recognition, T-maze and Morris water maze tests (Montes-Fernandez et al., 2020; Perez-Villegas et al., 2020). In fruit flies, a tight association between age-dependent memory impairment and structural changes in presynaptic AZs has been observed. Both structural changes and memory decline could be counteracted by treatment with the autophagy enhancer spermidine (Gupta et al., 2016; Liang and Sigrist, 2018). Finally, conditional knockout of the presynaptic AZ protein Bassoon only in excitatory neurons of the murine forebrain, which is supposed to cause enhanced autophagy exclusively in glutamatergic terminals, causes improved memory performance in dentate gyrus-dependent learning tasks, such as contextual fear memory or spatial pattern separation (Annamneedi et al., 2018). This memory improvement was associated with the maintenance of juvenile synaptic plasticity at relevant performant path to dentate gyrus synapses. These examples support the view that well-functioning presynaptic autophagy is a prerequisite for maintaining brain synapses plastic and healthy.

POTENTIAL SCENARIO FOR THE REGULATION OF PRESYNAPTIC AUTOPHAGY

An important unresolved question is how basal, activity-dependent and protein damage induced autophagy relate to each other? One potential answer is they are unrelated. A more parsimonious answer is they are intimately linked playing complementary and sometimes redundant roles. Moreover, the transition between them may primarily relate to the rate of flux and the pathways activated. Given the available data and emerging concepts in the field, we can conceive the following scenario for ubiquitination-dependent modes of protein turnover. It begins with a few knowns. First, that productive autophagy requires the generation of poly-ubiquitin tagged cargos (**Figure 5**), which can occur during use and natural aging of SVs and their associated proteins or through their acute damage, e.g., by ROS or nitrosylation among others. This could also occur during development, e.g., during synaptic pruning and/or trophic factor withdrawal via the E3 ligase MYCBP2/RPM-1/Highwire (Grill et al., 2016; Crawley et al., 2019). In principle, all this would be mediated by ubiquitin ligases, only a few of which are currently known. Second, that the degradation of these cargos requires the generation of phagophore membranes, which through adaptor proteins such as p62/SQSTM1, recruit the ubiquitinated cargos (**Figure 5**). This in turn requires the presence and activation of the machinery required to create the phagophore membrane. While there is a clear interdependency of these two arms of autophagy, as disruption of either blocks presynaptic autophagy, it is unclear how this is coordinated, regulated and/or what sensors are used. An attractive focal point for the generation of phagophore membranes and the sorting of ubiquitin-tagged cargos within presynaptic boutons are the early and sorting/recycling endosomal compartments, which maybe be used during basal, activity-dependent and protein damage induced autophagy. Here, it is well appreciated that these membranes operate as quality control stations, working to regenerate functional SVs with the correct complement of proteins. As such, it is easy to imagine that ubiquitin tagged proteins destined for destruction would be sorted into autophagic cargo vesicles at this point. Similarly, it would be a natural site for sorting the autophagy machinery (ATG9 among others), normally associated with SV-like vesicles, into precursor phagophore membranes that then mature into autophagosomes decorated with ATG8-like molecules (LC3, GABARAPs). In the event that there is little cargo, ATG9 would mostly be recycled back into the existing pool of SV-like membranes. Given the complexity of membrane trafficking, it would be important to entertain that many membranes could be used to generate autophagosomes and/or carry ubiquitinated cargos, including the plasma membrane, other endosomal compartments and/or the ER and potentially also SVs.

FURTHER OPEN QUESTIONS

It is well documented that accurate performance of all types of autophagy as well as the endolysosomal system are of utmost importance for cellular health. This applies particularly to neurons and their synapses with their extremely long lifespans. All major brain disorders are associated with failures of these clearance systems, either as causes or consequences of the pathology. In particular, neurodegenerative disorders, such as Parkinson's Disease or Alzheimer's can be directly linked with autophagy failures, though physiological aging is also associated with slow exhaustion of clearing systems. We have largely ignored this aspect in the present article and focused mainly on the molecular inventory of the presynapse, because disease-related issues have been the subject of numerous review articles during recent years (e.g., Rubinsztein, 2006; Mizushima et al., 2008; Bezprozvanny and Hiesinger, 2013; Michel et al., 2016; Deng et al., 2017; Menzies et al., 2017; Dikic and Elazar, 2018; Liang and Sigrist, 2018; Soukup et al., 2018; Lee and Kim, 2019; Malik et al., 2019; Pan et al., 2019; Giovedi et al., 2020; Tomoda et al., 2020). However, it is very obvious that there are multiple gaps in our knowledge about disease mechanisms. Therefore, a detailed understanding of the molecular organization of (pre-)synaptic protein turnover and clearance systems at the nanoscale is a major future challenge for the field.

Additional questions worth consideration include: Do clearance systems operate in a similar manner at all synapses? Do autophagic events occur near/within boutons or more remotely? On what time scales does autophagy operate? Which ubiquitin tagging systems (E2, E3 enzymes) are utilized? How many and when are the different lipidated ATG8-like conjugates used? Are different Unc-51-like kinase employed under specific conditions?

What autophagy receptors/cargo adaptors are tapped and at which synapses? What ubiquitin-independent mechanisms are in operation?

Further questions concern the sorting and routing of damaged proteins. Where does the sorting take place? Which organelles contribute membranes to the phagophore? Do SVs contribute to phagophore formation? Can SVs even act as a starting point for phagophore assembly? How can clearance pathways compensate for each other and is this controlled and regulated?

Finally, there are interesting recent observations that liquid phase separation might also play a role in PAS formation and the initiation of autophagy (Fujioka et al., 2020; Hollenstein and Kraft, 2020). For example, evidence from yeast indicates that the endocytic protein Ede1 (the yeast homolog of p115/Uso1) can mediate the formation endocytic protein condensates (ENDs) that then enter an autophagic degradation path (Wilfling et al., 2020). Another recent study revealed that condensed liquid droplets, formed from the AZ proteins RIM, RIM-binding protein and ELKS/CAST2 can tether SVs *in vitro* (Wu et al., 2021). The authors hypothesize that similar processes play a role in organelle biogenesis and autophagy. It will thus be interesting to see whether phase separation indeed triggers autophagy at the perisynaptic endocytic zone.

AUTHOR CONTRIBUTIONS

EG, CG, and MK wrote the article. AK designed and prepared the figures. RP provided bioinformatic and database analyses including **Figure 2**. All authors contributed to the conceptualization and the discussion of the content.

FUNDING

EG, AK, CG, and MK are supported by the Deutsche Forschungsgemeinschaft (DFG, FOR 5228 Syntophagy RP03 and RP06; and RTG 2413 SynAge TP04 and TP08). In addition, AK was supported by a LIN Special Project; RP by the state Saxony-Anhalt and the EU-EFRE program (ZS/2016/04/78113); CG was supported by the German Center for Neurodegenerative Diseases; the DFG CRC958 and the German Excellence Strategy (EXC-2049-390688087); and MK by grants from the Leibniz SAW program (SynERCa and SyMetAge).

REFERENCES

Ackermann, F., Schink, K. O., Bruns, C., Izsvak, Z., Hamra, F. K., Rosenmund, C., et al. (2019). Critical role for Piccolo in synaptic vesicle retrieval. *Elife* 8:e46629. doi: 10.7554/eLife.46629

Ackermann, F., Waites, C. L., and Garner, C. C. (2015). Presynaptic active zones in invertebrates and vertebrates. *EMBO Rep.* 16, 923–938. doi: 10.15252/embr.201540434

Alers, S., Loffler, A. S., Wesselborg, S., and Stork, B. (2012). The incredible ULKs. *Cell Commun. Signal.* 10:7. doi: 10.1186/1478-811X-10-7

Alirezaei, M., Kemball, C. C., Flynn, C. T., Wood, M. R., Whitton, J. L., and Kiosses, W. B. (2010). Short-term fasting induces profound neuronal autophagy. *Autophagy* 6, 702–710. doi: 10.4161/auto.6.6.12376

Andres-Alonso, M., Ammar, M. R., Butnaru, I., Gomes, G. M., Acuna Sanhueza, G., Raman, R., et al. (2019). SIPA1L2 controls trafficking and local signaling of TrkB-containing amphisomes at presynaptic terminals. *Nat. Commun.* 10:5448. doi: 10.1038/s41467-019-13224-z

Andres-Alonso, M., Kreutz, M. R., and Karpova, A. (2021). Autophagy and the endolysosomal system in presynaptic function. *Cell Mol. Life Sci.* 78, 2621–2639. doi: 10.1007/s00018-020-03722-5

Annamneedi, A., Caliskan, G., Muller, S., Montag, D., Budinger, E., Angenstein, F., et al. (2018). Ablation of the presynaptic organizer Bassoon in excitatory neurons retards dentate gyrus maturation and enhances learning performance. *Brain Struct. Funct.* 223, 3423–3445. doi: 10.1007/s00429-018-1692-3

Arias, E., Koga, H., Diaz, A., Mocholi, E., Patel, B., and Cuervo, A. M. (2015). Lysosomal mTORC2/PHLPP1/Akt Regulate Chaperone-Mediated Autophagy. *Mol. Cell* 59, 270–284. doi: 10.1016/j.molcel.2015.05.030

Azarnia Tehran, D., Kuijpers, M., and Haucke, V. (2018). Presynaptic endocytic factors in autophagy and neurodegeneration. *Curr. Opin. Neurobiol.* 48, 153–159. doi: 10.1016/j.conb.2017.12.018

Bakula, D., Muller, A. J., Zuleger, T., Takacs, Z., Franz-Wachtel, M., Thost, A. K., et al. (2017). WIPI3 and WIPI4 beta-propellers are scaffolds for LKB1-AMPK-TSC signalling circuits in the control of autophagy. *Nat. Commun.* 8:15637. doi: 10.1038/ncomms15637

Beese, C. J., Brynjolfsdottir, S. H., and Frankel, L. B. (2019). Selective Autophagy of the Protein Homeostasis Machinery: ribophagy, Proteaphagy and ER-Phagy. *Front. Cell Dev. Biol.* 7:373. doi: 10.3389/fcell.2019.00373

Behrends, C., Sowa, M. E., Gygi, S. P., and Harper, J. W. (2010). Network organization of the human autophagy system. *Nature* 466, 68–76. doi: 10.1038/nature09204

Bezprozvanny, I., and Hiesinger, P. R. (2013). The synaptic maintenance problem: membrane recycling, Ca2+ homeostasis and late onset degeneration. *Mol. Neurodegener.* 8:23. doi: 10.1186/1750-1326-8-23

Binotti, B., Jahn, R., and Chua, J. J. (2016). Functions of Rab Proteins at Presynaptic Sites. *Cells* 5:7. doi: 10.3390/cells5010007

Binotti, B., Pavlos, N. J., Riedel, D., Wenzel, D., Vorbruggen, G., Schalk, A. M., et al. (2015). The GTPase Rab26 links synaptic vesicles to the autophagy pathway. *Elife* 4:e05597. doi: 10.7554/eLife.05597

Bockaert, J., and Marin, P. (2015). mTOR in Brain Physiology and Pathologies. *Physiol. Rev.* 95, 1157–1187. doi: 10.1152/physrev.00038.2014

Boecker, C. A., and Holzbaur, E. L. (2019). Vesicular degradation pathways in neurons: at the crossroads of autophagy and endo-lysosomal degradation. *Curr. Opin. Neurobiol.* 57, 94–101. doi: 10.1016/j.conb.2019.01.005

Boland, B., Kumar, A., Lee, S., Platt, F. M., Wegiel, J., Yu, W. H., et al. (2008). Autophagy induction and autophagosome clearance in neurons: relationship to autophagic pathology in Alzheimer's disease. *J. Neurosci.* 28, 6926–6937. doi: 10.1523/JNEUROSCI.0800-08.2008

Borchers, A. C., Langemeyer, L., and Ungermann, C. (2021). Who's in control? Principles of Rab GTPase activation in endolysosomal membrane trafficking and beyond. *J. Cell Biol.* 220:e202105120. doi: 10.1083/jcb.202105120

Boucrot, E., Ferreira, A. P., Almeida-Souza, L., Debard, S., Vallis, Y., Howard, G., et al. (2015). Endophilin marks and controls a clathrin-independent endocytic pathway. *Nature* 517, 460–465. doi: 10.1038/nature14067

Boyken, J., Gronborg, M., Riedel, D., Urlaub, H., Jahn, R., and Chua, J. J. (2013). Molecular profiling of synaptic vesicle docking sites reveals novel proteins but few differences between glutamatergic and GABAergic synapses. *Neuron* 78, 285–297. doi: 10.1016/j.neuron.2013.02.027

Brodin, L., and Shupliakov, O. (2018). Retromer in Synaptic Function and Pathology. *Front. Synaptic Neurosci.* 10:37. doi: 10.3389/fnsyn.2018.00037

Cai, C. Z., Yang, C., Zhuang, X. X., Yuan, N. N., Wu, M. Y., Tan, J. Q., et al. (2021). NRBF2 is a RAB7 effector required for autophagosome maturation and mediates the association of APP-CTFs with active form of RAB7 for degradation. *Autophagy* 17, 1112–1130. doi: 10.1080/15548627.2020.1760623

Cai, Q., Lu, L., Tian, J. H., Zhu, Y. B., Qiao, H., and Sheng, Z. H. (2010). Snapin-regulated late endosomal transport is critical for efficient autophagy-lysosomal function in neurons. *Neuron* 68, 73–86. doi: 10.1016/j.neuron.2010.09.022

Cano, R., and Tabares, L. (2016). The Active and Periactive Zone Organization and the Functional Properties of Small and Large Synapses. *Front. Synaptic Neurosci.* 8:12. doi: 10.3389/fnsyn.2016.00012

Cao, M., Milosevic, I., Giovedi, S., and De Camilli, P. (2014). Upregulation of Parkin in endophilin mutant mice. *J. Neurosci.* 34, 16544–16549. doi: 10.1523/JNEUROSCI.1710-14.2014

Cason, S. E., Carman, P. J., Van Duyne, C., Goldsmith, J., Dominguez, R., and Holzbaur, E. L. F. (2021). Sequential dynein effectors regulate axonal autophagosome motility in a maturation-dependent pathway. *J. Cell Biol.* 220:e202010179. doi: 10.1083/jcb.202010179

Catanese, A., Garrido, D., Walther, P., Roselli, F., and Boeckers, T. M. (2018). Nutrient limitation affects presynaptic structures through dissociable Bassoon autophagic degradation and impaired vesicle release. *J. Cereb. Blood Flow Metab.* 38, 1924–1939. doi: 10.1177/0271678X18786356

Chang, C., Jensen, L. E., and Hurley, J. H. (2021). Autophagosome biogenesis comes out of the black box. *Nat. Cell Biol.* 23, 450–456. doi: 10.1038/s41556-021-00669-y

Chang, N. C., Nguyen, M., Germain, M., and Shore, G. C. (2010). Antagonism of Beclin 1-dependent autophagy by BCL-2 at the endoplasmic reticulum requires NAF-1. *EMBO J.* 29, 606–618. doi: 10.1038/emboj.2009.369

Chen, D., Fan, W., Lu, Y., Ding, X., Chen, S., and Zhong, Q. (2012). A mammalian autophagosome maturation mechanism mediated by TECPR1 and the Atg12-Atg5 conjugate. *Mol. Cell* 45, 629–641. doi: 10.1016/j.molcel.2011.12.036

Chen, S., Mari, M., Parashar, S., Liu, D., Cui, Y., Reggiori, F., et al. (2020). Vps13 is required for the packaging of the ER into autophagosomes during ER-phagy. *Proc. Natl. Acad. Sci. U. S. A.* 117, 18530–18539. doi: 10.1073/pnas.2008923117

Cheng, X. T., Zhou, B., Lin, M. Y., Cai, Q., and Sheng, Z. H. (2015). Axonal autophagosomes recruit dynein for retrograde transport through fusion with late endosomes. *J. Cell Biol.* 209, 377–386. doi: 10.1083/jcb.201412046

Cheong, H., Lindsten, T., Wu, J., Lu, C., and Thompson, C. B. (2011). Ammonia-induced autophagy is independent of ULK1/ULK2 kinases. *Proc. Natl. Acad. Sci. U. S. A.* 108, 11121–11126. doi: 10.1073/pnas.1107969108

Citri, A., and Malenka, R. C. (2008). Synaptic plasticity: multiple forms, functions, and mechanisms. *Neuropsychopharmacology* 33, 18–41. doi: 10.1038/sj.npp.1301559

Cohen, L. D., and Ziv, N. E. (2017). Recent insights on principles of synaptic protein degradation. *F1000Res.* 6:675. doi: 10.12688/f1000research.10599.1

Cohen, L. D., and Ziv, N. E. (2019). Neuronal and synaptic protein lifetimes. *Curr. Opin. Neurobiol.* 57, 9–16. doi: 10.1016/j.conb.2018.12.007

Crawley, O., Opperman, K. J., Desbois, M., Adrados, I., Borgen, M. A., Giles, A. C., et al. (2019). Autophagy is inhibited by ubiquitin ligase activity in the nervous system. *Nat. Commun.* 10:5017. doi: 10.1038/s41467-019-12804-3

Cremona, O., Di Paolo, G., Wenk, M. R., Luthi, A., Kim, W. T., Takei, K., et al. (1999). Essential role of phosphoinositide metabolism in synaptic vesicle recycling. *Cell* 99, 179–188. doi: 10.1016/s0092-8674(00)81649-9

David, Y., Ziv, T., Admon, A., and Navon, A. (2010). The E2 ubiquitin-conjugating enzymes direct polyubiquitination to preferred lysines. *J. Biol. Chem.* 285, 8595–8604. doi: 10.1074/jbc.M109.089003

De Gregorio, C., Delgado, R., Ibacache, A., Sierralta, J., and Couve, A. (2017). Drosophila Atlastin in motor neurons is required for locomotion and presynaptic function. *J. Cell Sci.* 130, 3507–3516. doi: 10.1242/jcs.201657

De Leo, M. G., Staiano, L., Vicinanza, M., Luciani, A., Carissimo, A., Mutarelli, M., et al. (2016). Autophagosome-lysosome fusion triggers a lysosomal response mediated by TLR9 and controlled by OCRL. *Nat. Cell Biol.* 18, 839–850. doi: 10.1038/ncb3386

De Pace, R., Britt, D. J., Mercurio, J., Foster, A. M., Djavaherian, L., Hoffmann, V., et al. (2020). Synaptic Vesicle Precursors and Lysosomes Are Transported by Different Mechanisms in the Axon of Mammalian Neurons. *Cell Rep.* 31:107775. doi: 10.1016/j.celrep.2020.107775

Deng, Z., Purtell, K., Lachance, V., Wold, M. S., Chen, S., and Yue, Z. (2017). Autophagy Receptors and Neurodegenerative Diseases. *Trends Cell Biol.* 27, 491–504. doi: 10.1016/j.tcb.2017.01.001

Diao, J., Liu, R., Rong, Y., Zhao, M., Zhang, J., Lai, Y., et al. (2015). ATG14 promotes membrane tethering and fusion of autophagosomes to endolysosomes. *Nature* 520, 563–566. doi: 10.1038/nature14147

Dikic, I., and Elazar, Z. (2018). Mechanism and medical implications of mammalian autophagy. *Nat. Rev. Mol. Cell Biol.* 19, 349–364. doi: 10.1038/s41580-018-0003-4

Ding, M., and Shen, K. (2008). The role of the ubiquitin proteasome system in synapse remodeling and neurodegenerative diseases. *Bioessays* 30, 1075–1083. doi: 10.1002/bies.20843

Dresbach, T., Hempelmann, A., Spilker, C., tom Dieck, S., Altrock, W. D., Zuschratter, W., et al. (2003). Functional regions of the presynaptic cytomatrix protein bassoon: significance for synaptic targeting and cytomatrix anchoring. *Mol. Cell Neurosci.* 23, 279–291. doi: 10.1016/s1044743103000150

Farfel-Becker, T., Roney, J. C., Cheng, X. T., Li, S., Cuddy, S. R., and Sheng, Z. H. (2019). Neuronal Soma-Derived Degradative Lysosomes Are Continuously Delivered to Distal Axons to Maintain Local Degradation Capacity. *Cell Rep.* 28, 51–64e54. doi: 10.1016/j.celrep.2019.06.013

Farias, G. G., Guardia, C. M., De Pace, R., Britt, D. J., and Bonifacino, J. S. (2017). BORC/kinesin-1 ensemble drives polarized transport of lysosomes into the axon. *Proc. Natl. Acad. Sci. U. S. A.* 114, E2955–E2964. doi: 10.1073/pnas.1616363114

Fernandes, A. C., Uytterhoeven, V., Kuenen, S., Wang, Y. C., Slabbaert, J. R., Swerts, J., et al. (2014). Reduced synaptic vesicle protein degradation at lysosomes curbs TBC1D24/sky-induced neurodegeneration. *J. Cell Biol.* 207, 453–462. doi: 10.1083/jcb.201406026

Fiesel, F. C., Moussaud-Lamodiere, E. L., Ando, M., and Springer, W. (2014). A specific subset of E2 ubiquitin-conjugating enzymes regulate Parkin activation and mitophagy differently. *J. Cell Sci.* 127, 3488–3504. doi: 10.1242/jcs.147520

Fimia, G. M., Stoykova, A., Romagnoli, A., Giunta, L., Di Bartolomeo, S., Nardacci, R., et al. (2007). Ambra1 regulates autophagy and development of the nervous system. *Nature* 447, 1121–1125. doi: 10.1038/nature05925

Fornasiero, E. F., Mandad, S., Wildhagen, H., Alevra, M., Rammner, B., Keihani, S., et al. (2018). Precisely measured protein lifetimes in the mouse brain reveal differences across tissues and subcellular fractions. *Nat. Commun.* 9:4230. doi: 10.1038/s41467-018-06519-0

Fujioka, Y., Alam, J. M., Noshiro, D., Mouri, K., Ando, T., Okada, Y., et al. (2020). Phase separation organizes the site of autophagosome formation. *Nature* 578, 301–305. doi: 10.1038/s41586-020-1977-6

Garner, C. C., Kindler, S., and Gundelfinger, E. D. (2000). Molecular determinants of presynaptic active zones. *Curr. Opin. Neurobiol.* 10, 321–327. doi: 10.1016/s0959-4388(00)00093-3

Gatica, D., Lahiri, V., and Klionsky, D. J. (2018). Cargo recognition and degradation by selective autophagy. *Nat. Cell Biol.* 20, 233–242. doi: 10.1038/s41556-018-0037-z

Geisler, S., Vollmer, S., Golombek, S., and Kahle, P. J. (2014). The ubiquitin-conjugating enzymes UBE2N, UBE2L3 and UBE2D2/3 are essential for Parkin-dependent mitophagy. *J. Cell Sci.* 127, 3280–3293. doi: 10.1242/jcs.146035

George, A. A., Hayden, S., Stanton, G. R., and Brockerhoff, S. E. (2016). Arf6 and the 5'phosphatase of synaptojanin 1 regulate autophagy in cone photoreceptors. *Bioessays* 38, S119–S135. doi: 10.1002/bies.201670913

Giovedi, S., Ravanelli, M. M., Parisi, B., Bettegazzi, B., and Guarnieri, F. C. (2020). Dysfunctional Autophagy and Endolysosomal System in Neurodegenerative Diseases: relevance and Therapeutic Options. *Front. Cell Neurosci.* 14:602116. doi: 10.3389/fncel.2020.602116

Gowrisankaran, S., Houy, S., Del Castillo, J. G. P., Steubler, V., Gelker, M., Kroll, J., et al. (2020). Endophilin-A coordinates priming and fusion of neurosecretory vesicles via intersectin. *Nat. Commun.* 11:1266. doi: 10.1038/s41467-020-14993-8

Grill, B., Murphey, R. K., and Borgen, M. A. (2016). The PHR proteins: intracellular signaling hubs in neuronal development and axon degeneration. *Neural Dev.* 11:8. doi: 10.1186/s13064-016-0063-0

Grumati, P., Dikic, I., and Stolz, A. (2018). ER-phagy at a glance. *J. Cell Sci.* 131:jcs217364. doi: 10.1242/jcs.217364

Guardia, C. M., Jain, A., Mattera, R., Friefeld, A., Li, Y., and Bonifacino, J. S. (2021). RUSC2 and WDR47 oppositely regulate kinesin-1-dependent distribution of ATG9A to the cell periphery. *Mol. Biol. Cell* 32:ar25. doi: 10.1091/mbc.E21-06-0295

Guardia, C. M., Tan, X. F., Lian, T., Rana, M. S., Zhou, W., Christenson, E. T., et al. (2020). Structure of Human ATG9A, the Only Transmembrane Protein of the Core Autophagy Machinery. *Cell Rep.* 31:107837. doi: 10.1016/j.celrep.2020.107837

Gundelfinger, E. D., and Fejtova, A. (2012). Molecular organization and plasticity of the cytomatrix at the active zone. *Curr. Opin. Neurobiol.* 22, 423–430. doi: 10.1016/j.conb.2011.10.005

Gundelfinger, E. D., Kessels, M. M., and Qualmann, B. (2003). Temporal and spatial coordination of exocytosis and endocytosis. *Nat. Rev. Mol. Cell Biol.* 4, 127–139. doi: 10.1038/nrm1016

Gundelfinger, E. D., Reissner, C., and Garner, C. C. (2016). Role of Bassoon and Piccolo in Assembly and Molecular Organization of the Active Zone. *Front. Synaptic Neurosci.* 7:19. doi: 10.3389/fnsyn.2015.00019

Gupta, V. K., Pech, U., Bhukel, A., Fulterer, A., Ender, A., Mauermann, S. F., et al. (2016). Spermidine Suppresses Age-Associated Memory Impairment by Preventing Adverse Increase of Presynaptic Active Zone Size and Release. *PLoS Biol.* 14:e1002563. doi: 10.1371/journal.pbio.1002563

Hakim, V., Cohen, L. D., Zuchman, R., Ziv, T., and Ziv, N. E. (2016). The effects of proteasomal inhibition on synaptic proteostasis. *EMBO J.* 35, 2238–2262. doi: 10.15252/embj.201593594

Han, S., Jeong, Y. Y., Sheshadri, P., Su, X., and Cai, Q. (2020). Mitophagy regulates integrity of mitochondria at synapses and is critical for synaptic maintenance. *EMBO Rep.* 21:e49801. doi: 10.15252/embr.201949801

Harris, J. J., Jolivet, R., and Attwell, D. (2012). Synaptic energy use and supply. *Neuron* 75, 762–777. doi: 10.1016/j.neuron.2012.08.019

Haucke, V., Neher, E., and Sigrist, S. J. (2011). Protein scaffolds in the coupling of synaptic exocytosis and endocytosis. *Nat. Rev. Neurosci.* 12, 127–138. doi: 10.1038/nrn2948

Hernandez, D., Torres, C. A., Setlik, W., Cebrian, C., Mosharov, E. V., Tang, G., et al. (2012). Regulation of presynaptic neurotransmission by macroautophagy. *Neuron* 74, 277–284. doi: 10.1016/j.neuron.2012.02.020

Hill, S. E., and Colon-Ramos, D. A. (2019). A specific ATG-4 isoform is required for autophagic maturation and clearance in C. elegans neurons. *Autophagy* 15, 1840–1842. doi: 10.1080/15548627.2019.1632123

Hill, S. E., and Colon-Ramos, D. A. (2020). The Journey of the Synaptic Autophagosome: a Cell Biological Perspective. *Neuron* 105, 961–973. doi: 10.1016/j.neuron.2020.01.018

Hill, S. E., Kauffman, K. J., Krout, M., Richmond, J. E., Melia, T. J., and Colon-Ramos, D. A. (2019). Maturation and Clearance of Autophagosomes in Neurons Depends on a Specific Cysteine Protease Isoform, ATG-4.2. *Dev. Cell* 49, 251–266.e8. doi: 10.1016/j.devcel.2019.02.013

Hoffmann, S., Orlando, M., Andrzejak, E., Bruns, C., Trimbuch, T., Rosenmund, C., et al. (2019). Light-Activated ROS Production Induces Synaptic Autophagy. *J. Neurosci.* 39, 2163–2183. doi: 10.1523/JNEUROSCI.1317-18.2019

Hoffmann-Conaway, S., Brockmann, M. M., Schneider, K., Annamneedi, A., Rahman, K. A., Bruns, C., et al. (2020). Parkin contributes to synaptic vesicle autophagy in Bassoon-deficient mice. *Elife* 9:e56590. doi: 10.7554/eLife.56590

Hollenstein, D. M., and Kraft, C. (2020). Autophagosomes are formed at a distinct cellular structure. *Curr. Opin. Cell Biol.* 65, 50–57. doi: 10.1016/j.ceb.2020.02.012

Holtmaat, A. J., Trachtenberg, J. T., Wilbrecht, L., Shepherd, G. M., Zhang, X., Knott, G. W., et al. (2005). Transient and persistent dendritic spines in the neocortex in vivo. *Neuron* 45, 279–291. doi: 10.1016/j.neuron.2005.01.003

Hwang, J. Y., Yan, J., and Zukin, R. S. (2019). Autophagy and synaptic plasticity: epigenetic regulation. *Curr. Opin. Neurobiol.* 59, 207–212. doi: 10.1016/j.conb.2019.09.010

Hyttinen, J. M., Niittykoski, M., Salminen, A., and Kaarniranta, K. (2013). Maturation of autophagosomes and endosomes: a key role for Rab7. *Biochim. Biophys. Acta* 1833, 503–510. doi: 10.1016/j.bbamcr.2012.11.018

Imai, K., Hao, F., Fujita, N., Tsuji, Y., Oe, Y., Araki, Y., et al. (2016). Atg9A trafficking through the recycling endosomes is required for autophagosome formation. *J. Cell Sci.* 129, 3781–3791. doi: 10.1242/jcs.196196

Inaguma, Y., Ito, H., Iwamoto, I., Matsumoto, A., Yamagata, T., Tabata, H., et al. (2016). Morphological characterization of Class III phosphoinositide 3-kinase during mouse brain development. *Med. Mol. Morphol.* 49, 28–33. doi: 10.1007/s00795-015-0116-1

Inoshita, T., Arano, T., Hosaka, Y., Meng, H., Umezaki, Y., Kosugi, S., et al. (2017). Vps35 in cooperation with LRRK2 regulates synaptic vesicle endocytosis through the endosomal pathway in Drosophila. *Hum. Mol. Genet.* 26, 2933–2948. doi: 10.1093/hmg/ddx179

Issa, A. R., Sun, J., Petitgas, C., Mesquita, A., Dulac, A., Robin, M., et al. (2018). The lysosomal membrane protein LAMP2A promotes autophagic flux and prevents SNCA-induced Parkinson disease-like symptoms in the Drosophila brain. *Autophagy* 14, 1898–1910. doi: 10.1080/15548627.2018.1491489

Itakura, E., Kishi-Itakura, C., and Mizushima, N. (2012). The hairpin-type tail-anchored SNARE syntaxin 17 targets to autophagosomes for fusion with endosomes/lysosomes. *Cell* 151, 1256–1269. doi: 10.1016/j.cell.2012.11.001

Jaber, N., Mohd-Naim, N., Wang, Z., DeLeon, J. L., Kim, S., Zhong, H., et al. (2016). Vps34 regulates Rab7 and late endocytic trafficking through recruitment of the GTPase-activating protein Armus. *J. Cell Sci.* 129, 4424–4435. doi: 10.1242/jcs.192260

Ji, C., Tang, M., Zeidler, C., Hohfeld, J., and Johnson, G. V. (2019). BAG3 and SYNPO (synaptopodin) facilitate phospho-MAPT/Tau degradation via autophagy in neuronal processes. *Autophagy* 15, 1199–1213. doi: 10.1080/15548627.2019.1580096

Jiang, P., Nishimura, T., Sakamaki, Y., Itakura, E., Hatta, T., Natsume, T., et al. (2014). The HOPS complex mediates autophagosome-lysosome fusion through interaction with syntaxin 17. *Mol. Biol. Cell* 25, 1327–1337. doi: 10.1091/mbc.E13-08-0447

Jin, E. J., Kiral, F. R., Ozel, M. N., Burchardt, L. S., Osterland, M., Epstein, D., et al. (2018). Live Observation of Two Parallel Membrane Degradation Pathways at Axon Terminals. *Curr. Biol.* 28, 1027–1038.e4. doi: 10.1016/j.cub.2018.02.032

Kannan, M., Bayam, E., Wagner, C., Rinaldi, B., Kretz, P. F., Tilly, P., et al. (2017). WD40-repeat 47, a microtubule-associated protein, is essential for brain development and autophagy. *Proc. Natl. Acad. Sci. U. S. A.* 114, E9308–E9317. doi: 10.1073/pnas.1713625114

Kaushik, S., and Cuervo, A. M. (2018). The coming of age of chaperone-mediated autophagy. *Nat. Rev. Mol. Cell Biol.* 19, 365–381. doi: 10.1038/s41580-018-0001-6

Kawabe, H., and Stegmuller, J. (2021). The role of E3 ubiquitin ligases in synapse function in the healthy and diseased brain. *Mol. Cell Neurosci.* 112:103602. doi: 10.1016/j.mcn.2021.103602

Khaminets, A., Behl, C., and Dikic, I. (2016). Ubiquitin-Dependent And Independent Signals In Selective Autophagy. *Trends Cell Biol.* 26, 6–16. doi: 10.1016/j.tcb.2015.08.010

Khaminets, A., Heinrich, T., Mari, M., Grumati, P., Huebner, A. K., Akutsu, M., et al. (2015). Regulation of endoplasmic reticulum turnover by selective autophagy. *Nature* 522, 354–358. doi: 10.1038/nature14498

Kirkin, V., Lamark, T., Sou, Y. S., Bjorkoy, G., Nunn, J. L., Bruun, J. A., et al. (2009). A role for NBR1 in autophagosomal degradation of ubiquitinated substrates. *Mol. Cell* 33, 505–516. doi: 10.1016/j.molcel.2009.01.020

Kitada, T., Asakawa, S., Hattori, N., Matsumine, H., Yamamura, Y., Minoshima, S., et al. (1998). Mutations in the parkin gene cause autosomal recessive juvenile parkinsonism. *Nature* 392, 605–608. doi: 10.1038/33416

Kohrs, F. E., Daumann, I. M., Pavlovic, B., Jin, E. J., Kiral, F. R., Lin, S. C., et al. (2021). Systematic functional analysis of rab GTPases reveals limits of neuronal robustness to environmental challenges in flies. *Elife* 10:e59594. doi: 10.7554/eLife.59594

Komatsu, M., Wang, Q. J., Holstein, G. R., Friedrich, V. L. Jr., Iwata, J., Kominami, E., et al. (2007). Essential role for autophagy protein Atg7 in the maintenance of axonal homeostasis and the prevention of axonal degeneration. *Proc. Natl. Acad. Sci. U. S. A.* 104, 14489–14494. doi: 10.1073/pnas.0701311104

Kononenko, N. L., Classen, G. A., Kuijpers, M., Puchkov, D., Maritzen, T., Tempes, A., et al. (2017). Retrograde transport of TrkB-containing autophagosomes via the adaptor AP-2 mediates neuronal complexity and prevents neurodegeneration. *Nat. Commun.* 8:14819. doi: 10.1038/ncomms14819

Kononenko, N. L., Puchkov, D., Classen, G. A., Walter, A. M., Pechstein, A., Sawade, L., et al. (2014). Clathrin/AP-2 mediate synaptic vesicle reformation from endosome-like vacuoles but are not essential for membrane retrieval at central synapses. *Neuron* 82, 981–988. doi: 10.1016/j.neuron.2014.05.007

Koopmans, F., van Nierop, P., Andres-Alonso, M., Byrnes, A., Cijsouw, T., Coba, M. P., et al. (2019). SynGO: an Evidence-Based, Expert-Curated Knowledge Base for the Synapse. *Neuron* 103, 217–234.e4. doi: 10.1016/j.neuron.2019.05.002

Kroll, J., Jaime Tobon, L. M., Vogl, C., Neef, J., Kondratiuk, I., Konig, M., et al. (2019). Endophilin-A regulates presynaptic Ca^{2+} influx and synaptic vesicle recycling in auditory hair cells. *EMBO J.* 38:e100116. doi: 10.15252/embj.2018100116

Kuijpers, M., Azarnia Tehran, D., Haucke, V., and Soykan, T. (2020). The axonal endolysosomal and autophagic systems. *J. Neurochem*. 158, 589–602. doi: 10.1111/jnc.15287

Kuijpers, M., Kochlamazashvili, G., Stumpf, A., Puchkov, D., Swaminathan, A., Lucht, M. T., et al. (2021). Neuronal Autophagy Regulates Presynaptic Neurotransmission by Controlling the Axonal Endoplasmic Reticulum. *Neuron* 109, 299–313.e9. doi: 10.1016/j.neuron.2020.10.005

Kulkarni, A., Dong, A., Kulkarni, V. V., Chen, J., Laxton, O., Anand, A., et al. (2020). Differential regulation of autophagy during metabolic stress in astrocytes and neurons. *Autophagy* 16, 1651–1667. doi: 10.1080/15548627.2019.1703354

Kwon, Y. T., and Ciechanover, A. (2017). The Ubiquitin Code in the Ubiquitin-Proteasome System and Autophagy. *Trends Biochem. Sci.* 42, 873–886. doi: 10.1016/j.tibs.2017.09.002

Lamb, C. A., Nuhlen, S., Judith, D., Frith, D., Snijders, A. P., Behrends, C., et al. (2016). TBC1D14 regulates autophagy via the TRAPP complex and ATG9 traffic. *EMBO J.* 35, 281–301. doi: 10.15252/embj.201592695

Lang, T., Reiche, S., Straub, M., Bredschneider, M., and Thumm, M. (2000). Autophagy and the cvt pathway both depend on AUT9. *J. Bacteriol.* 182, 2125–2133. doi: 10.1128/JB.182.8.2125-2133.2000

Lassek, M., Weingarten, J., Einsfelder, U., Brendel, P., Muller, U., and Volknandt, W. (2013). Amyloid precursor proteins are constituents of the presynaptic active zone. *J. Neurochem.* 127, 48–56. doi: 10.1111/jnc.12358

Lazarevic, V., Schone, C., Heine, M., Gundelfinger, E. D., and Fejtova, A. (2011). Extensive Remodeling of the Presynaptic Cytomatrix upon Homeostatic Adaptation to Network Activity Silencing. *J. Neurosci.* 31, 10189–10200. doi: 10.1523/JNEUROSCI.2088-11.2011

Lee, E. J., and Tournier, C. (2011). The requirement of uncoordinated 51-like kinase 1 (ULK1) and ULK2 in the regulation of autophagy. *Autophagy* 7, 689–695. doi: 10.4161/auto.7.7.15450

Lee, W., and Kim, S. H. (2019). Autophagy at synapses in neurodegenerative diseases. *Arch. Pharm. Res.* 42, 407–415. doi: 10.1007/s12272-019-01148-7

Li, W., Bengtson, M. H., Ulbrich, A., Matsuda, A., Reddy, V. A., Orth, A., et al. (2008). Genome-wide and functional annotation of human E3 ubiquitin ligases identifies MULAN, a mitochondrial E3 that regulates the organelle's dynamics and signaling. *PLoS One* 3:e1487. doi: 10.1371/journal.pone.0001487

Liang, Y. (2019). Emerging Concepts and Functions of Autophagy as a Regulator of Synaptic Components and Plasticity. *Cells* 8:34. doi: 10.3390/cells8010034

Liang, Y., and Sigrist, S. (2018). Autophagy and proteostasis in the control of synapse aging and disease. *Curr. Opin. Neurobiol.* 48, 113–121. doi: 10.1016/j.conb.2017.12.006

Lieberman, O. J., and Sulzer, D. (2020). The Synaptic Autophagy Cycle. *J. Mol. Biol.* 432, 2589–2604. doi: 10.1016/j.jmb.2019.12.028

Lin, B. C., Higgins, N. R., Phung, T. H., and Monteiro, M. J. (2021). UBQLN proteins in health and disease with a focus on UBQLN2 in ALS/FTD. *FEBS J.* [Online ahead of print] doi: 10.1111/febs.16129

Linares, J. F., Duran, A., Yajima, T., Pasparakis, M., Moscat, J., and Diaz-Meco, M. T. (2013). K63 polyubiquitination and activation of mTOR by the p62-TRAF6 complex in nutrient-activated cells. *Mol. Cell* 51, 283–296. doi: 10.1016/j.molcel.2013.06.020

Liu, N., Zhao, H., Zhao, Y. G., Hu, J., and Zhang, H. (2021). Atlastin 2/3 regulate ER targeting of the ULK1 complex to initiate autophagy. *J. Cell Biol.* 220:e202012091. doi: 10.1083/jcb.202012091

Lüningschrör, P., Binotti, B., Dombert, B., Heimann, P., Perez-Lara, A., Slotta, C., et al. (2017). Plekhg5-regulated autophagy of synaptic vesicles reveals a pathogenic mechanism in motoneuron disease. *Nat. Commun.* 8:678. doi: 10.1038/s41467-017-00689-z

Lüningschrör, P., and Sendtner, M. (2018). Autophagy in the presynaptic compartment. *Curr. Opin. Neurobiol.* 51, 80–85. doi: 10.1016/j.conb.2018.02.023

MacLeod, D. A., Rhinn, H., Kuwahara, T., Zolin, A., Di Paolo, G., McCabe, B. D., et al. (2013). RAB7L1 interacts with LRRK2 to modify intraneuronal protein sorting and Parkinson's disease risk. *Neuron* 77, 425–439. doi: 10.1016/j.neuron.2012.11.033

Maday, S., and Holzbaur, E. L. (2014). Autophagosome biogenesis in primary neurons follows an ordered and spatially regulated pathway. *Dev. Cell* 30, 71–85. doi: 10.1016/j.devcel.2014.06.001

Maday, S., and Holzbaur, E. L. (2016). Compartment-Specific Regulation of Autophagy in Primary Neurons. *J. Neurosci.* 36, 5933–5945. doi: 10.1523/JNEUROSCI.4401-15.2016

Maeda, S., Yamamoto, H., Kinch, L. N., Garza, C. M., Takahashi, S., Otomo, C., et al. (2020). Structure, lipid scrambling activity and role in autophagosome formation of ATG9A. *Nat. Struct. Mol. Biol.* 27, 1194–1201. doi: 10.1038/s41594-020-00520-2

Malik, B. R., Maddison, D. C., Smith, G. A., and Peters, O. M. (2019). Autophagic and endo-lysosomal dysfunction in neurodegenerative disease. *Mol. Brain* 12:100. doi: 10.1186/s13041-019-0504-x

Marat, A. L., and Haucke, V. (2016). Phosphatidylinositol 3-phosphates-at the interface between cell signalling and membrane traffic. *EMBO J.* 35, 561–579. doi: 10.15252/embj.201593564

Markson, G., Kiel, C., Hyde, R., Brown, S., Charalabous, P., Bremm, A., et al. (2009). Analysis of the human E2 ubiquitin conjugating enzyme protein interaction network. *Genome Res.* 19, 1905–1911. doi: 10.1101/gr.093963.109

Martens, S., and Fracchiolla, D. (2020). Activation and targeting of ATG8 protein lipidation. *Cell Discov.* 6:23. doi: 10.1038/s41421-020-0155-1

Martin, S., Papadopulos, A., Tomatis, V. M., Sierecki, E., Malintan, N. T., Gormal, R. S., et al. (2014). Increased polyubiquitination and proteasomal degradation of a Munc18-1 disease-linked mutant causes temperature-sensitive defect in exocytosis. *Cell Rep.* 9, 206–218. doi: 10.1016/j.celrep.2014.08.059

Matoba, K., Kotani, T., Tsutsumi, A., Tsuji, T., Mori, T., Noshiro, D., et al. (2020). Atg9 is a lipid scramblase that mediates autophagosomal membrane expansion. *Nat. Struct. Mol. Biol.* 27, 1185–1193. doi: 10.1038/s41594-020-00518-w

Matoba, K., and Noda, N. N. (2020). Secret of Atg9: lipid scramblase activity drives de novo autophagosome biogenesis. *Cell Death Differ.* 27, 3386–3388. doi: 10.1038/s41418-020-00663-1

Matsui, T., and Fukuda, M. (2013). Rab12 regulates mTORC1 activity and autophagy through controlling the degradation of amino-acid transporter PAT4. *EMBO Rep.* 14, 450–457. doi: 10.1038/embor.2013.32

McCabe, M. P., Cullen, E. R., Barrows, C. M., Shore, A. N., Tooke, K. I., Laprade, K. A., et al. (2020). Genetic inactivation of mTORC1 or mTORC2 in neurons reveals distinct functions in glutamatergic synaptic transmission. *Elife* 9:e51440. doi: 10.7554/eLife.51440

McMahon, H. T., and Boucrot, E. (2011). Molecular mechanism and physiological functions of clathrin-mediated endocytosis. *Nat. Rev. Mol. Cell Biol.* 12, 517–533. doi: 10.1038/nrm3151

Menzies, F. M., Fleming, A., Caricasole, A., Bento, C. F., Andrews, S. P., Ashkenazi, A., et al. (2017). Autophagy and Neurodegeneration: pathogenic Mechanisms and Therapeutic Opportunities. *Neuron* 93, 1015–1034. doi: 10.1016/j.neuron.2017.01.022

Mercer, T. J., and Tooze, S. A. (2021). The ingenious ULKs: expanding the repertoire of the ULK complex with phosphoproteomics. *Autophagy* 17, 4491–4493. doi: 10.1080/15548627.2021.1968615

Michel, P. P., Hirsch, E. C., and Hunot, S. (2016). Understanding Dopaminergic Cell Death Pathways in Parkinson Disease. *Neuron* 90, 675–691. doi: 10.1016/j.neuron.2016.03.038

Milosevic, I., Giovedi, S., Lou, X., Raimondi, A., Collesi, C., Shen, H., et al. (2011). Recruitment of endophilin to clathrin-coated pit necks is required for efficient vesicle uncoating after fission. *Neuron* 72, 587–601. doi: 10.1016/j.neuron.2011.08.029

Minowa-Nozawa, A., Nozawa, T., Okamoto-Furuta, K., Kohda, H., and Nakagawa, I. (2017). Rab35 GTPase recruits NDP52 to autophagy targets. *EMBO J.* 36, 2790–2807. doi: 10.15252/embj.201796463

Mizushima, N., Levine, B., Cuervo, A. M., and Klionsky, D. J. (2008). Autophagy fights disease through cellular self-digestion. *Nature* 451, 1069–1075. doi: 10.1038/nature06639

Mizushima, N., Yamamoto, A., Matsui, M., Yoshimori, T., and Ohsumi, Y. (2004). In vivo analysis of autophagy in response to nutrient starvation using transgenic mice expressing a fluorescent autophagosome marker. *Mol. Biol. Cell* 15, 1101–1111. doi: 10.1091/mbc.e03-09-0704

Montenegro-Venegas, C., Annamneedi, A., Hoffmann-Conaway, S., Gundelfinger, E. D., and Garner, C. C. (2020). BSN (bassoon) and PRKN/parkin in concert control presynaptic vesicle autophagy. *Autophagy* 16, 1732–1733. doi: 10.1080/15548627.2020.1801259

Montenegro-Venegas, C., Fienko, S., Anni, D., Pina-Fernandez, E., Frischknecht, R., and Fejtova, A. (2021). Bassoon inhibits proteasome activity via interaction

with PSMB4. *Cell Mol. Life Sci.* 78, 1545–1563. doi: 10.1007/s00018-020-03590-z

Montes-Fernandez, M. A., Perez-Villegas, E. M., Garcia-Gonzalo, F. R., Pedrazza, L., Rosa, J. L., de Toledo, G. A., et al. (2020). The HERC1 ubiquitin ligase regulates presynaptic membrane dynamics of central synapses. *Sci. Rep.* 10:12057. doi: 10.1038/s41598-020-68970-8

Moreau, K., Ravikumar, B., Puri, C., and Rubinsztein, D. C. (2012). Arf6 promotes autophagosome formation via effects on phosphatidylinositol 4,5-bisphosphate and phospholipase D. *J. Cell Biol.* 196, 483–496. doi: 10.1083/jcb.201110114

Mouatt-Prigent, A., Muriel, M. P., Gu, W. J., El Hachimi, K. H., Lucking, C. B., Brice, A., et al. (2004). Ultrastructural localization of parkin in the rat brainstem, thalamus and basal ganglia. *J. Neural Transm.* 111, 1209–1218. doi: 10.1007/s00702-004-0144-9

Murdoch, J. D., Rostosky, C. M., Gowrisankaran, S., Arora, A. S., Soukup, S. F., Vidal, R., et al. (2016). Endophilin-A Deficiency Induces the Foxo3a-Fbxo32 Network in the Brain and Causes Dysregulation of Autophagy and the Ubiquitin-Proteasome System. *Cell Rep.* 17, 1071–1086. doi: 10.1016/j.celrep.2016.09.058

Nandi, D., Tahiliani, P., Kumar, A., and Chandu, D. (2006). The ubiquitin-proteasome system. *J. Biosci* 31, 137–155. doi: 10.1007/BF02705243

Negrete-Hurtado, A., Overhoff, M., Bera, S., De Bruyckere, E., Schatzmuller, K., Kye, M. J., et al. (2020). Autophagy lipidation machinery regulates axonal microtubule dynamics but is dispensable for survival of mammalian neurons. *Nat. Commun.* 11:1535. doi: 10.1038/s41467-020-15287-9

Neisch, A. L., Neufeld, T. P., and Hays, T. S. (2017). A STRIPAK complex mediates axonal transport of autophagosomes and dense core vesicles through PP2A regulation. *J. Cell Biol.* 216, 441–461. doi: 10.1083/jcb.201606082

Nixon, R. A., Yang, D. S., and Lee, J. H. (2008). Neurodegenerative lysosomal disorders: a continuum from development to late age. *Autophagy* 4, 590–599. doi: 10.4161/auto.6259

Noda, T., Kim, J., Huang, W. P., Baba, M., Tokunaga, C., Ohsumi, Y., et al. (2000). Apg9p/Cvt7p is an integral membrane protein required for transport vesicle formation in the Cvt and autophagy pathways. *J. Cell Biol.* 148, 465–480. doi: 10.1083/jcb.148.3.465

Okerlund, N. D., Schneider, K., Leal-Ortiz, S., Montenegro-Venegas, C., Kim, S. A., Garner, L. C., et al. (2017). Bassoon Controls Presynaptic Autophagy through Atg5. *Neuron* 93, 897–913.e7. doi: 10.1016/j.neuron.2017.01.026

Orii, M., Tsuji, T., Ogasawara, Y., and Fujimoto, T. (2021). Transmembrane phospholipid translocation mediated by Atg9 is involved in autophagosome formation. *J. Cell Biol.* 220:e202009194. doi: 10.1083/jcb.202009194

Overhoff, M., De Bruyckere, E., and Kononenko, N. L. (2021). Mechanisms of neuronal survival safeguarded by endocytosis and autophagy. *J. Neurochem.* 157, 263–296. doi: 10.1111/jnc.15194

Palamiuc, L., Ravi, A., and Emerling, B. M. (2020). Phosphoinositides in autophagy: current roles and future insights. *FEBS J.* 287, 222–238. doi: 10.1111/febs.15127

Pan, P. Y., Zhu, Y., Shen, Y., and Yue, Z. (2019). Crosstalk between presynaptic trafficking and autophagy in Parkinson's disease. *Neurobiol. Dis.* 122, 64–71. doi: 10.1016/j.nbd.2018.04.020

Perez-Villegas, E. M., Perez-Rodriguez, M., Negrete-Diaz, J. V., Ruiz, R., Rosa, J. L., de Toledo, G. A., et al. (2020). HERC1 Ubiquitin Ligase Is Required for Hippocampal Learning and Memory. *Front. Neuroanat.* 14:592797. doi: 10.3389/fnana.2020.592797

Piccoli, G., and Volta, M. (2021). LRRK2 along the Golgi and lysosome connection: a jamming situation. *Biochem. Soc. Trans.* 49, 2063–2072. doi: 10.1042/BST20201146

Pielot, R., Smalla, K. H., Muller, A., Landgraf, P., Lehmann, A. C., Eisenschmidt, E., et al. (2012). SynProt: a Database for Proteins of Detergent-Resistant Synaptic Protein Preparations. *Front. Synaptic Neurosci.* 4:1. doi: 10.3389/fnsyn.2012.00001

Puri, C., Vicinanza, M., and Rubinsztein, D. C. (2018). Phagophores evolve from recycling endosomes. *Autophagy* 14, 1475–1477. doi: 10.1080/15548627.2018.1482148

Pyo, J. O., Jang, M. H., Kwon, Y. K., Lee, H. J., Jun, J. I., Woo, H. N., et al. (2005). Essential roles of Atg5 and FADD in autophagic cell death: dissection of autophagic cell death into vacuole formation and cell death. *J. Biol. Chem.* 280, 20722–20729. doi: 10.1074/jbc.M413934200

Qiao, Q., Ma, L., Li, W., Tsai, J. W., Yang, G., and Gan, W. B. (2016). Long-term stability of axonal boutons in the mouse barrel cortex. *Dev. Neurobiol.* 76, 252–261. doi: 10.1002/dneu.22311

Rao, Y., Perna, M. G., Hofmann, B., Beier, V., and Wollert, T. (2016). The Atg1-kinase complex tethers Atg9-vesicles to initiate autophagy. *Nat. Commun.* 7:10338. doi: 10.1038/ncomms10338

Ravikumar, B., Moreau, K., Jahreiss, L., Puri, C., and Rubinsztein, D. C. (2010). Plasma membrane contributes to the formation of pre-autophagosomal structures. *Nat. Cell Biol.* 12, 747–757. doi: 10.1038/ncb2078

Ravussin, A., Brech, A., Tooze, S. A., and Stenmark, H. (2021). The phosphatidylinositol 3-phosphate-binding protein SNX4 controls ATG9A recycling and autophagy. *J. Cell Sci.* 134:jcs250670. doi: 10.1242/jcs.250670

Rinetti, G. V., and Schweizer, F. E. (2010). Ubiquitination acutely regulates presynaptic neurotransmitter release in mammalian neurons. *J. Neurosci.* 30, 3157–3166. doi: 10.1523/JNEUROSCI.3712-09.2010

Rizalar, F. S., Roosen, D. A., and Haucke, V. (2021). A Presynaptic Perspective on Transport and Assembly Mechanisms for Synapse Formation. *Neuron* 109, 27–41. doi: 10.1016/j.neuron.2020.09.038

Rubinsztein, D. C. (2006). The roles of intracellular protein-degradation pathways in neurodegeneration. *Nature* 443, 780–786. doi: 10.1038/nature05291

Rubinsztein, D. C., and Nixon, R. A. (2010). Rapamycin induces autophagic flux in neurons. *Proc. Natl. Acad. Sci. U. S. A.* 107:E181. doi: 10.1073/pnas.1014633107

Saudou, F., and Humbert, S. (2016). The Biology of Huntingtin. *Neuron* 89, 910–926. doi: 10.1016/j.neuron.2016.02.003

Sawa-Makarska, J., Baumann, V., Coudevylle, N., von Bulow, S., Nogellova, V., Abert, C., et al. (2020). Reconstitution of autophagosome nucleation defines Atg9 vesicles as seeds for membrane formation. *Science* 369:eaaz7714. doi: 10.1126/science.aaz7714

Seto, S., Sugaya, K., Tsujimura, K., Nagata, T., Horii, T., and Koide, Y. (2013). Rab39a interacts with phosphatidylinositol 3-kinase and negatively regulates autophagy induced by lipopolysaccharide stimulation in macrophages. *PLoS One* 8:e83324. doi: 10.1371/journal.pone.0083324

Sheehan, P., and Waites, C. L. (2019). Coordination of synaptic vesicle trafficking and turnover by the Rab35 signaling network. *Small GTPases* 10, 54–63. doi: 10.1080/21541248.2016.1270392

Sheehan, P., Zhu, M., Beskow, A., Vollmer, C., and Waites, C. L. (2016). Activity-Dependent Degradation of Synaptic Vesicle Proteins Requires Rab35 and the ESCRT Pathway. *J. Neurosci.* 36, 8668–8686. doi: 10.1523/JNEUROSCI.0725-16.2016

Shehata, M., and Inokuchi, K. (2014). Does autophagy work in synaptic plasticity and memory?. *Rev. Neurosci.* 25, 543–557. doi: 10.1515/revneuro-2014-0002

Shen, Z. Q., Huang, Y. L., Teng, Y. C., Wang, T. W., Kao, C. H., Yeh, C. H., et al. (2021). CISD2 maintains cellular homeostasis. *Biochim. Biophys. Acta Mol. Cell Res.* 1868:118954. doi: 10.1016/j.bbamcr.2021.118954

Sheng, Y., Song, Y., Li, Z., Wang, Y., Lin, H., Cheng, H., et al. (2018). RAB37 interacts directly with ATG5 and promotes autophagosome formation via regulating ATG5-12-16 complex assembly. *Cell Death Differ.* 25, 918–934. doi: 10.1038/s41418-017-0023-1

Soukup, S. F., Kuenen, S., Vanhauwaert, R., Manetsberger, J., Hernandez-Diaz, S., Swerts, J., et al. (2016). A LRRK2-Dependent EndophilinA Phosphoswitch Is Critical for Macroautophagy at Presynaptic Terminals. *Neuron* 92, 829–844. doi: 10.1016/j.neuron.2016.09.037

Soukup, S. F., Vanhauwaert, R., and Verstreken, P. (2018). Parkinson's disease: convergence on synaptic homeostasis. *EMBO J.* 37:e98960. doi: 10.15252/embj.201898960

Soukup, S. F., and Verstreken, P. (2017). EndoA/Endophilin-A creates docking stations for autophagic proteins at synapses. *Autophagy* 13, 971–972. doi: 10.1080/15548627.2017.1286440

Soykan, T., Haucke, V., and Kuijpers, M. (2021). Mechanism of synaptic protein turnover and its regulation by neuronal activity. *Curr. Opin. Neurobiol.* 69, 76–83. doi: 10.1016/j.conb.2021.02.006

Stavoe, A. K., Gopal, P. P., Gubas, A., Tooze, S. A., and Holzbaur, E. L. (2019). Expression of WIPI2B counteracts age-related decline in autophagosome biogenesis in neurons. *Elife* 8:e44219. doi: 10.7554/eLife.44219

Stavoe, A. K., Hill, S. E., Hall, D. H., and Colon-Ramos, D. A. (2016). KIF1A/UNC-104 Transports ATG-9 to Regulate Neurodevelopment and Autophagy at Synapses. *Dev. Cell* 38, 171–185. doi: 10.1016/j.devcel.2016.06.012

Stavoe, A. K. H., and Holzbaur, E. L. F. (2018). Axonal autophagy: mini-review for autophagy in the CNS. *Neurosci. Lett.* 697, 17–23. doi: 10.1016/j.neulet.2018.03.025

Stavoe, A. K. H., and Holzbaur, E. L. F. (2019). Autophagy in Neurons. *Annu. Rev. Cell Dev. Biol.* 35, 477–500. doi: 10.1146/annurev-cellbio-100818-125242

Sturner, E., and Behl, C. (2017). The Role of the Multifunctional BAG3 Protein in Cellular Protein Quality Control and in Disease. *Front. Mol. Neurosci.* 10:177. doi: 10.3389/fnmol.2017.00177

Sudhof, T. C. (2012). The presynaptic active zone. *Neuron* 75, 11–25. doi: 10.1016/j.neuron.2012.06.012

Sumitomo, A., Yukitake, H., Hirai, K., Horike, K., Ueta, K., Chung, Y., et al. (2018). Ulk2 controls cortical excitatory-inhibitory balance via autophagic regulation of p62 and GABAA receptor trafficking in pyramidal neurons. *Hum. Mol. Genet.* 27, 3165–3176. doi: 10.1093/hmg/ddy219

Tada, H., Okano, H. J., Takagi, H., Shibata, S., Yao, I., Matsumoto, M., et al. (2010). Fbxo45, a novel ubiquitin ligase, regulates synaptic activity. *J. Biol Chem.* 285, 3840–3849. doi: 10.1074/jbc.M109.046284

Takahashi, Y., Meyerkord, C. L., Hori, T., Runkle, K., Fox, T. E., Kester, M., et al. (2011). Bif-1 regulates Atg9 trafficking by mediating the fission of Golgi membranes during autophagy. *Autophagy* 7, 61–73. doi: 10.4161/auto.7.1.14015

Takamori, S., Holt, M., Stenius, K., Lemke, E. A., Gronborg, M., Riedel, D., et al. (2006). Molecular anatomy of a trafficking organelle. *Cell* 127, 831–846. doi: 10.1016/j.cell.2006.10.030

Tang, G., Gudsnuk, K., Kuo, S. H., Cotrina, M. L., Rosoklija, G., Sosunov, A., et al. (2014). Loss of mTOR-dependent macroautophagy causes autistic-like synaptic pruning deficits. *Neuron* 83, 1131–1143. doi: 10.1016/j.neuron.2014.07.040

Taoufiq, Z., Ninov, M., Villar-Briones, A., Wang, H. Y., Sasaki, T., Roy, M. C., et al. (2020). Hidden proteome of synaptic vesicles in the mammalian brain. *Proc. Natl. Acad. Sci. U. S. A.* 117, 33586–33596. doi: 10.1073/pnas.2011870117

Taylor, M., and Alessi, D. R. (2020). Advances in elucidating the function of leucine-rich repeat protein kinase-2 in normal cells and Parkinson's disease. *Curr. Opin. Cell Biol.* 63, 102–113. doi: 10.1016/j.ceb.2020.01.001

Tian, X., Teng, J., and Chen, J. (2021). New insights regarding SNARE proteins in autophagosome-lysosome fusion. *Autophagy* 17, 2680–2688. doi: 10.1080/15548627.2020.1823124

Tian, Y., Chang, J. C., Fan, E. Y., Flajolet, M., and Greengard, P. (2013). Adaptor complex AP2/PICALM, through interaction with LC3, targets Alzheimer's APP-CTF for terminal degradation via autophagy. *Proc. Natl. Acad. Sci. U. S. A.* 110, 17071–17076. doi: 10.1073/pnas.1315110110

Tian, Y., Chang, J. C., Greengard, P., and Flajolet, M. (2014). The convergence of endosomal and autophagosomal pathways: implications for APP-CTF degradation. *Autophagy* 10, 694–696. doi: 10.4161/auto.27802

Tomoda, T., Yang, K., and Sawa, A. (2020). Neuronal Autophagy in Synaptic Functions and Psychiatric Disorders. *Biol. Psychiatry* 87, 787–796. doi: 10.1016/j.biopsych.2019.07.018

Toyofuku, T., Morimoto, K., Sasawatari, S., and Kumanogoh, A. (2015). Leucine-Rich Repeat Kinase 1 Regulates Autophagy through Turning On TBC1D2-Dependent Rab7 Inactivation. *Mol. Cell Biol.* 35, 3044–3058. doi: 10.1128/MCB.00085-15

Tsvetkov, A. S., Miller, J., Arrasate, M., Wong, J. S., Pleiss, M. A., and Finkbeiner, S. (2010). A small-molecule scaffold induces autophagy in primary neurons and protects against toxicity in a Huntington disease model. *Proc. Natl. Acad. Sci. U. S. A.* 107, 16982–16987. doi: 10.1073/pnas.1004498107

Uytterhoeven, V., Lauwers, E., Maes, I., Miskiewicz, K., Melo, M. N., Swerts, J., et al. (2015). Hsc70-4 Deforms Membranes to Promote Synaptic Protein Turnover by Endosomal Microautophagy. *Neuron* 88, 735–748. doi: 10.1016/j.neuron.2015.10.012

van der Beek, J., Jonker, C., van der Welle, R., Liv, N., and Klumperman, J. (2019). CORVET, CHEVI and HOPS - multisubunit tethers of the endo-lysosomal system in health and disease. *J. Cell Sci.* 132:jcs189134. doi: 10.1242/jcs.189134

Vanhauwaert, R., Kuenen, S., Masius, R., Bademosi, A., Manetsberger, J., Schoovaerts, N., et al. (2017). The SAC1 domain in synaptojanin is required for autophagosome maturation at presynaptic terminals. *EMBO J.* 36, 1392–1411. doi: 10.15252/embj.201695773

Verderio, C., Cagnoli, C., Bergami, M., Francolini, M., Schenk, U., Colombo, A., et al. (2012). TI-VAMP/VAMP7 is the SNARE of secretory lysosomes contributing to ATP secretion from astrocytes. *Biol. Cell* 104, 213–228. doi: 10.1111/boc.201100070

Verstreken, P., Koh, T. W., Schulze, K. L., Zhai, R. G., Hiesinger, P. R., Zhou, Y., et al. (2003). Synaptojanin is recruited by endophilin to promote synaptic vesicle uncoating. *Neuron* 40, 733–748. doi: 10.1016/s0896-6273(03)00644-5

Vijayan, V., and Verstreken, P. (2017). Autophagy in the presynaptic compartment in health and disease. *J. Cell Biol.* 216, 1895–1906. doi: 10.1083/jcb.201611113

Vukoja, A., Rey, U., Petzoldt, A. G., Ott, C., Vollweiter, D., Quentin, C., et al. (2018). Presynaptic Biogenesis Requires Axonal Transport of Lysosome-Related Vesicles. *Neuron* 99, 1216–1232.e7. doi: 10.1016/j.neuron.2018.08.004

Waites, C. L., Leal-Ortiz, S. A., Okerlund, N., Dalke, H., Fejtova, A., Altrock, W. D., et al. (2013). Bassoon and Piccolo maintain synapse integrity by regulating protein ubiquitination and degradation. *EMBO J.* 32, 954–969. doi: 10.1038/emboj.2013.27

Wan, H., Wang, Q., Chen, X., Zeng, Q., Shao, Y., Fang, H., et al. (2020). WDR45 contributes to neurodegeneration through regulation of ER homeostasis and neuronal death. *Autophagy* 16, 531–547. doi: 10.1080/15548627.2019.1630224

Wang, B., Iyengar, R., Li-Harms, X., Joo, J. H., Wright, C., Lavado, A., et al. (2018). The autophagy-inducing kinases, ULK1 and ULK2, regulate axon guidance in the developing mouse forebrain via a noncanonical pathway. *Autophagy* 14, 796–811. doi: 10.1080/15548627.2017.1386820

Wang, T., Martin, S., Papadopulos, A., Harper, C. B., Mavlyutov, T. A., Niranjan, D., et al. (2015). Control of autophagosome axonal retrograde flux by presynaptic activity unveiled using botulinum neurotoxin type a. *J. Neurosci.* 35, 6179–6194. doi: 10.1523/JNEUROSCI.3757-14.2015

Wang, Y., and Le, W. D. (2019). Autophagy and Ubiquitin-Proteasome System. *Adv. Exp. Med. Biol.* 1206, 527–550. doi: 10.1007/978-981-15-0602-4_25

Wang, Y. C., Lauwers, E., and Verstreken, P. (2017). Presynaptic protein homeostasis and neuronal function. *Curr. Opin. Genet. Dev.* 44, 38–46. doi: 10.1016/j.gde.2017.01.015

Watanabe, S., Mamer, L. E., Raychaudhuri, S., Luvsanjav, D., Eisen, J., Trimbuch, T., et al. (2018). Synaptojanin and Endophilin Mediate Neck Formation during Ultrafast Endocytosis. *Neuron* 98, 1184–1197e1186. doi: 10.1016/j.neuron.2018.06.005

Wei, F., and Duan, Y. (2019). Crosstalk between Autophagy and Nanomaterials: internalization, Activation, Termination. *Adv. Biosyst.* 3:e1800259. doi: 10.1002/adbi.201800259

Weingarten, J., Lassek, M., Mueller, B. F., Rohmer, M., Lunger, I., Baeumlisberger, D., et al. (2014). The proteome of the presynaptic active zone from mouse brain. *Mol. Cell Neurosci.* 59, 106–118. doi: 10.1016/j.mcn.2014.02.003

Wetzel, L., Blanchard, S., Rama, S., Beier, V., Kaufmann, A., and Wollert, T. (2020). TECPR1 promotes aggrephagy by direct recruitment of LC3C autophagosomes to lysosomes. *Nat. Commun.* 11:2993. doi: 10.1038/s41467-020-16689-5

Whang, M. I., Tavares, R. M., Benjamin, D. I., Kattah, M. G., Advincula, R., Nomura, D. K., et al. (2017). The Ubiquitin Binding Protein TAX1BP1 Mediates Autophagasome Induction and the Metabolic Transition of Activated T Cells. *Immunity* 46, 405–420. doi: 10.1016/j.immuni.2017.02.018

Wilfling, F., Lee, C. W., Erdmann, P. S., Zheng, Y., Sherpa, D., Jentsch, S., et al. (2020). A Selective Autophagy Pathway for Phase-Separated Endocytic Protein Deposits. *Mol. Cell* 80, 764–778.e7. doi: 10.1016/j.molcel.2020.10.030

Wojnacki, J., and Galli, T. (2018). A new actin-binding domain glues autophagy together. *J. Biol. Chem.* 293, 4575–4576. doi: 10.1074/jbc.H118.002041

Wojnacki, J., Nola, S., Bun, P., Cholley, B., Filippini, F., Presse, M. T., et al. (2021). Role of VAMP7-dependent secretion of reticulon 3 in neurite growth. *Cell Rep.* 35:109006. doi: 10.1016/j.celrep.2021.109006

Wu, X., Ganzella, M., Zhou, J., Zhu, S., Jahn, R., and Zhang, M. (2021). Vesicle Tethering on the Surface of Phase-Separated Active Zone Condensates. *Mol. Cell* 81, 13–24.e7. doi: 10.1016/j.molcel.2020.10.029

Xing, R., Zhou, H., Jian, Y., Li, L., Wang, M., Liu, N., et al. (2021). The Rab7 effector WDR91 promotes autophagy-lysosome degradation in neurons by regulating lysosome fusion. *J. Cell Biol.* 220:e202007061. doi: 10.1083/jcb.202007061

Xu, J., Fotouhi, M., and McPherson, P. S. (2015). Phosphorylation of the exchange factor DENND3 by ULK in response to starvation activates Rab12 and induces autophagy. *EMBO Rep.* 16, 709–718. doi: 10.15252/embr.201440006

Xu, J., Kozlov, G., McPherson, P. S., and Gehring, K. (2018). A PH-like domain of the Rab12 guanine nucleotide exchange factor DENND3 binds actin and is required for autophagy. *J. Biol. Chem.* 293, 4566–4574. doi: 10.1074/jbc.RA117.001446

Xuan, Z., Manning, L., Nelson, J., Richmond, J. E., Colon-Ramos, D. A., Shen, K., et al. (2017). Clarinet (CLA-1), a novel active zone protein required for synaptic vesicle clustering and release. *Elife* 6:e29276. doi: 10.7554/eLife.29276

Xuan, Z., Yang, S., Hill, S. E., Clark, B., Manning, L., and Colón-Ramos, D. A. (2021). The active zone protein Clarinet regulates ATG-9 trafficking at synapses and presynaptic autophagy. *bioRxiv* [Preprint]. doi: 10.1101/2021.08.19.457026

Yang, S., Park, D., Manning, L., Hill, S. E., Cao, M., Xuan, Z., et al. (2020). Presynaptic autophagy is coupled to the synaptic vesicle cycle via ATG-9. *bioRxiv* [Preprint]. doi: 10.1101/2020.12.28.424508

Yang, Y., and Calakos, N. (2013). Presynaptic long-term plasticity. *Front. Synaptic Neurosci.* 5:8. doi: 10.3389/fnsyn.2013.00008

Yao, I., Takagi, H., Ageta, H., Kahyo, T., Sato, S., Hatanaka, K., et al. (2007). SCRAPPER-dependent ubiquitination of active zone protein RIM1 regulates synaptic vesicle release. *Cell* 130, 943–957. doi: 10.1016/j.cell.2007.06.052

Yla-Anttila, P., Mikkonen, E., Happonen, K. E., Holland, P., Ueno, T., Simonsen, A., et al. (2015). RAB24 facilitates clearance of autophagic compartments during basal conditions. *Autophagy* 11, 1833–1848. doi: 10.1080/15548627.2015.1086522

Young, A. R., Chan, E. Y., Hu, X. W., Kochl, R., Crawshaw, S. G., High, S., et al. (2006). Starvation and ULK1-dependent cycling of mammalian Atg9 between the TGN and endosomes. *J. Cell Sci.* 119, 3888–3900. doi: 10.1242/jcs.03172

Young, J. E., Martinez, R. A., and La Spada, A. R. (2009). Nutrient deprivation induces neuronal autophagy and implicates reduced insulin signaling in neuroprotective autophagy activation. *J. Biol. Chem.* 284, 2363–2373. doi: 10.1074/jbc.M806088200

Conflict of Interest: The authors declare that the research was conducted in the absence of any commercial or financial relationships that could be construed as a potential conflict of interest.

Publisher's Note: All claims expressed in this article are solely those of the authors and do not necessarily represent those of their affiliated organizations, or those of the publisher, the editors and the reviewers. Any product that may be evaluated in this article, or claim that may be made by its manufacturer, is not guaranteed or endorsed by the publisher.

frontiers | Frontiers in Synaptic Neuroscience

REVIEW
published: 04 April 2022
doi: 10.3389/fnsyn.2022.861215

cAMP-Dependent Synaptic Plasticity at the Hippocampal Mossy Fiber Terminal

Meishar Shahoha[1,2†], Ronni Cohen[1,2†], Yoav Ben-Simon[3] and Uri Ashery[1,2*]*

[1] Faculty of Life Sciences, School of Neurobiology, Biochemistry and Biophysics, Tel Aviv University, Tel Aviv, Israel, [2] Sagol School of Neuroscience, Tel Aviv University, Tel Aviv, Israel, [3] Department of Neurophysiology, Vienna Medical University, Vienna, Austria

Cyclic adenosine monophosphate (cAMP) is a crucial second messenger involved in both pre- and postsynaptic plasticity in many neuronal types across species. In the hippocampal mossy fiber (MF) synapse, cAMP mediates presynaptic long-term potentiation and depression. The main cAMP-dependent signaling pathway linked to MF synaptic plasticity acts via the activation of the protein kinase A (PKA) molecular cascade. Accordingly, various downstream putative synaptic PKA target proteins have been linked to cAMP-dependent MF synaptic plasticity, such as synapsin, rabphilin, synaptotagmin-12, RIM1a, tomosyn, and P/Q-type calcium channels. Regulating the expression of some of these proteins alters synaptic release probability and calcium channel clustering, resulting in short- and long-term changes to synaptic efficacy. However, despite decades of research, the exact molecular mechanisms by which cAMP and PKA exert their influences in MF terminals remain largely unknown. Here, we review current knowledge of different cAMP catalysts and potential downstream PKA-dependent molecular cascades, in addition to non-canonical cAMP-dependent but PKA-independent cascades, which might serve as alternative, compensatory or competing pathways to the canonical PKA cascade. Since several other central synapses share a similar form of presynaptic plasticity with the MF, a better description of the molecular mechanisms governing MF plasticity could be key to understanding the relationship between the transcriptional and computational levels across brain regions.

Keywords: cAMP, PKA, synaptic plasticity, mossy fiber synapse, LTP, forskolin-induced potentiation

OPEN ACCESS

Edited by:
Lucia Tabares, Seville University, Spain

Reviewed by:
Tommaso Patriarchi, University of Zurich, Switzerland
Simon Chamberland, NYU Grossman School of Medicine, United States

***Correspondence:**
Yoav Ben-Simon
yoav.bensimon@meduniwien.ac.at
Uri Ashery
uriashery@gmail.com

† These authors have contributed equally to this work

Received: *24 January 2022*
Accepted: *23 February 2022*
Published: *04 April 2022*

Citation:
Shahoha M, Cohen R, Ben-Simon Y and Ashery U (2022) cAMP-Dependent Synaptic Plasticity at the Hippocampal Mossy Fiber Terminal. Front. Synaptic Neurosci. 14:861215. doi: 10.3389/fnsyn.2022.861215

CYCLIC ADENOSINE MONO-PHOSPHATE-AND PROTEIN KINASE A -DEPENDENT MECHANISMS OF SYNAPTIC PLASTICITY

The molecular mechanisms of synaptic transmission have been intensely studied in recent decades, resulting in the functional characterization of many synaptic proteins involved in vesicle docking, priming, fusion and recycling. These includes the SNARE proteins, synaptotagmin, regulatory proteins, such as RAB3a, Munc13, Munc18, tomosyn, and active zone proteins, such as Piccolo, Bassoon and RIM1a, as well as several structural and endocytotic proteins (Dresbach et al., 2001; Südhof, 2013; Rizo, 2018; Chanaday et al., 2019). In many cases, the order of interactions involving these proteins, as well as their roles at different stages of the synaptic vesicle cycle, have been extensively described (Brunger et al., 2019). However, the exact contribution of these proteins to synaptic plasticity is still poorly understood. Several second messengers, such as calcium (Ca^{2+}) and

cyclic adenosine mono-phosphate (cAMP), are known to produce short- and long-term changes in vesicle release probability (P_r), the number of release sites, and the clustering of calcium channels at the presynaptic terminal. However, whereas the role of Ca^{2+} in regulating both pre- and postsynaptic processes has been described in detail (Zucker, 1999; Schneggenburger and Neher, 2005; Lisman et al., 2007; Kavalali, 2020) the identities of cAMP downstream effectors, especially in the presynaptic terminal, are still largely unknown.

cAMP is a ubiquitous second-messenger found in the three domains of life, namely Eukarya, Bacteria and Archaea (Gehring, 2010; Kalia et al., 2013). A direct link between cAMP, synaptic transmission and potentiation was first demonstrated in a seminal work showing that exposing sensory neurons of the sea mollusk *Aplysia* to cAMP molecules resulted in increased neurotransmitter release, in turn affecting a short-term memory process known as sensitization (Cedar et al., 1972; Klein and Kandel, 1980; Schacher et al., 1988; Kandel et al., 2000). Later studies extended the connection between cAMP and synaptic plasticity to other model organisms, such as *Drosophila* (Davis et al., 1998) and mice (Nguyen and Kandel, 1997; Wong et al., 1999), where cAMP exposure was also shown to lead to an increase in P_r (Ariel et al., 2013; Fukaya et al., 2021), vesicle redistribution (Orlando et al., 2021) and changes in Ca^{2+} channel clustering (Midorikawa and Sakaba, 2017).

Until recently, research into the molecular cascades activated by cAMP focused on a single downstream effector—protein kinase A (PKA) (Corbin and Krebs, 1969). PKA is a tetrameric enzyme consisting of two regulatory and two catalytic subunits (Bauman and Scott, 2002; Taylor et al., 2012). Binding of cAMP to the PKA complex results in detachment of the regulatory subunits from the catalytic subunits, thereby removing inhibition from the latter (Turnham and Scott, 2016; Mucignat-Caretta and Caretta, 2020). Subsequently, the catalytic subunits of PKA are able to phosphorylate a myriad of protein targets, thus modifying their functions (Waltereit and Weller, 2003; Kandel, 2012). In *Aplysia*, injection of the PKA catalytic subunits yielded similar effects to those observed following injection of cAMP alone (Castellucci et al., 1980), leading to a prevailing consensus that PKA is the principal, and perhaps sole downstream effector of cAMP. In the mammalian brain, the hippocampal mossy fiber (MF) synapse was found to be particularly prone to cAMP-mediated regulation of neurotransmitter release, as will be discussed in detail below.

THE MOSSY FIBERS PATHWAY, CYCLIC ADENOSINE MONO-PHOSPHATE AND PROTEIN KINASE A-DEPENDENT PLASTICITY

The hippocampus is a central cortical structure in the mammalian brain known to mediate key mnemonic and cognitive functions. The hippocampus is classically divided into three unidirectional pathways, collectively known as the trisynaptic circuit. According to this notion of hippocampal information flow, neuronal activity originating in the adjacent entorhinal cortex (EC) is relayed via the perforant pathway (PP), primarily to the hippocampal dentate gyrus (DG), where it is processed and relayed to CA3 and CA2 pyramidal neurons via the mossy fibers (MF) pathway. From these regions, which are internally connected in an auto-associative network, the information is delivered almost exclusively to CA1 pyramidal neurons via Schaffer's collaterals (SC), which finally redistribute the processed signals across cortical and sub-cortical regions (**Figures 1A,B**; Lieberman, 1965; Witter, 2007). The MF synapse, corresponding to the second synapse in this circuit, is generally considered to be an important locus for the formation, storage and retrieval of contextual and episodic memories in mammals (Lieberman, 1965; Neves et al., 2008; Lisman et al., 2017), through a computational process termed "pattern separation" (Leutgeb et al., 2007; Schmidt et al., 2012; Rolls, 2013).

The MF pathway is characterized by non-myelinated axons that originate in dentate gyrus granule cells (DGCs) and travel immediately above and below the CA3 *Stratum Pyramidale (S.P.)*, forming the *Stratum Lucidum (S.L.)*. There, each axon forms about a dozen enormous synapses (up to several micrometers in diameter (Rollenhagen et al., 2007), termed mossy fiber boutons (MFB), onto the large proximal dendritic spines of CA3 neurons termed thorny excrescences (TEs) (Amaral and Dent, 1981; **Figures 1C,D**). A single large MFB contains 25 active zones on average and harbors some 16,000 synaptic vesicles, of which only about 600 are located within 60 nm from the AZ and are considered part of the readily releasable pool of vesicles, while an additional 4,000 vesicles are found at a short distance of 200 nm from the AZ and are considered part of the recycling pool (Hallermann et al., 2003; Rollenhagen et al., 2007). Though it has been speculated that this organization might be essential for supporting the various plasticity processes taking place at the MFB (Rollenhagen et al., 2007), the reason for such extreme redundancy of synaptic vesicles remains unclear.

In contrast to its prominent size, the MF synapse is characterized by a very low basal P_r (Jonas et al., 1993) and as a result, following a single action potential (AP) elicits weak excitatory post-synaptic potentials (EPSPs) in CA3 neurons (Lysetskiy et al., 2005). However, following a short train of high-frequency APs, the accumulation of Ca^{2+} in the MF synapse produces a dramatic increase in P_r, manifested as robust short-term synaptic facilitation (**Figures 1E,F**). This facilitation, together with the strategic location of the synapse in proximity to the CA3 somata, and its multiple release sites, allow a single MF synapse to elicit APs in its postsynaptic target following a short train of APs (Henze et al., 2000; Evstratova and Tóth, 2014; Chamberland et al., 2018). This trait has led researchers to describe the MF synapse as a "conditional detonator" or a "high-pass filter," due to the tendency of the synapse to selectively propagate high-frequency activity patterns (Pelkey and McBain, 2005; Vyleta et al., 2016).

While other hippocampal synapses have been shown to display primarily postsynaptic N-methyl-D-aspartate receptor (NMDAR)-dependent long-term potentiation (LTP) (Bliss and Collingridge, 2013), MF synapses are characterized by

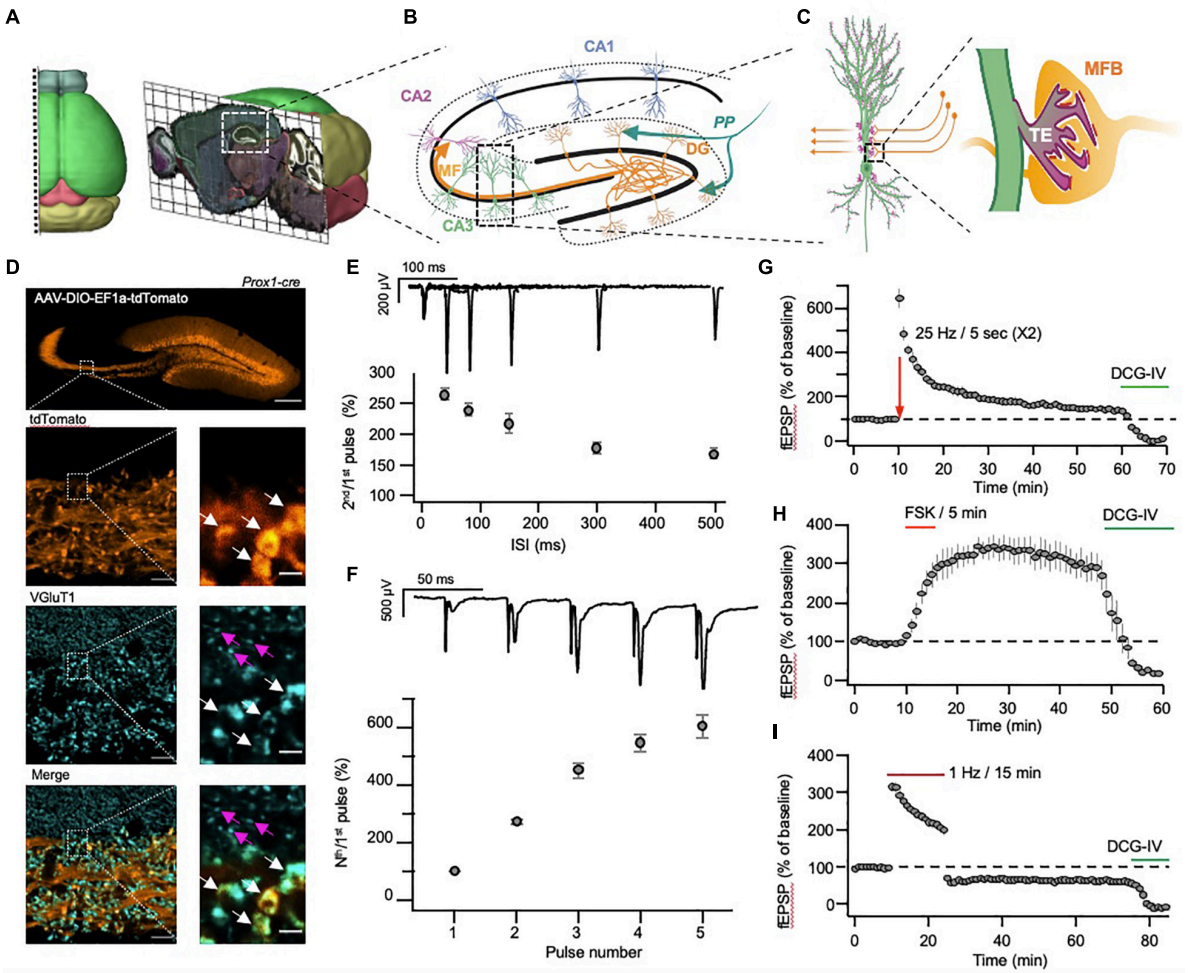

FIGURE 1 | Morphological and physiological properties of the hippocampal mossy fiber pathway. **(A)** Three-dimensional visualization of the anatomical location of the dorsal hippocampus in mouse brain. **(B)** Schematic representation of hippocampal sub-regions, with emphasis on the input and output to and from the DG. **(C)** Schematic representation of the unique anatomical and morphological structure of the MF-CA3 synapse. Insert: mossy fiber bouton (MFB, orange) and postsynaptic thorny excrescence (TE, light green). **(D)** A representative confocal image of the hippocampus following injection of AAV-DIO-EF1a-tdTomato into the DG of a Prox1-cre transgenic mouse (top). The images below show the MF tract at higher magnification (tdTomato, orange), following immunolabeling for VGluT1 (VGluT1, cyan), and demonstrate the size differences between the large MF terminals (white arrows) and the small S.R. terminals (magenta arrows). Scale bars represent 200, 10 and 2 μm for the top, right column and left column images, respectively. **(E,F)** MF-CA3 short-term plasticity demonstrated by measurements of paired-pulse **(E)** and a high-frequency burst **(F)** stimulation, delivered electrically to the DG while recording fEPSPs from the *S.L.* **(G,H)** MF-CA3 long-term plasticity demonstrated by measurements of FSK- **(G)** and tetanus- **(H)** induced potentiation, with subsequent application of DCG-IV, blocking synaptic transmission. **(I).** MF-CA3 long-term plasticity (LTD) following a prolonged low-frequency stimulation, with subsequent application of DCG-IV, blocking synaptic transmission. Images in **(A)** were adapted from the Allen institute's Brain Explorer 2 (http://mouse.brain-map.org/static/brainexplorer).

NMDAR-independent LTP (Zalutsky and Nicoll, 1990; Johnston et al., 1992; Huang et al., 1994; Salin et al., 1996b; Castillo, 2012). Long-term potentiation in the MF synapse (MF-LTP, **Figure 1G**) manifests as a long-term increase in the presynaptic P_r and is mediated by cAMP, evident by the robust potentiation observed also following application of the adenylyl cyclase (AC) agonist forskolin (FSK, **Figure 1H**; Weisskopf et al., 1994; Salin et al., 1996b; Villacres et al., 1998; Castillo, 2012). Using pharmacological tools that control cAMP levels, it was demonstrated that both cAMP and PKA are important for the induction and maintenance of MF-LTP (Huang et al., 1994; Weisskopf et al., 1994). These studies were followed by genetic perturbation of PKA subunits (Huang et al., 1995) that provided genetic evidence for the involvement of PKA in MF-LTP.

Like the MF-synapse, several other synapses in the mammalian brain display NMDAR independent presynaptic forms of LTP (Yang and Calakos, 2013). These include corticothalamic (Castro-Alamancos and Calcagnotto, 1999), thalamocortical (Andrade-Talavera et al., 2013), cortical interneuron (Chen et al., 2009; Sarihi et al., 2012) and subiculo-cortical synapses (Behr et al., 2009), as well as synapses of cerebellar parallel fibers (Salin et al., 1996a; Chen and Regehr, 1997; Bender et al., 2009), and several different inputs to the lateral amygdala (López de Armentia and Sah, 2007;

Fourcaudot et al., 2008). However, due to vast morphological and molecular differences between these synapses and the MF, it remains to be determined exactly how similar are the molecular mechanisms that underlie their presynaptic LTP.

In addition to MF-LTP, which is induced by a short train of high-frequency activity, long-term depression in the MF synapse (MF-LTD) can also be elicited, by applying a prolonged (15 min) low-frequency stimulation (**Figure 1I**). Like MF-LTP, MF-LTD is also NMDAR-independent, however, it is mediated by a reduction in cAMP levels and is manifested as a decrease in P_r (Tzounopoulos et al., 1998; Kobayashi, 2010). MF-LTD induction can be blocked by the metabotropic glutamate receptor (mGluR) antagonist MCPG (Fitzjohn et al., 1998) or *mGluR2/3* KO (Lyon et al., 2011). At the same time, application of the mGluR2/3 agonist DCG-IV completely blocks MF synaptic transmission synapses (**Figures 1G–I**), while having little to no effect on other hippocampal synapses (Yoshino et al., 1996; Kamiya and Ozawa, 1999). Since mGluR2/3 inhibits cAMP synthesis, it can be inferred that bidirectional changes in cAMP concentration control P_r at the MF synapse and can lead to LTP or LTD, depending on the direction of the change.

FSK is one of the main pharmacological tools for elevating cAMP levels that leads to synaptic potentiation. However, FSK affects both the presynaptic terminal and the postsynaptic cells, in addition to astrocytes, and is, therefore, not specific for the presynaptic terminal. New recently implemented tools, such as photoactivated adenylyl cyclase bPAC from the bacteria Beggiatoa (Stierl et al., 2011; Raffelberg et al., 2013) or pharmacogenetic tools, like Designer Receptors Exclusively Activated by Designer Drugs DREADDs (Roth, 2016; Campbell and Marchant, 2018), now enable control of cAMP levels with substantially better cellular, spatial and temporal precision than possible using pharmacological agents, such as FSK. Recently, photoactivation of a synaptically-translocated bPAC, termed SynaptoPAC, selectively in MF synapses, enabled cAMP synthesis with physiological kinetics and led to long-term changes in P_r, mimicking the effects of tetanus-induced LTP (Kees et al., 2021; Oldani et al., 2021). Such tools, together with new cAMP sensors (Odaka et al., 2014; Harada et al., 2017; Ohta et al., 2018; Linghu et al., 2020) will allow better understanding of the effects of cAMP on synaptic physiology at MF synapses.

MF synapses are characterized by additional forms of plasticity that should be briefly mentioned. Although MF-LTP is NMDA-independent, there are indications that presynaptic NMDA receptors support a different form of LTP in the MF synapse, which is dependent on Protein Kinase C (PKC) (Kwon and Castillo, 2008; Lituma et al., 2021). Furthermore, it should be noted that in addition to the large presynaptic MF terminal on pyramidal CA3 neurons, MF axons also innervate *S.L.* interneurons (SLINs) by small *en-passant* varicosities, also known as filopodial extensions (Acsády et al., 1998). These synapses on interneurons contribute to feed-forward inhibition and exhibit different forms of synaptic plasticity mediated by mGluR7 in a process only partially mediated by cAMP (Toth et al., 2000; Pelkey et al., 2008). MF-SLIN synapses also undergo cAMP-dependent plasticity changes, albeit in a unique way. These synapses reverse their polarity in an activity-dependent manner, with the internalization of mGluR7s serving as the switch between two states. In response to high frequency stimulation, naïve-state MF-IN synapses undergo cAMP-independent presynaptic LTD, whereas synapses that have internalized mGluR7s (LTD, resulting from previous high-frequency stimulation) undergo cAMP-dependent presynaptic LTP (Pelkey et al., 2008). This mechanism might allow initial bursts of APs to propagate uninhibited to CA3, yet prevents subsequent bursts from generating runaway excitation (Pelkey et al., 2008).

In addition, most previous research suggests that postsynaptic depolarization is not necessary for MF synapse LTP induction, although under certain conditions, such depolarization could still exert influence over presynaptic physiology (Castillo et al., 2012; Makani et al., 2021; Vandael et al., 2021). This implies that synchronous activation of pre- and postsynaptic neurons is not necessarily a prerequisite for this form of LTP, suggesting that MF synapse LTP is not Hebbian in nature. Together, these unique properties of the MF synapse are likely to support roles served by the hippocampus, such as the suggested role of MFs in spatial orientation through a mnemonic function known as pattern separation (Yassa and Stark, 2011; Schmidt et al., 2012; Rolls, 2013).

The ROLE OF Ca^{2+} AND ADENYLYL CYCLASE 1 IN MOSSY FIBERS PLASTICITY

As in most other synapses, vesicle release at the MF terminal depends on Ca^{2+} influx through voltage-dependent calcium channels (VGCC), such as the P/ Q-, N-, L-, and R-type calcium channels (Li et al., 2007; Vyleta and Jonas, 2014; Shin et al., 2018). In addition, the activation of presynaptic NMDA receptors during high frequency activity (Carta et al., 2018; Lituma et al., 2021) and release of Ca^{2+} from internal stores (Lauri et al., 2003; Scott and Rusakov, 2006) also contribute to Ca^{2+} dynamics at the MF synapse. These dynamic changes in presynaptic calcium drive MF short- and long-term synaptic plasticity (Castillo et al., 1994; Regehr et al., 1994; Kapur et al., 1998; Breustedt et al., 2003; Pelkey et al., 2006; Li et al., 2007; Vyleta and Jonas, 2014). In a mature MFB, it was demonstrated that synaptic vesicles are only loosely coupled to Ca^{2+} channels, allowing for a highly dynamic P_r range (Vyleta and Jonas, 2014; Böhme et al., 2018; Brockmann et al., 2019; Orlando et al., 2021). Changes in distances between calcium channels and the synaptic machinery, in channel density, and/or in concentrations of endogenous calcium buffers can enable rapid and dynamic modulation of synaptic strength, as discussed below.

In addition to its direct effects on vesicle fusion and neurotransmitter release, Ca^{2+} also exerts a powerful effect on MF synaptic strength through the Ca^{2+} sensor calmodulin and activation of AC, leading to increased levels of cAMP. Numerous studies have pointed to cAMP as the primary mediator of MF-LTP, given how the application of the potent AC agonist FSK or of cAMP analogs, such as Sp-8-CPT-cAMPs, elicit a strong and sustained increase in the basal P_r (Weisskopf et al., 1994;

Lonart et al., 1998; Tzounopoulos et al., 1998; Wang et al., 2003; Kaeser-Woo et al., 2013; Hashimotodani et al., 2017). In the mammalian brain, ten different isoforms of the *Adcy* gene encode for ten distinct AC enzymes (AC1-10). These are classified primarily according to their main upstream activator (Hanoune and Defer, 2001) and are differentially distributed across brain regions and cell types (Sanabra and Mengod, 2011). In the mouse hippocampus, *Adcy* isoforms 1 and 2 are strongly and selectively expressed in the DG but not in CA3 neurons (**Figures 2A,B**), and while KO of *Adcy8* was shown to affect MF synaptic plasticity (Wang et al., 2003), comparatively low mRNA levels in the DG (**Figures 2A,B**) suggest that further experiments are needed to validate these results. Of the two most abundant AC isoforms in the DG, AC1 is known to be activated by an increase in Ca^{2+} and its downstream effector calmodulin (Hanoune and Defer, 2001), whereas AC2 is largely Ca^{2+}-insensitive and is instead activated by PKC and the Gq protein-associated βγ subunit complex (Hanoune and Defer, 2001; Willoughby and Cooper, 2007; Halls and Cooper, 2011). Alongside these basic properties, additional evidence further supports a central role for AC1 in the MF synapse. First, AC1 is inhibited by the G_i cascade, such as that associated with mGluR2/3, leading to a reduction in cAMP levels (Sadana and Dessauer, 2009), an effect which potentially underlies the complete silencing of

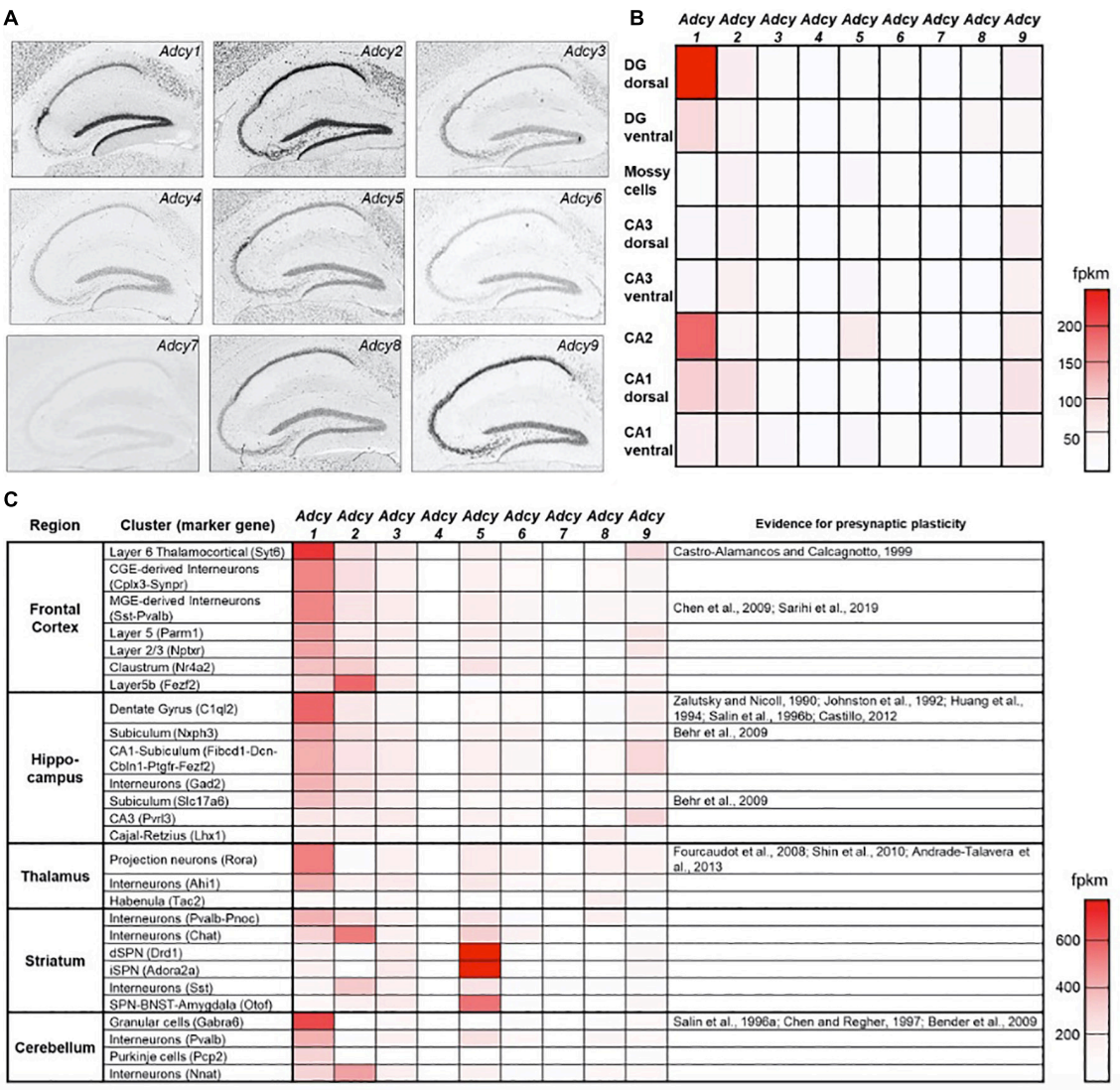

FIGURE 2 | Expression of AC isoforms across hippocampal sub-regions. **(A)** Distribution pattern of the ten AC isoforms in the hippocampus of adult mice following *in situ* hybridization (Lein et al., 2007). **(B)** A heat map showing the relative mRNA expression levels of *Adcy* isoforms 1–9 across different hippocampal sub-regions. fpkm—fragments per kilobase of transcript per million mapped reads (Cembrowski et al., 2016). **(C)** as in **(B)**, a heat map showing relative *Adcy* isoform 1–9 mRNA expression levels for the main cell clusters across several central brain regions. The right-most column specifies for which cell clusters evidence supports the existence of presynaptic LTP (Saunders et al., 2018). Data in **(A)** were adapted from the Allen institutes ISH brain atlas (http://mouse.brain-map.org/), data in **(B)** were adapted from hipposeq.janelia.org/and data in **(C)** were adapted from Dropviz.org.

MF synaptic transmission following application of DCG-IV. Furthermore, *Adcy1* KO mice were found to exhibit impaired MF-LTP but not PP-LTP and while MF short-term plasticity and FSK-induced potentiation were not altered in *Adcy1* KO mice (Villacres et al., 1998; **Table 1**), this effect could have still been mediated by other AC isoforms, being that FSK is not a selective AC1 agonist. Last, immunolabeling of AC1 in the hippocampus revealed it to be enriched in the hilus and mossy fibers (Conti et al., 2007), implying that AC1 is preferentially trafficked to MF synaptic domains.

Together, these observations suggest that AC1 is the dominant isoform mediating Ca^{2+} dependent increases, or mGluR2/3-dependent decreases in cAMP levels, to control MF synaptic plasticity. Interestingly, the distribution of AC1 mRNA across brain regions reveals strong correlation between cell types in which *Adcy1* is enriched, with such synapses having been previously shown to express a presynaptic form of LTP (**Figure 2C**). This correlation can potentially support the notion that shared molecular mechanisms, driven by up-stream AC1 activation, underlies presynaptic LTP across cell types. In the hippocampus, this conjuncture could apply to neurons of the CA2 sub-region, in which *Adcy1* is also enriched. While previous studies suggested that CA2 neurons do not display any form of postsynaptic plasticity (Zhao et al., 2007), the nature of the presynaptic mechanisms at play in their synapses onto CA1 neurons, corresponding to their principal output (Kohara et al., 2014), have not yet been investigated. Further experiments are required to determine whether cAMP- and PKA-dependent presynaptic LTP can also be induced there, and if so, one can ask what sort of functional relevance this might have on information processing in this pathway.

In addition to the Ca^{2+}-mediated activation of AC1, increased cAMP levels could also potentially arise from direct activation of AC2 and AC9 through the alpha subunit of G_s protein-coupled receptors (Hanoune and Defer, 2001), such as group 1 serotonin receptors (Hamblin et al., 1998), the beta sub-class of noradrenaline receptors (Johnson, 2006) and dopamine D1-like receptors (Girault and Greengard, 2004). In contrast, other G_i protein-coupled neuromodulator receptors, such as group 1 and 5 serotonin receptors, the alpha2 sub-class of noradrenergic receptors and the dopamine D2 receptor, would have an opposite effect on cAMP production, potentially supporting MF-LTD. It has previously been shown that neuromodulators can indeed exert effects on MF synaptic transmission in various manners (Yang and Calakos, 2013; Nozaki et al., 2016; Kobayashi et al., 2020). This contradictory mode of action of different receptors in response to the same ligand and their differential expression patterns across hippocampal sub-regions make it difficult to determine what would be the net effect of each receptor on synaptic transmission and plasticity. In addition, it has yet to be shown where these receptors are trafficked within the cells and whether they are enriched in presynaptic domains. Such knowledge is essential for determining whether neuromodulators could have a direct effect on neurotransmitter release at the MF-CA3 synapse, or whether the observed effects of neuromodulator application during recordings arise from changes in DGC somatic excitability or from various influences on CA3 postsynaptic domains. The use of specific cAMP sensors (Odaka et al., 2014; Harada et al., 2017; Ohta et al., 2018; Linghu et al., 2020) that can be targeted to the synapse will allow characterization of the spatiotemporal distribution of cMAP and can clarify the above debates.

MOLECULAR MECHANISMS OF PROTEIN KINASE A-DEPENDENT MOSSY FIBERS PLASTICITY

As mentioned above, MF-LTP depends on cAMP levels, with this effect having largely been attributed to downstream activation of PKA. This assessment was further supported by the observation that LTP is absent following KO of the PKA catalytic subunit-encoding gene (Huang et al., 1995) and that application of KT5720, a selective blocker of the PKA catalytic subunit, prevents MF-LTP (Weisskopf et al., 1994). In addition, it was suggested that FSK-induced potentiation interacts with LTP, as the two processes were shown to mutually occlude one another (Weisskopf et al., 1994). These findings led to the suggestion that activation of PKA is an essential step in MF-LTP. Accordingly, research conducted in recent decades identified several putative synaptic PKA targets thought to be involved in cAMP-dependent synaptic plasticity at MF synapses. These include RAB3a-interacting molecule 1a (RIM1a) and rabphilin, both acting through the vesicular GTPase Ras-related

TABLE 1 | The effects of manipulation of proteins on hippocampal mossy fiber synaptic plasticity.

KO/KD	STP	LTP	Fsk-induced potentiation (FIP)	Citations
Rab3A	Not affected	Abolished	Not affected	Castillo et al., 1997
RIM1a	Not affected	Abolished	Not affected	Castillo et al., 2002
Rabphilin	Not affected	No effect	Not determined	Schlüter et al., 1999
Synapsin	Not determined	No effect	Not affected	Spillane et al., 1995
Synaptotagmin-12	Not affected	Abolished	Impaired	Kaeser-Woo et al., 2013
Tomosyn	Impaired	Abolished	Impaired	Ben-Simon et al., 2015
PKAα	Not determined	Impaired	Not determined	De Lecea et al., 1998
AKAP7	Not determined	Abolished	Not determined	Jones et al., 2016
Epac2	Not affected	Abolished	Impaired	Fernandes et al., 2015
AC1	Not affected	Impaired	Not affected	Villacres et al., 1998

protein Rab-3A (RAB3a) (Takai et al., 1996; Wang et al., 2001), as well as synapsin (Bykhovskaia, 2011), synaptotagmin-12 (Maximov et al., 2007), and tomosyn-1 (Ashery et al., 2009). The involvement of these proteins in cAMP-dependent plasticity was mainly studied by examining the effects of deletion or mutations in each of the encoding genes on short-term plasticity (STP), FSK-induced potentiation, LTP and LTD (**Table 1** and **Figure 3**).

Earlier efforts paid substantial attention to the small vesicular GTPase RAB3a, which is seemingly involved in vesicle mobilization and fusion (Geppert et al., 1997; Lonart and Südhof, 1998). While RAB3a is not considered a putative PKA target, it is known to be regulated by other PKA targets, such as RIM1a and rabphilin and has, therefore, been linked to the PKA-mediated cascade. *RAB3a* KO was shown to block LTP, impair LTD formation in MF synapse and led to memory impairment (D'Adamo et al., 2004), although neither STP nor FSK-induced potentiation were affected (Castillo et al., 1997). These effects were thought to be the result of an enhanced effect of Ca^{2+} on the secretory apparatus (Lonart et al., 1998), although the precise mechanism involved was not identified.

RIM1a is an active zone protein and putative PKA target (Wang et al., 1997; Castillo et al., 2002; Lonart et al., 2003). Similar to what was seen in the absence of RAB3a, KO of *RIM1a* also prevented MF-LTP but not FSK-induced potentiation or STP (Castillo et al., 2002; **Figure 3** and **Table 1**), suggesting a direct link between PKA, RIM1a, RAB3a, and MF-LTP. However, this effect appears to be PKA-independent, as $RIM1a^{S413A}$, an isoform that carries a point mutation preventing RIM1a phosphorylation

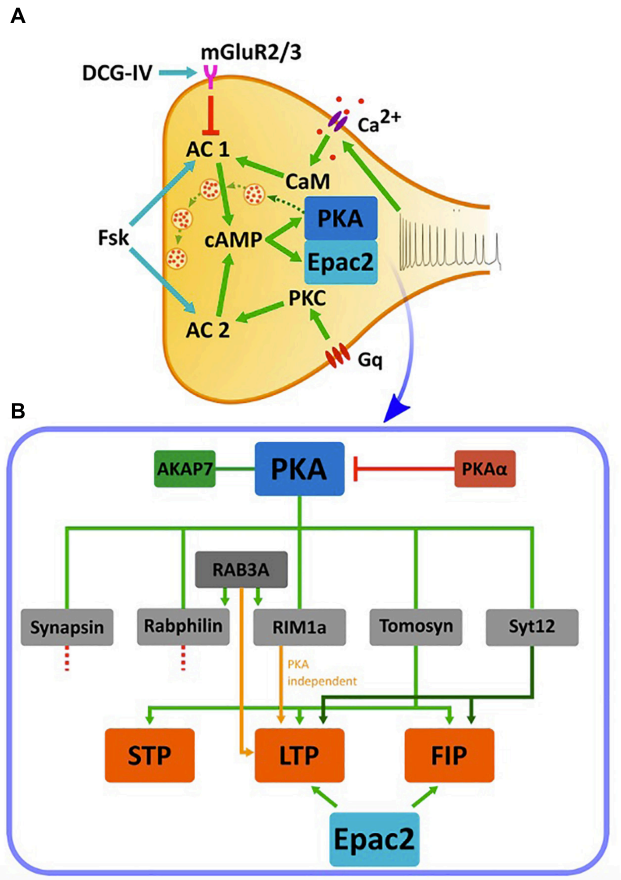

FIGURE 3 | cAMP cascades and cAMP-dependent synaptic plasticity in the MF synapse. **(A)** Cascades of activation of cAMP, PKA, and Epac2 in the MF terminal. A train of action potentials arriving at the MF synapse triggers a calcium influx through voltage-dependent calcium channels and subsequent activation of CaM that activates cAMP synthesis by AC1. AC1 acts on PKA or Epac2 to up regulate synaptic transmission (dashed green arrows between vesicles). Application of FSK activates both AC1 and AC2 and elevates cAMP. AC2 is also activated by PKC following the activation by a G-coupled protein. Application of DCG-IV, an agonist to mGluR2/3, leads to inhibition of AC1. Green arrows: activation, red arrow: inhibition, blue arrows: application of pharmacological reagents. **(B)** Downstream PKA cascades and their relation to synaptic plasticity. PKA activity is dependent on the anchoring protein AKAP7, and is inhibited by the negative regulator PKAα. PKA, in turn, phosphorylates multiple proteins including synapsin, rabphilin, tomosyn-1, synaptotagmin12 (Syt12) and RIM1a. Of these, deletion of synapsin and rabphilin does not impair MF synaptic plasticity. Ablation of RAB3A, although not a direct PKA target, and RIM1a abolishes MF-LTP but does not affect STP and FSK-induced potentiation (FIP). Synaptotagmin-12 KO abolishes MF-LTP and impairs FSK-induced potentiation but do not affect STP, while deletion of tomosyn-1 abolishes MF-LTP, impairs FSK-induced potentiation and also affects STP. Epac2 manipulation also abolishes LTP and impairs FSK-induced potentiation. STP- short-term potentiation, LTP- long-term potentiation, FIP- FSK-induced potentiation. Orange arrow represent PKA-independent pathway, Green arrows shades represent different pathways.

by PKA, was found to have no impact on either short- or long-term plasticity, nor on behavior (Kaeser et al., 2008). Hence, despite the dependence of LTP on RIM1a, the link through PKA is less defined and suggests that PKA operates either through a different mechanism, or via yet another unidentified parallel pathway/s.

Rabphilin, another RAB3a effector, regulates vesicle priming through interactions with RAB3a and the SNARE protein SNAP-25, with the former occurring in a GTP-dependent manner (Tsuboi and Fukuda, 2005; Deák et al., 2006). Rabphilin was found to be phosphorylated following application of FSK in the MF but not in the SC synapse (Lonart and Südhof, 1998), highlighting that significant differences exist in the molecular mechanisms underlying synaptic plasticity between these different hippocampal regions. However, KO of the *rph3a* gene encoding for rabphilin did not change either short-term facilitation or MF-LTP at the MF terminal (Schlüter et al., 1999; **Figure 3** and **Table 1**).

In addition to the RAB3a cascade, synapsin was considered as another candidate PKA downstream effector. Synapsins are among the most abundant synaptic proteins that are known to be phosphorylated by PKA, and are involved in both synaptic transmission and plasticity (De Camilli and Greengard, 1986; Gitler et al., 2004). Accordingly, synapsins were one of the first synaptic protein families to be examined as targets for cAMP and PKA-dependent plasticity at the MF. Synapsin binds synaptic vesicles and tethers them to the cytoskeleton, yet can release these vesicles following phosphorylation by PKA, enabling their translocation to the active zone in preparation for exocytosis (De Camilli et al., 1983; Spillane et al., 1995). A triple KO of all three synapsin isoform-encoding genes led to impaired plasticity in primary hippocampal neuronal cultures, with such changes being associated with PKA activity (Cheng et al., 2018). However, in the MF pathway of acute hippocampal slices, a double KO of the *syn*1 and *syn*2 genes, encoding the main isoforms expressed in CNS neurons, did not alter cAMP-dependent LTP or FSK-induced potentiation (**Figure 3B** and **Table 1**; Spillane et al., 1995). While further research is required to reconcile these contradicting results, these findings suggest that phosphorylation of synapsin1 and synapsin2 by PKA is unlikely to be required for cAMP-dependent MF synaptic plasticity.

More recent studies have examined other synaptic proteins thought to be involved in PKA-dependent LTP at the MF synapse. Synaptotagmin-12 differs from other synaptotagmins in that it does not bind Ca^{2+} (Wolfes and Dean, 2020). However, synaptotagmin-12 is phosphorylated by PKA and is involved in the regulation of synaptic vesicles fusion and P_r (Maximov et al., 2007). Synaptotagmin-12^{S97A} mutant mice, in which the site of PKA-mediated phosphorylation was mutated, displayed impaired MF-LTP and FSK-induced potentiation, although their STP remained unaltered (Kaeser-Woo et al., 2013). Consequently, synaptotagmin-12 can be regarded as the first protein shown to affect both LTP and FSK-induced potentiation in a PKA-dependent manner.

Tomosyn is a PKA-dependent negative regulator of P_r and its over-expression leads to an inhibition of vesicle priming, while knockdown, knockout, or mutations in the *tomosyn-1*-encoding gene led to an enhancement of vesicle fusion (Yizhar et al., 2004; Chevlet et al., 2006; Gracheva et al., 2006; McEwen et al., 2006; Ben-Simon et al., 2015). Tomosyn-1, which was shown to be enriched in the MF pathway (Barak et al., 2010, 2013), can be phosphorylated by PKA at Ser-724 (Baba et al., 2005) and its acute down-regulation in the MF synapse leads to reductions in both LTP and FSK-induced potentiation (Ben-Simon et al., 2015). Interestingly, this manipulation also strongly reduced MF facilitation and STP. These effects are likely the result of an increase in the basal P_r following down-regulation of tomosyn-1, which also led to occlusion of both potentiation and facilitation. Although acute KD of tomosyn reduced both LTP and FSK-induced potentiation (Ben-Simon et al., 2015), a direct link between PKA-driven tomosyn-1 phosphorylation and synaptic plasticity has yet to be demonstrated.

Although FSK-induced potentiation and MF-LTP are thought to be interlinked and are driven by cAMP elevation (Weisskopf et al., 1994), deletion of most PKA-dependent synaptic proteins abolished only MF-LTP and not FSK-induced potentiation. This could suggest the presence of additional parallel cAMP-dependent pathways that are not fully PKA-dependent. It is also possible that high frequency stimulation-induced LTP and FSK affect downstream events with different cAMP-mediated dynamics, which would differently affect MF-LTP and FSK-induced potentiation. However, the same does not apply to the loss of synaptic proteins, such as of tomosyn-1 or synaptotagmin-12, which impaired both MF-LTP and FSK-induced potentiation (Kaeser-Woo et al., 2013; Ben-Simon et al., 2015). It is reasonable to assume that the impact of the loss of tomosyn-1 on MF-LTP and FSK-induced potentiation can be explained through an increase in basal P_r that is further translated into a reduction in synaptic potentiation. What is clear is that further studies are needed to characterize the exact contributions of these and other synaptic proteins and pathways to the cAMP dependent plasticity of the MF.

Additional proteins that interact with PKA, like PKAα and AKAP7, have also been shown to affect MF plasticity. PKAα is a PKA inhibitor whose activity decreases following synaptic stimulation, leading to a relief of PKA inhibition during neuronal activity. Moreover, blocking this pathway with anti-sense oligonucleotides to *PKA*α resulted in elimination of MF-LTP in the synapse (De Lecea et al., 1998). AKAP7 is a PKA-anchoring protein also essential for the function of PKA. Ablation of AKAP7 results in even more pronounced effects than those seen with PKAα inhibition, specifically, not only the elimination of MF-LTP but also various measurable behavioral deficits (Huang et al., 1995; Jones et al., 2016; **Figure 3B** and **Table 1**).

CYCLIC ADENOSINE MONOPHOSPHATE AND RESTRUCTURING OF SYNAPTIC RELEASE SITES

Recent results obtained with isolated MF terminals indicate that cAMP can directly affect P_r via regulation of Ca^{2+} signaling (Midorikawa and Sakaba, 2017; Fukaya et al., 2021).

Applying cAMP to isolated MF terminals increased P_r, although the number of vesicles in the readily releasable pool and replenishment of this pool following depletion remained unchanged. It has been suggested that this increase in P_r is associated with changes in the physical coupling between of P/Q-type Ca^{2+} channels and readily releasable vesicles (Midorikawa and Sakaba, 2017), which can alter the synaptic properties at the terminal (Bucurenciu et al., 2008; Vyleta and Jonas, 2014). As such, following an action potential, Ca^{2+} concentrations near release sites are expected to be higher, thereby leading to synaptic potentiation. Such molecular rearrangements were recently shown to occur within 5–10 min following FSK application (Fukaya et al., 2021).

A recent paper showed that FSK-induced potentiation was associated with fast remodeling of MF synapse presynaptic ultrastructure. However, the distance between P/Q-type calcium channels and Munc13–1 as a proxy for the release machinery was not altered and was found to be 65 nm (Orlando et al., 2021). On the other hand, FSK-induced potentiation was associated with synaptic vesicle accumulation at active zones, increases in the numbers of docked and tethered vesicles and an overall increase in the number of active AZs. In addition, vesicles were more dispersed, possibly mediated by PKA phosphorylation of synapsin (Sihra et al., 1989; Pechstein et al., 2020), allowing for the mobilization of vesicles into the readily releasable vesicle pool. A similar increase in the number of docked vesicles was recently suggested to take place following high-frequency stimulation of MF synapses (Vandael et al., 2020) and was referred as a "pool engram," enabling post-tetanic potentiation. Reorganization of active zone and changes in the recycling vesicle pool also occurs after FSK-induced LTP at CA3-CA1 synapses and might represent a basic mechanism of presynaptic LTP in central synaptic synapses (Rey et al., 2020) and in the *Drosophila* neuromuscular junction (Weyhersmüller et al., 2011). Such processes are likely to be mediated by AZ proteins, such as RIM1a that interacts with Munnc13–1, or Rab3A together with calcium channels (Betz et al., 2001; Schoch et al., 2002; Han et al., 2011; Kaeser et al., 2011; Eggermann et al., 2012), via RIM-BP2 that stabilizes Munc13-1 protein clusters at MF AZs channels (Brockmann et al., 2019), or via synapsin phosphorylation. However, as mentioned above, PKA-mediated phosphorylation of RIM1a was shown to have no effect on MF synaptic transmission (Kaeser et al., 2008), while synapsin KO had no effect on MF-LTP. Additional super-resolution microscopy methods that can inspect organizational changes at the 10–20 nm range can resolve how the release machinery, AZ and calcium channels are restructured following elevations in cAMP levels.

ALTERNATIVE CYCLIC ADENOSINE MONOPHOSPHATE TARGETS

PKA is considered by many to be a master regulator of synaptic plasticity in the hippocampal MF synapse, as well as in many other synapses (Waltereit and Weller, 2003). Consequently, other than the intensive studies conducted on the involvement of PKA targets in MF-LTP, only few studies have considered other possible cAMP-dependent pathways. One such example is a study that linked Epac2, a member of a family of cAMP-dependent guanine nucleotide exchange proteins (GEFs), to synaptic plasticity at the MF synapse (Fernandes et al., 2015). The two cAMP-dependent GEFs, Epac1, and Epac2 (encoded by the *Rapgef3* and *Rapgef4* genes, respectively), were linked to several cAMP-dependent processes (Gloerich and Bos, 2010), and it was further suggested that these proteins are relevant to synaptic plasticity processes (De Rooij et al., 1998; Kawasaki et al., 1998; Fernandes et al., 2015). Epac was shown to activate a MAP-kinase called p38 (**Figure 4**) in cerebellar and hippocampal neurons and this was correlated with modulation of neuronal excitability (Ster et al., 2007, 2009). In a separate study, several experiments have demonstrated that blocking Epac2 signaling led to reduced levels of p38 phosphorylation (Emery et al., 2014). This suggests that Epac2 responds to cAMP by activating ERK and the small GTPase Rap, as well as its downstream kinase p38-MAPK, thereby bypassing the canonical PKA cascade (**Figure 4**). Epac2 plays a crucial role in MF-LTP, as KO of the encoding gene led to deficits in MF-LTP and impaired FSK-induced potentiation without affecting basal synaptic properties, as measured by changes in STP (Fernandes et al., 2015; **Figure 3B** and **Table 1**).

More recently, an additional member of the RAPGEF family, RapGEF2, was hypothesized to participate in neuronal and synaptic processes. Due to its unconventional cAMP-binding motif, RapGEF2 was long considered not to be a cAMP sensor (Liao et al., 1999; Kuiperij et al., 2003; Kannan et al., 2007). However, more recent studies have shown that a specific RAPGEF2 isoform expressed exclusively in neurons and endocrine cells, termed NCS-Rapgef2, can phosphorylate ERK in a cAMP-dependent manner in these cells (Emery et al., 2013; **Figure 4**). In neurons, this observed effect was modulated by activation of the dopamine receptor D1 (DRD1), potentially modulating postsynaptic sensitivity in response to dopamine release as well as in a dopamine receptor D1 (DRD1)-dependent manner (Jiang et al., 2017). In addition, KO of *NCS-Rapgef2* in $DRD1^+$ medium spiny neurons (MSN) of the nucleus accumbens was shown to have behavioral consequences, resulting in impairments in cocaine-induced locomotor sensitization (CILS) and in conditioned place preference (Jiang et al., 2021). Interestingly, CILS was previously shown to require ERK-dependent DRD1-MSN neuroplasticity (Ferguson et al., 2006; Girault et al., 2007), further supporting the contribution of ERK-dependent pathways and the possible involvement of NCS-RAPGEF2 in neuroplasticity. Still, the involvement of NCS-Rapgef2 in presynaptic plasticity has yet to demonstrated.

Based on current understanding, we can assume the existence of at least three main cAMP-dependent molecular pathways relevant to synaptic plasticity. These can be described according to the proteins directly activated by cAMP, and by the principal kinases or RAPGEFs downstream of these proteins, which execute many of the regulatory functions ascribed to their respective pathways. The three principal pathways are PKA → CREB, Epac → p38 and Rapgef2 → Erk (**Figure 4**). These pathways can work independently but can also interact and influence one another (Emery et al., 2014, 2016, 2017). Lastly,

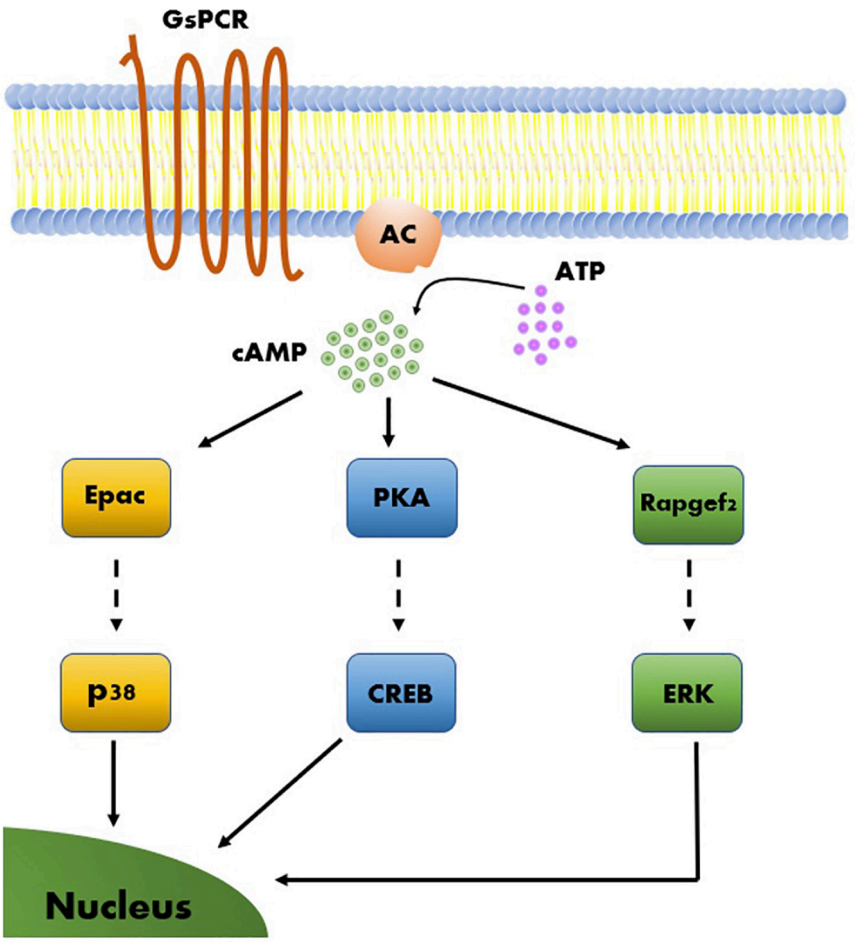

FIGURE 4 | Model of molecular mechanisms of cAMP-dependent LTP. Three cAMP-dependent effectors, Epac, PKA, and Rapgef2, give rise to three parallel molecular pathways. Each of the three cAMP-dependent molecular pathways include a transcription factor that upon activation leads to long-term effects on gene regulation that support synaptic plasticity.

these molecular pathways can activate plasticity processes that differ in several aspects, such as the locus of plastic changes (e.g., pre- vs. postsynaptic plasticity), resistance to pharmacological compounds, and even associated behavioral processes (Morozov et al., 2003; Fernandes et al., 2015).

CONCLUSION

In summary, the presynaptic forms of LTP and LTD that transpire in the hippocampal MF-CA3 synapse are thought to depend on cAMP-PKA-dependent cascades. Various synaptic proteins have been linked to these cascades, and manipulations of several of these proteins, such as RAB3a, RIM1a, synaptotagmin-12, and tomosyn-1, are crucial for signaling along these cascades. Interestingly, manipulations of these proteins mostly impact MF-LTP formation and only in some cases, FSK-induced potentiation or STP. This indicates the strong possibility of the existence of several parallel cAMP-dependent cascades, which are still only partially understood. Mechanistically, elevation of cAMP in the MF synapse involves the rearrangement of synaptic vesicles near release sites and the clustering of calcium channels near the release machinery, which lead to synaptic potentiation. Adopting additional methods that can detect nanometric-level organizational changes in the AZ will help resolve how the release machinery is restructured following elevation in cAMP with more detail. Such changes in synaptic plasticity can be mediated via other PKA targets or via non-canonical PKA-independent but cAMP-dependent pathways, like those involving the RAPGEF family of proteins. Combinations of cell type-specific manipulation of specific proteins, along with synapse-specific manipulation of cAMP by either optogenetic or pharmacogenetic approaches, as well as the ability to measure cAMP levels in response to natural stimulation patterns, will allow a more detailed understanding of the relationship between cAMP and synaptic plasticity at the MF synapse. Such findings could potentially be extrapolated to other synapses, which bear similar physiological hallmarks, to expand our understanding of the links between cellular transcriptomics, synaptic physiology and behavior.

AUTHOR CONTRIBUTIONS

All authors contributed to discussion, writing, and editing the manuscript.

FUNDING

This work was supported by the Israel Science Foundation (ISF grant 2141/20) to UA.

REFERENCES

Acsády, L., Kamondi, A., Sík, A., Freund, T., and Buzsáki, G. (1998). GABAergic cells are the major postsynaptic targets of mossy fibers in the rat hippocampus. *J. Neurosci.* 18, 3386–3403. doi: 10.1523/jneurosci.18-09-03386.1998

Amaral, D. G., and Dent, J. A. (1981). Development of the mossy fibers of the dentate gyrus: I. A light and electron microscopic study of the mossy fibers and their expansions. *J. Comp. Neurol.* 195, 51–86. doi: 10.1002/cne.901950106

Andrade-Talavera, Y., Duque-Feria, P., Sihra, T. S., and Rodríguez-Moreno, A. (2013). Pre-synaptic kainate receptor-mediated facilitation of glutamate release involves PKA and Ca2+-calmodulin at thalamocortical synapses. *J. Neurochem.* 126, 565–578. doi: 10.1111/jnc.12310

Ariel, P., Hoppa, M. B., and Ryan, T. A. (2013). Intrinsic variability in Pv, RRP size, Ca2+ channel repertoire, and presynaptic potentiation in individual synaptic boutons. *Front. Synaptic Neurosci.* 4:9. doi: 10.3389/fnsyn.2012.00009

Ashery, U., Bielopolski, N., Barak, B., and Yizhar, O. (2009). Friends and foes in synaptic transmission: the role of tomosyn in vesicle priming. *Trends Neurosci.* 32, 275–282. doi: 10.1016/j.tins.2009.01.004

Baba, T., Sakisaka, T., Mochida, S., and Takai, Y. (2005). PKA-catalyzed phosphorylation of tomosyn and its implication in Ca2+-dependent exocytosis of neurotransmitter. *J. Cell Biol.* 170, 1113–1125. doi: 10.1083/jcb.200504055

Barak, B., Okun, E., Ben-Simon, Y., Lavi, A., Shapira, R., Madar, R., et al. (2013). Neuron-specific expression of tomosyn1 in the mouse hippocampal dentate gyrus impairs spatial learning and memory. *Neuromolecular Med.* 15, 351–363. doi: 10.1007/s12017-013-8223-4

Barak, B., Williams, A., Bielopolski, N., Gottfried, I., Okun, E., Brown, M. A., et al. (2010). Tomosyn expression pattern in the mouse hippocampus suggests both presynaptic and postsynaptic functions. *Front. Neuroanat.* 4:149. doi: 10.3389/fnana.2010.00149

Bauman, A. L., and Scott, J. D. (2002). Kinase- and phosphatase-anchoring proteins: harnessing the dynamic duo. *Nat. Cell Biol.* 4, E203–E206. doi: 10.1038/ncb0802-e203

Behr, J., Wozny, C., Fidzinski, P., and Schmitz, D. (2009). Synaptic plasticity in the subiculum. *Prog. Neurobiol.* 89, 334–342. doi: 10.1016/J.PNEUROBIO.2009.09.002

Bender, V. A., Pugh, J. R., and Jahr, C. E. (2009). Presynaptically expressed long-term potentiation increases multivesicular release at parallel fiber synapses. *J. Neurosci.* 29, 10974–10978. doi: 10.1523/JNEUROSCI.2123-09.2009

Ben-Simon, Y., Rodenas-Ruano, A., Alviña, K., Lam, A. D., Stuenkel, E. L., Castillo, P. E., et al. (2015). A Combined Optogenetic-Knockdown Strategy Reveals a Major Role of Tomosyn in Mossy Fiber Synaptic Plasticity. *Cell Rep.* 12, 396–404. doi: 10.1016/j.celrep.2015.06.037

Betz, A., Thakur, P., Junge, H. J., Ashery, U., Rhee, J. S., Scheuss, V., et al. (2001). Functional interaction of the active zone proteins Munc13-1 and RIM1 in synaptic vesicle priming. *Neuron* 30, 183–196. doi: 10.1016/S0896-6273(01)00272-0

Bliss, T. V. P., and Collingridge, G. L. (2013). Expression of NMDA receptor-dependent LTP in the hippocampus: bridging the divide. *Mol. Brain* 6:5. doi: 10.1186/1756-6606-6-5

Böhme, M. A., Grasskamp, A. T., and Walter, A. M. (2018). Regulation of synaptic release-site Ca2+ channel coupling as a mechanism to control release probability and short-term plasticity. *FEBS Lett.* 592, 3516–3531. doi: 10.1002/1873-3468.13188

Breustedt, J., Vogt, K. E., Miller, R. J., Nicoll, R. A., and Schmitz, D. (2003). α1E-Containing Ca2+ channels are involved in synaptic plasticity. *Proc. Natl. Acad. Sci. U. S. A.* 100, 12450–12455. doi: 10.1073/pnas.2035117100

Brockmann, M. M., Maglione, M., Willmes, C. G., Stumpf, A., Bouazza, B. A., Velasquez, L. M., et al. (2019). RIM-BP2 primes synaptic vesicles via recruitment of Munc13-1 at hippocampal mossy fiber synapses. *Elife* 8:e43243. doi: 10.7554/eLife.43243

Brunger, A. T., Choi, U. B., Lai, Y., Leitz, J., White, K. I., and Zhou, Q. (2019). The pre-synaptic fusion machinery. *Curr. Opin. Struct. Biol.* 54, 179–188. doi: 10.1016/j.sbi.2019.03.007

Bucurenciu, I., Kulik, A., Schwaller, B., Frotscher, M., and Jonas, P. (2008). Nanodomain coupling between Ca2+ channels and Ca2+ sensors promotes fast and efficient transmitter release at a cortical GABAergic synapse. *Neuron* 57, 536–545. doi: 10.1016/j.neuron.2007.12.026

Bykhovskaia, M. (2011). Synapsin regulation of vesicle organization and functional pools. *Semin. Cell Dev. Biol.* 22, 387–392. doi: 10.1016/J.SEMCDB.2011.07.003

Campbell, E. J., and Marchant, N. J. (2018). The use of chemogenetics in behavioural neuroscience: receptor variants, targeting approaches and caveats. *Br. J. Pharmacol.* 175, 994–1003. doi: 10.1111/bph.14146

Carta, M., Srikumar, B. N., Gorlewicz, A., Rebola, N., and Mulle, C. (2018). Activity-dependent control of NMDA receptor subunit composition at hippocampal mossy fibre synapses. *J. Physiol.* 596, 703–716. doi: 10.1113/JP275226

Castellucci, V. F., Kandel, E. R., and Schwartz, J. H. (1980). Intracellular injection of the catalytic subunit of cyclic AMP-dependent protein kinase simulates facilitation of transmitter release underlying behavioral sensitization in Aplysia. *Proc. Natl. Acad. Sci. U. S. A.* 77, 7492–7496. doi: 10.1073/pnas.77.12.7492

Castillo, P. E. (2012). Presynaptic LTP and LTD of excitatory and inhibitory synapses. *Cold Spring Harb. Perspect. Biol.* 4:a005728. doi: 10.1101/cshperspect.a005728

Castillo, P. E., Schoch, S., Schmitz, F., Sudhof, T. C., and Malenka, R. C. (2002). RIM1 alpha is required for presynaptic long-term potentiation. *Nature* 415, 327–330. doi: 10.1038/415327a

Castillo, P. E., Weisskopf, M. G., and Nicoll, R. A. (1994). The role of Ca2+ channels in hippocampal mossy fiber synaptic transmission and long-term potentiation. *Neuron* 12, 261–269. doi: 10.1016/0896-6273(94)90269-0

Castillo, P. E., Younts, T. J., Chávez, A. E., and Hashimotodani, Y. (2012). Endocannabinoid signaling and synaptic function. *Neuron* 76, 70–81. doi: 10.1016/J.NEURON.2012.09.020

Castillo, P. E. E., Janz, R., Südhof, T. C., Tzounopoulos, T., Malenka, R. C. C., Nicoll, R. A. A., et al. (1997). Rab3A is essential for mossy fibre long-term potentiation in the hippocampus. *Nature* 388, 590–593. doi: 10.1038/41574

Castro-Alamancos, M. A., and Calcagnotto, M. E. (1999). Presynaptic Long-Term Potentiation in Corticothalamic Synapses. *J. Neurosci.* 19, 9090–9097. doi: 10.1523/JNEUROSCI.19-20-09090.1999

Cedar, H., Kandel, E. R., and Schwartz, J. H. (1972). Cyclic Adenosine Monophosphate in the Nervous System of Aplysia californica?: I. Increased synthesis in response to synaptic stimulation. *J. Gen. Physiol.* 60, 558–569. doi: 10.1085/jgp.60.5.558

Cembrowski, M. S., Wang, L., Sugino, K., Shields, B. C., and Spruston, N. (2016). Hipposeq: a comprehensive RNA-seq database of gene expression in hippocampal principal neurons. *eLife* 5:e14997. doi: 10.7554/eLife.14997

Chamberland, S., Timofeeva, Y., Evstratova, A., Volynski, K., and Tóth, K. (2018). Action potential counting at giant mossy fiber terminals gates information transfer in the hippocampus. *Proc. Natl. Acad. Sci. U. S. A.* 115, 7434–7439. doi: 10.1073/PNAS.1720659115

Chanaday, N. L., Cousin, M. A., Milosevic, I., Watanabe, S., and Morgan, J. R. (2019). The synaptic vesicle cycle revisited: new insights into the modes and mechanisms. *J. Neurosci.* 39, 8209–8216. doi: 10.1523/JNEUROSCI.1158-19.2019

Chen, C., and Regehr, W. G. (1997). The mechanism of cAMP-mediated enhancement at a cerebellar synapse. *J. Neurosci.* 17, 8687–8694. doi: 10.1523/jneurosci.17-22-08687.1997

Chen, H.-X., Jiang, M., Akakin, D., and Roper, S. N. (2009). Long-Term Potentiation of Excitatory Synapses on Neocortical Somatostatin-Expressing Interneurons. *J. Neurophysiol.* 102, 3251–3259. doi: 10.1152/JN.00641.2009

Cheng, Q., Song, S. H., and Augustine, G. J. (2018). Molecular mechanisms of short-term plasticity: role of synapsin phosphorylation in augmentation and

potentiation of spontaneous glutamate release. *Front. Synaptic Neurosci.* 10:33. doi: 10.3389/fnsyn.2018.00033

Chevlet, S., Bezzi, P., Ivarsson, R., Renström, E., Viertl, D., Kasas, S., et al. (2006). Tomosyn-1 is involved in a post-docking event required for pancreatic β-cell exocytosis. *J. Cell Sci.* 119, 2912–2920. doi: 10.1242/jcs.03037

Conti, A. C., Maas, J. W., Muglia, L. M., Dave, B. A., Vogt, S. K., Tran, T. T., et al. (2007). Distinct regional and subcellular localization of adenylyl cyclases type 1 and 8 in mouse brain. *Neuroscience* 146, 713–729. doi: 10.1016/J.NEUROSCIENCE.2007.01.045

Corbin, J. D., and Krebs, E. G. (1969). A cyclic AMP–stimulated protein kinase in adipose tissue. *Biochem. Biophys. Res. Commun.* 36, 328–336. doi: 10.1016/0006-291X(69)90334-9

D'Adamo, P., Wolfer, D. R., Kopp, C., Tobler, I., Toniolo, D., and Lipp, H. P. (2004). Mice deficient for the synaptic vesicle protein Rab3a show impaired spatial reversal learning and increased explorative activity but none of the behavioral changes shown by mice deficient for the Rab3a regulator Gdi1. *Eur. J. Neurosci.* 19, 1895–1905. doi: 10.1111/J.1460-9568.2004.03270.X

Davis, G. W., DiAntonio, A., Petersen, S. A., and Goodman, C. S. (1998). Postsynaptic PKA Controls Quantal Size and Reveals a Retrograde Signal that Regulates Presynaptic Transmitter Release in Drosophila. *Neuron* 20, 305–315. doi: 10.1016/S0896-6273(00)80458-4

López de Armentia, M. L., and Sah, P. (2007). Bidirectional synaptic plasticity at nociceptive afferents in the rat central amygdala. *J. Physiol.* 581, 961–970. doi: 10.1113/JPHYSIOL.2006.121822

De Camilli, P., Cameron, R., and Greengard, P. (1983). Synapsin I (protein I), a nerve terminal-specific phosphoprotein. I. Its general distribution in synapses of the central and peripheral nervous system demonstrated by immunofluorescence in frozen and plastic sections. *J. Cell Biol.* 96, 1337–1354. doi: 10.1083/jcb.96.5.1337

De Camilli, P., and Greengard, O. (1986). Synapsin I: a synaptic vesicle-associated neuronal phosphoprotein. *Biochem. Pharmacol.* 35, 4349–4357. doi: 10.1016/0006-2952(86)90747-1

De Lecea, L., Criado, J. R., Rivera, S., Wen, W., Soriano, E., Henriksen, S. J., et al. (1998). Endogenous protein kinase a inhibitor (PKIα) modulates synaptic activity. *J. Neurosci. Res.* 53, 269–278. doi: 10.1002/(SICI)1097-4547(19980801)53:3<269::AID-JNR1<3.0.CO;2-8

De Rooij, J., Zwartkruis, F. J. T., Verheijen, M. H. G., Cool, R. H., Nijman, S. M. B., Wittinghofer, A., et al. (1998). Epac is a Rap1 guanine-nucleotide-exchange factor directly activated by cyclic AMP. *Nature* 396, 474–477. doi: 10.1038/24884

Deák, F., Shin, O. H., Tang, J., Hanson, P., Ubach, J., Jahn, R., et al. (2006). Rabphilin regulates SNARE-dependent re-priming of synaptic vesicles for fusion. *EMBO J.* 25, 2856–2866. doi: 10.1038/sj.emboj.7601165

Dresbach, T., Qualmann, B., Kessels, M. M., Garner, C. C., and Gundelfinger, E. D. (2001). The presynaptic cytomatrix of brain synapses. *Cell. Mol. Life Sci.* 58, 94–116. doi: 10.1007/PL00000781

Eggermann, E., Bucurenciu, I., Goswami, S. P., and Jonas, P. (2012). Nanodomain coupling between Ca 2+ channels and sensors of exocytosis at fast mammalian synapses. *Nat. Rev. Neurosci.* 13, 7–21. doi: 10.1038/nrn3125

Emery, A. C., Eiden, M. V., and Eiden, L. E. (2014). Separate cyclic AMP sensors for neuritogenesis, growth arrest, and survival of neuroendocrine cells. *J. Biol. Chem.* 289, 10126–10139. doi: 10.1074/jbc.M113.529321

Emery, A. C., Eiden, M. V., and Eiden, L. E. (2016). Evaluating the Specificity and Potency of Activators and Inhibitors of the cAMP Sensors PKA, Epac2/Rapgef4, and NCS/Rapgef2 Using Cell-Based Assays for Activation of CREB, p38 MAPK, and ERK. *FASEB J.* 30, 1190.9–1190.9. doi: 10.1096/fasebj.30.1_supplement.1190.9

Emery, A. C., Eiden, M. V., Mustafa, T., and Eiden, L. E. (2013). Rapgef2 connects GPCR-mediated cAMP signals to ERK activation in neuronal and endocrine cells. *Sci. Signal.* 6:ra51. doi: 10.1126/scisignal.2003993

Emery, A. C., Xu, W., Eiden, M. V., and Eiden, L. E. (2017). Guanine nucleotide exchange factor Epac2-dependent activation of the GTP-binding protein Rap2A mediates cAMP-dependent growth arrest in neuroendocrine cells. *J. Biol. Chem.* 292, 12220–12231. doi: 10.1074/JBC.M117.790329

Evstratova, A., and Tóth, K. (2014). Information processing and synaptic plasticity at hippocampal mossy fiber terminals. *Front. Cell. Neurosci.* 8:28. doi: 10.3389/fncel.2014.00028

Ferguson, S. M., Fasano, S., Yang, P., Brambilla, R., and Robinson, T. E. (2006). Knockout of ERK1 enhances cocaine-evoked immediate early gene expression and behavioral plasticity. *Neuropsychopharmacology* 31, 2660–2668. doi: 10.1038/sj.npp.1301014

Fernandes, H. B., Riordan, S., Nomura, T., Remmers, C. L., Kraniotis, S., Marshall, J. J., et al. (2015). Epac2 mediates cAMP-dependent potentiation of neurotransmission in the hippocampus. *J. Neurosci.* 35, 6544–6553. doi: 10.1523/JNEUROSCI.0314-14.2015

Fitzjohn, S. M., Bortolotto, Z. A., Palmer, M. J., Doherty, A. J., Ornstein, P. L., Schoepp, D. D., et al. (1998). The potent mGlu receptor antagonist LY341495 identifies roles for both cloned and novel mGlu receptors in hippocampal synaptic plasticity. *Neuropharmacology* 37, 1445–1458. doi: 10.1016/S0028-3908(98)00145-2

Fourcaudot, E., Gambino, F., Humeau, Y., Casassus, G., Shaban, H., Poulain, B., et al. (2008). cAMP/PKA signaling and RIM1α mediate presynaptic LTP in the lateral amygdala. *Proc. Natl. Acad. Sci. U. S. A.* 105, 15130–15135. doi: 10.1073/pnas.0806938105

Fukaya, R., Maglione, M., Sigrist, S. J., and Sakaba, T. (2021). Rapid Ca2+ channel accumulation contributes to cAMP-mediated increase in transmission at hippocampal mossy fiber synapses. *Proc. Natl. Acad. Sci. U. S. A.* 118:e2016754118. doi: 10.1073/PNAS.2016754118

Gehring, C. (2010). Adenyl cyclases and cAMP in plant signaling - past and present. *Cell Commun. Signal.* 8:15. doi: 10.1186/1478-811X-8-15

Geppert, M., Goda, Y., Stevens, C. F., and Südhof, T. C. (1997). The small GTP-binding protein Rab3A regulates a late step in synaptic vesicle fusion. *Nature* 387, 810–814. doi: 10.1038/42954

Girault, J. A., and Greengard, P. (2004). The Neurobiology of Dopamine Signaling. *Arch. Neurol.* 61, 641–644. doi: 10.1001/archneur.61.5.641

Girault, J. A., Valjent, E., Caboche, J., and Hervé, D. (2007). ERK2: a logical AND gate critical for drug-induced plasticity?. *Curr. Opin. Pharmacol.* 7, 77–85. doi: 10.1016/j.coph.2006.08.012

Gitler, D., Takagishi, Y., Feng, J., Ren, Y., Rodriguiz, R. M., Wetsel, W. C., et al. (2004). Different Presynaptic Roles of Synapsins at Excitatory and Inhibitory Synapses. *J. Neurosci.* 24, 11368–11380. doi: 10.1523/JNEUROSCI.3795-04.2004

Gloerich, M., and Bos, J. L. (2010). Epac: defining a New Mechanism for cAMP Action. *Annu. Rev. Pharmacol. Toxicol.* 50, 355–375. doi: 10.1146/annurev.pharmtox.010909.105714

Gracheva, E. O., Burdina, A. O., Holgado, A. M., Berthelot-Grosjean, M., Ackley, B. D., Hadwiger, G., et al. (2006). Tomosyn inhibits synaptic vesicle priming in Caenorhabditis elegans. *PLoS Biol.* 4, 1426–1437. doi: 10.1371/journal.pbio.0040261

Hallermann, S., Pawlu, C., Jonas, P., and Heckmann, M. (2003). A large pool of releasable vesicles in a cortical glutamatergic synapse. *Proc. Natl. Acad. Sci. U. S. A.* 100, 8975–8980. doi: 10.1073/pnas.1432836100

Halls, M. L., and Cooper, D. M. F. (2011). Regulation by Ca2+-signaling pathways of adenylyl cyclases. *Cold Spring Harb. Perspect. Biol.* 3:a004143. doi: 10.1101/CSHPERSPECT.A004143

Hamblin, M. W., Guthrie, C. R., Kohen, R., and Heidmann, D. E. A. (1998). Gs protein-coupled serotonin receptors: receptor isoforms and functional differences. *Ann. N. Y. Acad. Sci.* 861, 31–37. doi: 10.1111/j.1749-6632.1998.tb10170.x

Han, Y., Kaeser, P. S., Südhof, T. C., and Schneggenburger, R. (2011). RIM determines Ca2+ channel density and vesicle docking at the presynaptic active zone. *Neuron* 69, 304–316. doi: 10.1016/j.neuron.2010.12.014

Hanoune, J., and Defer, N. (2001). Regulation and role of adenylyl cyclase isoforms. *Annu. Rev. Pharmacol. Toxicol.* 41, 145–174. doi: 10.1146/ANNUREV.PHARMTOX.41.1.145

Harada, K., Ito, M., Wang, X., Tanaka, M., Wongso, D., Konno, A., et al. (2017). Red fluorescent protein-based cAMP indicator applicable to optogenetics and in vivo imaging. *Sci. Rep.* 7:7351. doi: 10.1038/s41598-017-07820-6

Hashimotodani, Y., Nasrallah, K., Jensen, K. R., Chávez, A. E., Carrera, D., and Castillo, P. E. (2017). LTP at Hilar Mossy Cell-Dentate Granule Cell Synapses Modulates Dentate Gyrus Output by Increasing Excitation/Inhibition Balance. *Neuron* 95, 928–943.e3. doi: 10.1016/J.NEURON.2017.07.028

Henze, D. A., Urban, N. N., and Barrionuevo, G. (2000). The multifarious hippocampal mossy fiber pathway: a review. *Neuroscience* 98, 407–427. doi: 10.1016/s0306-4522(00)00146-9

Huang, Y. Y., Kandel, E. R., Varshavsky, L., Brandon, E. P., Qi, M., Idzerda, R. L., et al. (1995). A genetic test of the effects of mutations in PKA on mossy fiber LTP and its relation to spatial and contextual learning. *Cell* 83, 1211–1222. doi: 10.1016/0092-8674(95)90146-9

Huang, Y. Y., Li, X. C., and Kandel, E. R. (1994). cAMP contributes to mossy fiber LTP by initiating both a covalently mediated early phase and macromolecular synthesis-dependent late phase. *Cell* 79, 69–79. doi: 10.1016/0092-8674(94)90401-4

Jiang, S. Z., Sweat, S., Dahlke, S. P., Loane, K., Drossel, G., Xu, W., et al. (2021). Cocaine-Dependent Acquisition of Locomotor Sensitization and Conditioned Place Preference Requires D1 Dopaminergic Signaling through a Cyclic AMP, NCS-Rapgef2, ERK, and Egr-1/Zif268 Pathway. *J. Neurosci.* 41, 711–725. doi: 10.1523/JNEUROSCI.1497-20.2020

Jiang, S. Z., Xu, W., Emery, A. C., Gerfen, C. R., Eiden, M. V., and Eiden, L. E. (2017). NCS-Rapgef2, the Protein Product of the Neuronal *Rapgef2* Gene, Is a Specific Activator of D1 Dopamine Receptor-Dependent ERK Phosphorylation in Mouse Brain. *eNeuro* 4:ENEURO.248-ENEURO.217. doi: 10.1523/ENEURO.0248-17.2017

Johnson, M. (2006). Molecular mechanisms of β2-adrenergic receptor function, response, and regulation. *J. Allergy Clin. Immunol.* 117, 18–24. doi: 10.1016/j.jaci.2005.11.012

Johnston, D., Williams, S., Jaffe, D., and Gray, R. (1992). NMDA-receptor-independent long-term potentiation. *Annu. Rev. Physiol.* 54, 489–505. doi: 10.1146/annurev.ph.54.030192.002421

Jonas, P., Major, G., and Sakmann, B. (1993). Quantal components of unitary EPSCs at the mossy fibre synapse on CA3 pyramidal cells of rat hippocampus. *J. Physiol.* 472, 615–663. doi: 10.1113/jphysiol.1993.sp019965

Jones, B. W., Deem, J., Younts, T. J., Weisenhaus, M., Sanford, C. A., Slack, M. C., et al. (2016). Targeted deletion of AKAP7 in dentate granule cells impairs spatial discrimination. *Elife* 5:e20695. doi: 10.7554/ELIFE.20695

Kaeser, P. S., Deng, L., Wang, Y., Dulubova, I., Liu, X., Rizo, J., et al. (2011). RIM proteins tether Ca2+ channels to presynaptic active zones via a direct PDZ-domain interaction. *Cell* 144, 282–295. doi: 10.1016/j.cell.2010.12.029

Kaeser, P. S., Kwon, H. B., Blundell, J., Chevaleyre, V., Morishita, W., Malenka, R. C., et al. (2008). RIM1α phosphorylation at serine-413 by protein kinase A is not required for presynaptic long-term plasticity or learning. *Proc. Natl. Acad. Sci. U. S. A.* 105, 14680–14685. doi: 10.1073/pnas.0806679105

Kaeser-Woo, Y. J., Younts, T. J., Yang, X., Zhou, P., Wu, D., Castillo, P. E., et al. (2013). Synaptotagmin-12 phosphorylation by cAMP-dependent protein kinase is essential for hippocampal mossy fiber LTP. *J. Neurosci.* 33, 9769–9780. doi: 10.1523/JNEUROSCI.5814-12.2013

Kalia, D., Merey, G., Nakayama, S., Zheng, Y., Zhou, J., Luo, Y., et al. (2013). Nucleotide, c-di-GMP, c-di-AMP, cGMP, cAMP, (p)ppGpp signaling in bacteria and implications in pathogenesis. *Chem. Soc. Rev.* 42, 305–341. doi: 10.1039/C2CS35206K

Kamiya, H., and Ozawa, S. (1999). Dual mechanism for presynaptic modulation by axonal metabotropic glutamate receptor at the mouse mossy fibre-CA3 synapse. *J. Physiol.* 518, 497–506. doi: 10.1111/J.1469-7793.1999.0497P.X

Kandel, E. R. (2012). The molecular biology of memory: cAMP, PKA, CRE, CREB-1, CREB-2, and CPEB. *Mol. Brain* 5:14. doi: 10.1186/1756-6606-5-14

Kandel, E. R., Schwartz, J. H., Siegelbaum, S., and Jessell, T. M. (2000). *Principles of neural science*, 4th Edn. New York: McGraw-hill.

Kannan, N., Wu, J., Anand, G. S., Yooseph, S., Neuwald, A. F., Venter, J. C., et al. (2007). Evolution of allostery in the cyclic nucleotide binding module. *Genome Biol.* 8:R264. doi: 10.1186/gb-2007-8-12-r264

Kapur, A., Yeckel, M. F., Gray, R., and Johnston, D. (1998). L-type calcium channels are required for one form of hippocampal mossy fiber LTP. *J. Neurophysiol.* 79, 2181–2190. doi: 10.1152/jn.1998.79.4.2181

Kavalali, E. T. (2020). Neuronal Ca2+ signalling at rest and during spontaneous neurotransmission. *J. Physiol.* 598, 1649–1654. doi: 10.1113/JP276541

Kawasaki, H., Springett, G. M., Mochizuki, N., Toki, S., Nakaya, M., Matsuda, M., et al. (1998). A family of cAMP-binding proteins that directly activate Rap1. *Science* 282, 2275–2279. doi: 10.1126/science.282.5397.2275

Kees, A. L., Marneffe, C., and Mulle, C. (2021). Lighting up pre-synaptic potentiation: an Editorial for "SynaptoPAC, an optogenetic tool for induction of presynaptic plasticity" on page 324. *J. Neurochem.* 156, 270–272. doi: 10.1111/jnc.15236

Klein, M., and Kandel, E. R. (1980). Mechanism of calcium current modulation underlying presynaptic facilitation and behavioral sensitization in Aplysia. *Proc. Natl. Acad. Sci. U. S. A.* 77, 6912–6916. doi: 10.1073/pnas.77.11.6912

Kobayashi, K. (2010). Hippocampal Mossy Fiber Synaptic Transmission and Its Modulation. *Vitam. Horm.* 82, 65–85. doi: 10.1016/S0083-6729(10)82004-7

Kobayashi, K., Mikahara, Y., Murata, Y., Morita, D., Matsuura, S., Segi-Nishida, E., et al. (2020). Predominant Role of Serotonin at the Hippocampal Mossy Fiber Synapse with Redundant Monoaminergic Modulation. *iScience* 23:101025. doi: 10.1016/j.isci.2020.101025

Kohara, K., Pignatelli, M., Rivest, A. J., Jung, H. Y., Kitamura, T., Suh, J., et al. (2014). Cell type-specific genetic and optogenetic tools reveal hippocampal CA2 circuits. *Nat. Neurosci.* 17, 269–279. doi: 10.1038/nn.3614

Kuiperij, H. B., De Rooij, J., Rehmann, H., Van Triest, M., Wittinghofer, A., Bos, J. L., et al. (2003). Characterisation of PDZ-GEFs, a family of guanine nucleotide exchange factors specific for Rap1 and Rap2. *Biochim. Biophys. Acta Mol. Cell Res.* 1593, 141–149. doi: 10.1016/S0167-4889(02)00365-8

Kwon, H. B., and Castillo, P. E. (2008). Long-term potentiation selectively expressed by NMDA receptors at hippocampal mossy fiber synapses. *Neuron* 57, 108–120. doi: 10.1016/j.neuron.2007.11.024

Lauri, S. E., Bortolotto, Z. A., Nistico, R., Bleakman, D., Ornstein, P. L., Lodge, D., et al. (2003). A role for Ca2+ stores in kainate receptor-dependent synaptic facilitation and LTP at mossy fiber synapses in the hippocampus. *Neuron* 39, 327–341. doi: 10.1016/s0896-6273(03)00369-6

Lein, E. S., Hawrylycz, M. J., Ao, N., Ayres, M., Bensinger, A., Bernard, A., et al. (2007). Genome-wide atlas of gene expression in the adult mouse brain. *Nature* 445, 168–176. doi: 10.1038/nature05453

Leutgeb, J. K., Leutgeb, S., Moser, M. B., and Moser, E. I. (2007). Pattern separation in the dentate gyrus and CA3 of the hippocampus. *Science* 315, 961–966. doi: 10.1126/science.1135801

Li, L., Bischofberger, J., and Jonas, P. (2007). Differential gating and recruitment of P/ Q-, N-, and R-type Ca2+ channels in hippocampal mossy fiber boutons. *J. Neurosci.* 27, 13420–13429. doi: 10.1523/JNEUROSCI.1709-07.2007

Liao, Y., Kariya, K. I., Hu, C. D., Shibatohge, M., Goshima, M., Okada, T., et al. (1999). RA-GEF, a novel Rap1A guanine nucleotide exchange factor containing a Ras/Rap1A-associating domain, is conserved between nematode and humans. *J. Biol. Chem.* 274, 37815–37820. doi: 10.1074/jbc.274.53.37815

Lieberman, L. R. (1965). The Boy Who Wouldn't Say "Huh": A Suggested Area For Research. *J. Speech Hear. Disord.* 30, 184–186. doi: 10.1044/jshd.3002.184

Linghu, C., Johnson, S. L., Valdes, P. A., Shemesh, O. A., Park, W. M., Park, D., et al. (2020). Spatial Multiplexing of Fluorescent Reporters for Imaging Signaling Network Dynamics. *Cell* 183, 1682–1698.e24. doi: 10.1016/j.cell.2020.10.035

Lisman, J., Buzsáki, G., Eichenbaum, H., Nadel, L., Rangananth, C., and Redish, A. D. (2017). Viewpoints: how the hippocampus contributes to memory, navigation and cognition. *Nat. Neurosci.* 20, 1434–1447. doi: 10.1038/NN.4661

Lisman, J. E., Raghavachari, S., and Tsien, R. W. (2007). The sequence of events that underlie quantal transmission at central glutamatergic synapses. *Nat. Rev. Neurosci.* 8, 597–609. doi: 10.1038/nrn2191

Lituma, P. J., Kwon, H. B., Alviña, K., Luján, R., and Castillo, P. E. (2021). Presynaptic nmda receptors facilitate short-term plasticity and bdnf release at hippocampal mossy fiber synapses. *Elife* 10:e66612. doi: 10.7554/eLife.66612

Lonart, G., Janz, R., Johnson, K. M., and Südhof, T. C. (1998). Mechanism of action of rab3A in mossy fiber LTP. *Neuron* 21, 1141–1150. doi: 10.1016/s0896-6273(00)80631-5

Lonart, G., Schoch, S., Kaeser, P. S., Larkin, C. J., Südhof, T. C., and Linden, D. J. (2003). Phosphorylation of RIM1α by PKA Triggers Presynaptic Long-Term Potentiation at Cerebellar Parallel Fiber Synapses. *Cell* 115, 49–60. doi: 10.1016/S0092-8674(03)00727-X

Lonart, G., and Südhof, T. C. (1998). Region-Specific Phosphorylation of Rabphilin in Mossy Fiber Nerve Terminals of the Hippocampus. *J. Neurosci.* 18, 634–640. doi: 10.1523/JNEUROSCI.18-02-00634.1998

Lyon, L., Borel, M., Carrión, M., Kew, J. N. C., Corti, C., Harrison, P. J., et al. (2011). Hippocampal mossy fiber long-term depression in Grm2/3 double knockout mice. *Synapse* 65, 945–954. doi: 10.1002/SYN.20923

Lysetskiy, M., Földy, C., and Soltesz, I. (2005). Long- and short-term plasticity at mossy fiber synapses on mossy cells in the rat dentate gyrus. *Hippocampus* 15, 691–696. doi: 10.1002/hipo.20096

Makani, S., Lutzu, S., Lituma, P. J., Hunt, D. L., and Castillo, P. E. (2021). Retrograde Suppression of Post-Tetanic Potentiation at the Mossy Fiber-CA3 Pyramidal Cell Synapse. *eNeuro* 8:ENEURO.0450-20.2021. doi: 10.1523/ENEURO.0450-20.2021

Maximov, A., Shin, O. H., Liu, X., and Südhof, T. C. (2007). Synaptotagmin-12, a synaptic vesicle phosphoprotein that modulates spontaneous neurotransmitter release. *J. Cell Biol.* 176, 113–124. doi: 10.1083/JCB.200607021

McEwen, J. M., Madison, J. M., Dybbs, M., and Kaplan, J. M. (2006). Antagonistic Regulation of Synaptic Vesicle Priming by Tomosyn and UNC-13. *Neuron* 51, 303–315. doi: 10.1016/j.neuron.2006.06.025

Midorikawa, M., and Sakaba, T. (2017). Kinetics of Releasable Synaptic Vesicles and Their Plastic Changes at Hippocampal Mossy Fiber Synapses. *Neuron* 96, 1033–1040e3. doi: 10.1016/j.neuron.2017.10.016

Morozov, A., Muzzio, I. A., Bourtchouladze, R., Van-Strien, N., Lapidus, K., Yin, D., et al. (2003). Rap1 Couples cAMP Signaling to a Distinct Pool of p42/44MAPK Regulating Excitability, Synaptic Plasticity, Learning, and Memory. *Neuron* 39, 309–325. doi: 10.1016/S0896-6273(03)00404-5

Mucignat-Caretta, C., and Caretta, A. (2020). Protein kinase a catalytic and regulatory subunits interact differently in various areas of mouse brain. *Int. J. Mol. Sci.* 21:3051. doi: 10.3390/ijms21093051

Neves, G., Cooke, S. F., and Bliss, T. V. (2008). Synaptic plasticity, memory and the hippocampus: a neural network approach to causality. *Nat. Rev. Neurosci.* 9, 65–75. doi: 10.1038/nrn2303

Nguyen, P. V., and Kandel, E. R. (1997). Brief theta-burst stimulation induces a transcription-dependent late phase of LTP requiring cAMP in area CA1 of the mouse hippocampus. *Learn. Mem.* 4, 230–243. doi: 10.1101/lm.4.2.230

Nozaki, K., Kubo, R., and Furukawa, Y. (2016). Serotonin modulates the excitatory synaptic transmission in the dentate granule cells. *J. Neurophysiol.* 115, 2997–3007. doi: 10.1152/jn.00064.2016

Odaka, H., Arai, S., Inoue, T., and Kitaguchi, T. (2014). Genetically-encoded yellow fluorescent cAMP indicator with an expanded dynamic range for dual-color imaging. *PLoS One* 9:e100252. doi: 10.1371/journal.pone.0100252

Ohta, Y., Furuta, T., Nagai, T., and Horikawa, K. (2018). Red fluorescent cAMP indicator with increased affinity and expanded dynamic range. *Sci. Rep.* 8:1866. doi: 10.1038/s41598-018-20251-1

Oldani, S., Moreno-Velasquez, L., Faiss, L., Stumpf, A., Rosenmund, C., Schmitz, D., et al. (2021). SynaptoPAC, an optogenetic tool for induction of presynaptic plasticity. *J. Neurochem.* 156, 324–336. doi: 10.1111/jnc.15210

Orlando, M., Dvorzhak, A., Bruentgens, F., Maglione, M., Rost, B. R., Sigrist, S. J., et al. (2021). Recruitment of release sites underlies chemical presynaptic potentiation at hippocampal mossy fiber boutons. *PLoS Biol.* 19:e3001149. doi: 10.1371/journal.pbio.3001149

Pechstein, A., Tomilin, N., Fredrich, K., Vorontsova, O., Sopova, E., Evergren, E., et al. (2020). Vesicle Clustering in a Living Synapse Depends on a Synapsin Region that Mediates Phase Separation. *Cell Rep.* 30, 2594–2602.e3. doi: 10.1016/j.celrep.2020.01.092

Pelkey, K. A., and McBain, C. J. (2005). How to Dismantle a Detonator Synapse. *Neuron* 45, 327–329. doi: 10.1016/j.neuron.2005.01.018

Pelkey, K. A., Topolnik, L., Lacaille, J. C., and McBain, C. J. (2006). Compartmentalized Ca2+ Channel Regulation at Divergent Mossy-Fiber Release Sites Underlies Target Cell-Dependent Plasticity. *Neuron* 52, 497–510. doi: 10.1016/j.neuron.2006.08.032

Pelkey, K. A., Topolnik, L., Yuan, X. Q., Lacaille, J. C., and McBain, C. J. (2008). State-dependent cAMP sensitivity of presynaptic function underlies metaplasticity in a hippocampal feedforward inhibitory circuit. *Neuron* 60, 980–987. doi: 10.1016/J.NEURON.2008.11.018

Raffelberg, S., Wang, L., Gao, S., Losi, A., Gärtner, W., and Nagel, G. (2013). A LOV-domain-mediated blue-light-activated adenylate (adenylyl) cyclase from the cyanobacterium Microcoleus chthonoplastes PCC 7420. *Biochem. J.* 455, 359–365. doi: 10.1042/BJ20130637

Regehr, W. G., Delaney, K. R., and Tank, D. W. (1994). The role of presynaptic calcium in short-term enhancement at the hippocampal mossy fiber synapse. *J. Neurosci.* 14, 523–537. doi: 10.1523/jneurosci.14-02-00523.1994

Rey, S., Marra, V., Smith, C., and Staras, K. (2020). Nanoscale Remodeling of Functional Synaptic Vesicle Pools in Hebbian Plasticity. *Cell Rep.* 30, 2006–2017.e3. doi: 10.1016/j.celrep.2020.01.051

Rizo, J. (2018). Mechanism of neurotransmitter release coming into focus. *Protein Sci.* 27, 1364–1391. doi: 10.1002/pro.3445

Rollenhagen, A., Sätzler, K., Rodríguez, E. P., Jonas, P., Frotscher, M., and Lübke, J. H. R. (2007). Structural determinants of transmission at large hippocampal mossy fiber synapses. *J. Neurosci.* 27, 10434–10444. doi: 10.1523/JNEUROSCI.1946-07.2007

Rolls, E. T. (2013). The mechanisms for pattern completion and pattern separation in the hippocampus. *Front. Syst. Neurosci.* 7:74. doi: 10.3389/FNSYS.2013.00074

Roth, B. L. (2016). DREADDs for Neuroscientists. *Neuron* 89, 683–694. doi: 10.1016/j.neuron.2016.01.040

Sadana, R., and Dessauer, C. W. (2009). Physiological roles for G protein-regulated adenylyl cyclase isoforms: insights from knockout and overexpression studies. *Neurosignals.* 17, 5–22. doi: 10.1159/000166277

Salin, P. A., Scanziani, M., Malenka, R. C., and Nicoll, R. A. (1996b). Distinct short-term plasticity at two excitatory synapses in the hippocampus. *Proc. Natl. Acad. Sci. U. S. A.* 93, 13304–13309. doi: 10.1073/PNAS.93.23.13304

Salin, P. A., Malenka, R. C., and Nicoll, R. A. (1996a). Cyclic AMP Mediates a Presynaptic Form of LTP at Cerebellar Parallel Fiber Synapses. *Neuron* 16, 797–803. doi: 10.1016/S0896-6273(00)80099-9

Sanabra, C., and Mengod, G. (2011). Neuroanatomical distribution and neurochemical characterization of cells expressing adenylyl cyclase isoforms in mouse and rat brain. *J. Chem. Neuroanat.* 41, 43–54. doi: 10.1016/j.jchemneu.2010.11.001

Sarihi, A., Mirnajafi-Zadeh, J., Jiang, B., Sohya, K., Safari, M. S., Arami, M. K., et al. (2012). Cell type-specific, presynaptic LTP of inhibitory synapses on fast-spiking GABAergic neurons in the mouse visual cortex. *J. Neurosci.* 32, 13189–13199. doi: 10.1523/JNEUROSCI.1386-12.2012

Saunders, A., Macosko, E. Z., Wysoker, A., Goldman, M., Krienen, F. M., de Rivera, H., et al. (2018). Molecular diversity and specializations among the cells of the adult mouse brain. *Cell* 174, 1015–1030.e16. doi: 10.1016/j.cell.2018.07.028

Schacher, S., Castellucci, V. F., and Kandel, E. R. (1988). cAMP Evokes Long-Term Facilitation in Aplysia Sensory Neurons That Requires New Protein Synthesis. *Science* 240, 1667–1669. doi: 10.1126/science.2454509

Schlüter, O. M., Schnell, E., Verhage, M., Tzonopoulos, T., Nicoll, R. A., Janz, R., et al. (1999). Rabphilin knock-out mice reveal that rabphilin is not required for rab3 function in regulating neurotransmitter release. *J. Neurosci.* 19, 5834–5846. doi: 10.1523/JNEUROSCI.19-14-05834.1999

Schmidt, B., Marrone, D. F., and Markus, E. J. (2012). Disambiguating the similar: the dentate gyrus and pattern separation. *Behav. Brain Res.* 226, 56–65. doi: 10.1016/J.BBR.2011.08.039

Schneggenburger, R., and Neher, E. (2005). Presynaptic calcium and control of vesicle fusion. *Curr. Opin. Neurobiol.* 15, 266–274. doi: 10.1016/j.conb.2005.05.006

Schoch, S., Castillo, P. E., Jo, T., Mukherjee, K., Geppert, M., Wang, Y., et al. (2002). RIM1alpha forms a protein scaffold for regulating neurotransmitter release at the active zone. *Nature* 415, 321–326. doi: 10.1038/415321a

Scott, R., and Rusakov, D. A. (2006). Main determinants of presynaptic Ca2+ dynamics at individual mossy fiber-CA3 pyramidal cell synapses. *J. Neurosci.* 26, 7071–7081. doi: 10.1523/JNEUROSCI.0946-06.2006

Shin, M. C., Nonaka, K., Yamaga, T., Wakita, M., Akaike, H., and Akaike, N. (2018). Calcium channel subtypes on glutamatergic mossy fiber terminals synapsing onto rat hippocampal CA3 neurons. *J. Neurophysiol.* 120, 1264–1273. doi: 10.1152/jn.00571.2017

Sihra, T. S., Wang, J. K. T., Gorelick, F. S., and Greengard, P. (1989). Translocation of synapsin I in response to depolarization of isolated nerve terminals. *Proc. Natl. Acad. Sci. U. S. A.* 86, 8108–8112. doi: 10.1073/pnas.86.20.8108

Spillane, D. M., Rosahl, T. W., Sudhof, T. C., and Malenka, R. C. (1995). Long-term potentiation in mice lacking synapsins. *Neuropharmacology* 34, 1573–1579. doi: 10.1016/0028-3908(95)00107-h

Ster, J., de Bock, F., Bertaso, F., Abitbol, K., Daniel, H., Bockaert, J., et al. (2009). Epac mediates PACAP-dependent long-term depression in the hippocampus. *J. Physiol.* 587, 101–113. doi: 10.1113/jphysiol.2008.157461

Ster, J., De Bock, F., Guérineau, N. C., Janossy, A., Barrère-Lemaire, S., Bos, J. L., et al. (2007). Exchange protein activated by cAMP (Epac) mediates cAMP activation of p38 MAPK and modulation of Ca2+-dependent K+ channels in cerebellar neurons. *Proc. Natl. Acad. Sci. U. S. A.* 104, 2519–2524. doi: 10.1073/pnas.0611031104

Stierl, M., Stumpf, P., Udwari, D., Gueta, R., Hagedorn, R., Losi, A., et al. (2011). Light modulation of cellular cAMP by a small bacterial photoactivated adenylyl cyclase, bPAC, of the soil bacterium Beggiatoa. *J. Biol. Chem.* 286, 1181–1188. doi: 10.1074/jbc.M110.185496

Südhof, T. C. (2013). Neurotransmitter release: the last millisecond in the life of a synaptic vesicle. *Neuron* 80, 675–690. doi: 10.1016/j.neuron.2013.10.022

Takai, Y., Sasaki, T., Shirataki, H., and Nakanishi, H. (1996). Rab3A small GTP-binding protein in Ca(2+)-dependent exocytosis. *Genes Cells* 1, 615–632. doi: 10.1046/J.1365-2443.1996.00257.X

Taylor, S. S., Ilouz, R., Zhang, P., and Kornev, A. P. (2012). Assembly of allosteric macromolecular switches: lessons from PKA. *Nat. Rev. Mol. Cell Biol.* 13, 646–658. doi: 10.1038/nrm3432

Toth, K., Suares, G., Lawrence, J. J., Philips-Tansey, E., and McBain, C. J. (2000). Differential mechanisms of transmission at three types of mossy fiber synapse. *J. Neurosci.* 20, 8279–8289. doi: 10.1523/jneurosci.20-22-08279.2000

Tsuboi, T., and Fukuda, M. (2005). The C2B domain of rabphilin directly interacts with SNAP-25 and regulates the docking step of dense core vesicle exocytosis in PC12 cells. *J. Biol. Chem.* 280, 39253–39259. doi: 10.1074/jbc.M507173200

Turnham, R. E., and Scott, J. D. (2016). Protein kinase A catalytic subunit isoform PRKACA, History, function and physiology. *Gene* 577, 101–108. doi: 10.1016/j.gene.2015.11.052

Tzounopoulos, T., Janz, R., Südhof, T. C., Nicoll, R. A., and Malenka, R. C. (1998). A role for cAMP in long-term depression at hippocampal mossy fiber synapses. *Neuron* 21, 837–845. doi: 10.1016/S0896-6273(00)80599-1

Vandael, D., Borges-Merjane, C., Zhang, X., and Jonas, P. (2020). Short-Term Plasticity at Hippocampal Mossy Fiber Synapses Is Induced by Natural Activity Patterns and Associated with Vesicle Pool Engram Formation. *Neuron* 107, 509–521.e7. doi: 10.1016/j.neuron.2020.05.013

Vandael, D., Okamoto, Y., and Jonas, P. (2021). Transsynaptic modulation of presynaptic short-term plasticity in hippocampal mossy fiber synapses. *Nat. Commun.* 12:2912. doi: 10.1038/S41467-021-23153-5

Villacres, E. C., Wong, S. T., Chavkin, C., and Storm, D. R. (1998). Type I Adenylyl Cyclase Mutant Mice Have Impaired Mossy Fiber Long-Term Potentiation. *J. Neurosci.* 18, 3186–3194. doi: 10.1523/JNEUROSCI.18-09-03186.1998

Vyleta, N. P., Borges-Merjane, C., and Jonas, P. (2016). Plasticity-dependent, full detonation at hippocampal mossy fiber–CA3 pyramidal neuron synapses. *Elife* 5:e17977. doi: 10.7554/eLife.17977

Vyleta, N. P., and Jonas, P. (2014). Loose coupling between Ca2+ channels and release sensors at a plastic hippocampal synapse. *Science* 343, 665–670. doi: 10.1126/SCIENCE.1244811

Waltereit, R., and Weller, M. (2003). Signaling from cAMP/PKA to MAPK and synaptic plasticity. *Mol. Neurobiol.* 27, 99–106. doi: 10.1385/MN:27:1:99

Wang, H., Pineda, V. V., Chan, G. C. K., Wong, S. T., Muglia, L. J., and Storm, D. R. (2003). Type 8 Adenylyl Cyclase Is Targeted to Excitatory Synapses and Required for Mossy Fiber Long-Term Potentiation. *J. Neurosci.* 23, 9710–9718. doi: 10.1523/JNEUROSCI.23-30-09710.2003

Wang, X., Hu, B., Zimmermann, B., and Kilimann, M. W. (2001). Rim1 and rabphilin-3 bind Rab3-GTP by composite determinants partially related through N-terminal alpha -helix motifs. *J. Biol. Chem.* 276, 32480–32488. doi: 10.1074/JBC.M103337200

Wang, Y., Okamoto, M., Schmitz, F., Hofmann, K., and Südhof, T. C. (1997). Rim is a putative Rab3 effector in regulating synaptic-vesicle fusion. *Nature* 388, 593–598. doi: 10.1038/41580

Weisskopf, M. G., Castillo, P. E., Zalutsky, R. A., and Nicoll, R. A. (1994). Mediation of hippocampal mossy fiber long-term potentiation by cyclic AMP. *Science* 265, 1878–1882. doi: 10.1126/science.7916482

Weyhersmüller, A., Hallermann, S., Wagner, N., and Eilers, J. (2011). Rapid active zone remodeling during synaptic plasticity. *J. Neurosci.* 31, 6041–6052. doi: 10.1523/JNEUROSCI.6698-10.2011

Willoughby, D., and Cooper, D. M. F. (2007). Organization and Ca2+ regulation of adenylyl cyclases in cAMP microdomains. *Physiol. Rev.* 87, 965–1010. doi: 10.1152/PHYSREV.00049.2006

Witter, M. P. (2007). The perforant path: projections from the entorhinal cortex to the dentate gyrus. *Prog. Brain Res.* 163, 43–61. doi: 10.1016/S0079-6123(07)63003-9

Wolfes, A. C., and Dean, C. (2020). The diversity of synaptotagmin isoforms. *Curr. Opin. Neurobiol.* 63, 198–209. doi: 10.1016/J.CONB.2020.04.006

Wong, S. T., Athos, J., Figueroa, X. A., Pineda, V. V., Schaefer, M. L., Chavkin, C. C., et al. (1999). Calcium-Stimulated Adenylyl Cyclase Activity Is Critical for Hippocampus-Dependent Long-Term Memory and Late Phase LTP. *Neuron* 23, 787–798. doi: 10.1016/S0896-6273(01)80036-2

Yang, Y., and Calakos, N. (2013). Presynaptic long-term plasticity. *Front. Synaptic Neurosci.* 5:8. doi: 10.3389/fnsyn.2013.00008

Yassa, M. A., and Stark, C. E. L. (2011). Pattern separation in the hippocampus. *Trends Neurosci.* 34, 515–525. doi: 10.1016/j.tins.2011.06.006

Yizhar, O., Matti, U., Melamed, R., Hagalili, Y., Bruns, D., Rettig, J., et al. (2004). Tomosyn inhibits priming of large dense-core vesicles in a calcium-dependent manner. *Proc. Natl. Acad. Sci. U. S. A.* 101, 2578–2583. doi: 10.1073/pnas.0308700100

Yoshino, M., Sawada, S., Yamamoto, C., and Kamiya, H. (1996). A metabotropic glutamate receptor agonist DCG-IV suppresses synaptic transmission at mossy fiber pathway of the guinea pig hippocampus. *Neurosci. Lett.* 207, 70–72. doi: 10.1016/0304-3940(96)12486-1

Zalutsky, R. A., and Nicoll, R. A. (1990). Comparison of two forms of long-term potentiation in single hippocampal neurons. *Science* 248, 1619–1624. doi: 10.1126/science.2114039

Zhao, M., Choi, Y. S., Obrietan, K., and Dudek, S. M. (2007). Synaptic plasticity (and the lack thereof) in hippocampal CA2 neurons. *J. Neurosci.* 27, 12025–12032. doi: 10.1523/JNEUROSCI.4094-07.2007

Zucker, R. S. (1999). Calcium- and activity-dependent synaptic plasticity. *Curr. Opin. Neurobiol.* 9, 305–313. doi: 10.1016/S0959-4388(99)80045-2

Conflict of Interest: The authors declare that the research was conducted in the absence of any commercial or financial relationships that could be construed as a potential conflict of interest.

frontiers | Frontiers in Synaptic Neuroscience

ORIGINAL RESEARCH
published: 12 May 2022
doi: 10.3389/fnsyn.2022.858340

Presynaptic Mitochondria Communicate With Release Sites for Spatio-Temporal Regulation of Exocytosis at the Motor Nerve Terminal

*Mario Lopez-Manzaneda†, Andrea Fuentes-Moliz† and Lucia Tabares**

Department of Medical Physiology and Biophysics, School of Medicine, University of Seville, Seville, Spain

Presynaptic Ca^{2+} regulation is critical for accurate neurotransmitter release, vesicle reloading of release sites, and plastic changes in response to electrical activity. One of the main players in the regulation of cytosolic Ca^{2+} in nerve terminals is mitochondria, which control the size and spread of the Ca^{2+} wave during sustained electrical activity. However, the role of mitochondria in Ca^{2+} signaling during high-frequency short bursts of action potentials (APs) is not well known. Here, we studied spatial and temporal relationships between mitochondrial Ca^{2+} (mCa^{2+}) and exocytosis by live imaging and electrophysiology in adult motor nerve terminals of transgenic mice expressing synaptophysin-pHluorin (SypHy). Our results show that hot spots of exocytosis and mitochondria are organized in subsynaptic functional regions and that mitochondria start to uptake Ca^{2+} after a few APs. We also show that mitochondria contribute to the regulation of the mode of fusion (synchronous and asynchronous) and the kinetics of release and replenishment of the readily releasable pool (RRP) of vesicles. We propose that mitochondria modulate the timing and reliability of neurotransmission in motor nerve terminals during brief AP trains.

Keywords: mitochondria, synapse, exocytosis, calcium, synchronous release, asynchronous release, neuromuscular junction, active zones

OPEN ACCESS

Edited by:
Henrique Prado von Gersdorff, Oregon Health and Science University, United States

Reviewed by:
Robert B. Renden, University of Nevada, Reno, United States
Vincenzo Marra, University of Leicester, United Kingdom
Steve D. Meriney, University of Pittsburgh, United States

****Correspondence:***
Lucia Tabares
Ltabares@us.es

†These authors have contributed equally to this work and share first authorship

Received: *19 January 2022*
Accepted: *07 April 2022*
Published: *12 May 2022*

Citation:
Lopez-Manzaneda M, Fuentes-Moliz A and Tabares L (2022) Presynaptic Mitochondria Communicate With Release Sites for Spatio-Temporal Regulation of Exocytosis at the Motor Nerve Terminal. Front. Synaptic Neurosci. 14:858340. doi: 10.3389/fnsyn.2022.858340

INTRODUCTION

Synapses can broadly modulate their responses according to the pattern of the stimuli they receive, which has important consequences for information processing. Short-term synaptic plasticity is mostly presynaptic, and multiple mechanisms enhance or depress the synaptic output. Presynaptic Ca^{2+} is one of the main determinants of plasticity as it regulates exocytosis, endocytosis, and synaptic vesicle mobilization (Wu et al., 2014; Chamberland and Tóth, 2016; Leitz and Kavalali, 2016). For example, different electrical stimulation patterns generate distinct spatio-temporal increases in intracellular Ca^{2+} concentration [$(Ca^{2+})_i$], which, in turn, determine the number and timing of vesicle fusions. Among the multiple modes of neurotransmitter release, spontaneous, phasic, and asynchronous, the last two are action potential (AP) dependent. Phasic (synchronous) release is triggered by the arrival of one or more AP to the nerve terminal and the subsequent rapid and transient influx of Ca^{2+} through voltage-gated calcium channels in active zones (AZ), which

produces the fusion of primed synaptic vesicles with the plasma membrane on a submillisecond time scale. Following the fusion of vesicles, the AZs reorganize, and new vesicles are recruited and docked to the release sites so that neurotransmission can continue efficiently. Asynchronous release occurs during and after a stimulation train due to the accumulation of Ca^{2+} (residual Ca^{2+}) at release sites (Atluri and Regehr, 1998).

The large capacity of mitochondria to sequester and release Ca^{2+} is essential in many cell types to maintain Ca^{2+} homeostasis for different functions, from muscle contraction to secretion (Pallafacchina et al., 2021). In nerve cells, mitochondria are highly sensitive to increases in cytosolic [Ca^{2+}] (Chouhan et al., 2010; Ashrafi et al., 2019; Lopez-Manzaneda et al., 2021), making them good candidates to regulate synaptic activity and plasticity (MacAskill et al., 2010; Harris et al., 2012; Yang et al., 2021). Mitochondria have been shown to participate in the regulation of synchronous and asynchronous neurotransmitter release during an intense neuronal activity at motor nerve terminals (Tang and Zucker, 1997; David and Barrett, 2000, 2003; Talbot et al., 2003; Mironov and Symonchuk, 2006). However, the role of mitochondrial Ca^{2+} uptake in secretion properties during short-duration high-frequency AP bursts at mouse motor nerve terminals remained to be investigated.

Here, we used combined simultaneous real-time measurement of mitochondrial Ca^{2+} (mCa^{2+}) and exo-endocytosis to analyze the spatial and temporal relationships between release sites and mCa^{2+} uptake during electrical nerve activity. Furthermore, intracellular synaptic potential recordings were used to examine the effects of inhibiting mCa^{2+} uptake by carbonyl cyanide m-chlorophenylhydrazone (CCCP) on synaptic transmission. We found that mitochondria participate in establishing synaptic properties even during short bursts of AP.

MATERIAL AND METHODS

Animal Model

We generated an FVB/NJ mouse line that expressed the Synaptophysin-pHluorin (SypHy) protein endogenously in neurons under the Thy1.2 promoter[1]. SypHy mice appeared normal in size, weight, and behavior, and the morphology and functionality of their motor nerve terminals were indistinguishable from SypHy negative mice. The recordings were made in adult mice (2–3 months old). All experiments were carried out according to the guidelines of the Directive of the European Council for Laboratory Animal Care and the Animal Care and Ethics Committee of the University of Seville.

Acute Neuromuscular Preparation

Mice were killed with 100% CO_2. The levator auris longus (LAL) muscle, a fast-twitch muscle located in the rear part of the neck (Ojeda et al., 2020), was dissected as previously described (Tejero et al., 2016). The neuromuscular preparations were superfused with a solution of the following composition (in mM): NaCl 135, KCl 4, $CaCl_2$ 2, $MgCl_2$ 1, $NaHCO_3$ 15, NaH_2PO_4 0.33, and glucose 10. The solution was continuously gassed with 95% O_2 and 5% CO_2.

Mitochondrial Calcium Probe Loading

For mitochondrial calcium measurements, we used the membrane-permeable Rhod-2 AM probe (Thermo Fisher, R1245MP, Spain). The acetoxymethyl ester (AM) form is preferentially restricted to mitochondria because of its net positive charge. Rhod-2 is a single wavelength Ca^{2+} indicator with a maximum absorption/emission wavelength of ∼557/581 nm and a K_D of ∼570 nM. As described before (Lopez-Manzaneda et al., 2021), the probe was dissolved in dimethylsulfoxide (DMSO) and diluted to a final concentration of 5 μM in the solution that perfused the neuromuscular preparation. The preparation was incubated with the probe for 30 min at room temperature. After incubation, the preparation was washed with the physiological solution in the absence of the probe for 30 min at 28°C–32°C.

Live Imaging and Analysis

The nerve was stimulated using a suction electrode. Action potentials were elicited by square wave pulses of 0.15 ms duration and 2–10 mV amplitude at variable frequencies (20–100 Hz) and train durations (1–20 s)using an isolated pulse stimulator (A-M Systems, mo. 2100, USA). Muscle contractions were prevented by adding 10 μM D-tubocurarine (Sigma-Aldrich, T2379, Spain) to the bath solution. Intervals between trains were always ≥10 min unless otherwise stated to allow complete recovery of terminal resting values. Experiments were conducted at 28–32°C using a temperature controller (TC-344B) connected to a thermistor (SF-28 SloFlo, Warner Instruments, USA). Exo-endocytosis (SypHy) and mCa^{2+} (Rhod-2) images were acquired and analyzed similarly. SypHy and Rhod-2 were excited with a 488 nm laser line. The different emission signals were captured separately using a 525/50 nm emission filter for the SypHy signal and a 617/73 nm emission filter for the Rhod-2 signal. Both fluorescence signals were monitored with a Yokogawa CSU-X1 spinning disk system (3i, Germany) mounted on an upright BX61WI microscope (Olympus, Spain) equipped with a water-immersion LUMPlanFI objective (x60, NA: 0.9). The images were captured using an EM-CCD camera C9100-13 (Hamamatsu, Spain) with an effective number of pixels of 512(H) × 512(V) and a pixel size of 16 × 16 μm. The images were acquired up to four frames per second with commercial software (SlideBook™ 5.0, 3i, Germany), only in the best focus plane since the 3D simultaneous acquisition was not possible given the low fluorescent intensity of SypHy and the fast rise of the Rhod-2 signals.

Before analysis, images were aligned using the automatic routine of the Slidebook program. Images were exported to FIJI (ImageJ) and split into two separate channels. The regions of interest (ROI) were outlined with a threshold-based macro routine, and the data were exported to Microsoft Office Excel. The fluorescence intensity of each ROI was corrected by subtracting the mean background level in the corresponding channel. Fluorescence intensity values were plotted vs. time to

[1]https://idus.us.es/bitstream/handle/11441/24203/S_TD_PROV162.pdf?sequence%20=%201&isAllowed%20=%20y

calculate different parameters. Correction for time-dependent loss of the SypHy signal, primarily due to photobleaching, was performed by subtracting the exponential fits of the resting-state fluorescence before and after recovery from the stimuli. Although each ROI was analyzed individually, the characteristics of the different ROI responses of the same nerve terminal were usually similar and thus averaged together for plotting the mean response (**Figure 1C**). Baseline fluorescence (F_{basal}) was measured as the average fluorescence in ROIs before the stimulus (at least 10 frames). The change in fluorescence was expressed as ΔF ($\Delta F = F - F_{basal}$) or normalized to the baseline ($\Delta F/F_{basal}$). For mCa^{2+} (Rhod-2), the rise time was calculated as the time from 10 to 90% of the maximum fluorescence, and the decay time was calculated as the time required for the signal to return to half of its maximum value ($t_{1/2}$). For the colocalization analysis between Rhod-2 and SypHy fluorescence signals, the JACoP (Bolte and Cordelières, 2006) plugin was used.

Electrophysiology

The nerve was stimulated using a suction electrode. Action potentials were elicited by square wave pulses of 0.15 ms duration and 2–10 mV amplitude. A glass microelectrode (10–20 MΩ) filled with 3 M KCl was connected to an intracellular recording amplifier (TEC-05X; npi electronic, Germany) and used to impale single muscle fibers near the motor nerve endings. Evoked EPP and mEPP were recorded at room temperature (22°C–23°C), as previously described (Lopez-Manzaneda et al., 2021). Muscle contractions were prevented by including in the bath 2 μM μ-conotoxin GIIIB (Alomone Laboratories, C-270, Israel), a specific blocker of voltage-gated sodium channels in skeletal muscle. The recordings were sampled at 20 kHz, the mean amplitudes of the EPP and mEPP normalized to a resting membrane potential of −70 mV, and the EPP was corrected for nonlinear summation (McLachlan and Martin, 1981). Quantum content (*m*) was estimated by the direct method, which consists of recording mEPPs and EPPs (nerve stimulation 0.5 Hz) simultaneously and then calculating the ratio: *m* = Average EPP amplitude/Average mEPP amplitude. During a high-frequency train, *m* was estimated by calculating the ratio between each EPP and the average amplitude of the mEPPs for each experimental condition. To estimate the size of the RRP, *m* values during a train were plotted against time and fitted to a sequential model, as previously described (Ruiz et al., 2011). Briefly, the model assumes that quanta release on the stimulus came from the RRP, which subsequently was depleted along an exponential time course. The model also states that the recruitment process began after the first stimulus and rose sigmoidally to the plateau level as the original RRP became depleted. Then, we fitted the entire observed curve of quantal content along the train ($m(t)$) with two functions: a declining exponential plus a rising sigmoid, representing the contribution of the depletion of the RRP and the recruited vesicles, respectively: $m(t) = A^*\exp(-t/B) + C/(1 + \exp(-(t - D)/E))$, where A represents initial *m*; B, time constant of RRP depletion; C, mean amplitude of the plateau; D, half-time of refilling; and E, steepness of the refilling time course. We constrained the sigmoid to start at zero. Integration of the first exponential gives the size of the RRP.

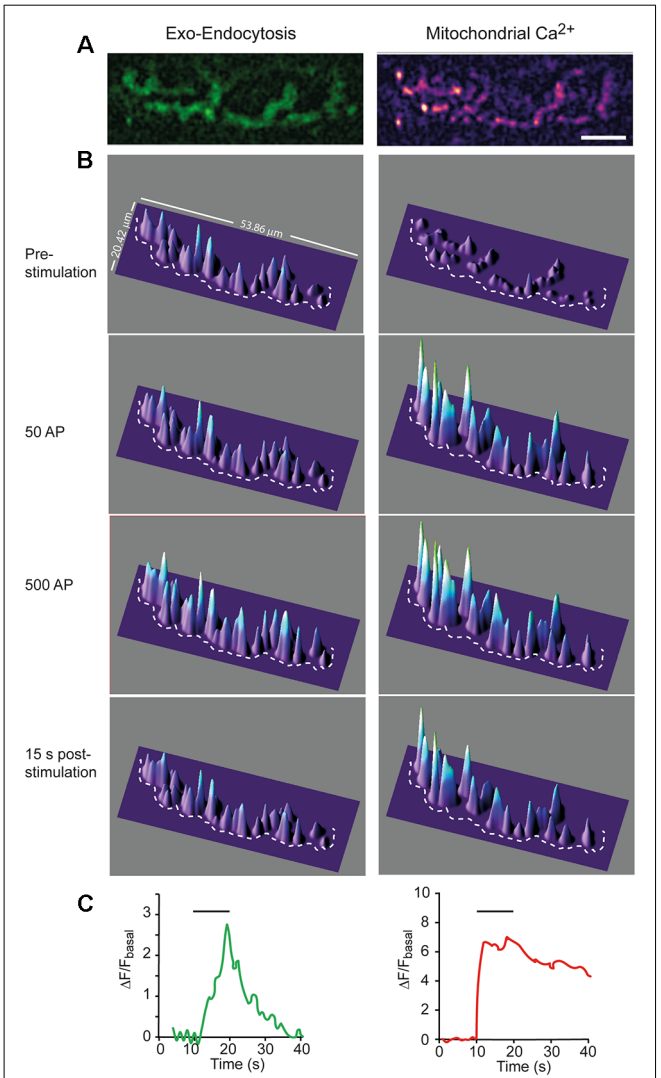

FIGURE 1 | Simultaneous recording of hot spots of exocytosis and mCa^{2+} in a single nerve terminal. **(A)** Representative example of SypHy (left) and Rhod-2 (right) fluorescence signals recorded from a nerve terminal at the end of a 10 s stimulation train at 50 Hz. Calibration bar: 10 μm. **(B)** 3D intensity plots of the same terminal before, during stimulation (after 50 and 500 AP), and after stimulation. The dotted line partially displays the boundary of the terminal. **(C)** Mean intensity changes of SypHy (left graph) and Rhod-2 (right graph) vs. time at the terminal in **(A)**. Horizontal lines show the start and end of the stimulation train.

The mitochondrial membrane potential (ψ_m) was depolarized with the protonophore carbonyl cyanide m-chlorophenylhydrazone (CCCP, 0.5–2 μM, Sigma-Aldrich C2759, Spain), which inhibits complex III of the electron transport chain preventing mCa^{2+} uptake and mitochondrial ATP synthesis. Mitochondrial complex V was inhibited with oligomycin (5 mg/ml, Sigma-Aldrich, Spain, O4876) to minimize ATP hydrolysis and partial ψ_m depolarization (David et al., 1998; David and Barrett, 2000). When possible, the

same fiber was first recorded in the absence of drugs (control), then with oligomycin alone (after 20–30 min of incubation), and finally with oligomycin plus CCCP. The addition of oligomycin alone did not affect the amplitude or frequency of mEPPs compared to the control. The exposition time to CCCP was restricted to a maximum of 20–30 min to minimize the possible effects of decreasing/interrupting the oxidative ATP synthesis.

Asynchronous release during 50 Hz trains was estimated by counting the events between the second half of the inter-stimulus interval and multiplying by two since asynchronous events during the evoked responses could not be detected accurately (Talbot et al., 2003). However, in CCCP, when the frequency of mEPP became too high to be resolved, we calculated the area under the baseline elevation after correcting for nonlinear summation and divided by the pretrain averaged mEPP area, as previously described (Van der Kloot, 1990; David et al., 2003). Asynchronous release peak rates were calculated as the mean number of asynchronous events during the last 60 ms of 1-s trains and expressed per millisecond.

The probability of release for synchronous release upon the first shock of a stimulation train was calculated as the ratio of initial *m* vs. the estimated RRP size.

Statistical Analysis

Statistical analysis of the imaging and electrophysiological data was performed using GraphPad Prism 5 (GraphPad Software). All values mentioned in the text and represented in the graphs are averages ± standard errors of the mean (SEM) unless otherwise stated. Parametric statistics were used whenever possible. The assumption of homogeneity of variances was assessed with the Levene test, using $\alpha = 0.05$ as the cutoff. The Kruskal-Wallis rank-sum test was used when the distribution was not normal, followed by the *post hoc* Dunns multiple comparison test.

Given that the number of nerve terminals analyzed per condition was typically six, each terminal was treated as statistically independent. The results were considered statistically different when the P-value was <0.05. Data in parentheses (*n, N*): *n*, the number of nerve terminals (imaging experiments) or muscle fibers (electrophysiological experiments) per group; *N*, the number of mice per group. All reported experiments include the results of at least three animals per condition.

RESULTS

Spatio-Temporal Relationship Between Exocytosis and mCa^{2+} Uptake

We simultaneously monitored mCa^{2+} with Rhod-2 AM and exo-endocytosis in adult transgenic mice expressing synaptophysin-pHluorin (SypHy; Lopez-Manzaneda et al., 2021). The acetoxymethyl (AM) ester group of Rhod-2, which facilitates its uptake, is removed by intracellular esterases, resulting in the selective accumulation of the calcium dye within mitochondria (David et al., 1998; Talbot et al., 2003).

Figures 1A,B show 2D and 3D images, respectively, for Syphy and mCa^{2+} signals in a representative nerve terminal, stimulated with a 500 AP train (50 Hz). The surface intensity plots of the SypHy signal (**Figure 1B**, green channel, left column) displayed multiple peaks distributed along the terminal surface, which amplitudes increased upon stimulation, especially in certain regions, which represent hot spots of exocytosis (Wu and Betz, 1999; Tabares et al., 2007; Gaffield et al., 2009; Cano et al., 2012; Lopez-Manzaneda et al., 2021), and remain stable with repeated trains (Tabares et al., 2007).

The time course of the SypHy increase was relatively slow. **Figure 1B**, second and third panels, shows the fluorescence increase, representing the excess of exocytosis over endocytosis, at 1 s (50 AP) and 10 s (500 AP) of the stimulation. When stimulation ceased, fluorescence decreased to the base level (lower panel) due to the endocytosis-reacidification process (Sankaranarayanan et al., 2000). **Figure 1C** (left graph) shows the average change in SypHy fluorescence vs. time at this terminal. The amplitude of the signal and the time constant of endocytosis (∼7 s) were similar to what has previously been described in this synapse (Cano et al., 2012; Cano and Tabares, 2016).

Similarly, the mCa^{2+} signal was distributed along the terminal surface, although its rising kinetics was much faster (**Figure 1B**, right column and **Figure 1C**, right graph) than the SypHy signal. The mCa^{2+} signal stayed high (plateau) during the stimulation train (second and third panels). The plateau represents the dynamic equilibrium between Ca^{2+} uptake, reversible formation of Ca^{2+}-phosphate complexes, and Ca^{2+} efflux (Gunter and Sheu, 2009). After stimulation, the signal slowly returned to the basal level, indicating mCa^{2+} release to the cytosol, a process mainly driven by the mitochondrial Na^+/Ca^{2+} exchanger. The average rise time was 1.07 ± 0.21 s, and the decay half-time was 17.67 ± 2.38 s ($n = 6$), which is consistent with previous measurements from presynaptic mitochondria of postnatal mouse motor nerve terminals (Lopez-Manzaneda et al., 2021). The slow release of Ca^{2+} from mitochondria has been shown to transitorily elevate cytosolic Ca^{2+} and promote post-tetanic potentiation at the mouse and crayfish motor nerve terminals (Tang and Zucker, 1997; García-Chacón et al., 2006) and at hippocampal mossy fiber synapses (Lee et al., 2007). In our recordings, Ca^{2+} efflux from mitochondria was slower than the endocytosis time course. Then, it would be of interest to determine in future studies whether mCa^{2+} release participates in the regulation of endocytosis.

Estimation of Inter-distances Between Mitochondria and Exocytosis Hot Spots by Quantitative Spatial Analysis

We performed an object-based approach analysis (Bolte and Cordelières, 2006) to examine the spatial relationship between mitochondria and exocytosis hot spots. The procedure was as follows: First, the maximum increase in fluorescence (ΔF_{exo} and $\Delta FmCa^{2+}$) at both channels was obtained by subtracting the intensity of their respective last images during the stimulation from the average intensity obtained before stimulation (mean of 10 images). Then, the regions of interest (ROIs) were established

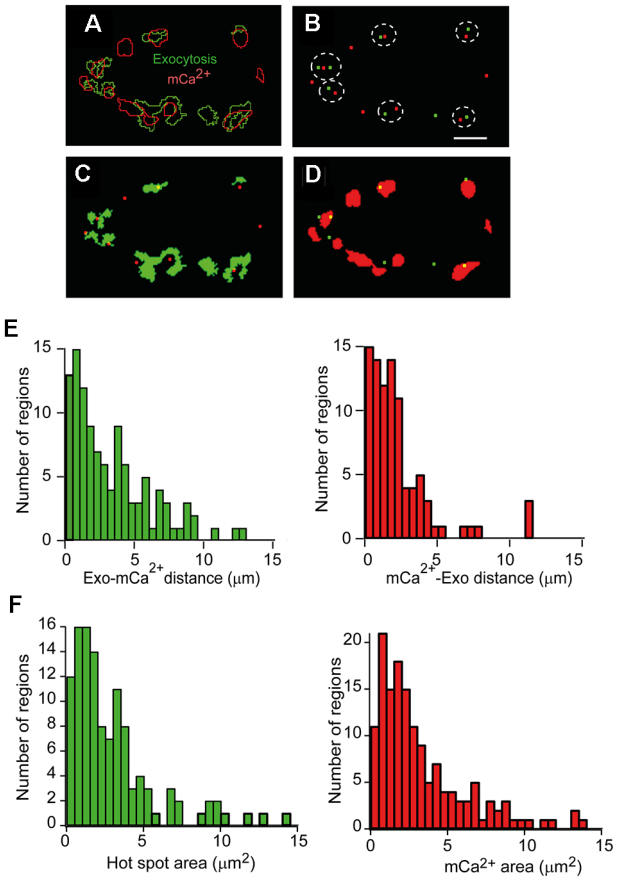

FIGURE 2 | Quantitative analysis of the spatial relationship between exocytosis hot spots and mCa^{2+}. **(A)** Representative image showing the outlines of hot spots of exocytosis regions (green) and mCa^{2+} increase regions (red) superimposed after a 500 AP train (50 Hz) of stimulation. **(B)** Spatial distribution of exocytosis hot spots centroids (green) and mCa^{2+} (red) centroids of the terminal in **A**. The dotted lines indicate the nearest neighbors between exocytosis hot spots and mCa^{2+}. **(C)** Location of mCa^{2+} centroids (red) and the exocytosis hot spot areas (green). **(D)** Location of exocytosis hot spots centroids (green) and the mCa^{2+} areas (red). Calibration bar **(A–D)**: 5 μm. **(E)** Distance distribution between nearest-neighbor centroids in 11 terminals (four mice). Left: exocytosis-mCa^{2+} distance. Right: mCa^{2+}-exocytosis hot spots distance. **(F)** Frequency histograms of the exocytosis hot spots areas (left) and mCa^{2+} region areas (right; 14 terminals, six mice) in each case.

using an intensity auto threshold macro (Lopez-Manzaneda et al., 2021), and the outlines were represented. Finally, the geometric center (centroid) of each ROI was obtained, and the inter-distances between objects were calculated (see "*Materials Methods*" Section). For example, **Figure 2A** shows the outlines from a representative nerve terminal containing 10 active mCa^{2+} regions (red outlines) and eight exocytosis hot spots (green outlines) merged in the same image.

Figure 2B shows the overlay of the centroids of the exocytosis hot spots (green) and the mCa^{2+} centroids (red) of the nerve terminal shown in **Figure 2A**. The dotted lines highlight the nearest neighbors' centroids between channels. The centroids in one channel and the ROIs in the other channel, and *vice versa*, are also shown for this terminal (**Figures 2C,D**). In general, most exocytosis hot spots were close to one or two active mitochondrial regions.

The distance distributions of the closest neighbor centroids between channels in a total of 11 nerve terminals from four experiments are shown in **Figure 2E**. The distances are represented in two histograms since the number of centroids in one channel and the other was not the same for a given terminal. The most frequent inter-distances between centroids of different channels were ∼0.5–1 μm, and ∼61% of exocytosis hot spots centroids were within 2 μm of a mCa^{2+} centroid, and ∼47% of mCa^{2+} centroids were within 2 μm from an exocytosis centroid.

Next, we wondered how many AZs could be within our exocytosis hot spots. In mouse motor nerve terminals, AZs are distributed throughout the surface terminal, and the mean density of AZs is $\sim 2.4/\mu m^2$ (Fukunaga et al., 1983; Nishimune et al., 2004; Ruiz et al., 2011). Since, in our experiments, 80% of the hot spots had a surface area of $\leq 4\ \mu m^2$ (**Figure 2F**, left histogram, 14 terminals, six mice), we estimate they may contain between ∼1 and 12 AZs. For comparison, the size distribution of the mCa^{2+} regions measured in our experiments is shown in the right histogram of **Figure 2F**.

Together, these observations suggest that hot spots of exocytosis and a subset of mitochondria are located in sub-synaptic functional domains (tandems). This distribution may contribute to the local regulation of $[Ca^{2+}]$ and facilitate the delivery of ATP at places of high exocytosis activity.

Presynaptic Mitochondria Efficiently Uptake Ca^{2+} in the Physiological Range of Neural Activity

To examine the capacity of presynaptic mitochondria to respond to physiological stimuli, we used short-duration stimulation trains and different stimulation frequencies. For example, **Figure 3A** shows a representative nerve terminal stimulated with six consecutive 1-s trains at 50 Hz, spaced 2–3 s. The plateau amplitude was essentially reached with the first train, confirming the high sensitivity of mitochondria to a brief high-frequency burst of APs. The plateau was not due to probe saturation since permeabilization of the membrane with digitonin increased the fluorescence above the plateau amplitude (data not shown, and Lopez-Manzaneda et al., 2021).

We also compared the amplitude and the rising kinetics of the mCa^{2+} responses at different stimulation frequencies while maintaining the number of action potentials constant (500 AP). The mean amplitude of the responses increased little with the stimulation frequency (3.7-fold ± 0.43 at 20 Hz, 4.01-fold ± 0.53 at 50 Hz, and 4.36-fold ± 0.46 at 100 Hz; n = 5–8 nerve terminals at each frequency; **Figure 3B**), indicating a powerful calcium buffering system in the matrix (David, 1999; David et al., 2003). However, the rising kinetics of the signal was very sensitive to the stimulation frequency. **Figure 3C** shows the average time course of mCa^{2+} rise at each frequency, normalized to the plateau amplitude ($\Delta F/F_{max}$). The half-maximum amplitudes were reached at ∼190 ms (100 Hz), ∼360 ms (50 Hz), and ∼650 ms (20 Hz), which correspond

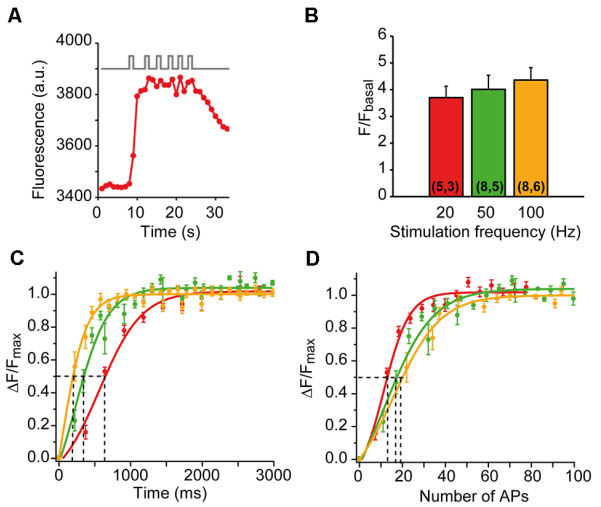

FIGURE 3 | mCa^{2+} responses to different patterns of nerve stimulation. **(A)** mCa^{2+} increases to six successive trains of 1-s duration at 50 Hz in a representative nerve terminal. **(B)** The average increase in fluorescence ($\Delta F/F_{basal}$) at 20, 50, and 100 Hz. The numbers of terminals and mice recorded are in parentheses. **(C,D)** Average fluorescence increase ($\Delta F/F_{max}$) as a function of time **(C)** and number of AP **(D)** at 20 (red symbols), 50 (green symbols), and 100 (yellow symbols) Hz. The solid lines are sigmoidal fit on the data. The time required to reach half-maximum mCa^{2+} (dotted lines in **C**) varies between 650 ms (20 Hz) and 190 ms (100 Hz). Half-increase in fluorescence is achieved with 13–19 AP (dotted lines in **D**). The apparent higher sensitivity of the response at 20 Hz in **(D)** is probably not such but reflects the time-dependent component of the response, as shown in **(C)**.

to the firing of 13–19 APs (**Figure 3D**). These results indicate that presynaptic mitochondria efficiently uptake calcium in the physiological range of neural activity of this synapse.

Reduction of mCa^{2+} Uptake May Alter Exocytosis

To explore the role of mitochondria in modulating synaptic strength, we recorded exocytosis and mCa^{2+} before and after adding CCCP to the bath solution. CCCP inhibits complex III of the electron transport chain, which depolarizes the mitochondrial membrane potential (ψm), reduces stimulation-induced mitochondrial Ca^{2+} uptake, and increases cytosolic $[Ca^{2+}]$ (Tang and Zucker, 1997; David et al., 1998; David, 1999; Suzuki et al., 2002; David and Barrett, 2003; Talbot et al., 2003; Lopez-Manzaneda et al., 2021). In addition, ψm depolarization reduces the electromotive force used for mitochondrial ATP synthesis and produces additional ATP depletion associated with ATP synthase (complex V) reversion. To prevent this extra hydrolysis of ATP, we added oligomycin (5 μg/ml) before CCCP, an inhibitor of complex V that does not depolarize ψm (David et al., 1998).

Figure 4 shows a representative example of a nerve terminal where mCa^{2+} and exocytosis were recorded first in oligomycin alone and then in oligomycin plus CCCP. As expected, the mCa^{2+} response to a 500 AP stimulation train (50 Hz) decreased considerably in the presence of CCCP (**Figure 4A**). On the contrary, the exo-endocytosis response increased (transitorily) over time (**Figure 4C**), compared to the oligomycin response alone (**Figure 4B**, purple trace: after 23 min in oligomycin; brown, blue, and orange traces: 5, 10, and 15 min in oligomycin plus CCCP). Normalizing the responses to their peak amplitudes (**Figure 4D**) revealed similar rise and decay kinetics in oligomycin (purple trace) and up to 10 min in CCCP (blue trace), and only slower relaxation after 15 min of CCCP (orange trace). The increases in the amplitude of the responses suggested an increase in exocytosis due to the elevation of cytosolic Ca^{2+}. However, this effect was followed by a marked decrease in the signal soon after, an effect varying greatly between different terminals. For this reason, we decided to further investigate the effect of mitochondria on secretion using an electrophysiological approach, which would allow us to use shorter stimulation trains and, therefore, minimize ATP consumption.

Mitochondria Limit Asynchronous Release During Short-Duration AP Trains

To further elucidate the role of mitochondria in neurotransmission during short-duration high-frequency nerve activity, we recorded endplate potentials (EPP) and miniature endplate potentials (mEPP) in the control solution, then in oligomycin, and finally with oligomycin plus CCCP in the same fiber. Stimulation in the control solution produced the typical response consisting of a progressive decrease in the EPP amplitude from an initial value to a plateau that was approximately one-half of the initial amplitude (**Figure 5A**, left recording). Stimulation after 20 min of incubation with oligomycin (5 mg/ml) did not significantly change the response (**Figure 5A**, central recording) nor the amplitude of EPP and mEPP. However, 5 min after adding oligomycin + CCCP (1 μM), there was an elevation on the baseline (**Figure 5A**, right recording) during the second half of the stimulation train and several seconds after the train due to the buildup of asynchronous release (David and Barrett, 2003). This response was never observed in control or oligomycin alone.

Before each train, the mEPP rates were similar in control (2.55 vesicles/s) and oligomycin (2.67 vesicles/s) but slightly elevated in CCCP (6.87 vesicles/s), which may represent a small increase in resting $[Ca^{2+}]_i$.

Estimation of the amount of intra-train asynchronous events (see "*Materials Methods*" Section) in this fiber showed two orders of magnitude higher peak vesicle release rates in CCCP (∼2,500 s^{-1}, **Figure 5B**) than in control and oligomycin (∼30 s^{-1}), indicating that the mean survival time of a vesicle before fusing asynchronously changed from ∼33 ms to a fraction of a ms after CCCP. On the contrary, on average, no statistical differences were found between control and oligomycin alone, which agrees with a previous report showing that the increase in asynchronous release with CCCP, in experiments lasting <1 h, is due to the increase in the $[Ca^{2+}]_i$ rather than inhibition of mitochondrial ATP synthesis (David and Barrett, 2003).

In contrast, cumulative synchronous release was reduced in CCCP compared to the control (**Figure 5C**). On average, the maximum vesicle release rate (**Figure 5D**) for synchronous release was approximately half in CCCP (1,649 ± 290 vesicles/s,

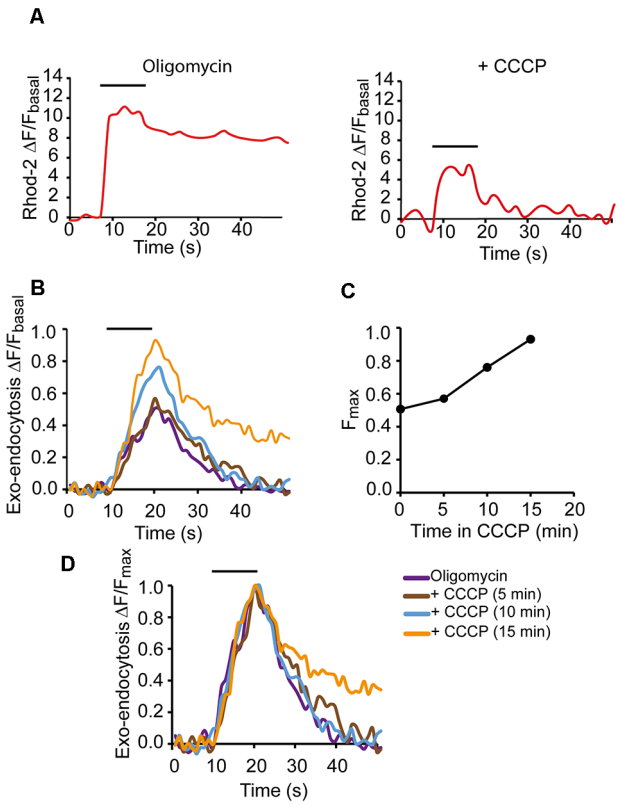

FIGURE 4 | Modification of the secretory response in depolarized mitochondria. **(A)** mCa^{2+} responses to 500 AP stimulation (50 Hz) in oligomycin only solution (left graph) and with oligomycin plus CCCP (right graph). **(B)** SypHy fluorescence increases in oligomycin alone (purple trace) and after 10 and 15 min in oligomycin plus CCCP (blue and yellow traces, respectively). Fluorescence increments were represented relative to the basal fluorescence in each case. **(C)** Fluorescent peak amplitudes of the SypHy signals vs. time in CCCP. **(D)** SypHy fluorescence for recordings in **(B)** normalized to their respective peak values to compare the kinetics of the responses. Horizontal lines show the start and end of the stimulation train (500 AP, 50 Hz).

n = 6 fibers) than in control (3,658 ± 346 vesicles/s, n = 10 fibers) or oligomycin alone (3,447 ± 277 vesicles/s, n = 8 fibers; $P_{Kruskal\text{-}Wallis}$ = 0.0034; **Figure 5D**).

Typically, total cumulative release (synchronous + asynchronous) in CCCP (**Figure 5E**, red line) was equivalent to release in oligomycin alone (blue line) during the first 500 ms of stimulation, suggesting that a proportion of the RRP vesicles fused asynchronously (see "*Discussion*" Section). However, during the second part of the train, total release in CCCP exceeded by <1,725 vesicles evoked release in oligomycin that could obey fusions of secondary docked vesicles (Nagwaney et al., 2009) or to the acceleration of the recruitment rate (Lu and Trussell, 2000).

Together, these data suggest that fast mitochondrial Ca^{2+} uptake restricts Ca^{2+} building up within microdomains and maintains the equilibrium between synchronous and asynchronous release during short bursts of AP.

Mitochondria Modulate Short-Term Plasticity and the Depletion and Refilling Kinetics of the RRP

Subsequently, we investigated whether mitochondrial uptake of cytosolic Ca^{2+} regulates short-term plasticity, vesicle loss and replenishment kinetics, and RRP size during short-duration AP trains. Since the degree of ψm depolarization produced by CCCP increases during the experiment (David et al., 2003; Talbot et al., 2003; Lopez-Manzaneda et al., 2021), we analyzed the modification of the release properties over time in CCCP in single fibers. For the analysis, we used a simple sequential kinetic model (Ruiz et al., 2011) that assumes that the primary docked vesicles (the RRP) would be the first to be released with repetitive nerve stimulation, that the RRP pool is depleted exponentially, and that the recruitment of new vesicles begins, increases, and maintains the plateau (Elmqvist and Quastel, 1965).

Examples of representative responses to two 1-s stimulation trains in a representative fiber, 1 and 10 min after adding CCCP (2 μM), are shown in **Figure 6A**. Note the high rates of mEPPs in the recordings (insets). The analysis performed is illustrated in **Figure 6B** (Ruiz et al., 2011). The thicker lines represent the quanta released synchronously (m) for each EPP. The loss of RRP (dotted exponential lines in **Figure 6B**) was estimated by adjusting the values of m during the first nine-10 stimuli in the train to a decaying exponential (see "*Materials Methods*" Section). The recruitment time course was then estimated by subtracting the exponential decay of the RRP from the entire observed curve and fitting the resulting curve with a rising sigmoid (dotted lines).

Nerve terminals recorded in control or oligomycin alone usually presented facilitation (increase in EPP size with the first two-three consecutive stimuli) in response to 50 Hz trains. Facilitation was still present at the beginning of the incubation with CCCP (**Figure 6B**, left recording) but generally disappeared later (**Figure 6B**, right graph). **Figure 6C** (open symbols) shows the number of quanta released after the first shock (initial m) vs. time for this experiment. The inset in **Figure 6B** shows the change in the probability of release (p_r), calculated as the ratio of initial m *vs.* the size of the pool. The increase in p_r (from 0.1 to 0.2), is correlated with a ∼40-fold increase in the pre-train mEPP rate in this fiber (from 1.2 to 47 vesicles/s), presumably caused by an elevation in residual [Ca^{2+}] within microdomains (Jackman and Regehr, 2017).

In contrast, the plateau amplitude, which reflects the equilibrium between depletion and vesicle replenishment, progressively depressed over time in CCCP (**Figures 6B,C**, filled symbols). For example, in this fiber, the steady-state to initial quanta ratio changed from ∼0.4 to ∼0.12 over time (**Figure 6D**). On average, the plateau amplitude after 5–10 min in CCCP was approximately half (25.5 ± 5.4 quanta) than in control (59.6 ± 5.7 quanta) or oligomycin alone (54.9 ± 4 quanta; $P_{Kruskal\text{-}Wallis}$ = 0.0032; **Figure 6E**). The increase in synaptic depression was not due to the desensitization of postsynaptic receptors, since the amplitude of mEPP did not

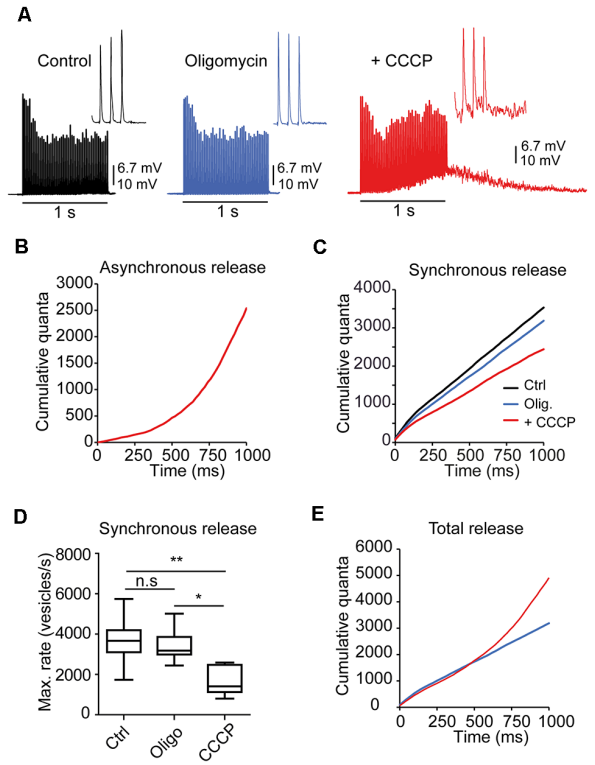

FIGURE 5 | Mitochondria regulate asynchronous release during brief AP trains. **(A)** Representative responses to 1-s stimulation trains (50 Hz) in a fiber recorded in control solution, oligomycin, and oligomycin plus CCCP. Note the elevation on the baseline during and after the train due to the prominent increase in asynchronous release in the presence of CCCP. The insets display the last three EPPs of the trains for each condition. **(B)** Cumulative asynchronous release during synaptic activity in CCCP (the same fiber as in **A**, estimated by integration, as described in "*Materials and Methods*" Section. **(C)** Cumulative synchronous quanta release from the fiber in **(A)** in all three solutions. **(D)** Average cumulative synchronous quanta release in control, oligomycin alone, and oligomycin plus CCCP (24 fibers, eight mice) ($P_{Kruskal\text{-}Wallis}$ = 0.0034). The box-whisker plot represents median (line), 25th–75th percentile (box), and min–max (whisker) for each condition. *:<0.05; **:<0.005; n.s., not significative. **(E)** Total quanta release (synchronous + asynchronous) in CCCP (red line). For comparison, release in oligomycin alone (blue line) is also shown.

change significantly over time in CCCP (for example, in the fiber of **Figure 6**, from 1.36 ± 0.27 mV to 1.34 ± 0.49 mV), or to severe failure of vesicle replenishment, since many vesicles still fused asynchronously (**Supplementary Figures 1A,B**).

Since ψm depolarization increases cytosolic [Ca^{2+}] and [Ca^{2+}] affects the priming of synaptic vesicles and the RRP size (Sakaba and Neher, 2001b; Burrone et al., 2002; Taschenberger et al., 2002; Habets and Borst, 2007; Hosoi et al., 2007; Ruiz et al., 2011; Thanawala and Regehr, 2013), we next examined the effect of CCCP on the number of available vesicles for synchronous release. For example, in the fiber of **Figure 6A**, the RRP decreased by ∼39% over time in CCCP, from ∼1,103 to ∼672 quanta (**Figure 6F**), despite the p_r increase (**Figure 6B**, inset). On average, the size of the RRP after 5–10 min in CCCP (889.7 ± 110.3 quanta, six fibers, four mice) was significantly smaller (**Figure 6G**) than in control (1,962 ± 150.1 quanta, 10 fibers, eight mice) or with oligomycin alone (1,847 ± 109.2 quanta, eight fibers, six mice; $P_{Kruskal\text{-}Wallis}$ = 0.0018).

The RRP size decrease was correlated with the concomitant increase in asynchronous release, which varied between different nerve terminals and over time in CCCP. For example, in the fiber shown in **Figure 6**, asynchronous release during the 1-s train accounted for ∼20% of total release after 1 min in CCCP (**Supplementary Figure 1C**) and ∼48% after 10 min (**Supplementary Figure 1D**). The asynchronous peak vesicle release rates went from ∼614 s^{-1} to 1,145 s^{-1}, and the synchronous ones from 2,429 s^{-1} to ∼1,235 s^{-1}.

Finally, we estimate the time constant of RRP depletion (τ_{RRP}, open symbols) and the half-time of refilling (dark symbols) during synaptic activity in control, oligomycin alone, and oligomycin plus CCCP (**Figure 6H**). RRP loss became approximately two times faster (from ∼195 to ∼90 ms), and reloading three times faster (from ∼370 to ∼113 ms) between the first and last recording in CCCP. On the contrary, no change was observed over time in control or oligomycin alone. On average, the τ_{RRP} in control was 266 ± 19.9 ms (n = 10 fibers) and 276 ± 30.1 ms (eight fibers) in oligomycin alone. The average refill half-time was 433 ± 34 ms and 415.7 ± 23.5 ms, respectively. In CCCP, the velocity of the RRP loss was inversely correlated with the frequency of mEPPs before stimulation (**Figure 6I**, n = 15 terminals, six mice). The τ_{RRP} became faster within a narrow range of mEPP frequencies, reaching an estimated minimum mean value of ∼129 ms for release rates ≥10 vesicles/s (**Figure 6I**, dotted line). Acceleration of the RRP loss in correlation to the increase in [Ca^{2+}] at release sites has been previously observed in the calyx of Held (Sakaba and Neher, 2001a).

Although the above results suggested that the RRP emptying kinetics through synchronous fusions is Ca^{2+}-dependent, we wondered whether the observed acceleration was due to the loss of vesicles through asynchronous fusions. Hence, we estimated the number of asynchronous events along each train and calculated the total release. **Supplementary Figures 1E,F** compare total quanta released (black traces), as well as that released synchronously (gray traces) and asynchronously (blue traces) during the 1-s AP train. The kinetics of RRP loss for vesicles going through the synchronous mode changed little despite the increase in asynchronous fusions. For example, the RRP depletion rate, the inverse of the time constant, for synchronous and total release after 10 min in CCCP was ∼0.0111 and ∼0.0092 vesicles/ms, respectively. Twice as fast as after 1 min in CCCP (∼0.0053 vesicles/ms), and approximately three times faster than in control and oligomycin alone (∼0.0037 vesicles/ms), indicating that the increase in asynchronous fusions along the 1-s train was not the main cause of the observed acceleration of synchronous release from the RRP.

Together, these results indicate that mitochondria limit the velocity of synchronous release under physiological conditions and participate in the regulation of synaptic plasticity during short-duration bursts of electrical activity.

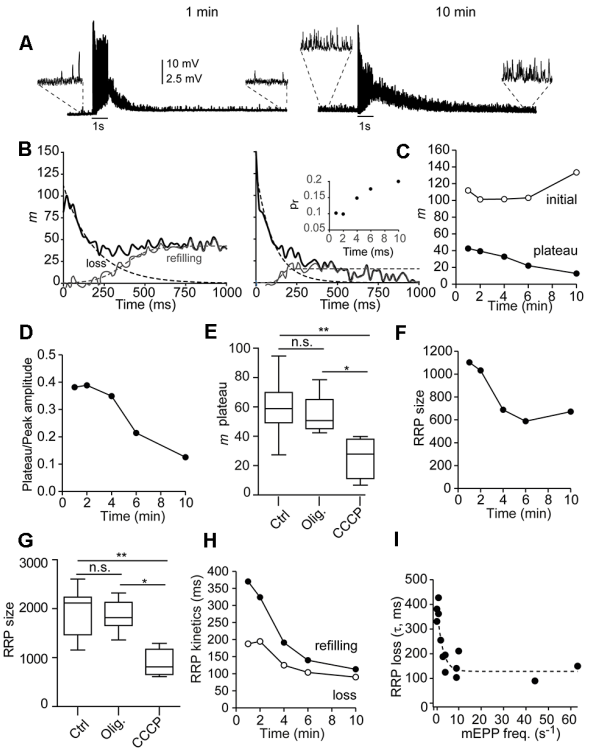

FIGURE 6 | Mitochondria modulate the depletion and refilling kinetics of the RRP and short-term plasticity during physiological stimuli. **(A)** Representative EPP responses of a single fiber to two 1-s stimulation trains, 1 and 10 min after adding CCCP to the recording chamber. Note the high frequency of asynchronous release before (insets), during, and after (insets) each train. **(B)** Curve fitting of *m* values during the trains (thick lines) to a function of the sum of exponential decay of the RRP plus the sigmoidal rise of recruitment (dotted lines) of the recordings in 6A for estimation of the RRP size, RRP depletion, and recruitment time. The inset on the right graph displays the probability of release (p_r) vs. time in the CCCP, estimated by dividing the number of quanta released with the first by the size of the RRP for each train. **(C)** Quanta released at the initial of the train (open symbols) and plateau amplitude (filled symbols) after 1, 2, 4, 6, and 10 min in CCCP. **(D)** Relationship between the plateau and the initial release amplitudes with time in CCCP. **(E,G)** Average plateau amplitude **(E)** and RRP size **(G)** in control (10 fibers, eight mice), oligomycin alone (eight fibers, six mice), and CCCP (5–10 min, six fibers, four mice). The box-whisker plots represent median (line), 25th–75th percentile (box), and min–max (whisker) for each condition ($P_{Kruskal\text{-}Wallis}$ = 0.0018). *: <0.05; **: <0.005; n.s.: not significative. **(F)** Decrease of the RRP over time in CCCP (same fiber as in **A**). **(H)** Acceleration of RRP depletion (τ_{RRP}, open symbols) and vesicle recruitment ($t_{1/2}$, filled symbols) over time in CCCP. **(I)** Correlation between the depletion of the RRP and the frequency of mEPP before the train. The data were fitted with an exponential function (dotted line).

DISCUSSION

This study examined the spatiotemporal and functional coupling between exocytosis and presynaptic mCa^{2+} at the motor nerve terminal of adult mice by a combination of techniques. Our results show that: *(i)* mitochondria and regions of high exocytosis (hot spots) are closely localized, *(ii)* mitochondria uptake Ca^{2+} upon arrival of a small number of APs at the terminal, and *(iii)* the inhibition of mCa^{2+} uptake increases the probability of release, accelerates the RRP depletion and refilling rates, and produces a rapid increase in asynchronous fusions during short bursts of APs. We propose that mitochondria regulate the synaptic response during the physiological activity of mature motor nerve terminals.

Spatial Relationship Between Hot Spots of Exocytosis and Mitochondria

Ca^{2+} microdomains are regions of an estimated size of 100 nm^{-1} μm across (Neher and Sakaba, 2008) where $[Ca^{2+}]$ rises and decays rapidly around voltage-dependent Ca^{2+} channels (Adler et al., 1991; Stanley, 1993; Neher, 1998; Bucurenciu et al., 2008). Multiple mechanisms participate in the spatiotemporal control of Ca^{2+} in microdomains, including mitochondria, which could be considered a part of the endogenous fixed Ca^{2+} buffer system. Positioning of mitochondria relative to AZs is critical for both local Ca^{2+} buffering and immediate energy source for synaptic vesicle functionality. Reports on the location of mitochondria within CNS axon terminals and crayfish and *Drosophila* motor nerve terminals show that most mitochondria are located in a central region of synaptic boutons, containing few synaptic vesicles (Gotow et al., 1991; King et al., 1996; Chouhan et al., 2010). However, a subset of mitochondria has also been reported to be spatially closely associated with clusters of synaptic vesicles at mouse motor nerve terminals (Torres-Benito et al., 2011, 2012) and the calyx of Held (Wimmer et al., 2006), forming rings or donut-like structures. Electron tomography in the calyx of Held synapse also shows mitochondria connected to the presynaptic membrane near AZs through cytoskeletal structures (Perkins et al., 2010). Our live imaging experiments showed spatial association of hot spots of exocytosis and mCa^{2+} signals (**Figure 2**); however, the relatively low resolution of our imaging system precludes us from estimating more accurately the distance between these two signals. Nevertheless, we started to detect an increase in mCa^{2+} with ∼5–10 AP (**Figure 3D**), that is, ∼50–100 ms from the onset of a train at 100 Hz (**Figure 3C**), in agreement with the findings that neuronal mitochondria can uptake Ca^{2+} in the submicromolar range (Chouhan et al., 2010; Ashrafi et al., 2019) and that a single AP can trigger mCa^{2+} influx at hippocampal neurons boutons (Gazit et al., 2016). In synapses, the high sensitivity of mitochondria to Ca^{2+} may be relevant not only to preventing Ca^{2+} accumulation in microdomains and their surroundings but also to modulate the range of responses to physiological stimuli during development and maturity. For example, in the mouse calyx of Held, mitochondrial volumes are increased to support high firing and secretion rates upon maturity (Kim et al., 2013; Thomas et al., 2019) and in *Drosophila* motor nerve terminals, presynaptic mitochondrial volume and packing density scale with presynaptic demands (Justs et al., 2022).

The Role of Mitochondria on the RRP Size and the Release Kinetics

We previously observed that the size of the functional (effective) RRP is frequency-dependent; the higher the stimulation frequency, the larger the RRP (Ruiz et al., 2011). An interpretation of this result is that the size of the RRP partially depends on the accumulation of Ca^{2+} during repetitive stimulation (Zucker and Regehr, 2002; Neher and Sakaba, 2008;

Thanawala and Regehr, 2013). Under this hypothesis, one might expect that mitochondrial depolarization will produce a larger accumulation of Ca^{2+} in nerve terminals and, concomitantly, an increase in the effective RRP size. However, we did not observe an enhancement of the RRP but a decrease (**Figures 6F,G**). On one side, the no increase in the RRP agrees with our previous observation that the maximum size of the RRP at this synapse comprises ∼1,700–2,000 vesicles, with no further increase when the stimulation frequency is above 50 Hz (Ruiz et al., 2011). Therefore, our present results also indicate that the upper limit of the RRP size in this synapse is reached at 50 Hz stimulation and that the reduction in mCa^{2+} uptake cannot increase it. On the other side, the progressive decrease in the RRP with CCCP could be due, among others, to the increase in asynchronous fusions (**Figure 5E**, **Supplementary Figures 1C,D**), reduction in the mitochondrial ATP production (Justs et al., 2022), partial inactivation of P/Q-type voltage-dependent Ca^{2+} channels by high Ca^{2+} (Forsythe et al., 1998; Demaria et al., 2001), moderate desensitization of postsynaptic receptors, or a combination of all. In all cases, mCa^{2+} uptake could minimize these effects during physiological stimuli.

Interestingly, together with the decrease in the RRP, we observed faster vesicle depletion and recruitment rates when the mCa^{2+} uptake was inhibiting (**Figure 6H**), suggesting a role of mitochondria in the regulation of these two processes. These observations agree with previous findings showing Ca^{2+}-dependent acceleration of vesicle recruitment in numerous types of synapses, including the calyx of Held (Wang and Kaczmarek, 1998; Sakaba and Neher, 2001a), the climbing fiber to cerebellar Purkinje cell synapses (Dittman and Regehr, 1998), excitatory hippocampal synapses (Stevens and Wesseling, 1998), the ribbon synapse in the retina (Von Gersdorff et al., 1998; Gomis et al., 1999), and the NMJ (Ruiz et al., 2011). Besides Ca^{2+}, the rate of vesicle recruitment at the steady-state is shortened by raising the temperature from 23°C to 37°C, both at the calyx of Held (Kushmerick et al., 2006) and the NMJ (Ruiz et al., 2011), what has no appreciable effect on the initial RRP size. These findings indicate that Ca^{2+} and temperature are two major determinants of short-term depression during high-frequency firing.

Mode of Fusion Change Upon mCa^{2+} Uptake Inhibition

The inverse synchronous and asynchronous release occurrence observed in our experiments during short AP trains (1-s) when the mCa^{2+} uptake was inhibited with CCCP (**Figures 5B,C**, and **Supplementary Figure 1**) suggests a switch in the mode of fusion of vesicles belonging to the RRP (Hagler and Goda, 2001; Otsu et al., 2004). Alternatively, or additionally, asynchronous fusions could result from secondary docked vesicles (Nagwaney et al., 2009) located outside AZ (Schneggenburger and Neher, 2005; Wen et al., 2013) and newly recruited vesicles from other pools that compete for the same release sites.

It has been found that synaptic vesicles are functionally and molecularly heterogeneous within the presynaptic terminal (Sakaba and Neher, 2001b; Hua et al., 2011) and that they could be spatially segregated according to their molecular identities (Wen et al., 2010). For example, asynchronous release has been reported to be triggered by a relatively low $[Ca^{2+}]$ (Otsu et al., 2004), indicating that vesicles that use this mode of release possess a high-affinity Ca^{2+} sensor (Sugita et al., 2002). Supposing that the vesicles that fuse asynchronously are located at a greater distance from voltage-dependent Ca^{2+} channels than the synchronous pool, it is expected they fuse after a relatively prolonged elevation of Ca^{2+} within microdomains. Alternatively, Ca^{2+} accumulation at microdomains during sustained activity may promote the integration of Synaptotagmin 7 and other synaptic proteins related to asynchronous release (Virmani et al., 2003; Sun et al., 2007) into the vesicular membrane *via* endocytosis, changing release towards the asynchronous mode while using the same release sites. In any case, controlling Ca^{2+} accumulation at the microdomains and their surroundings is crucial for determining the release mode.

In summary, our results suggest that mitochondria and release sites are organized in functional subsynaptic compartments for the spatial and temporal regulation of release during physiological neuronal activity. We propose that mitochondria uptake Ca^{2+} with high sensitivity and play a significant role in maintaining synaptic transmission strength and reliability in the NMJ under physiological activity.

DATA AVAILABILITY STATEMENT

The original contributions presented in the study are included in the article/**Supplementary Material**, further inquiries can be directed to the corresponding author.

ETHICS STATEMENT

The animal study was reviewed and approved by Ethics committee of the University of Seville and Junta de Andalucia.

AUTHOR CONTRIBUTIONS

ML-M, AF-M, and LT designed experiments, edited and approved the manuscript. ML-M and LT performed and analyzed live fluorescence imaging experiments. AF-M and LT performed and analyzed electrophysiological experiments. All authors contributed to the article and approved the submitted version.

FUNDING

This work was supported by SMA Europe and the Spanish Agencia Estatal de Investigación [grant number: PID2019-110272RB-100/AEI/10.13039/501100011033].

SUPPLEMENTARY MATERIAL

The Supplementary Material for this article can be found online at: https://www.frontiersin.org/articles/10.3389/fnsyn.2022.858340/full#supplementary-material.

Supplementary Figure 1 | Change of the release mode over time in the presence of ψm depolarization. **(A,B)** Cumulative release components,

asynchronous **(A)** and synchronous **(B)**, during 1-s train stimulation (50 Hz) after 1 min (blue lines) and 10 min (red lines) in CCCP (2 μM). **(C,D)** Comparison of cumulative total release (black) and synchronous release (gray) after 1 min **(C)** and 10 min **(D)** in CCCP calculated from **(A,B)**. **(E,F)** Time course of total (black), asynchronous (gray) and asynchronous (blue) quanta released during 1-s AP train.

REFERENCES

Adler, E. M., Augustine, G. J., Duffy, S. N., and Charlton, M. P. (1991). Alien intracellular calcium chelators attenuate neurotransmitter release at the squid giant synapse. *J. Neurosci.* 11, 1496–1507. doi: 10.1523/JNEUROSCI.11-06-01496.1991

Ashrafi, G., de Juan-Sanz, J., Farrell, R. J., and Ryan, T. A. (2019). Molecular tuning of the axonal mitochondrial Ca^{2+} uniporter ensures metabolic flexibility of neurotransmission. *Neuron* 105, 678–687. doi: 10.1016/j.neuron.2019.11.020

Atluri, P. P., and Regehr, W. G. (1998). Delayed release of neurotransmitter from cerebellar granule cells. *J. Neurosci.* 18, 8214–8227. doi: 10.1523/JNEUROSCI.18-20-08214.1998

Bolte, S., and Cordelières, F. P. (2006). A guided tour into subcellular colocalization analysis in light microscopy. *J. Microsc.* 224, 213–232. doi: 10.1111/j.1365-2818.2006.01706.x

Bucurenciu, I., Kulik, A., Schwaller, B., Frotscher, M., and Jonas, P. (2008). Nanodomain coupling between Ca^{2+} channels and Ca^{2+} sensors promotes fast and efficient transmitter release at a cortical gabaergic synapse. *Neuron* 57, 536–545. doi: 10.1016/j.neuron.2007.12.026

Burrone, J., Neves, G., Gomis, A., Cooke, A., and Lagnado, L. (2002). Endogenous calcium buffers regulate fast exocytosis in the synaptic terminal of retinal bipolar cells. *Neuron* 33, 101–112. doi: 10.1016/s0896-6273(01)00565-7

Cano, R., Ruiz, R., Shen, C., Tabares, L., and Betz, W. J. (2012). The functional landscape of a presynaptic nerve terminal. *Cell Calcium* 52, 321–326. doi: 10.1016/j.ceca.2012.04.012

Cano, R., and Tabares, L. (2016). The active and periactive zone organization and the functional properties of small and large synapses. *Front. Synaptic Neurosci.* 8, 1–7. doi: 10.3389/fnsyn.2016.00012

Chamberland, S., and Tóth, K. (2016). Functionally heterogeneous synaptic vesicle pools support diverse synaptic signalling. *J. Physiol.* 594, 825–835. doi: 10.1113/JP270194

Chouhan, A. K., Zhang, J., Zinsmaier, K. E., and Macleod, G. T. (2010). Presynaptic mitochondria in functionally different motor neurons exhibit similar affinities for Ca^{2+} but exert little influence as Ca^{2+} buffers at nerve firing rates *in situ*. *J. Neurosci.* 30, 1869–1881. doi: 10.1523/JNEUROSCI.4701-09.2010

David, G. (1999). Mitochondrial clearance of cytosolic Ca^{2+} in stimulated lizard motor nerve terminals proceeds without progressive elevation of mitochondrial matrix [Ca^{2+}]. *J. Neurosci.* 19, 7495–7506. doi: 10.1523/JNEUROSCI.19-17-07495.1999

David, G., and Barrett, E. F. (2000). Stimulation-evoked increases in cytosolic [Ca^{2+}] in mouse motor nerve terminals are limited by mitochondrial uptake and are temperature-dependent. *J. Neurosci.* 20, 7290–7296. doi: 10.1523/JNEUROSCI.20-19-07290.2000

David, G., and Barrett, E. F. (2003). Mitochondrial Ca^{2+} uptake prevents desynchronization of quantal release and minimizes depletion during repetitive stimulation of mouse motor nerve terminals. *J. Physiol.* 548, 425–438. doi: 10.1113/jphysiol.2002.035196

David, G., Barrett, J. N., and Barrett, E. F. (1998). Evidence that mitochondria buffer physiological Ca^{2+} loads in lizard motor nerve terminals. *J. Physiol.* 509, 59–65. doi: 10.1111/j.1469-7793.1998.059bo.x

David, G., Talbot, J., and Barrett, E. F. (2003). Quantitative estimate of mitochondrial [Ca^{2+}] in stimulated motor nerve terminals. *Cell Calcium* 33, 197–206. doi: 10.1016/s0143-4160(02)00229-4

Demaria, C. D., Soong, T. W., Alseikhan, B. A., Alvania, R. S., and Yue, D. T. (2001). Calmodulin bifurcates the local Ca^{2+} signal that modulates P/Q-type Ca^{2+} channels. *Nature* 411, 484–489. doi: 10.1038/35078091

Dittman, J. S., and Regehr, W. G. (1998). Calcium dependence and recovery kinetics of presynaptic depression at the climbing fiber to Purkinje cell synapse. *J. Neurosci.* 18, 6147–6162. doi: 10.1523/JNEUROSCI.18-16-06147.1998

Elmqvist, D., and Quastel, D. M. (1965). A quantitative study of end-plate potentials in isolated human muscle. *J. Physiol.* 178, 505–529. doi: 10.1113/jphysiol.1965.sp007639

Forsythe, I. D., Tsujimoto, T., Barnes-Davies, M., Cuttle, M. F., and Takahashi, T. (1998). Inactivation of presynaptic calcium current contributes to synaptic depression at a fast central synapse. *Neuron* 20, 797–807. doi: 10.1016/s0896-6273(00)81017-x

Fukunaga, H., Engel, A. G., Lang, B., Newsom-Davis, J., and Vincent, A. (1983). Passive transfer of Lambert-Eaton myasthenic syndrome with IgG from man to mouse depletes the presynaptic membrane active zones. *Proc. Natl. Acad. Sci. U S A* 80, 7636–7640. doi: 10.1073/pnas.80.24.7636

Gaffield, M. A., Tabares, L., and Betz, W. J. (2009). The spatial pattern of exocytosis and post-exocytic mobility of synaptopHluorin in mouse motor nerve terminals. *J. Physiol.* 587, 321–326. doi: 10.1113/jphysiol.2008.166728

García-Chacón, L. E., Nguyen, K. T., David, G., and Barrett, E. F. (2006). Extrusion of Ca^{2+} from mouse motor terminal mitochondria via a Na^{+}-Ca^{2+} exchanger increases post-tetanic evoked release. *J. Physiol.* 574, 663–675. doi: 10.1113/jphysiol.2006.110841

Gazit, N., Vertkin, I., Shapira, I., Helm, M., Slomowitz, E., Sheiba, M., et al. (2016). IGF-1 receptor differentially regulates spontaneous and evoked transmission via mitochondria at hippocampal synapses. *Neuron* 89, 583–597. doi: 10.1016/j.neuron.2015.12.034

Gomis, A., Burrone, J., and Lagnado, L. (1999). Two actions of calcium regulate the supply of releasable vesicles at the ribbon synapse of retinal bipolar cells. *J. Neurosci.* 19, 6309–6317. doi: 10.1523/JNEUROSCI.19-15-06309.1999

Gotow, T., Miyaguchi, K., and Hashimoto, P. H. (1991). Cytoplasmic architecture of the axon terminal: filamentous strands specifically associated with synaptic vesicles. *Neuroscience* 40, 587–598. doi: 10.1016/0306-4522(91)90143-c

Gunter, T. E., and Sheu, S. S. (2009). Characteristics and possible functions of mitochondrial Ca^{2+} transport mechanisms. *Biochim. Biophys. Acta* 1787, 1291–1308. doi: 10.1016/j.bbabio.2008.12.011

Habets, R. L. P., and Borst, J. G. G. (2007). Dynamics of the readily releasable pool during post-tetanic potentiation in the rat calyx of Held synapse. *J. Physiol.* 581, 467–478. doi: 10.1113/jphysiol.2006.127365

Hagler, D. J., and Goda, Y. (2001). Properties of synchronous and asynchronous release during pulse train depression in cultured hippocampal neurons. *J. Neurophysiol.* 85, 2324–2334. doi: 10.1152/jn.2001.85.6.2324

Harris, J. J., Jolivet, R., and Attwell, D. (2012). Synaptic energy use and supply. *Neuron* 75, 762–777. doi: 10.1016/j.neuron.2012.08.019

Hosoi, N., Sakaba, T., and Neher, E. (2007). Quantitative analysis of calcium-dependent vesicle recruitment and its functional role at the calyx of held synapse. *J. Neurosci.* 27, 14286–14298. doi: 10.1523/JNEUROSCI.4122-07.2007

Hua, Z., Leal-Ortiz, S., Foss, S. M., Waites, C. L., Garner, C. C., Voglmaier, S. M., et al. (2011). V-SNARE composition distinguishes synaptic vesicle pools. *Neuron* 71, 474–487. doi: 10.1016/j.neuron.2011.06.010

Jackman, S. L., and Regehr, W. G. (2017). The mechanisms and functions of synaptic facilitation. *Neuron* 94, 447–464. doi: 10.1016/j.neuron.2017.02.047

Justs, K. A., Lu, Z., Chouhan, A. K., Borycz, J. A., Lu, Z., Meinertzhagen, I. A., et al. (2022). Presynaptic mitochondrial volume and packing density scale with presynaptic power demand. *J. Neurosci.* 42, 954–967. doi: 10.1523/JNEUROSCI.1236-21.2021

Kim, J. H., Renden, R., and von Gersdorff, H. (2013). Dysmyelination of auditory afferent axons increases the jitter of action potential timing during high-frequency firing. *J. Neurosci.* 33, 9402–9407. doi: 10.1523/JNEUROSCI.3389-12.2013

King, M. J. R., Atwood, H. L., and Govind, C. K. (1996). Structural features of crayfish phasic and tonic neuromuscular terminals. *J. Comp. Neurol.* 372, 618–626. doi: 10.1002/(SICI)1096-9861(19960902)372:4<618::AID-CNE9>3.0.CO;2-7

Kushmerick, C., Renden, R., and Von Gersdorff, H. (2006). Physiological temperatures reduce the rate of vesicle pool depletion and short-term depression via an acceleration of vesicle recruitment. *J. Neurosci.* 26, 1366–1377. doi: 10.1523/JNEUROSCI.3889-05.2006

Lee, D., Lee, K. H., Ho, W. K., and Lee, S. H. (2007). Target cell-specific involvement of presynaptic mitochondria in post-tetanic potentiation at hippocampal mossy fiber synapses. *J. Neurosci.* 27, 13603–13613. doi: 10.1523/JNEUROSCI.3985-07.2007

Leitz, J., and Kavalali, E. T. (2016). Ca^{2+} dependence of synaptic vesicle endocytosis. *Neuroscientist* 22, 464–476. doi: 10.1177/1073858415588265

Lopez-Manzaneda, M., Franco-Espin, J., Tejero, R., Cano, R., and Tabares, L. (2021). Calcium is reduced in presynaptic mitochondria of motor nerve terminals during neurotransmission in SMA mice. *Hum. Mol. Genet.* 30, 629–643. doi: 10.1093/hmg/ddab065

Lu, T., and Trussell, L. O. (2000). Inhibitory transmission mediated by asynchronous transmitter release. *Neuron* 26, 683–694. doi: 10.1016/s0896-6273(00)81204-0

MacAskill, A. F., Atkin, T. A., and Kittler, J. T. (2010). Mitochondrial tracking and the provision of energy and calcium buffering at excitatory synapses. *Eur. J. Neurosci.* 32, 231–240. doi: 10.1111/j.1460-9568.2010.07345.x

McLachlan, E. M., and Martin, A. R. (1981). Non-linear summation of end-plate potentials in the frog and mouse. *J. Physiol.* 311, 307–324. doi: 10.1113/jphysiol.1981.sp013586

Mironov, S. L., and Symonchuk, N. (2006). ER vesicles and mitochondria move and communicate at synapses. *J. Cell Sci.* 119, 4926–4934. doi: 10.1242/jcs.03254

Nagwaney, S., Harlow, M. L., Jung, J. H., Szule, J. A., Ress, D., Xu, J., et al. (2009). Macromolecular connections of active zone material to docked synaptic vesicles and presynaptic membrane at neuromuscular junctions of mouse. *J. Comp. Neurol.* 513, 457–468. doi: 10.1002/cne.21975

Neher, E. (1998). Usefulness and limitations of linear approximations to the understanding of Ca^{++} signals. *Cell Calcium* 24, 345–357. doi: 10.1016/s0143-4160(98)90058-6

Neher, E., and Sakaba, T. (2008). Multiple roles of calcium ions in the regulation of neurotransmitter release. *Neuron* 59, 861–872. doi: 10.1016/j.neuron.2008.08.019

Nishimune, H., Sanes, J. R., and Carlson, S. S. (2004). A synaptic laminin-calcium channel interaction organizes active zones in motor nerve terminals. *Nature* 432, 580–587. doi: 10.1038/nature03112

Ojeda, J., Bermedo-García, F., Pérez, V., Mella, J., Hanna, P., Herzberg, D., et al. (2020). The mouse Levator Auris Longus muscle: an amenable model system to study the role of postsynaptic proteins to the maintenance and regeneration of the neuromuscular synapse. *Front. Cell. Neurosci.* 14, 1–13. doi: 10.3389/fncel.2020.00225

Otsu, Y., Shahrezaei, V., Li, B., Raymond, L. A., Delaney, K. R., and Murphy, T. H. (2004). Competition between phasic and asynchronous release for recovered synaptic vesicles at developing hippocampal autaptic synapses. *J. Neurosci.* 24, 420–433. doi: 10.1523/JNEUROSCI.4452-03.2004

Pallafacchina, G., Zanin, S., and Rizzuto, R. (2021). From the identification to the dissection of the physiological role of the mitochondrial calcium uniporter: an ongoing story. *Biomolecules* 11:786. doi: 10.3390/biom11060786

Perkins, G. A., Tjong, J., Brown, J. M., Poquiz, P. H., Scott, R. T., Kolson, D. R., et al. (2010). The micro-architecture of mitochondria at active zones: electron tomography reveals novel anchoring scaffolds and cristae structured for high-rate metabolism. *J. Neurosci.* 30, 1015–1026. doi: 10.1523/JNEUROSCI.1517-09.2010

Ruiz, R., Cano, R., Casañas, J. J., Gaffield, M. A., Betz, W. J., and Tabares, L. (2011). Active zones and the readily releasable pool of synaptic vesicles at the neuromuscular junction of the mouse. *J. Neurosci.* 31, 2000–2008. doi: 10.1523/JNEUROSCI.4663-10.2011

Sakaba, T., and Neher, E. (2001a). Calmodulin mediates rapid recruitment of fast-releasing synaptic vesicles at a calyx-type synapse. *Neuron* 32, 1119–1131. doi: 10.1016/s0896-6273(01)00543-8

Sakaba, T., and Neher, E. (2001b). Quantitative relationship between transmitter release and calcium current at the calyx of Held synapse. *J. Neurosci.* 21, 462–476. doi: 10.1523/JNEUROSCI.21-02-00462.2001

Sankaranarayanan, S., De Angelis, D., Rothman, J. E., and Ryan, T. A. (2000). The Use of pHluorins for optical measurements of presynaptic activity. *Biophys. J.* 79, 2199–2208. doi: 10.1016/S0006-3495(00)76468-X

Schneggenburger, R., and Neher, E. (2005). Presynaptic calcium and control of vesicle fusion. *Curr. Opin. Neurobiol.* 15, 266–274. doi: 10.1016/j.conb.2005.05.006

Stanley, E. F. (1993). Single calcium channels and acetylcholine release at a presynaptic nerve terminal. *Neuron* 11, 1007–1011. doi: 10.1016/0896-6273(93)90214-c

Stevens, C. F., and Wesseling, J. F. (1998). Activity-dependent modulation of the rate at which synaptic vesicles become available to undergo exocytosis. *Neuron* 21, 415–424. doi: 10.1016/s0896-6273(00)80550-4

Sugita, S., Shin, O. H., Han, W., Lao, Y., and Südhof, T. C. (2002). Synaptotagmins form a hierarchy of exocytotic Ca^{2+} sensors with distinct Ca^{2+} affinities. *EMBO J.* 21, 270–280. doi: 10.1093/emboj/21.3.270

Sun, J., Pang, Z., Qin, D., Fahim, A., Adachi, R., and Südhof, T. (2007). A dual-Ca^{2+}-sensor model for neurotransmitter release in a central synapse. *Nature* 450, 676–682. doi: 10.1038/nature06308

Suzuki, S., Osanai, M., Mitsumoto, N., Akita, T., Narita, K., Kijima, H., et al. (2002). Ca^{2+}-dependent Ca^{2+} clearance via mitochondrial uptake and plasmalemmal extrusion in frog motor nerve terminals. *J. Neurophysiol.* 87, 1816–1823. doi: 10.1152/jn.00456.2001

Tabares, L., Ruiz, R., Linares-Clemente, P., Gaffield, M. A. M. A., Toledo, G. A. d., Fernandez-Chacón, R., et al. (2007). Monitoring synaptic function at the neuromuscular junction of a mouse expressing synaptopHluorin. *J. Neurosci.* 27, 5422–5430. doi: 10.1523/JNEUROSCI.0670-07.2007

Talbot, J. D., David, G., and Barrett, E. F. (2003). Inhibition of mitochondrial Ca^{2+} uptake affects phasic release from motor terminals differently depending on external $[Ca^{2+}]$. *J. Neurophysiol.* 90, 491–502. doi: 10.1152/jn.00012.2003

Tang, Y. G., and Zucker, R. S. (1997). Mitochondrial involvement in post-tetanic potentiation of synaptic transmission. *Neuron* 18, 483–491. doi: 10.1016/s0896-6273(00)81248-9

Taschenberger, H., Leão, R. M., Rowland, K. C., Spirou, G. A., and Von Gersdorff, H. (2002). Optimizing synaptic architecture and efficiency for high-frequency transmission. *Neuron* 36, 1127–1143. doi: 10.1016/s0896-6273(02)01137-6

Tejero, R., Lopez-Manzaneda, M., Arumugam, S., and Tabares, L. (2016). Synaptotagmin-2 and -1, linked to neurotransmission impairment and vulnerability in spinal muscular atrophy. *Hum. Mol. Genet.* 25, 4703–4716. doi: 10.1093/hmg/ddw297

Thanawala, M. S., and Regehr, W. G. (2013). Presynaptic calcium influx controls neurotransmitter release in part by regulating the effective size of the readily releasable pool. *J. Neurosci.* 33, 4625–4633. doi: 10.1523/JNEUROSCI.4031-12.2013

Thomas, C. I., Keine, C., Okayama, S., Satterfield, R., Musgrove, M., Guerrero-Given, D., et al. (2019). Presynaptic mitochondria volume and abundance increase during development of a high-fidelity synapse. *J. Neurosci.* 39, 7994–8012. doi: 10.1523/JNEUROSCI.0363-19.2019

Torres-Benito, L., Neher, M. F. M. F., Cano, R., Ruiz, R., and Tabares, L. (2011). SMN requirement for synaptic vesicle, active zone and microtubule postnatal organization in motor nerve terminals. *PLoS One* 6, 1–16. doi: 10.1371/journal.pone.0026164

Torres-Benito, L., Ruiz, R., and Tabares, L. (2012). Synaptic defects in spinal muscular atrophy animal models. *Dev. Neurobiol.* 72, 126–133. doi: 10.1002/dneu.20912

Van der Kloot, W. (1990). Methods for estimating release rates during high frequency quantal secretion and for testing such methods. *J. Neurosci. Methods* 33, 33–39. doi: 10.1016/0165-0270(90)90079-u

Virmani, T., Han, W., Liu, X., Südhof, T. C., and Kavalali, E. T. (2003). Synaptotagmin 7 splice variants differentially regulate synaptic vesicle recycling. *EMBO J.* 22, 5347–5357. doi: 10.1093/emboj/cdg514

Von Gersdorff, H., Sakaba, T., Berglund, K., and Tachibana, M. (1998). Submillisecond kinetics of glutamate release from a sensory synapse. *Neuron* 21, 1177–1188. doi: 10.1016/s0896-6273(00)80634-0

Wang, L. Y., and Kaczmarek, L. K. (1998). High-frequency firing helps replenish the readily releasable pool of synaptic vesicles. *Nature* 394, 384–388. doi: 10.1038/28645

Wen, H., Hubbard, J. M., Rakela, B., Linhoff, M. W., Mandel, G., and Brehm, P. (2013). Synchronous and asynchronous modes of synaptic transmission utilize different calcium sources. *eLife* 2013:e01206. doi: 10.7554/eLife.01206

Wen, H., Linhoff, M. W., McGinley, M. J., Li, G. L., Corson, G. M., Mandel, G., et al. (2010). Distinct roles for two synaptotagmin isoforms in synchronous and

asynchronous transmitter release at zebrafish neuromuscular junction. *Proc. Natl. Acad. Sci. U S A* 107, 13906–13911. doi: 10.1073/pnas.1008598107

Wimmer, V. C., Horstmann, H., Groh, A., and Kuner, T. (2006). Donut-like topology of synaptic vesicles with a central cluster of mitochondria wrapped into membrane protrusions: A novel structure-function module of the adult calyx of held. *J. Neurosci.* 26, 109–116. doi: 10.1523/JNEUROSCI.3268-05.2006

Wu, L. G., and Betz, W. J. (1999). Spatial variability in release at the frog neuromuscular junction measured with FM1–43. *Can. J. Physiol. Pharmacol.* 77, 672–678.

Wu, L. G., Hamid, E., Shin, W., and Chiang, H. C. (2014). Exocytosis and endocytosis: modes, functions and coupling mechanisms*. *Annu. Rev. Physiol.* 76, 301–331. doi: 10.1146/annurev-physiol-021113-170305

Yang, C. H., Lee, K. H., Ho, W. K., and Lee, S. H. (2021). Inter-spike mitochondrial Ca^{2+} release enhances high frequency synaptic transmission. *J. Physiol.* 599, 1567–1594. doi: 10.1113/JP280351

Zucker, R. S., and Regehr, W. G. (2002). Short-term synaptic plasticity. *Annu. Rev. Physiol.* 64, 355–405. doi: 10.1146/annurev.physiol.64.092501.114547

Conflict of Interest: The authors declare that the research was conducted in the absence of any commercial or financial relationships that could be construed as a potential conflict of interest.

Publisher's Note: All claims expressed in this article are solely those of the authors and do not necessarily represent those of their affiliated organizations, or those of the publisher, the editors and the reviewers. Any product that may be evaluated in this article, or claim that may be made by its manufacturer, is not guaranteed or endorsed by the publisher.

frontiers | Frontiers in Synaptic Neuroscience

REVIEW
published: 16 May 2022
doi: 10.3389/fnsyn.2022.854957

Chemical Imaging and Analysis of Single Nerve Cells by Secondary Ion Mass Spectrometry Imaging and Cellular Electrochemistry

*Alicia A. Lork, Kim L. L. Vo and Nhu T. N. Phan**

Department of Chemistry and Molecular Biology, University of Gothenburg, Gothenburg, Sweden

A nerve cell is a unit of neuronal communication in the nervous system and is a heterogeneous molecular structure, which is highly mediated to accommodate cellular functions. Understanding the complex regulatory mechanisms of neural communication at the single cell level requires analytical techniques with high sensitivity, specificity, and spatial resolution. Challenging technologies for chemical imaging and analysis of nerve cells will be described in this review. Secondary ion mass spectrometry (SIMS) allows for non-targeted and targeted molecular imaging of nerve cells and synapses at subcellular resolution. Cellular electrochemistry is well-suited for quantifying the amount of reactive chemicals released from living nerve cells. These techniques will also be discussed regarding multimodal imaging approaches that have recently been shown to be advantageous for the understanding of structural and functional relationships in the nervous system. This review aims to provide an insight into the strengths, limitations, and potentials of these technologies for synaptic and neuronal analyses.

Keywords: neurons, synapses, single cells, SIMS, mass spectrometry imaging, electrochemistry, NanoSIMS

OPEN ACCESS

Edited by:
Silvio O. Rizzoli,
Max Planck Society, Germany

Reviewed by:
Vincenzo Marra,
University of Leicester,
United Kingdom
Eugenio Francesco Fornasiero,
University of Göttingen, Germany

***Correspondence:**
Nhu T. N. Phan
nhu.phan@chem.gu.se

Received: *14 January 2022*
Accepted: *14 March 2022*
Published: *16 May 2022*

Citation:
Lork AA, Vo KLL and Phan NTN (2022) Chemical Imaging and Analysis of Single Nerve Cells by Secondary Ion Mass Spectrometry Imaging and Cellular Electrochemistry. Front. Synaptic Neurosci. 14:854957. doi: 10.3389/fnsyn.2022.854957

INTRODUCTION

The molecular organization of neurons has been shown to play a regulatory role in neural communication. Investigation of this dynamic nanoscale architecture is crucially important for understanding the mechanistic insight into the brain activity and biology. Besides *in vivo* studies, neuronal cultures are widely used as models to study neuronal biology, for example, primary neuronal cultures, induced pluripotent stem cell-derived neurons, and neuronal cell lines. The main advantage of neuronal cultures is that their environmental factors, such as temperature, CO_2 and the culture medium, can be controlled and modified in a specific manner. In addition, it is a simplified model with only one or few cell types, allowing to focus on specific cellular mechanisms or particular cellular pathways while eliminating interference from complex interactions regarding the diversity of cells in the brain. To obtain highly spatially resolved images of single synapses, spines, vesicles, etc., imaging technologies with high spatial resolution are needed. To evaluate transmitter release in single synapses, analytical techniques with high temporal resolution are desirable. These criteria can be met using presently available technologies, for instance, fluorescence microscopy and super-resolution microscopy, mass spectrometry imaging (MSI), and cellular electrochemistry. While microscopic techniques have been widely used as established methods in neuroscience and biological research, MSI and cellular electrochemistry are less known in the field (**Figure 1**).

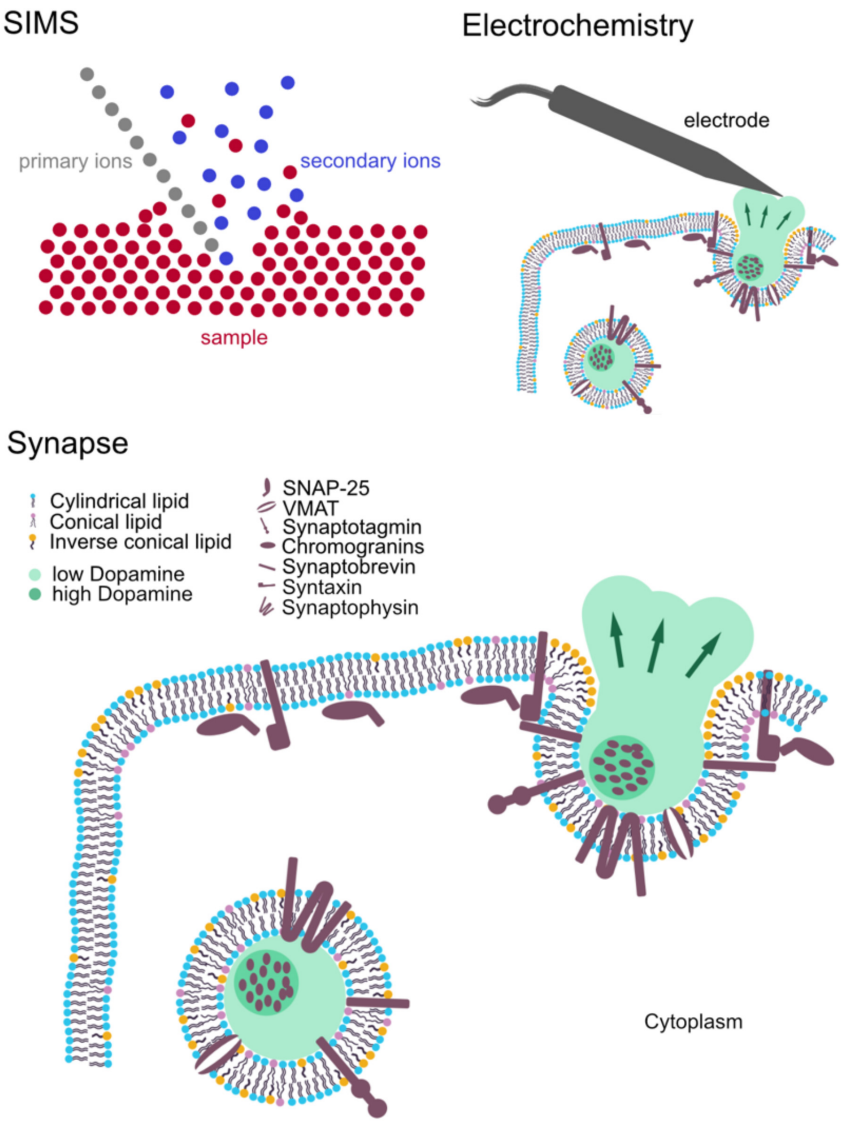

FIGURE 1 | Schematic of the main components of synaptic structure: synaptic vesicles and major associated molecules affecting synaptic activity. Secondary ion mass spectrometry (SIMS) and electrochemistry for measuring synaptic structure and activity, respectively.

Mass spectrometry imaging (MSI) is a powerful imaging tool for obtaining chemical information with cellular and subcellular spatial information. MSI is characterized by high chemical specificity, high sensitivity, high mass resolution, and, often, parallel detection of various compounds. Among different types of MSI, secondary ion mass spectrometry (SIMS) offers highest spatial resolution, which is suitable for subcellular imaging of neuronal cells. Unlike fluorescence imaging, SIMS allows for a label-free approach and elucidation of molecular structure (ToF-SIMS), although isotopic labeling is often employed to track the molecular turnover of cells and organelles (Lanekoff et al., 2011; Steinhauser et al., 2012). SIMS has continuously expanded its horizon of applications to study biomolecular organization in cell biology and neuroscience (Thomen et al., 2020; Agüi-Gonzalez et al., 2021; Jähne et al., 2021).

Electrochemical methods such as amperometry, cytometry, and voltametry measure the current or potential, which is changed by an electrochemical reaction related to an analyte, to quantify its concentration. Catecholaminergic neurotransmitters such as dopamine, epinephrine, and norepinephrine are all electroactive molecules, which can be oxidized or reduced and detected. With the excellent temporal resolution of electrochemical techniques (ns-ms range), single vesicular release events of live cells can be assessed to elucidate the mechanism of release. Electrochemical methods are, therefore, important techniques for studies on neural communication mechanisms and effects of exogeneous elements, e.g., drugs or plasticity inducing stimulation (Li et al., 2016b; Gu et al., 2019).

In this review, we present the principle, technical aspects of SIMS imaging and cellular electrochemistry, and their most

relevant applications in the research on synaptic biology. The goal of this review is to introduce these unfamiliar technologies to the neuroscience community, providing an insight of their strengths, limitations, and potentials for synaptic and neuronal imaging and analysis.

SECONDARY ION MASS SPECTROMETRY IMAGING

Secondary ion mass spectrometry utilizes a primary ion beam to bombard the surface of a sample pixel by pixel, sputtering secondary ions, which originate from the sample (Pacholski and Winograd, 1999; Vickerman and Briggs, 2013). Secondary ions will then be extracted and analyzed with a mass spectrometer and eventually be detected based on their mass to charge ratio (m/z). A mass spectrum is obtained for each pixel. Assembly of all spectra corresponding to their coordinates on the surface of the sample results in ion images showing the distribution of detected ions across the sample. During bombardment of the sample surface, the energy of the primary ion beam is partially transferred to the sample surface, the so called "collision cascade" phenomenon is taking place, and molecules in the sample are sputtered and ionized. It should be noted that only a small fraction of sputtered particles is ionized and analyzed. There are a variety of primary ion sources, for example, liquid metal ion guns (LMIGs) Au_3^+, Bi_3^+, polyatomic C_{60}^+, gas cluster ion beams (GCIBs), and monoatomic Cs^+ and O^-. Detailed development and performance of these primary ion sources can be found in comprehensive bodies of literature (Toyoda et al., 2003; Weibel et al., 2003; Kollmer, 2004; Rabbani et al., 2013). Depending on their properties, they have different performances in terms of spatial resolution, detected ions, destruction of the sample surface, and ionization efficiency. Larger cluster ion beams are softer than the small ones (Postawa et al., 2005; Winograd, 2013 and, thus, are less destructive to the sample and generate less fragmented secondary ions. However, large ion beams have a larger beam size, which hinders lateral resolution. Furthermore, there are several other parameters that also affect secondary ion yield, particularly, ionization probability, sputter yield, and concentration of analytes, and transmission of the instrument.

Time of Flight-Secondary Ion Mass Spectrometry and NanoSIMS

There are two main types of SIMS instruments available in the field. In the following section, distinct instrumental features of these two instruments are discussed. In time of flight (ToF)-SIMS, the primary ion beam impacts the sample at a 45° angle (**Figure 2A**), which is one of the factors limiting achieved lateral resolutions. On the other hand, nanoscale SIMS (NanoSIMS) benefits from its coaxial design, and combined with the monoatomic primary ion beam, it provides very high lateral resolution, ∼50 nm for a Cs^+ source (**Figure 2B**). SIMS generally has a depth resolution (z) of 1–10 nm. ToF-SIMS detects various analytes in parallel within a mass range of up to 2,000 Da, whereas NanoSIMS measures elements and small fragmented ions with up to 7 detectors. Mass resolution ($M/\Delta M$) is ∼10,000 for nanoSIMS and up to 10,000 for ToF-SIMS with delayed extraction (Vanbellingen et al., 2015; Nuñez et al., 2018). In addition, NanoSIMS employs Cs^+ and O^- as primary ion sources, whereas ToF-SIMS has more options from a wide range of primary ion sources mentioned above. Detailed discussion on the configuration of ToF-SIMS and NanoSIMS and their characteristics can be found in selected reviews of literature (Boxer et al., 2009; Nuñez et al., 2018; Agüi-Gonzalez et al., 2019).

Sample Preparation for Secondary Ion Mass Spectrometry Imaging

Sample preparation is a key aspect for SIMS analysis as molecules of interest and their locations need to be preserved well. Depending on the species of interest, different strategies for sample preparation should be considered. The simplest approach in terms of sample handling is the air-drying method in which preserved cells, after multiple washing steps to remove salts etc., are air-dried. This, however, could lead to shrinkage and deformation. Distinct sample preparation protocols could be performed for particular analytes of interest because of complex chemical distribution and topography in cultured neurons (Tucker et al., 2012). Paraformaldehyde fixation retained good lipid signals of *Aplysia californica* but produced low signals in the cell soma, whereas glycerol preserved well cell mophology and retained good lipid signals in the soma. On the other hand, formaldehyde increased background signal intensity but did not enhance lipid signals. The combination of glycerol and paraformadehyde was suitable for SIMS imaging of cultured neurons. Nevertheless, chemical fixation does not work well for all types of molecules and could potentially cause interferences. To avoid this, frozen hydrated samples have been used. Samples are snap-frozen and maintained in the frozen state during measurement; this is currently the best way to preserves the sample's molecular structure. However, it is less reproducible because of the inherent challenging procedure. One of the challenges is that samples need to be kept at a very low temperature throughout the preparation and away from the atmosphere to prevent the condensation of water on top of the samples. Another challenge is that the instrument needs to be cooled down with liquid nitrogen and maintained at equally low temperature during the entire analysis. This, in turn, causes difficulties in storing and transferring frozen samples into the analysis chamber of the SIMS instrument for analysis. A common alternative, which preserves samples well enough and is easily reproduced, is freeze-drying where samples are snap frozen in isopentane at −180°C to avoid the formation of larger water crystals. Subsequently, samples are dried in a vacuum at a low temperature so that the water slowly sublimates. Lee et al. (2019) propose covering samples with a graphene layer to let the samples dry slowly to better preserve cellular structures. The graphene layer can then be removed by air plasma treatment, and ion images can be taken with an improved quality compared to air drying. Most recently, Lim et al. (2021) showed that cells can be imaged in the wet state by covering them with grapheme, and that ions are sputtered through a transient hole while cells are still alive. Another possibility of sample preparation

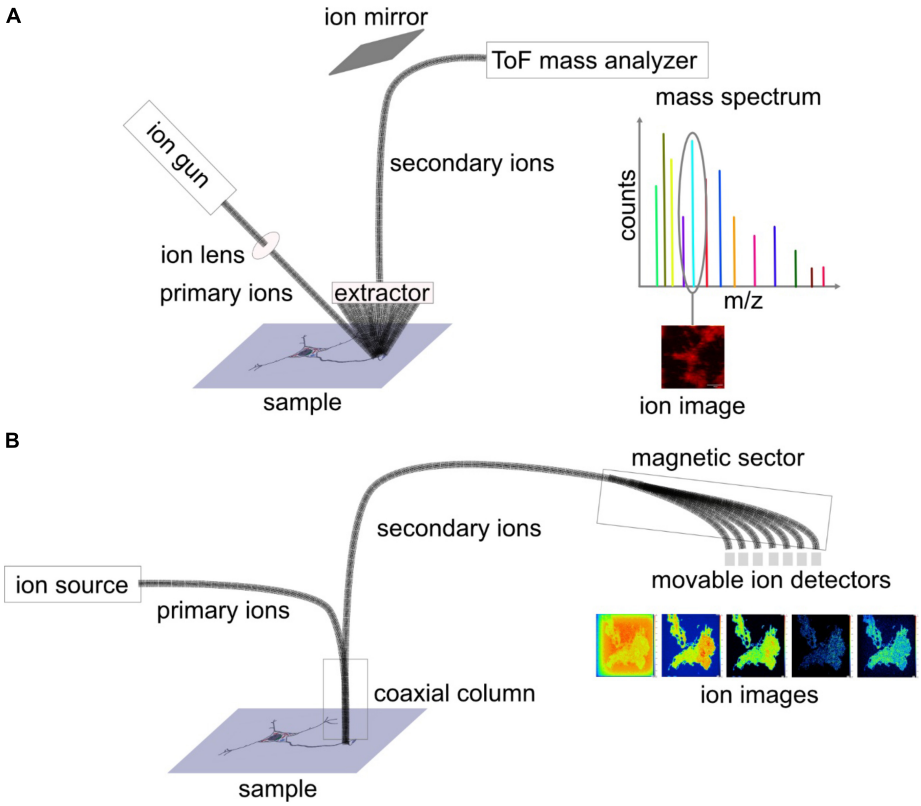

FIGURE 2 | Schematic diagram depicting the set-up of **(A)** ToF-SIMS and **(B)** nanoscale SIMS (NanoSIMS). In ToF-SIMS, sample surface is bombarded with primary ion beam at an angle of 45 degrees, and secondary ions are sputtered away, extracted, and transferred into the ToF mass analyser, where the ions are separated based on their mass to charge ratio (m/z). For each pixel, a mass spectrum is obtained, and for each mass peak, an ion image is depicted. NanoSIMS can achieve higher lateral resolution owing to the coaxial design of the primary and secondary ion beams. After being sputtered from the sample surface, the secondary ions are separated by a magnetic sector analyzer, and, eventually, seven masses are detected.

is to chemically fix cells with aldehydes and embed them in a resin (epoxy or acrylic resins), which has been commonly used for NanoSIMS. Samples can be contrasted, e.g., with osmium tetroxide to perform correlative transmission electron microscopy. Transparent resins can be used for correlative fluorescence microscopy (Saka et al., 2014).

Analyzing the spatial distribution of biomolecules across a biological sample has been demonstrated to be an important application for SIMS in general. Especially in highly polarized cells such as neurons, gaining the subcellular spatial distribution of cellular molecules is an important step in understanding their biology. SIMS is able to provide extensive atomic and molecular information at subcellular resolution, thus enabling the analysis of neurons, synapses, and vesicles.

Secondary Ion Mass Spectrometry Imaging of Single Nerve Cells

Vitamin E in Single Neurons

Many authors have studied the localization of vitamin E, an important antioxidative molecule, in neurons. The molecule is of great interest in neuroscience as low level of vitamin E affects axonal transport and can lead to axonal dystrophy and swelling. Monroe et al. (2005) identified vitamin E peaks with a vitamin E standard at m/z: 430, 205, and 165. Similar peaks were found in the *Aplysia* neuron with a distinct distribution; particularly, vitamin E localized in the soma. To minimize the effects of sample topography, the signal intensity of vitamin E was normalized to that of an ubiquitous evenly distributed ion, e.g., lipid acyl chain fragment (m/z 69). In addition, the authors highlight the importance of consistent sample preparation/analysis time as this distinct localization could not be observed when the samples were stored for a few days after freeze-drying before analysis (Monroe et al., 2005). The identification of vitamin E peaks was confirmed in *Aplysia* neurons by Passarelli and Ewing (2013) by tandem MS analysis. The localization of vitamin E was found to be in the soma, co-localizing with carotenoids, which were seen in an optical image. More recently, Bruinen et al. (2018) have imaged α-tocopherol, a type of vitamin E, in neurons (**Figure 3A**). Human-induced pluripotent stem cell (iPSC)-derived neurons were imaged in depth, and tandem MS analysis was performed for m/z 430. The data of MS/MS total ion current for m/z 430 as well as its product ions showed the localization of α-tocopherol predominantly in the soma but also in neurites (Bruinen et al., 2018). In addition, it was noted that peak assignments of molecules could be improved by the

MS/MS information of other molecules. In this case, m/z 772 was more confidently assigned to phosphatidylcholine (PC) (32:0) $[M + K]^+$ and m/z 551 as a fragment of PC (32.0) and DG (32:0). PC (32:0) $[M + K]^+$ localized evenly distributed in the soma and in central axes of neurites. Interestingly, m/z 551 showed a different distribution in the outer perimeter of the soma and neurites, which is likely to be attributed to DG (32:0).

Organization and Turnover of Membrane Lipids in PC12 Cells

PC12 rat pheochromocytoma cells are a common, well-studied cellular model system for the investigation of exocytosis mechanisms. They are easy to maintain in a culture. PC12 cells contain large dense core vesicles (LDCVs) with catecholamines (DeLellis et al., 1973). These vesicles can release their content upon extracellular stimulation in a conserved mechanism involving multiple proteins such as SNARE proteins. This has led to the investigation of PC12 cells with different SIMS techniques. Main emphases of the studies were lipid analysis mainly with ToF-SIMS and analysis of LDCV with NanoSIMS. In the study by Lanekoff et al. (2011), PC12 cells were incubated with isotopic phospholipids of two different shapes. Incubation with cylindrical-shaped lipid PC and conical-shaped phosphatidylethanolamine (PE) was shown to alter the exocytosis rate in opposing ways (Uchiyama et al., 2007); therefore, ToF-SIMS was conducted to assess the incorporation of these lipids. The cells were incubated with lipids containing rare isotopes [deuterated 16:0/16:0 PC (D75PC) and deuterated 16:0/16:0 PE (D62PE)], which incorporated into newly synthesized lipids in cells and could be distinguished from endogenous molecules. Lanekoff et al. showed that small changes in lipids (0.5% for PC, 1.3% for PE) were observed in the plasma membrane. With increasing concentrations of up to 300 μM during incubation, the relative amount of PC and PE in the membrane also increased to ∼ 2% for PC and ∼ 9% for PE. In 2018, relative quantification of isotopic fatty acids in PC12 cells as well as their lipid turnover, a process in which old lipid molecules are gradually replaced by newly synthesized ones to maintain proper cellular functions, were investigated by Philipsen et al. (2018). A-linolenic (omega 3 fatty acid) and linoleic acids (omega 6 fatty acid) are the precursors for polyunsaturated fatty acids and lipids and have been implicated in neurological disorders (Parletta et al., 2016). Incubation of PC12 cells with α-linolenic acid and linoleic acid leads to their uptake and incorporation into PCs, PEs, and phosphatidylinositols (PIs) (**Figure 3B**). Interestingly, it was shown that the formation of polyunsaturated fatty acids is different depending on which isotopically labeled fatty acid was incubated. Linoleic acid was only converted to 20 carbon polyunsaturated lipids, whereas α-linolenic acid could be converted to 20 carbon and 22 carbon polyunsaturated fatty acids. Furthermore, linoleic acid and its conversion product, arachidonic acid, were found to make up lipids with two and four double bonds, while α-linolenic acid and its product, eicosapentaenoic acid, make up lipids with three, five, and six double bonds, meaning that no addition of double bonds takes place during incorporation (Philipsen et al., 2018).

Structural Effects of Membrane Lipids on Synaptic Plasticity

Synaptic plasticity associated with lipid alterations has recently been investigated by Gu et al. (2020). PC12 cells were stimulated 0, 3, or 6 times with a 100-mM K^+ solution, and lipid fragments were analyzed with an ION-TOF V instrument. The authors focused on the fragments from PCs, PEs, and PIs, as they appear in higher abundance in the plasma membrane than other lipids. Interestingly, PC level reduced with increasing stimuli, whereas PE, PI, and cholesterol levels increased. It was hypothesized that this alteration might stabilize the fusion pore of vesicles during exocytosis owing to high abundance of high curvature, such as conical (PE), inverted cone shape (PI) lipids, and intrinsically negatively curved cholesterol. This, in turn, would lead to higher fraction of vesicular content to be released after multiple stimuli (Gu et al., 2020). The data agree with the results from previous studies on patients with Alzheimer's disease (Prasad et al., 1998), cocaine-treated flies (Philipsen et al., 2020), and cognitive-enhanced methylphenidate-treated flies (Philipsen et al., 2020), suggesting a link among dynamic lipid organization, synaptic plasticity, and memory.

Agüi-Gonzalez et al. (2021) investigated the effect of neuronal activity alterations on the lipid organization of the plasma membrane in primary hippocampal neurons. First, the spatial organization of lipids and lipid fragments across different parts of the cellular membrane was assessed. Independent component analysis and neighborhood cross correlation coefficient analysis was conducted to differentiate differences in lipid localization between neurites and the cell body. Second, neurons were treated with tetrodotoxin, a voltage-gated sodium channel blocker, to inhibit neuronal activity, or with bicuculine, a competitive antagonist of $GABA_A$ receptors, to increase neuronal activity. 51 lipid related peaks were found significantly different in their relative abundance between the activity inhibited cells and the control, and 41 lipid related peaks changed compared between the activity stimulated cells and the control. For example, ceramides, which are second messengers and components in the sphingolipid metabolic pathway, increased their abundance in inhibited cells. In addition, the total PC level decreased in the cell body while it increased in neurites in both activity-inhibited and enhanced cells. Furthermore, phosphatidylserine abundance reduced in low-activity cells, whereas it increased in high-activity ones. These distinct lipid alterations provide new insights into possible mechanisms of activity-dependent molecular organization in neurons.

CORRELATIVE SECONDARY ION MASS SPECTROMETRY AND OTHER TECHNIQUES FOR IMAGING SINGLE VESICLES AND SYNAPSES

Recently, emerging correlative imaging has expanded the perspectives of many complex biological questions that need multidimensional information, which cannot be achieved with a single technique. Correlative imaging combines several

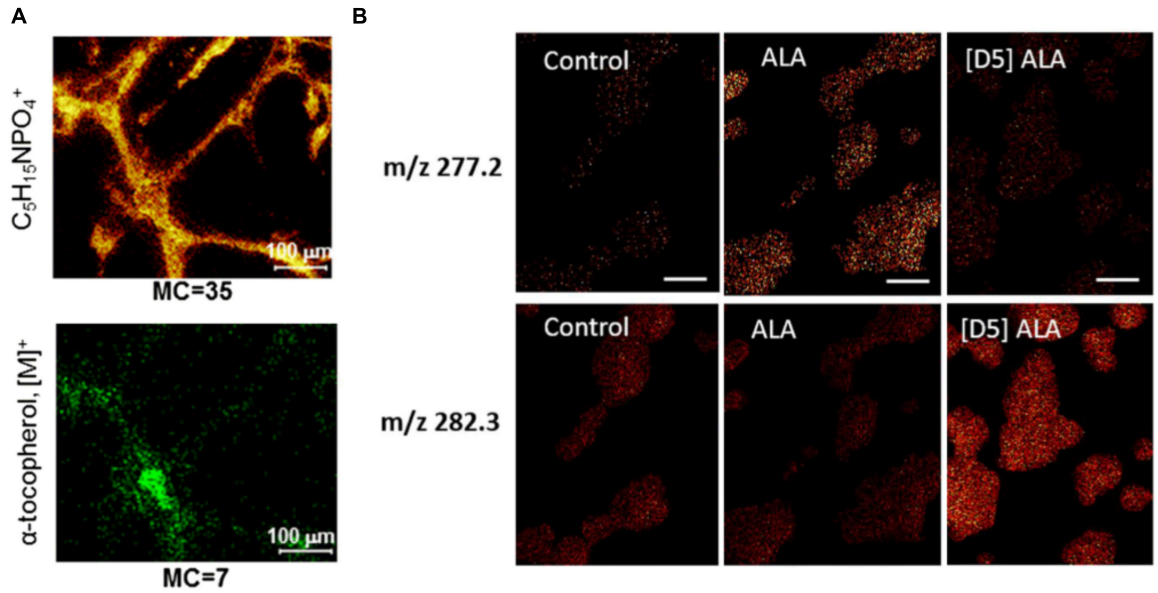

FIGURE 3 | Examples of ToF-SIMS imaging in nerve cells. **(A)** Ion images of phosphocholine head group $C_5H_{15}PO_4^+$ and α-tocopherol of human iPSC-derived neurons. **(B)** Ion images of masses m/z 277.2 and m/z 282.3 of PC12 cells incubated with α-linolenic acid (ALA) and isotopically labeled D_5-ALA. ALA-incubated cells show higher signal in m/z 277.2 than in 282.3, whereas for D_5-ALA the signal of incubated cells in m/z 282.3 is more dominant because of the contribution of the isotopic label. The Figures were reproduced and modified from Bruinen et al. (2018) and Philipsen et al. (2018) under the creative commons license.

different imaging and analysis technologies to connect different properties of cells, e.g., cellular structures, functions, and molecular dynamics to obtain an insight into their molecular mechanistic process. Various combinations such as SIMS, electron microscopy, and fluorescence microscopy have been optimized (Watanabe et al., 2011; Wilhelm et al., 2014; Salamifar and Lai, 2015; Lange et al., 2021). Here, we describe several correlative approaches, which have been applied for imaging single vesicles and synapses.

Correlative NanoSIMS and Fluorescence Microscopy

Correlative NanoSIMS and super resolution-stimulated emission depletion (STED) microscopic imaging was developed to study protein turnover in specific subcellular structures of rat hippocampal neurons (Saka et al., 2014). Neurons were incubated with ^{15}N-leucine, which was then incorporated into newly synthesized proteins as a marker for protein turnover in neurons. Several organelles and structures, particularly active zones, vesicles, mitochondria, Golgi, and endoplasmic reticulum, were immunostained and visualized by STED microscopy. Correlation between the map of protein turnover from NanoSIMS and protein localization from STED microscopy showed that the protein turnover in the synapse is significantly higher than that in axonal regions.

The combination of isotopic ^{15}N-leucine labeling and immunostaining for specific vesicular proteins in rat hippocampal neurons was used to study the protein turnover of recycling vesicles by NanoSIMS and STED microscopy (Truckenbrodt et al., 2018). By labeling recycling vesicles with an antibody against the intravesicular domain of synaptotagmins in different endocytosis cycles, the protein turnover of actively recycling vesicles could be compared to that of older vesicles. It was found that actively recycling vesicles are more enriched at the isotopic label and, therefore, have more newly produced proteins.

Correlative NanoSIMS and STED imaging was also performed to investigate protein turnover in single synapses with respect to synaptic activity in rat hippocampal neurons (Jähne et al., 2021). It was found that protein turnover is well-correlated with synaptic activity at the single synapse level. Combined with mathematical modeling of the synaptic vesicle cycle, the authors confirmed this observation by identifying the localization of synapses by STED microscopy and assessing their protein turnover by NanoSIMS using ^{15}N-labeled leucine incubation technique. Pre- and post-synapses were marked with synaptophysin1 and Homer1, respectively. The intensity of both markers was not correlated with protein turnover; however, when examining only vesicles undergoing exo- and endocytosis, their synaptotagmin intensity correlated strongly with presynaptic protein turnover (**Figures 4A–C**). Interestingly, this correlation was abolished when the synaptic activity was altered by tetrodotoxin and bicuculine. Both drugs had an opposite effect on both pre- and postsynaptic protein turnover, which indicates that synaptic protein turnover closely depends on synaptic activity (Jähne et al., 2021).

Correlative NanoSIMS and Electron Microscopy

The content of LDCVs has been evaluated by NanoSIMS imaging (Lovrić et al., 2017; Thomen et al., 2020; Nguyen et al., 2022;

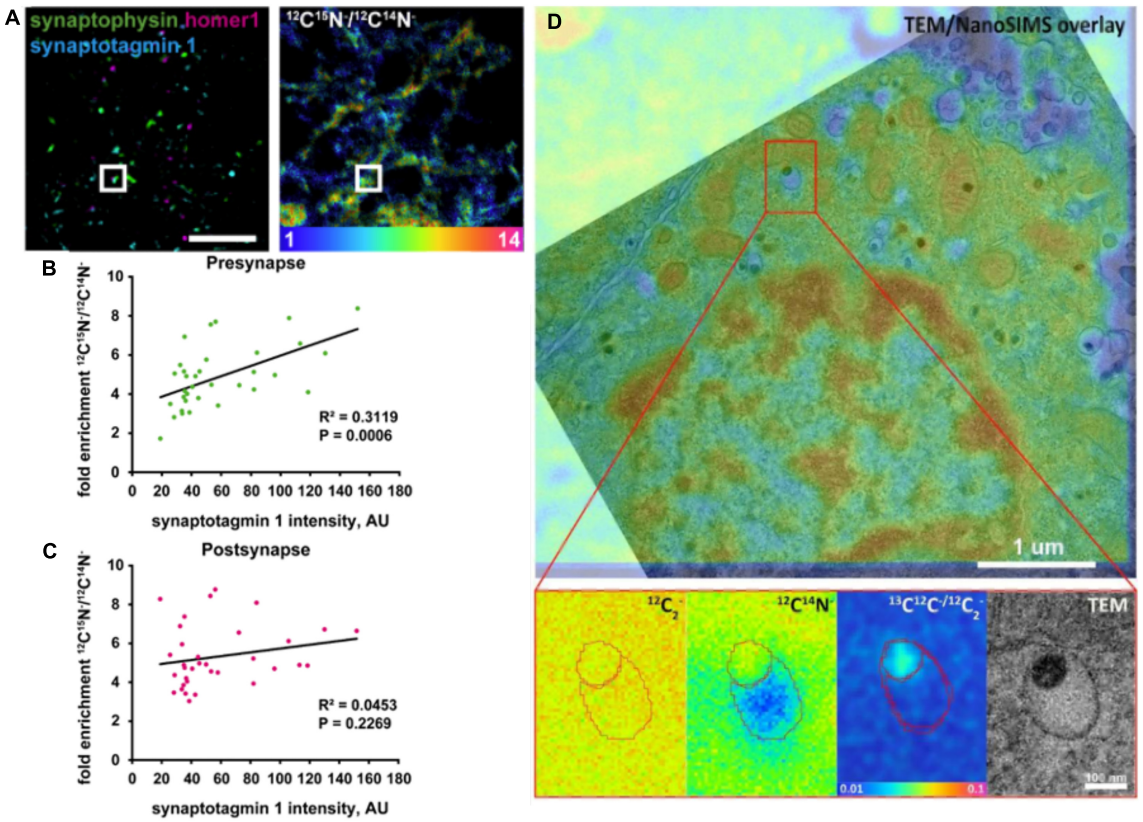

FIGURE 4 | Examples of correlative imaging with NanoSIMS in neurons and synapses. **(A–C)** Correlation of synaptic protein turnover with synaptic activity. **(A)** Stimulated emission depletion (STED) images localizing the pre- and post-synapses identified by presynaptic marker (Synaptophysin), postsynaptic marker (Homer 1), synaptic activity marker (Synaptotagmin 1), and their corresponding protein turnover shown in the $^{12}C^{15}N/^{12}C^{14}N$ NanoSIMS image. Scale bar is 5 μm. **(B)** Quantitative chart showing the correlation of presynaptic protein turnover with synaptic activity. **(C)** Quantitative chart showing no correlation of postsynaptic protein turnover with synaptic activity. **(D)** Correlative TEM and NanoSIMS imaging of dense core vesicles in a PC12 cell incubated with ^{13}C-labeled L-DOPA. A higher concentration of ^{13}C-dopamine (87.5 mM) was found in the dense core compared to the halo (16 mM). The Figures were reproduced from Jähne et al. (2021) and Rabasco et al. (2022) under the creative commons license.

Rabasco et al., 2022). Lovrić et al. investigated the distribution of dopamine across LDCVs by incubating PC12 cells with ^{13}C-labeled L-DOPA, which is then converted to dopamine and loaded into vesicles. Correlating transmission electron microscopy (TEM) and NanoSIMS, LDCVs could be identified, and their substructures, the dense core and halo, could be distinguished. The distribution of ^{13}C-labeled dopamine across these substructures could also be analyzed. In addition, reserpine, an inhibitor of the vesicular monoamine transporter (VMAT) for inhibiting the loading of dopamine into vesicles, was used in this study to modulate vesicular content. Interestingly, the results indicated that the protein-rich dense core (containing, e.g., chromogranins) traps more dopamine compared to an "expandable labile pool" of dopamine in the halo with increasing incubation time with ^{13}C-L-DOPA. NanoSIMS results were additionally confirmed by electrochemical data (Lovrić et al., 2017). Thomen et al. (2020) performed an absolute quantification of ^{13}C-labeled dopamine level in vesicles of PC12 cells. Importantly, the concentration of carbon in the embedding material, epoxy resin, measured *via* the $^{12}C^{12}C^-$ signal, was similar to that in PC12 cells including vesicles. In addition, to reach a steady state of sputtering, primary ion fluence must reach 1×10^{17} Cs^+cm^{-2}, which consumed a sample depth of ∼180 nm. Accumulation of dopamine in the dense core of vesicles was observed to be similar to the results from Lovrić et al. (2017). The determined concentration of ^{13}C-dopamine in vesicles was ∼60 mM, which is in agreement with the electrochemical data (Thomen et al., 2020). More recently, the absolute concentration of dopamine in each of two vesicle compartments was quantified (**Figure 4D**; Rabasco et al., 2022). It was found that the dense core contains a dopamine concentration of 87.5 mM, which is significantly higher compared to that in the halo (16 mM). Another study confirmed partial exocytotic release in PC12 cells, which is visualized by correlative NanoSIMS and TEM (Nguyen et al., 2022). ^{13}C-labeled L-DOPA was incubated in cells for visualization of ^{13}C-dopamine in vesicles. In addition, ^{127}I-di-*N*-desethylamiodarone was introduced to cell media during KCl stimulation of cells. Exocytosed vesicles were then identified by the co-localization of ^{127}I-di-*N*-desethylamiodarone and ^{13}C-labeled dopamine signals inside the vesicles in NanoSIMS images.

This allowed for the direct comparison of dopamine content of vesicles between stimulated and non-stimulated cells. The result showed that the dopamine content of vesicles reduces significantly after they undergo exocytosis, which confirmed the partial release of exocytosis.

AMPEROMETRY FOR STUDYING NEUROTRANSMITTER RELEASE DURING EXOCYTOSIS

Amperometry is one of the electrochemical methods that provides excellent sensitivity for quantification of neurotransmitters secreted from single cells at attomole to zeptomole (Chen et al., 1994; Jaffe et al., 1998; Pothos et al., 1998; Hochstetler et al., 2000), and an outstanding temporal resolution at sub-millisecond level (Robinson et al., 2008). In amperometry, a microelectrode is placed adjacent to a cell surface while a cell is stimulated with a potassium solution to initiate exocytosis. The potential is applied to an electrode surface and kept constant whereas a reduction and oxidation current will be recorded for the detection of an electroactive analyte, in this case the neurotransmitters released from the cell. A carbon fiber microelectrode was first introduced by Gonon et al. (1980) to record neurotransmitter release (Ponchon et al., 1979). In the early 1990s, single cell amperometry (SCA) was described by the Wightman group to study individual exocytosis events by placing a disk-shaped electrode on top of single bovine chromaffin cells (Leszczyszyn et al., 1991; Wightman et al., 1991). Carbon fibers have prominent mechanical and electrical properties, including high stability, long-term durability, and negligible temperature sensitivity. These electrodes can be constructed by aspirating carbon fibers (usually 5–10 μm in diameter) into glass or silica tubes to have a cylinder or a disk shaped with a 45° angle electroactive surface. Therefore, any electroactive molecules present on the surface of the electrode will react, causing a change in current (Bard and Faulkner, 2001; Borland and Michael, 2007). The recording of an amperometric peak with the presence of electroactive transmitters is shown in **Figure 5A**. According to Faraday's law, the number of transmitter molecules released from each exocytosis event can be calculated with $N = Q/nF$, where Q is the charge in coulombs, n is the number of electrons transferred per mole in the oxidation reaction (2 electrons for the oxidation of catecholamines and serotonin), and F is Faraday's constant (96,485 C mol^{-1}). The limitation of this method is that only neurotransmitters in vesicles with accessible redox waves such as dopamine, adrenaline, noradrenaline, serotonin, and histamine can be detected. Another drawback of the technique is the lack of a qualification analysis because the applied constant potential over time cannot distinguish different electroactive analytes measured at the same time (Borland and Michael, 2007). Therefore, it is necessary to identify molecules before amperometric measurements.

Different Modes of Exocytosis

SCA has been employed as a powerful tool to determine different modes of exocytosis. This phenomenon involves a fusion between a secretory vesicle and the plasma membrane, resulting in the release of its chemical content into the extracellular environment. The formation of a fusion pore is facilitated by SNARE proteins, but what exactly happens to the fusion pore afterward is still controversial (Ren et al., 2016). During quantal release, also called full release, a vesicle fully collapses and merges with the plasma membrane, leading to discharge of the entire content of the vesicle. The mechanism of exocytosis was thought to be an all-or-none process for a long time. However, more recent research has proved that this is not the only mode of release. There are a number of variations depending on how long the pore stays open and how much of the vesicular content is released. One of them is the kiss-and-run mechanism, in which an initial fusion pore can be transiently formed, and the vesicle releases a small amount of its content and closes. The third mode of exocytosis is referred to partial release, also known as sub-quantal release, or extended kiss and run, or open and closed. This mode involves the expansion of small sized fusion pores to a certain degree, allowing a larger amount of neurotransmitters to escape in comparison to that in the kiss and run mode. Illustrations of various modes of release are shown in **Figure 5B**. Flickering is another mode by which a pore opens and closes many times with only a very small fraction of catecholamine released (Staal et al., 2004). In this case, vesicles can open and close their fusion pores multiple times before expelling all the content. This phenomenon seems to appear more frequently than full release (Mellander et al., 2012).

Amperometry for Quantifying Neurotransmitters in Single Cell Models

Owing to outstanding spatial-temporal resolution and high sensitivity, amperometry has become a powerful tool to study exocytosis for many cell types, including primary cultures, nerve cells, other secretory cell models (chromaffin cells, pheochromocytoma cells, PC12 cells, mast cells, and pancreatic β cells), neurons, synapses, and single nerve cell varicosities (Keighron et al., 2020). Quantal release was observed from axonal varicosities of midbrain dopamine neurons consisting of small synaptic vesicles by Pothos et al. (1998). A 5-μm diameter carbon electrode was placed gently onto a varicosity, which was visualized by labeling neurites with Lucifer yellow. These results provided a new mean for direct measurement of the number of neurotransmitter molecules and release duration of quantal events in central nervous system (CNS) neurons. The data also demonstrated that synaptic strength can be modulated by changing the number of dopamine molecules, or quantal size, released per exocytotic event. Zhou and Misler reported the detection of quantal catecholamine release on the surface of somas of cultured neurons by placing a carbon fiber electrode into the cleft between the somas of superior cervical ganglion neurons (Zhou and Misler, 1995). They found that 3.5×10^4 catecholamine molecules were released per packet, or per quantum, indicating that release from neurons is almost 80-fold smaller than that from adrenal chromaffin cells. Another study on exocytosis events was carried out by Chen and Ewing in the cell body of single dopamine-containing neurons of *Planorbis*

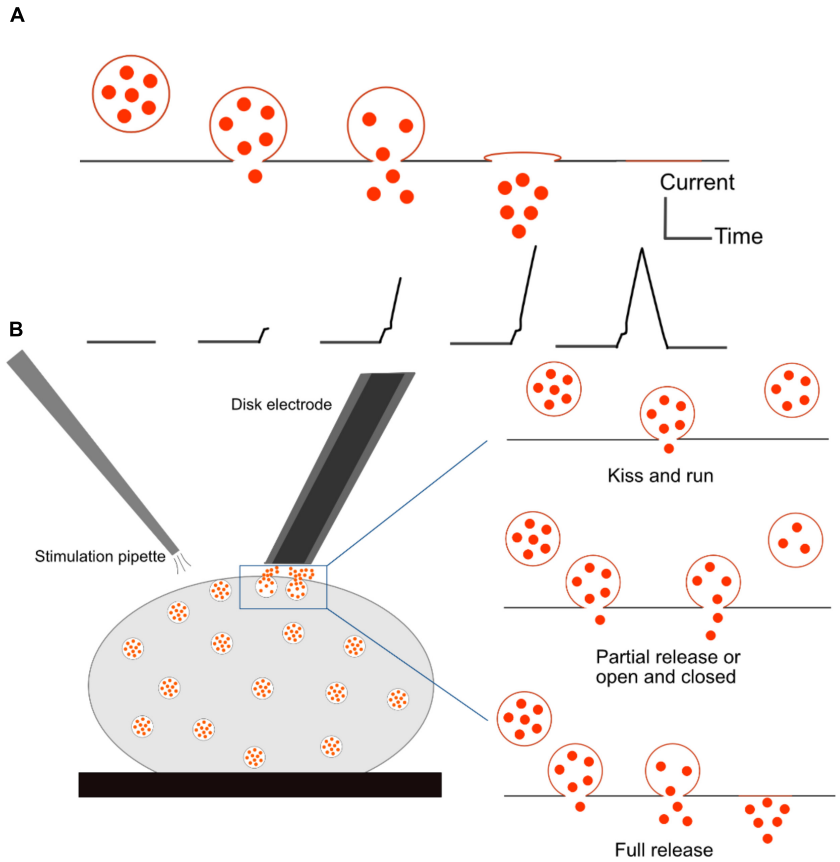

FIGURE 5 | Schematic of single cell amperometry (SCA) measurement and different modes of exocytosis. **(A)** Correlation of an exocytosis event of its recorded spike. **(B)** Schematic of disk electrode placement onto a cell and a stimulation pipette to initiate exocytosis (Left), and three different modes of exocytosis: kiss and run and partial release allow for a small fraction of neurotransmitters to be released from the vesicle, while full release expels all the transmitters (Right). The fraction of released transmitter is smaller in the kiss-and-run mode than in the partial release mode.

corneus (Chen and Ewing, 1995). Using a CNS stimulant, amphetamine, they manipulated the size and distribution of different classes of vesicles, which were distinguished by distinct distributions of the released dopamine from the neuron after the stimulation. Their results indicated a coexistence of two different classes of vesicles in dopamine containing neurons of *Planorbis*. Dopamine level was decreased by 40%, with changes in both vesicular content and distributions after amphetamine treatment. Moreover, amphetamine showed different effects on the two classes of vesicles, resulting in a third class of vesicles. The data demonstrated that multiple classes of vesicles are released, and that vesicular content can be independently manipulated with a psychostimulant. In 1995, Bruns and Jahn monitored the amount of transmitter released and kinetics of exocytosis from individual synaptic vesicles (Bruns and Jahn, 1995). The results indicated that the exocytosis of small vesicles appears more frequently and more quickly after a single action potential compared to large dense core vesicles because of different properties of their release events regarding charge, amplitude, and kinetics. Release rates of both types of vesicles are quite fast; large dense core vesicles discharge their content during the first millisecond, while small vesicles start releasing at a sub-millisecond timescale, suggesting rapid opening formation of a preassembled fusion pore. It was shown as a possible hypothesis that small vesicles are recycled without experiencing full fusion process.

Quantifying Neurotransmitters in Single Neuronal Varicosities and Synapses

Drosophila melanogaster, known as fruit fly, is an excellent model for studying brain function and neuronal communication due to its well-defined and easily manipulated nervous system. Despite its relatively simple genomes, the fly brain displays many high-order brain functions comparable to human counterparts. Therefore, *Drosophila* has been investigated to understand many important mechanisms of human developmental and physiological processes. Fly larva have been successfully developed to study the release in the field of *in vivo* electrochemistry. Majdi et al. (2015) reported a novel method to examine the octopamine release of exocytosis events in type 2 varicosities from a live, dissected larval system by amperometry. The neuromuscular junction is located peripherally and can be easily accessed with a small carbon fiber microelectrode. Furthermore, octopaminergic varicosities locate in the larval

body wall, which allows an electrode to be easily positioned on these boutons from a filet of the muscle wall (**Figures 6A–D**). The light-activated ion channel, channelrhodopsin-2, in neuronal varicosities (type 2 optopaminergic boutons) was expressed with the m-Cherry fluorescent protein. A 5-μm carbon fiber microelectrode was positioned on top of a bouton while it was visualized under red light, and exocytosis was evoked by the activation of channelrhodopsin-2 with blue light. The number of octopamine molecules released from the varicosity was determined to be ∼22,000 per vesicle. Interestingly, different modes of release were observed based on different shapes of transients, which was considered related to the mechanism of pore opening of a vesicle to form a nanometer-wide fusion pore (**Figure 6E**). It was also indicated that a vesicle fusion pore just opens to release the right amount of neurotransmitters at a necessary rate. This partial release of transmitters possibly affects presynaptic plasticity.

Because of the small distance of a synaptic cleft between neurons (20–30 nm) (Cox and Gabbiani, 2010), it has been very difficult to measure the neurotransmitters released in an individual synapse between two communicating cells. Recently, a novel finite conical nanoelectrode with a 50- to 200-nm tip diameter was introduced for measuring individual vesicular exocytosis events at the synaptic level (Li et al., 2014). The nanotip electrode was fabricated by flame-etching a carbon fiber to form a needle-shaped electrode with less than 100-nm radius and 1-μm shaft length. The release of norepinephrine from single synapses was probed by placing the electrode inside the space between neuronal varicosities and the soma of superior cervical ganglion cells (**Figure 7**). The results showed two types of amperometric peaks with approximately 42% of single events and 58% of complex events. This indicated the coexistence of different types of vesicle fusions in a single synapse. Additionally, a comparison between exocytosis events inside a synapse and on top of the corresponding varicosity denoted a non-uniform distribution of active zones corresponding to these two peak types. The results suggested that neurons can adopt different vesicle fusion modes in different locations of their axonal varicosities. In another study, a quantification of dopamine release inside single dopaminergic synapses with a nanoelectrode was performed for the first time (Tang et al., 2019). Harpagide, a natural product known to be a neuroprotective drug, was unambiguously demonstrated to enhance synaptic dopamine release and restore dopamine release to normal level from damaged neurons of a Parkinson's disease model. Phosphorylation and aggregation of α-synuclein monomers in neurons are suppressed by harpagide by inhibition of intracellular reactive oxygen level. This leads to an increase in exocytosed dopamine by increasing release frequency and total released amount, thus promoting synaptic activity.

Biosensors for Measuring Non-electroactive Neurotransmitters in Single Neurons

Amperometric techniques with carbon fiber micro- or nano-electrodes have been commonly used to directly quantify electroactive neurotransmitters in individual exocytotic events. However, it is impossible to monitor non-electroactive neurotransmitters such as acetylcholine, glutamate (Glu), and γ-aminobutyric acid (GABA). Shen et al. (2018) investigated acetylcholine concentration and release dynamics with a 15-nm nanopipette electrode without any modifications. The pipette electrode with nanoscale tip was filled with an organic reagent and then placed in a biological environment, recordings are obtained *via* ionic fluctuations caused by ion transfer between two immiscible electrolyte solution (ITIES) interfaces. With nanoscale scanning electrochemical microscope assistance, a nanoscale ITIES can be accurately positioned at a single living *Aplysia* synapse to measure the dynamics of cholinergic transmitter release. This study revealed that acetylcholine release from *Aplysia* varicosity is Ca^{2+}-dependent, and that it consists of singlet, doublet and multiplet spikes, which implies the possibility of multiple vesicle release or flickering of the fusion pore.

In another example, an enzymatic biosensor was successfully developed by co-modification of glutamate oxidase (GluOx) and platinum nanoparticles on the surface of a carbon fiber electrode by the Huang group (Qiu et al., 2018). This has been known as the first direct electrochemical detection of glutamate (Glu) released by exocytosis. The sensor was placed at a single hippocampal varicosity with stimulation of high K^+ concentration during SCA experiments. Multiple well-defined amperometric transients of exocytosis events were obtained in the presence of GluOx on the electrode. Recently, Yang et al. (2021) developed an electrochemical Glu-nanobiosensor to measure in real-time Glu fluxes released *via* exocytosis from individual living neurons. An enzyme, GluOx, was immobilized onto a carbon-modified *SiC* nanowire to convert Glu into H_2O_2, which is an electroactive molecule. The electrode was placed laterally on top of the varicosities of unpaired (without postsynaptic partner) rat hippocampal axons, and exocytosis release was triggered by a high potassium solution, leading to a series of amperometric spikes (46% occurrence frequency of single event, and the remaining had complex shapes). The study suggested a regulatory mechanism occurring during the exocytosis process to control the size, dynamics and lifetime of fusion pores, which, in turn, affects Glu release during synaptic transmission in the hippocampus.

VESICLE IMPACT ELECTROCHEMICAL CYTOMETRY AND INTRACELLULAR VESICLE IMPACT ELECTROCHEMICAL CYTOMETRY FOR MONITORING NEUROTRANSMITTER STORAGE IN INDIVIDUAL VESICLES

Amperometry provides an excellent method for quantification of the release process at the single cell level; however, it is unable to measure total vesicular content. This can be obtained by vesicle impact electrochemical cytometry (VIEC), and intracellular vesicle impact electrochemical cytometry (IVIEC) developed by the Ewing group (Dunevall et al., 2015; Li et al., 2016a;

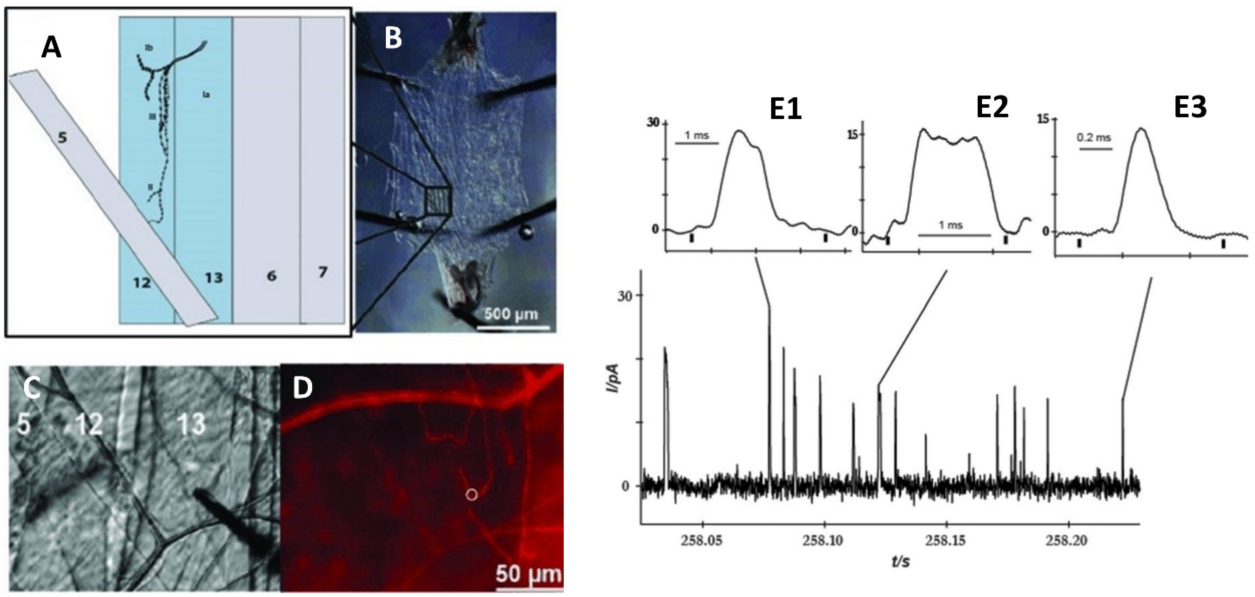

FIGURE 6 | Measurement of octopamine release from *Drosophila melanogaster* larvae by amperometry. **(A)** Schematic depicting muscles from the body wall, including muscles 12 and 13, which contain type 2 octopaminergic varicosities. **(B)** Dissection of the third instar larva revealing the body muscle wall. **(C)** Position of microelectrode on type 2 varicosities in muscle 13; **(D)** Same view as panel **(C)** but under red light to visualize mCherry in octopaminergic terminals, and the white ring indicates the location of the electrode. **(E)** Different amperometric peaks of the octopamine released from varicosity stimulated by blue light. **(E1)** Two overlapping peaks, **(E2)** plateau complex event, and **(E3)** single event. This Figure was reproduced from Majdi et al. (2015) under the creative commons license.

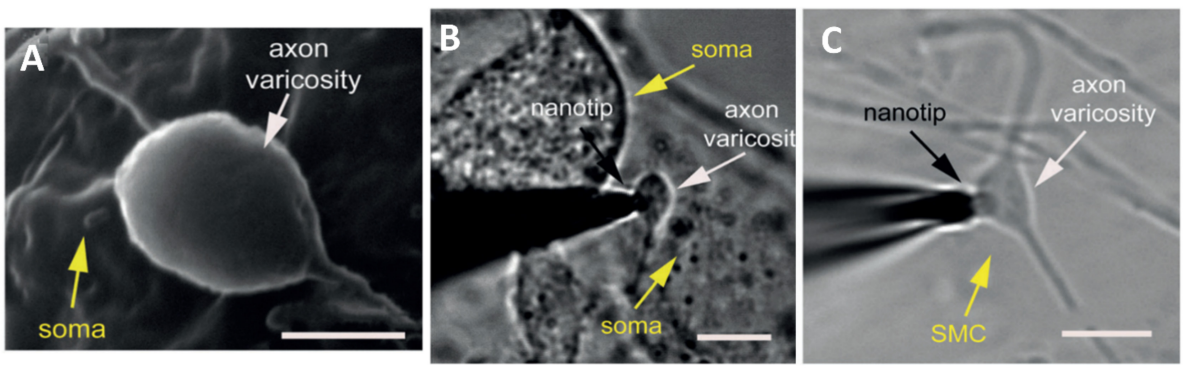

FIGURE 7 | Amperometric measurements of noradrenaline release at single synapses. **(A)** Scanning electron microscope image of a synapse formed between cultured superior cervical ganglion (SCG) sympathetic neurons. **(B)** Bright field photomicrograph of the nanotip at an individual synapse, between a varicosity of one SGC neuron and the soma of another neuron. **(C)** Photomicrograph of the nanotip electrode at a synapse, between a varicosity of a SGC neuron and smooth muscle cell. These Figures were reproduced from Li et al. (2014) under the creative commons license.

Figures 8A,B). These two methods share several similarities, but setups are different. In VIEC, a 33-µm disk-shaped electrode is directly dipped into a suspension of isolated vesicles. Vesicles are stochastically ruptured, and their transmitters are released to the surface of the electrode upon the application of a potential. With a similar principle, however, IVIEC employs a carbon fiber nanotip electrode (diameter < 100 nm), which allows for the electrode to penetrate into the cytosol of a living cell and measure the content of individual vesicles *in situ*. Using Faraday's law, the number of molecules stored inside individual vesicles can be determined similarly to SCA.

The combination of SCA and IVIEC can be applied to study transmitter release and storage in secretory vesicles, and helps to unambiguously certify the quantal or sub-quantal release in different modes of exocytosis in single living cells. Fraction release, the ratio of the amount released and total vesicle content, has been shown to be affected by drug treatments (Ye et al., 2018; Zhu et al., 2019). This provides powerful methodologies allowing for the analysis of the physical properties of vesicles in order to obtain a better understanding of vesicle dynamics. Additionally, these techniques enable the understanding of how alteration of the fraction of release, under

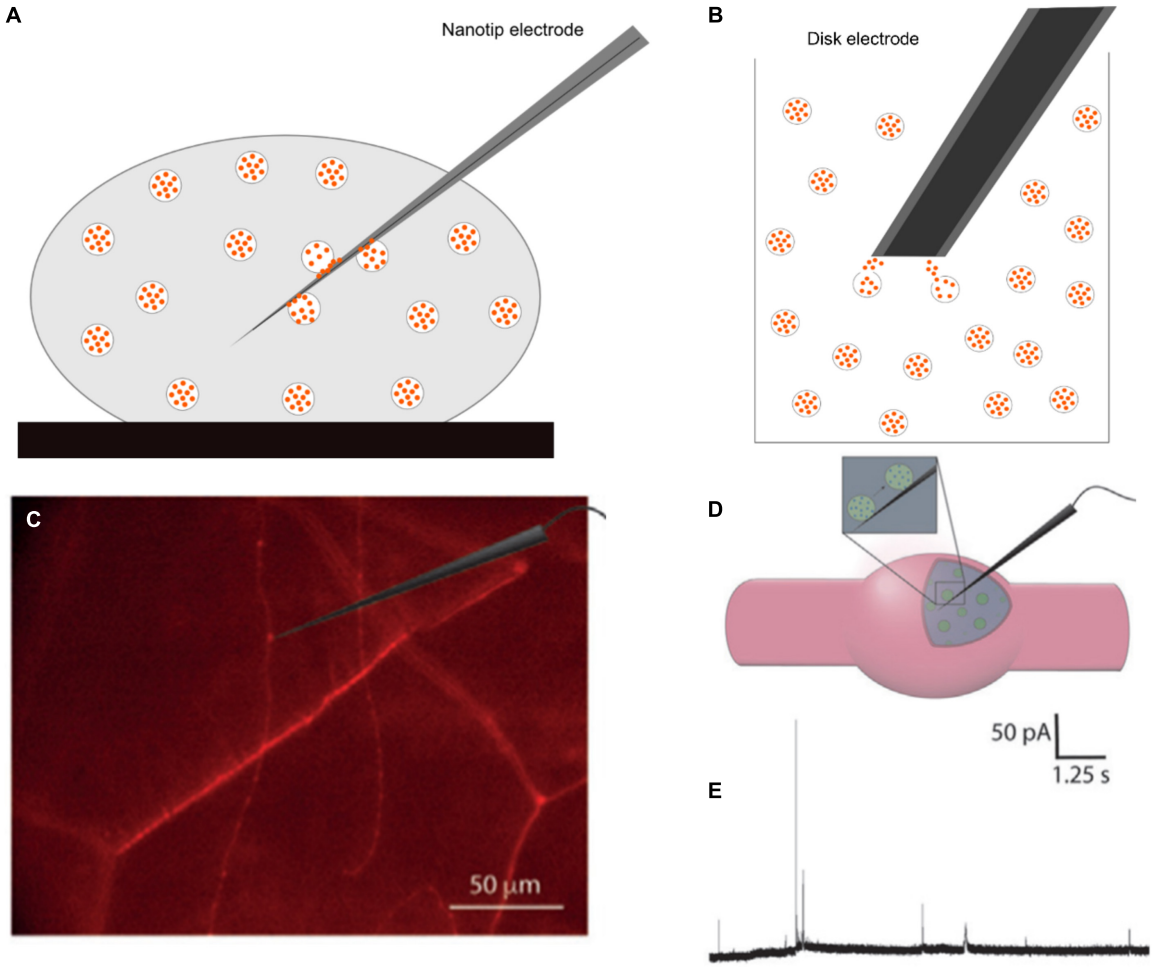

FIGURE 8 | Schematic of panel **(A)** intracellular vesicle impact electrochemical cytometry (IVIEC) with a nanotip electrode, **(B)** vesicle impact electrochemical cytometry with a 33-µm disk electrode, **(C)** mCherry-labeled neurons in Drosophila larva under a fluorescence microscope and an electrode placed on or inside a varicosity, **(D)** position of a nanotip electrode in the varicosity, and **(E)** Representative current transients for IVIEC measurements. Panels **(C–E)** were reproduced from Larsson et al. (2020) under the creative commons license.

the effects of an exogenous factor, can modulate synaptic and brain activities.

Using a combination of SCA and IVIEC, Larsson et al. (2020) showed that the release of octopamine during exocytosis in *Drosophila* larval neuromuscular junction is sub-quantal and complex. In this study, a nanotip electrode was used to pierce through the muscle into octopaminergic varicosities, which were observed under a fluorescence microscope (**Figures 8C–E**). Total vesicle content was detected in the range of 200,000 to 1.3 million molecules per vesicle, with a median of 411,000. This value is much higher than the amount released (22,700 molecules per vesicle) previously measured by SCA (Majdi et al., 2015). The fraction release of octopamine is, therefore, very small, and accounts for 4.5% for single events and 10.7% for complex events (oscillating or flickering) compared to the total vesicle content. A fusion pore can be adjusted *via* the opening-and-closing process to increase the released amount in complex spikes compared to simple ones. Their results strongly demonstrated that presynaptic plasticity can be regulated by fluctuations of fusion pores in the partial release.

Recently, intravesicular Glu was quantified using a novel Glu biosensor in living neurons (Yang et al., 2021). A combination of SCA and IVIEC enables the determination of Glu release and intracellular storage from rat hippocampal neurons following L-glutamine and Zn^{2+} treatments, which are known to be involved in the learning and memory processes. Intravesicular contents were strongly affected in opposite ways under the two treatments. Glu vesicular content and released amount dramatically increased by 259 and 183%, respectively, under the L-glutamine treatment. However, fraction release was at a similar level compared to the control group undergoing no L-glutamine treatment. In contrast, under the Zn^{2+}treatment, Glu content decreased by ca. one half, while the released amount increased by ca. one third of the total content. L-glutamine significantly enhanced the loading and synthesis of intracellular Glu but did

TABLE 1 | Common secondary ion mass spectrometry (SIMS) and electrochemical methods for neuronal and synaptic measurements.

Methods	Applications	Advantages/disadvantages
Time of flight secondary ion mass spectrometry (ToF-SIMS)	Imaging spatial distribution of ions up to ∼ 2,000 Da (metabolites, molecular lipids, small peptides) 2D and 3D imaging possible	+ Parallel detection within a large mass range (0-2,000 Da) +Suitable for non-targeted imaging (non-labeling) + Many primary ion sources available - Topographical sample effect - Spatial resolution possibly ∼ 250 nm
Nanoscale secondary ion mass spectrometry (NanoSIMS)	Imaging spatial distribution of monoatomic or diatomic ions at subcellular resolution 2D and 3D imaging possible	+ Spatial resolution ∼ 50 nm - Molecular information lost - Parallel detection up to 7 ions - Isotopic labeling often employed
Single cell amperometry (SCA)	Quantification of the number of neurotransmitters released from individual vesicles	+ High temporal resolution (sub-milliseconds to a few millisecond) - Cannot distinguish between catecholamine and other electroactive molecules at the same time
Vesicle impact electrochemical cytometry (VIEC)	Quantification of the total number of neurotransmitters stored inside individual vesicles Investigation of the effects of drug treatments on vesicle properties	+ easily manipulate the surrounding environment of vesicles - Risk of leakage of vesicular transmitters and changes of vesicle properties during the vesicle isolation process - Cannot distinguish between catecholamine and other electroactive molecules at the same time
Intracellular vesicle impact electrochemical cytometry (IVIEC)	*In situ* approach quantifying total vesicle content within their cellular environment (in the cytoplasm)	+ Possible to change external factors such as osmolarity, pH and pharmaceutical treatments with minimal impact on the cells - Cannot distinguish between catecholamine and other electroactive molecules at the same time
Fast scan cyclic voltammetry (FSCV)	Study of the behavior, addiction, and disease of live animals by measuring *in vivo* the rapid changes of neurotransmitters	+ Possible to simultaneously quantify and identify various analytes by selecting voltage limits of the interested analyte - Cannot measure basal levels of neurotransmitters, governed by phasic and tonic neuronal activity, only fast change of electroactive species because the background current can be only stable for a brief time

not affect the final fusion pore, whereas Zn^{2+} tended to enlarge pore sizes. The results strengthened the concept of sub-quantal release during exocytosis.

OTHER ELECTROCHEMICAL METHODS

Another common technique is fast scan cyclic voltammetry (FSCV), which is useful for monitoring neurotransmitter fluctuations in tissues or single cells *in vitro* because of interferences of complex environments. It has been considered as the most common method for monitoring neurotransmitter level in the brain (Robinson et al., 2003, 2008; Venton and Wightman, 2003; Rodeberg et al., 2017; Roberts and Sombers, 2018). Electroactive species are quickly reduced and oxidized on electrode surface by a triangular waveform applied to the electrode at high scan rate (>100 V/s). Electroactive compounds in the CNS of a rat brain were measured for the first time using implanted graphite paste microelectrodes by the Adam group (Kissinger et al., 1973). The Wightman group successfully introduced FSCV to determine electroactive transmitters such as dopamine, norepinephrine, epinephrine, serotonin, histamine, and adenosine, from various samples, including nucleus accumbens, bovine adrenal medullary cells, mast cells, and brain tissues (Bucher and Wightman, 2015). Venton and coworkers implemented a method for monitoring dopamine release in a ventral nerve cord from Drosophila larva (Vickrey et al., 2009). They also determined extracellular serotonin and dopamine levels in a single Drosophila larva ventral nerve cord (Borue et al., 2009). ChR2 was genetically expressed in octopaminergic and serotonergic neurons, neurotransmitter released was detected by FSCV with blue light stimulation. These studies show that dopamine and serotonin regulations are analogous to those in mammals.

Chronoamperometry and differential pulse voltammetry are available for measuring concentrations of neurotransmitters and different analytes. However, these methods show limited chemical selectivity and poor time resolution, as one scan takes more than 10 s for chronoamperometry and more than 30 s for differential pulse voltammetry. The fluctuation of neurotransmitters is on the sub-second time scale; therefore, these techniques are not commonly employed for monitoring chemical communication in the nervous system.

Capacitance measurement is also a useful approach for monitoring changes of cellular surface area after the vesicular membrane has fused with the plasma membrane during exocytosis (Lindau and Neher, 1988; Gillis, 1995). It allows for direct characterization of fusion pore properties. Capacitance measurements have been conducted for cells and neurons with complex branching (Kushmerick and von Gersdorff, 2003; Kim and Von Gersdorff, 2010). Example study is whole-cell recording from mossy fiber boutons in hippocampal neurons (Hallermann et al., 2003), in axon terminals of the brainstem calyx of Held (Sun and Wu, 2001; Wölfel and Schneggenburger, 2003), and in axon terminals of neurons in the posterior pituitary gland (Hsu and Jackson, 1996). Standard capacitance measurement, however, can only measure readily releasable vesicles and, thus, is not applicable for total releasable pools.

SUMMARY AND FUTURE PERSPECTIVES

Measurement of molecular organization, turnover, and dynamic change in single neuronal cells and single synapses is possible using current state-of-the-art analytical technologies (**Table 1**). SIMS allows for the visualization of non-targeted and targeted molecules and their metabolic turnover, whereas single cell amperometry and cytometry are ideal quantification methods with high temporal resolution for neuronal secretion. These technologies offer a unique opportunity to obtain an insight into the molecular mechanism that modulates synaptic activity and neuronal processes.

Challenges in neuronal and synaptic imaging are the required very high spatial resolution to visualize extremely small structures, sufficient sensitivity to detect analytes in a very small volume, and a suitable sample preparation strategy to preserve the intact molecular architecture of the sample. Technical developments in these technologies are still continuously ongoing to circumvent these challenges. For example, new primary ion sources and ion optics in SIMS are being developed to improve imaging sensitivity, spatial resolution, and mass resolution. Tandem MS SIMS, such as the recently developed OrbiSIMS (Passarelli et al., 2017), will be useful for elucidating molecular structures in complex molecular compositions of neurons and synapses. In addition, development of labeling tools for large biomolecules, such as proteins (Kabatas et al., 2019; Agüi-Gonzalez et al., 2021), will allow for targeted imaging of multiple proteins and lipids by SIMS at the single synapse level. Furthermore, standardization of data treatment and statistical analysis, as well as development of mass peak databases specific for neurons and synapses will ensure reliable data handling and interpretation performed by those who are not SIMS experts. This will play a vital role in realizing SIMS as a common imaging technique in neuroscience.

The development of new types of micro- and nanoelectrodes for electrochemical analysis is in continuous progress to expand its repertoire of detectable analytes, improve sensitivity and speed, and enable sub-vesicular measurements. Modification of electrochemical conditions, for example adding chaotropic anions (SCN^-) (He and Ewing, 2022), could change the opening nature of vesicles, facilitating the measurement of transmitter content in individual sub-vesicular compartments, the halo, and dense core.

Finally, a combination of different imaging and analysis techniques to obtain multidimensional information of the studied samples will be an increasingly favored trend. We will be able to correlate the organization of a wide range of targeted molecules, neuronal structures and morphology, dynamic metabolic processes, and synaptic activity in single neurons and synapses.

AUTHOR CONTRIBUTIONS

AL, KV, and NP wrote the manuscript. NP organized the manuscript, coordinated, and supervised the writing progress. All authors provided comments and refined the manuscript before the submission.

FUNDING

We acknowledge the grants from the VR (Swedish Research Council, 2020-00815), and the Hasselblad Foundation to N.T.N.P.

ACKNOWLEDGMENTS

We would like to thank the colleagues and collaborators who contributed to the studies cited in this review.

REFERENCES

Agüi-Gonzalez, P., Guobin, B., Gomes de Castro, M. A., Rizzoli, S. O., and Phan, N. T. N. (2021). Secondary ion mass spectrometry imaging reveals changes in the lipid structure of the plasma membranes of hippocampal neurons following drugs affecting neuronal activity. *ACS Chem. Neurosci.* 12, 1542–1551. doi: 10.1021/acschemneuro.1c00031

Agüi-Gonzalez, P., Jähne, S., and Phan, N. T. N. (2019). SIMS imaging in neurobiology and cell biology. *J. Analyt. Atomic. Spec.* 34, 1355–1368. doi: 10.1039/C9JA00118B

Bard, A. J., and Faulkner, L. J. (2001). *Electrochemical Methods: Fundamentals and Applications*, 2nd Edn. Hoboken, NJ: John Wiley & Sons, Inc.

Borland, L. M., and Michael, A. C. (2007). "An introduction to electrochemical methods in neuroscience," in *Electrochemical Methods for Neuroscience*, eds A. C. Michael and L. M. Borland (Boca Raton, FL: CRC Press).

Borue, X., Cooper, S., Hirsh, J., Condron, B., and Venton, B. J. (2009). Quantitative evaluation of serotonin release and clearance in *Drosophila*. *J. Neurosci. Methods* 179, 300–308. doi: 10.1016/j.jneumeth.2009.02.013

Boxer, S. G., Kraft, M. L, and Weber, P. K. (2009). Advances in imaging secondary ion mass spectrometry for biological samples. *Annu. Rev. Biophys.* 38, 53–74. doi: 10.1146/annurev.biophys.050708.133634

Bruinen, A. L., Fisher, G. L., Balez, R., van der Sar, A. M., Ooi, L., and Heeren, R. M. A. (2018). Identification and high-resolution imaging of α-tocopherol from human cells to whole animals by TOF-SIMS tandem mass spectrometry. *J. Am. Soc. Mass Spectrom.* 29, 1571–1581. doi: 10.1007/s13361-018-1979-x

Bruns, D., and Jahn, R. (1995). Real-time measurement of transmitter release from single synaptic vesicles. *Nature* 377, 62–65. doi: 10.1038/377062a0

Bucher, E. S., and Wightman, R. M. (2015). Electrochemical analysis of neurotransmitters. *Annu. Rev. Anal. Chem.* 8, 239–261. doi: 10.1146/annurev-anchem-071114-040426

Chen, G., and Ewing, A. G. (1995). Multiple classes of catecholamine vesicles observed during exocytosis from the Planorbis cell body. *Brain Res.* 701, 167–174. doi: 10.1016/0006-8993(95)00989-9

Chen, T. K., Luo, G. O., and Ewing, A. G. (1994). Amperometric monitoring of stimulated catecholamine release from rat pheochromocytoma (Pc12) cells at the zeptomole level. *Anal. Chem.* 66, 3031–3035. doi: 10.1021/ac00091a007

Cox, S. J., and Gabbiani, F. (eds). (2010). "Synaptic transmission and quantal release," in *Mathematics for Neuroscientists*, (Cambridge, MA: Academic Press), 175–191. doi: 10.1016/b978-0-12-374882-9.00012-5

DeLellis, R., Merk, F., Deckers, P., Warren, S., and Balogh, K. (1973). Ultrastructure and in vitro growth characteristics of a transplantable rat

pheochromocytoma. *Cancer* 32, 227–235. doi: 10.1002/1097-0142(197307)32:1<227::aid-cncr2820320134>3.0.co;2-w

Dunevall, J., Fathali, H., Najafinobar, N., Lovric, J., Wigstrom, J., Cans, A. S., et al. (2015). Characterizing the catecholamine content of single mammalian vesicles by collision-adsorption events at an electrode. *J. Am. Chem. Soc.* 137, 4344–4346. doi: 10.1021/ja512972f

Gillis, K. D. (1995). "Techniques for membrane capacitance measurements," in *Single-Channel Recording*, ed. E. Sakmann Bertand Neher (New York, NY: Springer), 155–198. doi: 10.1007/978-1-4419-1229-9_7

Gonon, F., Buda, M., Cespuglio, R., Jouvet, M., and Pujol, J. F. (1980). In vivo electrochemical detection of catechols in the neostriatum of anaesthetized rats: dopamine or DOPAC? *Nature* 286, 902–904. doi: 10.1038/286902a0

Gu, C., Larsson, A., and Ewing, A. G. (2019). Plasticity in exocytosis revealed through the effects of repetitive stimuli affect the content of nanometer vesicles and the fraction of transmitter released. *Proc. Natl. Acad. Sci.* 116, 21409–21415. doi: 10.1073/PNAS.1910859116

Gu, C., Philipsen, M. H., and Ewing, A. G. (2020). Mass spectrometric imaging of plasma membrane lipid alteration correlated with amperometrically measured activity-dependent plasticity in exocytosis. *Int. J. Mol. Sci.* 21:9519. doi: 10.3390/ijms21249519

Hallermann, S., Pawlu, C., Jonas, P., and Heckmann, M. (2003). A large pool of releasable vesicles in a cortical glutamatergic synapse. *Proc. Natl. Acad. Sci. U.S.A.* 100, 8975–8980. doi: 10.1073/pnas.1432836100

He, X., and Ewing, A. G. (2022). Simultaneous counting of molecules in the halo and dense-core of nanovesicles by regulating dynamics of vesicle opening. *Angew. Chem. Int. Ed. Engl.* 61:e202116217. doi: 10.1002/anie.202116217

Hochstetler, S. E., Puopolo, M., Gustincich, S., Raviola, E., and Wightman, R. M. (2000). Real-time amperometric measurements of zeptomole quantities of dopamine released from neurons. *Anal. Chem.* 72, 489–496. doi: 10.1021/ac991119x

Hsu, S. F., and Jackson, M. B. (1996). Rapid exocytosis and endocytosis in nerve terminals of the rat posterior pituitary. *J. Physiol.* 494, 539–553. doi: 10.1113/jphysiol.1996.sp021512

Jaffe, E. H., Marty, A., Schulte, A., and Chow, R. H. (1998). Extrasynaptic vesicular transmitter release from the somata of substantia nigra neurons in rat midbrain slices. *J. Neurosci.* 18, 3548–3553. doi: 10.1523/JNEUROSCI.18-10-03548.1998

Jähne, S., Mikulasch, F., Heuer, H. G. H., Truckenbrodt, S., Agüi-Gonzalez, P., Grewe, K., et al. (2021). Presynaptic activity and protein turnover are correlated at the single-synapse level. *Cell Rep.* 34:108841. doi: 10.1016/j.celrep.2021.108841

Kabatas, S., Agüi-Gonzalez, P., Saal, K. A., Jähne, S., Opazo, F., Rizzoli, S. O., et al. (2019). Boron-containing probes for non-optical high resolution imaging of biological samples. *Angew. Chem. Int. Ed.* 58, 3438–3443. doi: 10.1002/anie.201812032

Keighron, J. D., Wang, Y., and Cans, A.-S. (2020). Electrochemistry of single-vesicle events. *Annu. Rev. Anal. Chem.* 13, 159–181. doi: 10.1146/annurev-anchem-061417-010032

Kim, M., and Von Gersdorff, H. (2010). Extending the realm of membrane capacitance measurements to nerve terminals with complex morphologies. *J. Physiol.* 588, 2011–2012. doi: 10.1113/jphysiol.2010.191270

Kissinger, P. T., Hart, J. B., and Adams, R. N. (1973). Voltammetry in brain-tissue - new neurophysiological measurement. *Brain Res.* 55, 209–213. doi: 10.1016/0006-8993(73)90503-9

Kollmer, F. (2004). Cluster primary ion bombardment of organic materials. *Appl. Surf. Sci.* 231, 153–158. doi: 10.1016/j.apsusc.2004.03.101

Kushmerick, C., and von Gersdorff, H. (2003). Exo-endocytosis at mossy fiber terminals: toward capacitance measurements in cells with arbitrary geometry. *Proc. Natl. Acad. Sci. U.S.A.* 100, 8618–8620. doi: 10.1073/pnas.1633427100

Lanekoff, I., Sjövall, P., and Ewing, A. G. (2011). Relative quantification of phospholipid accumulation in the PC12 cell plasma membrane following phospholipid incubation using TOF-SIMS imaging. *Anal. Chem.* 83, 5337–5343. doi: 10.1021/ac200771g

Lange, F., Agüi-Gonzalez, P., Riedel, D., Phan, N. T. N., Jakobs, S., and Rizzoli, S. O. (2021). Correlative fluorescence microscopy, transmission electron microscopy and secondary ion mass spectrometry (CLEM-SIMS) for cellular imaging. *PLoS One* 16:e0240768. doi: 10.1371/journal.pone.0240768

Larsson, A., Majdi, S., Oleinick, A., Svir, I., Dunevall, J., Amatore, C., et al. (2020). Intracellular electrochemical nanomeasurements reveal that exocytosis of molecules at living neurons is subquantal and complex. *Angew. Chem.* 59, 6711–6714. doi: 10.1002/anie.201914564

Lee, S. Y., Lim, H., Moon, D. W., and Kim, J. Y. (2019). Improved ion imaging of slowly dried neurons and skin cells by graphene cover in time-of-flight secondary ion mass spectrometry. *Biointerphases* 14:051001. doi: 10.1116/1.5118259

Leszczyszyn, D. J., Jankowski, J. A., Viveros, O. H., Diliberto, E. J. Jr., Near, J. A., and Wightman, R. M. (1991). Secretion of catecholamines from individual adrenal medullary chromaffin cells. *J. Neurochem.* 56, 1855–1863. doi: 10.1111/j.1471-4159.1991.tb03441.x

Li, X., Dunevall, J., and Ewing, A. G. (2016a). Quantitative chemical measurements of vesicular transmitters with electrochemical cytometry. *Acc. Chem. Res.* 49, 2347–2354. doi: 10.1021/acs.accounts.6b00331

Li, X., Dunevall, J., and Ewing, A. G. (2016b). Using single-cell amperometry to reveal how cisplatin treatment modulates the release of catecholamine transmitters during exocytosis. *Ange. Chem.* 55, 9041–9044. doi: 10.1002/anie.201602977

Li, Y. T., Zhang, S. H., Wang, L., Xiao, R. R., Liu, W., Zhang, X. W., et al. (2014). Nanoelectrode for amperometric monitoring of individual vesicular exocytosis inside single synapses. *Angew. Chem. Int. Ed. Engl.* 53, 12456–12460. doi: 10.1002/anie.201404744

Lim, H., Lee, S. Y., Park, Y., Jin, H., Seo, D., Jang, Y. H., et al. (2021). Mass spectrometry imaging of untreated wet cell membranes in solution using single-layer graphene. *Nat. Methods* 18, 316–320. doi: 10.1038/s41592-020-01055-6

Lindau, M., and Neher, E. (1988). Patch-clamp techniques for time-resolved capacitance measurements in single cells. *Pflugers Arch.* 411, 137–146. doi: 10.1007/BF00582306

Lovrić, J., Dunevall, J., Larsson, A., Ren, L., Andersson, S., Meibom, A., et al. (2017). Nano secondary ion mass spectrometry imaging of dopamine distribution across nanometer vesicles. *ACS Nano* 11, 3446–3455. doi: 10.1021/acsnano.6b07233

Majdi, S., Berglund, E. C., Dunevall, J., Oleinick, A. I., Amatore, C., Krantz, D. E., et al. (2015). Electrochemical measurements of optogenetically stimulated quantal amine release from single nerve cell varicosities in drosophila larvae. *Angew. Chem. Int. Ed. Engl.* 54, 13609–13612. doi: 10.1002/anie.201506743

Mellander, L. J., Trouillon, R., Svensson, M. I., and Ewing, A. G. (2012). Amperometric post spike feet reveal most exocytosis is via extended kiss-and-run fusion. *Sci. Rep.* 2:907. doi: 10.1038/srep00907

Monroe, E. B., Jurchen, J. C., Lee, J., Rubakhin, S. S., and Sweedler, J. V. (2005). Vitamin E imaging and localization in the neuronal membrane. *J. Am. Chem. Soc.* 127, 12152–12153. doi: 10.1021/ja051223y

Nguyen, T., Mellander, L., Lork, A., Philipsen, M., Kurczy, M. E., Phan, N. T. N., et al. (2022). Visualization of partial exocytotic content release and chemical transport into nanovesicles in cells. *ACS Nano* 16, 4831–4842. doi: 10.1021/acsnano.2c00344

Nuñez, J., Renslow, R., Cliff, J. B., and Anderton, C. R. (2018). NanoSIMS for biological applications: current practices and analyses. *Biointerphases* 13:03B301. doi: 10.1116/1.4993628

Pacholski, M. L., and Winograd, N. (1999). Imaging with mass spectrometry. *Chem. Rev.* 99, 2977–3006. doi: 10.1021/cr980137w

Parletta, N., Niyonsenga, T., and Duff, J. (2016). Omega-3 and omega-6 polyunsaturated fatty acid levels and correlations with symptoms in children with attention deficit hyperactivity disorder, autistic spectrum disorder and typically developing controls. *PLoS One* 11:e0156432. doi: 10.1371/journal.pone.0156432

Passarelli, M. K., and Ewing, A. G. (2013). Single-cell imaging mass spectrometry. *Curr. Opin. Chem. Biol.* 17, 854–859. doi: 10.1016/j.cbpa.2013.07.017

Passarelli, M. K., Pirkl, A., Moellers, R., Grinfeld, D., Kollmer, F., Havelund, R., et al. (2017). The 3D OrbiSIMS–Label-free metabolic imaging with subcellular lateral resolution and high mass resolving power. *Nat. Methods* 14, 1175–1183. doi: 10.1038/nmeth.4504

Philipsen, M. H., Phan, N. T. N., Fletcher, J. S., and Ewing, A. G. (2020). Interplay between cocaine, drug removal, and methylphenidate reversal on phospholipid alterations in drosophila brain determined by imaging mass spectrometry. *ACS Chem. Neurosci.* 11, 806–813. doi: 10.1021/acschemneuro.0c00014

Philipsen, M. H., Sämfors, S., Malmberg, P., and Ewing, A. G. (2018). Relative quantification of deuterated omega-3 and -6 fatty acids and their lipid turnover in PC12 cell membranes using TOF-SIMS. *J. Lipid Res.* 59, 2098–2107. doi: 10.1194/jlr.M087734

Ponchon, J. L., Cespuglio, R., Gonon, F., Jouvet, M., and Pujol, J. F. (1979). Normal pulse polarography with carbon fiber electrodes for in vitro and in vivo determination of catecholamines. *Anal. Chem.* 51, 1483–1486. doi: 10.1021/ac50045a030

Postawa, Z., Czerwinski, B., Winograd, N., and Garrison, B. J. (2005). Microscopic insights into the sputtering of thin organic films on Ag111 induced by C_{60} and ga bombardment. *J. Phys. Chem. B.* 109, 11973–11979. doi: 10.1021/jp050821w

Pothos, E. N., Davila, V., and Sulzer, D. (1998). Presynaptic recording of quanta from midbrain dopamine neurons and modulation of the quantal size. *J. Neurosci.* 18, 4106–4118. doi: 10.1523/JNEUROSCI.18-11-04106.1998

Prasad, M. R., Lovell, M. A., Yatin, M., Dhillon, H., and Markesbery, W. R. (1998). Regional membrane phospholipid alterations in Alzheimer's disease. *Neurochem. Res.* 23, 81–88. doi: 10.1023/A:1022457605436

Qiu, Q. F., Zhang, F. L., Tang, Y., Zhang, X. W., Jiang, H., Liu, Y. L., et al. (2018). Real-time monitoring of exocytotic glutamate release from single neuron by amperometry at an enzymatic biosensor. *Electroanalysis* 30, 1054–1059. doi: 10.1002/elan.201700656

Rabasco, S., Nguyen, T. D. K., Gu, C., Kurczy, M. E., Phan, N. T. N., and Ewing, A. G. (2022). Localization and absolute quantification of dopamine in discrete intravesicular compartments using nanoSIMS imaging. *Int. J. Mol. Sci.* 23:160. doi: 10.3390/ijms23010160

Rabbani, S. S., Barber, A., Fletcher, J. S., Lockyer, N. P. and Vickerman, J. C. (2013). Enhancing secondary ion yields in time of flight-secondary ion mass spectrometry using water cluster primary beams. *Anal. Chem.* 85, 5654–5658. doi: 10.1021/ac4013732

Ren, L., Mellander, L. J., Keighron, J., Cans, A. S., Kurczy, M. E., Svir, I., et al. (2016). The evidence for open and closed exocytosis as the primary release mechanism. *Q. Rev. Biophys.* 49:e12. doi: 10.1017/S0033583516000081

Roberts, J. G., and Sombers, L. A. (2018). Fast-scan cyclic voltammetry: chemical sensing in the brain and beyond. *Anal. Chem.* 90, 490–504. doi: 10.1021/acs.analchem.7b04732

Robinson, D. L., Hermans, A., Seipel, A. T., and Wightman, R. M. (2008). Monitoring rapid chemical communication in the brain. *Chem. Rev.* 108, 2554–2584. doi: 10.1021/cr068081q

Robinson, D. L., Venton, B. J., Heien, M. L., and Wightman, R. M. (2003). Detecting subsecond dopamine release with fast-scan cyclic voltammetry in vivo. *Clin. Chem.* 49, 1763–1773. doi: 10.1373/49.10.1763

Rodeberg, N. T., Sandberg, S. G., Johnson, J. A., Phillips, P. E., and Wightman, R. M. (2017). Hitchhiker's guide to voltammetry: acute and chronic electrodes for in vivo fast-scan cyclic voltammetry. *ACS Chem. Neurosci.* 8, 221–234. doi: 10.1021/acschemneuro.6b00393

Saka, S. K., Vogts, A., Kröhnert, K., Hillion, F., Rizzoli, S. O., and Wessels, J. T. (2014). Correlated optical and isotopic nanoscopy. *Nat. Commun.* 5:3664. doi: 10.1038/ncomms4664

Salamifar, S. E., and Lai, R. Y. (2015). Scanning electrochemical and fluorescence microscopy for detection of reactive oxygen species in living cells. *ACS Symposium Ser.* 1200, 415–430. doi: 10.1021/bk-2015-1200.ch017

Shen, M., Qu, Z., DesLaurier, J., Welle, T. M., Sweedler, J. V., and Chen, R. (2018). Single synaptic observation of cholinergic neurotransmission on living neurons: concentration and dynamics. *J. Am. Chem. Soc.* 140, 7764–7768. doi: 10.1021/jacs.8b01989

Staal, R. G., Mosharov, E. V., and Sulzer, D. (2004). Dopamine neurons release transmitter via a flickering fusion pore. *Nat. Neurosci.* 7, 341–346. doi: 10.1038/nn1205

Steinhauser, M. L., Bailey, A. P., Senyo, S. E., Guillermier, C., Perlstein, T. S., Gould, A. P., et al. (2012). Multi-isotope imaging mass spectrometry quantifies stem cell division and metabolism. *Nature* 481, 516–519. doi: 10.1038/nature10734

Sun, J.-Y., and Wu, L.-G. (2001). Fast kinetics of exocytosis revealed by simultaneous measurements of presynaptic capacitance and postsynaptic currents at a central synapse. *Neuron* 30, 171–182.

Tang, Y., Yang, X. K., Zhang, X. W., Wu, W. T., Zhang, F. L., Jiang, H., et al. (2019). Harpagide, a natural product, promotes synaptic vesicle release as measured by nanoelectrode amperometry. *Chem. Sci.* 11, 778–785. doi: 10.1039/c9sc05538j

Thomen, A., Najafinobar, N., Penen, F., Kay, E., Upadhyay, P. P., Li, X., et al. (2020). Subcellular mass spectrometry imaging and absolute quantitative analysis across organelles. *ACS Nano* 14, 4316–4325. doi: 10.1021/acsnano.9b09804

Toyoda, N., Matsuo, J., Aoki, T., Yamada, I., and Fenner, D. B. (2003). Secondary ion mass spectrometry with gas cluster ion beams. *Appl. Surf. Sci.* 203, 214–218. doi: 10.1016/S0169-4332(02)00628-1

Truckenbrodt, S., Viplav, A., Jähne, S., Vogts, A., Denker, A., Wildhagen, H., et al. (2018). Newly produced synaptic vesicle proteins are preferentially used in synaptic transmission. *EMBO J.* 37, 1–24. doi: 10.15252/embj.201798044

Tucker, K. R., Li, Z., Rubakhin, S. S., and Sweedler, J. V. (2012). Secondary ion mass spectrometry imaging of molecular distributions in cultured neurons and their processes: comparative analysis of sample preparation. *J. Am. Soc. Mass Spectrom.* 23, 1931–1938. doi: 10.1007/s13361-012-0472-1

Uchiyama, Y., Maxson, M. M., Sawada, T., Nakano, A., and Ewing, A. G. (2007). Phospholipid mediated plasticity in exocytosis observed in PC12 cells. *Brain Res.* 1151, 46–54. doi: 10.1016/j.brainres.2007.03.012

Vanbellingen, Q. P., Elie, N., Eller, M. J., Della-Negra, S., Touboul, D., and Brunelle, A. (2015). Time-of-flight secondary ion mass spectrometry imaging of biological samples with delayed extraction for high mass and high spatial resolutions. *Rapid Commun. Mass Spectrom.* 29, 1187–1195.

Venton, B. J., and Wightman, R. M. (2003). Psychoanalytical electrochemistry: dopamine and behavior. *Anal. Chem.* 75, 414a–421a. doi: 10.1021/ac031421c

Vickerman, J. C., and Briggs, D. (2013). *ToF-SIMS: Surface Analysis by Mass Spectrometry*. IM Pulication.

Vickrey, T. L., Condron, B., and Venton, B. J. (2009). Detection of endogenous dopamine changes in *Drosophila melanogaster* using fast-scan cyclic voltammetry. *Anal. Chem.* 81, 9306–9313. doi: 10.1021/ac901638z

Watanabe, S., Punge, A., Hollopeter, G., Willig, K. I., Hobson, J. R., Davis, M. W., et al. (2011). Protein localization in electron micrographs using fluorescence nanoscopy. *Nat. Methods* 1, 80–84. doi: 10.1038/nmeth.1537

Weibel, D., Wong, S., Lockyer, N., Blenkinsopp, P., Hill, R., and Vickerman, J. C. (2003). A C_{60} primary ion beam system for time of flight secondary ion mass spectrometry: its development and secondary ion yield characteristics. *Anal. Chem.* 75, 1754–1764. doi: 10.1021/ac026338o

Wightman, R. M., Jankowski, J. A., Kennedy, R. T., Kawagoe, K. T., Schroeder, T. J., Leszczyszyn, D. J., et al. (1991). Temporally resolved catecholamine spikes correspond to single vesicle release from individual chromaffin cells. *Proc. Natl. Acad. Sci. U.S.A.* 88, 10754–10758. doi: 10.1073/pnas.88.23.10754

Wilhelm, B. G., Mandad, S., Truckenbrodt, S., Kröhnert, K., Schäfer, C., Rammner, B., et al. (2014). Composition of isolated synaptic boutons reveals the amounts of *Vesicle trafficking* proteins. *Science* 344, 1023–1028. doi: 10.1126/science.1252884

Winograd, N. (2013). "The magic of cluster SIMS," in *Fundamentals of Mass Spectrometry*, ed. K. Hiraoka (New York, NY: Springer), 199–230. doi: 10.1007/978-1-4614-7233-9_10

Wölfel, M., and Schneggenburger, R. (2003). Presynaptic capacitance measurements and Ca^{2+} uncaging reveal submillisecond exocytosis kinetics and characterize the Ca^{2+} sensitivity of vesicle pool depletion at a fast CNS synapse. *J. Neurosci.* 23, 7059–7068. doi: 10.1523/JNEUROSCI.23-18-07059.2003

Yang, X. K., Zhang, F. L., Wu, W. T., Tang, Y., Yan, J., Liu, Y. L., et al. (2021). Quantitative nano-amperometric measurement of intravesicular glutamate content and its sub-quantal release by living neurons. *Angew. Chem.* 60, 15803–15808. doi: 10.1002/anie.202100882

Ye, D. X., Gu, C., and Ewing, A. Y. (2018). Using single-cell amperometry and intracellular vesicle impact electrochemical cytometry to shed light on the biphasic effects of lidocaine on exocytosis. *ACS Chem. Neurosci.* 9, 2941–2947. doi: 10.1021/acschemneuro.8b00130

Zhou, Z., and Misler, S. (1995). Amperometric detection of stimulus-induced quantal release of catecholamines from cultured superior cervical ganglion neurons. *Proc. Natl. Acad. Sci. U.S.A.* 92, 6938–6942. doi: 10.1073/pnas.92.15.6938

Zhu, W. Y., Gu, C. Y., Dunevall, J., Ren, L., Zhou, X. M., and Ewing, A. G. (2019). Combined amperometry and electrochemical cytometry reveal differential effects of cocaine and methylphenidate on exocytosis and the fraction of chemical release. *Angew. Chem.* 58, 4238–4242. doi: 10.1002/anie.201813717

Conflict of Interest: The authors declare that the research was conducted in the absence of any commercial or financial relationships that could be construed as a potential conflict of interest.

The handling editor SR declared a past co-authorship/collaboration with the author NP.

Publisher's Note: All claims expressed in this article are solely those of the authors and do not necessarily represent those of their affiliated organizations, or those of the publisher, the editors and the reviewers. Any product that may be evaluated in this article, or claim that may be made by its manufacturer, is not guaranteed or endorsed by the publisher.

Advantages of publishing in Frontiers

OPEN ACCESS
Articles are free to read for greatest visibility and readership

FAST PUBLICATION
Around 90 days from submission to decision

HIGH QUALITY PEER-REVIEW
Rigorous, collaborative, and constructive peer-review

TRANSPARENT PEER-REVIEW
Editors and reviewers acknowledged by name on published articles

Frontiers
Avenue du Tribunal-Fédéral 34
1005 Lausanne | Switzerland

Visit us: www.frontiersin.org
Contact us: frontiersin.org/about/contact

REPRODUCIBILITY OF RESEARCH
Support open data and methods to enhance research reproducibility

DIGITAL PUBLISHING
Articles designed for optimal readership across devices

FOLLOW US
@frontiersin

IMPACT METRICS
Advanced article metrics track visibility across digital media

EXTENSIVE PROMOTION
Marketing and promotion of impactful research

LOOP RESEARCH NETWORK
Our network increases your article's readership